# EMERGING INFECTIOUS DISEASES®

U.S. CENTERS FOR DISEASE CONTROL AND PREVENTION

**Parasitic Infections**

**July 2026**



**Sherri Richards (1955–), *An Everlasting Love*, 2024.** Acrylic and oil on gallery-wrapped canvas. 36 in × 36 in (91.44 cm × 91.44 cm). Used with permission of the artist.

Pages 1039–1230

# EMERGING INFECTIOUS DISEASES

A Peer-Reviewed Journal Tracking and Analyzing Disease Trends



*Emerging Infectious Diseases* is published monthly by the Centers for Disease Control and Prevention, 1600 Clifton Rd NE, Mailstop H16-2, Atlanta, GA 30329-4018, USA. Telephone 404-639-1960; email eideditor@cdc.gov

# EMERGING INFECTIOUS DISEASES®

**Parasitic Infections** **July 2026**


## On the Cover

**Sherri Richards (1955–), *An Everlasting Love*, 2024.** Acrylic and oil on gallery-wrapped canvas. 36 in x 36 in (91.44 cm x 91.44 cm). Used with permission of the artist.

**About the Cover p. 1226**

## Synopses


**Outbreak of Legionnaires' Disease Linked to Newly Installed Residential Water Heaters, the Netherlands, 2022–2023**
D.F.M. Reukers et al. **1039**

Medscape EDUCATION ACTIVITY

**Trichinellosis Outbreak Linked to Undercooked Bear Jerky, North Carolina, USA, 2024**
Three cases were caused by *Trichinella spiralis* infection.
C.D. Gowler et al. **1046**

**Emerging Risk for Human T-Cell Leukemia Virus Type 1 Transmission with HIV-Positive Breastfeeding Support**
A. Meybeck et al. **1052**

**Epidemiology and Clinical Features of *Balamuthia mandrillaris* Infection, China**
T. Yang et al. **1058**

**Neurosurgical Biopsy and Resection for Diagnosis and Treatment of *Balamuthia mandrillaris* Amebic Encephalitis, United States**
B. Rubbab et al. **1065**


## Research


**Adeno-Associated Virus Type 2 and Human Adenovirus Species F Type 41 Co-infection Associated with Acute Severe Hepatitis in Children, California, USA**
R. Zhuo et al. **1074**

**National Surveillance of Enterovirus D68 Upsurge, France, 2024**
M. Jeannoël et al. **1082**

**Clinical Predictors of Fatal Outcomes from Human Leptospirosis, Thailand, 2015–2024**
U. Limothai et al. **1094**

**Prognostic Value of PCR Cycle Threshold Value in Crimean-Congo Hemorrhagic Fever, Iraq, 2022–2023**
R.I. Khaleel et al. **1104**

**Predictive Approach to Mapping *Angiostrongylus cantonensis* Nematode Distribution, Canary Islands, Spain**
L. Anettová et al. **1113**



EMERGING INFECTIOUS DISEASES®

July 2026

**Molecular Epidemiology of Skin-Dwelling Filariae and Risk Factors for *Mansonella streptocerca* infection, Gabon**
C.M. Sicard et al. **1123**

**Investigation of Donor-Transmitted *Strongyloides stercoralis* Infections in Solid Organ Transplant Recipients, United States, 2012–2024**
K.R. Gainor et al. **1133**

## Historical Review

**Discovery of *Cinchona* as Antimalarial, Viceroyalty of Peru, Circa 1630**
J. Rojas-Jaimes et al. **1141**

## Dispatches

***Phormia regina* Fly as Vector for *Ignatzschineria* spp. Bacteremia in Persons Experiencing Homelessness, Canada, 2025**
E.C.L. Finlayson-Trick et al. **1150**

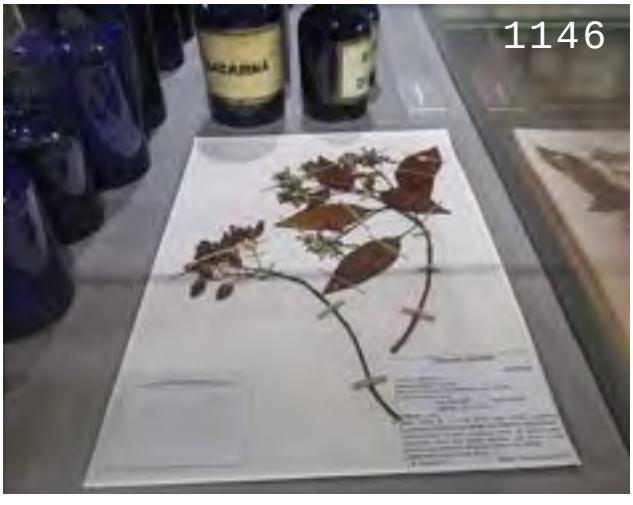


**Cat Scratch Disease Associated with Acute Hearing Loss, Israel**
M. Yakubovsky et al. **1155**

**Cluster of Human Tanapox Cases in Wildlife Reserve, South Africa, 2024**
M. Birkhead et al. **1159**


**Vascularized Iris Mass as Sentinel Manifestation of Syphilis in Patient with HIV Infection, Spain, 2025**
M. Caminal-Caramés et al. **1163**

**Nipah Virus Shedding in Urine from Fruit Bats, Sri Lanka, 2018–2019**
C. Kohl et al. **1167**


**Recurrent Facial Folliculities Caused by *Klebsiella aerogenes* Sequence Type 117 in Men who Have Sex with Men**
G. Monsel et al. **1172**

**Trends in Congenital Syphilis Cases by Maternal Country of Birth, Spain, 2016–2024**
V. Hernando et al. **1177**


**Household Transmission of Enterovirus D68 in Washington and Oregon, USA, 2022–2024**
P. Roychoudhury et al. **1182**

***Angiostrongylus cantonensis* Rat Lungworm Detected in Rats, Madagascar, 2022–2023**
S.F. Randrianarisoa et al. **1188**

## Research Letters

**New World Ocular Dirofilariasis Caused by *Dirofilaria repens* Infection, United States**
B.J. Glasgow et al. **1193**

**Human Pulmonary Dirofilariasis, North Queensland, Australia, 2023**
K. Murray et al. **1196**

**Detection of and Early Genomic Insights into Chikungunya Virus, Bolivia, 2025**
J.A.C. Valdez et al. **1198**

**Ophthalmomyiasis Outbreak Caused by *Oestrus ovis* Infection, Algeria, 2025**
Y. Zeng et al. **1201**

**Molecular Confirmation of Autochthonous *Taenia saginata* Infection, Timor-Leste, 2019**
H. Jin et al. **1204**

**Emergence of West African Human T-Lymphotropic Virus 1aC Subgroup, Brazilian Amazon**
J. de Melo Silva et al. **1207**


EMERGING INFECTIOUS DISEASES®
July 2026

**Neurologic Alveolar Echinococcosis in Postpartum Zoo-Housed Gorilla, the Netherlands, 2024**
L.A.N. Derks et al. **1211**

***Dracunculus* sp. PantanalBr Infection in Florida Panthers and Bobcat, Florida, USA**
M.J. Yabsley et al. **1214**

***Ancylostoma ceylanicum* Hookworm, Rural Papua New Guinea, 2020**
Jessica L. Scott et al. **1217**

**Autochthonous Neurocysticercosis Brain Lesions Mimicking Metastatic Disease, Spain**
E. Hernández-Sánchez et al. **1188**


**Chikungunya Outbreak, Cuba, July 2025**
M.M. Perez et al. **1217**

## About the Cover

**Jimmy Carter and Eradication of Guinea Worm Disease**
S. O'Connor et al. **1226**

## Etymologia

***Fasciolopsis buski***
M. Calatri **1051**

## Online Report

**Inconsistent Strategies to Mitigate the Effects of *Batrachochytrium salamandrivorans*, Europe**
P. Böning et al.
**https://wwwnc.cdc.gov/eid/article/32/7/25-1271_article**

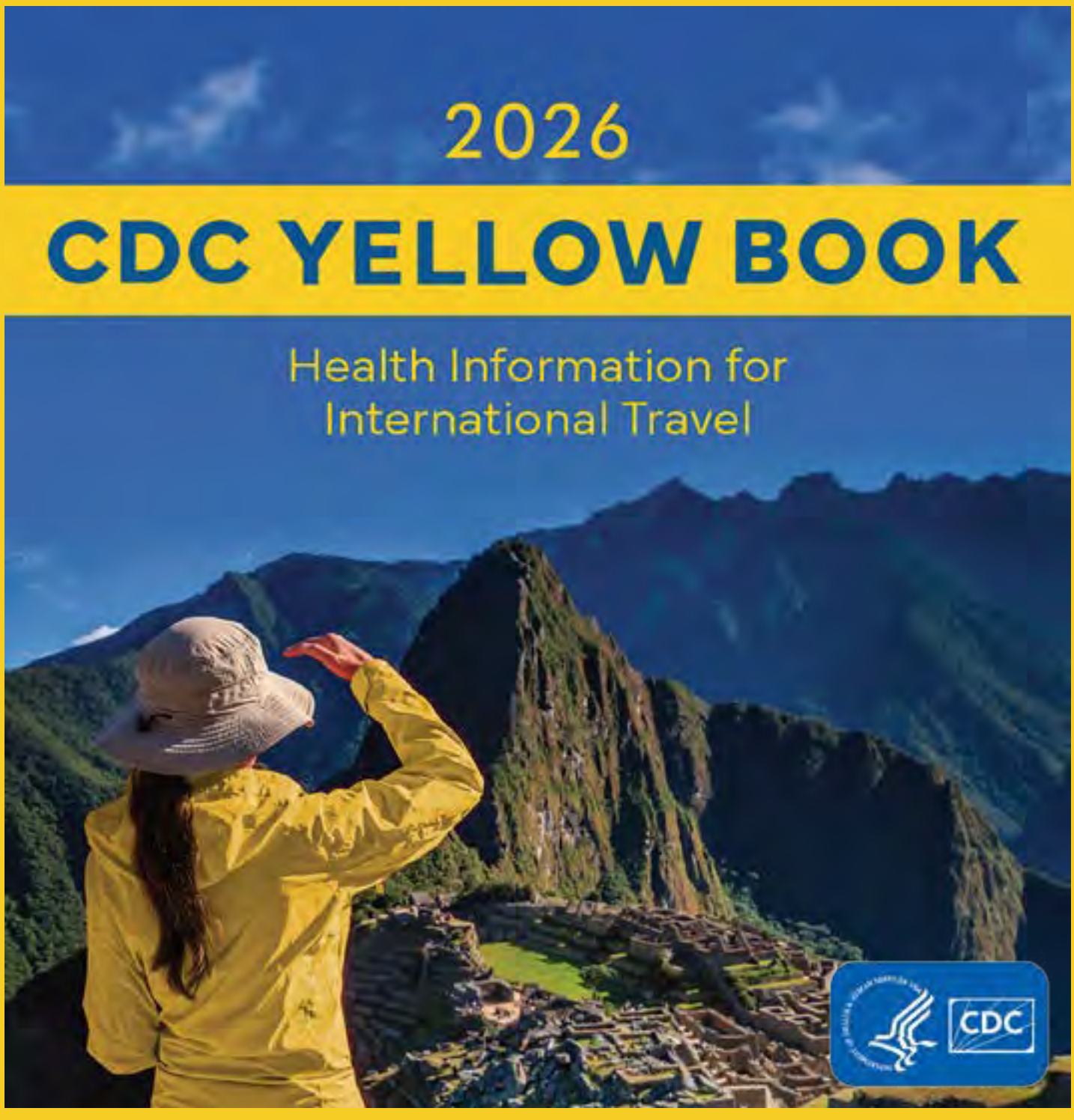


# Launch of CDC Yellow Book 2026– A Trusted Travel Medicine Resource

CDC is pleased to announce the launch of the **CDC Yellow Book 2026**. The CDC Yellow Book is a resource containing the U.S. government's travel medicine recommendations and has been trusted by the travel medicine community for over 50 years. Healthcare professionals can use the print and digital versions to find the most up-to-date travel medicine information to better serve their patients' healthcare needs.

The CDC Yellow Book is available online now at www.cdc.gov/yellowbook and in print starting in June 2025 through Oxford University Press and other major online booksellers.

# Outbreak of Legionnaires' Disease Linked to Newly Installed Residential Water Heaters, the Netherlands, 2022–2023

Daphne F.M. Reukers, Sjoerd M. Euser, Alvin A. Bartels, Martijn G. Keet, Marijke Boot, Wilhelmina L.M. Ruijs, Petra S. Brandsema

During 2022–2023, two small Legionnaires' disease (LD) clusters (2 and 4 cases) occurred in 2 residential apartment buildings in the Netherlands. All case-patients recently installed a new brand A water heater. Environmental sampling revealed *Legionella pneumophila* serogroup 1 sequence type 37 in the hot water system of each case-patient's apartment, matching 1 clinical isolate. We conducted a case–control study to evaluate whether brand A water heaters were linked to cases in the 2 clusters. We identified 23 LD case-patients, 21 of whom had a brand A water heater installed ≤6 months before illness onset. Four cases had a genotypic match between clinical and environmental isolates; none of 31 control-patients had recently installed a water heater. Analyses showed that LD cases were strongly associated with new brand A water heaters (OR 542 [95% CI 24.76–11,854.03]); the manufacturer implemented control measures. Residential water heaters could serve as *L. pneumophila* transmission sources.

Legionnaires' disease (LD) is pneumonia caused by infection with *Legionella* spp. bacteria (*1*). Legionellae can be found in water and soil in natural environments or in water installations, such as tap water, cooling towers, or wastewater treatment plants (*2*–*4*). If water from those systems or small soil particles containing *Legionella* spp. bacteria are aerosolized, the aerosols can be inhaled and subsequently cause disease. More than 60 different *Legionella* species have been identified, half of which are known to be pathogenic (*5*,*6*). In most countries, including the Netherlands, LD is primarily caused by *L. pneumophila*, of which serogroup 1 (SG1) is detected most often in patients (*7*,*8*).

LD is a notifiable disease in the Netherlands, and LD incidence has been increasing in the Netherlands and in Europe. In 2023, LD incidence reached a peak of 5.0 notifications/100,000 inhabitants in the Netherlands and 3.2 notifications/100,000 inhabitants in Europe (*8*). LD has a seasonal pattern that peaks in summer in most countries in Europe, including the Netherlands, likely because of favorable weather conditions for legionellae transmission from environmental sources (*7*,*8*).

In the Netherlands, most LD notifications are sporadic (i.e., not cluster or outbreak-related), and the source of infection, despite source tracing, remains unknown. In the Netherlands, only 1%–2% of LD cases have a source confirmed by a genotypic match between the patient's isolate and an environmental isolate (*7*); showers and drinking water systems in patients' homes are the most often sampled sources for LD cases, representing 31% of sampled sources during 2013–2022 (*7*). However, on average, <1 case/year had a genotypic match to the home water system (*7*).

At the beginning of 2023, two small clusters of LD cases emerged within 2 residential apartment buildings in the Netherlands. Cluster 1 included 4 cases in 1 building, and cluster 2 had 2 cases in another building. Because >1 LD case is rarely notified from a residential building, the unusual event of 2 clusters in a short period was reason for further investigation.

For 1 case, a clinical isolate was available and typed as *L. pneumophila* SG1 sequence type (ST) 37. ST37 is not common in drinking water in the Netherlands and is not often identified among LD patients in the country (*7*). Environmental sampling in patients' homes revealed ST37 in the hot water systems of

Author affiliations: Centre for Infectious Disease Control, National Institute for Public Health and the Environment (RIVM), Bilthoven, the Netherlands (D.F.M. Reukers, A.A. Bartels, M.G. Keet, M. Boot, W.L.M. Ruijs, P.S. Brandsema); Regional Public Health Laboratory Kennemerland, Haarlem, the Netherlands (S.M. Euser)

DOI: https://doi.org/10.3201/eid3207.260171

case-patients in both buildings, which matched with 1 clinical isolate. The concentration of *L. pneumophila* bacteria in most samples was 100–1,000 CFU/L, and it was detected in taps and shower hoses. At the building of cluster 1, the drinking water company, a certified water consultancy company, and the owners' association of the apartment building conducted an extensive examination of the building's hot and cold water systems. No legionellae were detected in the water samples from plumbing entering the building or the cold water samples in the apartments, except for 1 cold water sample from a mixed water tap. In addition, the building of cluster 2 was served by a different drinking water company; therefore, the drinking water supply was ruled out as the primary source. Furthermore, the drinking water company could not identify any incidents or repairs to the water supply that might have caused contamination from groundwater.

In view of the short period (2.5 months) in which the patients fell ill and the age of the buildings (16 years), previously existing defects were unlikely to be the primary cause. The only recent change in the apartments that could explain the LD clusters was replacement of the water heaters in each apartment; all LD patients had installed a new water heater of the same brand (brand A) ≤3 months before onset of illness. During the examination of the water system for cluster 1, cluster 2 emerged in another building where the same brand A water heaters were installed ≤2 months before illness onset. Here, we describe a case–control study that we initiated to investigate whether more LD cases in the Netherlands were linked to newly installed brand A water heaters.

## Methods

In the Netherlands, all laboratory-confirmed LD cases are notifiable and reported by clinicians or medical microbiologists to the public health service (PHS). The PHS uses a structured questionnaire to conduct a source finding investigation and collects all relevant data, including demographic, diagnostic, underlying conditions, smoking, travel history, and all possible locations, activities, or other potential sources of exposure in the 14 days before illness onset. Using those data, the PHS in collaboration with the National Reference Laboratory for *Legionella* (*Legionella* Source Identification Unit) decides which water or soil samples should be collected from potential sources of infection. The reference laboratory collects and analyzes all samples, including genotyping of *Legionella* isolates.

### Case Definitions and Epidemiologic Investigation

We initiated a case–control study at the beginning of 2023. All reported LD cases included in this study were laboratory-confirmed according to the 2018 European Union/European Economic Area case definition (*9*). The PHS obtained production dates of the water heaters from the serial numbers. Because the water heaters implicated in the 2 LD clusters were all produced in 2022, we included LD patients reported from 2022 on; therefore, we retrospectively conducted some case and control finding.

We defined cases as LD patients reported in the Netherlands during 2022–2023 who had *L. pneumophila* SG1 ST37 detected in a clinical isolate or in the water system of the patient's home, which included the 6 cases from clusters 1 and 2. We defined controls as reported LD cases during 2021–2023 without *L. pneumophila* ST37 identified (i.e., a non-ST37 clinical isolate or no clinical isolate), for which the residential water system tested *L. pneumophila* ST37–negative or had low water temperature or a technical problem reported in the 14 days before onset of illness. We added the criteria on water heaters to obtain enough controls because we retrospectively selected controls and environmental sampling might not have been considered necessary at that time.

### Water Heater Inquiries

For cases and controls, the PHS made additional inquiries about water heaters ≤6 months before illness onset. Those inquiries collected information on the brand and type, installation date, setting (e.g., tap water temperature, ECO setting designed to save energy), and any issues or errors with the heater remembered by the patient or by their legal representative in case the patient was unable to provide information.

### Environmental Sampling and Microbiological Investigation

The reference laboratory collected environmental samples, then genotyped those samples and clinical isolates by using sequence-based typing and compared against European Working Group for *Legionella* Infections sequence-based typing database (*10*). To increase typing resolution, we calculated molecular serogroups, multilocus sequence typing (MLST) STs, and 1,521 locus core genome MLST (cgMLST) complex types in Seqsphere+ software version 7.7.5 (Ridom, https://www.ridom.de) by automated allele submission to the *Legionella pneumophila* cgMLST server (*11*,*12*).

We used allelic profiles to calculate distance matrices by using a Hamming distance and ignoring pairwise missing loci. We used the allelic profile out-

put to create minimum-spanning neighbor-joining trees on the basis of 1,535 core genomes, including the 7 housekeeping genes for sequence-based MLST typing and 1,521 genomes for cgMLST. For context, we added cgMLST results of 3 randomly selected clinical ST37 isolates (1 each from 2012, 2015, and 2019) to the minimum-spanning tree.

### Statistical Analyses

We calculated odds ratios (ORs), SEs, and 95% CIs to measure the strength of the association between newly installed brand A water heaters and LD cases with a ST37 clinical isolate, environmental sample, or both. Because ≥1 cell frequency was 0, we applied a Haldane-Anscombe correction (i.e., addition of 0.5 to each cell of the 2 × 2 table) (*13*,*14*). As a sensitivity analysis, we calculated an OR assuming all controls with missing data on the water heating system had a newly installed brand A water heater.

## Results

### Identification of Cases and Controls

We identified 23 LD cases with an illness onset date during May 2022–August 2023 (Figure 1). The median age of case-patients was 76 years; 10 (43%) were male and 13 (57%) were female. All case-patients were hospitalized, and 4 (17%) died. Underlying conditions were reported for 16 (70%) and smoking for 5 (22%) case-patients. All LD cases were diagnosed by urine antigen test, 2 were also diagnosed by PCR, and 8 had an ST37 clinical isolate available (Table).

We identified a total of 56 persons with illness onset during December 2021–May 2023. The PHS was able to collect information about the home water heaters for 31 of those patients, which we included as controls; 14 (45%) of them had reported technical problems with the water heater, and 17 (55%) had *L. pneumophila* ST37–negative home sampling. The median age of the 31 control-patients was 70 years; 18 (58%) were male and 13 (42%) were female. Most (97%, 30/31) control-patients were hospitalized, and 3 (10%) died. Underlying conditions were reported for 14 (45%) control-patients and smoking was reported for 12 (39%). Most (28/31; 90%) control cases were diagnosed using urine antigen test, 3 (10%) were diagnosed with PCR, and 7 (23%) had a clinical isolate available.

### Environmental and Microbiological Investigation

Among the 23 case-patients, 21 (91%) had a brand A water heater installed ≤6 months before illness onset (Table, Figure 1). Two cases had a different water heater brand; 1 had traveled abroad, and their infection likely was travel-associated. Environmental sampling was conducted for homes of 21 cases, and *L. pneumophila* ST37 was detected in 20 (95%), all of which had a brand A water heater. No legionellae were detected in the home of the case-patient who had a different water heater brand. The homes of the travel-associated case-patient and 1 case-patient with a brand A water heater could not be sampled. Of the 8 cases with a clinical *L. pneumophila* ST37 isolate, 4 had a genotypic match with environmental samples from the home water system; environmental sampling of the home was not performed for 3 cases,

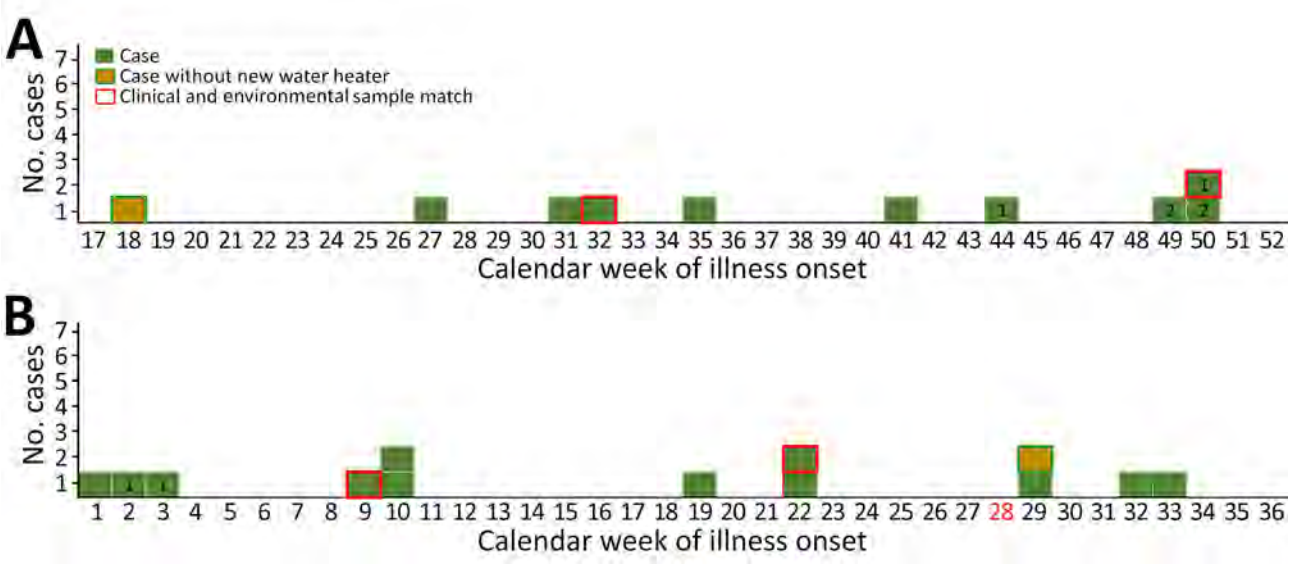


**Figure 1.** Timeline of cases in an outbreak of Legionnaires' disease linked to newly installed residential water heaters, the Netherlands, 2022–2023. Timelines show calendar weeks for case-patient illness onset in 2022 (A) and 2023 (B). Numbered cases are from 2 clusters (cluster 1 and cluster 2) in separate apartment buildings in the Netherlands. Red date is week public warning was issued.

**Table.** Case characteristics in outbreak of Legionnaires' disease linked to newly installed residential water heaters, the Netherlands, 2022–2023*

| Case no. | Cluster no. | Illness onset date | Age, y/sex | Died | Diagnostic method | *Legionella pneumophila* serogroup 1 detected, sequence type | | | New brand A water heater | Installation date |
|---|---|---|---|---|---|---|---|---|---|---|
| | | | | | | Clinical | Environmental | Match† | | |
| 1 | 1 | 2022 Nov | 76/F | N | UAT | Y, ND | Y, ST37 | N | Y | 2022 Oct |
| 2 | 1 | 2022 Dec | 70/F | N | Culture, UAT | Y, ST37 | Y, ST37 | Y | Y | 2022 Oct |
| 3 | 1 | 2023 Jan | 73/F | N | UAT | Y, ND | Y, ST37 | N | Y | 2023 Jan |
| 4 | 1 | 2023 Jan | 84/F | N | UAT | Y, ND | Y, ST37 | N | Y | 2022 Oct |
| 5 | 2 | 2022 Dec | 70/M | N | UAT | Y, ND | Y, ST37 | N | Y | 2022 Oct |
| 6 | 2 | 2022 Dec | 63/M | Y | UAT | Y, ND | Y, ST37 | N | Y | 2022 Oct |
| 7 | NA | 2022 May | 59/M | N | Culture, UAT | Y, ST37 | No sampling | NA | N; probable travel-associated case | NA |
| 8 | NA | 2022 Jul | 88/M | N | Culture, UAT | Y, ST37 | No sampling | NA | Y | 2022 Jul |
| 9 | NA | 2022 Aug | 62/M | N | Culture, PCR, UAT | Y, ST37 | No sampling | NA | Y | 2022 Jul |
| 10 | NA | 2022 Sep | 90/M | Y | UAT | Y, ND | Y, ST37 | N | Y | 2022 Jun |
| 11 | NA | 2022 Oct | 57/M | N | UAT | Y, ND | Y, ST37 | N | Y | 2022 Oct |
| 12 | NA | 2023 Jan | 85/M | Y | UAT | Y, ND | Y, ST37 | N | Y | 2022 Nov |
| 13 | NA | 2023 Feb | 76/F | N | Culture, UAT | Y, ST37 | Y, ST37 | Y | Y | 2022 Aug |
| 14 | NA | 2023 Feb | 82/F | Y | Culture, UAT | Y, ST37 | Y, ST37 | Y | Y | 2022 Oct |
| 15 | NA | 2023 Mar | 93/M | N | UAT | Y, ND | Y, ST37 | N | Y | 2023 Jan |
| 16 | NA | 2023 Mar | 71/F | N | UAT | Y, ND | Y, ST37 | N | Y | 2023 Jan |
| 17 | NA | 2023 May | 55/F | N | UAT | Y, ND | Y, ST37 | N | Y | 2023 Mar |
| 18 | NA | 2023 May | 69/M | N | UAT | Y, ND | Y, ST37 | N | Y | 2023 Apr |
| 19 | NA | 2023 Jun | 77/F | N | Culture, PCR, UAT | Y, ST37 | Y, ST37 | Y | Y | <6 mo before illness onset |
| 20 | NA | 2023 Jul | 58/F | N | UAT | Y, ND | Y, ST37 | N | Y | 2023 Mar |
| 21 | NA | 2023 Jul | 81/F | N | Culture, UAT | Y, ST37 | Negative | N | N | >2 y before illness onset |
| 22 | NA | 2023 Aug | 80/F | N | UAT | Y, ND | Y, ST37 | N | Y | 2023 Jul |
| 23 | NA | 2023 Aug | 77/F | N | UAT | Y, ND | Y, ST37 | N | Y | 2023 Jul |

*NA, not applicable; ND, not determined; ST, sequence type; UAT, urinary antigen test.
†Genotypical match between the clinical and environmental isolate, both containing *Legionella pneumophila* serogroup 1 sequence type 37.

and for 1 case, the home sample was negative. The cases were geographically spread across the Netherlands (Figure 2).

### Odds of LD

None of the 31 controls had installed a new water heater of any brand ≤6 months before illness onset. Analysis showed that LD cases had a statistically significant association with a newly installed brand A water heater (OR 541.80 [95% CI 24.76–11,854.03]). That association might be overestimated because we identified the 56 controls retrospectively, and 25 could not be contacted. However, we conducted a sensitivity analysis by using the assumption that all 25 controls with missing data had a newly installed brand A water heater, which still showed a statistically significant association (OR 13.02 [95% CI 2.78–60.92]).

### Whole-Genome Sequencing

We included 8 *L. pneumophila* ST37 isolates from LD cases related to this outbreak and 4 environmental isolates collected during source investigations for this outbreak in the whole-genome sequencing analysis. In addition, we included 3 *L. pneumophila* ST37 isolates unrelated to this outbreak from LD cases reported in 2012, 2015, and 2019 for context. All isolates showed close relationships on the basis of cgMLST results and had a maximum of 6 alleles difference (Figure 3).

### Outbreak Control Measures

The National Institute for Public Health and the Environment informed the Netherlands Food and Consumer Product Safety Authority (NVWA) in early 2023 about the 2 LD clusters. After the case–control study and additional research at the water heater distributor in the Netherlands, the NVWA and the manufacturer issued safety warnings on July 13, 2023. The NVWA ordered the distributor to contact all clients with brand A water heaters produced during January 1, 2022–March 31, 2023, and to take necessary actions. The company implemented control measures, which included chemical disinfection of the residential water systems and thermostatic mixer valves. Pending that disinfection, clients received a shower head with a filter to prevent exposure to legionellae.

## Discussion

Newly installed brand A water heaters were identified as the most probable source of infection in this outbreak because all the available data from epidemiologic and

environmental investigations showed a clear link between the water heaters and cases of *L. pneumophila* ST37 infection. Our case–control study confirmed that cases were associated with newly installed brand A water heaters with a large and highly significant OR. However, because of the partially retrospective design, data on the brand of water heater were missing for many (25/56) controls. Therefore, we performed a sensitivity analysis assuming strong bias toward the null, which still showed a statistically significant association (OR 13.02 [95% CI 2.78–60.92]). Of note, the *L. pneumophila* ST37 patient isolates and environmental strains found in this cluster were also closely related by cgMLST to isolates from 3 LD cases reported in 2012, 2015, and 2019 in patients not related to this cluster. That finding aligns with previous studies reporting on the genomic population structure of *L. pneumophila* isolates that made similar observations for some STs, indicating that isolates can be genetically closely related but not epidemiologically linked (*15*–*17*).

At the start of the outbreak, the drinking water supply was also considered as a possible source of infection but was swiftly ruled out after assessing the geographic distribution of the cases, the ORs, and detection of *L. pneumophila* ST37 only in warm, not cold, water samples. The geographic distribution of the LD cases and their homes across the country showed that they were connected to various drinking water companies and nothing indicated that *L. pneumophila* ST37 was in drinking water supplied by those companies. That observation is supported by environmental samples taken during 2012–2021 as part of source investigation by the reference laboratory of the Netherlands. The reference laboratory sampled 984 sources, including the homes of 316 LD patients, and found *L. pneumophila* ST37 in only 0.4% of all sources (*18*,*19*). Furthermore, only 3.4% of *L. pneumophila* clinical isolates during that period were ST37 (*18*,*19*). Of note, the sampling results in cluster 1 indicated this strain possibly has a high virulence because a low concentration (<1.000 CFU/L) of ST37 caused multiple LD cases. Therefore, ST37 would have been found more often in potential sources or in the clinical isolates if the strain were commonly in drinking water in the Netherlands, even in low concentrations. Finally, we also looked at possible introduction of ST37 in the drinking water system by other sources. In the building of cluster 1, a device to control the water pressure had been replaced during 2022, but that device was not replaced in the building in cluster 2 or for any of the other cases. Source finding history did not show any other sources of *L. pneumophila* ST37 introduction into the water system of the homes of the patients or any other common sources of exposure.

On the basis of the questionnaire and temperatures measured at sampling, we did not find specific risk factors related to the temperature settings or other common issues or errors with the water heaters. At most homes, the hot water temperatures at the tap were ≥55°C. Some water heaters were set on Eco mode (energy efficient), resulting in low temperatures for the first few minutes. How often and for how long the patients used the hot water is not known.

The brand A water heater is also sold in several other countries in Europe. To identify possible cases in those countries, we issued a warning through EpiPulse, an online infectious disease surveillance portal for Europe managed by the ECOC, but no other countries reported LD cases. However, several countries communicated that they might be unable to detect such cases because detailed case finding information with environmental investigations and typing of isolates are not routinely performed in those countries. Furthermore, unlike the Netherlands, many countries use biocides in their drinking water system, which could explain why no cases have been observed in other countries. In the Netherlands, chemical or thermal disinfection is also not mandatory after water heater installation, which could explain why no cases have been observed in other countries.

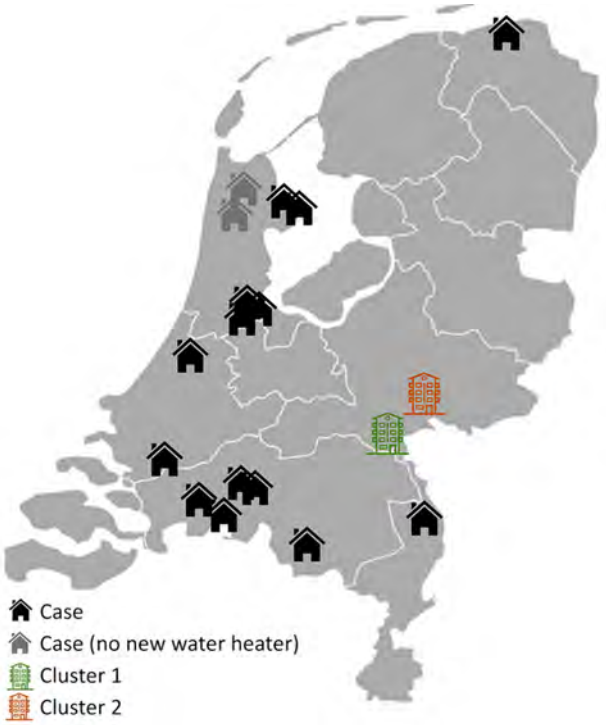


**Figure 2.** Locations of Legionnaires' disease cases linked to newly installed residential water heaters, the Netherlands, 2022–2023. Two clusters (cluster 1 [4 cases] and cluster 2 [2 cases]) were identified in 2 apartment buildings.

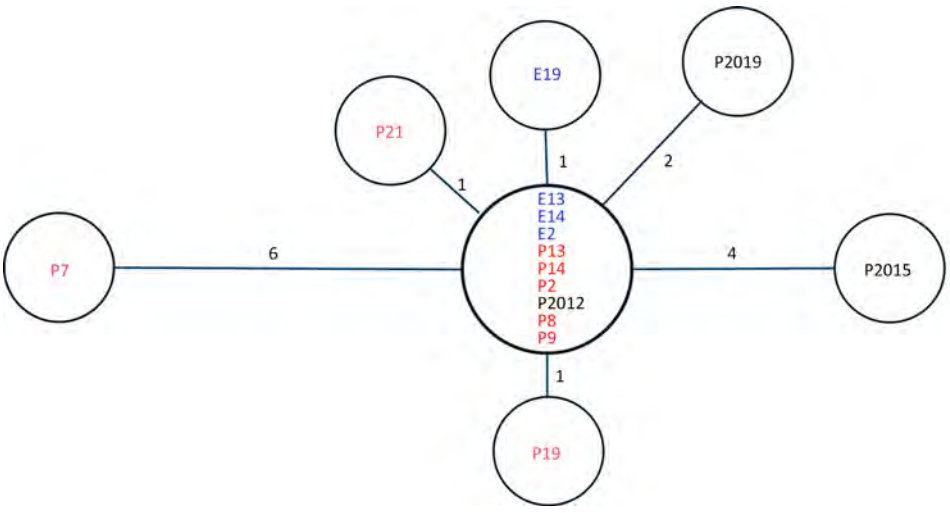


**Figure 3.** Genomic links among *Legionella pneumophila* isolates from reference sources and from an outbreak of Legionnaires' disease linked to newly installed residential water heaters, the Netherlands, 2022–2023. Minimum-spanning tree was based on 1,521 core genome sequencing typing targets showing genomic links between *L. pneumophila* isolates from 8 clinical (red font) and 4 environmental (blue font) sequence type 37 isolates related to the outbreak, as well as 3 randomly selected non–outbreak-related sequence type 37 isolates from 2012, 2015, and 2019 for context (black font). Numbers on nodes indicate allele differences.

The brand A water heater had a flow-through system without a storage tank, so the legionellae growth cannot be explained by stagnant water with temperatures of 25°C–50°C degrees or thermal stratification in the hot water storage tank, which is known to pose a higher risk for legionellae growth (*20*). However, a plausible explanation for introduction of legionellae into the water system is that a small amount of test water containing *L. pneumophila* ST37 remained in the heater after the production process and that microorganisms were able to create a biofilm, enabling *L. pneumophila* to survive. All heaters are tested with water for possible leakage before distribution. During the investigation into the clusters, the reference laboratory confirmed that a small (≈30 mL) amount of water was in new water heaters still in storage. We hypothesize that after water heater installation, *L. pneumophila* was released into the hot water system in the home and was able to grow in the pipes, shower hoses, and shower heads, subsequently causing infection. However, before the safety warning, no *L. pneumophila* ST37 was detected by the reference laboratory in samples from the small amount of water in the water heaters still in storage.

Further research is necessary to assess the risk for *L. pneumophila* contamination in water heaters causing infections and provide evidence-based policy recommendations for infection prevention and control. Previous research has documented that *L. pneumophila* is able to enter a viable but nonculturable state and later resuscitate in the right environment (*21*,*22*), which might explain how the bacteria in the LD clusters survived in storage for months. However, more data are needed to elucidate how *L. pneumophila* ST37 entered the water heaters, how the bacteria were able to grow in the plumbing system despite high water temperatures, and whether energy-saving designs like Eco Mode result in lower temperatures and an increased risk for bacterial growth. Further research also is needed to determine whether *L. pneumophila* infection is specific to brand A water heaters or if similar infections could occur in water heaters from other brands as well.

In conclusion, *L. pneumophila* in plumbing systems is widely reported, often in relation to water temperatures of 25°C–50°C, stagnant water, or low biocide levels. The risk for legionellae growth in thermostatic valves and biofilms in shower hoses also is well known (*23*–*26*). This study demonstrated the value of legionellae control measures during production or installation of water devices and that a new device could pose a risk for introduction of *L. pneumophila* into a water system. Manufacturers of water heaters or fittings for plumbing systems that are tested with water should ensure devices are clean and dry before packaging and should control for *L. pneumophila* growth in the test water. Furthermore, this outbreak emphasizes how vital an adaptable surveillance system, environmental investigations, typing of isolates, and alert public health workers are for detecting previously unrecognized sources of *L. pneumophila*.

Ethical approval was not obtained for the study because these data were collected as part of routine surveillance.

Raw sequence data was submitted to the National Center for Biotechnology Information Sequence Read Archive (https://www.ncbi.nlm.nih.gov/sra; accession no. PRJNA1453490).

## About the Author

Dr. Reukers is an epidemiologist at the National Institute for Public Health and the Environment in the Netherlands.

Her work focuses on infectious disease surveillance and research of respiratory infections, such as legionellosis, Q fever, and psittacosis.

## References


1. Steinert M, Hentschel U, Hacker J. *Legionella pneumophila*: an aquatic microbe goes astray. FEMS Microbiol Rev. 2002; 26:149–62. https://doi.org/10.1111/j.1574-6976.2002.tb00607.x
2. National Academies of Sciences, Engineering, and Medicine; Health and Medicine Division; Division on Earth and Life Studies; Board on Population Health and Public Health Practice; Board on Life Sciences; Water Science and Technology Board; Committee on Management of Legionella in Water Systems. Management of *Legionella* in water systems. Washington: National Academies Press; 2019.
3. van Heijnsbergen E, Schalk JAC, Euser SM, Brandsema PS, den Boer JW, de Roda Husman AM. Confirmed and potential sources of *Legionella* reviewed. Environ Sci Technol. 2015;49:4797–815. https://doi.org/10.1021/acs.est.5b00142
4. Orkis LT, Harrison LH, Mertz KJ, Brooks MM, Bibby KJ, Stout JE. Environmental sources of community-acquired Legionnaires' disease: a review. Int J Hyg Environ Health. 2018;221:764–74. https://doi.org/10.1016/j.ijheh.2018.04.013
5. Yu VL, Plouffe JF, Pastoris MC, Stout JE, Schousboe M, Widmer A, et al. Distribution of *Legionella* species and serogroups isolated by culture in patients with sporadic community-acquired legionellosis: an international collaborative survey. J Infect Dis. 2002;186:127–8. https://doi.org/ 10.1086/341087
6. Fields BS, Benson RF, Besser RE. *Legionella* and Legionnaires' disease: 25 years of investigation. Clin Microbiol Rev. 2002;15:506–26. https://doi.org/10.1128/CMR.15.3.506-526.2002
7. Reukers DFM, Bartels AA, Mulder AC, Berry DSF, Euser S, Laarman C, et al. Surveillance of legionellosis in the Netherlands. Overview of clusters, sources and environmental factors between 2013 and 2022 [in Dutch]. Bilthoven: National Institute for Public Health and the Environment; 2024.
8. European Centre for Disease Prevention and Control. Legionnaires' disease. Annual epidemiological report for 2023. Stockholm: The Centre; 2026.
9. European Commission. Case definitions of communicable diseases: Legionnaires' disease. Official Journal of the European Union. 2018 Jul 7 [cited 2025 Jan 27]. https://eur-lex.europa.eu/legal-content/EN/TXT/PDF/?uri=CELEX:32018D0945&from=EN#page=26
10. Gaia V, Fry NK, Afshar B, Lück PC, Meugnier H, Etienne J, et al. Consensus sequence-based scheme for epidemiological typing of clinical and environmental isolates of *Legionella pneumophila*. J Clin Microbiol. 2005;43:2047–52. https://doi.org/10.1128/JCM.43.5.2047-2052.2005
11. Jünemann S, Sedlazeck FJ, Prior K, Albersmeier A, John U, Kalinowski J, et al. Updating benchtop sequencing performance comparison. Nat Biotechnol. 2013;31:294–6. https://doi.org/10.1038/nbt.2522
12. Moran-Gilad J, Prior K, Yakunin E, Harrison TG, Underwood A, Lazarovitch T, et al. Design and application of a core genome multilocus sequence typing scheme for investigation of Legionnaires' disease incidents. Euro Surveill. 2015;20:28. https://doi.org/10.2807/1560-7917.ES2015.20.28.21186
13. Haldane JB. The estimation and significance of the logarithm of a ratio of frequencies. Ann Hum Genet. 1956;20:309–11. https://doi.org/10.1111/j.1469-1809.1955.tb01285.x
14. Anscombe FJ. On estimating binomial response relations. Biometrika. 1956;43:461–4. https://doi.org/10.1093/biomet/43.3-4.461
15. Quero S, Párraga-Niño N, Barrabeig I, Sala MR, Pedro-Botet ML, Monsó E, et al. Population structure of environmental and clinical *Legionella pneumophila* isolates in Catalonia. Sci Rep. 2018;8:6241. https://doi.org/10.1038/s41598-018-24708-1
16. David S, Mentasti M, Tewolde R, Aslett M, Harris SR, Afshar B, et al. Evaluation of an optimal epidemiological typing scheme for *Legionella pneumophila* with whole-genome sequence data using validation guidelines. J Clin Microbiol. 2016;54:2135–48. https://doi.org/10.1128/JCM.00432-16
17. Schjørring S, Stegger M, Kjelsø C, Lilje B, Bangsborg JM, Petersen RF, et al.; ESCMID Study Group for Legionella Infections (ESGLI). Genomic investigation of a suspected outbreak of *Legionella pneumophila* ST82 reveals undetected heterogeneity by the present gold-standard methods, Denmark, July to November 2014. Euro Surveill. 2017;22:25. https://doi.org/10.2807/1560-7917.ES.2017.22.25.30558
18. Den Boer JW, Euser SM, Brandsema P, Reijnen L, Bruin JP. Results from the National *Legionella* Outbreak Detection Program, the Netherlands, 2002–2012. Emerg Infect Dis. 2015;21:1167–73. https://doi.org/10.3201/eid2107.141130
19. Euser SM, Bruin JP, Brandsema P, Reijnen L, Boers SA, Den Boer JW. Legionella prevention in the Netherlands: an evaluation using genotype distribution. Eur J Clin Microbiol Infect Dis. 2013;32:1017–22. https://doi.org/10.1007/s10096-013-1841-9
20. Roman FA Jr, Martin RL, Rhoads WJ, Pearce A, Smeltz RE, Pruden A, et al. Water heater type, temperature setting, operational conditions, and insulation affect ecological niches for *Legionella* growth. ACS ES T Water. 2024;5:377–86. https://doi.org/10.1021/acsestwater.4c00894
21. Steinert M, Emödy L, Amann R, Hacker J. Resuscitation of viable but nonculturable *Legionella pneumophila* Philadelphia JR32 by *Acanthamoeba castellanii*. Appl Environ Microbiol. 1997;63:2047–53. https://doi.org/10.1128/aem.63.5.2047-2053.1997
22. García MT, Jones S, Pelaz C, Millar RD, Abu Kwaik Y. *Acanthamoeba polyphaga* resuscitates viable non-culturable *Legionella pneumophila* after disinfection. Environ Microbiol. 2007;9:1267–77. https://doi.org/10.1111/j.1462-2920.2007.01245.x
23. Whiley H, Giglio S, Bentham R. Opportunistic pathogens *Mycobacterium avium* complex (MAC) and *Legionella* spp. colonise model shower. Pathogens. 2015;4:590–8. https://doi.org/10.3390/pathogens4030590
24. Proctor CR, Reimann M, Vriens B, Hammes F. Biofilms in shower hoses. Water Res. 2018;131:274–86. https://doi.org/10.1016/j.watres.2017.12.027
25. Hayes-Phillips D, Bentham R, Ross K, Whiley H. Factors influencing *Legionella* contamination of domestic household showers. Pathogens. 2019;8:27. https://doi.org/10.3390/pathogens8010027
26. Cavallaro A, Rhoads WJ, Sylvestre É, Marti T, Walser JC, Hammes F. *Legionella* relative abundance in shower hose biofilms is associated with specific microbiome members. FEMS Microbes. 2023;4:xtad016. https://doi.org/10.1093/femsmc/xtad016


Address for correspondence: Daphne Reukers, Centre for Infectious Disease Control, National Institute for Public Health and the Environment, A. van Leeuwenhoeklaan 9, 3721 MA Bilthoven, the Netherlands; email: daphne.reukers@rivm.nl

# Trichinellosis Outbreak Linked to Undercooked Bear Jerky, North Carolina, USA, 2024

Camden D. Gowler, Nicole Lee, Meghan Phillips, Sarah G.H. Sapp, Tammra Morrison, Melanie D'Angelo, Margaret Neja, Billy A. Watson, Susan P. Montgomery, Anne Straily, Carl Williams, Erica Wilson

Medscape CME Activity

In support of improving patient care, this activity has been planned and implemented by Medscape, LLC and Emerging Infectious Diseases. Medscape, LLC is jointly accredited with commendation by the Accreditation Council for Continuing Medical Education (ACCME), the Accreditation Council for Pharmacy Education (ACPE), and the American Nurses Credentialing Center (ANCC), to provide continuing education for the healthcare team.

Medscape, LLC designates this Journal-based CME activity for a maximum of 1.00 ***AMA PRA Category 1 Credit(s)™***. Physicians should claim only the credit commensurate with the extent of their participation in the activity.

Successful completion of this CME activity, which includes participation in the evaluation component, enables the participant to earn up to 1.0 MOC points in the American Board of Internal Medicine's (ABIM) Maintenance of Certification (MOC) program. Participants will earn MOC points equivalent to the amount of CME credits claimed for the activity. It is the CME activity provider's responsibility to submit participant completion information to ACCME for the purpose of granting ABIM MOC credit.

All other clinicians completing this activity will be issued a certificate of participation. To participate in this journal CME activity: (1) review the learning objectives and author disclosures; (2) study the education content; (3) take the post-test with a 75% minimum passing score and complete the evaluation at http://www.medscape.org/journal/eid; and (4) view/print certificate. For CME questions, see page 1230.

NOTE: It is the policy of Medscape Education to avoid the mention of brand names or specific manufacturers in accredited educational activities. However, trade and manufacturer names in this activity are provided in an effort to provide clarity. The use of brand or manufacturer names should not be viewed as an endorsement by Medscape of any specific product or manufacturer.

**Release date: June 24, 2026; Expiration date: June 24, 2027**

**Learning Objectives**

Upon completion of this activity, participants will be able to:

1. Assess the epidemiology and parasitology of trichinellosis
2. Distinguish the diagnostic criteria for trichinellosis
3. Identify the attack rate of *Trichinella spiralis* after exposure in the current study

**CME Editor**

**Bryce Simons, MPH,** Technical Writer/Editor, Emerging Infectious Diseases. *Disclosure: Bryce Simons, MPH, has no relevant financial relationships.*

**CME Author**

**Charles P. Vega, MD,** Health Sciences Clinical Professor of Family Medicine, University of California, Irvine School of Medicine, Irvine, California, USA. *Charles P. Vega, MD, has the following relevant financial relationships: consultant or advisor for Boehringer Ingelheim; Exact Sciences; GlaxoSmithKline.*

**Authors**

***Camden D. Gowler, PhD; Nicole Lee, MPH; Meghan Phillips, BSN, RN; Sarah G. H. Sapp, PhD; Tammra Morrison, BSN, RN, NCCPHN; Melanie D'Angelo, MPH; Margaret A. Neja, BS; Billy A. Watson, PhD; Susan P. Montgomery, DVM, MPH; Anne Straily, DVM, MPH; Carl J. Williams, DVM; Erica Wilson, MD.***

Author affiliations: North Carolina Department of Health and Human Services, Raleigh, North Carolina, USA (C.D. Gowler, N. Lee, T. Morrison, M. D'Angelo, C. Williams, E. Wilson); Centers for Disease Control and Prevention, Atlanta, Georgia, USA (C.D. Gowler, S.G.H. Sapp, M. Neja, B.A. Watson, S.P. Montgomery, A. Straily); Graham County Department of Public Health, Robbinsville, North Carolina, USA (M. Phillips)

DOI: https://doi.org/10.3201/eid3207.260062

*Trichinella* spp. nematodes are parasites that can cause trichinellosis in humans after consumption of infected, undercooked meat. A November 2024 trichinellosis outbreak in western North Carolina, USA, resulted in 3 cases (2 probable, 1 confirmed), all linked to undercooked bear jerky. In total, 6 persons consumed the implicated meat (attack rate 50%). Molecular testing identified *Trichinella spiralis* in leftover meat from the same bear. This outbreak provides evidence of changing trichinellosis patterns. Low-cost safety measures and prevention efforts regarding safe wild game preparation are needed to avoid future outbreaks.

*Trichinella* spp. are parasitic nematodes that can cause trichinellosis (also called trichinosis) when humans consume infected, undercooked meat. Trichinellosis is a reportable disease in North Carolina, USA. Only 3 cases were reported during 1991–2022, and no outbreaks were reported during the same period. Historical reports suggest very low incidence locally (*1*,*2*). In November 2023, a probable trichinellosis outbreak was reported, and undercooked bear meat was the likely source (*3*). A year later, in November 2024, a public health investigation was initiated when a clinician reported a hospitalized patient with suspected trichinellosis. This patient had shared wild bear meat with 5 other persons in the form of jerky (desiccated meat). The Graham County Health Department and North Carolina Division of Public Health (NCDPH) investigated to characterize cases and provide public health guidance to prevent further illness.

## Methods

The week after the November 2024 report, public health officials identified and interviewed 6 persons who consumed the bear jerky. We used the 2014 case definition from the Council for State and Territorial Epidemiologists (*4*) for case classification. We defined probable cases as the presence of clinically compatible symptoms in a person who shared an epidemiologically implicated meal or ate a meat product in which the parasite was found. We defined confirmed cases as the presence of clinically compatible symptoms with a positive laboratory test such as *Trichinella* antibody screening. Clinically compatible signs and symptoms included fever, myalgia, periorbital edema, and eosinophilia. This activity was reviewed by the Centers for Disease Control and Prevention (CDC), was deemed not research, and was conducted consistent with applicable federal law and CDC policy.

The bear was hunted in Graham County in western North Carolina at the start of bear season (October). Approximately half the meat was frozen as various cuts and half was prepared as jerky without prior freezing. Because the process involved only marination and dehydration, the jerky preparation likely did not reach the suggested ≥165°F (≥74°C) internal temperature necessary to kill *Trichinella* spp. parasites. At the time of notification, purportedly no jerky remained, but 4 remaining frozen meat pieces were sent for testing at the CDC's Division of Parasitic Diseases and Malaria, National Center for Emerging and Zoonotic Infectious Diseases.

The implicated bear jerky was shared among 6 persons. Trichinellosis symptoms developed in 3 persons, including 1 who was hospitalized with severe symptoms characteristic of trichinellosis: periorbital edema, eosinophilia, and muscle weakness. The patient's physician had read of an outbreak of trichinellosis in western North Carolina reported in Morbidity and Mortality Weekly Report (*3*) and informed NCDPH. Public health officials advised those involved to cease further jerky consumption. State wildlife officials emailed a notice to a listserv of registered hunters about proper handling and cooking of bear meat.

**Table 1.** Case classification, demographics, and symptoms for all persons who consumed undercooked bear jerky in trichinellosis outbreak in North Carolina, USA, 2024 *

| | Age grouping | | | | | |
|---|---|---|---|---|---|---|
| Characteristics | 20–29 | 50–59 | 20–29 | 30–39 | 20–29 | Unknown |
| Sex | M | M | F | M | M | M |
| Classification | Confirmed | Probable | Probable | Not a case | Not a case | Not a case |
| Symptomatic | Yes | Yes | Yes | No | No | No |
| Hospitalization | Yes | No | No | NA | NA | NA |
| Treatment† | Yes | Yes | Yes | NA | NA | NA |
| Symptom onset, days | 25 | 38 | 31 | NA | NA | NA |
| Eosinophil count, K/μL (%)‡ | 3.69 (22) | Not performed | Not performed | NA | NA | NA |
| Symptoms | Fever, myalgia, photophobia, muscle weakness, periorbital edema, subungual and retinal hemorrhage, elevated CRP, eosinophilia | Fever, myalgia | Myalgia | NA | NA | NA |

*CRP, C-reactive protein; NA, not applicable.
†Primary treatment was albendazole.
‡Reference range 0.00–0.50 K/μL (0.0%–7.0%).

**Table 2.** Trichinella antibody testing timeline and results from patient who consumed undercooked bear jerky in trichinellosis outbreak in North Carolina, USA, 2024

| Age group | Sex | Classification | First IgG test timepoint | First IgG test result | Second IgG test timepoint | Second IgG test result |
|---|---|---|---|---|---|---|
| 20–29 | M | Confirmed | 37 days after meal* | Negative | 56 days after meal* | Positive |

*On the basis of initial consumption of bear jerky.

## Results

The overall attack rate was 50% (n = 3), including probable cases in persons who ate the implicated meal and reported symptoms (Table 1). For confirmed cases only, the attack rate was 16% (n = 1). Median incubation period for symptomatic cases was 33 (range 27–40) days. The hospitalized patient was tested for *Trichinella* IgG twice. The first results were negative (collected 12 days after symptom development), but convalescent serum results (collected 31 days after symptom development) were positive (Table 2). Public health officials advised the remaining symptomatic persons of the value of testing, including convalescent testing, because of potential early false negatives. However, because they did not have health insurance, both were discouraged by the high cost (>$200) of testing. All symptomatic persons were treated with albendazole and recovered (Table 1).

CDC's Division of Parasitic Diseases and Malaria tested 4 bear meat specimens. The meat was frozen at an unknown temperature for >57 days. Testing found encapsulated *Trichinella* spp. larvae in all 4 specimens; the parasite loads ranged from 18.6 to 47.9 larvae/g (Figure; Table 3). Two specimens contained a few larvae with very slight motility. Molecular testing using real-time PCR targeting the encapsulated North American *Trichinella* spp. identified the larvae as *T. spiralis* nematodes (Table 3).

## Discussion

We describe a trichinellosis outbreak in western North Carolina, providing additional evidence of changing trichinellosis patterns. Trichinellosis was rarely reported in North Carolina until 2023, when a probable outbreak of trichinellosis resulted in 10 symptomatic cases (*3*). However, the causative *Trichinella* species could not be determined. In the outbreak described in this article, *T. spiralis* nematodes were identified from leftover meat. This finding was somewhat unexpected because *T. spiralis* infection is rarely reported from bear meat, compared with rates for other *Trichinella* spp.(*6*). Wildlife disease surveillance is needed to update our knowledge of *Trichinella* prevalence, host affinities, and associated public health risks.

The outbreak we report also underscores the need for prevention to avoid painful, debilitating infections. Despite the risk for severe disease from trichinellosis, including persistent myalgia or even death, persons preparing wild game and other potentially affected meats for consumption still neglect to follow the recommended cooking measures. Furthermore, provider awareness of trichinellosis can help enable appropriate treatment and guide public health action. Treatment of trichinellosis is typically with albendazole or mebendazole and can be supplemented with steroid drugs for severe cases (*7*).

Trichinellosis is rare in the United States. The disease was once mostly associated with pork, but changes in husbandry practices coincided with a decrease in trichinellosis cases domestically (*8*). More recently, the few cases reported each year are mostly associated with consumption of wild game meat (*8*), with bear meat being the suspected or confirmed food source for recently reported outbreaks in the United States (*9*). The trichinellosis outbreak reported in this article and the 2023 probable outbreak in North Carolina (*3*) were both linked to undercooked bear meat harvested in-state. An increasing number of bears are harvested each year in North Carolina;

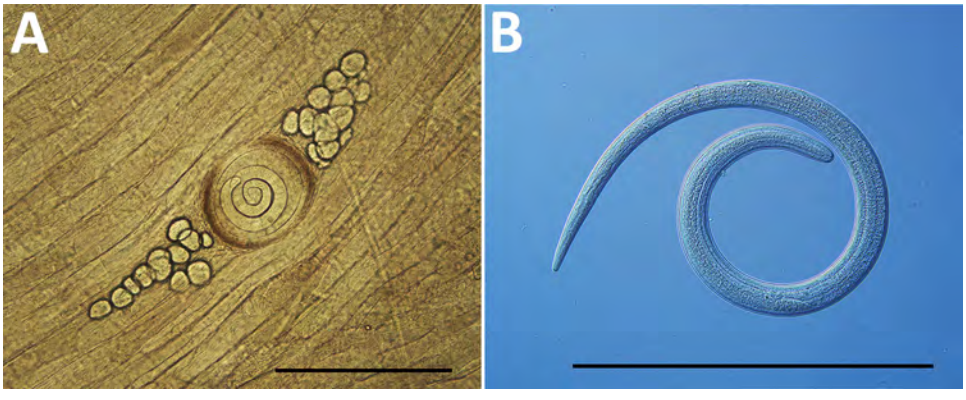


**Figure.** *Trichinella spiralis* larva from contaminated bear meat recovered from investigation into trichinellosis outbreak in North Carolina, USA, 2024. A) Encapsulated *T. spiralis* larva in squash prep of bear meat. B) Liberated *T. spiralis* larva after artificial pepsin-hydrochloric acid digestion shown under differential interference contrast. Scale bars equal 500 µm.

**Table 3.** Molecular and parasite load results for frozen bear meat quantified at Centers for Disease Control and Prevention from investigation into trichinellosis outbreak in North Carolina, USA, 2024

| Specimen ID | Meat cut | Molecular identification* | Parasite load, larvae/g | Motile larvae |
|---|---|---|---|---|
| A | Tenderloin | *Trichinella spiralis* | 32.7 | No |
| B | Ham | *T. spiralis* | 47.9 | No |
| C | Ham | *T. spiralis* | 46.7 | Yes |
| D | Ham | *T. spiralis* | 18.6 | Yes |

*Tested by using a previously published real-time PCR designed to target encapsulated North American *Trichinella* species (*5*).

≈1,500 were harvested in 2023 (*10*). In the United States and Canada, human trichinellosis outbreaks associated with bear meat are more commonly attributed to infection with *T. nativa* nematodes (*9*,*11*), whereas contemporary outbreaks of *T. spiralis* infection are mostly associated with consumption of wild boar (*6*). A report from 2003 suggested that 2 *T. nativa* trichinellosis cases in Tennessee occurred because of a bear hunted in Canada (*11*), rather than in the southeastern United States. In Canada, polar bears and grizzly bears have been confirmed to carry *Trichinella* spp. nematodes (*6*).

Trichinellosis outbreaks associated with jerky prepared from bear (*12*) and other wild game (*13*) have been reported previously. In the outbreak described in this article, jerky preparation consisted of marinade and drying steps that likely did not reach sufficient temperatures for safe consumption. Freezing wild game meat before jerky preparation is sometimes recommended as a treatment step (https://nchfp.uga.edu) but might not be sufficient for killing freeze-resistant *Trichinella* spp. nematodes, such as *T. nativa* (*7*,*9*). Although *T. spiralis* nematodes are usually considered freeze-susceptible, experimental infection trials have demonstrated persistent larval motility after several weeks of freezing, albeit with declining infectivity over time (*14*). The weak motility noted in larvae from this report is not evidence of persistent infectivity after freezing, but because of the uncertainties and potential diversity of *Trichinella* in bear meat, freezing alone cannot be assumed to reliably eliminate infection risk. Cooking meat to an internal temperature ≥165°F (≥74°C) verified by a meat thermometer remains the best method for killing all *Trichinella* species across different types of meat. Safe food handling practices, such as processing raw or undercooked meat separately from other foods, can prevent trichinellosis spread by cross-contamination (*9*,*15*).

Trichinellosis symptoms can be severe, and diagnosis can be challenging. Serologic testing for *Trichinella* IgG is often used to diagnose trichinellosis; however, IgG seroconversion might not be detectable until weeks after infection, potentially causing false negatives if serum is collected during acute infection. Convalescent serum samples are crucial for diagnostic and public health purposes, but their acquisition remains challenging. In addition, healthcare visits, diagnostic tests, and treatment are more difficult for uninsured patients, as demonstrated by the 2 symptomatic patients who did not receive testing during this outbreak.

In conclusion, we report an outbreak of trichinellosis in North Carolina that resulted from undercooked, locally harvested bear prepared as jerky, providing evidence of changing trichinellosis patterns. Low-cost safety measures can help prevent illness, and communication of disease prevention through safe wild game preparation is critical to avoid future outbreaks.

## About the Author

Dr. Gowler is a communicable disease epidemiologist at the Chicago Department of Public Health and previously worked as an Epidemic Intelligence Service Officer with the Centers for Disease Control and Prevention, assigned to the North Carolina Department of Health and Human Services. His research interests include infectious diseases, disease surveillance, and mathematical modeling.

## References

1. Bailey TM, Schantz PM. Trends in the incidence and transmission patterns of trichinosis in humans in the United States: comparisons of the periods 1975–1981 and 1982–1986. Rev Infect Dis. 1990;12:5–11. https://doi.org/10.1093/clinids/12.1.5
2. Sawitz W. Prevalence of trichinosis in the United States. Public Health Rep. 1938;11:365–83. https://doi.org/10.2307/4582479
3. Gowler CD, Lee N, Morrison T, Mears V, Williams C, Fleischauer A, et al. Notes from the field: suspected outbreak of trichinellosis associated with undercooked bear meat—North Carolina, November 2023. MMWR Morb Mortal Wkly Rep. 2024;73:906–7. https://doi.org/10.15585/mmwr.mm7340a4
4. McLaughlin J, Castrodale L, Cooper M. 13-ID-06, revised surveillance case definition for trichinellosis (*Trichinosis*) (*Trichinella spp.*) [cited 2026 May 25]. https://cdn.ymaws.com/www.csteorg/resource/resmgr/PS/13-ID-06Updated.pdf
5. Almeida MD, Bishop H, Nascimento FS, Mathison B, Bradbury RS, Silva AD. Multiplex TaqMan qPCR assay for specific identification of encapsulated *Trichinella* species prevalent in North America. Memórias do Instituto Oswaldo Cruz. 2018;113:e180305. https://doi.org/10.1590/0074-02760180305

6. Malone CJ, Oksanen A, Mukaratirwa S, Sharma R, Jenkins E. From wildlife to humans: the global distribution of *Trichinella* species and genotypes in wildlife and wildlife-associated human trichinellosis. Int J Parasitol Parasites Wildl. 2024;24:100934. https://doi.org/10.1016/j.ijppaw.2024.100934
7. Gottstein B, Pozio E, Nöckler K. Epidemiology, diagnosis, treatment, and control of trichinellosis. Clin Microbiol Rev. 2009;22:127–45. https://doi.org/10.1128/CMR.00026-08
8. Wilson NO, Hall RL, Montgomery SP, Jones JL. Trichinellosis surveillance—United States, 2008–2012. MMWR Surveill Summ. 2015;64:1–8.
9. Cash-Goldwasser S, Ortbahn D, Narayan M, Fitzgerald C, Maldonado K, Currie J, et al. Outbreak of human trichinellosis—Arizona, Minnesota, and South Dakota, 2022. MMWR Morb Mortal Wkly Rep. 2024;73:456–9. https://doi.org/10.15585/mmwr.mm7320a2
10. Olfenbuttel C. North Carolina black bear annual report: updated with 2023 data (North Carolina Wildlife Research Commission) [cited 2026 May 25]. https://www.ncwildlife.gov/hunting/harvest-statistics#ByCounty-1163
11. Smith P, Eidson M, Willsey A, Wallace B, Kacica M, Johnson G, et al.; Centers for Disease Control and Prevention (CDC). Trichinellosis associated with bear meat—New York and Tennessee, 2003. MMWR Morb Mortal Wkly Rep. 2004;53:606–10.
12. Walker AT. Trichiniasis: report of an outbreak caused by eating trichinous bear meat in the form of jerky. J Am Med Assoc. 1932;98:2051–3. https://doi.org/10.1001/jama.1932.02730500017006
13. Dworkin MS, Gamble HR, Zarlenga DS, Tennican PO. Outbreak of trichinellosis associated with eating cougar jerky. J Infect Dis. 1996;174:663–6. https://doi.org/10.1093/infdis/174.3.663
14. Hill DE, Forbes L, Gajadhar AA, Gamble HR. Viability and infectivity of *Trichinella spiralis* muscle larvae in frozen horse tissue. Vet Parasitol. 2007;146:102–6. https://doi.org/10.1016/j.vetpar.2007.02.001
15. Hall RL, Lindsay A, Hammond C, Montgomery SP, Wilkins PP, da Silva AJ, et al. Outbreak of human trichinellosis in Northern California caused by *Trichinella murrelli*. Am J Trop Med Hyg. 2012;87:297–302. https://doi.org/10.4269/ajtmh.2012.12-0075


Address for correspondence: Camden Gowler, Centers for Disease Control and Prevention, 1600 Clifton Rd NE, Mailstop H23-9, Atlanta, GA 30329-4018, USA; email: camdengowler@gmail.com

etymologia

# *Fasciolopsis buski*

## [fas″-ē-ō-lōp′sis buh′-skī]

Michele Calatri

The intestinal fluke *Fasciolopsis buski* is the largest trematode that parasitizes humans, reaching up to 75 mm in length (Figure 1). The genus *Fasciolopsis* was established by Arthur Looss in 1899 and the term derived from the Latin word *fasciola*, meaning small band, and the Ancient Greek suffix *-οψις* (-opsis), meaning resemblance, referring to the similarity with the members of the genus *Fasciola*. The species was named for the English surgeon George Busk (Figure 2), who identified the adult worm in 1852 from the duodenum of a sailor from India. The first comprehensive description of the species was provided by Edwin Lankester in 1857, and the parasite's lifecycle was definitively clarified by Koan Nakagawa in 1921.


**Figure 1.** Adult *Fasciolopsis buski* fluke. Photograph credit: DPDx (https://www.cdc.gov/dpdx).

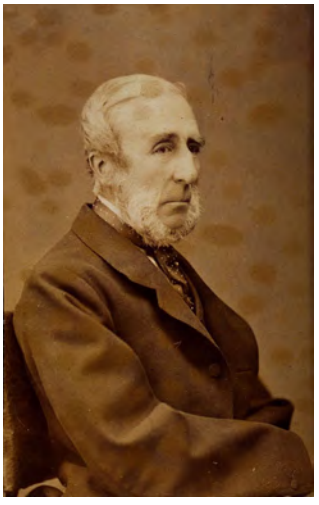

**Figure 2.** Photograph of George Busk for whom *Fasciolopsis buski* is named. Source: Wellcome Library, London, UK.

Fasciolopsiasis is a foodborne trematodiasis that is endemic in rural areas of South and Southeast Asia. The parasite affects both humans and pigs, and the latter acts as the main zoonotic reservoir for the parasite. The cercariae, released into the water by various species of planorbid snails, encyst on underwater vegetation. Infection occurs via ingestion of metacercariae on the surface of the water or encysted on freshwater edible plants.

## Sources

1. Groove DI. A history of human helminthology. Wallingford (UK): C.A.B. International; 1990.
2. Siles-Lucas M, Becerro-Recio D, Serrat J, González-Miguel J. Fascioliasis and fasciolopsiasis: current knowledge and future trends. Res Vet Sci. 2021;134:27–35. https://doi.org/10.1016/j.rvsc.2020.10.011

Author affiliation: University of Cagliari Faculty of Medicine and Surgery, Cagliari, Italy

DOI: https://doi.org/10.3201/eid3207.241403

Address for correspondence: Michele Calatri, Faculty of Medicine and Surgery, University of Cagliari, S.S. 554 bivio per Sestu Monserrato, Cagliari 09042, Italy; email: mcalatri@gmail.com

# Emerging Risk for Human T-Cell Leukemia Virus Type 1 Transmission with HIV-Positive Breastfeeding Support

Agnes Meybeck, Nathalie Viget, Emmanuelle Aïssi, Roxane Vanspranghels, Yasmine Clermont-Hama, Marion Lagrée, Enagnon Kazali Alidjinou, Olivier Robineau

Human T-cell leukemia virus 1 (HTLV-1) is a neglected retrovirus affecting 5–10 million persons worldwide. Most infections are asymptomatic, but HTLV-1 can cause adult T-cell leukemia or lymphoma and HTLV-1–associated myelopathy. Although mother-to-child transmission through breastfeeding is preventable, few countries have policies that include antenatal screening. The World Health Organization recommends integrating HTLV-1 into HIV and sexually transmitted infection strategies. HIV guidelines in high-income countries increasingly support breastfeeding under controlled conditions, creating increased risk for unrecognized HTLV-1 transmission. We reviewed existing policies for HTLV-1 mother-to-child transmission and considered integration of HTLV prevention into HIV response. We discovered inconsistent guidance across HIV, pediatric, and obstetric fields, leading to conflicting counseling of expectant mothers. Integration of HTLV-1 prevention into HIV guidelines and harmonization with maternal and child health policies is essential for awareness among providers. Prevention through screening and avoiding breastfeeding remains the cornerstone of HTLV-1 control.

Human T-cell leukemia virus 1 (HTLV-1) remains a neglected retrovirus, despite its potentially severe consequences: adult T-cell leukemia or lymphoma and HTLV-1–associated myelopathy. In addition to those 2 severe diseases, ≥14 clinical conditions have been shown to be associated with HTLV-1, including infective dermatitis, uveitis, lung disease, tuberculosis, and severe strongyloidiasis. Persons with HTLV-1 experienced higher risk of death (*1*). Transmission occurs through breastfeeding, sexual contact, needle sharing, and blood products (*2*). Most persons infected with HTLV-1 remain asymptomatic. The risk for adult T-cell leukemia or lymphoma, the most severe disease caused by HTLV-1, is estimated to be up to 20% after early life infection (*3*). HTLV-1 has no current effective treatment; therefore, emphasis should be placed on detection and prevention. We reviewed knowledge about HTLV-1 mother-to-child transmission (MTCT) and existing policies for HTLV-1 prevention and consider why and how the HIV management field should play a role in the prevention of HTLV-1 MTCT.

Author affiliation: Centre Hospitalier de Tourcoing, Tourcoing, France (A. Meybeck, N. Viget, E. Aïssi, Y. Clermont-Hama, O. Robineau); Centre Hospitalier Universitaire de Lille, Lille, France (R. Vanspranghels, M. Lagrée, E.K. Alidjinou); Université de Lille, Lille (E.K. Alidjinou, O. Robineau).

DOI: https://doi.org/10.3201/eid3207.251525

## Epidemiology of HTLV-1 Infection and Risk for MTCT

The total estimate of people living with HTLV-1 infection ranged from 5 to 10 million in 2012, but that number was probably underestimated (*2*). In collaboration with member states and partners, the World Health Organization (WHO) works to develop guidance on HTLV-1 surveillance methods, including those used to determine prevalence. Distribution of HTLV-1 infection prevalence varies widely throughout the world. High-prevalence countries are defined by a prevalence in the general population of >1%. Regions identified as high endemicity areas include southern Japan, the Caribbean, areas of South America and tropical Africa, and foci in the Middle East, Australia, and Melanesia (*4*). In Europe, prevalence is low except in Romania and possibly Moldova (*4*,*5*).

HTLV-1 is mainly transmitted sexually (more often male-to-female) or vertically by breastfeeding.

Approximately 20% of breastfed infants of HTLV-1 infected mothers acquire HTLV-1, compared with <5% if breastfeeding is avoided (*2*,*6*).

### Existing Policies and Guidelines for Prevention of HTLV-1 MTCT

Recently, WHO has recognized HTLV-1 as a global concern and listed prevention of HTLV-1 MTCT as a goal for 2030 (*7*). WHO has undertaken consultations with member states and partners and published a 2021 technical report that summarized existing policies and guidelines for preventing HTLV-1 transmission and treating those with HTLV-1–associated diseases (*8*). According to the report, Japan has implemented a nationwide program for preventing HTLV-1 MTCT, including universal antenatal screening and counseling for breastfeeding avoidance if positive (*9*). Some territories in the Caribbean also screen pregnant women for HTLV-1 (e.g., Grenada, Saint Lucia), and the Organisation of Eastern Caribbean States recommends screening pregnant women and exclusive formula feeding (*10*). Among high-prevalence countries, Seychelles also screens all pregnant women for HTLV-1 and recommends avoiding breastfeeding in case of positivity. The Pan American Health Organization (PAHO) and its member states established targets and goals for the elimination of HTLV vertical transmission through public health programs. The PAHO goal is to achieve a <5% of vertical transmission rate through an expected HTLV screening coverage of 95% of pregnant women and >90% of babies exposed to possible vertical transmission and intervention implementation of >90% to prevent transmission (*11*).

Among low-prevalence countries, France recommends screening of breast milk donors and pregnant women from endemic regions, such as the Caribbean, Africa, Japan, and Southeast Asia (*12*). Despite those recommendations, implementation of HTLV-1 antenatal screening is low in France except in overseas territories in South America (French Guiana) and the Caribbean (Martinique and Guadeloupe) (*13*). In the United Kingdom, screening of all breast milk donors is mandatory (*14*). However, the UK National Screening Committee advised against HTLV-1 universal antenatal screening and is currently assessing targeted antenatal screening for pregnant women who are at high risk for living with HTLV-1 (*15*). Testing for HTLV-1 is already recommended in women from high endemic regions in the UK health migrants guide (*16*). Experts from Spain advocate for expanding HTLV-1 screening in Europe (*17*).

### Epidemiologic Similarities Between HIV and HTLV-1

WHO suggested integrating HTLV-1 control measures into existing HIV and sexually transmitted infection interventions (*7*). A first step of this implementation could be HTLV-1 antenatal screening in women living with HIV, in agreement with guidelines that recommend HTLV-1 testing in high-risk pregnant women. HTLV-1 and HIV share the same transmission routes and similar high prevalence regions. In a study conducted in Brazil in several epidemiologically relevant groups, the prevalence of HTLV-1 infection was higher among HIV-positive persons (*18*). In Gabon, screening for HTLV-1 infection in those living with HIV revealed a high rate of co-infections, reaching 7% of the population (*19*). Co-infections were far more prevalent in women. In HTLV-1 low prevalence countries, HTLV-1 infection might be higher in women living with HIV. The last report from the European Centre for Disease Prevention and Control regarding HIV/AIDS surveillance revealed an increased number of HIV diagnoses in the European Union and European economic area and countries to the west of the region in 2023 compared with 2022. The increase is primarily because of a rise in persons diagnosed with HIV originating from sub-Saharan Africa and continued high rates among those originating from central and eastern Europe, Latin America, and the Caribbean (*20*). Several studies conducted in Europe suggest a higher prevalence of HTLV-1 infection in migrants, especially in women (*21*). In France, similar to the United Kingdom, HTLV-1 testing is included in the health screen of newly arrived migrant women of reproductive age (*16*,*22*). The European Centre for Disease Prevention and Control, however, did not mention HTLV-1 infection in its guidelines on screening and vaccination for infectious diseases in newly arrived migrants within the European Union and European economic area (*23*).

### HIV and Breastfeeding, the Evolving Context

Current WHO guidelines recommend lifelong antiretroviral treatment for pregnant and breastfeeding women living with HIV. Mothers living with HIV who are on antiretroviral therapy should exclusively breastfeed their infants for the first 6 months, introducing appropriate complementary foods thereafter, and continue breastfeeding for ≥12 months (*24*). In low- and middle-income countries, the decision regarding whether mothers living with HIV should breastfeed is made on the basis of balancing the risk for HIV transmission through breastfeeding with the increased risk for illness and death in the absence of

a safe diet without breast milk. Most Latin American countries recommend mothers living with HIV to avoid breastfeeding and provide infant formula (*25*). Exclusive breastfeeding for the first 6 months is an alternative guideline when formula feeding is not acceptable, feasible, affordable, sustainable, and safe (*25*). In Guatemala, mothers are given the option to choose breastfeeding or formula feeding after being fully informed about the risks and benefits of different feeding methods. Argentina and the Caribbean nation of Trinidad and Tobago have recently updated their breastfeeding HIV guidelines to state that mothers living with HIV who choose to breastfeed are closely monitored and should adhere strictly to antiretroviral treatment (*25*). Similarly, recent changes in high-income countries HIV guidelines have marked a shift in favor of breastfeeding under controlled conditions. For decades, formula feeding was the standard, but the accumulated evidence has demonstrated that the risk for HIV transmission is negligible when undetectable viremia is maintained during pregnancy. Because of this negligible risk, countries such as the United Kingdom and Switzerland now recommend or enable breastfeeding with appropriate monitoring (*26*,*27*). A survey conducted in 2022 by the European AIDS Clinical Society revealed that 23 of 25 countries in Europe had specifically mentioned breastfeeding in their HIV and pregnancy guidelines (*28*). Among those countries, 11 offered breastfeeding as an option under certain conditions. Since publication of the survey, France has also begun enabling breastfeeding in women living with HIV under strict virologic and clinical criteria (*29*). The last update of European AIDS Clinical Society guidelines, however, generally discouraged breastfeeding, stating it should only be considered if maternal viral load is undetectable and with close follow-up (*30*). Similarly, the US Department of Health and Human Services, the Canadian Paediatric and Perinatal HIV/AIDS Research Group, and the Australasian Society for HIV, Viral Hepatitis and Sexual Health Medicine continue to support exclusive formula feeding as the preferred method for infants born to women living with HIV; although they have included in their guidelines breastfeeding options for women on antiretroviral therapy with sustained undetectable viral load (*31*–*33*).

### Prevention of HTLV-1 MTCT in Guidelines

This evolution in practice regarding HIV and breastfeeding requires maintaining attention to other vertically transmitted viruses, particularly HTLV-1 (*34*). Indeed, there is a potential overlap of women living with HIV in high-income countries and those at high risk for having HTLV-1 infection. WHO's guidance is clear: HIV-positive women on antiretroviral treatment with suppressed viral load should breastfeed for ≥12 months in low- and middle-income countries (*24*). WHO does not have guidance yet regarding HTLV-1 MTCT. In WHO's technical report summarizing existing policies for preventing HTLV-1 transmission, breastfeeding appeared to be contraindicated for HTLV-1–infected mothers (*8*). Similarly, in the technical note of PAHO on good practices, the preferred recommendation for HTLV-1–infected mothers is exclusive formula feeding, short-term breastfeeding being an alternative in settings where formula feeding is not acceptable, feasible, affordable, sustainable, and safe (ideally <3 months) (*11*). Because HIV care increasingly includes breastfeeding in high-income countries, the risk of unrecognized HTLV-1 transmission in migrant or co-infected populations is real (*18*,*19*,*21*). Pregnant women living with HIV, especially those from HTLV-1 endemic regions, should be offered HTLV-1 screening as part of routine antenatal care. Early diagnosis enables informed counseling and infant feeding alternatives.

HTLV-1 prevention messages remain fragmented across disciplines (*22*,*35*). Pediatric and gyneco-obstetric guidelines might recommend screening of at-risk women or infants and contraindicate breastfeeding in infants born to mothers infected with HTLV-1, yet HIV-specific guidelines often fail to mention HTLV-1 altogether (*29*,*30*,*35*–*45*). High-income countries should take advantage of low- and middle-income countries' experience. In Brazil, for example, HTLV-1 testing is recommended for all persons living with HIV, at baseline visit, in the HIV clinical protocol and therapeutic guidelines (*46*). In the Organisation of Eastern Caribbean States guidelines for sexually transmitted infections, HTLV testing is recommended for anyone living with HIV (*47*).

We illustrate the divergence between HIV guidelines, which increasingly support breastfeeding, and national breastfeeding guidelines, and often contraindicate it for HTLV-1 (Appendix Table, http://wwwnc.cdc.gov/EID/article/32/7/25-1525-App1.pdf). Only Japan integrated HTLV-1 into both HIV and maternal–child health policies. In addition, HIV guidelines almost never mention HTLV-1, whereas obstetric and pediatric guidance might list it as a formal contraindication. In 2024, the PAHO included HTLV-1 in the mother-to-child HIV, syphilis, hepatitis B and C, and Chagas elimination protocol (*11*).

Integration of HTLV-1 information into HIV guidelines is essential but should also be accompanied by dissemination through obstetric, midwife,

pediatric, infectious disease, and migrant healthcare pathways to ensure visibility and implementation (*7*,*8*). Implementation of counseling regarding HTLV-1 could be easier in the context of HIV infection, because breastfeeding counseling on transmissible infections is already routinely done (*48*). Implementation could also enable specific research, including evaluating the effect of certain antiretroviral treatments and their role in elimination of HTLV-1 MTCT (*49*,*50*).

In conclusion, HTLV-1 MTCT is preventable but neglected. Because HIV guidelines increasingly support breastfeeding, not including HTLV-1 represents a missed opportunity and a public health risk. Women living with HIV, particularly from HTLV-1–endemic regions, should be systematically offered HTLV-1 screening as part of antenatal care. To be effective, prevention strategies should not remain isolated. Articulation and harmonization between HIV, obstetrics, pediatrics, and public health guidelines are urgently needed to ensure consistent counseling, avoid contradictory messages, and to raise awareness among all healthcare providers. Leveraging HIV MTCT programs offers the most practical pathway to reduce HTLV-1 transmission. The HIV field has the expertise and infrastructure to lead the way. Failure to integrate HTLV-1 prevention can result in a silent epidemic of preventable infections.

N.V. was partially supported to attend HIV meetings by Gilead, ViiV Healthcare, and Merck Sharp and Dohme. E.K.A. was partially supported by honoraria and travel grants for HIV conferences from Gilead, ViiV Healthcare, and Merck Sharp and Dohme.

Author contributions: study conception, O.R., A.M., N.V., and E.A.; original manuscript draft, A.M. and O.R.; drafting of specific manuscript sections, R.G., Y.C.H., M.L., and E.K.A.; review of first draft and final manuscript approval, all authors.

## About the Author

Dr. Meybeck is a senior physician in the Department of Infectious Diseases in Tourcoing Hospital. Her research interests are the management of HIV, infectious diseases relevant to migrant populations, and reproductive health.

### References:

1. Schierhout G, McGregor S, Gessain A, Einsiedel L, Martinello M, Kaldor J. Association between HTLV-1 infection and adverse health outcomes: a systematic review and meta-analysis of epidemiological studies. Lancet Infect Dis. 2020;20:133–43. https://doi.org/10.1016/S1473-3099(19)30402-5
2. Legrand N, McGregor S, Bull R, Bajis S, Valencia BM, Ronnachit A, et al. Clinical and public health implications of human T-lymphotropic virus type 1 infection. Clin Microbiol Rev. 2022;35:e0007821. https://doi.org/10.1128/cmr.00078-21
3. Imaizumi Y, Iwanaga M, Nosaka K, Ishitsuka K, Ishizawa K, Ito S, et al.; for collaborative Investigators. Prognosis of patients with adult T-cell leukemia/lymphoma in Japan: a nationwide hospital-based study. Cancer Sci. 2020;111:4567–80. https://doi.org/10.1111/cas.14658
4. European Centre for Disease Prevention and Control. Geographical distribution of areas with a high prevalence of HTLV-1 infection. 2015 [cited 2025 Aug 7]. https://www.ecdc.europa.eu/sites/default/files/media/en/publications/Publications/geographical-distribution-areas-high-prevalence-HTLV1.pdf
5. Rosadas C, Harvala H, Davison K, Taylor GP. HTLV-1 screening of blood donations: we are systematically missing opportunities. Br J Haematol. 2023;202:1220–3. https://doi.org/10.1111/bjh.18988
6. Rosadas C, Taylor GP. Current interventions to prevent HTLV-1 mother-to-child transmission and their effectiveness: a systematic review and meta-analysis. Microorganisms. 2022;10:2227. https://doi.org/10.3390/microorganisms10112227
7. World Health Organization. Global health sector strategies on, respectively, HIV, viral hepatitis and sexually transmitted infections for the period 2022–2030. 2022 [cited 2025 Aug 7]. https://www.who.int/publications/i/item/9789240053779
8. World Health Organization. Human T-lymphotropic virus type 1: technical report. March 3, 2021 [cited 2025 Aug 7]. https://www.who.int/publications/i/item/9789240020221
9. Japanese Ministry of Health, Labour and Welfare. Manual on preventing HTLV-1 infection among mothers and children. 2017 [cited 2025 Aug 7]. https://www.mhlw.go.jp/ bunya/kodomo/boshi-hoken16/dl/06.pdf
10. Pan American Health Organization. The diagnosis of human T lymphotropic virus (HTLV) and strategies to expand HTLV screening in the context of maternal and child health, meeting report, 7 July 2023. 2024 [cited 2025 Aug 7]. https://iris.paho.org/handle/10665.2/59463
11. Pan American Health Organization. Technical note on good practices to prevent mother-to-child transmission of HTLV-1 in the context of the EMTCT Plus initiative. 2024 [cited 2025 Aug 7]. https://iris.paho.org/handle/10665.2/62014
12. Director-General of Health Professor J. Menard. Circular DGS/SP 2 No. 97–785 of 16 December 1997 on the personalized donation of milk from a mother to her hospitalized child and a reminder of the provisions in force concerning breastfeeding. 1996 [cited 2025 Aug 7]. https://affairesjuridiques.aphp.fr/textes/circulaire-dgssp-2-n-97-785-du-16-decembre-1997-relative-au-don-de-lait-personnalise-dune-mere-a-son-enfant-hospitalise-et-rappel-des-dispositions-en-vigueur-en-matiere-dallaitement-materne
13. Moquet O, Faye I, Auffret N, Garin B, Brichler S, Césaire R. Human T-cell lymphotropic virus screening in France: missed opportunities? A retrospective multicenter study of serological testing in hospital laboratories. IJID Reg. 2024;12:100387. https://doi.org/10.1016/j.ijregi.2024.100387
14. Centre for Clinical Practice. Donor breast milk banks: the operation of donor milk bank services. 2010 [cited 2025 Aug 7]. https://www.ncbi.nlm.nih.gov/ books/NBK66142
15. National Screening Committee. Antenatal screening programme: HTLV. 2022 [cited 2025 Aug 7].

https://view-health-screening-recommendations.service.gov.uk/htlv
16. Office for Health Improvement and Disparities. Women's health: migrant health guide. [cited 2026 Mar 22]. www.gov.uk/guidance/womens-health-migrant-health-guide
17. Soriano V, de Mendoza C; Spanish HTLV Network. Screening for HTLV-1 infection should be expanded in Europe. Int J Infect Dis. 2024;140:99–101. https://doi.org/10.1016/j.ijid.2024.01.015
18. Brites C, Tonto PB, Vallinoto AC, Dos Santos Oliveira O, Simionatto S, Bay M, et al. Multicenter cross-sectional study of HTLV-1 prevalence and associated risk factors in epidemiologically relevant groups across Brazil. Front Public Health. 2025;13:1511374. https://doi.org/10.3389/fpubh.2025.1511374
19. Mouinga-Ondémé A, Boundenga L, Koumba Koumba IP, Idam Mamimandjiami A, Diané A, Engone-Ondo JD, et al. Human T-lymphotropic virus type 1 and human immunodeficiency virus co-infection in rural Gabon. PLoS One. 2022;17:e0271320. https://doi.org/10.1371/journal.pone.0271320
20. World Health Organization Regional Office for Europe, European Centre for Disease Prevention and Control. HIV/AIDS surveillance in Europe 2024–2023 data. 2024 [cited 2025 Aug 7]. https://www.who.int/europe/publications/i/item/9789289061551
21. Norman FF, Salvador F, Gullón B, Díaz-Menéndez M, Pérez-Ayala A, Rodriguez-Guardado A, et al. Frequency and characteristics of HTLV in migrants: results from the +Redivi collaborative network in Spain. J Travel Med. 2022;29:taac019. https://doi.org/10.1093/jtm/taac019
22. Migrant Commission, French Society of Infectious Pathology, French Paediatric Society, French Society for the Fight against AIDS. Recommendation of the French Society of Infectious Pathology in French (SPILF), the French Paediatric Society (SFP) and the French Society for the Fight against AIDS (SFLS) on the health check-up to be carried out on all newly arrived migrants (adults and children) [in French]. June 2024 [cited 2025 Aug 7]. https://www.sfls.fr/ckfinder/userfiles/files/NEW/commission-migrants/Recommandation_Bilan_de_Sante_vfinale.pdf
23. European Centre for Disease Prevention and Control. Public health guidance on screening and vaccination for infectious diseases in newly arrived migrants within the EU/EEA. 2018 [cited 2025 Aug 7]. https://www.ecdc.europa.eu/en/publications-data/public-health-guidance-screening-and-vaccination-infectious-diseases-newly
24. World Health Organization. Guidelines on HIV and infant feeding: 2021 update. Guideline: updates on HIV and infant feeding: the duration of breastfeeding, and support from health services to improve feeding practices among mothers living with HIV, 2016 [cited 2025 Aug 7]. https://iris.who.int/bitstream/handle/10665/246260/9789241549707-eng.pdf
25. Pérez-Escamilla R, Hernández-Cordero S, Gupta T. Perspective: infant feeding policies among women living with HIV in Latin America and the Caribbean: should they be updated? Adv Nutr. 2026;17:100469. https://doi.org/10.1016/j.advnut.2025.100469
26. British HIV Association. BHIVA guidelines for the management of HIV in pregnancy. July 2024 [cited 2025 Aug 7]. https://bhiva.org/clinical-guideline/pregnancy-guidelines
27. Aebi-Popp K, Bernasconi E, Kahlert C, Martinez De Tejada B, Nadal D, Rudin C, et al. Recommendations of the Federal Commission for Sexual Health (FCSG) for the medical care of HIV-infected women and their children [in German]. Bull Swiss Federal Office of Public Health. 2018;50:10–22.
28. Keane A, Lyons F, Aebi-Popp K, Feiterna-Sperling C, Lyall H, Martínez Hoffart A, et al. Guidelines and practice of breastfeeding in women living with HIV—results from the European INSURE survey. HIV Med. 2024;25:391–7. https://doi.org/10.1111/hiv.13583
29. Haute Autorité de Santé. Pregnancy and HIV: desire for a child, care of the pregnant woman and prevention of mother-to-child transmission [in French]. April 2024 [cited 2025 Aug 7]. https://www.has-sante.fr/upload/docs/application/pdf/2024-05/recommandations_vih_grossesse_22_mai_2024.pdf
30. European AIDs Clinical Society. EACS guidelines version 12.0. October 2023 [cited 2025 Aug 7]. https://www.eacsociety.org/guidelines/eacs-guidelines
31. US Department of Health and Human Services. Panel on treatment of HIV-infected pregnant women and prevention of perinatal transmission. Recommendations for use of antiretroviral drugs in pregnant HIV-1-infected women for maternal health and interventions to reduce perinatal HIV transmission in the United States [cited 2025 Aug 7]. https://clinicalinfo.hiv.gov/en/guidelines/perinatal/antepartum-care
32. Khan S, Tsang K, Brophy J. Canadian peadiatric and perinatal HIV/AIDS research group consensus recommendations for infant feeding in the HIV context. J Assoc Med Microbiol Infect Dis Can. 2022;8(1):7-17. https://doi.org/10.3138/jammi-2022-11-03
33. The Australasian Society of HIV Viral Hepatitis and Sexual Health Medicine. The optimal scenario and context of care. ASHM guidance for healthcare providers regarding infant feeding options for people living with HIV with highlights from breatfeeding and women living with HIV in Australia. 2021 [cited 2025 Aug 7]. https://ashm.org.au/wp-content/uploads/2022/04/Resource_ASHM-HIV-Infant-feeding-Guidance_FINAL.pdf
34. Rosadas C, Taylor GP. Mother-to-Child HTLV-1 Transmission: Unmet Research Needs. Front Microbiol. 2019;10:999. https://doi.org/10.3389/fmicb.2019.00999
35. World Health Organization. Governance for the validation of elimination of mother-to-child transmission of HIV, syphilis and hepatitis B virus: an overview of validation structures and responsibilities at national, regional and global levels. 2022 [cited 2025 Aug 7]. https://iris.who.int/bitstream/handle/10665/362636/9789240056961-eng.pdf
36. Hernández-Aguilar MT, Bartick MC, Schreck PK, Chapin EM. Academy of breastfeeding medicine clinical protocol #7: model maternity policy supportive of breastfeeding. Breastfeed Med. 2025;20:771–804. https://doi.org/10.1177/15568253251375964
37. National Health and Medical Research Council. Infant feeding guidelines. Information for healthworkers. 2012 [cited 2025 Aug 7]. https://www.eatforhealth.gov.au/sites/default/files/2022-09/170131_n56_infant_feeding_guidelines.pdf
38. Health Canada. Draft nutrition for healthy term infants—recommendations from birth to six months: guidelines and recommendations. [cited 2025 Aug 7]. https://www.canada.ca/en/health-canada/programs/consultation-draft-nutrition-healthy-term-infants-0-6-months-guidelines/guidelines-recommendations.html
39. Cattaneo A, Fallon M, Kewitz G, Mikiel-Kostyra K, Robertson A. Infant and young child feeding: standard recommendations for the European Union [cited 2025 Aug 7]. https://cnol.kobiety.med.pl/wp-content/

uploads/2019/11/EUNUTNET_Infant_and_young_child_feeding.pdf
40. Haut Conseil de Santé Publique. Report on breastfeeding. Summary of key points [in French]. 12 June 2024 [cited 2025 Aug 7]. https://www.gifa.org/publications/hcsp-rapport-sur-lallaitement-maternel-2024/
41. Minakami H, Hiramatsu Y, Koresawa M, Fujii T, Hamada H, Iitsuka Y, et al.; Japan Society of Obstetrics and Gynecology; Japan Association of Obstetricians and Gynecologists. Guidelines for obstetrical practice in Japan: Japan Society of Obstetrics and Gynecology (JSOG) and Japan Association of Obstetricians and Gynecologists (JAOG) 2011 edition. J Obstet Gynaecol Res. 2011;37:1174–97. https://doi.org/10.1111/j.1447-0756.2011.01653.x
42. Interdisciplinary Working Group. Feeding the healthy newborn [in French] [cited 2025 Aug 7]. https://www.paediatrieschweiz.ch/fr/alimentation-du-nouveau-ne-sain
43. Centers for Disease Control and Prevention. Breastfeeding: contraindications. 2024 [cited 2025 Aug 7]. https://www.cdc.gov/breastfeeding-special-circumstances/hcp/contraindications/index.html
44. UK Department of Health. Infant feeding recommendation 2003. [cited 2025 Aug 7]. https://abm.me.uk/wp-content/uploads/Department-of-Health-Infant-Feeding-recommendation.pdf
45. National Aboriginal Community Controlled Health Organisation. Australian clinical guidelines on HTLV-1 for Aboriginal primary health care settings [cited 2026 Mar 28]. https://ashm.org.au
46. Ministerio da Saude do Brasil. Protocolo clínico e diretrizes terapêuticas para manejo da infecção pelo hiv em adultos [cited 2026 Mar 28]. https://www.gov.br/aids/pt-br/central-de-conteudo/pcdts/pcdt_hiv_modulo_1_2024.pdf/@@display-file/file
47. Organisation of Eastern Caribbean States. OECS HIV STI guidelines. 2018 [cited 2026 Mar 28]. https://oecs.int/en/our-work/knowledge/library/health/hiv-tb/hiv
48. Rosadas C, Senna K, da Costa M, Assone T, Casseb J, Nukui Y, et al. Women living with HTLV-1 should have the opportunity to make informed decisions on prevention of mother-to-child transmission. Lancet Glob Health. 2023; 11:e1181. https://doi.org/10.1016/S2214-109X(23)00268-1
49. Maertens GN, Purcell DFJ, Rosadas C, Bradshaw D, Biglione M, Taylor GP, et al. Why not eliminate HTLV-1 while eliminating HIV-1? Lancet. 2024;403:2288–9. https://doi.org/10.1016/S0140-6736(24)00295-2
50. O'Donnell JS, Jaberolansar N, Chappell KJ. Human T-lymphotropic virus type 1 and antiretroviral therapy: practical considerations for pre-exposure and post-exposure prophylaxis, transmission prevention, and mitigation of severe disease. Lancet Microbe. 2024;5:e400–8. https://doi.org/10.1016/S2666-5247(23)00359-2

Address for correspondence: Agnès Meybeck, Centre Hospitalier de Tourcoing, 135 rue du Président Coty, 59200 Tourcoing, France; email: ameybeck@ch-tourcoing.fr

# etymologia revisited

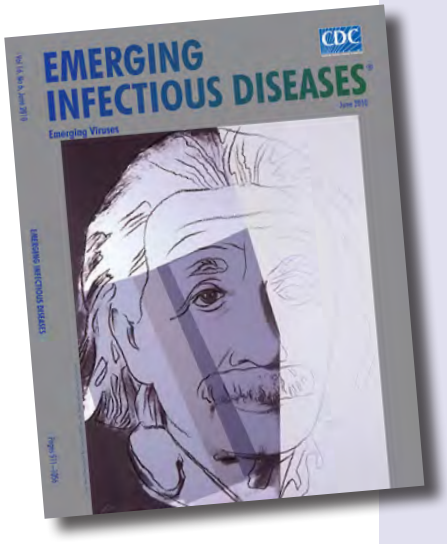


*Originally published in June 2010*

## Lassa Virus

[lah sə] virus

This virus was named after the town of Lassa at the southern end of Lake Chad in northeastern Nigeria, where the first known patient, a nurse in a mission hospital, had lived and worked when she contracted this infection in 1969. The virus was discovered as part of a plan to identify unknown viruses from Africa by collecting serum specimens from patients with fevers of unknown origin. Lassa virus, transmitted by field rats, is endemic in West Africa, where it causes up to 300,000 infections and 5,000 deaths each year.

**References:**

1 Frame JD, Baldwin JM Jr, Gocke DJ, Troup JM. Lassa fever, a new virus disease of man from West Africa. I. Clinical description and pathological findings. Am J Trop Med Hyg. 1970;19:670–6.
2. Mahy BW. The dictionary of virology, 4th ed. Burlington (MA): Elsevier; 2009.

**https://wwwnc.cdc.gov/eid/article/16/6/et-1606_article**

# Epidemiology and Clinical Features of *Balamuthia mandrillaris* Infection, China

Tzuyi Yang,[1] Yan Lei,[1] Xiaobo Feng, Zhirong Yao, Zhen Zhang

*Balamuthia mandrillaris* is a highly lethal free-living ameba that primarily affects the skin and central nervous system, manifesting clinically as chronic granulomatous lesions and granulomatous encephalitis. Once the central nervous system is involved, the mortality rate exceeds 90%. No standardized treatment regimen has yet been established. In this review, we summarized 66 cases reported from China. The median patient age was 36 years (range 10 months–77 years); 62.12% patients were male and 37.88% female. Fifty-five (83.33%) patients were immunocompetent. For 42 (63.64%) patients, initial symptoms were cutaneous manifestations; of those, central nervous system involvement subsequently developed in 25 (59.52%) patients. Twenty-four (36.36%) patients were hospitalized initially with encephalitis. Among the 63 patients with a known outcome, 43 (68.25%) succumbed to infection. For patients with cutaneous-only disease, the survival rate was 93.75%, whereas once the central nervous system was affected, mortality reached 96.00%.

*Balamuthia mandrillaris* is a free-living ameba classified within the phylum Amoebozoa, class Discosea, order Centramoebida, and family Balamuthiidae (*1*,*2*). *B. mandrillaris* are ubiquitously distributed in nature and exhibit 2 developmental stages: the trophozoite and the cyst. The trophozoite is 12–60 μm in diameter and is characterized by a round nucleus with a large, spherical, densely staining nucleolus. However, trophozoites with 2 or 3 nucleolar bodies have been seen, especially in infected tissues, which is a distinguishing feature in early diagnosis of *B. mandrillaris* infection (*3*). Trophozoites often display prominent spiny projections and pseudopodia. Under unfavorable environmental conditions, such as desiccation, extreme temperatures, or exposure to chemicals, trophozoites differentiate into cysts (*4*). The cysts are spherical, measuring 12–30 μm in diameter, with a single nucleus. The cyst wall appears double-layered under light microscopy and triple-layered under electron microscopy (*3*).

Previous studies have established that soil, water, and dust are the principal environmental reservoirs of *B. mandrillaris* and that the organism can enter the human body through breaches in the cutaneous barrier or through the lower respiratory tract (*5*). An additional report suggested that *B. mandrillaris* might invade the central nervous system through the olfactory nerve (*6*). Several case reports have also confirmed possible transmission through solid organ transplantation (*7*,*8*).

Globally, cases of *B. mandrillaris* infection have been reported on 5 continents, excluding just Africa and Antarctica. Most cases occur in hot, arid tropical and subtropical regions, particularly in the warm climate of the southwestern United States, tropical areas of Peru, and subtropical regions of China (*9*).

*B. mandrillaris* infection predominantly involves 2 organ systems in humans, the skin and the central nervous system (CNS). Cutaneous disease most frequently affects the nose, followed by the knees; other sites, such as the buttocks, thighs, arms, and chest, might also be involved. Lesions can be solitary or multifocal and usually manifest as asymptomatic, well-demarcated plaques with slightly raised annular borders; ulceration is uncommon (*3*). Lesion size ranges from 1 cm to several centimeters, and lesions typically have a reddish to dark red hue. The affected skin typically retains normal sensation and demonstrates a firm, rubbery, cartilaginous, or stone-like consistency on palpation (*10*). The cutaneous course is generally chronic, persisting for months to years. Without timely intervention, hematogenous dissemination to the CNS may occur (*4*). When the CNS is involved, the predominant clinical manifestation is granulomatous amebic encephalitis (GAE), also referred to as *B. mandrillaris* amebic encephalitis. The disease typically

Author affiliation: Xinhua Hospital, Shanghai Jiaotong University School of Medicine, Shanghai, China

DOI: https://doi.org/10.3201/eid3207.251771

[1]These first authors contributed equally to this article.

follows an acute to subacute course and manifests with nonspecific neurologic symptoms. Early features include headache, nausea, vomiting, fever, somnolence, gait disturbance, and impairments of consciousness and speech. When infection progresses rapidly, seizures, coma, and ultimately death can ensue (*3*,*10*). Once the CNS is affected, the mortality rate approaches 90% (*11*). Because of the nonspecific manifestation, CNS infection is often initially misdiagnosed as brain abscess, tumor, neurocysticercosis, or acute disseminated encephalomyelitis (*11*). *Balamuthia* appears capable of infecting both immunocompetent and immunocompromised persons. Previous reports in the United States have indicated that only 39% of patients were immunocompromised (*11*).

Given the rarity of this disease, the epidemiology and clinical features for *B. mandrillaris* infection in China remain incompletely characterized. To address this gap, we summarized all reported cases of *B. mandrillaris* infection in China, with the objective of delineating the epidemiology and clinical features.

## Methods

We conducted a comprehensive literature review to identify reported cases of *B. mandrillaris* infection in China. We included published articles in PubMed and the China National Knowledge Infrastructure through September 2025 using the following search terms: free-living amoebae, *Balamuthia mandrillaris*, infection, encephalitis, case report, diagnosis, treatment, and China. We conducted searches in English and Chinese. Two authors (T.Y. and Y.L.) independently reviewed the retrieved articles. Inclusion criteria were case reports or case series reporting ≥1 confirmed case of *B. mandrillaris* infection. We excluded duplicate publications and studies not involving *B. mandrillaris* infection. We extracted relevant data, such as patient characteristics, epidemiologic features, clinical manifestations, treatment strategies, and clinical outcomes. We reviewed 39 publications through September 2025 and identified 66 confirmed cases of *B. mandrillaris* infection in China beginning in 2002 (Appendix Table 1, https://wwwnc.cdc.gov/EID/article/32/7/25-1771-App1.pdf).

We classified the certainty of exposure sources on the basis of the descriptions provided in the literature. We defined the certainty of exposure sources as confirmed when a specific traumatic event or exposure was reported, the site of injury or exposure was consistent with the location of clinical manifestations, and the diagnosis was confirmed by histopathologic examination of the corresponding site. We considered the certainty of exposure sources probable when a specific traumatic event or exposure was described but the exact site of injury or exposure was not specified or when diagnosis was based on next-generation sequencing (NGS) only or histopathologic confirmation was not obtained from the corresponding site. We classified the certainty of exposure sources as possible when a suspected exposure was reported but lacked sufficient supporting evidence. The analyses in this study focused on confirmed and probable cases.

We also categorized the certainty of diagnosis on the basis of available evidence. We defined the certainty of diagnosis as confirmed when the diagnosis was established by histopathological examination but classified certainty of diagnosis diagnosed solely by NGS as probable, given that NGS alone can be insufficient to confirm a case because of the potential for cross-contamination. We calculated descriptive statistics and frequency distributions using SPSS Statistics for Windows version 17.0 (IBM, https://www.ibm.com).

## Results

### Epidemiology

We identified 39 articles from the literature search. All the included articles were case reports or case series. As of September 2025, the earliest reported case had disease onset in 2002; a total of 66 cases of *B. mandrillaris* infection in China have been reported in published English and Chinese language literature (Appendix Table 1).

Of the 66 cases, 41 (62.12%) patients were male and 25 (37.88%) female, yielding a male-to-female ratio of 1.64:1. Ages ranged from 10 months to 77 years (mean 36 years); 28 (42.42%) cases occurred in persons <18 years of age. Regarding occupational background, 8 (12.12%) patients were farmers, 1 was involved in animal husbandry, 1 was employed as a miner, and 1 worked in waste management. In the case of the remaining patients, 27 (40.91%) patients had no reported occupation and 28 (42.42%) were children <18 years of age. Among the 66 cases, only 23 had clearly reported dates of disease onset. Even within those 23 cases, we observed no apparent seasonal pattern of *B. mandrillaris* infection (Figure).

Cases were distributed across multiple provinces and municipalities in China. We determined distribution on the basis of clearly reported exposure locations; when such information was unavailable, we categorized cases according to the treatment location. Previous studies have faced similar limitations and therefore applied the same approach for

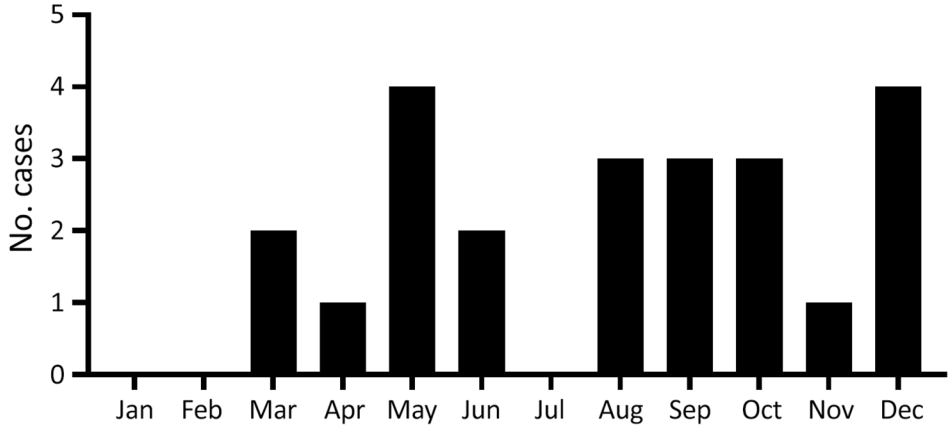


**Figure.** Monthly distribution of *Balamuthia mandrillaris* cases in study of epidemiology and clinical features of *B. mandrillaris* infection, China. Onset dates were specified in 23 case reports but unspecified in 43 others.

case classification (*11*). Of the 66 cases, 38 cases had a clearly documented province of origin, whereas 28 were inferred from the treating hospital.

Among 66 cases, 55 (83.33%) patients were immunocompetent, 5 (7.58%) were immunocompromised or receiving immunosuppressive therapy (2 patients were receiving immunosuppressive therapy after kidney transplantation, 2 had type 2 diabetes mellitus, and 1 had breast cancer), and 2 (3.03%) had concomitant infections (1 patient had concurrent human herpesvirus 6 encephalitis and 1 had previous SARS-CoV-2 infection); the immune status of 4 (6.06%) patients was not specified. Among the 2 patients who received immunosuppressive therapy after kidney transplantation, 1 (case 52) underwent kidney transplantation 13 days before disease onset because of uremia and received tacrolimus, mycophenolate sodium enteric-coated tablets, methylprednisolone, and antithymocyteglobulin for antirejection therapy beginning on the first postoperative day (*12*). The other patient (case 57) had been on long-term immunosuppression for 14 years and was treated with cyclosporine, mycophenolate mofetil, and prednisone acetate; the patient also had a 2-month history of type 2 diabetes mellitus (*13*). The immunosuppressive therapy given to transplant recipients likely predisposes them to rapid progression of disease. Overall, 42 (63.64%) of 66 patients lived in rural areas, 3 (4.55%) lived in urban settings, and the remaining 21 (31.82%) had unspecified residence.

Regarding the certainty of transmission routes among the 66 cases, we classified 20 (30.30%) as confirmed, 4 (6.06%) as probable, 4 (6.06%) as possible, and 38 (57.58%) as unknown. Among the confirmed cases, 19 (95.83%) cases had a documented history of cutaneous trauma, and 1 (4.17%) case was linked to water exposure, in which previous nasal trauma followed by water contact resulted in nasal infection (*14*). Among the 4 probable cases, 2 had a documented history of skin trauma but without a clearly specified site corresponding to the location of clinical manifestations, and 2 had a documented history of skin trauma with a clearly identified site, but the diagnosis was established by NGS performed on specimens obtained from the brain. Among the 4 possible cases, 3 were suspected to be associated with water exposure: 1 patient had been exposed to rainwater 1 day before the onset of neurologic symptoms, 1 reported habitual consumption of untreated mountain spring water, and 1 was associated with accidental seawater aspiration. The remaining possible case-patient (case 52), who underwent kidney transplantation 13 days before disease onset, was classified as having a possible association with organ transplantation, given that donor-derived transmission and infection in other organ recipients from the same donor could not be confirmed (*12*). In contrast, case-patient 57, in whom infection developed 14 years after kidney transplantation, was considered less likely to have a transplant-related infection; the infection might instead have been associated with long-term immunosuppressive therapy, and the route of transmission remained unknown (*13*).

### Clinical Manifestations

Regarding clinical manifestations, 42 (63.64%) patients had initial symptoms of cutaneous lesions, most commonly plaques (85.71%), followed by scales (4.76%), erythema (2.38%), ulcers (2.38%), crusts (2.38%), and unspecified lesions (9.52%). Lesions were located on the face (78.57%), lower limbs (9.52%), upper limbs (7.14%), waist (2.38%), back (2.38%), or unspecified sites (2.38%). Among those 42 patients, CNS involvement subsequently occurred in 25 (59.52%) persons. For a total of 24 (36.36%) patients, initial manifestation was CNS disease, most frequently with headache (62.50%), fever (62.50%), vomiting (41.67%), gait instability or

motor disturbance (29.17%), consciousness disturbance (25.00%), fatigue (20.83%), dizziness (16.67%), nausea (12.50%), speech disorders (12.50%), somnolence (8.33%), epilepsy (8.33%), blurred vision (4.17%), limb numbness (4.17%), personality or behavioral changes such as irritability (4.17%), delayed reaction (4.17%), and convulsions (4.17%). Among the 25 patients with both cutaneous and CNS involvement, the interval from the onset of skin lesions to neurologic manifestations ranged from 2 months to 9 years (mean 3.67 years); time interval was unspecified in 5 cases.

Regarding the certainty of relationship between clinical manifestations and transmission routes, among the 42 patients with cutaneous manifestations, 19 (45.24%) were classified as having a confirmed association with skin trauma. Four (9.52%) patients were classified as having a probable association with skin trauma, including 2 cases without a clearly specified site of exposure and 2 cases diagnosed by NGS of brain tissue. The remaining 19 (45.24%) patients had no detailed exposure information. Among the 24 patients who initially had CNS manifestations, 3 (12.50%) were classified as having a possible association with water exposure, and 1 (4.17%), who underwent transplantation 13 days before disease onset, was classified as having a possible association with organ transplantation (*12*). The remaining 20 (83.33%) had no documented exposure history.

### Diagnosis

Among the 66 reported cases, 38 (57.58%) were confirmed by histopathologic examination (with or without supporting NGS results). The remaining 28 (42.42%) were considered probable on the basis of NGS of brain tissue or cerebrospinal fluid only.

### Treatment

Among 66 reported patients, 44 (66.67%) received pharmacologic therapy, 9 (13.64%) underwent combined pharmacologic and surgical treatment, and 9 (13.64%) died before treatment could be initiated; for 4 (6.06%) patients, the treatment approach was unknown. For patients with cutaneous manifestations alone, treatment regimens have typically included ≥1 antibiotic from the lincosamide, macrolide, or tetracycline classes, administered with or without interferon and, in some cases, combined with surgical excision. For patients with CNS involvement, treatment regimens have generally consisted of surgical intervention (lesion resection or decompressive craniectomy) in combination with fluconazole, flucytosine, azithromycin (or tetracycline), and trimethoprim/sulfamethoxazole; metronidazole is added in some cases (Appendix Table 2).

### Outcome

Among 66 patients, outcome was known for 63 patients; 43 (68.25%) patients died and 20 (31.75%) survived (Appendix Table 1). Among 17 patients with cutaneous-only manifestations, 15 (93.75%) survived, 1 (6.25%) died from drug-induced liver failure after treatment with diminazene aceturate (*15*), and 1 had an unknown outcome. Among survivors, 11 received ≥1 lincosamide, macrolide, or tetracycline, with or without interferon and surgical excision.

Among 25 patients who initially demonstrated cutaneous manifestations and subsequently progressed to CNS involvement, 24 (96.00%) died and 1 (4.00%) survived. Of note, 11 of those patients received treatment regimens similar to those for patients demonstrating only cutaneous manifestations. However, although their skin lesions showed partial or marked improvement after treatment, all of them ultimately died after the development of neurologic symptoms.

Among 24 patients with CNS-only manifestations, 18 (81.82%) died, 4 (18.18%) survived, and 2 had unknown outcomes. Among 5 surviving patients with CNS involvement, with or without cutaneous lesions, 3 received combination treatment regimens consisting of fluconazole, flucytosine, azithromycin (or tetracyclines), and trimethoprim/sulfamethoxazole, with or without surgical excision; metronidazole was added in some cases. One patient underwent surgical excision followed by treatment with miltefosine, fluconazole, rifampin, albendazole, and amphotericin B; the treatment regimen for 1 patient was unknown. However, 2 patients who died received treatment regimens similar to those of the survivors, consisting of fluconazole, flucytosine, azithromycin, and trimethoprim/sulfamethoxazole, with or without surgical excision. Despite that treatment, their neurologic symptoms deteriorated and ultimately resulted in death. After CNS symptom onset, time to death ranged from 5 days to 6 months (mean 41.79 days); 24 patients (48.98%) died within 1 month.

## Discussion

In China, *B. mandrillaris* infections occur predominantly in men; most cases have been reported in northern regions and rural settings. A substantial proportion of affected persons are engaged in occupations such as farming, animal husbandry, and horticulture. The higher prevalence among men is likely attributable to their role as the primary labor force in rural areas, a

pattern consistent with observations from the southwestern United States and Peru, where most infected patients were also male agricultural workers. Most cases have been reported in temperate climatic zones at latitudes comparable to those of the southwestern United States, consistent with environmental conditions favorable for the growth of *B. mandrillaris*.

In contrast to the United States, where ≈39% of reported cases have occurred in immunocompromised persons, most patients in China with *B. mandrillaris* infection have been immunocompetent; only 10.61% had underlying conditions such as hepatitis C, malignancy, viral infections, diabetes, uremia, or long-term immunosuppressive therapy. Those patients appear more likely to experience rapid progression to *B. mandrillaris* GAE, which might contribute to poor therapeutic outcomes. For example, in one case, a patient with a 2-year history of cutaneous lesions on the left knee underwent radical mastectomy for breast cancer. Although no postoperative immunosuppressive therapy was administered, the disease progressed rapidly to CNS involvement within 1 week of surgery and ultimately resulted in death (*16*).

In China, 63.64% of patients initially sought care for cutaneous manifestations, consistent with epidemiologic observations from Peru, where chronic granulomatous skin lesions also predominate. The lesions typically manifested as plaques, most frequently on the face, and many patients had a documented history of cutaneous trauma; lesions often developed at the site of injury. Those findings support the soil contact–skin injury hypothesis and align with the agricultural context of both China and Peru, where frequent soil exposure increases the risk for infection after traumatic skin injury. One reported case (case 52) was considered to have possibly acquired a donor-derived infection through hematogenous transmission through organ transplantation (*12*). A minority of cases have been possibly attributed to waterborne transmission; those patients had initial CNS symptoms such as headache, fever, and vomiting, resembling the clinical manifestations reported in the United States. A previous US study reported that 35 (85%) of 41 case-patients with documented soil exposure had engaged in soil-related activities, providing evidence supporting the soil contact–skin injury hypothesis. In addition, the same study also noted that 66% of patients in the United States who reported *B. mandrillaris* infection had a history of water exposure (*11*). In another previously reported case, infection with *B. mandrillaris* was associated with the use of nonsterile water for nasal lavage (*17*). In addition, another study reported that 57% of infected patients had exposure to stagnant water (*18*). Those reports suggest that water exposure might be a potential source of *B. mandrillaris* infection. Although the suspected water sources were not tested for *B. mandrillaris*, those findings indicate that water-related activities, such as swimming in ponds or rivers, might allow the organism to enter the body through breaches in the cutaneous barrier, through the nasal mucosa, or through the lower respiratory tract.

Patients initially demonstrating cutaneous disease achieved a survival rate of 93.75%. Most survivors received treatment regimens including 2 classes of antibiotics, with or without interferon, diminazene aceturate, or surgical excision. Diminazene aceturate, an antiprotozoal agent primarily used in veterinary medicine, has been reported in China to achieve favorable outcomes in the treatment of cutaneous *B. mandrillaris* infection. In those cases, the drug was used to reduce lesion size, often followed by surgical resection or adjunctive therapy (*15*). However, because of the lack of reported use in human treatment, available evidence is primarily derived from animal studies, in which its clinical application has been limited by potential adverse effects, including gastrointestinal symptoms (abdominal distension, nausea, and vomiting), cardiovascular manifestations (palpitations), hepatic and renal dysfunction (elevated liver enzymes and proteinuria), and severe neurotoxicity (myalgia, weakness, and polyneuritis) (*19*,*20*). Of note, among the 4 patients who were treated with diminazene aceturate reported in China, gastrointestinal and neurologic adverse effects developed in all patients, and 1 patient ultimately died of drug-related hepatic failure, underscoring concerns regarding its safety (*15*). Hepatotoxicity has not been reported with other commonly used therapeutic agents for this disease.

In cases where complete or near-complete surgical excision of intracranial lesions was achieved, surgery not only provided definitive confirmation of the infectious etiology but also might have contributed to disease management. In patients with rapidly increasing intracranial pressure because of extensive cerebral edema or space-occupying lesions, neurosurgical procedures such as decompressive craniectomy were used to relieve intracranial pressure, thereby affording critical time for pharmacologic therapy and host immune response. With regard to agents recommended by the US Centers for Disease Control and Prevention (such as miltefosine) and additional agents reported in the literature, such as pentamidine and nitroxoline, those drugs are not currently available

in China. One patient survived after combined surgical and pharmacologic therapy with miltefosine, fluconazole, rifampin, albendazole, and amphotericin B (*21*). However, another patient succumbed to infection despite receiving a treatment regimen consisting of miltefosine, pentamidine, flucytosine, fluconazole, clarithromycin, amphotericin B, and trimethoprim/sulfamethoxazole (*16*).

Among the 66 cases of *B. mandrillaris* infection in mainland China summarized in this study, the survival rate was 93.75% for patients with cutaneous manifestations alone. However, once the disease progressed to CNS involvement, the mortality rate increased sharply to 96.00%, consistent with previous reports in other countries. In addition, when CNS symptoms were the initial manifestation, the mortality rate was as high as 81.82%. Of note, 11 patients still progressed to fatal neurologic involvement despite improvement in cutaneous manifestations after treatment, indicating that controlling cutaneous symptoms does not completely prevent neurologic involvement. It is likely owing to the limited ability of therapeutic agents to penetrate the blood–brain barrier.

An epidemiologic survey conducted in the United States reported that the mean interval from onset of CNS symptoms to death for *B. mandrillaris* GAE was 24 days (range 4–450 days; n = 43) (*11*). In contrast, among the cases from China included in this study, the mean interval from CNS symptom onset to death was 39.45 days (range 7–180 days; n = 33), and 48.98% of patients died within 1 month of CNS symptom onset. Those findings underscore the extremely poor prognosis of *Balamuthia mandrillaris* infection once the CNS becomes involved.

With advances in diagnostic technology and improved detection capacity, the number of confirmed cases of *B. mandrillaris* infection in China has gradually increased, underscoring the need for heightened clinical awareness. Given the exceedingly high mortality rate associated with this disease, further in-depth research is urgently needed to enable earlier prevention and more timely detection, with the ultimate goal of reducing both the incidence and mortality of this devastating infection. When patients display suspicious epidemiologic exposures or cutaneous manifestations, *B. mandrillaris* infection should be considered in the differential diagnosis.

Z.Z. was supported by the National Natural Science Foundation of China (grant no. 82203937) and the Shanghai Sailing Program (grant no. 22YF1427000). Z.Y. was supported by the National Natural Science Foundation of China (grant no. 82230106).

T.Y., Y.L., X.F., and Z.Z. contributed equally to this work. T.Y. and Y.L. searched the scientific literature, collected and analyzed data, prepared figures, and cowrote and edited the manuscript. X.F., Z.Y., and Z.Z. designed the study, collected and interpreted data, and cowrote and edited the manuscript. All authors had access to the data in this manuscript. Z.Y. and Z.Z. accessed and verified the data.

## About the Author

Dr. Yang is a clinician and researcher in the department of dermatology at Xinhua Hospital, Shanghai Jiaotong University School of Medicine. His research interests focus on emerging infectious diseases. Dr. Lei is a clinician and researcher in the department of dermatology at Xinhua Hospital, Shanghai Jiaotong University School of Medicine. His research interests focus on emerging infectious diseases.

## References

1. Adl SM, Simpson AGB, Lane CE, Lukeš J, Bass D, Bowser SS, et al. The revised classification of eukaryotes. J Eukaryot Microbiol. 2012;59:429–93. https://doi.org/10.1111/j.1550-7408.2012.00644.x
2. National Center for Biotechnology Information. *Balamuthia mandrillaris* (taxonomy ID: 66527) [cited 2026 Mar 12]. https://www.ncbi.nlm.nih.gov/Taxonomy/Browser/wwwtax.cgi?id=66527
3. Visvesvara GS, Moura H, Schuster FL. Pathogenic and opportunistic free-living amoebae: *Acanthamoeba* spp., *Balamuthia mandrillaris, Naegleria fowleri*, and *Sappinia diploidea.* FEMS Immunol Med Microbiol. 2007;50:1–26. https://doi.org/10.1111/j.1574-695X.2007.00232.x
4. Matin A, Siddiqui R, Jayasekera S, Khan NA. Increasing importance of *Balamuthia mandrillaris.* Clin Microbiol Rev. 2008;21:435–48. https://doi.org/10.1128/CMR.00056-07
5. Sarink MJ, van der Meijs NL, Denzer K, Koenderman L, Tielens AGM, van Hellemond JJ. Three encephalitis-causing amoebae and their distinct interactions with the host. Trends Parasitol. 2022;38:230–45. https://doi.org/10.1016/j.pt.2021.10.004
6. Kiderlen AF, Laube U. *Balamuthia mandrillaris*, an opportunistic agent of granulomatous amebic encephalitis, infects the brain via the olfactory nerve pathway. Parasitol Res. 2004;94:49–52. https://doi.org/10.1007/s00436-004-1163-z
7. Farnon EC, Kokko KE, Budge PJ, Mbaeyi C, Lutterloh EC, Qvarnstrom Y, et al.; Balamuthia Transplant Investigation Teams. Transmission of *Balamuthia mandrillaris* by organ transplantation. Clin Infect Dis. 2016;63:878–88. https://doi.org/10.1093/cid/ciw422
8. Gupte AA, Hocevar SN, Lea AS, Kulkarni RD, Schain DC, Casey MJ, et al. Transmission of *Balamuthia mandrillaris* through solid organ transplantation: utility of organ recipient serology to guide clinical management. Am J Transplant. 2014;14:1417–24. https://doi.org/10.1111/ajt.12726
9. Zhang Z, Liang J, Wei R, Feng X, Wang L, Wang L, et al. Facial *Balamuthia mandrillaris* infection with neurological involvement in an immunocompetent child. Lancet Infect

Dis. 2022;22:e93–100. https://doi.org/10.1016/S1473-3099(21)00334-0
10. Wang L, Cheng W, Li B, Jian Z, Qi X, Sun D, et al. *Balamuthia mandrillaris* infection in China: a retrospective report of 28 cases. Emerg Microbes Infect. 2020;9:2348–57. https://doi.org/10.1080/22221751.2020.1835447
11. Cope JR, Landa J, Nethercut H, Collier SA, Glaser C, Moser M, et al. The epidemiology and clinical features of *Balamuthia mandrillaris* disease in the United States, 1974–2016. Clin Infect Dis. 2019;68:1815–22. https://doi.org/10.1093/cid/ciy813
12. Qin S, Lu X, Li L, Huang D. Nursing care in intensive care unit of a patient infected with *Balamuthia mandrillaris* after renal transplantation: a case report. Transplant Proc. 2024;56:1183–7. https://doi.org/10.1016/j.transproceed.2024.02.019
13. Wang S, Zhang Y, Yan M, Wu Y, Li Y, Yue X, et al. *Balamuthia mandrillaris* amoebic encephalitis: a case report [in Chinese]. Zhonghua Ganran Yu Hualiao Zazhi. 2024;24:85–8.
14. Ai J, Zhang H, Yu S, Li J, Chen S, Zhang W, et al. A case of fatal amoebic encephalitis caused by *Balamuthia mandrillaris*, China. Infect Genet Evol. 2022;97:105190. https://doi.org/10.1016/j.meegid.2021.105190
15. Wang L, Li B, Zhao T, Wang L, Jian Z, Cheng W, et al. Treatment of cutaneous *Balamuthia mandrillaris* infection with diminazene aceturate: a report of 4 cases. Clin Infect Dis. 2022;75:1637–40. https://doi.org/10.1093/cid/ciac356
16. Hu J, Zhang Y, Yu Y, Yu H, Guo S, Shi D, et al. Encephalomyelitis caused by *Balamuthia mandrillaris* in a woman with breast cancer: a case report and review of the literature. Front Immunol. 2022;12:768065. https://doi.org/10.3389/fimmu.2021.768065
17. Roy SL, Lopez AS, Schuster FL, Glaser CA, Reynolds JP, Lyon GM. Fatal *Balamuthia mandrillaris* brain infection associated with improper nasal lavage. Clin Infect Dis. 2004;38:e94–6.
18. Bravo FG, Gotuzzo E, Castillo M, Cabrera J, Anselmo M. Cutaneous balamuthiasis: a clinicopathological study. Clin Infect Dis. 2007;44:258–62.
19. Alli A, Ortiz JF, Morillo Cox Á, Armas M, Orellana VA. Miltefosine: a miracle drug for meningoencephalitis caused by free-living amoebas. Cureus. 2021;13:e13698. https://doi.org/10.7759/cureus.13698
20. Lewis KM, Cohn LA, Marr HS, Birkenheuer AJ. Failure of efficacy and adverse events associated with dose-intense diminazene diaceturate treatment of chronic *Cytauxzoon felis* infection in five cats. J Feline Med Surg. 2014;16:157–63. https://doi.org/10.1177/1098612X13502974
21. Mei J, Sheng F, Zhang C, Chen X. Imaging monitoring of Balamuthia granulomatous amoebic encephalitis. Clin Neurol Neurosurg. 2025;254:108917. https://doi.org/10.1016/j.clineuro.2025.108917

Address for correspondence: Zhen Zhang or Zhirong Yao, Department of Dermatology, Xinhua Hospital, Shanghai Jiaotong University School of Medicine, 1665 Kongjiang Rd, Yangpu District, Shanghai 200092, China; email: zhangzhen4027@163.com or yaozhirong@xinhuamed.com.cn

# etymologia revisited

## Plague

[plāg]

Plague (from the Latin *plaga*, "stroke" or "wound") infections are believed to have been common since at least 3000 BCE. Plague is caused by the ancestor of current *Yersinia* (named for Swiss bacteriologist Alexandre Yersin, who first isolated the bacterium) *pestis* strains. However, this ancestral *Y. pestis* lacked the critical *Yersinia* murine toxin (*ymt*) gene that enables vectorborne transmission. After acquiring this gene (sometime during 1600–950 BCE), which encodes a phospholipase D that protects the bacterium inside the flea gut, *Y. pestis* evolved the ability to cause pandemics of bubonic plague. The first recoded of these, the Justinian Plague, began in 541 CE and eventually killed more than 25 million persons.

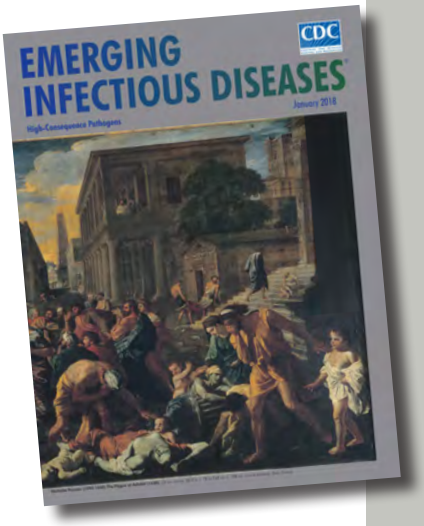


*Originally published in January 2018*

### References

1. Alexandre Yersin BW. Etymologia: yersinia. Emerg Infect Dis. 2010;16:496.
2. Centers for Disease Control and Prevention. History of plague [cited 2017 Oct 19]. https://www.cdc.gov/plague/history/index.html.
3. Rasmussen S, Allentoft ME, Nielsen K, Orlando L, Sikora M, Sjögren K-G, et al. Early divergent strains of *Yersinia pestis* in Eurasia 5,000 years ago. Cell. 2015;163:571–82.

**https://wwwnc.cdc.gov/eid/article/24/1/et-2401_article**

# Neurosurgical Biopsy and Resection for Diagnosis and Treatment of *Balamuthia mandrillaris* Amebic Encephalitis, United States

Beenish Rubbab,[1] Ammar Adenwalla,[1] Natasha Spottiswoode, Julia C. Haston, Sarah Firmani, Sumit Singh, Veena Rajaram, Jay Ramos, Ibne Karim M. Ali, Brett Whittemore, Natasha W. Hanners

We report a systematic case review of antemortem neurosurgical resections and biopsies and outcomes including new lesions after procedure and survival in *Balamuthia mandrillaris* granulomatous amebic encephalitis. The investigation was prompted by a 5-year-old patient in the southwestern United States who was treated with nitroxoline, the 2021 Centers for Disease Control and Prevention regimen, and underwent 2 resections; initial resection site recurrence and a new lesion after resection prompted the question whether complete resection versus biopsy is associated with better outcomes. We conducted a literature review and found no substantial difference between neurosurgical resection versus biopsy-only groups. Limitations include case review, number of cases, and incomplete data available. Additional analyses comparing neurosurgical outcomes with outcomes of those diagnosed via blood or cerebrospinal fluid and metagenomic next-generation sequencing might provide more definitive answers. This case and systematic review provide evidence that treatment with nitroxoline and neurosurgical resection could contribute to survival in *Balamuthia* encephalitis case-patients.

Free-living amebae (FLA) are soil- and water-dwelling unicellular organisms found throughout the world that cause rare but often fatal infections (*1*,*2*). *Acanthamoeba* and *Balamuthia* are 2 genera of FLA that cause granulomatous amebic encephalitis (GAE), a subacute disease characterized by focal neurologic deficits, altered mental status, and ≥1 parenchymal brain lesions on imaging. The true incidence is unclear because of diagnostic and reporting limitations, but in the United States, <20 cases are reported annually; however, >90% of infected patients who have central nervous system (CNS) involvement die (*1*,*2*).

*Acanthamoeba* spp. FLA primarily affect immunocompromised hosts, whereas *Balamuthia mandrillaris* amebae also infect immunocompetent hosts. *Balamuthia* spp. amebae exist as environmentally stable cysts and infectious trophozoites, entering the body through the respiratory tract or open skin wounds and spreading hematogenously to the organs, most notably the brain (*2*–*9*). *Balamuthia* was first identified in a pregnant mandrill (*Papio sphinx*) in 1990, but as a result, posthumous human diagnoses were made dating back to 1974 (*10*). Since then, *B. mandrillaris* GAE cases have been diagnosed worldwide, many among children, and often with fatal outcomes. A review of 109 US cases during 1974–2016 revealed a 90% mortality rate (*2*). Even when infections are diagnosed antemortem and patients receive antiamebic medications, the fatality rate exceeds 75% (*11*).

The Centers for Disease Control and Prevention (CDC) recommends a regimen for *B. mandrillaris* GAE including pentamidine, sulfadiazine, azithromycin or clarithromycin, a triazole, flucytosine, and miltefosine (*12*). In 2025, CDC added nitroxoline to the recommended regimen (*12*). A study published in 2018 screened 2,177 clinically approved compounds (including the CDC-recommended regimen) for in vitro activity against *B. mandrillaris* amebae (*13*). A quinoline antibiotic, nitroxoline, was found to be the most potent and selective of all agents tested (including the drugs in the recommended regimen) against

Author affiliations: University of Texas Southwestern Medical Center, Dallas, Texas, USA (B. Rubbab, A. Adenwalla, S. Singh, V. Rajaram, B. Whittemore, N.W. Hanners); University of California San Francisco, San Francisco, California, USA (N. Spottiswoode); Centers for Disease Control and Prevention, Atlanta, Georgia, USA (J.C. Haston, I.K.M. Ali); Children's Health, Dallas (S. Firmani, J. Ramos)

DOI: https://doi.org/10.3201/eid3207.260725

[1]These authors contributed equally to this article.

both cystic and trophozoite forms and at pharmacologically relevant concentrations (*13*). Nitroxoline has been used with a favorable side effect profile for human urinary tract infection treatment since the 1970s, including in pediatric patients (*14*). In 2021, an adult patient treated with nitroxoline for *Balamuthia* GAE survived (*15*). Herein, we describe a pediatric patient successfully treated with a combination of nitroxoline, the 2021 CDC recommended regimen, and 2 neurosurgical resections. We also conducted a literature review of previously published cases to determine any difference between neurosurgical resection versus biopsy-only groups.

## Case Report

In autumn 2021, a previously healthy 5-year-old was brought to care with new-onset seizures and headaches. Persisting symptoms prompted brain magnetic resonance imaging (MRI), revealing a heterogeneously enhancing cortical mass at the junction between the left temporal and occipital lobes with a large region of surrounding T2 fluid attenuated inversion recovery (FLAIR) hyperintensity (Figure 1).

With malignant tumor on the differential diagnosis, the patient underwent left occipital craniotomy and the specimen was removed en bloc and sent to pathology. The neurosurgeon chose resection margins on the basis of intraoperative frameless stereotactic navigation and the appearance and feel of normal-appearing, soft, edematous brain. Postoperative MRI confirmed an enhancing mass with no change in the surrounding edema. The neurosurgery team consulted the pediatric infectious diseases service because the preliminary pathology report was concerning for infection rather than tumor. We suspected *Balamuthia* GAE because of course chronicity, immunocompetent host, and extensive soil exposures, including making mudpies. However, we also considered in the initial consultation *Acanthamoeba* (considered less likely because the patient was immunocompetent), *Naegleria* (considered less likely because the patient had no typical acute manifestations), mycobacterial diseases

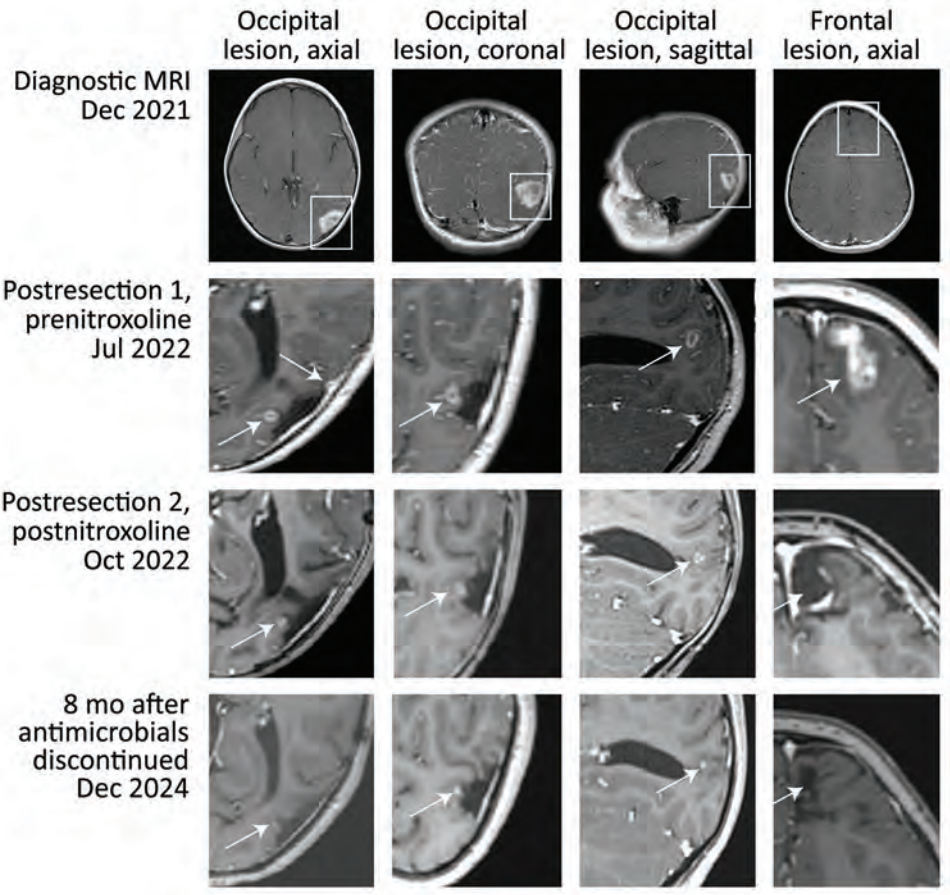


**Figure 1.** Axial, coronal, and sagittal postcontrast T1-weighted MRI images from study of neurosurgical biopsy and resection for diagnosis and treatment of *Balamuthia mandrillaris* amebic encephalitis, United States. Top row images show patient's primary occipital and frontal lesions (boxes). Three weeks after resection of the first occipital lesion (second row), recurrent nodules (arrows) developed around the resection cavity. Before nitroxoline initiation, those nodules were enlarging. MRI in July 2022 (second row) showed a new, 7-mm diameter, indistinct, fluid attenuated inversion recovery–hyperintense, enhancing focus in the anterior aspect of the left superior frontal gyrus. After nitroxoline (third row), the occipital lesions retracted (arrows) and were no longer ring-enhancing. No recurrent lesions were noted at the resection site of the frontal lesion, which was resected while the patient was on multidrug therapy and 4 weeks before starting nitroxoline. Follow-up imaging 8 months after antimicrobial treatment was discontinued (fourth row), a stable, residual nodule (arrows) in the medial resection cavity remained, thought to represent gliosis. MRI, magnetic resonance imaging.

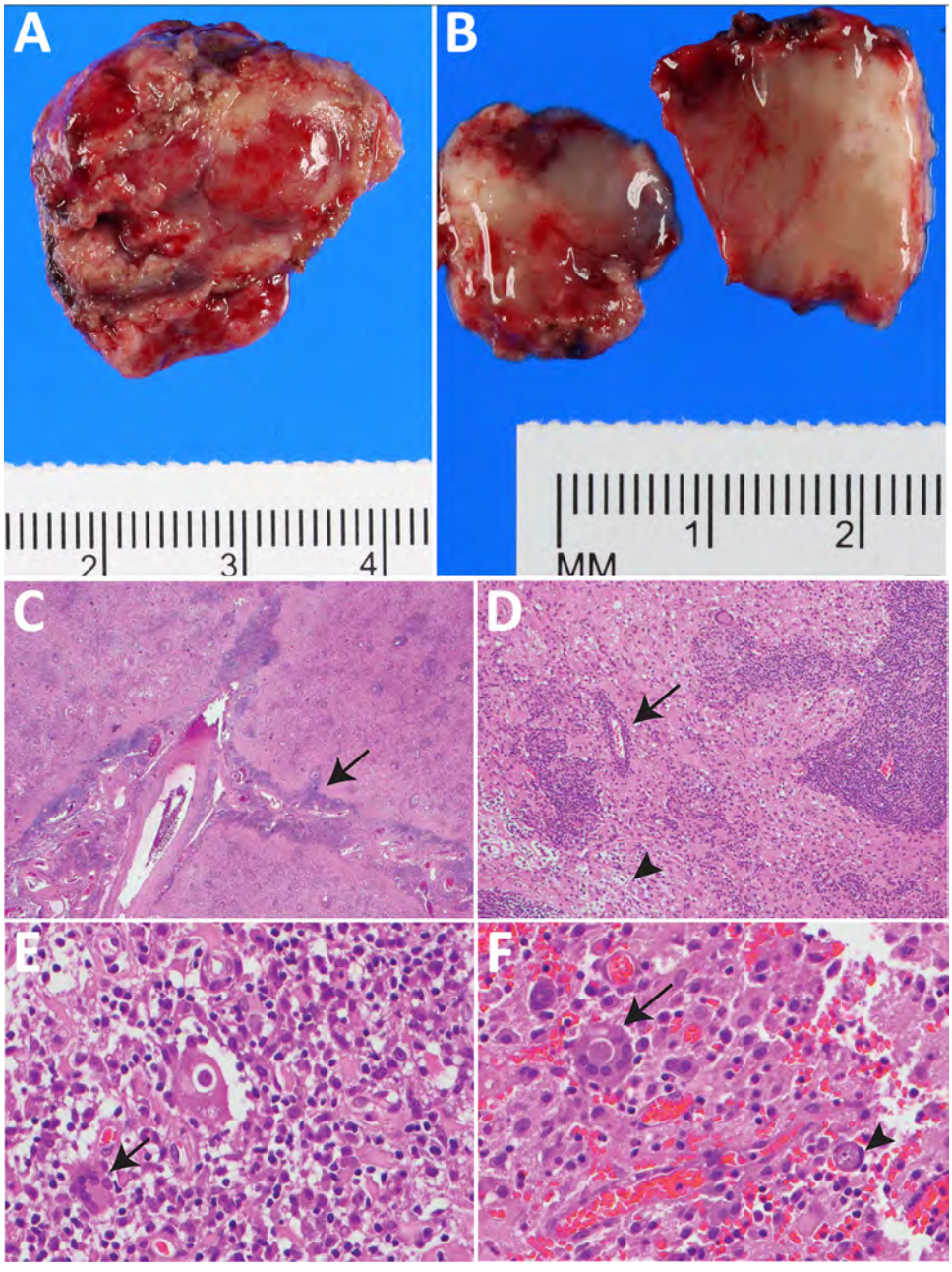


**Figure 2.** Resected occipital lesion gross and histopathology from patient in study of neurosurgical biopsy and resection for diagnosis and treatment of *Balamuthia mandrillaris* amebic encephalitis, United States. A) Gross pathology revealed pink-tan, firm tissue fragments. B) Cut sections reveal a heterogenous, tan-pink, and soft surface with effacement of the white and gray matter demarcation. C, D) Hematoxylin and eosin stained sections of the brain show leptomeningeal thickening with striking perivascular lymphocytic infiltrate (C, arrow) extending into the cortical parenchyma with foci of lymphocytic infiltration into the vessel wall, consistent with vasculitis (D, arrow). The architecture of the cortical gray matter is obliterated by neuronal loss, reactive gemistocytic astrocytes and infiltration by macrophages, multinucleated giant cells, and lymphocytes. This involves the adjacent white matter with areas of parenchymal loss/liquefactive necrosis (D, arrowhead). Original magnification ×2 for panel C, ×10 for panel D. E, F) Many of the multinucleated giant cells (E, arrow) contain large round thick-walled parasites (F, arrow) containing granular material and an occasional inconspicuous, dot like nucleus (F, arrowhead). Original magnification ×40 for panels E and F. Occasional structures resembling engulfed organisms are seen in the parenchyma (D–F).

including nontuberculous (NTM) and tuberculosis (TB) (considered less likely because the patient was immunocompetent [NTM] and had no specific exposure [TB]), and endemic fungal infections with spread to the CNS (again considered less likely because the patient was immunocompetent). Histopathology revealed leptomeningeal lymphocytic infiltrate extending into the cortical parenchyma with focal vasculitis, along with lymphocytes and multinucleated giant cells containing large, round, thick-walled parasites, consistent with GAE (Figure 2). Special tissue stains were negative for acid-fast bacillus and fungal elements, but a sample of brain tissue sent to CDC's Free-living and Intestinal Amebas laboratory (National Center for Emerging and Zoonotic Infectious Diseases, Division of Foodborne, Waterborne, and Environmental Diseases) was positive for *B. mandrillaris* amebae by PCR (*24*).

On the basis of CDC recommendations at diagnosis, the patient was started on pentamidine (4 mg/kg [80 mg] every 24 h), sulfadiazine (50 mg/kg [1,000 mg] every 6 h), azithromycin (20 mg/kg [400 mg] every 24 h), fluconazole (12 mg/kg [240 mg] every 24 h), flucytosine (37.5 mg/kg [750 mg] every 6 h), and

miltefosine (2.5 mg/kg [50 mg] every 24 h) (Figure 3). On this regimen, 5 months later, new frontal headaches developed. Repeat MRI at that time showed a new, 7-mm diameter, enhancing focus in left superior frontal gyrus and 3 enhancing nodules at the peripheral resection margins of the primary left occipital site. The multidrug regimen was continued, and repeat MRI 2 months later showed interval increase in the size of the left frontal lesion and surrounding T2/FLAIR hyperintensity (Figure 1). The patient subsequently underwent a left frontal craniotomy for en bloc resection using intraoperative frameless stereotactic navigation. Intraoperative ultrasound revealed no residual hyperechoic tissue. Pathology resembled first resection, and the tissue was again positive for *B. mandrillaris* amebae by PCR testing at CDC.

Given concern for progressive disease on existing therapy, along with promising in vitro data and a published successful case report (*13*,*15*), we decided to add nitroxoline to the regimen. We obtained Institutional review board approval, Food and Drug Administration emergency investigational drug designation, and parental consent. After emergency designation, we identified a foreign nitroxoline manufacturer. However, because the patient's imaging and clinical status were worsening and obtaining the drug directly from the manufacturer would have meant a delay of several weeks, to ensure timely administration, we procured a small supply produced by the same manufacturer via University of California San Francisco Investigational Drug Services. The patient received the first dose of nitroxoline 1 month after second resection. We sourced subsequent treatment directly from the manufacturer and established a formal contractual agreement to secure ongoing access to the investigational agent.

While monitoring the patient in the hospital for both medication side effects and worsening symptoms, we titrated the nitroxoline dose over 1 week to a total of 30 mg/kg/day (3×/d). We chose that dose because it is the maximum pediatric dose described in published nitroxoline reviews and was comparable to dosing used for an adult *B. mandrillaris* patient treated with nitroxoline (*14*,*15*). Clinical, laboratory, electrocardiogram, and dental monitoring showed that the patient tolerated nitroxoline without substantial side effects.

MRI at 6 weeks after nitroxoline initiation showed considerable improvement in the ring-enhancing lesions at the margin of the left occipital surgical cavity, no recurrence of left frontal lesion, and no new

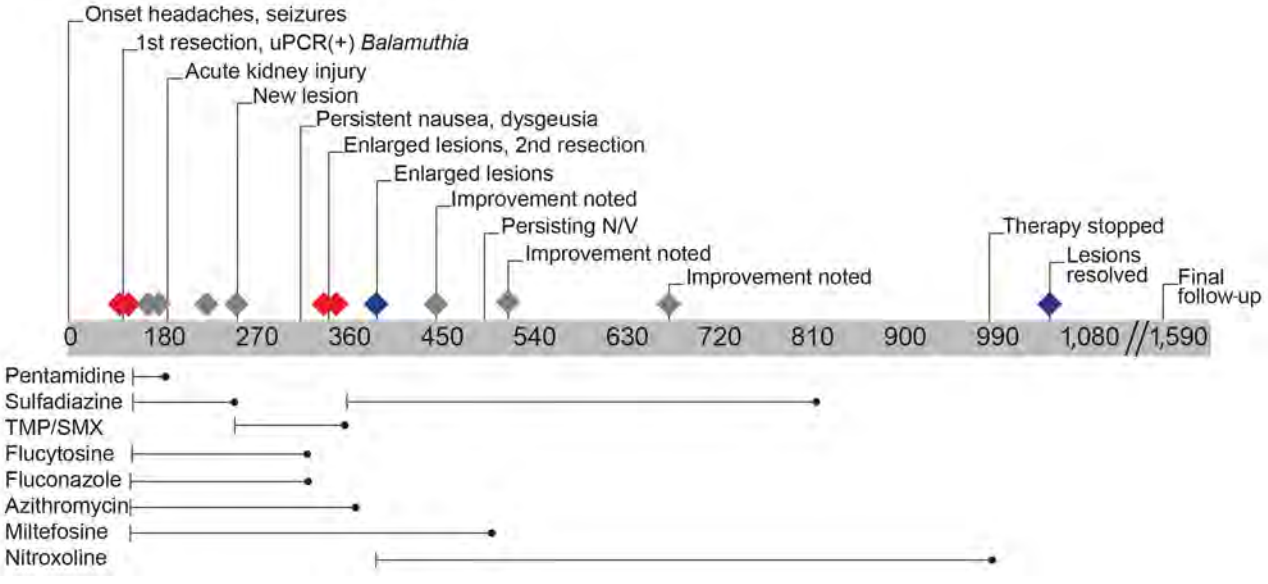


**Figure 3.** Timeline of events and medications for patient in study of neurosurgical biopsy and resection for diagnosis and treatment of *Balamuthia mandrillaris* amebic encephalitis, United States. Gray bar shows days since initial evaluation; red diamonds indicate magnetic resonance imaging (MRI) obtained before and after surgical dates; gray diamonds indicate interval MRI; blue diamonds indicate MRI before and after end date of nitroxoline. Nitroxoline dosing was titrated over 1 week to a total of 30 mg/kg/day 3 times/day; other medication dosing was pentamidine, 4 mg/kg (80 mg) every 24 hours; sulfadiazine, 50 mg/kg (1,000 mg) every 6 hours; azithromycin, 20 mg/kg (400 mg) every 24 hours; fluconazole, 12 mg/kg (240 mg) every 24 hours; flucytosine, 37.5 mg/kg (750 mg) every 6 hours; and miltefosine, 2.5 mg/kg (50 mg) every 24 hours. Pentamidine was discontinued after 8 weeks because of concern for renal toxicity. Sulfadiazine was briefly switched to trimethoprim/sulfamethoxazole because of manufacturer supply shortage and ultimately discontinued because of cost and administration concerns. Because of persistent nausea, vomiting, dysgeusia, and anorexia, flucytosine, fluconazole, azithromycin, and miltefosine were each discontinued, and the patient remained on nitroxoline for a total of 19 months. N/V, nausea and vomiting; TMP/SMX, trimethoprim/sulfamethoxazole; uPCR, universal broad-range PCR amplicon sequencing.

lesions. Her next MRI scans, at 3 and 9 months after nitroxoline initiation, showed continued improvement in the ring-enhancing lesions of the occipital region and no new lesions. MRI 1 year after nitroxoline initiation showed expected encephalomalacia and gliosis at previous resection cavities, resolution of ring-enhancing occipital lesions, and no new lesions. In total, the patient was treated for 2 years and 4 months with antiamebic therapy, including nitroxoline for the final 19 months of therapy. At 8 months after therapy ended, a tiny residual nodule in the medial resection cavity was stable and thought to represent gliosis (Figure 1). Clinical follow-up 4 years after diagnosis revealed a healthy, active child without focal neurologic findings but with mild neurocognitive and learning delays on neuropsychiatric testing.

### Systematic Literature Review

The progression of disease and need for a second resection in this case raised the question whether complete resection, versus biopsy only, might be beneficial to outcomes of *B. mandrillaris* GAE. We hypothesized that because of the prevalence of vasculitis in and proposed hematogenous spread of *Balamuthia* disease, biopsy might promote spread by disruption of the blood–brain barrier and transection of affected vessels, whereas complete resection, aided by reducing the burden of organisms, could be associated with better outcomes. To evaluate that possibility, we performed a systematic review of the literature according to the guidelines for Preferred Reporting Items for Systematic Reviews and Meta-Analyses (*16*,*17*). We searched for published articles via PubMed (last reverified 2026 Jun 4) to identify cases in which *B. mandrillaris* GAE was diagnosed using specimens obtained antemortem via neurosurgical procedures, including complete resection (group 1) or subtotal resection or biopsy (group 2). We used the following search terms: Balamuthia AND (biopsy OR neurosurgery OR neurosurgical OR excision OR resection OR brain mass OR tumor). That initial search returned 231 articles (Appendix 1 Table 1, https://wwwnc.cdc.gov/EID/article/32/7/26-0725-App1.xlsx). We then filtered the list by English language to 223 articles and then further filtered for human cases, bringing the number of articles to 161. We also found 6 published articles not captured in the PubMed search (*15*,*18*–*23*); all were noted in the course of reviewing other articles and considered pertinent to this topic. However, noting the absence of those articles in the PubMed search, to avoid omission of articles or bias, we reviewed the nonhuman filtered cases to identify erroneously omitted cases and conducted another search using terms "Balamuthia AND case report." Those searches identified no additional articles that did not meet exclusion criteria. In total, we reviewed 168 articles (Appendix 1 Table 2).

This study was confined to antemortem neurosurgical procedures only because of the hypothesis that cutting into diseased tissue without (presumptively) substantially diminishing the burden of ameba might worsen disease outcomes in *Balamuthia* GAE. Therefore, we excluded the following types of cases: no neurosurgical specimen obtained antemortem (n = 36), only cutaneous disease (n = 3), infection not verified by the definitions we devised or cases of other FLA (n = 3), and co-infections (which might alter the pathogenesis) (n = 2). We also excluded the following types of studies: primary purpose of subject review (n = 30), in vitro studies (n = 22), primary purpose to report specimen data or imaging findings without substantial clinical descriptions (n = 7), environmental specimens (n = 5), duplicated cases (n = 4), editorials (n = 2), mouse studies (n = 1), nonhuman cases (n = 1), retracted articles (n = 1), articles for which we could not obtain the full text (n = 1), or case reports that did not include the targeted data (n = 1) (Appendix 1 Table 3).

We defined a confirmed case of *B. mandrillaris* GAE as a patient with clinical encephalitis with imaging findings supportive of diagnosis and either molecular diagnostics (PCR or metagenomic next-generation sequencing; Karius, https://kariusdx.com) or immunofluorescence or immunohistochemistry staining positive on pathologic specimens for *B. mandrillaris.* Cases that had only positive serologic results or morphologic evidence of ameba were not considered diagnostic for *B. mandrillaris* GAE.

We defined resection cases as cases in which the article defined the procedure as resection or complete excision or en bloc in an antemortem neurosurgical procedure. We defined biopsy cases as cases in which the article reported biopsy, excisional biopsy, or subtotal resection of the lesion in an antemortem neurosurgical procedure. Cases involving only blood, cerebrospinal fluid (CSF) specimens, or skin or other organ biopsies were outside the scope of this study.

We reviewed and extracted data from the 68 articles meeting inclusion and exclusion criteria. Of those, 20 were resection cases; data collected included clinical manifestation description (country of residence, age, sex, initial symptoms, notable medical history), number and location of lesions at evaluation, site of lesion resected, antiamebic medications (if used and with details to the extent published), presence of vasculitis on biopsy, additional lesions

identified after procedure, and use of steroids before *Balamuthia* diagnosis. The remaining 48 articles were on biopsy cases; data collected included clinical manifestation description, whether ≥1 lesion was present at diagnosis, whether additional lesions were identified after procedure, and whether steroids were used before *Balamuthia* diagnosis.

For resection and biopsy studies including resection cases, we recorded the number that had additional lesions identified on brain imaging (most advanced obtained, either computed tomography or MRI) after the antemortem neurosurgical specimen collection. We also recorded the number for whom steroids were reported to be given and the number who survived the infection. For the steroid use and survival analyses, we calculated percentages on the basis of the total number of resection cases or biopsy cases. For the lesion number analysis, the denominator was the number of cases for which information was available by imaging reports, because some patients died before follow-up imaging after the procedure could be obtained.

We used GraphPad Prism (https://www.graphpad.com) for statistical analysis. We examined for statistical differences between resection cases and biopsy cases using Fisher exact tests.

## Results

From our systematic review of the literature, plus the case we report here, we found 7 published articles describing 1 or 2 cases of *B. mandrillaris* intracranial lesions that were surgically resected and the patient survived (*18*,*19*,*25*–*29*). Of 13 cases in which the patient subsequently died, each was associated with ≥1 of the following: multiple CNS lesions at initial evaluation (n = 5) (Appendix 2 Table 1 references *5*,*17*–*19*, https://wwwnc.cdc.gov/EID/article/32/7/26-0725-App2.pdf), advanced neurologic symptoms (i.e., hemiparesis, seizures, signs of increased intracranial pressure or herniation, loss of consciousness) (n = 9) (Appendix 2 Table 1 references *5*,*6*,*10*,*13*,*17*–*19*), vasculitis on imaging or pathology (n = 5) (Appendix 2 Table 1 references *5*–*7*,*10*,*17*), a regimen distinct from the 2021 CDC medication regimen (≤4 agents used) (n = 11) (Appendix 2 Table 1, references *5*–*7*,*12*,*13*,*16*–*19*), or steroid use preceding diagnosis and antiamebic treatment (n = 6) (Appendix 2 Table 1 references *5*,*10*,*12*,*17-19*).

We questioned whether resection, either subtotal or biopsy or complete resection, increased likelihood of patient death or additional lesions arising after the neurosurgical procedure. Vasculitis is a prominent feature of *B. mandrillaris* GAE (*30*). We hypothesized that incision into infected tissue might promote spread of ameba if total resection is not achieved. Therefore, we conducted an additional review of the cases that had biopsy or subtotal resections for outcomes of survival or death and whether additional lesions were discovered on follow-up imaging after the procedure. We found no statistical difference between the groups, however (Table; Appendix 2 Table 2), and similar rates of steroid use before *B. mandrillaris* GAE diagnosis.

## Discussion

We report the excellent outcome for a pediatric patient with *B. mandrillaris* GAE treated with nitroxoline. Factors contributing to GAE survival are not clear, but we believe that nitroxoline and neurosurgical interventions were important to this patient's survival. A multidisciplinary team, including pharmacy, psychology, and child life services, individualized the patient's complex medication schedule, which, along with family vigilance, undoubtedly contributed to the success of this regimen. Our findings of clinical and radiographic improvement add to a growing body of literature suggesting that nitroxoline, in combination with

**Table.** Analyses of outcomes between resection and biopsy groups in study of neurosurgical biopsy and resection for diagnosis and treatment of *Balamuthia mandrillaris* amebic encephalitis, United States

| Category | No. (%) cases* | | Statistically significant difference between groups† |
|---|---|---|---|
| | Resection, n = 20 | Biopsy, n = 48 | |
| New lesions after procedure | | | |
| Y | 9 (45) | 17 (35) | N (p = 0.75)‡ |
| N | 6 (20) | 9 (19) | |
| Not clear | 5 (25) | 22 (46) | |
| Survival | | | |
| Y | 7 (35) | 8 (17) | N (p = 0.12) |
| N | 13 (65) | 40 (83) | |
| Steroids | | | |
| Y | 9 (45) | 27 (56) | N (p = 0.43) |
| Not reported | 11 (55) | 21 (44) | |

*Includes case from this study.
†For yes/no responses only. Method used Fisher exact test.
‡For new lesions, the "not clear" cases were omitted from statistical analysis.

other antiamebic drugs and surgical resection, could improve outcomes from this rare, highly fatal disease. Nitroxoline has better tolerability and in vitro efficacy against *B. mandrillaris* infection than other antiamebic agents (*13*,*31*). In a review of safety and efficacy of nitroxoline in UTI treatment, only 9.8% of patients reported adverse effects (primarily nausea) (*13*,*14*,*31*). In contrast, the standard regimen, which includes pentamidine, miltefosine, a triazole, flucytosine, azithromycin, and sulfadiazine, has substantial toxicities, often limiting use and leading to other adverse conditions. Indeed, acute kidney injury and hypertension occurred in this patient, but resolved after discontinuation of pentamidine. In addition, gastrointestinal side effects of dysgeusia, anorexia, nausea, vomiting, and diarrhea necessitated placing a gastrostomy tube for nutrition; those symptoms resolved after sequential discontinuation of miltefosine, fluconazole, flucytosine, and azithromycin and did not recur during nitroxoline monotherapy.

Nitroxoline was continued throughout the final 19 months' duration of this patient's antiamebic therapy, and clinical and radiographic improvement continued even during the final 6 months on nitroxoline monotherapy, suggesting that nitroxoline could be a contributor to her survival. Our review of the literature subsequent to this case identified 2 other reported uses of nitroxoline, in addition to the adult case reported in the introduction (*15*). Those 2 cases were pediatric as well, but neither included neurosurgical resection. In the first case, a 4-year-old had *B. mandrillaris* infection diagnosed by Karius testing of blood and confirmed by CSF PCR. Nitroxoline was started 1 month into diagnosis, but the patient died 1 month later (*32*). The other pediatric case, in a 2-year-old, was diagnosed by biopsy and was included in this systematic review; the patient survived, as reported at 1 year after manifestation (*33*).

We cannot definitively determine the independent contribution of nitroxoline to treatment success on the basis of the case we report or the few others that have been published. However, a lack of recurrence or progression over a period of 19 months on nitroxoline, including 6 months of nitroxoline alone, supports the possibility that nitroxoline contributed to recovery. Before nitroxoline was initiated, testing showed a new frontal lesion and progression of that lesion (Figures 1, 3), but after nitroxoline treatment began, no new progression or lesions developed, and occipital residual lesions shrank. In addition, at the resection margins of the frontal lesion addressed in the second resection, surrounding residual nodules did not develop during nitroxoline treatment, unlike after the first resection before nitroxoline treatment. Variations in the success of complete resection microscopically, brief steroid use postoperatively after first resection, and being on any antiamebic therapy at the second resection all likely contributed as well.

The role of neurosurgical intervention for *Balamuthia* infections remains unclear. Whereas Karius testing and metagenomic next-generation sequencing can provide new opportunities for diagnosis without neurosurgical intervention (*20*,*32*,*34*–*42*), brain biopsy can lead to definitive diagnosis and early therapy. However, few cases manifest with lesions amenable to complete resection (*18*,*19*,*25*–*29*). Lesion recurrence after this patient's first surgery, despite using the CDC-recommended regimen, suggests that infection might have extended into normal-appearing tissue, beyond resection margins (i.e. incomplete resection); the previous CDC-recommended regimen could be insufficient to treat *Balamuthia* GAE; or vasculitis or resection in the setting of steroids or vasculitis without concurrent medication against *Balamuthia* amebae might contribute to dissemination (*30*). Of interest, we saw no recurrence from the patient's second resection, but at that time, the patient had concurrent treatment with antiamebic medications, including nitroxoline shortly thereafter. Our review and analyses suggest that variations in completeness of excision might not determine the recurrence or development of new lesions because no substantial difference in new lesions after biopsy or resection were noted between the 2 groups. We did find a trend toward association of excision with survival that warrants further investigation; however, the data did not show a statistically significant survival benefit to excision.

Our study is limited by the nature of literature reviews, including incomplete information and relatively small numbers, given the rarity of the disease. For example, with respect to steroid use, some articles (3 cases of the biopsy-only group) reported that the patients were initially treated for CNS TB. Providing steroids is the standard of care for such cases, so the lack of steroids reported in many of those cases exemplifies possible missing data in the literature (*43*). Future studies comparing the outcomes of patients who have antemortem neurosurgical resections or biopsies with those who only have non-CNS procedures for diagnosis or therapy (i.e., skin biopsies, blood or CSF specimens only) will be further informative on the risks of neurosurgical intervention in *Balamuthia* GAE. In addition to that theorized risk, risks of neurosurgery must always be considered before surgical intervention, but lack of recurrent or new lesions

in this patient case report after the second resection might have been the result of the multidrug regimen used before resection, and the addition of nitroxoline shortly after resection.

In this systematic review and analysis, we found no statistically significant outcomes between the group for whom biopsy was conducted for diagnosis and the group for whom complete resection for diagnosis and therapy was used. However, we did find a trend toward benefit in survival in complete resection group that warrants further study.

In conclusion, we report a systematic review of survival in *B. mandrillaris* GAE after antemortem neurosurgical resections and biopsies, including successful treatment of a pediatric patient in the southwestern United States. For patients with *B. mandrillaris* GAE, neurosurgical management, multidrug therapy, and nitroxoline treatment could improve outcomes associated with this deadly infection.

### Acknowledgments

We thank the patient and the family for participating in this study. The parents gave written consent to the publication of the patient's clinical manifestations, treatment, and follow-up as described in this manuscript. Asieris Pharmaceuticals provided nitroxoline. We appreciate the advice and guidance of Joseph L. DeRisi and the information received by direct communication from Joshua Cuoco.

This activity was reviewed by CDC and was conducted consistent with applicable federal law and CDC policy. See e.g., 45 C.F.R. part 46.102(I)(2), 21 C.F.R. part 56; 42 U.S.C. §241(d); 5 U.S.C. §552a; 44 U.S.C. §3501 et seq. The University of Texas Southwestern Medical Center Institutional Review Board reviewed and approved use of nitroxoline for this patient.

The authors acknowledge using ChatGPT in this manuscript for the sole purpose of assistance in concise wording, not in a generative capacity.

## About the Author

Dr. Rubbab is an assistant professor of pediatrics in the Division of Infectious Diseases at Baylor College of Medicine. Her clinical and research interests include pediatric infectious diseases, antimicrobial stewardship, infections in immunocompromised children, and improving patient safety. Dr. Adenwalla is a neurosurgery resident at UT Southwestern Medical Center. His work centers on neurosurgical outcomes and surgical innovation, with a particular interest in advancing techniques that improve patient care.

### References:

1. Haston JC, O'Laughlin K, Matteson K, Roy S, Qvarnstrom Y, Ali IKM, et al. The epidemiology and clinical features of non-keratitis *Acanthamoeba* infections in the United States, 1956–2020. Open Forum Infect Dis. 2023;10:ofac682. https://doi.org/10.1093/ofid/ofac682
2. Cope JR, Landa J, Nethercut H, Collier SA, Glaser C, Moser M, et al. The epidemiology and clinical features of *Balamuthia mandrillaris* disease in the United States, 1974–2016. Clin Infect Dis. 2019;68:1815–22. https://doi.org/10.1093/cid/ciy813
3. Martinez AJ, Visvesvara GS. Free-living, amphizoic and opportunistic amebas. Brain Pathol. 1997;7:583–98. https://doi.org/10.1111/j.1750-3639.1997.tb01076.x
4. Shehab KW, Aboul-Nasr K, Elliott SP. *Balamuthia mandrillaris* granulomatous amebic encephalitis with renal dissemination in a previously healthy child: case report and review of the pediatric literature. J Pediatric Infect Dis Soc. 2018;7:e163–8. https://doi.org/10.1093/jpids/pix089
5. Matin A, Siddiqui R, Jayasekera S, Khan NA. Increasing importance of *Balamuthia mandrillaris*. Clin Microbiol Rev. 2008;21:435–48. https://doi.org/10.1128/CMR.00056-07
6. Siddiqui R, Matin A, Warhurst D, Stins M, Khan NA. Effect of antimicrobial compounds on *Balamuthia mandrillaris* encystment and human brain microvascular endothelial cell cytopathogenicity. Antimicrob Agents Chemother. 2007;51:4471–3. https://doi.org/10.1128/AAC.00373-07
7. Matin A, Siddiqui R, Jung SY, Kim KS, Stins M, Khan NA. *Balamuthia mandrillaris* interactions with human brain microvascular endothelial cells in vitro. J Med Microbiol. 2007;56:1110–5. https://doi.org/10.1099/jmm.0.47134-0
8. Matin A, Stins M, Kim KS, Khan NA. *Balamuthia mandrillaris* exhibits metalloprotease activities. FEMS Immunol Med Microbiol. 2006;47:83–91. https://doi.org/10.1111/j.1574-695X.2006.00065.x
9. Jayasekera S, Matin A, Sissons J, Maghsood AH, Khan NA. *Balamuthia mandrillaris* stimulates interleukin-6 release in primary human brain microvascular endothelial cells via a phosphatidylinositol 3-kinase-dependent pathway. Microbes Infect. 2005;7:1345–51. https://doi.org/10.1016/j.micinf.2005.05.001
10. Visvesvara GS, Martinez AJ, Schuster FL, Leitch GJ, Wallace SV, Sawyer TK, et al. Leptomyxid ameba, a new agent of amebic meningoencephalitis in humans and animals. J Clin Microbiol. 1990;28:2750–6. https://doi.org/10.1128/jcm.28.12.2750-2756.1990
11. Spottiswoode N, Haston JC, Hanners NW, Gruenberg K, Kim A, DeRisi JL, et al. Challenges and advances in the medical treatment of granulomatous amebic encephalitis. Ther Adv Infect Dis. 2024;11:20499361241228340. https://doi.org/10.1177/20499361241228340
12. Centers for Disease Control and Prevention. Clinical care of *Balamuthia* infection. 2025 [cited 2025 Apr 1]. https://www.cdc.gov/balamuthia/hcp/clinical-care
13. Laurie MT, White CV, Retallack H, Wu W, Moser MS, Sakanari JA, et al. Functional assessment of 2,177 U.S. and international drugs identifies the quinoline nitroxoline as a potent amoebicidal agent against the pathogen *Balamuthia mandrillaris*. MBio. 2018;9:e02051-18. https://doi.org/10.1128/mBio.02051-18
14. Naber KG, Niggemann H, Stein G, Stein G. Review of the literature and individual patients' data meta-analysis on efficacy and tolerance of nitroxoline in the treatment of uncomplicated urinary tract infections. BMC Infect Dis. 2014;14:628. https://doi.org/10.1186/s12879-014-0628-7

15. Spottiswoode N, Pet D, Kim A, Gruenberg K, Shah M, Ramachandran A, et al. Successful treatment of *Balamuthia mandrillaris* granulomatous amebic encephalitis with nitroxoline. Emerg Infect Dis. 2023;29:197–201. https://doi.org/10.3201/eid2901.221531
16. Page MJ, Moher D, Bossuyt PM, Boutron I, Hoffmann TC, Mulrow CD, et al. PRISMA 2020 explanation and elaboration: updated guidance and exemplars for reporting systematic reviews. BMJ. 2021;372:n160. https://doi.org/10.1136/bmj.n160
17. Page MJ, McKenzie JE, Bossuyt PM, Boutron I, Hoffmann TC, Mulrow CD, et al. The PRISMA 2020 statement: an updated guideline for reporting systematic reviews. BMJ. 2021;372:n71. https://doi.org/10.1136/bmj.n71
18. Mei J, Sheng F, Zhang C, Chen X. Imaging monitoring of *Balamuthia* granulomatous amoebic encephalitis. Clin Neurol Neurosurg. 2025;254:108917. https://doi.org/10.1016/j.clineuro.2025.108917
19. Lehmer LM, Ulibarri GE, Ragsdale BD, Kunkle J. Cutaneous *Balamuthia mandrillaris* infection as a precursor to *Balamuthia* amoebic encephalitis (BAE) in a healthy 84-year-old Californian. Dermatol Online J. 2017;23:13030/qt8c8720qm. https://doi.org/10.5070/D3237035732
20. Edminster SY, Rebbe RW, Khatchadourian C, Hurth KM, Mathew AJ, Huss-Bawab J, et al. The role of plasma metagenomic sequencing in identification of *Balamuthia mandrillaris* encephalitis. Acta Neuropathol Commun. 2025;13:60. https://doi.org/10.1186/s40478-025-01963-8
21. Tello-Zavala MC, Bravo-Oro A, Falcón-Escobedo R. Central nervous system infection in an immunocompetent Mexican child. Pediatr Infect Dis J. 2014;33:991, 995–6.
22. Li Q, Yang XH, Qian J. September 2004: a 6-year-old girl with headache and stiff neck. Brain Pathol. 2005;15:93–5. https://doi.org/10.1111/j.1750-3639.2005.tb00109.x
23. Atay Ünal N, Kuzucu P, Bedir Demirdağ T, Aykur M, Günsoy Kiliç Y, Güdeloğlu E, et al. 12-year-old boy with fever, headache and vomiting. Pediatr Infect Dis J. 2024;43:88–90. https://doi.org/10.1097/INF.0000000000004068
24. Qvarnstrom Y, Visvesvara GS, Sriram R, da Silva AJ. Multiplex real-time PCR assay for simultaneous detection of *Acanthamoeba* spp., *Balamuthia mandrillaris*, and *Naegleria fowleri*. J Clin Microbiol. 2006;44:3589–95. https://doi.org/10.1128/JCM.00875-06
25. Peng L, Zhou Q, Wu Y, Cao X, Lv Z, Su M, et al. A patient with granulomatous amoebic encephalitis caused by *Balamuthia mandrillaris* survived with two excisions and medication. BMC Infect Dis. 2022;22:54. https://doi.org/10.1186/s12879-021-07020-8
26. Cuoco JA, Klein BJ, LeBel DP, Faulhaber J, Apfel LS, Witcher MR. Successful treatment of a *Balamuthia mandrillaris* cerebral abscess in a pediatric patient with complete surgical resection and antimicrobial therapy. Pediatr Infect Dis J. 2022;41:e54–7. https://doi.org/10.1097/INF.0000000000003418
27. Doyle JS, Campbell E, Fuller A, Spelman DW, Cameron R, Malham G, et al. *Balamuthia mandrillaris* brain abscess successfully treated with complete surgical excision and prolonged combination antimicrobial therapy. J Neurosurg. 2011;114:458–62. https://doi.org/10.3171/2010.10.JNS10677
28. Botterill E, Yip G. A rare survivor of *Balamuthia* granulomatous encephalitis. Clin Neurol Neurosurg. 2011;113:499–502. https://doi.org/10.1016/j.clineuro.2011.01.013
29. Mei J, Sheng F, Zhang C, Chen X. Corrigendum to "Imaging monitoring of Balamuthia granulomatous amoebic encephalitis". Clin Neurol Neurosurg. 2025;256:109015. https://doi.org/10.1016/j.clineuro.2025.109015
30. Guarner J, Bartlett J, Shieh WJ, Paddock CD, Visvesvara GS, Zaki SR. Histopathologic spectrum and immunohistochemical diagnosis of amebic meningoencephalitis. Mod Pathol. 2007;20:1230–7. https://doi.org/10.1038/modpathol.3800973
31. Dubey P, Kobpornchai P, Tongkrajang N, Chaiyaloom S, Lu C, Rice CA, et al. Drug susceptibility of a clinical isolate of *Balamuthia mandrillaris*, a pathogenic free-living amoeba. Antimicrob Agents Chemother. 2026;70:e0148225. https://doi.org/10.1128/aac.01482-25
32. Aboubechara JP, Kantamneni T, Pasao K. *Balamuthia Mandrillaris* central nervous system vasculitis in an immunocompetent child: case report. J Child Neurol. 2025;40:366–70. https://doi.org/10.1177/08830738241307058
33. Degese MF, Prieto MP, Nigro MG, Perazzo J, Pérez Garófalo M, Lemir G, et al. Free-living amoebae infections: case reports identified at a reference parasitology laboratory in Argentina. Acta Parasitol. 2025;70:240. https://doi.org/10.1007/s11686-025-01198-6
34. Vollmer ME, Glaser C. A *Balamuthia* survivor. JMM Case Rep. 2016;3:e005031. https://doi.org/10.1099/jmmcr.0.005031
35. Deetz TR, Sawyer MH, Billman G, Schuster FL, Visvesvara GS. Successful treatment of *Balamuthia* amoebic encephalitis: presentation of 2 cases. Clin Infect Dis. 2003;37:1304–12. https://doi.org/10.1086/379020
36. Schuster FL, Yagi S, Gavali S, Michelson D, Raghavan R, Blomquist I, et al. Under the radar: *Balamuthia* amebic encephalitis. Clin Infect Dis. 2009;48:879–87. https://doi.org/10.1086/597260
37. Cary LC, Maul E, Potter C, Wong P, Nelson PT, Given C II, et al. *Balamuthia mandrillaris* meningoencephalitis: survival of a pediatric patient. Pediatrics. 2010;125:e699–703. https://doi.org/10.1542/peds.2009-1797
38. Moriarty P, Burke C, McCrossin D, Campbell R, Cherian S, Shahab MS, et al. *Balamuthia mandrillaris* encephalitis: survival of a child with severe meningoencephalitis and review of the literature. J Pediatric Infect Dis Soc. 2014;3:e4–9. https://doi.org/10.1093/jpids/pit033
39. Orozco L, Hanigan W, Khan M, Fratkin J, Lee M. Neurosurgical intervention in the diagnosis and treatment of *Balamuthia mandrillaris* encephalitis. J Neurosurg. 2011;115:636–40. https://doi.org/10.3171/2011.4.JNS102057
40. Yang Y, Hu X, Min L, Dong X, Guan Y. *Balamuthia mandrillaris*–related primary amoebic encephalitis in China diagnosed by next generation sequencing and a review of the literature. Lab Med. 2020;51:e20–6. https://doi.org/10.1093/labmed/lmz079
41. Yi Z, Zhong J, Wu H, Li X, Chen Y, Chen H, et al. *Balamuthia mandrillaris* encephalitis in a child: case report and literature review. Diagn Microbiol Infect Dis. 2021;100:115180. https://doi.org/10.1016/j.diagmicrobio.2020.115180
42. Hu J, Zhang Y, Yu Y, Yu H, Guo S, Shi D, et al. Encephalomyelitis caused by *Balamuthia mandrillaris* in a woman with breast cancer: a case report and review of the literature. Front Immunol. 2022;12:768065. https://doi.org/10.3389/fimmu.2021.768065
43. American Academy of Pediatrics Committee on Infectious Diseases. Kimberlin DW, Banerjee R, Barnett ED, Lynfield R, Sawyer MH, editors. Red Book: 2024–2027 Report of the Committee on Infectious Diseases. 33rd edition. Elk Grove Village (IL): American Academy of Pediatrics; 2024.

Address for correspondence: Natasha W. Hanners, University of Texas Southwestern Medical Center, 5323 Harry Hines Blvd, Dallas, TX 75390, USA; email: natasha.hanners@utsouthwestern.edu

# Adeno-Associated Virus Type 2 and Human Adenovirus Species F Type 41 Co-infection Associated with Acute Severe Hepatitis in Children, California, USA

Ran Zhuo,[1] Colette J. Matysiak Match,[1] Sanchi Malhotra, Huan Vinh Dong, Kristina Adachi, Robert S. Venick, Grace Aldrovandi, Shangxin Yang

Since late 2021, clusters of acute severe hepatitis of unknown etiology in previously healthy children, including some requiring liver transplantation, have been reported worldwide. Co-infection with adeno-associated virus type 2 (AAV2) and human adenovirus species F type 41 (HAdV-F41) has been identified in most cases. Global incidence peaked in 2022, and pediatric liver failure involving co-infection with AAV2 and HAdV-F41 has remained rare in recent years. We report 2 cases of pediatric liver failure associated with AAV2 and HAdV-F41 in California, USA, in March 2024 and January 2025. The patients had high adenovirus loads (393,000 and 480,000 copies/mL), extended adenovirus viremia (2 and 3.5 months), and high AAV2 viral loads (1.3 and 1.0 × $10^6$ copies/mL). One patient required liver transplantation; both patients recovered. Our findings underscore the need for heightened physician awareness and expanded surveillance to identify and characterize new cases, improve understanding of underlying pathophysiology, clarify risk factors, and inform therapeutic strategies.

Since late 2021, clusters of severe acute hepatitis in children have been linked to adeno-associated virus type 2 (AAV2) and co-infection with helper viruses, most frequently human adenovirus species F type 41 (HAdV-F41) but also Epstein–Barr virus (EBV), human herpesvirus 6, or both (*1*–*6*). This unexpected surge of severe disease, uncharacteristic of AAV2 infection alone, has been hypothesized to result from altered patterns of childhood viral exposure during the COVID-19 pandemic, possibly coupled with host immunogenetic susceptibility (*3*,*7*). More than 1,000 suspected cases of severe acute hepatitis across 35 countries were reported to the World Health Organization (WHO); ≈6% of patients required liver transplantation, and the mortality rate was 1.8% (*8*–*10*). Environmental surveillance (e.g., wastewater sampling) has demonstrated parallel peaks in community circulation of AAV2 and HAdV-F41 during outbreak periods (*11*,*12*). By June 2023, the outbreak seemingly dissipated, with only rare reports of AAV2-associated hepatitis (*13*). We report 2 cases of acute non-A–E hepatitis with liver failure in previously healthy 3-year-old children in California, USA, in March 2024 and January 2025.

Author affiliations: University of California Los Angeles David Geffen School of Medicine, Los Angeles, California, USA (R. Zhuo, C.J. Matysiak Match, S. Malhotra, H.V. Dong, K. Adachi, R.S. Venick, G. Aldrovandi, S. Yang); Duke University School of Medicine, Durham, North Carolina, USA (R. Zhuo); University of California San Francisco School of Medicine, San Francisco, California, USA (C.J.M. Match)

DOI: https://doi.org/10.3201/eid3207.260284

## The Cases

### Case 1

In March 2024, a previously healthy girl, 3 years and 8 months of age, was brought to a hospital 3 days after she had jaundice scleral icterus, nonbloody nonbilious emesis, and fatigue develop. Over the next 2 days, pale stools and dark urine had developed. At home, her 2 older siblings reportedly had conjunctivitis, but she remained afebrile without sore throat, cough, congestion, abdominal pain, diarrhea, rash, or conjunctivitis. She had not recently taken new medications, specifically no acetaminophen, and no suggestion of accidental substance ingestion was apparent. Her birth, medical, surgical, and family

[1]These authors contributed equally to this article.

histories were unremarkable for liver, autoimmune, or metabolic disease, as well as for immunodeficiency or recurrent infections. She had no allergies, and her immunizations were up to date except for COVID-19. Social and exposure history included household exposure to dogs and cats.

On examination, she was comfortable and afebrile (36.3°C). Heart rate was 110 beats/min, respiratory rate 27 breaths/min, blood pressure 98/59 mm Hg, and oxygen saturation 95% on room air. Findings included scleral icterus and jaundiced skin; results of cardiopulmonary and neurologic examinations were unremarkable. Laboratory results showed leukocyte count of 7.46 × $10^9$ cells/L (reference range 5.0–16.0 × $10^9$ cells/L), hemoglobin 12.4 g/dL (reference range 11.5–14.0 g/dL), platelets 90 × $10^9$/L (reference range 140–400 × $10^9$/L); alanine transaminase (ALT) was 3,667 U/L (reference range 8–24 U/L), aspartate transaminase (AST) 4,945 U/L (reference range 20–39 U/L), total bilirubin 10.8 mg/dL (reference range 0.2–0.8 mg/dL), direct bilirubin 9.2 mg/dL (reference range ≤0.2 mg/dL), prothrombin time (PT) 21 seconds (reference range 12.1–14.5 seconds), partial thromboplastin time (PTT) 32.2 seconds (reference range 25.1–36.5 seconds), international normalized ratio (INR) 1.9 (therapeutic range 2–3), ferritin 3,612 ng/mL (reference range 8–180 ng/mL), ammonia 35 μmol/L (reference range 18–90 mcg/dL), and gamma glutamyl transferase (GGT) 108 U/L (reference range 7–68 U/L).

Results of standard viral hepatitis panels (A–E), herpesvirus testing, and BioFire FilmArray Gastrointestinal and Respiratory panels (bioMérieux, https://www.biomerieux.com) including HAdV as a target were all negative; QuantiFERON-TB Gold (QIAGEN, https://www.qiagen.com) result was indeterminate (Table 1). Abdominal ultrasound showed increased hepatic echogenicity without biliary obstruction.

The patient was empirically treated with N-acetylcysteine, cefepime, and metronidazole. Autoimmune serologies revealed a positive antinuclear antibody titer (1:160) and elevated IgG for her age (1,360 mg/dL, reference range 320–990 mg/dL). Results were negative for liver kidney microsomal 1, liver cytosol type 1, mitochondrial, and smooth muscle antibodies.

On hospitalization day 2, her coagulation profile worsened; PT and INR rose in subsequent days to a peak of 51.9 seconds for PT and 5.6 for INR on day 4. A percutaneous liver biopsy was performed after her coagulopathy was corrected with fresh frozen plasma and recombinant coagulation factor 7a that demonstrated panlobular severe acute hepatitis with lymphocytic predominance and 70%–80% hepatocyte loss. No viral inclusions were seen, and an adenovirus antibody probe was negative.

On day 3, qualitative plasma PCR for adenovirus returned a positive result, prompting initiation of cidofovir (5 mg/kg/wk intravenously). Quantitative whole-blood adenovirus PCR (ARUP Laboratories, https://www.aruplab.com) on day 8 measured 393,000 copies/mL (log 5.6).

Given clinical and biochemical concern for progressive liver failure, she was listed for transplant on day 4 (with a calculated Pediatric End-Stage Liver Disease Score of 25). On day 5, hyperammonemia, altered mental status, and worsening coagulopathy developed, necessitating intubation and continuous renal replacement therapy for ammonia clearance; her transplant status was upgraded to 1A. She underwent ABO compatible, whole-graft orthotopic liver transplantation on day 10. Weekly cidofovir was continued before and after transplantation for 40 days because of persistent adenovirus viremia, although PCR of explanted liver tissue was negative for adenovirus.

### Case 2

In January 2025, a previously healthy boy, 3 years and 1 month of age, was brought to a hospital with a 1-day history of jaundice and scleral icterus. He had experienced 1 week of postprandial abdominal discomfort and 2 days of pale, foul-smelling stools. Three weeks before care was sought, he had 1 day of emesis and a subjective fever, without concurrent or subsequent respiratory symptoms, rash, conjunctivitis, or diarrhea. His medical history was only notable for mild speech delay of unknown etiology without concerns for other growth or developmental delay. There was no reported family history of liver, autoimmune, metabolic, disease, immunodeficiency, or history of recurrent infections.

At admission, he was found to be afebrile; vital signs included heart rate 115 beats/min, respiratory rate 22 breaths/min, blood pressure 98/56 mm Hg, and oxygen saturation 100% on room air. He appeared comfortable. Examination showed diffuse jaundice, scleral icterus, and hepatomegaly. Initial laboratory results included leukocytes 10.55 × $10^9$ cells/L, hemoglobin 10.6 g/dL, and platelets 281 × $10^9$/L. Other notable laboratory results were ALT 3,371 U/L, AST 5,651 U/L, total bilirubin 6.6 mg/dL, direct bilirubin 6.0 mg/dL, PT 17 seconds, PTT 33.4 seconds, INR 1.5, ferritin 694, GGT 82 U/L, and ammonia 44 μmol/L. Results of autoimmune hepatitis workup (smooth muscle, liver kidney microsomal 1, mitochondrial, systemic panel) and urine toxicology were negative. Routine infectious hepatitis panels

were likewise negative (Table 1), except for plasma adenovirus, which was PCR positive at 49 copies/mL (from referring hospital); rhinovirus/enterovirus detected by a respiratory pathogen multiplex PCR; and sapovirus detected by BioFire FilmArray Gastrointestinal Panel. However, results of both initial respiratory and stool panels were negative for adenovirus. Cytomegalovirus was detectable by blood PCR but below the limit of quantification (<35 copies/mL).

The patient remained afebrile and clinically stable throughout his admission. Initial adenovirus testing suggested low risk for severe or disseminated disease, given the low plasma viral load (49 copies/mL) and negative respiratory and stool panel results. On hospitalization day 6, a percutaneous liver biopsy revealed marked lobular inflammation, frequent acidophil bodies, ballooned hepatocytes, and focal bridging necroinflammatory activity; bile ducts were spared. Mixed inflammatory infiltrates (predominantly lymphocytes with eosinophils, neutrophils, and plasma cells) were noted. Results of special stains (Trichrome, periodic acid–Schiff, $\alpha_1$-antitrypsin, iron) and immunohistochemistry for cytomegalovirus, adenovirus, and EBV (EBER) were all negative. Concern for acute liver failure prompted treatment with cidofovir (1 mg/kg on hospital days 7, 9, and 11) alongside standard hydration and probenecid for renal protection. Intravenous methylprednisolone (1 mg/kg 2×/d) was also initiated on day 7; the dose was lowered on day 11 (0.5 mg/kg 2×/d) and then transitioned to oral prednisolone on day 14. The patient tolerated cidofovir well without renal toxicities.

Subsequent testing demonstrated new adenovirus positivity in stool, and on day 11, repeat quantitative whole-blood adenovirus PCR showed 480,000 copies/mL. Despite persistent high-level viremia, liver enzymes steadily improved. To enable transfer to outpatient therapy, cidofovir was adjusted to 5 mg/kg/wk beginning on day 17. At discharge on day 18, jaundice and scleral icterus had markedly resolved, and transaminase levels had declined (AST 218 U/L; ALT 360 U/L), although quantitative adenovirus PCR returned 564,000 copies/mL after discharge. The patient was discharged on oral steroids with plans for weekly cidofovir infusions and weekly adenovirus PCR monitoring. Despite clinical improvement, adenovirus viremia persisted for 3 months; cidofovir was continued for 6 months given prolonged steroid wean (Figure).

**Table 1.** Initial infectious workups for 2 pediatric cases of acute severe hepatitis of unknown etiology associated with adeno-associated virus type 2 and human adenovirus species F type 41 co-infection, California, USA

| Pathogen | Sample type | Testing modality | Result | |
|---|---|---|---|---|
| | | | Case 1 | Case 2 |
| Cytomegalovirus | Blood | PCR | Negative | Positive <35 copies/mL |
| Cytomegalovirus IgG and IgM | Blood | Serology | Negative | IgG positive, IgM negative |
| Epstein-Barr virus | Blood | PCR | Negative | Negative |
| | Blood | Monospot | Negative | Negative |
| Hepatitis A virus IgM | Blood | Serology | Negative | Negative |
| Hepatitis B virus surface antigen | Blood | Serology | Negative | Negative |
| Hepatitis B virus core antibody | Blood | Serology | Negative | Negative |
| Hepatitis C virus antibody | Blood | Serology | Negative | Negative |
| Hepatitis C virus | Blood | PCR | Negative | Not performed |
| Hepatitis E virus | Blood | PCR | Negative | Not performed |
| Hepatitis E virus IgG and IgM | Blood | Serology | Negative | Negative |
| Parvovirus B19 | Blood | PCR | Negative | Negative |
| Enterovirus | Blood | PCR | Negative | Negative |
| Human herpes virus 6 | Blood | PCR | Negative | Negative |
| Parechovirus | Blood | PCR | Negative | Negative |
| Varicella-zoster virus IgM | Blood | Serology | Negative | Negative |
| West Nile virus | Blood | PCR | Negative | Not performed |
| West Nile virus IgG and IgM | Blood | Serology | Negative | Not performed |
| Herpes simplex virus type 1 and 2 | Blood | PCR | Negative | Negative |
| SARS-CoV-2 | Mid-turbinate swab | PCR | Negative | Negative |
| *Bartonella henselae* IgG and IgM | Blood | Serology | Negative | Not performed |
| *Coccidioides* IgG/IgM EIA | Blood | Serology | Negative | Not performed |
| Cryptococcal antigen | Blood | Serology | Negative | Not performed |
| QuantiFERON-TB Gold* | | | Indeterminant | Indeterminant |
| Leptospira | | | | Negative |
| BioFire Gastrointestinal Panel† | Stool | PCR | Negative | Positive, sapovirus |
| ePlex Respiratory Pathogen Panel‡ | Nasopharyngeal swab | PCR | Negative | Positive, rhinovirus/enterovirus |

*QuantiFERON-TB Gold, QIAGEN, https://www.qiagen.com.
†BioFire FilmArray Gastrointestinal Panel, bioMérieux, https://www.biomerieux.com.
‡ePlex Respiratory Pathogen Panel, Roche, https://www.roche.com.

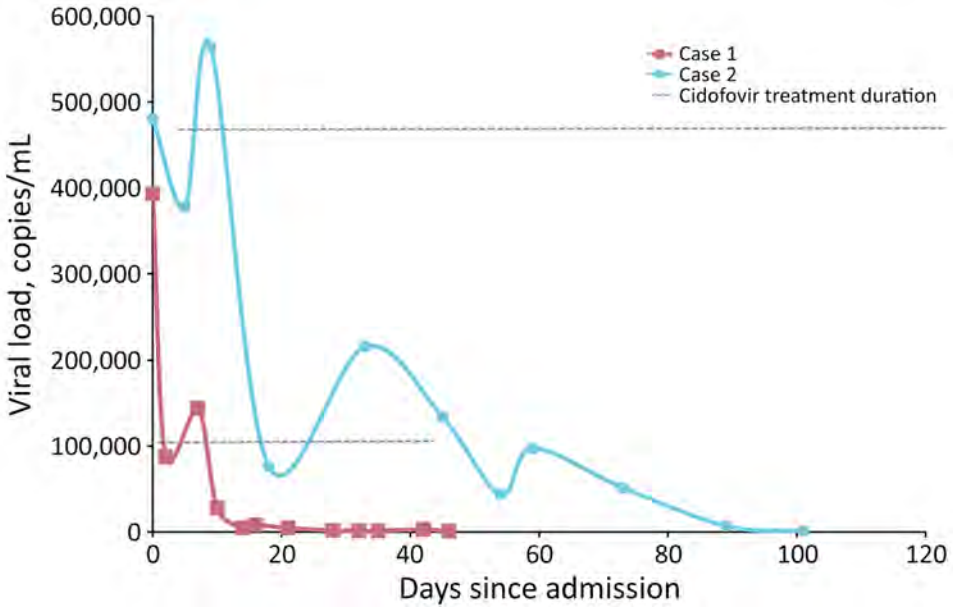


**Figure.** Longitudinal human adenovirus species F type 41 viral loads measured by quantitative PCR in whole-blood specimens from 2 pediatric cases of acute severe hepatitis of unknown etiology associated with adeno-associated virus type 2 and human adenovirus species F type 41 co-infection, California, USA. Viral loads are plotted against hospital day, illustrating high viremia preceding antiviral therapy and liver transplantation in case 1, the subsequent decline during cidofovir treatment, and persistent low-level detection despite clinical improvement in case 2.

## Materials and Methods

Our goal was to track the microbial etiology of acute hepatitis in both patients. We employed shotgun metagenomic next-generation sequencing (mNGS), targeted next-generation sequencing (tNGS), and quantitative PCR (qPCR) to track AAV2 load.

### Genomic DNA Extraction and Sequencing

We extracted DNA from whole blood, plasma, and liver tissue (liver tissue available only from patient 1) by using either the EZ1 Tissue Kit (QIAGEN) or the easyMAG system (bioMérieux). We then prepared indexed libraries on a MagicPrep NGS System (Tecan, https://www.tecan.com) and sequenced on a MiSeq platform (Illumina, https://www.illumina.com) using a 2 × 250 bp pair-end protocol. We analyzed raw reads with the Chan Zuckerberg ID (CZ ID) cloud-based metagenomic pipeline (https://www.czid.org).

### AAV2 Detection and Quantification by qPCR

We detected AAV2 by using a published primer-probe set (*14*). In brief, we performed real-time PCR in a 5-μL reaction volume containing 2.5 μL of 2X PrimeTime Gene Expression Master Mix (Integrated DNA Technologies, https://www.idtdna.com), 0.25 μL of AAV2-specific assay mix (10 μmol primers, 5 μmol probe), 1.25 μL of nuclease-free water (Thermo Fisher Scientific, https://www.thermofisher.com), and 1 μL of template DNA. We conducted amplification on an Applied Biosystems 7500 Fast Dx Real-Time PCR System (Thermo Fisher Scientific) under the following conditions: 95°C for 3 minutes, 40 cycles of 95°C for 5 seconds, and 60°C for 30 seconds. We quantified AAV2 viral load by using a standard curve generated from 10-fold serial dilutions of a custom oligonucleotide (Integrated DNA Technologies) with the following sequence: 5′-CGGCCTCAGTGAGCGAGCGAGCGCGCAGAGAGGGAGTGGCCAACTCCATCACTAGGGGTTCC-3′.

### Adenovirus tNGS and Genotyping

We performed adenovirus genotyping by targeted amplification and sequencing of the hexon hypervariable region using published primers (*15*). We performed PCR in a 20-μL reaction containing lyophilized High Fidelity PCR ecoDry Premix (TaKaRa Bio USA, https://www.takarabio.com), 1.6 μL of each primer (AD1 and AD2, 10 μmol), 16.8 μL of nuclease-free water (Thermo Fisher Scientific), and 5 μL of template DNA. We performed amplification on a ProFlex PCR System (Thermo Fisher Scientific) under the following conditions: 95°C for 1 minute; 35 cycles of 95°C for 30 seconds, 51°C for 1 minute, and 68°C for 1 minute; and a final extension at 68°C for 3 minutes.

We purified amplicons with AMPure XP beads (Beckman Coulter, https://www.beckman.com), according to the manufacturer's instructions, and sequenced on an Illumina MiSeq platform, as we described. We processed sequence reads using the CZ ID pipeline and mapped resulting hexon sequences against the human adenovirus 41 reference genome (GenBank accession no. OR628209) using Geneious Prime 2023.2.1 (https://www.geneious.com). We confirmed genotype assignment BLAST analysis (https://blast.ncbi.nlm.nih.gov) against the

National Center for Biotechnology Information nucleotide database. We deposited sequence files generated in this study into GenBank (BioProject no. PRJNA1455204).

## Results

For patient 1, shotgun mNGS identified AAV2 in both plasma and liver tissue. BLAST analysis revealed closest homology to AAV2 isolate CHC3511 (GenBank accession no. MK163942.1), and genome mapping analysis showed 81.3% whole-genome coverage and 95.4% identity (Table 2). AAV2 qPCR demonstrated high viral loads ($1.3 \times 10^6$ copies/mL) in plasma and liver before liver transplantation and AAV2 clearance from plasma after transplantation. tNGS detected HAdV-F41 in whole blood but not in the liver, consistent with the PCR results. The HAdV-F41 strain bears the closest similarity to human adenovirus 41 isolate 2330/N.Nov/RU/2009 hexon gene, partial coding sequence 2330/N.Nov/RU/2009 (GenBank accession no. HM588740.1; 100% coverage, 96.7% identity). Adenovirus quantitative real-time PCR at a reference laboratory (ARUP Laboratories) demonstrated high-level HAdV-F41 viremia before transplantation and a decline during antiviral therapy but persistent low-level detection for weeks thereafter (Figure). The patient experienced an episode of mild T-cell mediated rejection 1 month after transplantation, treated with intravenous steroid pulse for 1 week. She was discharged on day 36 receiving tacrolimus, prednisolone, and antimicrobial prophylaxis, with plans to continue weekly cidofovir until blood adenovirus PCR was negative (Figure). She was weaned off steroids and managed on tacrolimus monotherapy at 12 months after transplantation. At 2 years after transplantation, she had maintained normal biochemical graft function with no recent hospital admissions.

For patient 2, we identified AAV2 in plasma by using shotgun mNGS. BLAST analysis revealed closest homology to the AAV2 complete genome (GenBank accession no. NC_001401); genome mapping analysis showed 35.1% whole-genome coverage and 90.9% identity (Table 2). We also identified AAV2 in plasma ($1 \times 10^5$ copies/mL), stool ($1 \times 10^5$ copies/mL), and whole blood ($1 \times 10^6$ copies/mL) by qPCR. Targeted sequencing of the adenovirus hexon hypervariable region identified HAdV-F41 in whole blood with the closest homology to HAdV-F41 isolate 2330/N.Nov/RU/2009 hexon gene, partial coding sequence (accession no. HM588740; 86% query coverage and 99.5% identity).

Clinically, the patient's hepatic function panel normalized biochemically by late February 2025. Prednisone and cidofovir were continued for 6 months at gradually lower doses (for prednisone) and longer intervals between infusions (for cidofovir). Treatments were discontinued in July 2025, and the patient continued to have normal liver function tests for the next 6 months.

## Discussion

An outbreak of acute severe hepatitis of unknown etiology (ASHUE) predominantly in children <5 years of age was first recognized in 2021 (*8*,*16*). AAV2, a dependoparvovirus that requires a helper virus (most commonly adenoviruses or herpesviruses) for productive replication, has been implicated (*17*,*18*). In the ASHUE cases, HAdV-F41 commonly provides this helper function. Proposed pathogenic mechanisms include a tropism shift of HAdV-F41 permitting hepatic co-infection and activation of AAV2 replication in hepatocytes and immune-mediated injury, potentially driven by high AAV2 antigen loads in the liver and shaped by host human leukocyte antigen (HLA) genotype (e.g., enrichment for HLA-DRB1*04:01) (*1*,*3*,*19*). Initial surveillance in the United Kingdom detected adenovirus in 68% of ASHUE cases, predominately type 41F (*20*). An early case series from the United States found adenovirus in 8 (89%) of 9 children with ASHUE and detected 3 distinct HAdV-F41 variants

**Table 2.** Genomic analysis for 2 pediatric cases of acute severe hepatitis of unknown etiology associated with AAV2 and HAdV-F41 co-infection, California, USA*

| Case no. | Source | NGS method | Virus identified | % Genome/ gene coverage | % Identity | Reference genome/gene | GenBank accession no. Reference isolate | GenBank accession no. Patient isolate |
|---|---|---|---|---|---|---|---|---|
| 1 | Plasma and liver | Shotgun | AAV2 | 81.3 | 95.4 | AAV isolate CHC3511_AAV.FL.circular, complete genome | MK163942 | SRX33017783 |
| | Whole blood | Amplicon (hexon gene) | HAdV-F41 | 100 | 96.7 | HAdV-F41 isolate 2330/N.Nov/RU/2009 hexon gene, partial cds | HM588740 | SRX33034982 |
| 2 | Plasma | Shotgun | AAV2 | 35.1 | 90.9 | AAV2, complete genome | NC_001401 | SRX33017784 |
| | Whole blood | Amplicon (hexon gene) | HAdV-F41 | 86 | 99.5 | HAdV-F41isolate 2330/N.Nov/RU/2009 hexon gene, partial cds | HM588740 | SRX33034983 |

*AAV2, adeno-associated virus type 2; HAdV-F41, human adenovirus species F type 41; cds, coding sequence; NGS, next-generation sequencing.

among 5 sequenced isolates; none showed viral inclusions or positive immunohistochemical staining in liver biopsies (*21*). In a larger analysis of >200 pediatric patients with hepatitis of unknown etiology over a 7.5-month period, only 45% of cases were positive for adenovirus (*16*), so adenovirus infection alone did not explain that outbreak. That analysis also investigated whether the hepatitis resulted from change in immune response secondary to COVID-19 or COVID-19 vaccination, but <40% of patients had evidence of ever having been infected with SARS-CoV-2, and only 4% had received ≥1 vaccine dose (*16*).

In the 2 cases we report, liver biopsies were negative for adenovirus by immunohistochemistry. Moreover, initial microbiological results identified high levels ($10^5$–$10^6$ copies/mL) of adenovirus in patient blood but failed to detect adenovirus in the explanted liver tissue from patient 1, supporting the likelihood that HAdV-F41 did not directly cause severe hepatitis in the children. Of note, patient 1 experienced a very rapid disease course, just 3 days from symptom onset to fulminant liver failure, whereas prior AAV2 case series reported prodromal period lasting 2–12 weeks (*3*). The 2 patients also had significantly higher adenovirus levels (393,000 copies/mL and 480,000 copies/mL) than were found in previous reports, which showed a maximum of 156,400 copies/mL (*21*). Patient 1's duration of adenovirus viremia for 2 months was likely affected by need for increased immunosuppression after liver transplantation. Patient 2's profound adenovirus viremia persisted for 3.5 months despite rapid clinical recovery and improved transaminase levels. Prolonged corticosteroid usage is suspected to have contributed to the prolonged viremia, although duration was longer than typically observed on antiviral treatment.

HAdV-F41 is an enteric adenovirus classically associated with acute gastroenteritis. Early in both cases we report, stool specimens were negative for adenovirus, but patient 2 later shed adenovirus in stool on hospital day 11, despite earlier detection of high-level viremia ($10^5$–$10^6$ copies/mL) in whole blood. Delayed enteric detection alongside marked viremia suggests possible altered tropism for HAdV-F41. Given that AAV2 integrates into human chromosome 19 and human peripheral blood mononuclear cells and hepatocytes serve as targets (*22*–*25*), we hypothesize that HAdV-F41 acts as a helper in hematopoietic cells, amplifying AAV2 replication that subsequently infects hepatocytes either directly causing liver injury or indirectly via immune-mediated mechanisms (*26*). That possibility is supported by the findings of high AAV2 loads (≈$10^6$ copies/mL) in liver tissue despite undetectable HAdV-F41 in the same sample. After transplantation, AAV2 cleared rapidly in plasma in parallel with clinical recovery, whereas adenovirus viremia persisted for weeks, further implicating AAV2 as the primary driver of liver injury. After discharge, we did not obtain sufficient specimens from patient 2 for AAV2 quantification in blood. Future in vitro studies of the HAdV-F41 and AAV2 strains isolated from the patients are warranted to elucidate their cell tropism, cellular pathogenesis, and underlying mechanisms contributing to ASHUE in children.

Multiple case–control studies employing mNGS have implicated AAV2 in acute pediatric hepatitis (*1*–*3*). In 1 US cohort, 93% of affected children tested positive for AAV2, compared with only 3.5% of matched controls (*1*). Another study found AAV2 in all 5 patients who required liver transplantation (*2*). Historically, AAV2 has been viewed as hepatotropic, and transient hepatitis after AAV-based gene therapy vectors is well documented (*27*). Given AAV2's known liver tropism, those observations strengthen the hypothesis that, under specific conditions, primary AAV2 infection can precipitate severe liver injury. Seroprevalence of AAV2 peaks among children 3–5 years of age (*3*), aligning with both our cases and the median age in the 2021–2022 outbreak and suggesting that AAV2-associated hepatitis reflects acute rather than reactivated infection.

One study identified class II HLA-DRB1*04:01 variant allele as a risk factor for AAV2-associated hepatitis (*3*). In the cases we report, patient 1 was found to have the HLA-DRB1*04:07 variant allele, differing by only 2 amino acids by preliminary typing. However, high-resolution NGS is needed for confirmation. Further investigation is required to delineate the molecular mechanisms by which specific HLA class II variants confer increased susceptibility and to define the spectrum of immunogenetic risk alleles in AAV2-related liver disease.

Clinically, given the relatively high severity of illness among children with ASHUE associated with AAV2–HAdV-F41, many patients are treated with cidofovir and concomitant intravenous steroids. Steroids are used to control dysregulated immune responses; for some patients, the treatment normalizes liver function tests completely, and they can be weaned off steroids altogether. Other patients, however, remain immune-reactive and could go on to develop autoimmune hepatitis, requiring long-term maintenance immunosuppression and vigilant follow-up.

In conclusion, we identified HAdV-F41 and AAV2 co-infections in 2 pediatric ASHUE cases in California in 2024 and 2025, years after global outbreaks subsided in 2022. AAV2 testing is not readily available in most clinical settings, but our case studies

suggest it remains in circulation and should be considered as a co-pathogen in ASHUE cases. The cases we report highlight the importance of equipping clinical laboratories with molecular tools such as PCR and NGS to identify HAdV-F41 and AAV2 infections in children who have non-A–E hepatitis. Beyond laboratory diagnosis, clinicians are encouraged to report unexpected ASHUE cases or clusters to public health authorities, even in the absence of official reporting requirements, because that practice is critical for effective surveillance. Our findings underscore the need for heightened physician awareness for pediatric liver failure associated with AAV2 and HAdV-F41 and expanded surveillance to promptly identify and characterize new cases, improve understanding of the underlying pathophysiology, clarify risk factors, and inform future therapeutic strategies.

This case report describes <3 patients and, per UCLA institutional policy, does not require Institutional Review Board (IRB) approval. Written informed consent for publication was not obtained. All identifying information has been removed, and the case has been fully anonymized to protect patient privacy. Publication is considered ethically appropriate in accordance with institutional and journal guidelines.

This study was funded by the UCLA Department of Pathology and Laboratory Medicine. H.V.D.'s contribution was supported by the National Institutes of Health (award no. T32 AI177290). The content is solely the responsibility of the authors and does not necessarily represent the official views of the National Institutes of Health.

## About the Author

Dr. Zhuo is a medical microbiology director at the Duke University Health System Clinical Microbiology Laboratories and assistant professor of pathology at the Duke University School of Medicine. Her research focuses on clinical application of next-generation sequencing for infectious diseases and diagnostic stewardship. Dr. Match is director of microbiology at Zuckerberg San Francisco General Hospital and assistant professor of laboratory medicine at UCSF. Her research focuses on development of rapid molecular tests and next-generation sequencing assays, particularly to solve unmet clinical needs in resource-limited settings and improve global health.

## References

1. Servellita V, Sotomayor Gonzalez A, Lamson DM, Foresythe A, Huh HJ, Bazinet AL, et al.; Pediatric Hepatitis of Unknown Etiology Working Group. Adeno-associated virus type 2 in US children with acute severe hepatitis. Nature. 2023;617:574–80. https://doi.org/10.1038/s41586-023-05949-1
2. Morfopoulou S, Buddle S, Torres Montaguth OE, Atkinson L, Guerra-Assunção JA, Moradi Marjaneh M, et al.; DIAMONDS Consortium; PERFORM Consortium; ISARIC 4C Investigators. Genomic investigations of unexplained acute hepatitis in children. Nature. 2023; 617:564–73. https://doi.org/10.1038/s41586-023-06003-w
3. Ho A, Orton R, Tayler R, Asamaphan P, Herder V, Davis C, et al.; DIAMONDS Consortium; ISARIC4C Investigators. Adeno-associated virus 2 infection in children with non-A–E hepatitis. Nature. 2023;617:555–63. https://doi.org/10.1038/s41586-023-05948-2
4. Iwata KI, Torii Y, Sakai A, Fukuda Y, Haruta K, Yamaguchi M, et al. Association between adeno-associated virus 2 and severe acute hepatitis of unknown etiology in Japanese children. J Infect Chemother. 2025;31:102462. https://doi.org/10.1016/j.jiac.2024.07.002
5. Kawada JI, Higashimoto Y, Kawamura Y, Hattori F, Ite M, Kawasaki Y, et al. Association between adeno-associated virus 2 and neurologic complications of pediatric human herpesvirus-6b infection. Pediatr Infect Dis J. 2025;44:1231–6. https://doi.org/10.1097/INF.0000000000004924
6. Boster JM, Dominguez SR, Messacar K, Adams M, Weinberg A, Black JO, et al. Acute liver failure in a child with adenovirus detected by PCR in the explanted liver. Pediatrics. 2023;151:e2022059237. https://doi.org/10.1542/peds.2022-059237
7. Shteyer E, Mor O, Waisbourd-Zinman O, Mozer-Glazberg Y, Arnon R, Hecht Sagie L, et al. The outbreak of unexplained acute hepatitis in children: the role of viral infections in view of the COVID-19 pandemic. Viruses. 2024;16:808. https://doi.org/10.3390/v16050808
8. World Health Organization. Disease outbreak news: severe acute hepatitis of unknown aetiology in children—multi-country. 2022 Jul 12 [cited 2026 Feb 9]. https://www.who.int/emergencies/disease-outbreak-news/item/2022-DON400
9. Phan J, Eslick GD, Elliott EJ. Demystifying the global outbreak of severe acute hepatitis of unknown aetiology in children: a systematic review and meta-analysis. J Infect. 2024;88:2–14. https://doi.org/10.1016/j.jinf.2023.11.011
10. Gurdasani D, Trent M, Ziauddeen H, Mnatzaganian E, Turville S, Chen X, et al. Acute hepatitis of unknown aetiology in children: evidence for and against causal relationships with SARS-CoV-2, HAdv and AAV2. BMJ Paediatr Open. 2024;8:e002410. https://doi.org/10.1136/bmjpo-2023-002410
11. Martin NA, Gonzalez G, Reynolds LJ, Bennett C, Campbell C, Nolan TM, et al. Adeno-associated virus 2 and human adenovirus F41 in wastewater during outbreak of severe acute hepatitis in children, Ireland. Emerg Infect Dis. 2023;29:751–60. https://doi.org/10.3201/eid2904.221878
12. Rodríguez RA, Garza FM, Birch ON, Greaves JCJ. Co-occurrence of adeno-associated virus 2 and human enteric adenovirus (group F) in wastewater after worldwide outbreaks of acute hepatitis of unknown etiology (AHUE). Sci Total Environ. 2024;955:176806. https://doi.org/10.1016/j.scitotenv.2024.176806
13. Almendares O, Baker JM, Sugerman DE, Parashar UD, Reagan-Steiner S, Kirking HL, et al.; Hepatitis of Unknown Etiology Group2. Deaths associated with pediatric hepatitis of unknown etiology, United States, October 2021–June 2023. Emerg Infect Dis. 2024;30:644–53. https://doi.org/10.3201/eid3004.231140
14. Aurnhammer C, Haase M, Muether N, Hausl M, Rauschhuber C, Huber I, et al. Universal real-time PCR for the detection and quantification of adeno-associated virus

serotype 2-derived inverted terminal repeat sequences. Hum Gene Ther Methods. 2012;23:18–28. https://doi.org/10.1089/hgtb.2011.034
15. Sarantis H, Johnson G, Brown M, Petric M, Tellier R. Comprehensive detection and serotyping of human adenoviruses by PCR and sequencing. J Clin Microbiol. 2004; 42:3963–9. https://doi.org/10.1128/JCM.42.9.3963-3969.2004
16. Cates J, Baker JM, Almendares O, Kambhampati AK, Burke RM, Balachandran N, et al.; Hepatitis of Unknown Etiology Group. Interim analysis of acute hepatitis of unknown etiology in children aged <10 years—United States, October 2021–June 2022. MMWR Morb Mortal Wkly Rep. 2022;71:852–8. https://doi.org/10.15585/mmwr.mm7126e1
17. Tacke F. Severe hepatitis outbreak in children linked to AAV2 virus. Nature. 2023;617:471–2. https://doi.org/10.1038/d41586-023-00570-8
18. Sant'Anna TB, Araujo NM. Adeno-associated virus infection and its impact in human health: an overview. Virol J. 2022;19:173. https://doi.org/10.1186/s12985-022-01900-4
19. Liddy E, Murphy N, Mereckiene J, Fitzpatrick E, Broderick A, Egan R, et al.; Incident Management Team. Investigation of an outbreak of novel hepatitis of unknown aetiology in children and adolescents, Ireland, 2021 to 2023. Euro Surveill. 2025;30:2400536. https://doi.org/10.2807/1560-7917.ES.2025.30.14.2400536
20. UK Health Security Agency. Investigation into acute hepatitis of unknown aetiology in children in England. 2022 [cited 2026 Feb 8]. https://assets.publishing.service.gov.uk/media/646b4271382a5100139fc4da/AHUA-EEI.pdf
21. Gutierrez Sanchez LH, Shiau H, Baker JM, Saaybi S, Buchfellner M, Britt W, et al. A case series of children with acute hepatitis and human adenovirus infection. N Engl J Med. 2022;387:620–30. https://doi.org/10.1056/NEJMoa2206294
22. Kotin RM, Siniscalco M, Samulski RJ, Zhu XD, Hunter L, Laughlin CA, et al. Site-specific integration by adeno-associated virus. Proc Natl Acad Sci U S A. 1990;87:2211–5. https://doi.org/10.1073/pnas.87.6.2211
23. Henckaerts E, Dutheil N, Zeltner N, Kattman S, Kohlbrenner E, Ward P, et al. Site-specific integration of adeno-associated virus involves partial duplication of the target locus. Proc Natl Acad Sci U S A. 2009;106:7571–6. https://doi.org/10.1073/pnas.0806821106
24. Ponnazhagan S, Mukherjee P, Yoder MC, Wang XS, Zhou SZ, Kaplan J, et al. Adeno-associated virus 2-mediated gene transfer in vivo: organ-tropism and expression of transduced sequences in mice. Gene. 1997;190:203–10. https://doi.org/10.1016/S0378-1119(96)00576-8
25. Hüser D, Gogol-Döring A, Lutter T, Weger S, Winter K, Hammer EM, et al. Integration preferences of wildtype AAV-2 for consensus rep-binding sites at numerous loci in the human genome. PLoS Pathog. 2010;6:e1000985. https://doi.org/10.1371/journal.ppat.1000985
26. de Kleine RH, Carbo EC, Lexmond WS, Zhou XW, de Kroon A, Mei H, et al. Metagenomic and transcriptomic investigation of pediatric acute liver failure cases reveals a common pathway predominated by monocytes. MBio. 2025;16:e0391324. https://doi.org/10.1128/mbio.03913-24
27. Maina A, Foster GR. Hepatitis after gene therapy, what are the possible causes? J Viral Hepat. 2024;31(Suppl 1):14–20. https://doi.org/10.1111/jvh.13919

Address for correspondence: Shangxin Yang, UCLA David Geffen School of Medicine, 11633 San Vicente Blvd, Los Angeles, CA 90049, USA; email: shangxinyang@mednet.ucla.edu

# National Surveillance of Enterovirus D68 Upsurge, France, 2024

Marion Jeannoël, Maxime Bisseux, Stéphanie Dan, Elisa Creuzet, Delphine Parraud, Jean-Luc Bailly, Jérémie Lebeurre, Amélie Brebion, Hélène Chabrolles, Laurence Josset, Cécile Henquell, Isabelle Schuffenecker, Audrey Mirand; Enterovirus Surveillance Network[1]

In 2024, an early and rapid rise in enterovirus D68 (EV-D68) infections in France prompted the implementation of enhanced nationwide surveillance to characterize the outbreak. EV-D68 screening was performed as part of the routine hospital strategy of the 2 national reference laboratories and of the national surveillance of enterovirus infections. Of 919 patients, 49.1% (451/919) were adults. Severe infection was reported in 169 patients (102 children and 67 adults). We observed neurologic complications in 7 children (seizures and encephalitis) and 4 adults (myelitis). Infections peaked in week 38 and were associated with subgenotypes A2 and B3; A2 predominated, particularly in adults (317/457 [69.3%] A2 infections). Complete genome analyses identified a new A2-derived lineage with mutations clustering in exposed regions of viral capsid protein 1. Our findings highlight the substantial clinical impact of EV-D68 in adults as well as children, underscoring the need for broad clinical and genomic surveillance.

Although enterovirus D68 (EV-D68), first isolated in 1962, has been considered an emerging pathogen since 2008 (*1*), it attracted attention after the US Centers for Disease Control and Prevention (CDC) issued alerts in 2014 (*2*), which were followed by reports of numerous cases worldwide (*3*). EV-D68 causes severe respiratory infections in children and adults, particularly in patients with underlying respiratory disease (*3*,*4*). Neurologic complications can occur, and some constitute a specific neurologic entity, acute flaccid myelitis (AFM), characterized by frequent sequelae (*5*). Several countries have thus strengthened existing surveillance of enterovirus infections by combining it with respiratory, syndromic (asthma-like illness, AFM, or both) or even environmental surveillance (*6*–*9*). After markedly reduced circulation in 2020, EV-D68 infections resurged in autumn 2021, 2022, and 2023 in Europe (*4*,*8*,*10*–*12*) and in 2022 across the United States with increase in respiratory illness in pediatric patients (*13*). More recently, enhanced genomic surveillance evidenced EV-D68 upsurges in 2024 in Italy (*9*), Spain (*14*), and the United States (*15*).

To date, EV-D68 strains are divided into 3 genotypes and 5 subgenotypes, designated A (A1 and A2, also referred to as clade D in some studies), B (B1–B3), and C. Since 2017, EV-D68 epidemics have been associated with the cocirculation of the subgenotypes B3 and A2 on all continents (*16*). In France, enterovirus surveillance involves a network of 32–36 hospital virology laboratories, the Enterovirus Surveillance Network (ESN), including the 2 enterovirus national reference laboratories (NRLs), based in Clermont-Ferrand (University Hospital of Clermont-Ferrand, France, coordinator) and in Lyon (Hospices Civils de Lyon, France, associate). Since the reemergence of EV-D68 in 2014, network members are regularly encouraged to screen respiratory specimens for EV-D68 at least in patients with severe infection (*17*). Such screening enabled the detection of EV-D68 epidemics in 2014, 2016, and 2018 (*4*,*17*,*18*), and then in 2021, 2022, and 2024 (*19*). Here, we describe the 2024

Author affiliations: Hospices Civils de Lyon, Centre National de Référence des Entérovirus–Laboratoire Associé, Lyon, France (M. Jeannoël, S. Dan, D. Parraud, J. Lebeurre, L. Josset, I. Schuffenecker); Université Clermont Auvergne, Clermont-Ferrand (M. Bisseux, E. Creuzet, H. Chabrolles, C. Henquell, A. Mirand); Centre Hospitalier Universitaire de Clermont-Ferrand, Centre National de Référence des Entérovirus–Laboratoire Coordonnateur, Clermont-Ferrand, France (M. Bisseux, E. Creuzet, A. Brebion, H. Chabrolles, C. Henquell, A. Mirand); Université Claude Bernard Lyon 1, Villeurbanne, France (S. Dan, D. Parraud, L. Josset); Université Clermont Auvergne, Clermont-Ferrand (J.L. Bailly)

DOI: https://doi.org/10.3201/eid3207.260044

[1]Additional members of Enterovirus Surveillance Network who contributed data are listed at the end of this article.

EV-D68 upsurge in France characterized by early circulation, detected as early as June, as well its effect on the adult population, and the cocirculation of B3 and A2 subgenotypes, including a new A2-derived lineage.

## Methods

### Patient Population, Study Design and Molecular Testing of Clinical Specimens

Respiratory specimens were tested for EV-D68 either by an EV-D68 real-time reverse transcription PCR or by sequencing the viral protein (VP) 4/VP2 coding region (*20*–*22*). EV-D68 testing was done as part of the routine hospital diagnostic and genotyping strategies for enterovirus/rhinovirus-positive respiratory specimens from patients of all ages and year-round at NRL1, or for all respiratory specimens from children <5 years of age during September–November at NRL2. Both NRLs also analyzed enterovirus-positive samples from the ESN throughout the year, regardless of the sample type. The observation of early circulation and the increased detection of EV-D68 cases prompted the NRLs to implement an enhanced EV-D68 surveillance nationwide in France during September 2–December 1, 2024 (weeks 36–48). Enhanced surveillance consisted of extended EV-D68 screening to children <10 years of age starting week 36 in NRL2 and asking the ESN to retroactively and prospectively send enterovirus- or rhinovirus-positive respiratory specimens for EV-D68 screening by prioritizing samples from patients with severe infection. To determine whether the 2024 upsurge displayed distinct epidemiologic features compared with previous years, we compared the EV-D68 positivity rate of samples in 2024 with those in 2021–2023 (weeks 36–48) in both NRLs, whose strategies remained unchanged during 2021–2024. We considered 3 age groups: children <5 years of age (separated data for each NRL), children 5–17 years of age (data for NRL1), and adults ≥18 years of age (data for NLR1).

### Patients and Clinical Characteristics

We retrospectively collected demographic and clinical characteristics from medical charts. Severity criteria included admission to intensive care when not attributable to another cause, respiratory disease requiring intravenous corticosteroids, high-flow

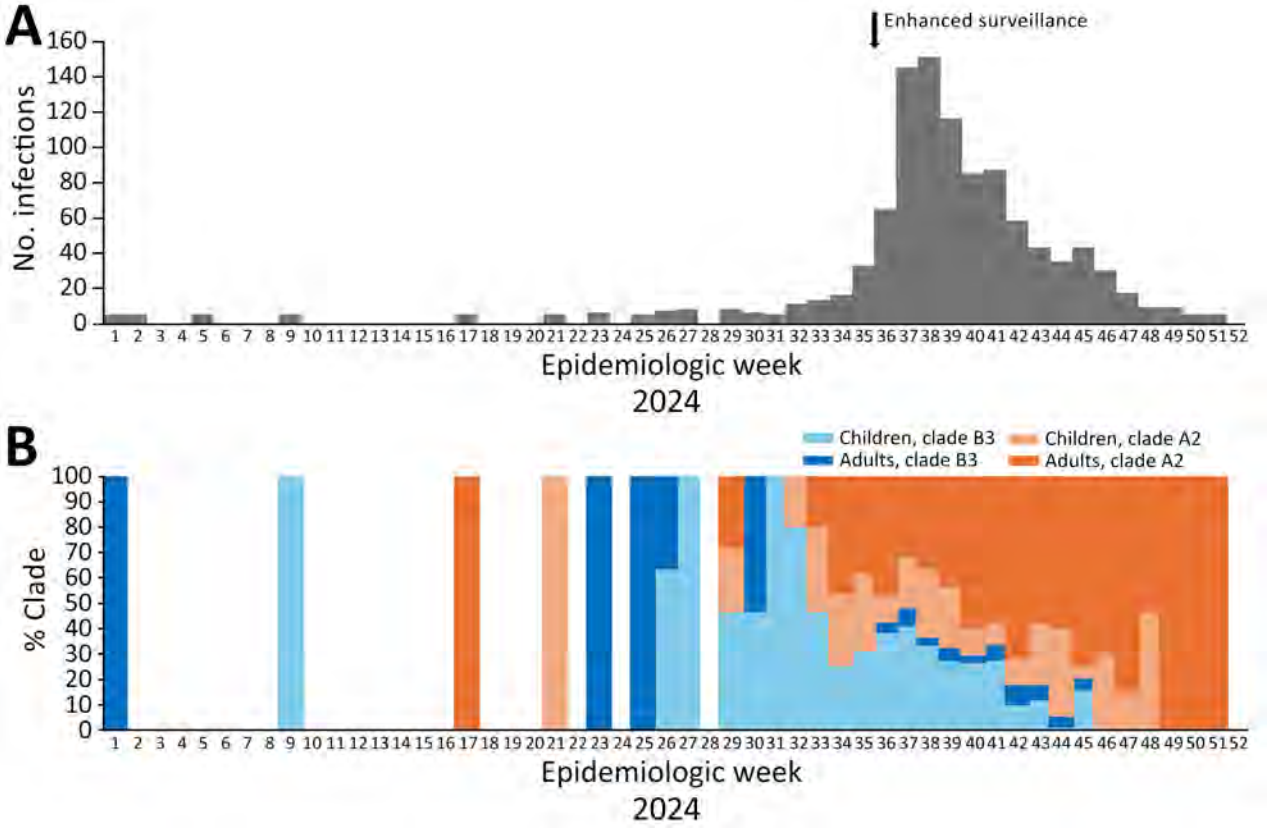


**Figure 1.** Distribution of infections from report on national surveillance of enterovirus D68 upsurge, France, 2024. A) Weekly distribution of infections in 2024. B) Distribution of subgenotype percentages. Each genotype is represented by a color, the intensity of which indicates the age group (children <18 years of age, adults ≥18 years of age).

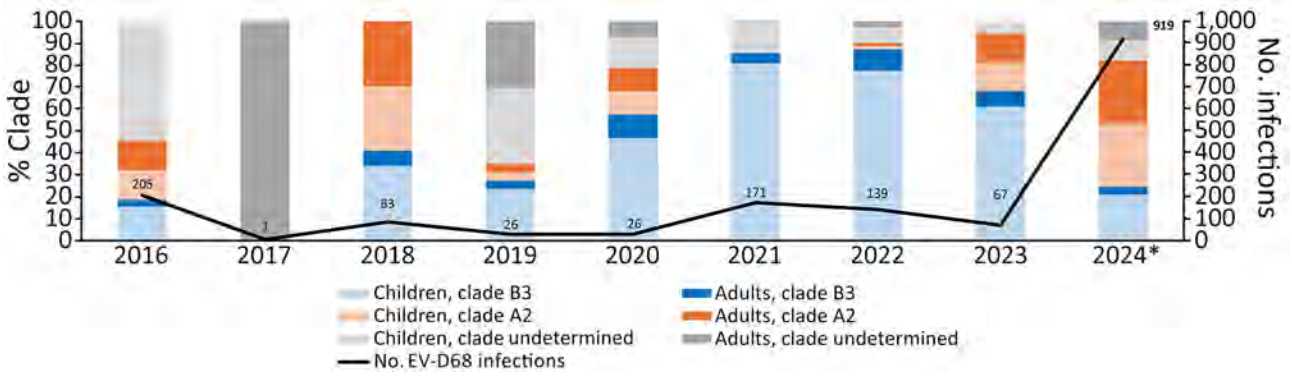


**Figure 2.** Distribution of EV-D68 subgenotype infections by year from report on national surveillance of enterovirus D68 upsurge, France, 2016–2024. Curve shows total number of infections per year. Children are defined as patients <18 years of age, adults ≥18 years of age. EV-D68, enterovirus D68.

oxygen therapy or intubation, encephalitis, complex seizures, myelitis, and death, including sudden infant death. The ethics committee of Centre Hospitalier Universitaire de Clermont Ferrand approved this study (IRB00013412; CHU de Clermont Ferrand IRB #1, IRB no. 2024-CF393).

### VP1 and Complete Enterovirus Genome Sequencing

We determined the complete or partial VP1 sequences of EV-D68–positive specimens by in-house gene amplification and Sanger sequencing to assign a phylogenetic subgenotype (*4*). We compared the proportions of the different subgenotypes identified nationally among children and adults in 2024 with those of the 2016–2023 period. We performed whole-genome sequencing by next-generation sequencing (NGS) methods on a subset of samples representing the full genetic diversity observed in the 1D sequences (encoding the VP1 capsid protein) in 2021–2024, either after amplification of full-length genome (at NRL1) or using a metatranscriptomic approach (at NRL2) (*23*) (Appendix, https://wwwnc.cdc.gov/EID/article/32/6/26-0044-App1.pdf). We deposited all complete genome sequences in GenBank (accession nos. PQ612496–575, PP947790–800, and PP548243–8).

### Data Collection, Sequence Processing, and Bayesian Inference

As of June 1, 2025, we retrieved all available EV-D68 sequences >6,000-nt long that were deposited in GenBank, yielding a total of 1,813 sequences, including the 97 sequences obtained in this study from 2021–

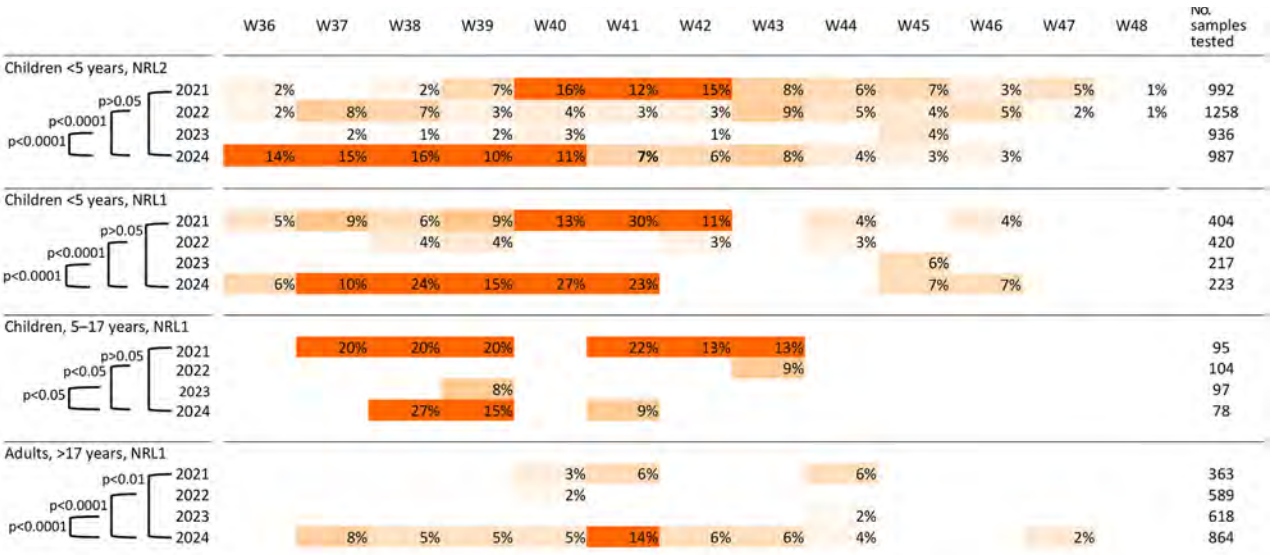


**Figure 3.** Percentages of positive samples, by week and by age group, from report on national surveillance of enterovirus D68 upsurge, France, 2021–2024. Data are based on routine hospital strategies of each of the 2 NRLs. To determine whether the 2024 upsurge had distinct epidemiologic features compared with previous years, we compared the positivity rate of samples in 2024 with those in 2021–2023 (weeks 36–48) in both NRLs. We included 3 age groups: children <5 years of age (data for both NRLs), children 5–17 years of age (data only for NRL1), and adults >17 years old (data only for NRL1). NRL, national reference laboratory; W, week.

**Table 1.** Patient characteristics and clinical outcomes in study of EV-D68 upsurge, France, 2024*

| Characteristic | Children 0–17 y, n = 363 | Adults | | |
|---|---|---|---|---|
| | | 18–64 y, n = 155 | ≥65 y, n = 134 | Total, n = 289 |
| Median age, y (IQR) | 2.0 (0.04–7) | 45 (34–56) | 76 (70–82) | 62 (43–75) |
| Female/male ratio | 0.76 | 0.49 | 0.55 | 1.08 |
| EV-D68 severe infections | 102/363 (28.1) | 38/155 (24.5) | 29/134 (21.6) | 67/289 (23.2) |
| Hospitalization† | 308/358 (86.0) | 126/150 (84.0) | 127/131 (96.9) | 253/281 (90.04) |
| Intensive care unit‡ | 85/343 (24.78) | 42/143 (29.4) | 27/125 (21.6) | 69/268 (25.75) |
| Death | 2/363 (0.6)§ | 3/155 (1.9) | 6/134 (4.5) | 9/289 (3.1)¶ |

*Values are no. (%) except as indicated. EV-D68, enterovirus D68; IQR, interquartile range.
†Hospitalization requirement was reported for 358 children and 281 adults.
‡Intensive care requirement was reported for 343 children and 268 adults.
§Sudden infant death syndrome. Although EV-D68 was the only detected pathogen, EV-D68 infection was considered as the possible cause of death; attributing causality can be challenging without thorough investigation in such contexts.
¶Among the 9 adults, the EV-D68 infection was considered as the probable cause of death in 4 patients (EV-D68 was the only detected pathogen) and as possible in 5 patients (evidence or strong suspicion of bacterial co-infection).

2024. After filtering steps (i.e., exclusion of sequences <6,495 nt and clusters of sequences collected in the same country and year that displayed <0.5% genetic differences), we obtained a final alignment comprising 449 high-quality EV-D68 sequences, including 42 study sequences (2024, n = 19; 2023, n = 8; 2022, n = 13, 2021, n = 2). We analyzed Bayesian inference using an uncorrelated lognormal relaxed molecular clock model to accommodate rate variation among lineages. We used the coalescent Bayesian Skyline model as the tree before accounting for demographic history. We modeled nucleotide substitutions using the general time reversible substitution model. We jointly estimated phylogenetic parameters through a Markov chain Monte Carlo process that ran for 500 million generations.

### Complete Genome and P1 Region Amino Acid Sequence Analyses

We compared the consensus of complete coding sequences indicating the predominant amino acids between historical strains A2-I and B3-I and the 2024 study strains A2-II and B3-II. We determined the positions of the mutations by aligning sequences with the prototype sequence (GenBank accession no. AY426531; Fermon strain). We predicted the 3-dimensional pentameric structure of A2 strains from 5 copies of the VP1–VP4 protein sequences using AlphaFold (https://alphafoldserver.com).

### Statistical Analysis

We conducted group comparisons by Fisher exact test; $p<0.05$ indicated a statistically significant difference.

**Table 2.** Clinical characteristics of cases in study of enterovirus D68 upsurge, France, 2024*

| Characteristic | Children 0–17 y, n = 363 | | Adults ≥18 y, n = 289 | | Total, N = 652 | |
|---|---|---|---|---|---|---|
| | No. (%) patients | No. (%) severity criteria | No. (%) patients | No. (%) severity criteria | No. (%) patients | No. (%) severity criteria |
| Respiratory symptoms | 332 (91.5) | 91 (25.1) | 278 (96.2) | 55 (19.0) | 610 (93.6) | 146 (22.4) |
| URTI | 100 (27.5) | 3 (0.8) | 81 (28.0) | 0 | 181 (27.8) | 3 (0.5) |
| Asthma | 147 (40.5) | 61 (16.8) | 33 (11.4) | 11 (3.8) | 180 (27.6) | 72 (11.0) |
| Bronchiolitis, bronchitis, bronchial syndrome | 45 (12.4) | 12 (3.3) | 24 (8.3) | 0 | 69 (10.6) | 12 (1.8) |
| Pneumonia | 18 (5.0) | 4 (1.1) | 52 (18.0) | 15 (5.2) | 70 (10.7) | 19 (2.9) |
| Dyspnea | 5 (1.4) | 0 | 15 (5.2) | 0 | 20 (3.1) | 0 |
| Neonatal apnea/distress | 3 (0.8) | 0 | NA | NA | 3 (0.5) | 0 |
| Acute exacerbation of COPD | NA | NA | 41 (14.2) | 12 (4.2) | 41 (6.3) | 12 (1.8) |
| Respiratory distress | 15 (4.1) | 7 (1.9) | 31 (10.7) | 17 (5.9) | 46 (7.1) | 24 (3.7) |
| Neurologic symptoms | 17 (4.7) | 7 (1.9) | 5 (1.7) | 4 (1.4) | 22 (3.4) | 11 (1.7) |
| Seizures | 14 (3.9) | 7 (1.9) | 1 (0.3) | 0 | 15 (2.3) | 7 (1.1) |
| Encephalitis | 4 (1.1) | 4 (1.1) | 0 | 0 | 4 (0.6) | 4 (0.6) |
| Meningitis | 1 (0.3) | 0 | 0 | 0 | 1 (0.2) | 0 |
| Myelitis, Guillain-Barré syndrome | 0 | 0 | 4 (1.4) | 4 (1.4) | 4 (0.6) | 4 (0.6) |
| Other | 1 (0.3)† | 0 | 0 | 0 | 1 (0.2) | 0 |
| Cardiovascular symptoms | 2 (0.6) | 2 (0.6) | 21 (7.3) | 14 (4.8) | 23 (3.5) | 16 (2.5) |
| Decompensated heart failure | 1 (0.3) | 1 (0.3) | 15 (5.2) | 7 (2.4) | 16 (2.5) | 8 (1.2) |
| Myocarditis | 1 (0.3) | 1 (0.3) | 0 | 0 | 1 (0.2) | 1 (0.2) |
| Sepsis, shock | 0 | 0 | 12 (4.2) | 11 (3.8) | 12 (1.8) | 11 (1.7) |
| Enteric symptoms | 57 (15.7)‡ | 0 | 25 (8.7)‡ | 0 | 82 (12.6) | 0 |
| Isolated fever | 6 (1.7) | 0 | 7 (2.4) | 0 | 13 (2.0) | 0 |

*A given patient may experience >1 clinical item. COPD, chronic obstruction pulmonary disease; NA, not applicable; URTI, upper respiratory tract infection.
†Irritability and hypotonia.
‡Acute gastroenteric symptoms were the only clinical signs in 9 children and 2 adults.

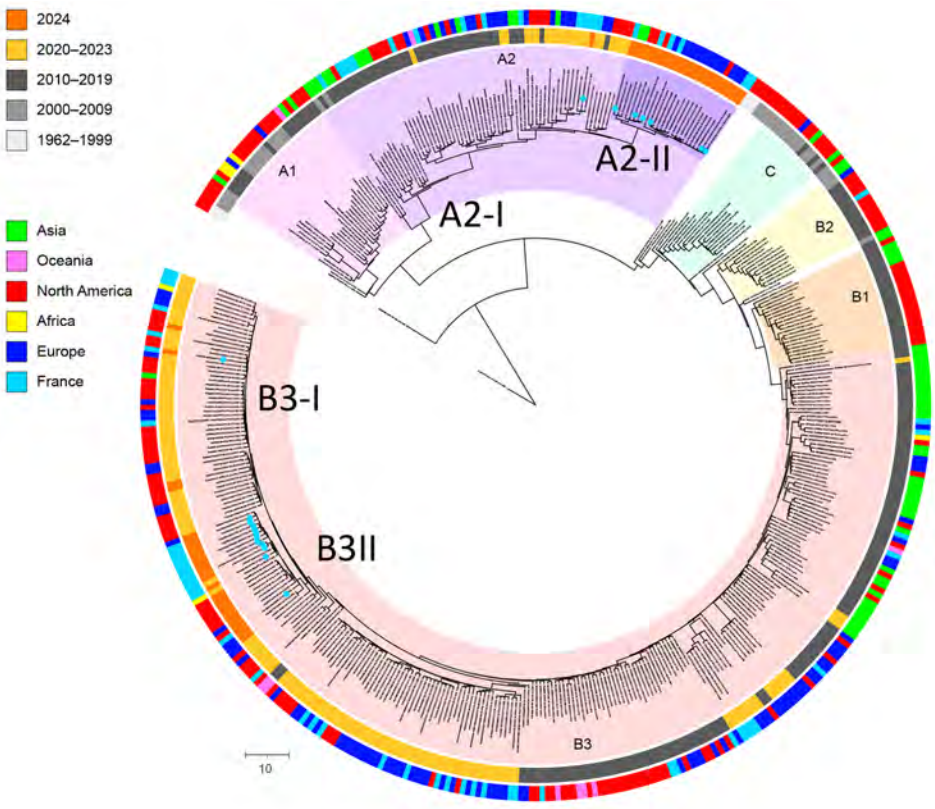


**Figure 4.** Time-scaled phylogeny of enterovirus D68 from report on national surveillance of enterovirus D68 upsurge, France, 2024. We reconstructed a time-calibrated phylogenetic tree based on all available complete or near-complete (<6,495 nt) ORF sequences retrieved from GenBank, along with the sequences generated in this study. We subsampled and analyzed a total of 449 sequences using Bayesian inference with BEAST version 2.6.3 (https://beast.community), running a Markov chain of 500 million generations. We summarized the maximum clade credibility tree using TreeAnnotator (https://beast.community/treeannotator), and visualized with iTOL (https://itol.embl.de). We added 2 outer annotation rings, the outer ring for the continent or country of origin and the inner ring for the year of sampling. Previously defined clades (A1, A2, B1–B3, and C) are labeled and highlighted for branches and taxa: pink for clade A1, light purple for A2 and darker purple for sequences from the newly identified 2024 A2 subgroup A2-II, light orange for B1, yellow for B2, peach for B3, and light green for C. We identified the 2 groups of B3 sequences in this study as B3-I (ancestral) and B3-II. Blue dots indicated at the taxon names indicate sequences generated in this study in 2024. Scale bar represents the divergence in years relative to 2024.

We used GraphPad Prism version 8.0.2 (GraphPad Software, https://www.graphpad.com) for all analyses.

## Results

### Epidemiologic Characteristics of the 2024 EV-D68 Epidemic

We detected a total of 919 EV-D68 infections, 468 (50.9%) of which occurred in children. The EV-D68 epidemic peaked in week 38; the first consecutive weekly seasonal cases were detected starting week 29 (Figure 1, panel A). The age distribution of EV-D68 infections shifted over time. Whereas 332/532 (60.7%) samples collected during weeks 26–39 were from children, 247/378 (65.3%) samples collected from week 39 onward were from adults. Clade subgenotyping was possible for 721 (78.5%) of the 919 samples, among which 367 were from children and 354 from adults. Subgenotypes B3 and A2 cocirculated; A2 was predominant in 457/721 (63.3%) samples. Subgenotype B3 was more frequently detected in children (227/367 [61.8%]) than in adults (37/354 [10.5%]; p<0.0001); adults were more frequently infected with subgenotype A2 (317/354 [89.5%]) (Figure 1, panel B; Appendix Table). Subgenotype A2 became predominant from week 34, accounting for 64% of samples during weeks 34–48, and seemed to expand again after 5 years of B3 predominance (Figure 2).

To further characterize the upsurge, we compared the EV-D68 positivity rate of samples collected during weeks 36–48 of 2021–2024, exclusively using data from the routine hospital activity of the NRLs whose strategies have remained unchanged since 2021 (Figure 3). Among children <5 years of age, we observed a significant increase in EV-D68 prevalence in 2024 compared with 2022 and 2023, regardless of the testing strategy in each NRL. In 2024, a sustained circulation (≥10% positivity rate) was documented earlier and over a longer period than in 2021, at 6 weeks versus 3 weeks. In the adult population, the 2024 epidemic was characterized by a higher positivity rate (2021–2024, p<0.01; 2022–2024 and 2023–2024, p<0.0001) and a broader temporal amplitude than in previous years.

### Demographic and Clinical Characteristics of EV-D68 Infections

Clinical data were available for 668/919 patients with EV-D68 infections. We excluded 16 patients,

7 children and 9 adults, because EV-D68 was considered unlikely on the basis of their clinical symptoms. We analyzed demographics, clinical outcomes (Table 1), and clinical characteristics (Table 2) for the 652 remaining patients. A total of 308/358 children and 253/281 adults required hospitalization; of the adults, 126/150 were 18–64 years of age and 127/131 ≥65 years of age. Hospitalization rate was significantly higher in adults ≥65 years of age (96.9%) than in children (86.0%; p = 0.0003) and than in adults 18–64 years of age (84.0%; p = 0.0002) (Table 1). Intensive care was needed for 85/343 children and 69/268 adults; of the adults, 42/143 were 18–64 years of age and 27/125 were ≥65 years of age. Infections met severity criteria in 102/363 (28.1%) children and 67/289 (23.2%) adults. We observed no association between clade and severity.

Respiratory symptoms were predominant in both children and adults. Eleven patients (1.7%) experienced severe neurologic symptoms associated with respiratory signs. Although none of the children experienced AFM, 4 adults were hospitalized with myelitis, 1 case of facial paralysis with left motor deficit and 3 cases of Guillain-Barré syndrome (GBS). All 3 GBS patients experienced abolished osteotendinous reflexes and rapidly progressive motor paralysis, followed by acute respiratory failure requiring intensive care. GBS was documented on electroneuromyography for 2 patients. EV-D68 was the only pathogen detected in 2 patients with GBS and was associated with multiple pathogens in the third patient. All adult neurologic cases were associated with subgenotype A2 infection.

### Phylogenetic and Amino Acid Variation Analyses

Phylogenetic analysis of 449 near-complete coding sequences showed that most of the 2024 sequences clustered into 2 defined, well-supported groups, designated A2-II and B3-II in this study, distinct from other sequences among subgenotypes A2 and B3 (Figure 4). B3-II included most of the study sequences and recent 2024 outbreak strains from the United States and Italy and 2023 strains from the Netherlands, Senegal, and France (Figure 5). It likely emerged around early 2021 (time to most recent common ancestor 2021.2 [95% high posterior probability 2020.7–2021.6]) and is

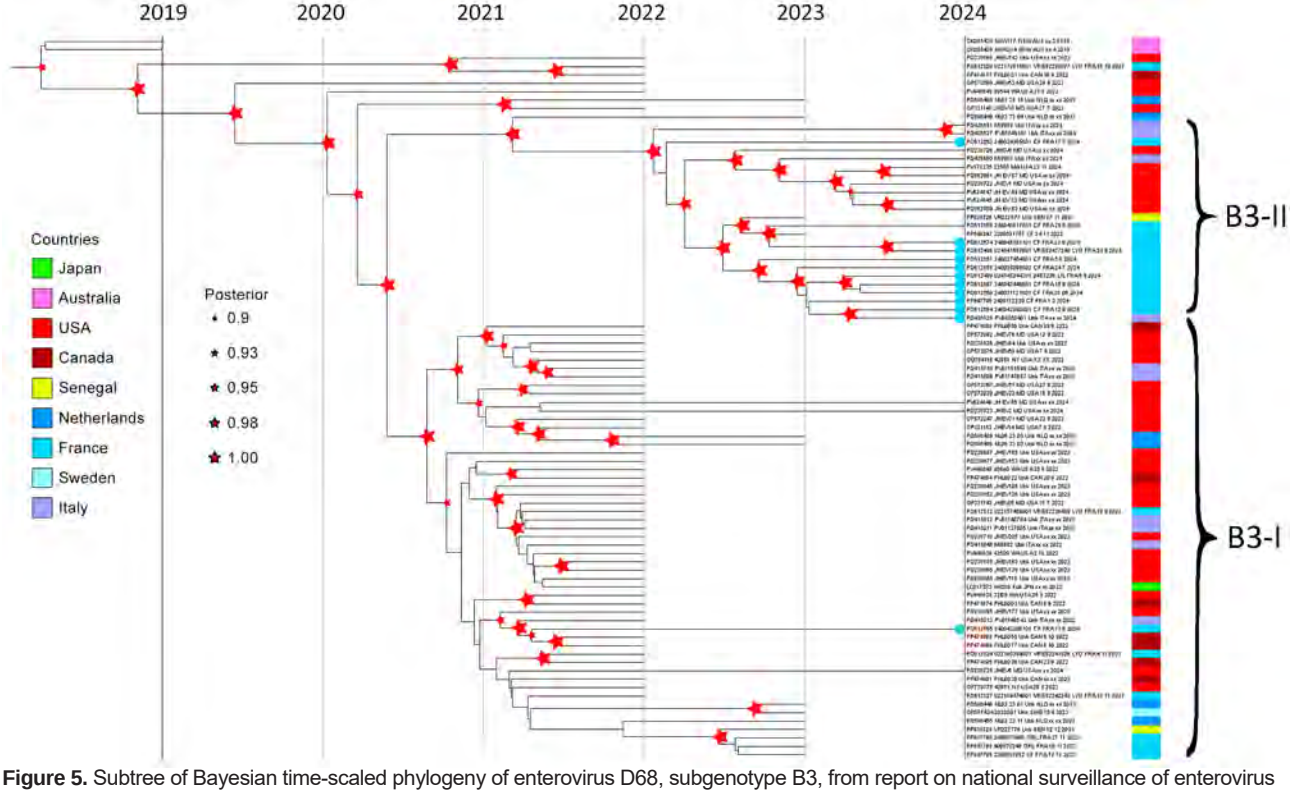


**Figure 5.** Subtree of Bayesian time-scaled phylogeny of enterovirus D68, subgenotype B3, from report on national surveillance of enterovirus D68 upsurge, France, 2024. Phylogeny created using BEAST version 2.6.3 (https://beast.community). Subtree focusing on the study strains belonging to subgenotype B3 was extracted from the complete time-calibrated phylogenetic tree. The estimated ages of the most recent common ancestors from the root of each clade to the year 2024 are indicated. Red stars at nodes indicate posterior probabilities >0.9, star sizes are proportional to posterior probability (larger symbols indicate values closer to 1). Colors at right indicate country of origin for each strain. Blue dots indicated at the taxon names indicate sequences generated in this study in 2024. GenBank accession numbers are provided. An expanded version of this figure is available online (https://wwwnc.cdc.gov/EID/article/32/7/26-0044-F5.htm).

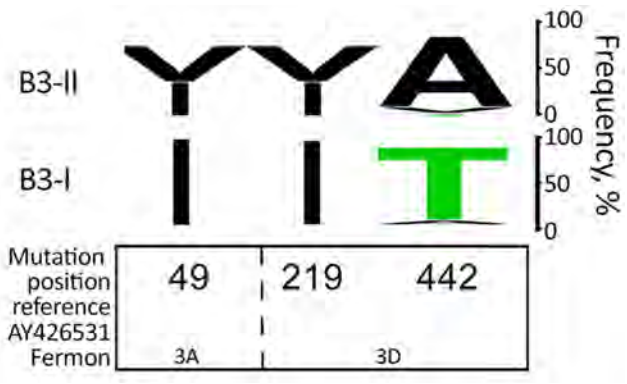


**Figure 6.** Amino acid change analysis of enterovirus D68, subgenotype B3, from report on national surveillance of enterovirus D68 upsurge, France, 2024. Amino acid substitutions leading to changes in the predominant residues between B3-II (n = 61 sequences) and the monophyletic clade corresponding to the nearest common ancestor B3-I (n = 106 sequences) are shown. Mutation positions are numbered according to the reference Fermon strain (GenBank accession no. AY426531) and annotated by the corresponding nonstructural viral proteins (3A and 3D). For each of the positions showing a mutation in the new group, the frequency of each amino acid was visualized using WebLogo (https://weblogo.threeplusone.com). A, alanine; I, isoleucine; T, threonine; Y, tyrosine; V, valine.

distinct of a broader B3 lineage, B3-I, mainly composed of strains collected in 2022–2023 worldwide. Three amino acid changes distinguished the B3-II group from B3-I group (Figure 6), all located outside the capsid region. The group A2-II formed a new A2 lineage comprising only sequences from 2024 strains collected mostly in France and Italy (*9*) (Figure 7). Time to most recent common ancestor was estimated at 2022.1 (95% high posterior probability 2021.2–2022.6); it shared a common ancestor with a lineage composed primarily of strains collected since 2019 in Europe and in the United States. That A2-II lineage exhibited 4.4% nucleotide and 1.4% amino acid divergence; 25 amino acid positions shifted in predominant residues of several proteins, compared with ancient A2 strains (Figure 8). In 15/25 positions, the dominant amino acids in 2024 strains (>90% prevalence) were previously minor variant in historical A2 sequences. Mutations in VP1 were located in key structural regions: the BC loop (residues 90–103), DE loop (110–169), GH loop (178–218), and the C-terminal domain (277–311) (*24*). Structural mapping onto a capsid pentamer model revealed that these capsid mutations are surface exposed (Figure 9, panels A, B).

## Discussion

We report the 2024 EV-D68 upsurge in France, which was characterized by an early onset, with the first consecutive weekly cases detected at the beginning of summer, and the highest number of cases detected by hospital-based surveillance since the reappearance of this virus in 2014. Those features can be partly explained by the enhanced laboratory surveillance and the intensive participation of the ESN, which sent 11 times more samples in 2024 than in 2021–2023. However, we observed higher EV-D68 positivity rates in 2024 than in 2021–2023 in both NRLs; each laboratory applied comparable strategies over the period. The adult population was particularly affected, as already observed for the EV-D68 surge reported in Italy in 2024 compared with 2023 (*9*).

US multimodal surveillance of EV-D68 infections showed that the syndromic surveillance for asthmatic illness provided the best estimate of EV-D68 disease burden because of continued limited and selective sampling and testing for EV-D68 (*6*). However, that approach focused mainly on the pediatric population (*13*). In a Europe-based study, the combination of clinical enterovirus and respiratory surveillance was the most effective for detecting EV-D68 cases (*11*). In our study, year-round systematic screening for enterovirus/rhinovirus in respiratory samples using a diagnostic method capable of detecting EV-D68, followed by genotyping of positive samples, enabled the timely detection of EV-D68 upsurge. Of note, that surveillance approach, even when implemented across a limited number of laboratories, could therefore trigger an alert to the public health authorities.

It is also important to raise clinician awareness about the need to reinforce EV-D68 screening not only in children but also in adults, particularly those with underlying or severe conditions, to enable a more accurate assessment of the effect of EV-D68 on this often underrecognized population (*4*,*25*,*26*). It has been widely reported that children are at greater risk of developing severe forms of EV-D68 infections (*3*,*5*); however, the resurgence observed in France in 2024 was associated with significant illness in adults. In the 2024 outbreak, 25.8% of adults required admission to intensive care departments, similar to the rate among children (24.8%). Regarding neurologic complications associated with EV-D68 infections, 7 (1.9%) children and 4 adults (1.4%) experienced severe neurologic signs; none of the children had signs of AFM but they did have seizures and signs of encephalitis. Among EV-D68 cases reported by 13 countries in 2021–2022 in Europe, 43 patients (6.8%) displayed neurologic disorders and half of those were diagnosed with seizures, encephalitis, meningitis, or AFM (*8*). The decrease in incidence of neurologic complications was also observed in the United States, where EV-D68 upsurges have not been asso-

ciated with resurgences of myelitis since 2019, despite an effective surveillance of AFM cases (*6*,*7*). Since 2019, circulating EV-D68 viruses might be less neurotropic or less likely to cause neurologic disease than were viruses from 2014, 2016, and 2018 (*11*). All mutations, except for VP1:D283E, which was previously associated with neurovirulence traits (*27*), were absent in 2024 strains, including those of subgenotype A2 associated with the 4 adult cases of myelitis. Three of those adult cases were reported to be GBS. Because the AFM criteria are mainly based on pediatric cases (*7*,*28*) and that distinction between AFM and GBS might be challenging (*27*) particularly in adults, it is relevant to retain a broad and nonspecific definition such as acute flaccid paralysis, for the surveillance of EV-D68–associated myelitis.

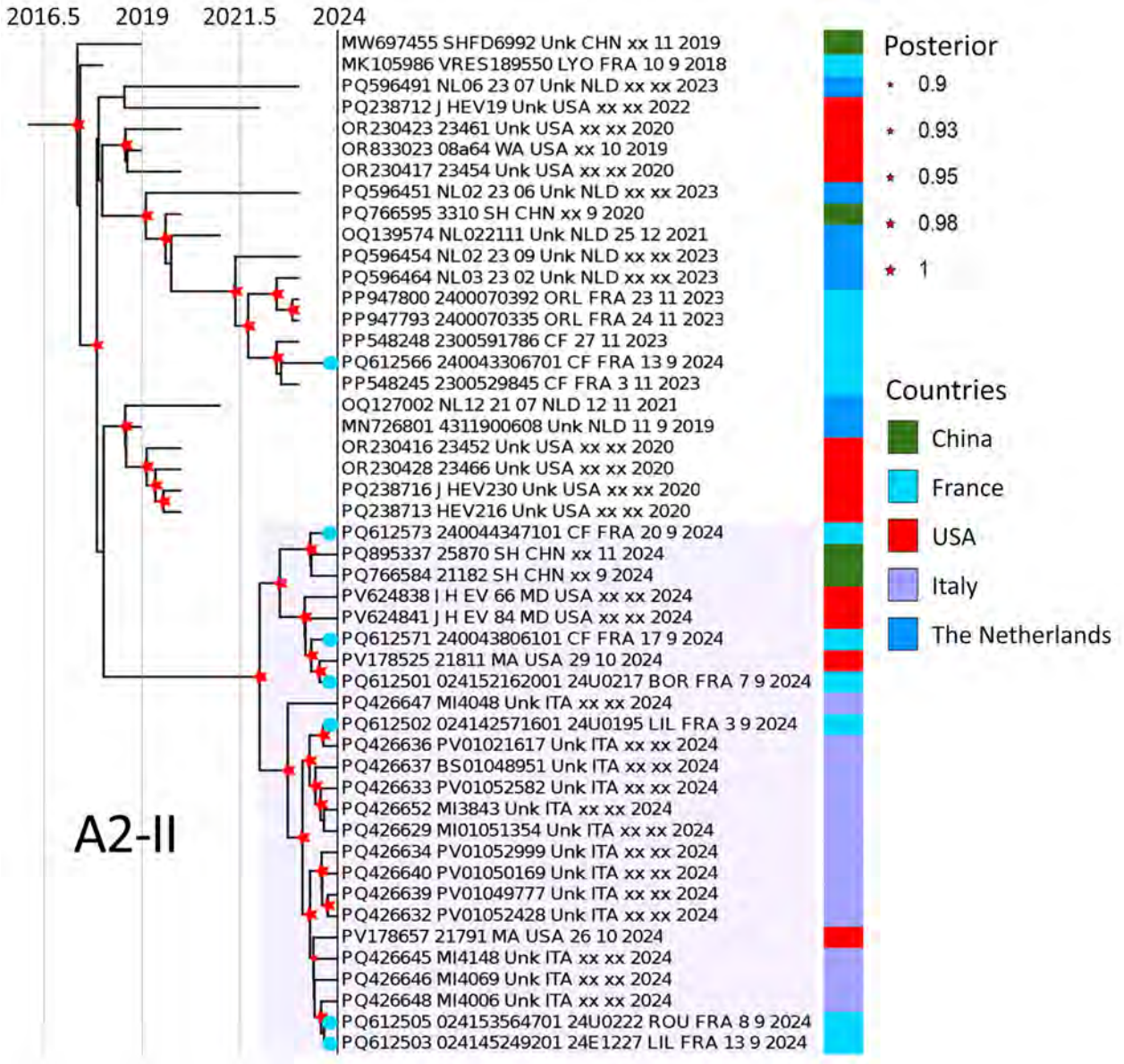


**Figure 7.** Subtree of Bayesian time-scaled phylogeny of EV-D68, subgenotype A2, from report on national surveillance of enterovirus D68 upsurge, France, 2024. Phylogeny created using BEAST version 2.6.3 (https://beast.community). A subtree focusing on the most recent strains of subgenotype A2 was extracted from the complete time-calibrated phylogenetic tree of EV-D68. The estimated ages of the most recent common ancestors (MRCAs) from the root of each clade to the year 2024 are indicated. Red stars at nodes indicate posterior probabilities >0.9, star sizes are proportional to posterior probability (larger symbols indicate values closer to 1). Colors at right indicate country of origin for each strain. Blue dots indicated at the taxon names indicate sequences generated in this study in 2024. GenBank accession numbers are provided. An expanded version of this figure is available online (https://wwwnc.cdc.gov/EID/article/32/7/26-0044-F7.htm).

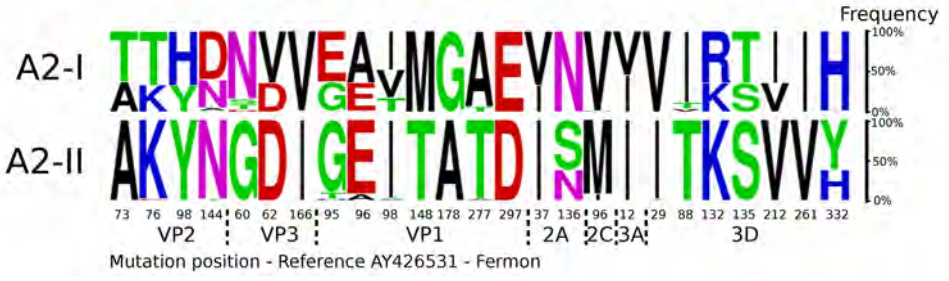


**Figure 8.** Amino acid change analysis of enterovirus D68, subgenotype A2, from report on national surveillance of enterovirus D68 upsurge, France, 2024. Amino acid substitutions leading to changes in the predominant residues between the newly identified A2-II group (n = 50 sequences) and the previously circulating A2-I (n = 75 sequences) clade are shown. Mutation positions are numbered according to the reference Fermon strain (GenBank accession no. AY426531) and annotated by the corresponding viral proteins (structural proteins VP2, VP3, and VP1 and nonstructural proteins 2A, 2C, 3A, and 3D). A, alanine; D, aspartate; E, glutamate; G, glycine; H, histidine; I, isoleucine; K, lysine; M, methionine; N, asparagine; R, arginine; S, serine; T, threonine; V, valine; VP, viral protein; Y, tyrosine.

B3-derived lineages were predominantly associated with recent EV-D68 outbreaks in Europe; an A2-derived lineage dominated the second part of the 2024 outbreak and was detected elsewhere in Europe, in North America, and in Asia. Since 2016, the main circulation of clade A2 in France had been observed only in 2018 (51% of EV-D68 infection), mainly in adults (*4*). Despite a new circulating lineage, the previously reported association of infection by the A2 subgenotype with adult patients (*4*,*29*) remained true in 2024 (*12*). Genomes of 2024 A2 viruses were genetically close to strains that simultaneously circulated in Italy, where the median age of cases with EV-D68 A2 lineage was 10-fold higher than that of cases with B3 subgenotype (*9*). Extensive genomic surveillance demonstrated periodic replacement of B3-derived lineages between epidemics and rapid renewal of epitopes in capsid proteins (particularly the BC and DE loops, and C-terminal end of the VP1 protein), potentially associated with antigenic evolution (*1*,*8*,*10*–*12*,*29*). Meanwhile, evolution of A2 viruses was also ongoing (*11*,*12*); numerous amino acid mutations accumulated that concentrate in VP1 surface loops and adjacent VP2 and VP3 surfaces, where neutralizing epitopes and receptor interaction cluster (*15*,*29*). In addition to functional implications, such as changes in receptor binding and increased transmissibility, those mutations could also have immunologic consequences that could explain the age–subgenotype association (*4*,*9*,*29*,*30*). The amino acid changes in the surface of recent A2 viruses could reduce cross-clade immunity (*31*) and foster reinfection of adults. Seroprevalence studies in adults that include strains from different subgenotypes are needed to determine the level of immunity to different and recent viruses. Adults could also be more susceptible to infection because of underlying conditions or specific mutations elsewhere in the

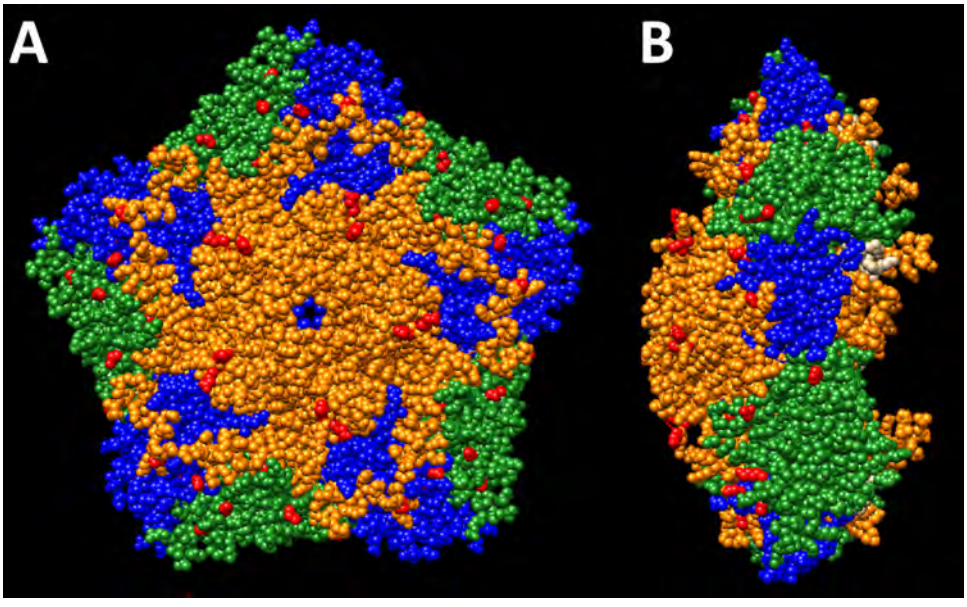


**Figure 9.** Structural models of the capsid pentamer of the newly identified A2 clade of enterovirus D68, from report on national surveillance of enterovirus upsurge, France, 2024. On the basis of a consensus sequence of the newly identified A2 clade, we reconstructed pentameric capsid subunit using AlphaFold (https://alphafoldserver.com) and validated it by structural comparison with the crystal structure of the reference enterovirus D68 strain (structure 4WM8; RCSB Protein Data Bank, https://www.rcsb.org). A) Outer surface view. B) Side view. Structural models of the capsid pentamer are shown with proteins colored as follows: orange, viral protein (VP) 1; green, VP2; blue, VP3; white, VP4. Red indicates amino acid substitutions.

viral genome promoting more severe infection or inflammation, leading them to seek medical attention.

The continued and sustained circulation of EV-D68 in recent years underlines the importance of comprehensive genomic surveillance of EV-D68 to track the spread of different subgenotypes and to understand their geographic distribution; Nextclade (https://github.com/enterovirus-phylo/nextclade_d68) is one useful tool for EV-D68 analysis (*29*,*32*). Adequate virologic and clinical surveillance, regardless of age and season, is essential to give a complete picture of the epidemiologic and clinical spectrum of EV-D68 and other emerging enterovirus type–associated infections.

Additional members of Enterovirus Surveillance Network who contributed data: Laurent Andreoletti, Véronique Brodard (CHU Reims, Laboratoire de Virologie, Reims, France); Christelle Auvray, Alexis de Rougemont (CHU Dijon Bourgogne, Laboratoire de Virologie-Sérologie, Dijon, France); Thomas Bourlet, Sylvie Pillet (CHU de Saint-Etienne, Service des agents infectieux et d'hygiène, Saint-Etienne, France); Eline Bremond, Léa Pilorge (CHU de Brest, Unité de Virologie, Brest, France); Céline Bressollette Bodin, Thomas Drumel (CHU Nantes, Service de Virologie, Hôtel Dieu, Nantes, France); Marianne Burgard, Nicolas Veyrenche (Hôpital Necker-Enfants Malades, AP-HP, Laboratoire de Virologie, Paris, France); Sonia Burrel, Mathilde Gay (GH Pellegrin, Université de Bordeaux, Service de Virologie, CNRS UMR 5234, Fundamental Microbiology and Pathogenicity, Bordeaux, France); Anne Cady (CH Brocéliande Atlantique, Laboratoire de Biologie Médicale, Vannes, France); Cyril Debuysschere, Mouna Lazrek (CHU de Lille, Laboratoire de Virologie ULR, Univ Lille, Lille, France); Laura Djamdjian, Soraya Metref (CH de Gonesse, Laboratoire de Biologie Médicale, Gonesse, France); Violaine Doat, Charlotte Tellini (CH Bourgoin-Jallieu, Laboratoire de Biologie Médicale, Bourgoin-Jallieu, France); Joséphine Dorin (CH Antibes-Juan-les-Pins, Laboratoire de Biologie médicale, Antibes, France); Alexandra Ducancelle, Caroline Lefeuvre (CHU d'Angers, Laboratoire de Virologie, Département de Biologie des Agents Infectieux, Angers, France); Ilka Engelmann, Vincent Foulongne (CHU Montpellier, Site Unique de Biologie, Laboratoire de Virologie, Montpellier, France); Eric Farfour (Hôpital Foch, Service de biologie clinique, Suresnes, France); Agathe Francart, Caroline Vaudron (CH Libourne Robert Moulin, Laboratoire de Biologie Médicale, Libourne, France); Floriane Gallais, Morgane Solis (CHU Strasbourg, Laboratoire de virologie, Strasbourg, France); Magali Garcia, Nicolas Leveque (CHU de Poitiers, Laboratoire de virologie et mycobactériologie, Poitiers, France); Catherine Gaudy-Graffin, Lynda Handala (CHRU de Tours, Unité Emergence, Service de bactériologie, virologie et hygiène hospitalière, Tours, France); Juliette Gillon (CH Frejus, CHI Frejus, Frejus, France); Geraldine Gonfrier (CHU de Nice, Laboratoire de Virologie Archet 2, Nice, France); Marie Gueudin, Véronique Lemee (CHU Rouen, Laboratoire de Virologie, Rouen, France); Pascal Guiet (CH Montargis, Laboratoire de Biologie Médicale, Amilly, France); Clémence Guillaume, Victoria Marie (CHU d'Orléans, Laboratoire de Microbiologie, Orléans, France); Anne Christine Jaouen, David Leyssene (CH de la Côte Basque, Laboratoire de Biologie médicale, Bayonne, France); Marine Jourdain (Hôpitaux Nord-Ouest, Villefranche sur Saône, France); Gisèle Lagathu, Vincent Thibault (CHU Rennes, Laboratoire de Virologie, Rennes, France); Sylvie Larrat, Aurélie Truffot (CHU Grenoble-Alpes, Laboratoire de Virologie, Institut de Biologie et Pathologie, Grenoble, France); Quentin Lepiller, Solène Marty-Quinternet (CHU de Besançon, Laboratoire de Virologie, Besançon, France); Anne-Sophie L'honneur, Alice-Andrée Mariaggi (CHU Cochin, AP-HP, Service de virologie, Paris); Marie Louchet-Ducoroy (CHU Amiens, Laboratoire de Virologie, Amiens, France); Léa Luciani (CHU Marseille, Laboratoire de virologie aigue et tropicale, LAI AP-HM, Marseille, France); Sarah Mafi, Sylvie Rogez (CHU Limoges, Laboratoire de Virologie, Limoges, France); Stéphanie Marque Juillet, Alexandra Teboul (CH de Versailles, Laboratoire de Biologie Médicale, Le Chesnay, France); Yanne Michel, Aurélie Schnuriger (CHU St Antoine-Tenon-Trousseau, AP-HP, Laboratoire de Virologie, Paris); Marion Migueres, Pauline Tremeaux (CHU de Toulouse, Laboratoire de Virologie, Toulouse, France); Menel Mohamedi, Maud Salmona (Hôpital Saint Louis, AP-HP, Laboratoire de Virologie, Paris); Jean-Benjamin Murat (CH de Roanne, Laboratoire de Biologie médicale, Roanne, France); Emeline Riverain (CH François Quesnay, Laboratoire de Biologie médicale, Mantes la Jolie, France); Cécile Schanen (CHU de Caen, Service de Virologie, Caen, France); Evelyne Schvoerer, Véronique Venard (CHRU de Nancy, Laboratoire de virologie, Vandeouvre-les-Nancy, France); Anne-Lise Toyer (CHI Toulon, Laboratoire de Biologie Médicale, Toulon, France); Nicolas Traversier (CHU Réunion, Laboratoire de microbiologie, St Denis, France).

**Acknowledgments**

We thank Adeline Duard, Laetitia Gardette and Floriane Serre (NRL1) and Delphine Falcon, Emmanuelle Groscarret, Laure Zanghellini, Isabelle Rousset, Thibaut Corsin, Eva Oddoux, and Quentin Semanas (NRL2 and GenEPII sequencing platform) for helpful technical assistance in EV-D68 screening and genome sequencing. We thank all the medical and technical staff involved in

the enterovirus surveillance within each laboratory of the Enterovirus Surveillance Network. We thank the Mésocentre Clermont Auvergne University for providing computing and storage resources.

This research received no external funding. The National Reference Center for Enteroviruses and Parechoviruses is supported by an annual grant from the national public health institute (Santé publique France).

## About the Author

Dr Jeannoël is a virologist at the National Center for Enteroviruses and Parechoviruses at the Hospices Civils de Lyon, Lyon, France. Her research interests are enterovirus and parechovirus diagnosis and epidemiology.

## References

1. Imamura T, Okamoto M, Nakakita S, Suzuki A, Saito M, Tamaki R, et al. Antigenic and receptor binding properties of enterovirus 68. J Virol. 2014;88:2374–84. https://doi.org/10.1128/JVI.03070-13
2. Midgley CM, Jackson MA, Selvarangan R, Turabelidze G, Obringer E, Johnson D, et al. Severe respiratory illness associated with enterovirus D68—Missouri and Illinois, 2014. MMWR Morb Mortal Wkly Rep. 2014;63:798–9.
3. Holm-Hansen CC, Midgley SE, Fischer TK. Global emergence of enterovirus D68: a systematic review. Lancet Infect Dis. 2016;16:e64–75. https://doi.org/10.1016/S1473-3099(15)00543-5
4. Duval M, Mirand A, Lesens O, Bay JO, Caillaud D, Gallot D, et al. Retrospective study of the upsurge of enterovirus D68 Clade D1 among adults (2014–2018). Viruses. 2021;13:1607. https://doi.org/10.3390/v13081607
5. Murphy OC, Messacar K, Benson L, Bove R, Carpenter JL, Crawford T, et al.; AFM Working Group. Acute flaccid myelitis: cause, diagnosis, and management. Lancet. 2021;397:334–46. https://doi.org/10.1016/S0140-6736(20)32723-9
6. Messacar K, Matzinger S, Berg K, Weisbeck K, Butler M, Pysnack N, et al. Multimodal surveillance model for enterovirus D68 respiratory disease and acute flaccid myelitis among children in Colorado, USA, 2022. Emerg Infect Dis. 2024;30:423–31. https://doi.org/10.3201/eid3003.231223
7. Whitehouse ER, Lopez A, English R, Getachew H, Ng TFF, Emery B, et al. Surveillance for acute flaccid myelitis—United States, 2018–2022. MMWR Morb Mortal Wkly Rep. 2024;73:70–6. https://doi.org/10.15585/mmwr.mm7304a1
8. Simoes MP, Hodcroft EB, Simmonds P, Albert J, Alidjinou EK, Ambert-Balay K, et al. Epidemiological and clinical insights into the enterovirus D68 upsurge in Europe 2021–2022 and emergence of novel B3-derived lineages, ENPEN Multicentre Study. J Infect Dis. 2024;230:e917–28. https://doi.org/10.1093/infdis/jiae154
9. Pariani E, Piralla A, Pellegrinelli L, Giardina F, Porrello VN, Romano G, et al.; Respiratory Viruses Pandemic Preparedness Group Lombardy. Enhanced laboratory surveillance of respiratory infection disclosed the rapid rise of enterovirus D68 cases, northern Italy, August to September 2024. Euro Surveill. 2024;29:2400645. https://doi.org/10.2807/1560-7917.ES.2024.29.41.2400645
10. Benschop KS, Albert J, Anton A, Andrés C, Aranzamendi M, Armannsdóttir B, et al. Re-emergence of enterovirus D68 in Europe after easing the COVID-19 lockdown, September 2021. Euro Surveill. 2021;26:2100998. https://doi.org/10.2807/1560-7917.ES.2021.26.45.2100998
11. Hirvonen A, Johannesen CK, Simmonds P, Fischer TK, Harvala H, Benschop KSM, et al.; ENPEN study collaborators. Sustained circulation of enterovirus D68 in Europe in 2023 and the continued evolution of enterovirus D68 B3-lineages associated with distinct amino acid substitutions in VP1 protein. J Clin Virol. 2025;178:105785. https://doi.org/10.1016/j.jcv.2025.105785
12. Andrés C, Prats-Méndez I, Midgley S, Berginc N, González-Sánchez A, Johannesen CK, et al. Circulation patterns, genetic diversity, and public health implications of enterovirus D68, Europe, 2014-2024. Emerg Infect Dis. 2026;32:491–9. https://doi.org/10.3201/eid3204.251022
13. Fall A, Han L, Abdullah O, Norton JM, Eldesouki RE, Forman M, et al. An increase in enterovirus D68 circulation and viral evolution during a period of increased influenza like illness, the Johns Hopkins Health System, USA, 2022. J Clin Virol. 2023;160:105379. https://doi.org/10.1016/j.jcv.2023.105379
14. Garcia-Pedemonte D, Carcereny A, Andrés C, Antón A, Pérez I, Blanco A, et al. Unveiling the enterovirus diversity in Barcelona, Spain (2020–2024) through wastewater and clinical surveillance. Emerg Microbes Infect. 2025;14:2589547. https://doi.org/10.1080/22221751.2025.2589547
15. Fall A, Norton JM, Abdullah O, Pekosz A, Klein E, Mostafa HH. Enhanced genomic surveillance of enteroviruses reveals a surge in enterovirus D68 cases, the Johns Hopkins Health System, Maryland, 2024. J Clin Microbiol. 2024:63:e00469-25. https://doi.org/10.1128/jcm.00469-25
16. Hadfield J, Megill C, Bell SM, Huddleston J, Potter B, Callender C, et al. Nextstrain: real-time tracking of pathogen evolution. Bioinformatics. 2018;34:4121–3. https://doi.org/10.1093/bioinformatics/bty407
17. Schuffenecker I, Mirand A, Josset L, Henquell C, Hecquet D, Pilorgé L, et al. Epidemiological and clinical characteristics of patients infected with enterovirus D68, France, July to December 2014. Euro Surveill. 2016;21. https://doi.org/10.2807/1560-7917.ES.2016.21.19.30226
18. Kramer R, Sabatier M, Wirth T, Pichon M, Lina B, Schuffenecker I, et al. Molecular diversity and biennial circulation of enterovirus D68: a systematic screening study in Lyon, France, 2010 to 2016. Euro Surveill. 2018;23:1700711. https://doi.org/10.2807/1560-7917.ES.2018.23.37.1700711
19. National Reference Center for Enteroviruses and Parechoviruses. Activity reports. 2026 [cited 2026 May 26]. https://www.chu-clermontferrand.fr/liste-services/centre-national-de-reference-des-enterovirus-et-parechovirus/rapports-dactivites
20. Savolainen C, Blomqvist S, Mulders MN, Hovi T. Genetic clustering of all 102 human rhinovirus prototype strains: serotype 87 is close to human enterovirus 70. J Gen Virol. 2002;83:333–40. https://doi.org/10.1099/0022-1317-83-2-333
21. Linsuwanon P, Payungporn S, Samransamruajkit R, Posuwan N, Makkoch J, Theanboonlers A, et al. High prevalence of human rhinovirus C infection in Thai children with acute lower respiratory tract disease. J Infect. 2009;59:115–21. https://doi.org/10.1016/j.jinf.2009.05.009
22. Poelman R, Schölvinck EH, Borger R, Niesters HGM, van Leer-Buter C. The emergence of enterovirus D68 in a Dutch university medical center and the necessity for routinely screening for respiratory viruses. J Clin Virol. 2015;62:1–5. https://doi.org/10.1016/j.jcv.2014.11.011
23. Destras G, Sabatier M, Bal A, Simon B, Semanas Q, Regue H, et al. Comparison between metatranscriptomics

and viral metagenomics, 16S, and host transcriptomics for comprehensive profiling of the respiratory microbiome and host response. Front Microbiol. 2026;16:1685035. https://doi.org/10.3389/fmicb.2025.1685035
24. Li F, Lu RJ, Zhang YH, Shi P, Ao YY, Cao LF, et al. Clinical and molecular epidemiology of enterovirus D68 from 2013 to 2020 in Shanghai. Sci Rep. 2024;14:2161. https://doi.org/10.1038/s41598-024-52226-w
25. Lau SKP, Yip CCY, Zhao PSH, Chow WN, To KKW, Wu AKL, et al. Enterovirus D68 infections associated with severe respiratory illness in elderly patients and emergence of a novel clade in Hong Kong. Sci Rep. 2016;6:25147. https://doi.org/10.1038/srep25147
26. Mallet MC, Trottier S, Baz M, Redah I, Duvvuri VR, Kozak R, et al. Clinical presentation of Enterovirus D68 in adults with acute respiratory infections consulting emergency departments in Quebec, Canada. IJID Reg. 2025;15:100669. https://doi.org/10.1016/j.ijregi.2025.100669
27. Leser JS, Frost JL, Wilson CJ, Rudy MJ, Clarke P, Tyler KL. VP1 is the primary determinant of neuropathogenesis in a mouse model of enterovirus D68 acute flaccid myelitis. J Virol. 2024;98:e00397–24. https://doi.org/10.1128/jvi.00397-24
28. Helfferich J, Neuteboom RF, de Lange MMA, Benschop KSM, Van Leer-Buter CC, Meijer A, et al. Pediatric acute flaccid myelitis: evaluation of diagnostic criteria and differentiation from other causes of acute flaccid paralysis. Eur J Paediatr Neurol. 2023;44:28–36. https://doi.org/10.1016/j.ejpn.2023.03.002
29. Hodcroft EB, Dyrdak R, Andrés C, Egli A, Reist J, García Martínez De Artola D, et al. Evolution, geographic spreading, and demographic distribution of enterovirus D68. PLOS Pathog. 2022;18:e1010515. https://doi.org/10.1371/journal.ppat.1010515
30. Mengual-Chuliá B, Tamayo-Trujillo R, Mira-Iglesias A, Cano L, García-Esteban S, Ferrús ML, et al.; VAHNSI network. Enterovirus D68 disease burden and epidemiology in hospital-admitted influenza-like illness, Valencia region of Spain, 2014–2020 influenza seasons. J Med Virol. 2024;96:e29810. https://doi.org/10.1002/jmv.29810
31. Harrison CJ, Weldon WC, Pahud BA, Jackson MA, Oberste MS, Selvarangan R. Neutralizing antibody against enterovirus D68 in children and adults before 2014 outbreak, Kansas City, Missouri, USA. Emerg Infect Dis. 2019;25:585–8. https://doi.org/10.3201/eid2503.180960
32. Aksamentov I, Roemer C, Hodcroft E, Neher R. Nextclade: clade assignment, mutation calling and quality control for viral genomes. J Open Source Softw. 2021;6:3773. https://doi.org/10.21105/joss.03773

Address for correspondence: Audrey Mirand, CHU Clermont-Ferrand, Centre National de Référence des Entérovirus et Parechovirus, 58 Rue Montalembert, 63003 Clermont-Ferrand, France; email: amirand@chu-clermontferrand.fr

# Clinical Predictors of Fatal Outcomes from Human Leptospirosis, Thailand, 2015–2024

Umaporn Limothai, Nathan E. Stone, Sasipha Tachaboon, Janejira Dinhuzen, Jason W. Sahl, Theerapon Sukmark, Chayomon Dokpong, David M. Wagner, David A. Haake, Nattachai Srisawat

Early predictors of fatal leptospirosis and the role of pathogen lineages remain poorly defined, limiting clinical risk stratification, genomic surveillance, and public health response in leptospirosis-endemic settings. We conducted a multicenter prospective cohort study of hospitalized patients with suspected leptospirosis in Thailand during 2015–2024. Among 459 patients with laboratory-confirmed cases, 25 (5.4%) died during hospitalization. Older age, higher total bilirubin, and higher leptospiremia were independently associated with in-hospital death, and a combined model demonstrated good discriminatory performance. We performed targeted amplicon sequencing analysis directly on clinical samples and whole-genome sequencing on available isolates. Genomic analysis identified *Leptospira interrogans* as the predominant species; clonal group 272 sequence type 34 was the predominant lineage and was observed in all patients with fatal cases for whom genomic data were available. Our findings support integration of clinical predictors and pathogen load for early risk stratification and highlight the potential value of genomic surveillance in leptospirosis-endemic settings.

Leptospirosis is a widespread zoonotic disease caused by pathogenic *Leptospira* bacteria species. It is responsible for an estimated 1.03 million cases and 58,900 deaths annually worldwide and has a mean case-fatality rate (CFR) of ≈6.8% (*1*). The disease prevalence is highest in tropical regions, where environmental exposure and occupational risk factors contribute to transmission through contaminated water, soil, and animal reservoirs (*2*–*4*). Despite its global impact, leptospirosis remains a neglected tropical disease with substantial public health and socioeconomic burdens in resource-limited settings (*5*). In Thailand, leptospirosis remains endemic, particularly among agricultural workers (*6*), and continues to cause severe illness characterized by multiorgan failure and high CFRs. National surveillance data from 2013 through 2022 reported an overall CFR of 1.46% (*7*), and our previous multicenter cohort of hospitalized patients with laboratory-confirmed cases documented a 7% mortality rate with frequent multiorgan dysfunction (*8*). Those findings highlight the substantial clinical burden of leptospirosis in endemic settings.

The wide clinical spectrum of leptospirosis probably is influenced by both host factors and the genomic diversity of *Leptospira* strains. Prior studies have shown that host clinical and inflammatory responses are major determinants of disease severity (*9*–*17*). In contrast, pathogen-related determinants, such as the contributions of specific *Leptospira* species, strains, and lineages, have been less well characterized. Infecting *Leptospira* species and serogroups or serovars have been associated with clinical syndromes (*18*), but severe disease has been reported across multiple serogroups, and our previous multicenter cohort in Thailand found no statistically significant difference

Author affiliations: Chulalongkorn University Faculty of Medicine, Center of Excellence in Critical Care Nephrology, Bangkok, Thailand (U. Limothai, S. Tachaboon, J. Dinhuzen, N. Srisawat); King Chulalongkorn Memorial Hospital–Thai Red Cross Society, Excellence Center for Critical Care Nephrology, Bangkok (U. Limothai, S. Tachaboon, J. Dinhuzen, N. Srisawat); Northern Arizona University Pathogen and Microbiome Institute, Flagstaff, Arizona, USA (N.E. Stone, J.W. Sahl, D.M. Wagner); Thungsong Hospital, Nakhon Si Thammarat, Thailand (T. Sukmark); Khukhan Hospital, Sisaket, Thailand (C. Dokpong); Veterans Affairs Greater Los Angeles Healthcare System, Los Angeles, California, USA (D.A. Haake); University of California David Geffen School of Medicine, Los Angeles (D.A. Haake); University of Pittsburgh School of Medicine, Pittsburgh, Pennsylvania, USA (N. Srisawat); Royal Society of Thailand Academy of Science Bangkok (N. Srisawat)

DOI: https://doi.org/10.3201/eid3207.260014

in serogroup distribution between severe and nonsevere leptospirosis (*8*). That finding suggests that serogroup alone is insufficient to explain clinical phenotype and underscores the need to investigate lineage-level characteristics and host–pathogen interactions when studying severe disease. Recent molecular epidemiologic work has identified substantial genetic heterogeneity within *L. interrogans*; some lineages showed distinct geographic distributions (*18*,*19*) and potential clinical associations (*20*,*21*). However, direct evidence linking specific bacterial lineages to severe or fatal disease remains limited. A clearer understanding of pathogen diversity and how it interacts with host responses is important for improving genomic surveillance, targeted risk stratification, and public health response in endemic settings.

To address those gaps, we aimed to identify clinical, laboratory, and pathogen-load factors associated with in-hospital death in patients with confirmed leptospirosis. We also characterized *Leptospira* species and lineage diversity using targeted amplicon sequencing directly from clinical samples and whole-genome sequencing (WGS) of isolates. This integrated clinical and genomic approach is intended to improve risk prediction, inform genomic surveillance across animal reservoirs, and deepen understanding of pathogen diversity contributing to severe leptospirosis.

## Methods

### Study Design and Setting

We conducted a multicenter prospective cohort study of patients hospitalized with suspected leptospirosis during September 1, 2015–December 31, 2024, in Sisaket and Nakhon Si Thammarat, 2 leptospirosis-endemic provinces in Thailand (Appendix 1, https://wwwnc.cdc.gov/EID/article/32/7/26-0014-App1.pdf; Appendix 2, https://wwwnc.cdc.gov/EID/article/32/7/26-0014-App1.xlsx). We used demographic, clinical, laboratory, and outcome data that were collected during hospitalization. The primary objectives were to identify predictors of in-hospital death and to characterize infecting *Leptospira* species and lineages among laboratory-confirmed cases.

### Case Definition and Laboratory Confirmation

We defined laboratory-confirmed leptospirosis as ≥1 positive result by *lipL32* quantitative PCR (qPCR), culture, or microscopic agglutination test (MAT), as previously described (*22*). We included clinically suspected but non–laboratory-confirmed patients from the same cohort as a comparator group for clinical outcome analyses. We defined severe leptospirosis by death, intensive care unit (ICU) admission, mechanical ventilation, pulmonary hemorrhage, or organ failure on the basis of a modified Sequential Organ Failure Assessment score (*23*–*25*) (Appendix 1).

### DNA Extraction and qPCR Detection

We extracted total DNA from whole blood or urine specimens. We detected *Leptospira* DNA by using qPCR targeting the *lipL32* gene, as previously described (*26*) (Appendix 1).

### Genomic Subset and Sequencing Workflow

Among 473 laboratory-confirmed cases, to ensure sufficient bacterial DNA for genotyping we selected DNA extracts from 93 whole blood samples and 2 urine samples with *lipL32* qPCR cycle threshold values <35 for targeted amplicon sequencing by using the *Leptospira* AmpSeq (amplicon sequencing) assay (*27*). To minimize selection bias, we randomly selected samples meeting the cycle threshold with clinical severity blinded to the laboratory team. The selection included qPCR-positive patients across the clinical severity spectrum. In parallel, we performed WGS on 13 *L. interrogans* whole blood isolates. Seven patients had both AmpSeq and culture isolates available, enabling direct cross-validation between methods. Baseline characteristics of the genotyped subset did not meaningfully differ from the overall cohort, supporting the representativeness of the subset. We have summarized the study design and sample selection (Appendix 1 Figure 1). Phylogenetic analyses included publicly available *L. interrogans* reference genomes representing diverse lineages, together with *L. kirschneri* as an outgroup, to provide evolutionary context for lineage assignment (Appendix 1).

### Statistical Analysis

We performed group comparisons, logistic regression, receiver operating characteristic analysis, and bootstrap internal validation by using standard methods (Appendix 1). We excluded 14 laboratory-confirmed cases with missing clinical data from the primary analysis.

## Results

### Study Population and Case Confirmation

We screened a total of 641 patients with suspected leptospirosis (Appendix 1 Figure 1). Of those, 473 (73.8%) were laboratory-confirmed based on ≥1 positive diagnostic test: blood qPCR (385 [81.4%]), urine qPCR (195 [41.2%]), culture (22 [5.1%]), or MAT (179 [38.3%]). After excluding 14 confirmed cases because

of missing clinical data, 459 patients remained, and we included them in the primary analysis. Among those, 434 (94.6%) survived and 25 (5.4%) died during hospitalization, corresponding to an overall in-hospital CFR of 5.4% among patients with laboratory-confirmed cases.

The median age of the study population was 47 years, and most patients were male (82.9% vs. 17.1% female) (Appendix 1 Table 1). Patients who died were significantly older than survivors (median 60 years vs. 47 years; p = 0.007). The median time from fever onset to hospital admission was 3 days in both groups. Most participants were agricultural workers (70.6%), and the percentage was significantly higher among patients with fatal cases compared with survivors (88.0% vs. 69.6%; p = 0.049). Flood exposure was common (85.0% overall) and similar between groups. Active smoking also was frequent in the cohort (45.2%) but did not differ significantly between survivors and patients with fatal cases (45.4% vs. 41.7%; p = 0.720). The prevalence of other underlying conditions was low and comparable between groups. At admission, patients with fatal cases had markedly lower blood pressures compared with survivors, including lower systolic blood pressure (median 93.0 vs. 110.0 mm Hg), diastolic blood pressure (53.0 vs. 64.0 mm Hg), and mean arterial pressure (66.7 vs. 80.0 mm Hg). Most clinical symptoms were comparable between groups, although headache was less common among patients with patients with fatal cases (p = 0.046).

Laboratory findings revealed pronounced abnormalities among patients with fatal cases, including more severe thrombocytopenia (platelets 30.0 vs. 128.0 × $10^3$/μL; p<0.001), higher levels of blood urea nitrogen (51.0 vs. 17.0 mg/dL; p<0.001) and creatinine (4.6 vs. 1.2 mg/dL; p<0.001), and markedly reduced estimated glomerular filtration rate (17.6 vs. 71.6 mL/min/1.73 $m^2$; p<0.001). Patients with fatal cases also exhibited more severe hepatic dysfunction, having significantly higher total bilirubin (4.1 vs. 1.1 mg/dL; p<0.001), direct bilirubin (4.2 vs. 0.5 mg/dL; p<0.001), and elevated aspartate aminotransferase levels (141.0 vs. 53.0 U/L; p<0.001) and lower serum albumin (2.6 vs. 3.4 g/dL; p<0.001) and total protein levels (6.4 vs. 6.9 g/dL; p = 0.004). We also observed lower bicarbonate levels in patients with fatal cases (17.0 vs. 23.0 mEq/L; p<0.001). Regarding diagnostics, a higher proportion of patients with fatal cases had positive blood qPCR (96.0% vs. 73.5%; p = 0.012) and significantly higher leptospiremia levels (median 4.5 vs. 2.9 $\log_{10}$ copies/mL, p<0.001).

**Table 1.** Clinical outcomes of 459 hospitalized patients with confirmed leptospirosis, Thailand, 2015–2024*

| Outcome | No. (%) patients |
|---|---|
| ICU admission | 87 (19.3) |
| Mechanical ventilation | 54 (11.9) |
| Pulmonary hemorrhage | 48 (10.6) |
| Cardiovascular SOFA ≥3† | 84 (18.6) |
| Coagulation SOFA ≥3† | 113 (25.1) |
| Renal SOFA ≥3† | 75 (16.7) |
| Hepatic SOFA ≥3† | 43 (9.8) |
| Multiorgan failure | 105 (22.9) |
| Severe leptospirosis‡ | 197 (43.7) |
| In-hospital death§ | 25 (5.4) |

*ICU, intensive care unit; SOFA, Sequential Organ Failure Assessment score.
†Organ-specific SOFA subscores ≥3 indicate severe dysfunction.
‡Defined as death, ICU admission, mechanical ventilation, pulmonary hemorrhage, or organ failure (modified SOFA ≥3).
§Defined as death during hospitalization for leptospirosis.

### Clinical Outcomes and Organ Dysfunction

Among 459 hospitalized patients with confirmed leptospirosis, acute complications and organ dysfunction were common (Table 1). Nearly 1 in 5 patients required ICU admission (19.3%), and 54 patients (11.9%) required mechanical ventilation. Pulmonary hemorrhage occurred in 48 patients (10.6%).

Organ-specific severe dysfunction, defined as modified Sequential Organ Failure Assessment subscores ≥3, also was frequent: cardiovascular dysfunction in 84 (18.6%) patients, coagulation dysfunction in 113 (25.1%), renal dysfunction in 75 (16.7%), and hepatic dysfunction in 43 (9.8%). We documented multiorgan failure in 105 (22.9%) patients. Overall, 197 (43.7%) patients met criteria for severe leptospirosis. The overall in-hospital CFR was 5.4% (25/459 patients). Clinically suspected but non–laboratory-confirmed patients from the same cohort generally had less severe outcomes, including a lower in-hospital CFR (3.0%) (Appendix 1 Table 2).

For patients with fatal cases, length of hospitalization varied widely, reflecting both early and late deaths (Appendix 2 Table 1). The most frequently documented causes of death included septic shock, pulmonary hemorrhage, acute respiratory failure, metabolic acidosis, acute kidney injury, and disseminated intravascular coagulation.

### Independent Predictors of In-Hospital Death in Leptospirosis Case-Patients

In the univariate analyses (Table 2), several admission variables were significantly associated with in-hospital death. Those variables included older age, lower mean arterial pressure, lower platelet count, higher creatinine, higher total bilirubin, lower albumin, lower bicarbonate, and higher leptospiremia (p<0.001 for all).

**Table 2.** Factors associated with in-hospital death in patients with confirmed leptospirosis, Thailand, 2015–2024

| Variable | Unadjusted OR (95% CI) | p value | Adjusted OR (95% CI) | p value |
|---|---|---|---|---|
| Age | 1.03 (1.01–1.06) | 0.013 | 1.05 (1.01–1.09) | 0.022 |
| Sex | 1.09 (0.36–3.26) | 0.880 | | |
| Days of fever at admission | 0.95 (0.77–1.16) | 0.604 | | |
| Mean arterial pressure | 0.95 (0.92–0.98) | <0.001 | 0.99 (0.96–1.02) | 0.446 |
| Platelet count | 0.75 (0.66–0.86) | <0.001 | 0.99 (0.97–1.00) | 0.056 |
| Creatinine level | 1.34 (1.16–1.54) | <0.001 | 0.97 (0.75–1.25) | 0.791 |
| Total bilirubin | 1.11 (1.05–1.18) | <0.001 | 1.09 (1.01–1.19) | 0.039 |
| Albumin level | 0.21 (0.10–0.43) | <0.001 | 0.57 (0.20–1.65) | 0.304 |
| Bicarbonate level | 0.84 (0.77–0.91) | <0.001 | 0.91 (0.80–1.04) | 0.158 |
| Leptospiremia | 2.12 (1.54–2.91) | <0.001 | 1.87 (1.26–2.75) | 0.002 |

*Variables with p<0.10 in univariate analysis were considered for inclusion in the multivariable model. OR, odds ratio.

In the multivariable logistic regression model, age, total bilirubin, and leptospiremia remained independently associated with in-hospital death. Each 1-year increase in age was associated with a 5% increase in the odds of death (adjusted OR [aOR] 1.05 [95% CI 1.01–1.09]; p = 0.022). Higher total bilirubin on admission also was associated with increased death (aOR 1.09 [95% CI 1.01–1.19]; p = 0.039). Of note, higher leptospiremia was a strong independent predictor of death; each 1 $\log_{10}$ increase in bacterial load increased the odds of death by nearly 2-fold (aOR 1.87 [95% CI 1.26–2.75]; p = 0.002).

To further evaluate the discriminatory performance of these predictors, we performed receiver operating characteristic analysis. Age showed modest discrimination for in-hospital death (area under the curve [AUC] 0.66 [95% CI 0.56–0.77]; p = 0.003). Total bilirubin demonstrated good discrimination (AUC 0.79 [95% CI 0.70–0.88]; p<0.001), as did leptospiremia (AUC 0.78 [95% CI 0.67–0.88]; p<0.001). A combined model incorporating age, total bilirubin, and leptospiremia showed good discrimination (AUC 0.86 [95% CI 0.78–0.94]; p<0.001), outperforming each individual predictor. We summarized corresponding cutoff values and diagnostic performance metrics (Appendix 1 Tables 3). Bootstrap internal validation using 1,000 replications demonstrated stable regression coefficients and robust discrimination of the multivariable model incorporating age, total bilirubin, and leptospiremia.

### Secondary Analysis of Genomic Subset

To explore pathogen-related factors, we performed a secondary analysis in the subset of patients for whom genomic data were available. We conducted targeted amplicon sequencing on a total of 95 qPCR-positive clinical samples and conducted WGS on 13 *L. interrogans* isolates recovered from culture (Appendix 1 Figure 1). Because AmpSeq was applied directly to qPCR-positive clinical samples, we did not restrict lineage assignment to culturable isolates. We compared the characteristics of the genotyped subset with those of the overall cohort (Appendix 1 Table 4). We also summarized all metadata for all AmpSeq samples and characteristics of the sequenced isolates (Appendix 1 Table 5; Appendix 2 Tables 2). We analyzed 7 cases by using both AmpSeq and WGS, enabling direct comparison of lineage assignments. AmpSeq and WGS showed precise concordance; 6 of 7 paired samples yielded identical clonal-group classifications, and 1 sample showed evidence suggestive of mixed infection (Appendix 1 Tables 6).

In total, 84 clinical specimens yielded assignable genomic data, of which 82 (97.6%) were *L. interrogans* and 2 (2.4%) were *L. kirschneri*. Clonal-group classification identified 54 samples (64.3%) as *L. interrogans* clonal group 272 (CG272) and 30 samples (35.7%) as non-CG272. Multilocus sequence typing (MLST) and core genome MLST analyses assigned 11 of the 13 isolates to sequence type (ST) 34, corresponding to *L. interrogans* CG272, whereas 2 isolates assigned to other sequence types within *L. interrogans* (ST264 and ST76) (Appendix 1 Table 5).

Phylogenies generated from WGS data (Figure 1), high-coverage AmpSeq data (Figure 2), and the broader AmpSeq dataset (Appendix 1 Figure 2) for samples identified as *L. interrogans* yielded a consistent structure; most samples were assigned to a well-supported CG272 clade. All 9 patients with fatal cases represented in the genomic subset had isolate genomes that were located within the CG272 clade. CG272 and non-CG272 infections had broadly similar admission characteristics (Appendix 1 Tables 7). Mean leptospiremia was slightly higher among CG272 infections compared with non-CG272 infections (4.3 $\pm$ SD 1.1 versus 4.0 $\pm$ SD 1.1 $\log_{10}$ copies/mL; p = 0.198), although this difference was not statistically significant. We also examined the relationship between age and admission leptospiremia and found no significant correlation (Spearman $\rho$ = 0.048; p = 0.313).

Collectively, those results identify CG272 as the dominant *L. interrogans* lineage in the sequenced cohort and highlight that all genotyped patients with fatal cases with available genomic data were infected

with isolates that clustered within that clade. Although the sample size limits formal inference, this observation warrants further investigation in larger and more systematically sampled cohorts. Of note, our exploratory analysis of single-nucleotide polymorphisms (SNPs) specific to CG272 identified 6 nonsynonymous substitutions in putative virulence-associated genes (*28*), including *Leptospira* immunoglobulin-like protein B (Appendix 2 Table 3), an immunoglobulin-like protein associated with host interaction.

## Discussion

In this multicenter cohort of 459 hospitalized patients with laboratory-confirmed leptospirosis, acute complications were frequent: 19.3% required ICU admission, 11.9% required mechanical ventilation, and 22.9% developed multiorgan failure. The in-hospital CFR was 5.4%, close to the reported global mean CFR of 6.8% (*1*), suggesting that our cohort is broadly representative of severe hospitalized leptospirosis patients rather than patient populations with unusually mild or extreme disease. For comparison, clinically suspected but non–laboratory-confirmed patients from the same hospitals had a lower in-hospital mortality rate (3.0%), indicating that confirmed leptospirosis carries a disproportionate burden of severe outcomes among patients admitted with suspected leptospirosis.

We identified 3 admission variables (age, total bilirubin, and leptospiremia) that were independently associated with in-hospital death and together provided strong discriminatory performance (AUC

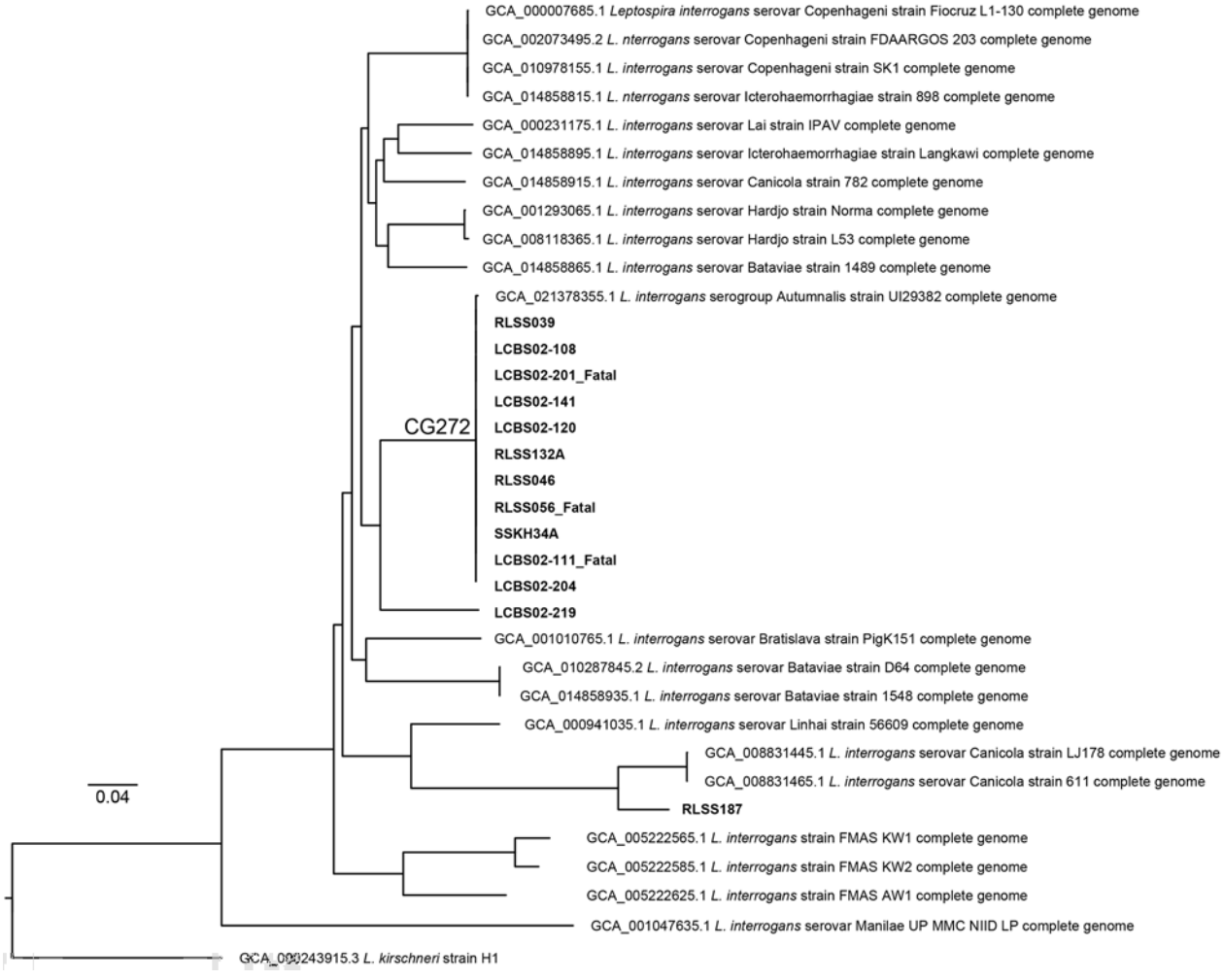


**Figure 1.** Whole-genome phylogeny of *Leptospira interrogans* isolates, Thailand, 2015–2024. Maximum-likelihood phylogenetic tree was generated by using 102,654 variable sites across a 3.9-Mb core genome of 13 *L. interrogans* isolates from this study (in bold font) plus 21 publicly available *L. interrogans* reference genomes. The tree was rooted with *L. kirschneri*. Eleven of the 13 isolates clustered within CG272, including 3 from patients with fatal cases. The remaining 2 isolates grouped outside CG272, indicating the presence of additional *L. interrogans* lineages in the region. Scale bar represents nucleotide substitutions per site. CG272, clonal group 272.

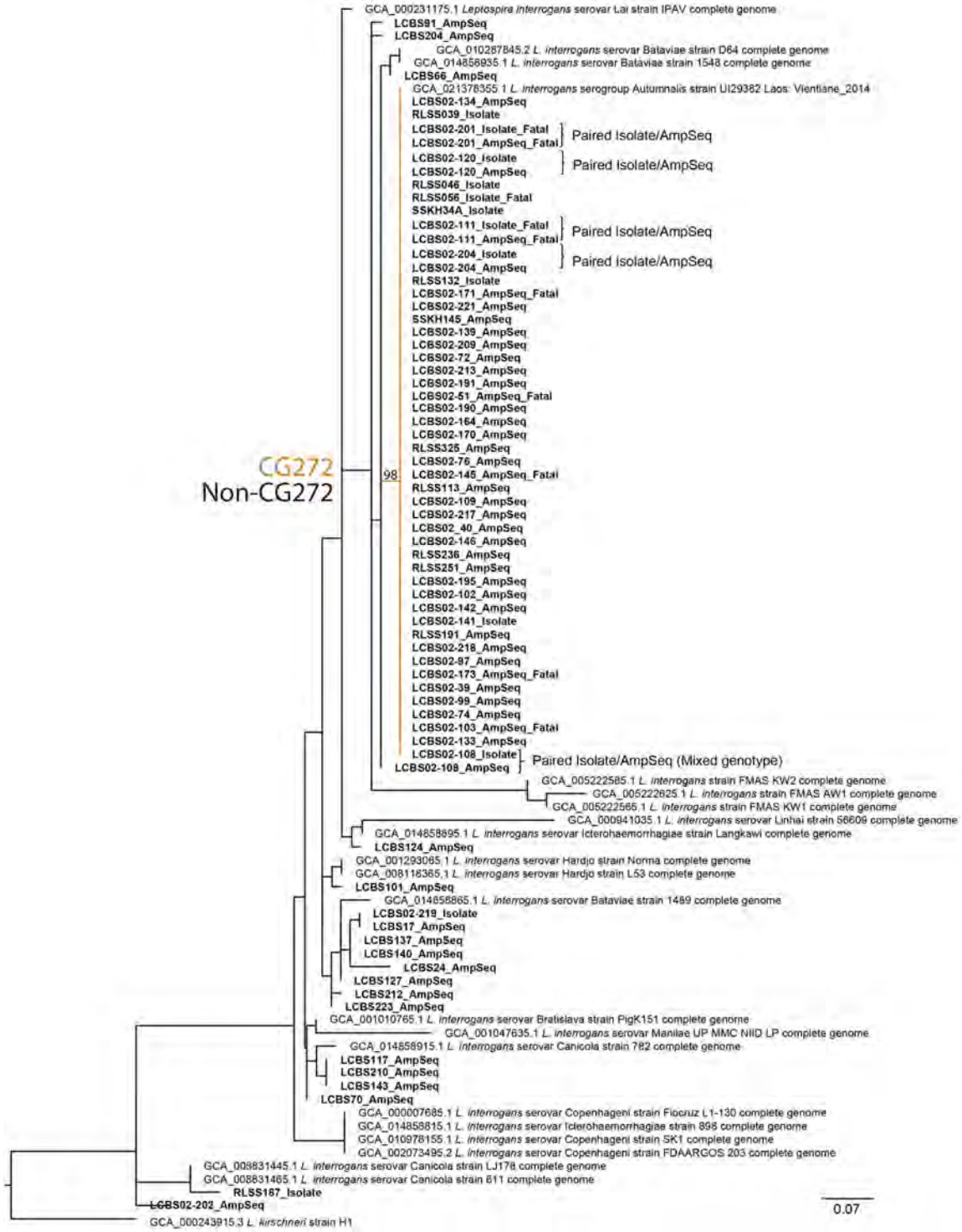


**Figure 2.** Phylogenetic analysis of *Leptospira interrogans* from AmpSeq (*27*) and isolate genome data, Thailand, 2015–2024. Maximum-likelihood phylogenetic tree was generated for high breadth of coverage AmpSeq samples (≥25 loci amplified with >10× coverage) by using 59 variable sites across a 1,813-nt core genome of 57 *L. interrogans* AmpSeq samples, 13 *L. interrogans* isolates, and 21 publicly available *L. interrogans* reference genomes. The tree was rooted with *L. kirschneri*. Five isolate or AmpSeq pairs demonstrate the phylogenetic concordance between methods. A major clade corresponding to CG272 contained most of the clinical samples, including those from several patients with fatal cases, whereas the remaining samples fell into other non-CG272 lineages. A bootstrap value of 98 supports placement in the CG272 clade. CG272 and non-CG272 lineages are color-coded in gold and black. Bold font indicates sequences generated during this study. Scale bar represents nucleotide substitutions per site. AmpSeq, amplicon sequencing; CG272, clonal group 272.

0.86). Older age (*9*,*11*,*29*,*30*) and hyperbilirubinemia (*31*,*32*) are well-established predictors of severe leptospirosis and death, and our findings confirm their prognostic value in a contemporary, multicenter cohort in Thailand. Leptospiremia at admission emerged as an important pathogen-derived predictor of in-hospital death in our cohort; each 1 $\log_{10}$ increase in bacterial load nearly doubled the odds of death, and leptospiremia alone provided good discrimination (AUC 0.78). These findings suggest that combining host vulnerability (age), early hepatic dysfunction (bilirubin), and pathogen load (leptospiremia) may provide a practical and biologically plausible approach for early risk stratification in hospitalized leptospirosis patients, particularly in endemic, resource-limited settings.

The relationship between quantitative leptospiremia and disease severity has been heterogeneous across previous studies. In Sri Lanka, a 16S rRNA–gene-based qPCR did not demonstrate a clear correlation between leptospiral load and clinical manifestations or outcome (*33*). By contrast, studies from New Caledonia (*34*) and Martinique (*35*) using *lfb1*-targeted qPCR found significantly higher early leptospiremia among patients with severe disease, and a Thailand multicenter cohort employing a *lipL32* assay reported higher baseline leptospiremia was independently associated with severe leptospirosis (*8*). Our data extend this latter body of work by showing that higher admission leptospiremia, measured by using a *lipL32*-based qPCR, also is a strong independent predictor of in-hospital death. Methodologic differences in qPCR platforms (including distinct gene targets, primer–probe sets, instruments, and sample types), along with variation in infecting *Leptospira* genotypes and timing of sampling, may partly explain the inconsistent associations reported across studies. Taken together, those data support early leptospiremia as a useful, although not universally consistent, marker of severity and highlight the importance of evaluating pathogen load in parallel with other factors when investigating determinants of severe and fatal leptospirosis. This integrated approach may help clarify whether observed differences in clinical outcomes reflect variation in pathogen load, genotype, or host–pathogen interactions.

Genomic characterization revealed limited species diversity; we identified *L. interrogans* in nearly all genotyped samples, consistent with prior reports from Southeast Asia and other endemic settings (*19*,*21*,*36*,*37*). Within *L. interrogans*, CG272 (ST34) was the predominant lineage and formed a well-supported clade in both amplicon and WGS analyses. We did not observe significant differences in early clinical severity or leptospiremia between CG272 and non-CG272 infections, but all patients with fatal cases in the genomic subset had infecting isolate genomes that clustered within CG272. The genomic subset in our study was small, so this observation should be interpreted cautiously, but lineage assignment was not based solely on cultured isolates, given that targeted amplicon sequencing also was applied directly to qPCR-positive and culture-negative clinical samples. This lineage has been linked to rodent reservoirs, including both *Bandicota indica* rats and *Mus cookii* mice in northern Thailand, indicating that the lineage is not restricted to a single host species (*20*,*39*). In addition, historical and regional data further support the persistence of ST34 or CG272 across Thailand and Laos over more than a decade, including in outbreak settings and fatal infections (*19*,*21*). Together, those findings suggest that pathogen lineage may contribute to clinical heterogeneity, although whether lineage-specific factors influence disease severity remains uncertain, so the findings should therefore be considered hypothesis-generating rather than causal.

To further explore potential CG272-specific features, exploratory analysis of lineage-defining SNPs identified 6 nonsynonymous substitutions in putative virulence-associated genes, including adhesins such as *Leptospira* immunoglobulin-like protein B and *lsa30* and related host-interaction proteins (Appendix 2 Table 3). Those 6 CG272-specific variants were conserved across CG272 isolates but absent in non-CG272 strains. The functional importance of those mutations remains unknown, and no direct link to increased virulence can be inferred; however, they provide preliminary hypotheses for future mechanistic investigation.

The strengths of this study include its multicenter prospective design across 2 endemic provinces, standardized clinical assessment and management according to national guidelines, and rigorous case confirmation using qPCR, culture, and MAT. Comprehensive clinical phenotyping that included organ dysfunction scores, complications, and objective outcomes provided a robust foundation for evaluating disease severity. Of note, this study examined both host and pathogen determinants of outcome. Host factors such as age and total bilirubin were evaluated alongside pathogen factors including leptospiremia and lineage-level genomic characterization. The integration of targeted amplicon sequencing and WGS added a valuable genomic dimension that enabled detailed investigation of circulating leptospiral populations. High-resolution genomic data of this kind rarely are available

in leptospirosis cohorts and enabled identification of CG272 as the predominant lineage in the sequenced subset and the only lineage observed among patients with fatal cases for whom genomic data were available. Further, the development of an admission death prediction model with excellent discriminatory performance (AUC 0.86) highlights the potential for early and practical risk stratification in routine clinical care.

One limitation of this study is that because amplicon-based sequencing and culture isolation require a minimum bacterial load, we restricted genomic analyses to samples with sufficient pathogen quantity or to cases with available isolates. That approach might lead to underrepresentation of certain lineages or low pathogen-load infections, and therefore the associations between lineage and clinical outcomes should be interpreted with caution. Larger and more systematically sampled genomic datasets, including expanded WGS of non-CG272 lineages, will be needed to clarify whether the observed clustering of isolates from patients with fatal cases within CG272 persists after minimizing potential technical and sampling biases. To reduce selection bias, we randomly selected samples with severity status blinded. In addition, we did not design the exploratory analysis of CG272-specific SNPs to establish functional relevance, and the observed variants require further functional characterization. In addition, we did not observe significant differences in leptospiremia or early clinical severity markers between CG272 and non-CG272 infections. However, those comparisons were limited by the small number of sequenced samples and the limited number of deaths, which reduced statistical power to detect modest lineage-associated effects. Larger genomic datasets will be needed to clarify whether CG272 is associated with differences in bacterial load, host response, or clinical outcomes. Moreover, because this study was conducted in district-level hospitals, the findings may not be fully generalizable to community cases, milder infections, or healthcare settings with different referral pathways. Further, although this was a prospective cohort study, there may be relevant factors that were not measured, such as additional host characteristics, environmental exposures, or differences in treatment, that could have influenced the results.

Our findings provide direction for integrated public health surveillance integrating human clinical, environmental, and reservoir data. Future studies should combine clinical predictors with pathogen genotype in broader populations and across different healthcare settings. Expanded genomic surveillance will be important for tracking the distribution and evolution of potentially high-risk lineages such as CG272. Integrative studies that combine host biomarkers, pathogen load, and genomic data may help clarify mechanisms of severe disease. Functional experiments also are needed to determine how specific lineages influence pathogenicity and immune responses. Further, developing practical clinical tools that incorporate both host and pathogen information may improve early recognition and management of patients in endemic regions who are at high risk.

In conclusion, this multicenter prospective study identified key host and pathogen factors associated with death in hospitalized patients with leptospirosis. Older age, elevated total bilirubin, and higher leptospiremia at admission were independently associated with in-hospital death, and a combined model demonstrated excellent discrimination. Genomic analysis identified CG272 as the predominant lineage in the sequenced subset and the only lineage observed among patients with fatal cases for whom genomic data were available, although this association remains exploratory. Our findings support the integration of clinical and pathogen data to improve early risk stratification and guide public health surveillance in endemic settings.

**Acknowledgments**

We thank the directors, officers, and healthcare workers of Thungsong Hospital and Khukhan Hospital for their collaboration during patient enrollment and data collection.

Genomic data generated in this study have been deposited in the National Center for Biotechnology Information under BioProject accession number PRJNA1377651, including both whole-genome sequencing and amplicon sequencing data.

This work was supported by the National Institutes of Health/National Institute of Allergy and Infectious Diseases under awards R01 AI183353 (N.S., D.A.H., U.L., S.T., J.D.), P01 AI168148 (N.S., D.A.H., N.E.S., D.M.W.), and R01 AI172924 (N.E.S) and by Chulalongkorn University's Second Century Fund (U.L., N.S.). The funders had no role in study design, data collection, analysis, interpretation, or manuscript preparation.

Author contributions: U.L. and N.S. conceived and designed the study. U.L., J.D., and S.T. developed the methodology and performed laboratory analyses. J.D. and S.T. curated clinical data, and U.L. conducted statistical analyses. T.S. and C.D. coordinated patient enrollment and clinical data collection at the study sites. N.E.S. performed the AmpSeq and initial genomic processing. N.E.S. and J.W.S. conducted the bioinformatic and phylogenetic analyses. D.M.W. supervised the genomic and

bioinformatic components of the project. U.L. drafted the original manuscript and prepared figures. All authors reviewed and approved the final manuscript. N.S. and D.A.H. provided overall project supervision. N.S. and D.A.H. acquired the funding.

Artificial intelligence tools were used for language editing and clarity; no content generation or data analysis was performed by artificial intelligence.

## About the Author

Dr. Limothai is a postdoctoral research fellow at Chulalongkorn University's Faculty of Medicine in Bangkok, Thailand. Her research focuses on clinical and molecular epidemiology of tropical infectious diseases, particularly leptospirosis and dengue.

## References


1. Costa F, Hagan JE, Calcagno J, Kane M, Torgerson P, Martinez-Silveira MS, et al. Global morbidity and mortality of leptospirosis: a systematic review. PLoS Negl Trop Dis. 2015;9:e0003898. https://doi.org/10.1371/journal.pntd.0003898
2. Haake DA, Levett PN. Leptospirosis in humans. Curr Top Microbiol Immunol. 2015;387:65–97. https://doi.org/10.1007/978-3-662-45059-8_5
3. Picardeau M. Virulence of the zoonotic agent of leptospirosis: still terra incognita? Nat Rev Microbiol. 2017;15:297–307. https://doi.org/10.1038/nrmicro.2017.5
4. Baharom M, Ahmad N, Hod R, Ja'afar MH, Arsad FS, Tangang F, et al. Environmental and occupational factors associated with leptospirosis: a systematic review. Heliyon. 2024;10:e23473.
5. Muñoz-Zanzi C, Dreyfus A, Limothai U, Foley W, Srisawat N, Picardeau M, et al. Leptospirosis—improving healthcare outcomes for a neglected tropical disease. Open Forum Infect Dis. 2025;12:ofaf035. https://doi.org/10.1093/ofid/ofaf035
6. Narkkul U, Thaipadungpanit J, Srisawat N, Rudge JW, Thongdee M, Pawarana R, et al. Human, animal, water source interactions and leptospirosis in Thailand. Sci Rep. 2021;11:3215. https://doi.org/10.1038/s41598-021-82290-5
7. Sawangpol C, Aimyong N, Phosri A. Epidemiological changes in the incidence of human leptospirosis in Thailand: findings from the National Disease Surveillance System from 2013 to 2022. Infect Dis Now. 2025;55:105108. https://doi.org/10.1016/j.idnow.2025.105108
8. Limothai U, Lumlertgul N, Sirivongrangson P, Kulvichit W, Tachaboon S, Dinhuzen J, et al. The role of leptospiremia and specific immune response in severe leptospirosis. Sci Rep. 2021;11:14630. https://doi.org/10.1038/s41598-021-94073-z
9. Spichler AS, Vilaça PJ, Athanazio DA, Albuquerque JO, Buzzar M, Castro B, et al. Predictors of lethality in severe leptospirosis in urban Brazil. Am J Trop Med Hyg. 2008;79:911–4. https://doi.org/10.4269/ajtmh.2008.79.911
10. Petakh P, Rostoka L, Isevych V, Kamyshnyi A. Identifying risk factors and disease severity in leptospirosis: a meta-analysis of clinical predictors. Trop Doct. 2023;53:464–9. https://doi.org/10.1177/00494755231187673
11. Daher EF, Soares DS, Galdino GS, Macedo ÊS, Gomes PEAC, Pires Neto RDJ, et al. Leptospirosis in the elderly: the role of age as a predictor of poor outcomes in hospitalized patients. Pathog Glob Health. 2019;113:117–23. https://doi.org/10.1080/20477724.2019.1621729
12. Dupont H, Dupont-Perdrizet D, Perie JL, Zehner-Hansen S, Jarrige B, Daijardin JB. Leptospirosis: prognostic factors associated with mortality. Clin Infect Dis. 1997;25:720–4. https://doi.org/10.1086/513767
13. Galdino GS, de Sandes-Freitas TV, de Andrade LGM, Adamian CMC, Meneses GC, da Silva Junior GB, et al. Development and validation of a simple machine learning tool to predict mortality in leptospirosis. Sci Rep. 2023;13:4506. https://doi.org/10.1038/s41598-023-31707-4
14. Tubiana S, Mikulski M, Becam J, Lacassin F, Lefèvre P, Gourinat AC, et al. Risk factors and predictors of severe leptospirosis in New Caledonia. PLoS Negl Trop Dis. 2013;7:e1991. https://doi.org/10.1371/journal.pntd.0001991
15. Abgueguen P, Delbos V, Blanvillain J, Chennebault JM, Cottin J, Fanello S, et al. Clinical aspects and prognostic factors of leptospirosis in adults. Retrospective study in France. J Infect. 2008;57:171–8. https://doi.org/10.1016/j.jinf.2008.06.010
16. Reis EA, Hagan JE, Ribeiro GS, Teixeira-Carvalho A, Martins-Filho OA, Montgomery RR, et al. Cytokine response signatures in disease progression and development of severe clinical outcomes for leptospirosis. PLoS Negl Trop Dis. 2013;7:e2457. https://doi.org/10.1371/journal.pntd.0002457
17. Senavirathna I, Rathish D, Agampodi S. Cytokine response in human leptospirosis with different clinical outcomes: a systematic review. BMC Infect Dis. 2020;20:268. https://doi.org/10.1186/s12879-020-04986-9
18. Boonsilp S, Thaipadungpanit J, Amornchai P, Wuthiekanun V, Bailey MS, Holden MT, et al. A single multilocus sequence typing (MLST) scheme for seven pathogenic *Leptospira* species. PLoS Negl Trop Dis. 2013;7:e1954. https://doi.org/10.1371/journal.pntd.0001954
19. Thaipadungpanit J, Wuthiekanun V, Chierakul W, Smythe LD, Petkanchanapong W, Limpaiboon R, et al. A dominant clone of *Leptospira interrogans* associated with an outbreak of human leptospirosis in Thailand. PLoS Negl Trop Dis. 2007;1:e56. https://doi.org/10.1371/journal.pntd.0000056
20. Jolley KA, Bray JE, Maiden MCJ. Open-access bacterial population genomics: BIGSdb software, the PubMLST.org website and their applications. Wellcome Open Res. 2018;3:124. https://doi.org/10.12688/wellcomeopenres.14826.1
21. Grillová L, Robinson MT, Chanthongthip A, Vincent AT, Nieves C, Oppelt J, et al. Genetic diversity of *Leptospira* isolates in Lao PDR and genome analysis of an outbreak strain. PLoS Negl Trop Dis. 2021;15:e0010076. https://doi.org/10.1371/journal.pntd.0010076
22. World Health Organization (WHO). Human leptospirosis: guidance for diagnosis, surveillance and control. 2003 [cited 2026 Jan 5]. https://www.who.int/publications/i/item/human-leptospirosis-guidance-for-diagnosis-surveillance-and-control
23. Moreno R, Rhodes A, Piquilloud L, Hernandez G, Takala J, Gershengorn HB, et al. The Sequential Organ Failure Assessment (SOFA) score: has the time come for an update? Crit Care. 2023;27:15. https://doi.org/10.1186/s13054-022-04290-9
24. Singer M, Deutschman CS, Seymour CW, Shankar-Hari M, Annane D, Bauer M, et al. The Third International Consensus Definitions for Sepsis and Septic Shock (Sepsis-3). JAMA. 2016;315:801–10. https://doi.org/10.1001/jama.2016.0287

25. Vincent JL, Moreno R, Takala J, Willatts S, De Mendonça A, Bruining H, et al. The SOFA (Sepsis-related Organ Failure Assessment) score to describe organ dysfunction/failure. Intensive Care Med. 1996;22:707–10. https://doi.org/10.1007/BF01709751
26. Stoddard RA, Gee JE, Wilkins PP, McCaustland K, Hoffmaster AR. Detection of pathogenic *Leptospira* spp. through TaqMan polymerase chain reaction targeting the LipL32 gene. Diagn Microbiol Infect Dis. 2009;64:247–55. https://doi.org/10.1016/j.diagmicrobio.2009.03.014
27. Stone NE, Hamond C, Clegg JR, McDonough RF, Bourgeois RM, Ballard R, et al. Host population dynamics influence *Leptospira* spp. transmission patterns among *Rattus norvegicus* in Boston, Massachusetts, US. PLoS Negl Trop Dis. 2025;19:e0012966. https://doi.org/10.1371/journal.pntd.0012966
28. Giraud-Gatineau A, Nieves C, Harrison LB, Benaroudj N, Veyrier FJ, Picardeau M. Evolutionary insights into the emergence of virulent *Leptospira* spirochetes. PLoS Pathog. 2024; 20:e1012161. https://doi.org/10.1371/journal.ppat.1012161
29. Al Hariri YK, Sulaiman SAS, Khan AH, Adnan AS, Al-Ebrahem SQ. Determinants of prolonged hospitalization and mortality among leptospirosis patients attending tertiary care hospitals in northeastern state in peninsular Malaysia: a cross sectional retrospective analysis. Front Med (Lausanne). 2022;9:887292. https://doi.org/10.3389/fmed.2022.887292
30. Gancheva GI. Leptospirosis in elderly patients. Braz J Infect Dis. 2013;17:592–5. https://doi.org/10.1016/j.bjid.2013.01.012
31. Mikulski M, Boisier P, Lacassin F, Soupé-Gilbert ME, Mauron C, Bruyere-Ostells L, et al. Severity markers in severe leptospirosis: a cohort study. Eur J Clin Microbiol Infect Dis. 2015;34:687–95. https://doi.org/10.1007/s10096-014-2275-8
32. Petakh P, Nykyforuk A. Predictors of lethality in severe leptospirosis in Transcarpathian region of Ukraine. Infez Med. 2022;30:272–6.
33. Agampodi SB, Matthias MA, Moreno AC, Vinetz JM. Utility of quantitative polymerase chain reaction in leptospirosis diagnosis: association of level of leptospiremia and clinical manifestations in Sri Lanka. Clin Infect Dis. 2012;54:1249–55. https://doi.org/10.1093/cid/cis035
34. Tubiana S, Mikulski M, Becam J, Lacassin F, Lefèvre P, Gourinat A-C, et al. Risk factors and predictors of severe leptospirosis in New Caledonia. PLoS Negl Trop Dis. 2013;7:e1991. https://doi.org/10.1371/journal.pntd.0001991
35. Hochedez P, Theodose R, Olive C, Bourhy P, Hurtrel G, Vignier N, et al. Factors associated with severe leptospirosis, Martinique, 2010–2013. Emerg Infect Dis. 2015;21:2221–4. https://doi.org/10.3201/eid2112.141099
36. Philip N, Bahtiar Affendy N, Ramli SNA, Arif M, Raja P, Nagandran E, et al. *Leptospira interrogans* and *Leptospira kirschneri* are the dominant *Leptospira* species causing human leptospirosis in Central Malaysia. PLoS Negl Trop Dis. 2020;14:e0008197. https://doi.org/10.1371/journal.pntd.0008197
37. Ravindranathan AT, Mukundan A, Puthanpurayil SNT, Kavuthodi B, Karunakaran S, John R. Molecular and genomic characterization of *Leptospira* isolates in humans and its relation to disease severity. Indian J Med Microbiol. 2025;56:100910. https://doi.org/10.1016/j.ijmmb.2025.100910


Address for correspondence: Nattachai Srisawat, Center of Excellence in Critical Care Nephrology, Faculty of Medicine, Chulalongkorn University, 1873 Rama IV Rd, Pathumwan, Bangkok 10330, Thailand; email: nattachai.sr@chula.ac.th

# Prognostic Value of PCR Cycle Threshold Value in Crimean-Congo Hemorrhagic Fever, Iraq, 2022–2023

Raghad I. Khaleel, Ihab R. Aakef, Riyadh A. Al-hilfi, Hussein A. Hasan, Iman M. Aufi, Hawraa A. Shakir, Ahmed A. Hussein, Noora A. Abdulhadi, Zainb A. Mohsin, Amal A. Raheem, Sarah W. Ahmed, Ghazwan A. Baghdadi, Chiori Kodama, Antoine Chaillon, Anaïs Legand, Pierre Formenty, Sinan G. Mahdi, Adnan Khamasi

Using laboratory and epidemiologic data collected in 2022 and 2023 in Iraq, we aimed to evaluate the diagnostic and prognostic performance of reverse transcription PCR (RT-PCR) in Crimean-Congo hemorrhagic fever (CCHF) patients and to identify factors associated with disease outcomes. CCHF was confirmed in 955 hospitalized patients. Among those, RT-PCR analysis showed that blood specimens from deceased patients had a lower median cycle threshold (Ct) value than did those who recovered; we used those data to determine a cutoff value. Univariate and multivariate logistic regression analysis indicated that low Ct values, hemorrhagic symptoms at admission, and age ≥15 years were independent determinants of fatal CCHF outcome. Viral load and patient age play key roles in the outcome of CCHF in Iraq. Ct value at admission, as a proxy for viral load, serves as a practical indicator to guide clinicians in managing CCHF patients.

Crimean-Congo hemorrhagic fever (CCHF) is a severe tickborne disease caused by CCHF virus (CCHFV; family Nairoviridae, genus *Orthonairovirus*) (*1*). CCHF is endemic across Africa, southern and eastern Europe, the Middle East, and countries in Asia south of the 50th parallel north, which represents the geographic limit of detection of the principal vector and natural reservoir, the *Hyalomma* species tick (*2*,*3*). Reported case-fatality rates (CFRs) vary by region and country, from 5% to as high as 30% (*4*). CCHFV is primarily transmitted to humans through bites of infected ticks or direct contact with blood or tissues of viremic livestock or infected individual animals (*5*,*6*).

As of June 2026, no antiviral drug or licensed vaccine is available for CCHF; however, several therapeutic and vaccines candidates are under development. Outbreak control primarily relies on preventing transmission through isolating persons with suspected and confirmed CCHF, early detection via surveillance and laboratory diagnostics, intensive supportive care, infection prevention and control in health facilities, and community engagement (*7*).

CCHF cases were first reported in 1979 in Iraq; ≈50 cases were detected annually during 1986–1996. Reported cases declined during 1998–2020 (*8*–*10*), but major outbreaks occurred in 2022 and 2023 (*11*–*13*).

The Central Public Health Laboratory (CPHL) viral hemorrhagic fevers unit, CCHF laboratory (Baghdad, Iraq), serves as the national reference laboratory for CCHF diagnosis in Iraq. The Iraq Communicable Disease Control Center (Iraq-CDC) coordinates the national response to CCHF outbreaks. The Iraq-CDC has developed an epidemiologic database to analyze data and guide control and prevention interventions. Here, we present an analysis of CPHL-generated data from 2022–2023, in conjunction with epidemiologic data collected by Iraq-CDC. Patients' data were recorded as part of Ministry of Health guidelines on

Author affiliations: Central Public Health Laboratory, Baghdad, Iraq (R.I. Khaleel, H.A. Hasan, I.M. Aufi, H.A. Shakir, A.A. Hussein, N.A. Abdulhadi, Z.A. Mohsin, A.A. Raheem, S.W. Ahmaed); Communicable Disease Control Center, Baghdad (I.R. Aakef, G.A. Baghdadi, S.G. Mahdi); Directorate of Public Health, Ministry of Health, Baghdad (R.A. Al-hilfi); World Health Organization Eastern Mediterranean Regional Office, Cairo, Egypt (C. Kodama); World Health Organization Emergencies Programme, Geneva, Switzerland (A. Chaillon, A. Legand, P. Formenty); World Health Organization Country Office, Baghdad (A. Khamasi)

DOI: https://doi.org/10.3201/eid3207.251284

CCHF management. We conducted the study under the supervision of the Ministry of Health of Iraq and with appropriate ethics approval obtained from the MOH. We used anonymized data for analysis.

## Methods

### Patients and Specimens

The Iraq-CDC case definition for a suspected CCHF case was as follows: any person with acute onset of fever with ≥1 of the following symptoms: headache, backache, joint pain, stomach pain, vomiting; and with history of exposure to one of the following risk factors within the previous 14 days: contact with animal, animal tissues or fluids during slaughtering, raw meat during preparation; or tick bite history or involvement in the removal of a tick from a person or an animal; or contact with a suspected or confirmed case of CCHF. A blood specimen was collected from live patients with suspected CCHF to establish the diagnosis. All suspected and laboratory-confirmed CCHF cases were admitted to general hospitals across governorates in Iraq and managed in their intensive care units.

Blood samples were collected from patients with suspected CCHF at hospital admission; they were admitted into the specialized unit for patients with suspected CCHF. Samples were shipped to CPHL and tested by reverse transcription PCR (RT-PCR). Blood samples from patients with negative RT-PCR results were retested by ELISA IgM serology.

### Diagnostic Assays

Blood specimens were collected on gel and clot activator tube. After separation, 10 mL serum from each specimen was transferred to plain tubes and transported, cooled in ice, to the CPHL in Baghdad for diagnosis. We extracted viral RNA from whole serum samples by using the QIAamp viral RNA mini kit (QIAGEN, https://www.qiagen.com), according to the manufacturer's instructions.

We performed RT-PCR testing using the RealStar CCHFV RT-PCR Kit 1.0 detection kit (Altona Diagnostics GmbH, https://www.altona-diagnostics.com), which targets the small segment of the CCHFV virus, on the QuantStudio 5 PCR thermocycler (ThermoFisher, https://www.thermofisher.com), according to the manufacturer's instructions. We added the internal control template of the kit to the sample before RNA extraction; only results with a valid run control were communicated. In brief, the protocol runs as a reverse transcription holding step at 50°C for 10 minutes, denaturation holding phase at 95°C for 2 minutes, then 45 cycles of amplification each at 95°C, 55°C, and 72°C. We used 10 µL of extracted RNA per reaction for a final volume of 25 µL. Assay conditions were consistent throughout the study period, using the same diagnostic kit, standardized protocol, and calibration procedures. We used ELISA IgM serology test (Abbexa LTD, https://www.abbexa.com) in accordance with manufacturer's protocol to determine levels of CCHFV IgM in the serum of suspected patients with negative RT-PCR results.

### Data Management

General hospitals and Iraq-CDC provided patients' demographic data, included on the laboratory request form accompanying each sample. Laboratory results were provided to Iraq-CDC and the hospital by CPHL. Data were captured in both CPHL's and Iraq-CDC's databases (Microsoft Excel, https://www.microsoft.com). Variables included age, sex, governorate of residence, hospital patient identifier, sample identifier, sample type, collection date, date of symptom onset, patient's outcome, date of death, laboratory result, and cycle threshold (Ct) values in patients who tested positive by RT-PCR.

To validate the demographic information and document disease outcome, we merged the CPHL and Iraq-CDC databases using hospital patient and sample identifiers recorded in both databases. We resolved all inconsistencies through thorough investigation, examining all available records. A full dataset was not available for 13 confirmed cases that are not included in this report.

We classified patients into 2 main groups for analysis: non-CCHF cases, defined as suspected cases of CCHF with subsequent negative CCHF results by RT-PCR and negative IgM serology; or CCHF confirmed cases, defined as suspected CCHF cases with subsequent positive RT-PCR result, positive IgM serology, or both. We excluded patients with missing or conflicting data that prevented classification into either category from the analysis. The final database comprised 3,546 patients; all 3,546 samples were collected during January 2022–December 2023.

### Statistical Analysis

We described categorical variables as percentages. The denominator varied between variables because of missing data. We described continuous variables by medians and interquartile range (IQRs) and associations between independent variables and the dichotomous outcome (survival or death) with crude (unadjusted) odds ratios (ORs).

We used logistic regression models to investigate factors associated with patient outcomes and hemorrhagic conditions. We conducted initial analyses using univariate regression to explore the relationship between individual predictors and the outcome variable. We used univariate analysis to explore unadjusted associations between variables and outcome and used ORs and 95% CIs to quantify the strength of those associations. We considered a p value <0.25 and other variables of known clinical relevance (including those not statistically significant in univariate analysis) for inclusion in the multivariable model. We then used multivariate logistic regression models to adjust for potential confounders. The final model included the following covariates: Ct value, sex, age, hemorrhagic signs, time from onset to admission, tick bite, contact with a confirmed patient, contact with raw meat, contact with animal, and year of outbreaks. We assessed model fit using the Akaike Information Criterion and likelihood ratio tests. We defined statistical significance as p<0.05. We performed all analyses in R version 4.4.1 (The R Project for Statistical Computing, https://www.r-project.org) using the stats (https://www.rdocumentation.org/packages/stats/versions/3.6.2) and gtsummary (https://www.danieldsjoberg.com/gtsummary) packages. We conducted receiver operating characteristic (ROC) analysis to determine the optimal Ct cutoff for predicting patient outcome using the pROC package in R (*14*,*15*).

## Results

### CCHF Confirmation by Testing Methods

Our analysis includes a total of 3,546 suspected CCHF patients who sought care at hospitals in Iraq during 2022–2023. CCHF infection was confirmed in 955 (27%) suspected cases; 915 were confirmed by RT-PCR, and an additional 40 that were negative by RT-PCR were confirmed by IgM ELISA (Table 1; Figure 1). In 2022, among 1,370 symptomatic suspected cases, CCHF infection was confirmed in 380 (27%) patients, 354 confirmed by RT-PCR and 26 by IgM ELISA. In 2023, among 2,176 symptomatic suspected cases, CCHF infection was confirmed in 575 (26%) patients, 561 confirmed by RT-PCR and 14 by IgM ELISA.

**Table 1.** Characteristics of CCHF-confirmed patients in study of prognostic value of PCR cycle threshold for Crimean-Congo hemorrhagic fever, Iraq, 2022–2023

| Characteristic | Values | | p value† |
|---|---|---|---|
| | 2022 | 2023 | |
| Age | | | 0.10 |
| <15 | 17/380 (4.5) | 16/575 (3) | |
| 15–24 | 99/380 (26) | 133/575 (23) | |
| 25–34 | 61/380 (16) | 131/575 (23) | |
| 35–44 | 85/380 (22) | 130/575 (23) | |
| 45–54 | 73/380 (19) | 92/575 (16) | |
| ≥55 | 45/380 (12) | 73/575 (13) | |
| Median (range) | 35 (1–90) | 35 (2–80) | |
| Sex | | | 0.35 |
| F | 149/380 (39) | 243/575 (42) | |
| M | 231/380 (61) | 332/575 (58) | |
| Residency status | | | 1.00 |
| Rural | 1/1 (100) | 262/575 (46) | |
| Semiurban | 0/1 (0) | 81/575 (14) | |
| Urban | 0/1 (0) | 232/575 (40) | |
| Ct value, median (range) | 25.8 (11.4–36.9) | 27.4 (12.9–38.9) | <0.001 |
| Exposures and clinical features | | | <0.001 |
| Median time from onset to admission, d (range) | 3 (0–13) | 4 (0–20) | |
| Fever | 359/380 (94) | 567/575 (99) | <0.001 |
| Contact with confirmed case | 18/375 (5) | 15/567 (3) | 0.08 |
| Contact with animals | 212/375 (57) | 297/575 (52) | 0.14 |
| Slaughtering | 127/375 (34) | 315/574 (55) | <0.001 |
| Contact with raw meat | 207/375 (55) | 359/575 (63) | 0.02 |
| Tick bite | 134/374 (36) | 42/575 (7) | <0.001 |
| Hemorrhagic | 145/380 (38) | 195/575 (34) | 0.18 |
| Ecchymosis | 104/380 (27) | 134/575 (23) | 0.16 |
| Bleeding at injection site | 109/379 (29) | 145/575 (25) | 0.23 |
| Injected eyes | 1/1 (100) | 41/575 (7) | 0.07 |
| Ribavirin | 1/1 (100) | 190/535 (36) | 0.36 |
| Outcome | | | 0.02 |
| Cured | 305/380 (80) | 494/575 (86) | |
| Death | 75/380 (20) | 81/575 (14) | |

*Values are no. (%) except as indicated, Percentages may not sum to 100% due to rounding. Ct, cycle threshold
†Determined by Pearson $\chi^2$ test, Wilcoxon rank-sum test, or Fisher exact test.

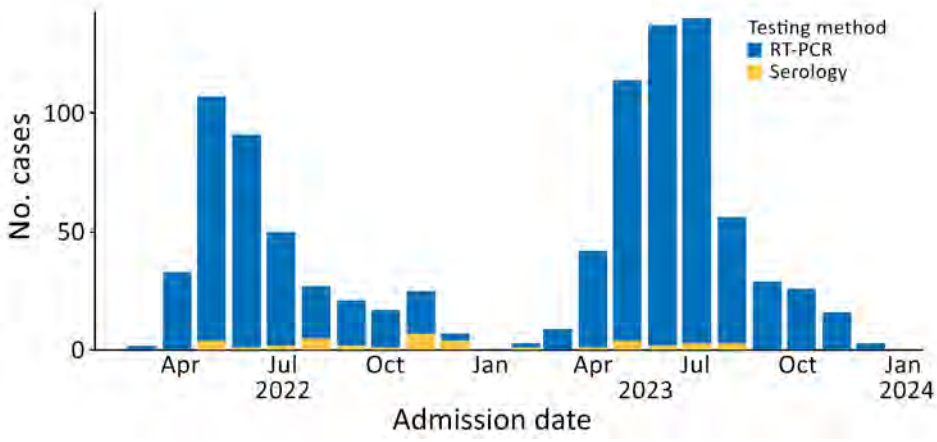


**Figure 1.** Distribution of confirmed Crimean-Congo hemorrhagic fever patients by testing method in study of prognostic value of PCR cycle threshold value for Crimean-Congo hemorrhagic fever, Iraq, 2022–2023. RT-PCR, reverse transcription PCR.

### Admission and Rate of Confirmation by Month

In 2022–2023, among all suspected cases with available month of admission data (n = 3,514), a total of 3,096 (88%) were admitted during April–September (Figure 1). During that period, mean positivity rate was 29% (median 27%, range 22%–41%). Outside of the period, mean positivity rate was 19% (median 23%, range 0%–31%) (Appendix Figure 1, https://wwwnc.cdc.gov/EID/article/32/7/25-1284-App1.pdf). Among the 955 confirmed cases, 848 (89%) patients were admitted during April–September. The average number of confirmed patients admitted per month during April–September was 141, whereas during October–March, the monthly average was 21.

### CFR over Time

In 2022–2023, the CFR of confirmed CCHF hospitalized cases was 16%. The mean monthly CFR among confirmed cases was 22% (median 17%, range 10%–50%). During April–September, the mean monthly CFR among confirmed cases was 15% (median 15%, range 10%–21%), whereas during October–March, the mean monthly CFR among confirmed cases was 27% (median 21%, range 14%–50%) (Figure 2).

### Distribution of Cases and CFRs by Governorate

In 2022–2023, confirmed CCHF cases were admitted in hospitals of 19 governorates. Three governorates accounted for most cases, reporting a combined total of 523 (55%) cases; Thi-Qar reported 302 (32%), Baghdad reported 116 (12%), and Basra reported 105 (11%). Babylon, Missan, Muthana, and Wassit governorates reported 5%–8% of all confirmed cases (Figure 3).

CFR varied by governorate; the range was 0%–41% (Figure 3). CFR decreased from 2022 to 2023 in all but 4 governorates (Appendix Figure 2). There was no statistical difference in Ct value at admission across governorates (Appendix Figure 3).

### Ct Value and Outcome

Of the patients with CCHF diagnosis, 915 had their diagnosis confirmed by RT-PCR. RT-PCR analysis of blood specimens from patients who died yielded a lower median Ct value (22.1 [range 12.9–37.0]) than those from patients who recovered (27.7 [range 11.4–38.9]). When plotting the CFR versus Ct categories to assess the relationship between Ct value and outcome, we noted an inverse correlation between Ct and CFR ($p<0.001$) (Figure 4). That finding

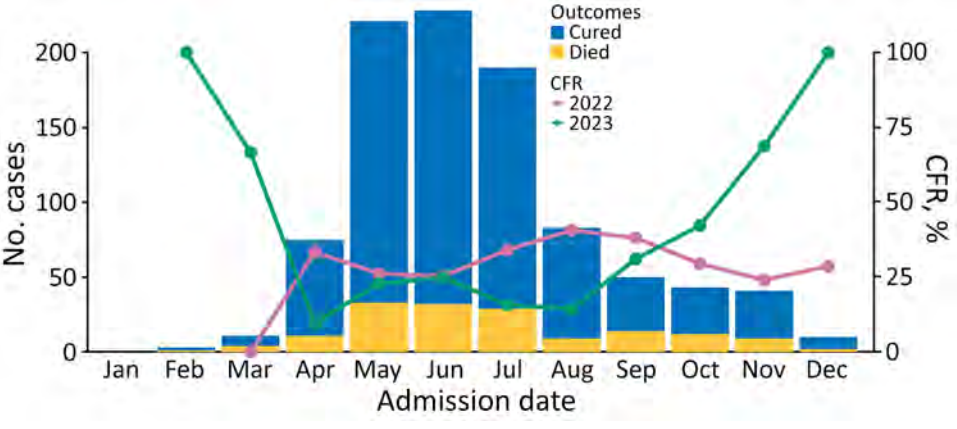


**Figure 2.** Confirmed Crimean-Congo hemorrhagic fever cases and CFRs by month in study of prognostic value of PCR cycle threshold for Crimean-Congo hemorrhagic fever, Iraq, 2022–2023. CFR was reported if ≥5 cases were confirmed in that month. CFR, case-fatality ratio.

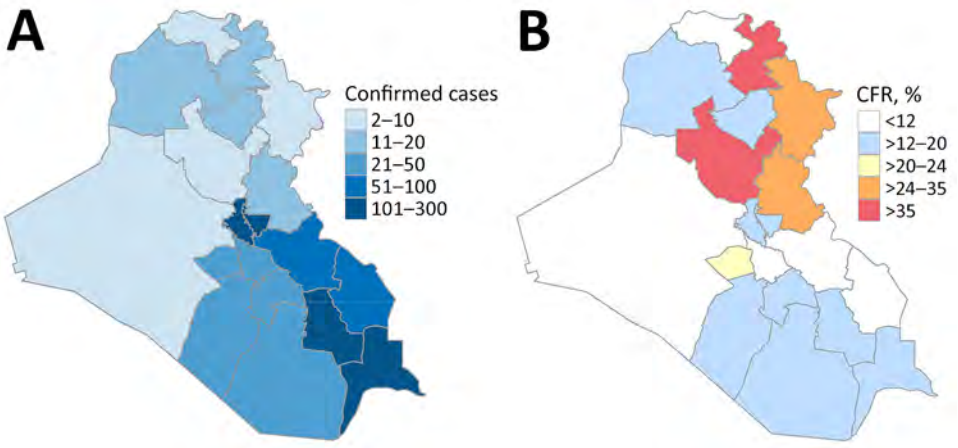


**Figure 3**. Distribution of confirmed Crimean-Congo hemorrhagic fever (CCHF) patients and CFRs by governorate in study of prognostic value of PCR cycle threshold for CCHF, Iraq, 2022–2023. A) CCHF-confirmed patients by governorate. B) CFR among confirmed CCHF patients by governorate. CFR, case-fatality ratio.

suggests that the Ct value at admission has a strong prognostic value. We performed ROC analyses to determine the optimal Ct value to predict participant outcome, using an area under the curve value of 0.76 (Appendix Figure 4); we determined an optimal Ct cutoff of 26 by ROC analysis by Youden method for predicting patients' outcome (sensitivity 81.6%, specificity 60.9%). The median Ct value on admission to the hospital showed no trend over time (Appendix Figure 5), but median Ct value was overall lower in 2022 than in 2023 (25.8 vs. 27.4; p<0.001) (Figure 1).

### Age and CFR

Among patients <15 years of age (n = 33), median Ct value was 29.9 (range 13.9–38), and no deaths were reported. In older patients (n = 922), CFR fluctuated from 13% to 19%; median Ct value was 26.7 (range 11.4–38.9) (Appendix Figures 6, 7).

### Logistic Regression Analysis

We used logistic regression models to determine factors associated with fatal outcomes. We performed a univariate analysis to explore unadjusted associations between laboratory (Ct value) and relevant demographics (age, sex), clinical and epidemiologic data (hemorrhagic signs, time from onset to admission, tick bites, contact with confirmed cases, animal or raw meat, year of outbreak), and patient outcomes. Characteristics associated with an unfavorable outcome included lower Ct value (OR 0.83 [95% CI 0.8–0.86]; p<0.001), hemorrhagic signs (OR 2.18 [95% CI 1.54–3.09]; p<0.001), and age (OR 1.01 [95% CI 1.0–1.02]; p = 0.041). Receiving a diagnosis in 2023 was also associated with a lower risk for a fatal outcome (OR 0.67 [95% CI 0.47–0.94]; p = 0.022). Those results remained significant for all but age and year of outbreak after false discovery rate correction. Sex; contact with confirmed cases, animal, or raw meat; and history of tick bites were not associated with an unfavorable outcome in the univariate analyses (p>0.5); therefore, we removed those variables from the multivariate analyses (Appendix Table 1). Characteristics associated with a higher risk for unfavorable outcome by multivariate modeling included lower Ct (OR 0.82 [95% CI 0.79–0.86]; p<0.001) and hemorrhagic signs (OR 2.75 [95% CI] 1.86–4.08; p<0.001) (Table 2).

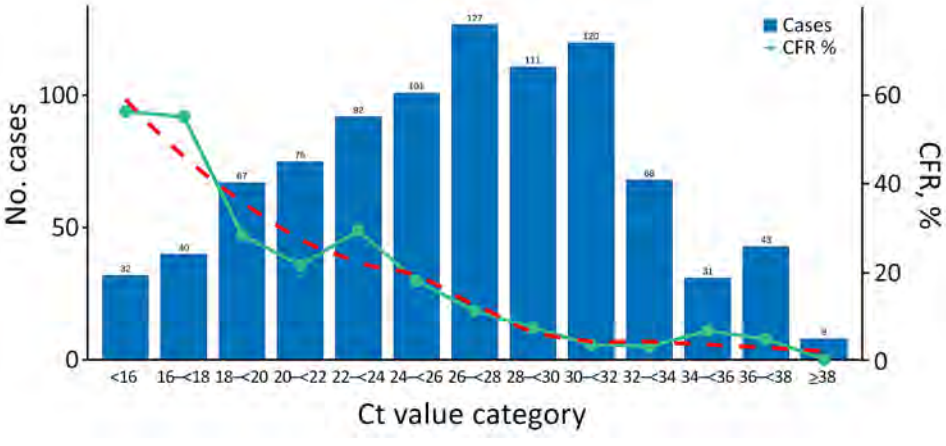


**Figure 4.** Distribution of confirmed Crimean-Congo hemorrhagic fever patients (n = 915) by Ct value category and corresponding CFR in study of prognostic value of PCR cycle threshold for Crimean-Congo hemorrhagic fever, Iraq, 2022–2023. Case fatality ratio is plotted for each Ct values category, indicating an inverse correlation between Ct value and outcome. Red dashed line shows the smoothed CFR trend across categories ($p = 3.28 \times 10^{-5}$; locally estimated scatterplot smoothing fit, p<0.05). CFR, case-fatality ratio; Ct, cycle threshold.

**Table 2.** Multivariate logistic regression results from study of prognostic value of PCR cycle threshold value for Crimean-Congo hemorrhagic fever, Iraq, 2022–2023*

| Characteristic | OR (95% CI) | p value | q value† |
|---|---|---|---|
| Ct | 0.83 (0.79–0.86) | <0.001 | **<0.001** |
| Hemorrhagic | | <0.001 | **<0.001** |
| N | NA | | |
| Y | 2.72 (1.82–4.07) | | |
| Age | 1.01 (1.00–1.02) | 0.094 | 0.31 |
| Sex | | 0.73 | 0.92 |
| M | NA | | |
| F | 0.93 (0.62–1.39) | | |
| Time from onset to admission | 0.97 (0.89–1.06) | 0.56 | 0.79 |
| Tick bite | | 0.98 | 0.98 |
| N | NA | | |
| Y | 1.0 (0.56–1.73) | | |
| Contact with confirmed case | | 0.38 | 0.71 |
| N | NA | | |
| Y | 0.61 (0.17–1.77) | | |
| Contact with raw meat | | 0.38 | 0.71 |
| N | NA | | |
| Y | 1.20 (0.80–1.80) | | |
| Contact with animal | | 0.86 | 0.96 |
| N | NA | | |
| Y | 1.04 (0.68–1.57) | | |
| Year of outbreak | | 0.42 | 0.71 |
| 2022 | NA | | |
| 2023 | 0.84 (0.55–1.29) | | |

*We analyzed data from 896 cases confirmed by reverse transcription PCR. A total of 150 of those case-patients were deceased. Bold text indicates statistical significance after false discovery rate correction. Ct, cycle threshold; NA, not applicable; OR, odds ratio.
†False discovery rate correction for multiple testing.

## Discussion

### CCHF Trends in 2022 and 2023

Our study observed a clear seasonal pattern consistent with previous reports (*13*); during April–September, 89% of all patients with confirmed cases were admitted to a hospital. Similar trends have been documented in studies on tick seasonality in southern Iraq (*16*), where tick populations increased from spring to autumn, whereas winter months recorded the lowest rates. The observed seasonal variation in tick density appears to correlate with the frequency of CCHF cases. However, further research is needed to better understand the factors contributing to the apparent population increase of the primary CCHFV vector, ticks of the genus *Hyalomma*, and to identify effective control measures.

We observed notable differences between 2022 and 2023. The overall CFR was higher in 2022 than in 2023 (20% vs. 14%), despite a greater number of reported cases in 2023. In addition, median Ct value was lower in 2022 than in 2023 (25.8 vs. 27.4). In 2023, the median monthly CFR was lower during April–September than during the rest of the year (12% vs. 32%). That pattern contrasts with 2022, when the median monthly CFR fluctuated from 14% to 35% throughout the year, showing no clear difference between the epidemic season and other periods.

Those differences noted in 2023 may reflect, in part, strengthened public health response, including improved case detection, clinical management, and community engagement over the course of 2023 (*13*), along with sensitization efforts before the 2023 epidemic season. Improved clinical awareness and recognition of milder forms of disease, along with faster and more effective management of severe cases, likely contributed to the observed decrease in CFR. However, those interventions were not uniformly implemented across all governorates, and their relative contribution to CFR reduction cannot be quantified in this analysis.

### Factors Associated with Disease Outcome

In Iraq, the logistic regression analysis showed that low Ct value, hemorrhagic symptoms at admission, and age ≥15 years were independent determinants of a poor CCHF outcome. Our findings are consistent with those of previous studies reporting an association between hemorrhagic symptoms, in particular melena and hematemesis, and fatal outcome (*17*). Systematic standardized clinical data collection and analysis would help assess additional factors that may affect disease outcomes.

### Ct Value as a Key Indicator for Disease Prognosis

Previous studies have indicated association with high viral load (>$10^8$copies/mL) and poor outcome

(*17*–*19*). Our findings further suggest that low Ct values at admission are also associated with fatal outcome. Similar to the case for Ebola virus disease (*20*) or Lassa fever (*21*), viral load, using Ct value as a proxy, is closely correlated with CCHF outcome. We found a significant difference of 5.6 Ct between median Ct values persons who died from CCHF (median 22.1, range 12.9–37.0) and survivors (median 27.7, range 11.4–38.9), roughly corresponding to a difference in virus RNA concentration of 1.7 $\log_{10}$ units ($p<0.01$). However, further analysis of Ct values across affected countries, considering different CCHF viral genotypes and CFR, is needed.

Among patients with CCHF, those with a Ct value <26 had a 33% CFR, whereas those with a Ct value >26 had a 6% CFR. Between those extremes, Ct values showed a strong negative correlation with CFR. That finding suggests that Ct values are predictive of CCHF CFR and serve as a key indicator of disease prognosis, which is crucial information for clinicians in assessing disease severity and guiding prognosis evaluation. We observed a higher CFR in patients whose Ct values were in the 22–24 range compared with patients whose Ct value was 18–22. A possible explanation is that patients with Ct value of 18–22 had more severe clinical manifestations, prompting more immediate medical intervention, whereas those with Ct values of 22–24 may have exhibited milder initial symptoms, leading to delayed treatment.

Given the strong correlation between Ct values and CCHF CFR, distribution of Ct should be considered when comparing CFRs across districts, governorates, and countries but also across seasons or years. For example, when comparing the CCHF CFR in Iraq between 2022 (20%) and 2023 (14%), standardizing CFR by Ct values can provide more accurate and meaningful comparisons.

Ct values should be interpreted with caution because they are influenced by several factors, including the timing of sample collection relative to symptom onset and underlying viral kinetics. In our analysis, we accounted for those factors by including time from symptom onset to admission in the multivariable model; however, that variable is subject to recall bias and may not fully capture the timing of infection. Therefore, although Ct value at admission appears to be a robust prognostic marker, residual confounding related to disease stage at sampling cannot be excluded.

Ct values can provide a pragmatic and immediately actionable marker for clinicians, particularly in resource-limited settings. They can serve as a useful tool to rapidly assess disease severity at admission and support early clinical decision making, including the timely initiation or intensification of supportive care.

### Lower CCHF CFR in Patients <15 Years of Age

In our cohort, we observed a 0% mortality rate among the 33 pediatric cases, compared with 17% in adults ($p<0.001$). Similar trends have been reported in regional studies from Turkey: CFR of 0% (n = 31) (*22*) and 2.1% (n = 47) (*23*) for pediatric cases. Although the biological mechanism for that age-related disparity remains a subject of investigation, our findings reinforce the observation that pediatric CCHF cases often have more favorable clinical outcomes than adult cases. However, those results should be interpreted cautiously and viewed as consistent with regional observations rather than definitive evidence of age-related differences in CFR.

The lower CFR reported in children infected with CCHF in this study contrasts with findings from studies on Ebola virus disease, in which higher CFRs have been documented in younger children, particularly those <5 years of age. That trend was partly attributed to malaria co-infection (*20*) and higher viral loads in pediatric patients (*24*). Conversely, our findings are more consistent with studies on Lassa fever in Nigeria, where children <15 years of age showed lower CFRs than adults (2.9% vs. 13%) (*25*).

Given the rarity of fatal CCHF cases in children in both Iraq and Turkey, a deeper understanding of the clinical and laboratory characteristics of pediatric CCHF is needed. As highlighted previously (*23*), comprehensive multicountry observational studies involving both children and adults are essential. Such studies should investigate host and viral factors that may explain those differences, providing insights into disease progression and pathogenesis.

A limitation of our study is that data were collected retrospectively and collated manually. Although we carefully reviewed the data, we cannot completely rule out the possibility that some mismatches may have occurred. In the different governorates, hospital attendance might have been influenced by factors such as information campaigns, the hospital's reputation, perceived disease severity, willingness and financial ability to seek treatment and testing, and distance to the healthcare center. Variation in those factors could help explain some of the observed variations in CFR in terms of person, place, and time. Future investigations should also include other circulating genotypes of CCHFV.

In summary, Ct value at admission is a useful indicator of CCHF disease severity to guide clinicians

in managing patients; lower Ct values are indicators of poor outcomes. Ct value should be communicated to clinicians to support optimized supportive care for affected patients.

### Acknowledgments

We thank the clinicians and the public health officers from the general hospitals and the Iraq- Communicable Disease Control Center health workers across governorates for their commitment and excellent cooperation. We also thank Nadia Wauquier for her thorough technical review of the manuscript and her significant contributions to improving the clarity of this manuscript.

The Central Public Health Laboratory in Baghdad and Iraq Communicable Disease Control Center supported this work as part of national activities against Crimean-Congo hemorrhagic fever.

## About the Author

Dr. Khaleel oversees CCHF diagnostic testing at the Central Public Health Laboratory in Baghdad and serves as Iraq's national focal point for WHO's International Health Regulations, collaborating with national and international health authorities to strengthen compliance and health security. Her research interests include virology, parasitology sequencing and infectious diseases.

### References

1. Garrison AR, Smith DR, Golden JW. Animal models for Crimean-Congo hemorrhagic fever human disease. Viruses. 2019;11:590. https://doi.org/10.3390/v11070590
2. Hoogstraal H. The epidemiology of tick-borne Crimean-Congo hemorrhagic fever in Asia, Europe, and Africa. J Med Entomol. 1979;15:307–417. https://doi.org/10.1093/jmedent/15.4.307
3. Gargili A, Estrada-Peña A, Spengler JR, Lukashev A, Nuttall PA, Bente DA. The role of ticks in the maintenance and transmission of Crimean-Congo hemorrhagic fever virus: a review of published field and laboratory studies. Antiviral Res. 2017;144:93–119. https://doi.org/10.1016/j.antiviral.2017.05.010
4. Bente DA, Forrester NL, Watts DM, McAuley AJ, Whitehouse CA, Bray M. Crimean-Congo hemorrhagic fever: history, epidemiology, pathogenesis, clinical syndrome and genetic diversity. Antiviral Res. 2013;100:159–89. https://doi.org/10.1016/j.antiviral.2013.07.006
5. Ergönül O. Treatment of Crimean-Congo hemorrhagic fever. Antiviral Res. 2008;78:125–31. https://doi.org/10.1016/j.antiviral.2007.11.002
6. Hawman DW, Feldmann H. Crimean-Congo haemorrhagic fever virus. Nat Rev Microbiol. 2023;21:463–77. https://doi.org/10.1038/s41579-023-00871-9
7. World Health Organization. Crimean-Congo haemorrhagic fever fact sheet. 2025 [2025 Aug 20]. https://www.who.int/news-room/fact-sheets/detail/crimean-congo-haemorrhagic-fever
8. Tantawi HH, Al-Moslih MI, Al-Janabi NY, Al-Bana AS, Mahmud MI, Jurji F, et al. Crimean-Congo haemorrhagic fever virus in Iraq: isolation, identification and electron microscopy. Acta Virol. 1980;24:464–7.
9. Tantawi HH, Shony MO, Al-Tikriti SK. Antibodies to Crimean-Congo haemorrhagic fever virus in domestic animals in Iraq: a seroepidemiological survey. Int J Zoonoses. 1981;8:115–20.
10. Majeed B, Dicker R, Nawar A, Badri S, Noah A, Muslem H. Morbidity and mortality of Crimean-Congo hemorrhagic fever in Iraq: cases reported to the National Surveillance System, 1990–2010. Trans R Soc Trop Med Hyg. 2012;106:480–3. https://doi.org/10.1016/j.trstmh.2012.04.006
11. Alhilfi RA, Khaleel HA, Raheem BM, Mahdi SG, Tabche C, Rawaf S. Large outbreak of Crimean-Congo haemorrhagic fever in Iraq, 2022. IJID Reg. 2023;6:76–9. https://doi.org/10.1016/j.ijregi.2023.01.007
12. Atwan Z, Alhilfi R, Mousa AK, Rawaf S, Torre JDL, Hashim AR, et al. Alarming update on incidence of Crimean-Congo hemorrhagic fever in Iraq in 2023. IJID Reg. 2024;10:75–9. https://doi.org/10.1016/j.ijregi.2023.11.018
13. Kodama C, Alhilfi RA, Aakef I, Khamasi A, Mahdi S, Hasan HM, et al. Epidemiological analysis and potential factors affecting the 2022–23 Crimean-Congo hemorrhagic fever outbreak in Iraq. Eur J Public Health. 2025;35(Supplement_1):i6–13. https://doi.org/10.1093/eurpub/ckae147
14. Perkins NJ, Schisterman EF. The inconsistency of "optimal" cutpoints obtained using two criteria based on the receiver operating characteristic curve. Am J Epidemiol. 2006;163:670–5. https://doi.org/10.1093/aje/kwj063
15. Robin X, Turck N, Hainard A, Tiberti N, Lisacek F, Sanchez JC, et al. pROC: an open-source package for R and S+ to analyze and compare ROC curves. BMC Bioinformatics. 2011;12:77. https://doi.org/10.1186/1471-2105-12-77
16. Hatem A, Abou Turab M, Abdulzahra H. Diversity and seasonal occurrence of ticks from some wild mammals in South of Iraq. J Entomol Zool Stud. 2018;6:2788–91.
17. Akinci E, Bodur H, Sunbul M, Leblebicioglu H. Prognostic factors, pathophysiology and novel biomarkers in Crimean-Congo hemorrhagic fever. Antiviral Res. 2016;132:233–43. https://doi.org/10.1016/j.antiviral.2016.06.011
18. Sahay RR, Shete AM, Yadav PD, Patil S, Majumdar T, Jain R, et al. Sequential determination of viral load, humoral responses and phylogenetic analysis in fatal and non-fatal cases of Crimean-Congo hemorrhagic fever patients from Gujarat, India, 2019. PLoS Negl Trop Dis. 2021;15:e0009718. https://doi.org/10.1371/journal.pntd.0009718
19. Ahmeti S, Berisha L, Halili B, Ahmeti F, von Possel R, Thomé-Bolduan C, et al. Crimean-Congo hemorrhagic fever, Kosovo, 2013–2016. Emerg Infect Dis. 2019;25:321–4. https://doi.org/10.3201/eid2502.171999
20. Kerber R, Krumkamp R, Diallo B, Jaeger A, Rudolf M, Lanini S, et al. Analysis of diagnostic findings from the European Mobile Laboratory in Guéckédou, Guinea, March 2014 through March 2015. J Infect Dis. 2016;214(suppl 3):S250–7. https://doi.org/10.1093/infdis/jiw269
21. Strampe J, Asogun DA, Speranza E, Pahlmann M, Soucy A, Bockholt S, et al. Factors associated with progression to death in patients with Lassa fever in Nigeria: an observational study. Lancet Infect Dis. 2021;21:876–86. https://doi.org/10.1016/S1473-3099(20)30737-4
22. Tezer H, Sucakli IA, Sayli TR, Celikel E, Yakut I, Kara A, et al. Crimean-Congo hemorrhagic fever in children. J Clin Virol. 2010;48:184–6. https://doi.org/10.1016/j.jcv.2010.04.001

23. Bozkurt I, Erdeniz EH, Riley MJ, Şensoy L, Beeching NJ, Aydogdu S, et al. A comparison of clinical and laboratory features of Crimean-Congo hemorrhagic fever in children and adults: a retrospective single-center cohort study and literature review. Vector Borne Zoonotic Dis. 2025;25:81–91. https://doi.org/10.1089/vbz.2024.0066
24. Nanclares C, Kapetshi J, Lionetto F, de la Rosa O, Tamfun JJ, Alia M, et al. Ebola virus disease, Democratic Republic of the Congo, 2014. Emerg Infect Dis. 2016;22:1579–86. https://doi.org/10.3201/eid2209.160354
25. Duvignaud A, Etafo IC, Jaspard M, Salau Q, Serra B, Kareem AJ, et al. Presentation and outcomes of Lassa fever in children in Nigeria: a prospective cohort study (LASCOPE). J Pediatric Infect Dis Soc. 2024;13:513–22. https://doi.org/10.1093/jpids/piae083

Address for correspondence: Anaïs Legand, World Health Organization Av. Appia 20, 1211 Genève, Switzerland; email: leganda@who.int

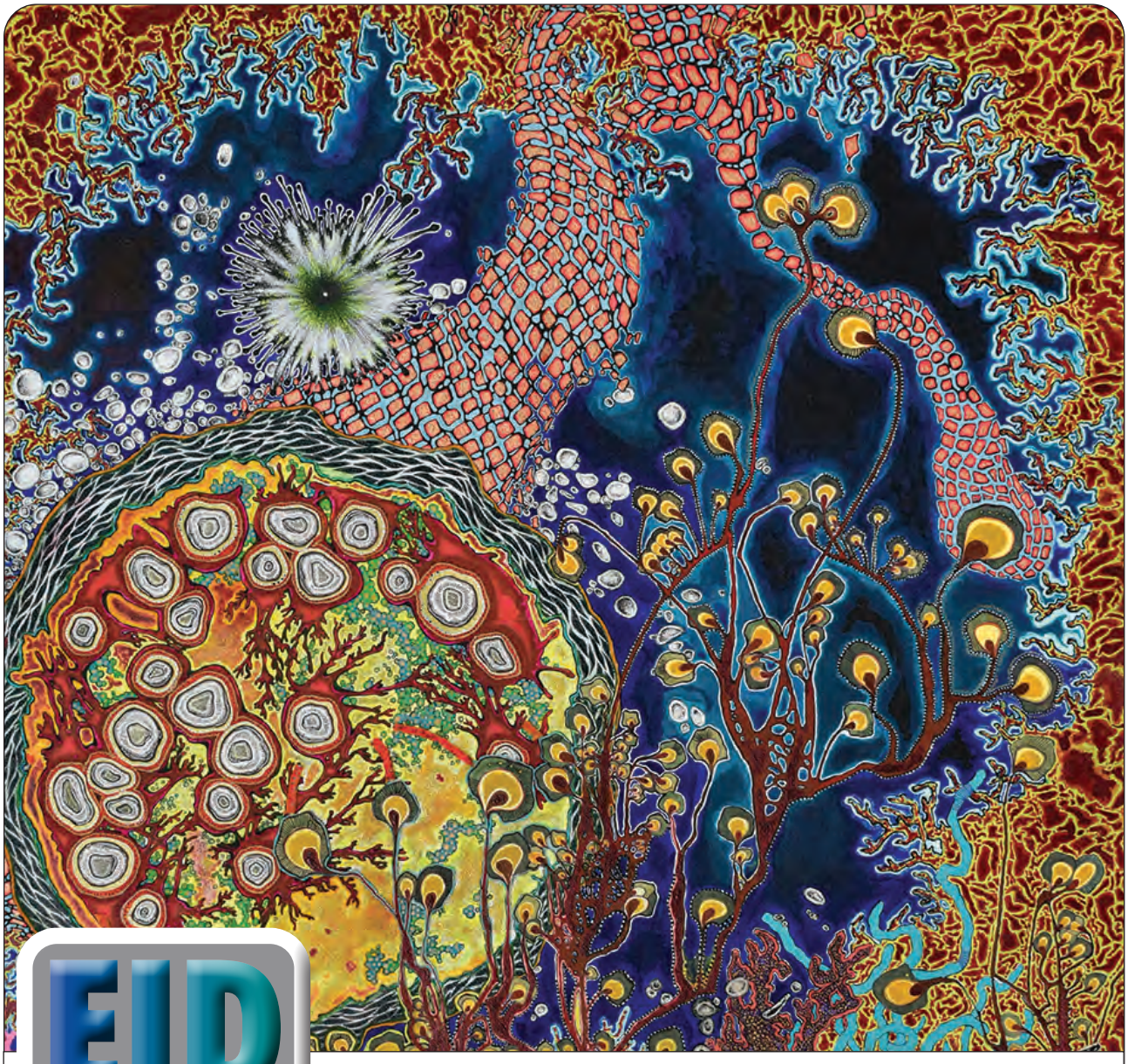

# Predictive Approach to Mapping *Angiostrongylus cantonensis* Nematode Distribution, Canary Islands, Spain

Lucia Anettová, Jan Divíšek, Radovan Coufal, Anna Šipková, Jana Kačmaříková, Michal Horsák, Vojtech Baláž, Elena Izquierdo-Rodriguez, Barbora Červená, Pilar Foronda, David Modrý

The invasive nematode *Angiostrongylus cantonensis* (rat lungworm) can cause eosinophilic meningitis in humans. Once restricted to Southeast Asia, *A. cantonensis* nematodes are now widespread across the tropics and have been reported in Europe. Tenerife, in the Canary Islands, and the Mediterranean region are emerging hotspots. We surveyed gastropods, rats, and lizards across Tenerife and detected the parasite in all host groups at 2.4%–41.6% prevalence. Using species distribution models, we identified precipitation seasonality as the main driver of habitat suitability; tree cover and climatic variability primarily shaped prevalence patterns. Modeling showed suitable habitats in northeastern Tenerife and several western Canary Islands but limited overlap with areas of dense human population. Multivariate environmental similarity surface analysis comparison with another *A. cantonensis* hotspot, Hawaii, USA, revealed similar environments across the archipelago, except for the novel northeastern Tenerife area. Although no human infections have been reported, continued vigilance is warranted because *A. cantonensis* nematodes are established in Tenerife.

*Angiostrongylus cantonensis* (the rat lungworm) is an invasive parasitic nematode originally endemic to Southeast Asia. Since its original description in China in the 1930s (*1*), the species has exhibited a remarkable capacity for global dispersal. Its range has steadily expanded, and *A. cantonensis* nematodes have been detected on all continents except Antarctica (*2*). Recent records suggest that the parasite is approaching or has already established new foci in or near Europe (*2*–*5*). The rat lungworm is considered a highly successful invader because of its widespread distribution and the invasive potential of its 2 primary host groups: rats as definitive hosts and gastropods as intermediate hosts. Representatives of those host groups are globally invasive and thrive in a wide range of environments (*6*–*9*). The close ecologic association with other successful invaders makes the *A. cantonensis* nematode a striking example of parallel biologic invasion, whereby the parasite expands its range in tandem with the global spread of its hosts.

The rat lungworm is an ecologically successful invader and zoonotic pathogen. In humans, the parasite is the primary cause of eosinophilic meningitis, which is increasingly recognized as a serious infectious disease known as neuroangiostrongyliasis (*10*). Clinical manifestations of *A. cantonensis* infection range from mild influenza-like symptoms to severe neurologic impairment and, in rare cases, death (*10*). In addition to humans, *A. cantonensis* nematodes can infect a wide range of accidental hosts, including other mammals and birds, in which it can cause neurologic symptoms (*11*–*14*).

Despite detection of the parasite in the Mediterranean and Macaronesia, Europe has only had a single reported case of likely autochthonous human neuroangiostrongyliasis, in France (*15*). That single case is in stark contrast to other affected regions, such as Southeast Asia, southern China, and the Pacific

Author affiliations: Czech University of Life Sciences, Prague, Czech Republic (L. Anettová, D. Modrý); Masaryk University, Brno, Czech Republic (J. Divíšek, R. Coufal, A. Šipková, M. Horsák, D. Modrý); University of Veterinary Sciences, Brno (J. Kačmaříková, V. Baláž, B. Červená); University of La Laguna, Tenerife, Spain (E. Izquierdo-Rodriguez, P. Foronda); Czech Academy of Sciences, Brno (B. Červená); Czech Academy of Sciences, České Budějovice, Czech Republic (D. Modrý)

DOI: https://doi.org/10.3201/eid3207.251930

Islands, where human cases are relatively common (*16*,*17*). One possible explanation for those differences lies in differences in cultural and dietary practices. In several endemic regions of Asia especially, traditional cuisine includes consumption of raw or undercooked gastropods and paratenic hosts, such as freshwater shrimp, frogs, and monitor lizards, increasing the risk for infection (*18*–*22*), but such practices are rare in Europe. Nevertheless, transmission can occur through accidental ingestion of small, infected gastropods contaminating fresh produce. Infective *A. cantonensis* larvae in gastropod mucus trails has been proposed as a possible route (*23*,*24*), but remains insufficiently demonstrated. Likewise, waterborne *A. cantonensis* transmission has been hypothesized (*25*) but lacks clear supporting evidence. Those possible transmission routes highlight the need for food hygiene and public awareness, even in regions where risky culinary practices are uncommon.

In addition to the newly recognized hotspots within Europe (*3*,*5*,*26*), the Canary Islands, an autonomous community of Spain located in the Atlantic Ocean ≈100 km northwest of Africa, represent a crucial focus of *A. cantonensis* nematodes. Rat lungworm was first reported in Tenerife, Canary Islands, from its definitive hosts in 2010 (*27*) and has been studied extensively in its intermediate and paratenic hosts (*4*,*28*–*30*). By 2025, high *A. cantonensis* prevalences had been reported in host species from the northeastern tip of Tenerife (*28*,*29*), but in the southern part of the island, only 1 positive sample had been documented, from an endemic *Gallotia galloti* lizard (*4*). That apparent spatial disparity might reflect both environmental influences and uneven sampling effort because host collection is generally easier in the humid north.

In contrast to other rat lungworm hotspots with similarly high prevalence in intermediate and paratenic hosts that can serve as sources of human infection (*31*–*33*), no human infection has been reported in the Canary Islands. In comparison, the Pacific Island of Hawaii, USA, another archipelago where *A. cantonensis* nematodes have been established and studied for decades, human infections have been reported since 1959 (*34*). Underdiagnosis cannot be entirely ruled out in the Canary Islands, but this well-developed region has a high standard of healthcare, making underdiagnosis less likely. Although the parasite has almost certainly been in Hawaii longer than in the Canary Islands (*31*), a comparison between climatic conditions could clarify differences in human infections between these 2 invaded archipelagos.

Despite extensive study, the probable distribution and key factors influencing *A. cantonensis* nematode prevalence across the Canary Islands is still unclear, limiting implementation of targeted surveillance. To shed more light on the occurrence of rat lungworm across in the archipelago, and to explain the apparent absence of human infections, we conducted a comprehensive analysis of parasites in 3 different host groups: definitive, intermediate, and paratenic. We also modeled spatial patterns in the distribution and prevalence of *A. cantonensis* nematodes in the Canary Islands and compared climatic conditions between the Canary Islands and Hawaii to assess relative contributions of environmental factors driving those patterns.

## Materials and Methods

### Sample Collection

Because Tenerife and the Canary Islands are characterized by diverse landscapes, a wide range of vegetation types, and substantial altitudinal variation (Figure 1), we hypothesized that the presence and prevalence of the nematode would vary considerably across the island. Thus, during April–May 2022, we collected samples from 3 host groups across 41 locations throughout the island, aiming to cover a range of altitude and vegetation zones with varying levels of anthropogenic influence (Figure 2). We considered an area of ≤400 $m^2$ as 1 location. We met all ethical requirements, and animal captures were authorized by the government of the Canary Islands in accordance with applicable law no. 42/2007, under expedient nos. 2022/14555 and 2022/11052.

### Rat Collection

We collected definitive rat hosts at 11 locations. We captured rats in live traps set at dusk, left overnight, and retrieved by dawn. A person authorized to handle and euthanize animals euthanized rats by using medetomidine (0.2 mg/kg) and ketamine (3.5 mg/kg), followed by intracardial T61 injection.

We dissected rats and collected adult nematodes from the heart or pulmonary arteries. We preliminarily identified recovered nematodes as *A. cantonensis* on the basis of macroscopic characteristics and preserved nematodes for subsequent molecular confirmation. We also collected brain samples and stored in 70% ethanol for molecular analysis. We considered rats positive if we confirmed adult nematodes from pulmonary arteries or heart.

### Lizard Sample Collection

For lizard samples, we used data from our previous study on *A. cantonensis* prevalence in *G. galloti* lizards

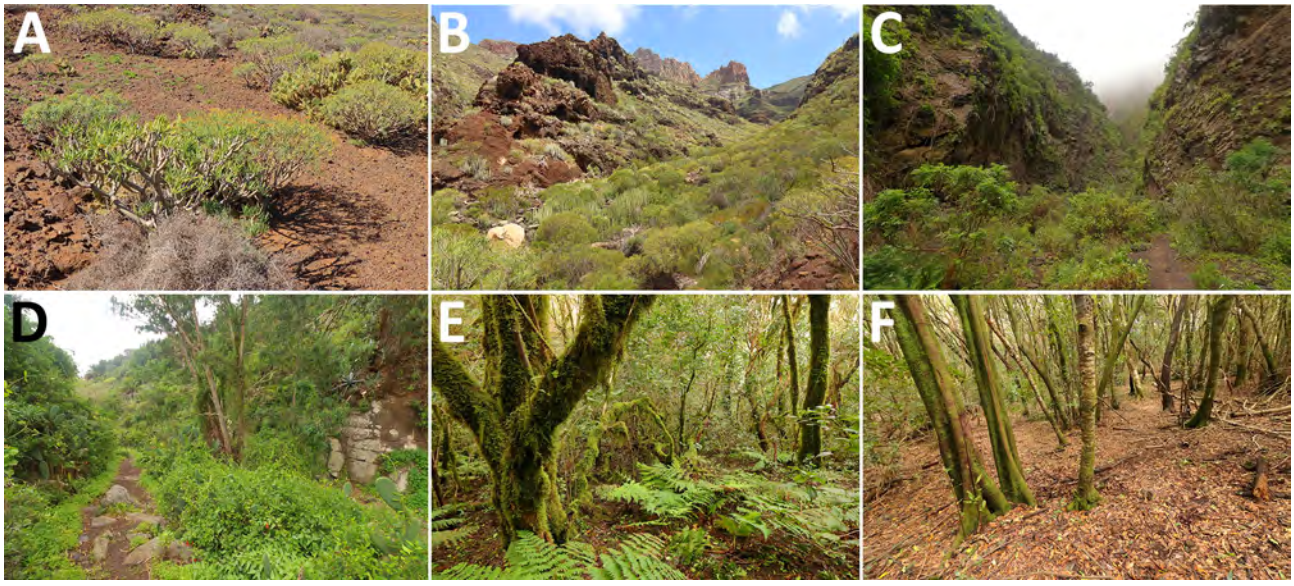


**Figure 1.** Examples of sampling sites for definitive, intermediate, and paratenic hosts used in a predictive approach to mapping *Angiostrongylus cantonensis* nematode distribution, Canary Islands, Spain. Hosts were collected and sampled in 2022 on Tenerife. A, B) Xeric vegetation types, including bare volcanic rocks with scattered succulents (A) and sparse xerophytic bushland (B). C, D) Bush vegetation, including continuous bush without tree cover (C) and continuous bush interspersed with isolated trees (D). E, F) Laurel forest in Anaga, Tenerife.

on Tenerife (*4*). For that study, we collected only tail tissue before releasing lizards. In brief, we captured lizards live in traps baited with a ripe tomato. Traps were checked hourly; we removed captured lizards, grasped the tail to induce caudal autotomy, then released the lizard (*4*). We retained the separated tail, approximately two thirds of the total length, and froze for *A. cantonensis* DNA testing (*4*).

### Gastropod Collection

We collected gastropods at 37 sites. One person searched each site, an area of ≈20 $m^2$ of homogeneous habitat, for ≈60 minutes. We collected both native and nonnative gastropods by handpicking. We did not use the litter sieving method because it primarily captures minute gastropod species that are unlikely to contribute substantially to *A. cantonensis* transmission dynamics.

We euthanized collected gastropods by freezing and subsequently preserved gastropods in molecular-grade 99% ethanol. We later performed species identification in the laboratory by following the MolluscaBase (https://www.molluscabase.org) nomenclature. Of all collected gastropods, we selected 697 for molecular analysis.

### Molecular Analysis

For molecular analysis, we defrosted lizard tails and weighed, using ≈25 mg of the proximal part of the tail (*4*). For gastropods, we used ≈25 μg of foot tissue; we processed a similar amount of cerebral tissue from the rats. We used the DNeasy Blood & Tissue Kit (QIAGEN, https://www.qiagen.com) to extract DNA from gastropod, lizard, and rat tissues using an extended overnight prelysis step.

We performed quantitative PCR by using a LightCycler 480 instrument (Roche Life Science, https://lifescience.roche.com), following previously published protocols (*35*). For positive controls, we extracted DNA from a single third-stage *A. cantonensis* larva by the same method used for the samples and diluted ×100. We used nuclease-free water as a negative control. We ran the assay in duplicate and calculated the average cycle threshold (Ct) values between positive sample duplicates by performing absolute quantification analysis of the 2nd derivative maximum. We only considered amplification curves with a Ct value <35 positive to avoid false-positive results caused by amplification and fluorescence artifacts or by cross-contamination.

For adult nematodes, we extracted DNA from approximately the middle third of the body by using innuPREP Forensic Kit (Innuscreen GmbH, https://innuscreen.ist-ag.com). We amplified the complete cytochrome c oxidase subunit I (COI) gene, as previously described (*5*). We separated PCR products and visualized by using agarose gel electrophoresis and subsequently purified by using ExoSAP-IT reagent (Thermo Fisher Scientific, https://www.thermofisher.com). We submitted samples to SEQme

(https://www.seqme.eu) for Sanger sequencing. We checked, trimmed and aligned sequences in Geneious Prime 2025.2.2 (https://www.geneious.com) and checked their identity against the GenBank database by using BLASTn (https://blast.ncbi.nlm.nih.gov), according to described methods (*36*).

### Species Distribution Modeling

To model the potential distribution of *A. cantonensis* in the Canary Islands, we used data derived from field surveys. We considered locations positive if we detected the parasite's DNA by molecular methods in any host species (rats, lizards, or gastropods) or if we found adult nematodes in the pulmonary arteries of rats.

We performed species distribution modeling by using the maximum entropy algorithm in Maxent software version 3.4.4 (American Museum of Natural History, https://biodiversityinformatics.amnh.org/open_source/maxent). Environmental predictor variables included bioclimatic data, land cover, vegetation indices, and topographic characteristics (Appendix Table 1, https://wwwnc.cdc.gov/EID/article/32/7/25-1930-App1.pdf). We resampled all raster layers to a common resolution of ≈100 m² (0.0012555749) and kept in World Geodetic System 1984 (GIS Geography, https://gisgeography.com/wgs84-world-geodetic-system) to match the coordinate format of occurrence data. To ensure model calibration focused on Tenerife, we used a bias file to constrain background point selection to this island.

We obtained the bioclimatic variables for Tenerife from 1981–2010 from the CHELSA database (https://www.chelsa-climate.org). CHELSA variables included annual mean temperature in degrees Celsius (bio1), temperature seasonality (bio4), annual precipitation in kilograms per square meter (bio12), and precipitation seasonality (bio15) (*37*). We used a 2018 tree cover density (TCD) layer and CORINE land cover (CLC) categories from the European Union's Copernicus Land Monitoring Service (https://land.copernicus.eu) to represent the landscape structure and transformed TCD and CLC into binary layers. We aggregated CLC classes to define land categories as urban areas (class 1), agricultural land (classes 21, 22, and 24), forests (class 31), scrub vegetation (class 32), pastures and grasslands (classes 231 and 321), and nonvegetated areas (class 33).

We represented local site moisture conditions by a topographic wetness index (TWI), calculated in SAGA GIS version 8.3.0 (https://sagagis.com) on the basis of the Copernicus global and European digital elevation model (Copernicus Data Space Ecosystem, https://dataspace.copernicus.eu) at 90 meters resolution (*38*). We incorporated vegetation dynamics via

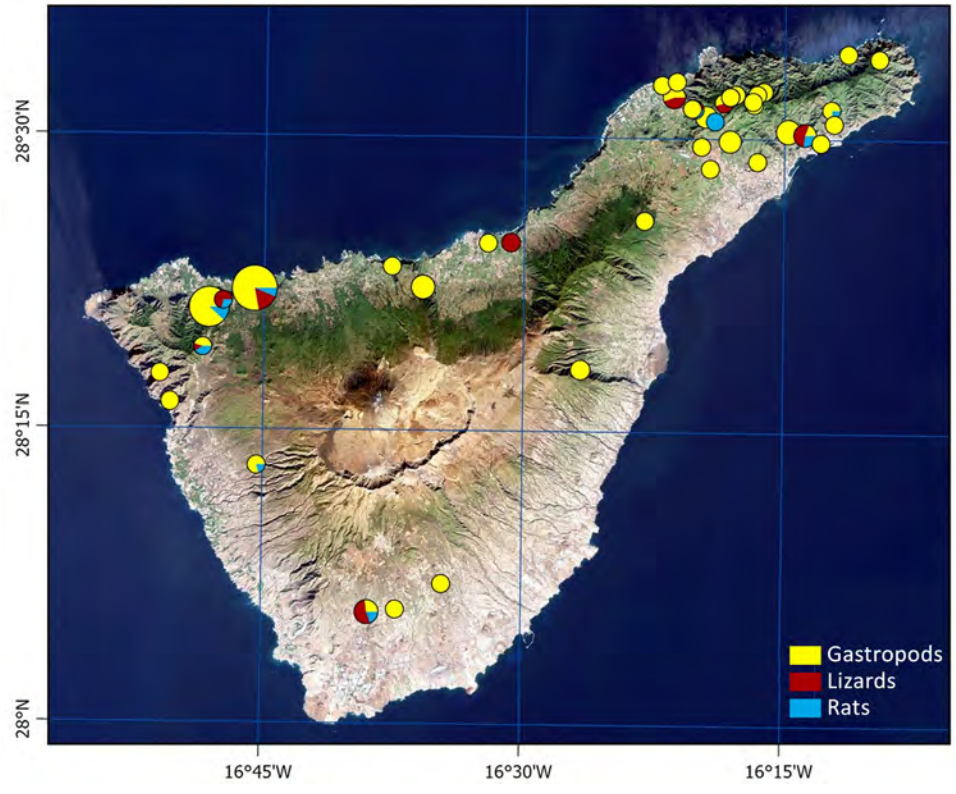


**Figure 2.** Host sampling sites used in a predictive approach to mapping *Angiostrongylus cantonensis* nematode distribution, Canary Islands, Spain. Host sampling included gastropods intermediate hosts, lizards paratenic hosts, and rats definitive hosts across Tenerife in 2022. We used those samples as the basis for prevalence estimates and species distribution modeling of *A. cantonensis*.

mean (SD) normalized difference vegetation index (NDVI) for 2022 (*39*). We also included a terrain ruggedness index (TRI) as a topographic predictor. We resampled all raster layers to a common resolution of ≈100 m² (0.0012555749) by using B-spline interpolation in SAGA GIS.

We trained models with default Maxent settings unless stated otherwise. We excluded variables contributing <0.5% to the model to improve model parsimony. We projected the final model to all Canary Islands to identify suitable habitats beyond Tenerife.

We calculated *A. cantonensis* prevalence as the percentage of positive samples for 37 locations in Tenerife. We excluded locations with <6 samples or with samples marked as failed or dubious. To model prevalence, we used a boosted regression tree (BRT) algorithm and the same set of environmental predictors as in the Maxent modeling. We used Mann-Whitney U test to assess differences in prevalence between locations with overlapping host groups and those with a single host group. To assess the overlap between areas with high human population density and predicted suitability for *A. cantonensis* nematodes, we overlaid the Maxent and the prevalence model outputs with land cover data on urban areas from CLC class 1.

We ran the BRT model in R (The R Project for Statistical Computing, https://www.r-project.org) by using the gbm.step function from the dismo package (https://r-packages.io/packages/dismo/circles). We used the following parameters in the BRT model: family = gaussian, tree.complexity = 3, learning.rate = 0.001, bag.fraction = 0.75, and step.size = 10. We selected the optimal number of boosted regression trees via 5-fold cross-validation. We weighted locations by the number of host samples collected per site, ranging from 6 to 106 (mean 23.84) host samples. We ran an initial model with all predictors, then removed predictors with zero contribution before refitting the final model using the same settings.

To assess climatic similarity between the Canary Islands and the Hawaiian Islands, we performed a multivariate environmental similarity surface (MESS) analysis in R by using the dismo and raster packages (https://r-packages.io/packages/dismo/circles). In that analysis, we used bioclimatic variables bio1, bio4, bio12, and bio15, as described. We obtained climatic data for Hawaii and the Canary Islands from the CHELSA database (1981–2010). We trained MESS on climatic data from Hawaii, then projected to the Canary Islands to identify areas of environmental similarity and novelty relative to the training region.

## Results

### *A. cantonensis* Distribution

Of 41 surveyed locations, we confirmed ≥1 positive host species in 35 locations. In total, we collected 78 rats (both *Rattus rattus* and *R. norvegicus*) from 11 sites; 13 (16.7%) rates tested positive. We observed the highest *A. cantonensis* prevalence in rats in Tegueste, the humid northeast of the island, where half of the examined rats carried the parasite. We confirmed all adult nematodes collected from rats were *A. cantonensis*, and COI sequences were identical across all specimens (GenBank accession no. PX496382).

Among 129 *G. galloti* lizards examined, 35 (27.1%) were *A. cantonensis* positive (*4*). For lizards, the highest infection rate (63.6%) was in Anaga National Park in the humid northeast.

Gastropods represented the largest sample set. Among 697 individual gastropods tested from 41 locations, 185 (26.7%) were *A. cantonensis* positive; results for 4 were inconclusive, showing weak or inconsistent amplification signals (Ct values ≥35) upon repeated quantitative PCR analysis. The Anaga region showed the highest *A. cantonensis* prevalence (43.3%) in gastropods.

After excluding sites with <6 samples or with failed or dubious results, prevalence estimates calculated for 37 sites ranged from 0 to 0.70 (mean 0.28). Sampling of multiple host groups overlapped in 11 locations, and 30 locations included only 1 host group (Appendix Table 2). Mean prevalence was lower in locations with multiple host groups (17.6%) compared with locations with a single host group (33.7%); however, that difference was not statistically significant ($p = 0.15$ by Mann-Whitney U test).

### Predicted Environmental Suitability

Maxent predictions showed that the highest habitat suitability is in the northeastern tip of the island, with scattered patches in mid-altitude zones. We retained 8 variables in the final model: precipitation seasonality, annual mean temperature, topographic wetness, terrain ruggedness, TCD, vegetation indices (mean NDVI [SD]), and temperature seasonality. The most influential predictors for *A. cantonensis* detection were precipitation seasonality (52.1% contribution), annual mean temperature (18.1% contribution), and terrain ruggedness (9.5% contribution) (Table 1). Response curves indicated that the parasite favored intermediate temperatures and lower rainfall variability (Appendix Figures 1–3). Intersecting the Maxent prediction with urbanized areas showed limited overlap between highly suitable habitats and densely urbanized zones (i.e., areas of high population

**Table 1.** Percent contribution and permutation importance of environmental variables retained in a predictive approach to mapping *Angiostrongylus cantonensis* nematode distribution, Canary Islands, Spain*

| Variable | % Contribution | Permutation |
|---|---|---|
| Precipitation seasonality | 52.1 | 9.6 |
| Mean annual temperature | 18.1 | 49.8 |
| Topographic wetness index | 10.4 | 9.4 |
| Terrain ruggedness index | 9.5 | 20.3 |
| Tree cover density, 2018 | 8.4 | 0.9 |
| Mean NDVI (SD), 2022 | 0.8 (0.5) | 1.6 (0.4) |
| Temperature seasonality | 0.4 | 7.9 |

*Predictions of habitat suitability (probability of occurrence) were made in MaxEnt mode on the basis of data from *A. cantonensis* field surveys conducted on Tenerife in 2022. We used bioclimatic variables from the CHELSA database (https://www.chelsa-climate.org) for 1981–2010 (*37*), including annual mean temperature in degrees Celsius (bio1), temperature seasonality (bio4), annual precipitation in kilograms per square meter (bio12), and precipitation seasonality (bio15). NDVI, normalized difference vegetation index.

density), and overlap mainly is restricted to small patches in the northeastern outcrop (Figure 3).

### Influences on Parasite Prevalence

The BRT model (pseudo-$R^2$ = 26%, mean squared error = 0.0412) confirmed that TCD (30.9%), precipitation seasonality (22.2%), and temperature seasonality (17.0%) were the strongest predictors of prevalence variation among sites. Vegetation indices also contributed notably (NDVI mean 12.7% [SD 6.9%]). In contrast, annual precipitation and topographic wetness had minimal influence (1%). The BRT model predicted prevalence values ranged from 20% to 32% across Tenerife. Predicted prevalence maps highlighted foci overlapping with the northeast but also indicated suitable mid-elevation habitats outside the current known *A. cantonensis* distribution (Table 2, Figure 3).

### Climatic Conditions Associated with *A. cantonensis* Distribution

MESS projections using bioclimatic variables bio1, bio4, bio12, and bio15 indicated relatively high environmental similarity to Hawaii in the drier leeward areas of southern Tenerife, southern Gran Canaria, and El Hierro, but the humid northeast of Tenerife showed low similarity and had novel conditions relative to Hawaii (Figure 4). Those projections suggest that climatic analogy to conditions in Hawaii occur primarily in drier Canary Island habitats, whereas the humid northeastern sector represents a distinct

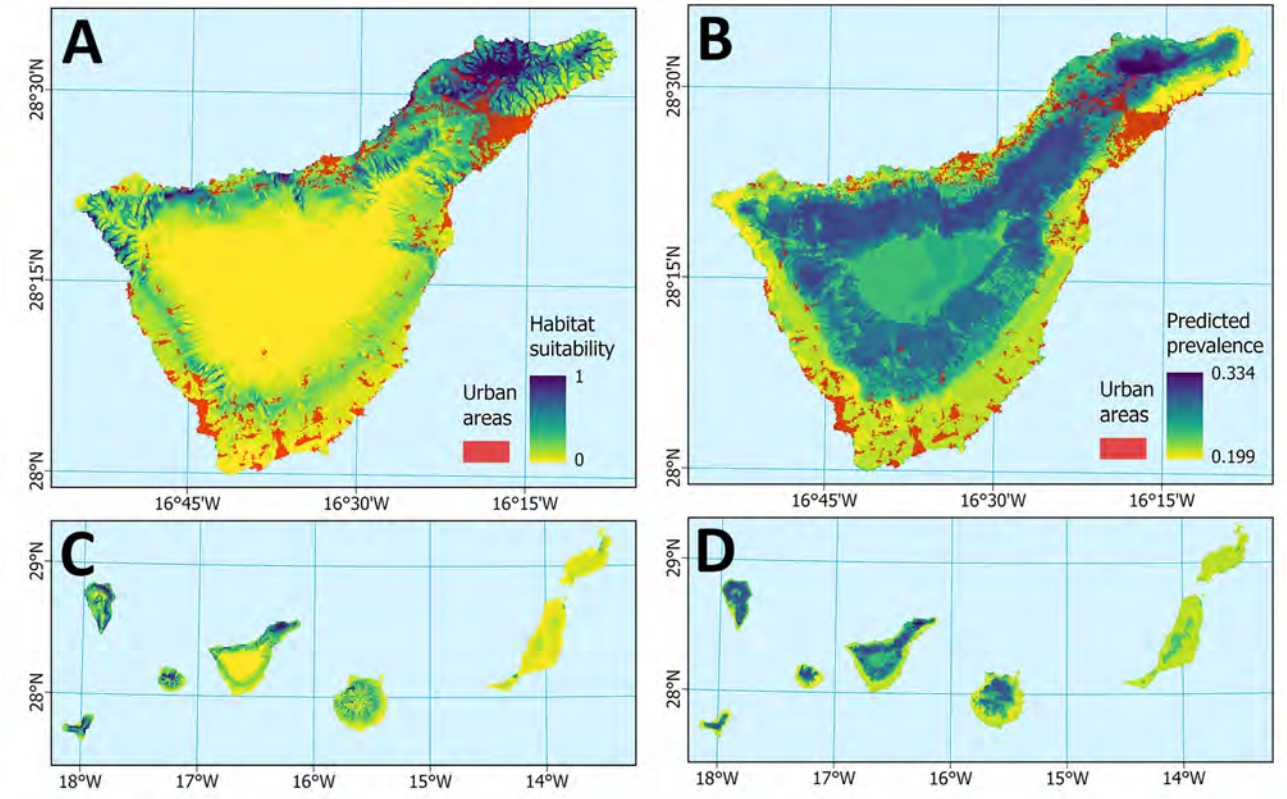


**Figure 3.** Modeled habitat suitability from a predictive approach to mapping *Angiostrongylus cantonensis* nematode distribution, Canary Islands, Spain, and prevalence of *A. cantonensis* across Tenerife and the Canary Islands based on field survey data (2022). A, C) MaxEnt model predicting habitat suitability (probability of occurrence), with overlap of urban areas (CORINE Land Cover, class 1), for Tenerife detail (A) and the Canary Islands archipelago (C). B, D) Boosted regression tree model predicting prevalence in Tenerife (B) and the Canary Islands archipelago (D).

environmental space that might follow its own transmission pathways.

## Discussion

Our survey confirms that *A. cantonensis* is now firmly established across Tenerife. The parasite was detected across the island, and 35 of 41 surveyed locations tested positive, including arid southern sites where the parasite was previously reported in endemic lizards (*4*).

The invasion process is typically described as a sequence of 5 stages: transport, introduction, establishment, spread, and negative impacts (*40*). Establishment can be recognized by the successful exploitation of local hosts and an increasing number of infected host species over time (*41*,*42*). Since the parasite was first recorded on Tenerife in 2010 (*27*), it circulated among both endemic and invasive species, involving intermediate as well as paratenic hosts (*28*,*30*). Therefore, we consider *A. cantonensis* nematodes to be well established on Tenerife. Distribution on the remaining Canary Islands is less clear, but the parasite has been documented in intermediate and accidental hosts on other islands in the archipelago (*43*). Involvement of multiple host taxa, including numerous gastropods species, lizards, and rats (Appendix Table 2), raises concerns not only for zoonotic risk but also for potential impacts on wildlife that could suffer from neurologic disease caused by *A. cantonensis* infection.

Although locations with multiple host groups might be expected to enable completion of the parasite life cycle, we did not observe higher *A. cantonensis* prevalence in those sites. That observation might reflect differences in sampling effort, host-specific infection dynamics, or environmental conditions rather than true transmission intensity. Thus, the presence of multiple host types alone might not be a sufficient indicator of elevated transmission risk.

Despite the well-documented presence of *A. cantonensis* nematodes in animal hosts, no human neuroangiostrongyliasis cases have been reported from Tenerife, mirroring a pattern from the Mediterranean where the parasite has been confirmed but no cases of human infection have been reported (*3*,*5*). One plausible explanation lies in local cultural and culinary practices. In contrast to Southeast Asia and parts of the Pacific, where raw or undercooked gastropods (including small or hidden gastropods on vegetation or produce), freshwater shrimp, frogs, or lizards are often consumed (*18*–*21*), such practices are not common in Europe. Sporadic cases in the future cannot be entirely ruled out, and although dietary habits and food preparation standards likely reduce infection risk, accidental exposure via produce contaminated with small gastropods remains possible.

In Tenerife specifically, our models highlight another potential factor: limited overlap between areas of highest predicted environmental suitability for *A. cantonensis* nematodes and densely populated urban zones. That overlap was restricted to small patches in the humid northeast. Instead, most of the suitable habitat is associated with forested or seminatural areas, where human–gastropod contact is expected to be less frequent. The parasite's dependence on precipitation seasonality and TCD, as identified by Maxent and BRT analyses, reinforces that pattern because those conditions are most pronounced in natural

**Table 2.** Relative influence of environmental variables in boosted regression tree model used in a predictive approach to mapping *Angiostrongylus cantonensis* nematode distribution, Canary Islands, Spain*

| Variable | % Relative influence |
|---|---|
| Tree cover density | 30.95 |
| Precipitation seasonality | 22.19 |
| Temperature seasonality | 17.03 |
| Mean NDVI (SD) | 12.74 (6.88) |
| Mean annual temperature | 5.83 |
| Terrain ruggedness index | 3.21 |
| Annual precipitation | 0.79 |
| Topographic wetness index | 0.36 |

*Model used local prevalence of *A. cantonensis* nematode detection among multiple host groups across Tenerife on the basis of 2022 field surveillance data. NDVI, normalized difference vegetation index.

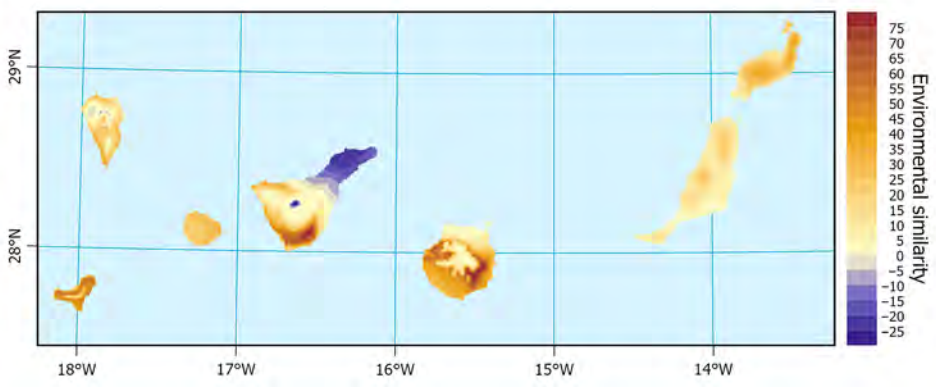


**Figure 4.** Multivariate Environmental Similarity Surface (MESS) analysis assessing climatic similarity between Hawaii, USA (training region with known human cases of neuroangiostrongyliasis), and the Canary Islands using selected bioclimatic variables in a predictive approach to mapping *Angiostrongylus cantonensis* nematode distribution, Canary Islands, Spain. Values indicate areas of environmental similarity and novelty relative to Hawaii.

and forested landscapes rather than in croplands or densely urbanized areas.

Of note, the BRT model explained only 26% of variation in prevalence values and produced predictions in a narrow range of 20%–32%, rather than across the full 0%–70% prevalence spectrum. Although the model was unable to predict exceptionally high prevalences, the spatial pattern was well captured, confirming the results of Maxent modeling.

The MESS analysis revealed variable climatic similarity across the Canary Islands. Drier leeward zones climatically resemble Hawaii, but the humid northeastern tip of Tenerife, where *A. cantonensis* prevalence is highest, falls outside the Hawaii reference climate. That apparent paradox illustrates that bioclimatic factors alone cannot predict parasite presence or human infection risk. Thus, distinction is needed between parasite establishment in natural hosts, shaped by climate and rat ecology, and human case emergence, which depends on ecologic, cultural, and socioeconomic exposure drivers.

Comparisons with other regions support that view. In Hawaii, where the parasite was introduced and is now widespread, cases of human infection have been reported (*31*), possibly related to anthropologic and ecologic factors, including fresh produce carrying small infected gastropods or, potentially, their mucus. On the other hand, in Australia, neuroangiostrongyliasis cases are more commonly reported in dogs (*44*), again reflecting local exposure pathways rather than climate alone. Those examples suggest that the parasite's broad ecologic tolerance and ability to persist in rats and snails effectively decouple its distribution from strict climatic boundaries. *A. cantonensis* nematodes have the capacity to overwinter in rodents because of long patent periods and have been experimentally shown to persist in snails (*45*), further widening the climatic niche beyond those captured by environmental predictors.

Limitations of this study include nonuniform host sampling across locations, single time-point prevalence estimates, and a MESS analysis restricted to climatic similarity without accounting for ecologic differences. Nonetheless, integrating field data with modeling offers a practical framework for identifying areas of potential risk.

In conclusion, our results highlight that species distribution models are useful for identifying environmental hotspots for *A. cantonensis* nematodes and guiding surveillance but cannot predict human infection risk alone. Future research should integrate ecologic modeling with epidemiologic and anthropologic perspectives, addressing dietary practices, food safety, water systems, and human behaviors that modulate zoonotic potential. The absence of human cases despite locally established host cycles in Tenerife, Mallorca, Valencia, and Naples suggests exposure-related factors are critical determinants. Nonetheless, continued vigilance for human *A. cantonensis* infection is warranted in areas with established host populations.

This article was preprinted at https://doi.org/10.1101/2025.11.28.691155.

The study was supported by SEAEUROPEJFS19IN-053 and the Czech Science Foundation grant no. 22-26136S. L.A. was also supported by specific research support of student projects (no. MUNI/ IGA/1182/2021). E.I.-R. was supported by M-ULL scholarship (M-ULL, convocatoria 2019). P.F. was supported by Consejería de Transición Ecológica, Lucha contra el Cambio Climático y Planificación Territorial (Gobierno de Canarias) "Estudio de patógenos en aves migratorias y en especies exóticas en un escenario de cambio climático."

Author contributions: D.M., L.A., and M.H. conceptualized the study; L.A., A.Š., V.B., J.D., D.M., and L.A. devised the methodology; L.A., R.C., A.Š., V.B., J.K., E.I.-R., and B.Č. conducted the investigation; D.M., J.D., and M.H. curated data; J.D., M.H., and D.M. supervised the study; J.D., M.H., and D.M. validated results; L.A., J.D., R.C., M.H., and D.M. wrote the manuscript; L.A., J.D., and R.C. created visualizations; D.M. acquired funding; P.F. administered the project and obtained resources.

## About the Author

Dr. Anettová is a researcher and assistant professor at the Czech University of Life Sciences in Prague, Czech Republic. Her research interests focus on zoonotic parasites, wildlife infectious diseases, and ecologic modelling of host–parasite systems.

## References

1. Chen HT. A new lungworm, *Pulmonema cantonensis*, n. g., n. sp. of Canton rats [in French]. Ann Parasitol Hum Comp. 1935;13:312–7. https://doi.org/10.1051/parasite/1935134312
2. Jaume-Ramis S, Martínez-Ortí A, Delgado-Serra S, Bargues MD, Mas-Coma S, Foronda P, et al. Potential intermediate hosts of *Angiostrongylus cantonensis* in the European Mediterranean region (Mallorca, Spain). One Health. 2023;17:100610. https://doi.org/10.1016/j.onehlt.2023.100610
3. Galán-Puchades MT, Gómez-Samblás M, Osuna A, Sáez-Durán S, Bueno-Marí R, Fuentes MV. Update on the first finding of the rat lungworm, *Angiostrongylus cantonensis*, in *Rattus* spp. in continental Europe, Valencia, Spain, 2022. Pathogens. 2023;12:567. https://doi.org/10.3390/pathogens12040567
4. Anettová L, Baláž V, Coufal R, Horsák M, Izquierdo-Rodriguez E, Šipková A, et al. Lizards as

sentinels for the distribution of *Angiostrongylus cantonensis*. Epidemiol Infect. 2024;152:e168. https://doi.org/10.1017/S0950268824000931
5. Pandian D, Šipková A, Scarcelli S, Sgroi G, Kačmaříková J, Buono F, et al. Detection of rat lungworm (*Angiostrongylus cantonensis*) in rats and gastropods, Italy. Emerg Infect Dis. 2025;31:1833–7. https://doi.org/10.3201/eid3109.250648
6. Thiengo SC, Faraco FA, Salgado NC, Cowie RH, Fernandez MA. Rapid spread of an invasive snail in South America: the giant African snail, *Achatina fulica*, in Brasil. Biol Invasions. 2007;9:693–702. https://doi.org/10.1007/s10530-006-9069-6
7. Martín PR, Burela S, Seuffert ME, Tamburi NE, Saveanu L. Invasive *Pomacea* snails: actual and potential environmental impacts and their underlying mechanisms. Perspect Agric Vet Sci Nutr Nat Resour. 2019;14:1–11. https://doi.org/10.1079/PAVSNNR201914042
8. Harper GA, van Dinther M, Russell JC, Bunbury N. The response of black rats (*Rattus rattus*) to evergreen and seasonally arid habitats: informing eradication planning on a tropical island. Biol Conserv. 2015;185:66–74. https://doi.org/10.1016/j.biocon.2014.11.044
9. Teles WS, Silva DP, Vilela B, Lima-Junior DP, Pires-Oliveira JC, Miranda MS. How will the distributions of native and invasive species be affected by climate change? Insights from giant South American land snails. Diversity (Basel). 2022;14:467. https://doi.org/10.3390/d14060467
10. Wang QP, Lai DH, Zhu XQ, Chen XG, Lun ZR. Human angiostrongyliasis. Lancet Infect Dis. 2008;8:621–30. https://doi.org/10.1016/S1473-3099(08)70229-9
11. Edwards EE, Borst MM, Lewis BC, Gomez G, Flanagan JP. *Angiostrongylus cantonensis* central nervous system infection in captive callitrichids in Texas. Vet Parasitol Reg Stud Reports. 2020;19:100363. https://doi.org/10.1016/j.vprsr.2019.100363
12. Rivory P, Pillay K, Lee R, Taylor D, Ward MP, Šlapeta J. Fatal neural angiostrongyliasis in the Bolivian squirrel monkey (*Saimiri boliviensis boliviensis*) leading to defining *Angiostrongylus cantonensis* risk map at a zoo in Australia. One Health. 2023;17:100628. https://doi.org/10.1016/j.onehlt.2023.100628
13. Burns RE, Bicknese EJ, Qvarnstrom Y, DeLeon-Carnes M, Drew CP, Gardiner CH, et al. Cerebral *Angiostrongylus cantonensis* infection in a captive African pygmy falcon (*Polihierax semitorquatus*) in southern California. J Vet Diagn Invest. 2014;26:695–8. https://doi.org/10.1177/1040638714544499
14. Monks DJ, Carlisle MS, Carrigan M, Rose K, Spratt D, Gallagher A, et al. *Angiostrongylus cantonensis* as a cause of cerebrospinal disease in a yellow-tailed black cockatoo (*Calyptorhynchus funereus*) and two tawny frogmouths (*Podargus strigoides*). J Avian Med Surg. 2005;19:289–93. https://doi.org/10.1647/2004-024.1
15. Nguyen Y, Rossi B, Argy N, Baker C, Nickel B, Marti H, et al. Autochthonous case of eosinophilic meningitis caused by *Angiostrongylus cantonensis*, France, 2016. Emerg Infect Dis. 2017;23:1045–6. https://doi.org/10.3201/eid2306.161999
16. Kliks MM, Palumbo NE. Eosinophilic meningitis beyond the Pacific Basin: the global dispersal of a peridomestic zoonosis caused by *Angiostrongylus cantonensis*, the nematode lungworm of rats. Soc Sci Med. 1992;34:199–212. https://doi.org/10.1016/0277-9536(92)90097-A
17. Wang QP, Wu ZD, Wei J, Owen RL, Lun ZR. Human *Angiostrongylus cantonensis*: an update. Eur J Clin Microbiol Infect Dis. 2012;31:389–95. https://doi.org/10.1007/s10096-011-1328-5
18. Tsai HC, Lai PH, Sy CL, Lee SSJ, Yen CM, Wann SR, et al. Encephalitis caused by *Angiostrongylus cantonensis* after eating raw frogs mixed with wine as a health supplement. Intern Med. 2011;50:771–4. https://doi.org/10.2169/internalmedicine.50.4193
19. Banerjee P, Chatterjee N, Chen JS, Dey G, Sharma R, Maity J, et al. Consumption of invasive apple snails (*Pomacea* spp.): a public health concern for neuroangiostrongyliasis in Taiwan. J. Environ Pharm Sustain Sci. 2025;2:1–17. https://doi.org/10.52756/jepss.2025.v02.i03.001
20. Li TM, Liu YH, Fang W, Zhao SH, Li T, Jiang L, et al. Monitoring the trends of *Angiostrongylus cantonensis* infection in humans and *Pomacea* spp. snails in Dali, Yunnan, China, 2007–2021. PLoS Negl Trop Dis. 2025;19:e0013065. https://doi.org/10.1371/journal.pntd.0013065
21. Yang L, Darasavath C, Chang K, Vilay V, Sengduangphachanh A, Adsamouth A, et al. Cluster of angiostrongyliasis cases following consumption of raw monitor lizard in the Lao People's Democratic Republic and review of the literature. Trop Med Infect Dis. 2021;6:107. https://doi.org/10.3390/tropicalmed6030107
22. Federspiel F, Skovmand S, Skarphedinsson S. Eosinophilic meningitis due to *Angiostrongylus cantonensis* in Europe. Int J Infect Dis. 2020;93:28–39. https://doi.org/10.1016/j.ijid.2020.01.012
23. Šipková A, Anettová L, Izquierdo-Rodriguez E, Velič V, Modrý D. Release of *Angiostrongylus cantonensis* larvae from live intermediate hosts under stress. Parasitol Res. 2024;123:212. https://doi.org/10.1007/s00436-024-08232-y
24. Rollins RL, Medeiros MCI, Cowie RH. Stressed snails release *Angiostrongylus cantonensis* (rat lungworm) larvae in their slime. One Health. 2023;17:100658. https://doi.org/10.1016/j.onehlt.2023.100658
25. Howe K, Kaluna L, Lozano A, Torres Fischer B, Tagami Y, McHugh R, et al. Water transmission potential of *Angiostrongylus cantonensis*: larval viability and effectiveness of rainwater catchment sediment filters. PLoS One. 2019;14:e0209813. https://doi.org/10.1371/journal.pone.0209813
26. Paredes-Esquivel C, Sola J, Delgado-Serra S, Puig Riera M, Negre N, Miranda MÁ, et al. *Angiostrongylus cantonensis* in North African hedgehogs as vertebrate hosts, Mallorca, Spain, October 2018. Euro Surveill. 2019;24:1900489. https://doi.org/10.2807/1560-7917.ES.2019.24.33.1900489
27. Foronda P, López-González M, Miquel J, Torres J, Segovia M, Abreu-Acosta N, et al. Finding of *Parastrongylus cantonensis* (Chen, 1935) in *Rattus rattus* in Tenerife, Canary Islands (Spain). Acta Trop. 2010;114:123–7. https://doi.org/10.1016/j.actatropica.2010.02.004
28. Martin-Alonso A, Abreu-Yanes E, Feliu C, Mas-Coma S, Bargues MD, Valladares B, et al. Intermediate hosts of *Angiostrongylus cantonensis* in Tenerife, Spain. PLoS One. 2015;10:e0120686. https://doi.org/10.1371/journal.pone. 0120686
29. Martín-Carrillo N, Feliu C, Abreu-Acosta N, Izquierdo-Rodriguez E, Dorta-Guerra R, Miquel J, et al. A peculiar distribution of the emerging nematode *Angiostrongylus cantonensis* in the Canary Islands (Spain): recent introduction or isolation effect? Animals (Basel). 2021;11:1267. https://doi.org/10.3390/ani11051267
30. Anettová L, Izquierdo-Rodriguez E, Foronda P, Baláž V, Novotný L, Modrý D. Endemic lizard *Gallotia galloti* is a paratenic host of invasive *Angiostrongylus cantonensis* in Tenerife, Spain. Parasitology. 2022;149:934–9. https://doi.org/10.1017/S0031182022000336
31. Johnston DI, Dixon MC, Elm JL, Calimlim PS, Sciulli RH, Park SY. Review of cases of angiostrongyliasis in Hawaii,

2007–2017. Am J Trop Med Hyg. 2019;101:608–16. https://doi.org/10.4269/ajtmh.19-0280
32. Kim JR, Wong TM, Curry PA, Yeung NW, Hayes KA, Cowie RH. Modelling the distribution in Hawaii of *Angiostrongylus cantonensis* (rat lungworm) in its gastropod hosts. Parasitology. 2019;146:42–9. https://doi.org/10.1017/S0031182018001026
33. Todaka T, Oshiro Y, Shinzato T. A case of human angiostrongyliasis manifesting as eosinophilic meningitis in Okinawa, Japan. Parasitol Int. 2020;77:102124. https://doi.org/10.1016/j.parint.2020.102124
34. Horio SR, Alicata JE. Parasitic meningo-encephalitis in Hawaii. A new parasitic disease of man. Hawaii Med J. 1961;21:139–40.
35. Sears WJ, Qvarnstrom Y, Dahlstrom E, Snook K, Kaluna L, Baláž V, et al. AcanR3990 qPCR: a novel, highly sensitive, bioinformatically-informed assay to detect *Angiostrongylus cantonensis* infections. Clin Infect Dis. 2021;73:e1594–600. https://doi.org/10.1093/cid/ciaa1791
36. Altschul SF, Gish W, Miller W, Myers EW, Lipman DJ. Basic local alignment search tool. J Mol Biol. 1990;215:403–10. https://doi.org/10.1016/S0022-2836(05)80360-2
37. Karger DN, Conrad O, Böhner J, Kawohl T, Kreft H, Soria-Auza RW, et al. Climatologies at high resolution for the earth's land surface areas. Sci Data. 2017;4:170122. https://doi.org/10.1038/sdata.2017.122
38. European Environment Agency. Copernicus global digital elevation models [cited 2026 Mar 19]. https://portal.opentopography.org/datasetMetadata?otCollectionID=OT.032021.4326.1 doi:10.5069/G9028PQB
39. Copernicus Land Monitoring Service. Normalised difference vegetation index 2020–2025 (raster 300 m), global, 10-daily—ersion 2 [cited 2026 Mar 19]. https://land.copernicus.eu/en/products/vegetation/normalised-difference-vegetation-index-v2-0-300m
40. Blackburn TM, Pyšek P, Bacher S, Carlton JT, Duncan RP, Jarošík V, et al. A proposed unified framework for biological invasions. Trends Ecol Evol. 2011;26:333–9. https://doi.org/10.1016/j.tree.2011.03.023
41. Lomolino MV, Brown JH, Sax DF. Island biogeography theory. In: Losos JB, Ricklefs RE eds. The theory of island biogeography revisited. Woodstock (UK): Princeton University Press; 2010. p. 13–51.
42. Fridley JD, Stachowicz JJ, Naeem S, Sax DF, Seabloom EW, Smith MD, et al. The invasion paradox: reconciling pattern and process in species invasions. Ecology. 2007;88:3–17. https://doi.org/10.1890/0012-9658(2007)88[3:TIPRPA]2.0.CO;2
43. Martin-Carrillo N, Baz-González E, García-Livia K, Amaro-Ramos V, Abreu-Acosta N, Miquel J, et al. Data on new intermediate and accidental hosts naturally infected with *Angiostrongylus cantonensis* in La Gomera and Gran Canaria (Canary Islands, Spain). Animals (Basel). 2023;13:1969. https://doi.org/10.3390/ani13121969
44. Lunn JA, Lee R, Smaller J, MacKay BM, King T, Hunt GB, et al. Twenty two cases of canine neural angiostrongylosis in eastern Australia (2002–2005) and a review of the literature. Parasit Vectors. 2012;5:70. https://doi.org/10.1186/1756-3305-5-70
45. Anettová L, Šipková A, Izquierdo-Rodriguez E, Velič V, Modrý D. Rat lungworm survives winter: experimental overwintering of *Angiostrongylus cantonensis* larvae in European slugs. Parasitology. 2023;150:950–5. https://doi.org/10.1017/S0031182023000781

Address for correspondence: Lucia Anettová, Department of Veterinary Sciences, Faculty of Agrobiology, Food and Natural Resources, Czech University of Life Sciences, Kamýcká 129, Prague 16500, Czech Republic; email: lucia.anettova@gmail.com

# Molecular Epidemiology of Skin-Dwelling Filariae and Risk Factors for *Mansonella streptocerca* Infection, Gabon

Capucine Marie Sicard, Mara Fischer, Chiara Wizemann, Marilen Bartling, Linda Martin, Miriam Rodi, Juliana Inoue, Sabrina Valeria Sinopoli, Esther Mehmel, Andrea Kreidenweiss, Pierre Blaise Matsiegui, Michael Ramharter, Selidji Todagbe Agnandji, Jana Held

*Mansonella streptocerca* is a species of neglected skin-dwelling filarial nematode parasite with scarce epidemiologic data from Central Africa. We conducted a cross-sectional survey of 1,007 adults from 51 rural and semiurban communities in Gabon to update prevalence estimates and identify risk factors. Molecular analyses by quantitative PCR detected filarial DNA in 18.3% of skin snips; *M. streptocerca* predominated (14.2%), and *Onchocerca volvulus* (3.4%) occurred focally in a single rural area. Blood-dwelling parasite species such as *Loa loa*, *M. perstans*, and *Mansonella* sp. "DEUX" were rarely detected. *M. streptocerca* infection was 4 times more frequent in rural areas than in semiurban areas and independently associated with male sex, urticaria, and poor housing conditions. *Wolbachia* DNA occurred in 28% of *M. streptocerca*–positive samples, suggesting endosymbiosis. Our findings reveal a substantial but overlooked burden of *M. streptocerca* nematodes in Gabon and emphasize the need for integrated surveillance of skin-dwelling filarial infections in Central Africa.

*Mansonella streptocerca* is a species of neglected, skin-dwelling filarial nematode that is transmitted by biting midges of the genus *Culicoides*. *M. streptocerca* is one of the least studied human filariae species; epidemiologic data are scarce compared with other species (*1*,*2*). Although often asymptomatic, infections can cause pruritus, papular dermatitis, or lymphadenopathy (*3*,*4*). Whether this species induces immunomodulatory effects, as for *M. perstans* nematodes, is unclear (*5*). Risk factors for infection with this parasite are unknown.

Central Africa presents a relevant epidemiologic context because of the dense rainforest ecosystem that promotes vector populations and human exposure (*6*,*7*). In Gabon, a country recognized as filarial-endemic, data on *M. streptocerca* nematodes are limited. A few parasitologic surveys in the 1970s and 1980s detected dermal filarial species in several regions (J. Chandenier, doctoral thesis, University of Paris VI, 1983), but large-scale molecular investigations have been lacking since. Coendemic filarial species complicate local epidemiology. *Onchocerca volvulus* nematodes, transmitted by *Simulium* black flies, cause major dermatologic and ocular disease, but data from Gabon remain scarce (*8*–*10*). In contrast to *Simulium* black flies, which require fast-flowing rivers for larval development (*11*), *Culicoides* midges typically breed in moist, organically rich substrates, such as damp soil and decaying vegetation (*12*). Those ecologic differences suggest that environmental determinants of transmission might vary substantially between skin-dwelling filariae. The *Loa loa* nematode, a blood-dwelling species, can occasionally be detected in skin in cases with high

Author affiliations: Institute of Tropical Medicine Tübingen, University Hospital Tübingen, Tübingen, Germany (C.M. Sicard, M. Fischer, C. Wizemann, M. Bartling, L. Martin, M. Rodi, J. Inoue, S.V. Sinopoli, A. Kreidenweiss, J. Held); Bernhard-Nocht Institute for Tropical Medicine, Hamburg, Germany (E. Mehmel, M. Ramharter); Centre de Recherches Médicales de Lambaréné (CERMEL), Lambaréné, Gabon (A. Kreidenweiss, M. Ramharter, S.T. Agnandji, J. Held); German Center for Infection Research (DZIF), partner site Tübingen, Tübingen (A. Kreidenweiss, J. Held); Centre de Recherches Médicales de la Ngounié, Fougamou, Gabon (P.B. Matsiegui); German Center for Infection Research, Partner Sites Hamburg-Lübeck-Borstel-Riems, Hamburg (M. Ramharter); Institute for Medical Microbiology, University Hospital Münster, Münster, Germany (S.T. Agnandji)

DOI: https://doi.org/10.3201/eid3207.251800

parasitemia (*13*,*14*). Loiasis is widespread in Gabon; hyperendemic areas are characterized by high microfilarial loads (*15*–*17*). Its coendemicity with onchocerciasis is programmatically relevant because ivermectin, the standard antiparasitic used for onchocerciasis control, can cause severe adverse events in persons with high *L. loa* microfilaremia (*18*). In addition, other blood-dwelling filaria such as *M. perstans* and the recently described *Mansonella* sp. "DEUX" nematodes are frequent blood parasites in populations in Gabon (*19*,*20*), yet their detection in skin snips is not documented. Among those human filariases, only onchocerciasis is currently included in the World Health Organization (WHO) list of neglected tropical diseases. No evidence of sustained large-scale antifilarial mass drug administration programs in Gabon was identified in the literature; the lack of evidence might partly reflect the difficulty of implementing such programs in the context of limited data on disease distribution and *L. loa* coendemicity (*21*).

Skin snipping has historically been the diagnostic standard of skin-dwelling filariae such as *O. volvulus* and *M. streptocerca*. Molecular tools have improved sensitivity and specificity of skin-snip analysis, enabling simultaneous detection of multiple species and clearer mapping of parasitic distributions.

This study was designed to update prevalence estimates of skin-dwelling filarial infections in 2 provinces of central Gabon, with a particular focus on *M. streptocerca* nematodes. We aimed to establish the risk factors and symptoms associated with this parasite. By combining population-based skin snip sampling with molecular assays and standardized questionnaires, we sought to better characterize the burden of these neglected filariae and inform future control strategies.

## Methods

### Ethics Approval

This cross-sectional study was conducted by convenience sampling during May 2022–December 2024. Ethical approval was granted by the Institutional Ethics Committee of the Centre de Recherches Médicales de Lambaréné (reference no. CEI-001/2022). All participants provided written informed consent before enrollment. Participation was voluntary, and participants were informed of their test results. *Onchocerca*-positive persons were offered doxycycline as treatment. The study followed the International Conference on Harmonization of Good Clinical Practice and the Declaration of Helsinki.

### Study Area and Population

The study took place in Ngounié and Moyen-Ogooué provinces in central Gabon, covering rural and semiurban communities around Lambaréné, Bifoun, Sindara, and Fougamou. Gabon is a country in Central Africa dominated by rainforest ecosystems, providing suitable conditions for filarial transmission.

Study sites were classified as rural or semiurban. Semiurban sites were the towns of Fougamou, Lambaréné, and Bifoun, defined by population size of ≥1,400 inhabitants (*22*) and partial access to infrastructure such as healthcare, electricity, or sanitation. Rural sites were small, often isolated villages with limited to absent public services. In total, we sampled 51 locations (35 rural and 16 semiurban) (Figure 1).

Adults (≥18 years of age) residing in the area who provided written consent were eligible to participate. Recruitment was community-based and conducted in public space. Each participant received a pseudonymized study identification.

### Sample Collection

We collected a superficial skin snip (≈2 mg) from the scapular region under local anesthesia (EMLA; Aspen Pharmacare, https://www.aspenpharma.com). We took snips using sterile cannulas and scalpels and disinfected wound sites before and after sampling. We stored snips in DNA/RNA Shield (Zymo Research, https://www.zymoresearch.com) at −20°C until further on-site procedures.

### Questionnaire Data

Trained interviewers administered a structured questionnaire in French language. Demographic information included sex, age, occupation, and type of residence. Occupations were grouped into 5 categories: agriculture/forest labor, non-agricultural manual labor, health/public sector, commerce, and other (students, irregular work, unemployment). Vector exposure was assessed by self-reported frequency of bites by *Culicoides* midges (fourous in French) per day (>50, 10–50, <10, or never).

Self-reported clinical data included symptoms associated with filarial infections (pruritus, rash, urticaria, fatigue, joint pain, subcutaneous nodules, stomach pain, headaches); frequency was scored on an ordinal scale (daily, weekly, monthly, never). We recorded eye symptoms (yes/no), uncommon in *M. streptocerca* infections, to explore potential overlap with *O. volvulus* or *L. loa* infections. Participants reported medical history (chronic illness, filarial diagnosis in the past year), recent antiparasitic treatment (Appendix, https://wwwnc.

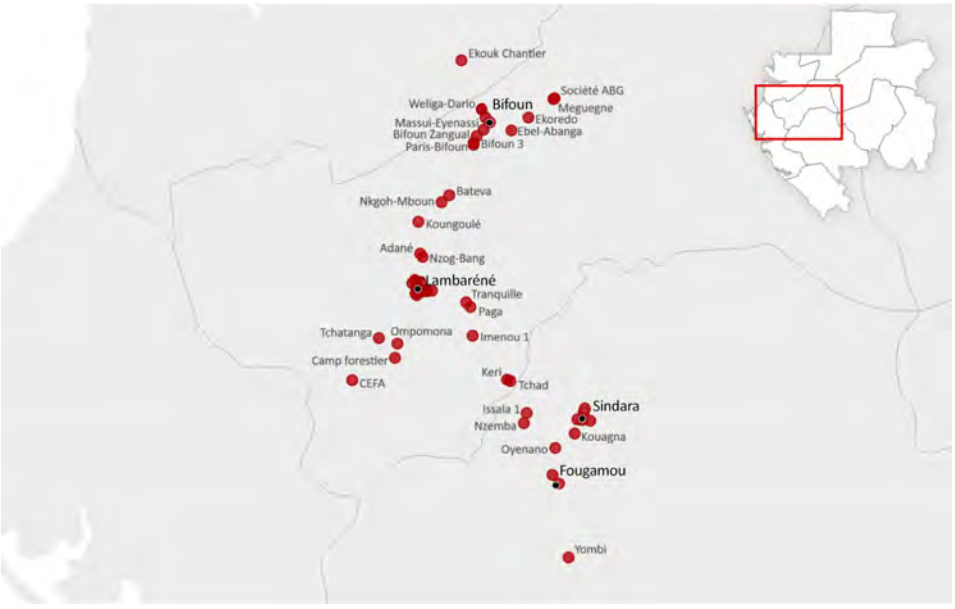


**Figure 1.** Sampling sites across central Gabon in study of molecular epidemiology of skin-dwelling filariae and risk factors for *Mansonella streptocerca* infection, Gabon. For clarity in labeling, nearby semiurban sampling sites were grouped under their respective town names (e.g., Lambaréné, Bifoun, Fougamou). Although Sindara is a cluster of rural villages, not a town, it was labeled as a town because of the high number of sampling sites in the area and its central role in the analysis. Inset map shows location of study area in Gabon.

cdc.gov/EID/article/32/7/25-1800-App1.pdf), travel outside their region within 1 year, and presence of domestic animals or rodents in the household. We assessed housing quality with 4 binary indicators: protected drinking water, electricity, cement flooring, and improved sanitation. A composite housing score (0–4) reflected infrastructure quality; higher scores indicated better housing conditions. Participants also rated the effects of skin problems on daily life (not at all, a little, a lot, very much).

### Laboratory Procedures and Quantitative PCR Assay Design

We extracted DNA from skin snips using the Monarch Genomic DNA Purification Kit (New England Biolabs, https://www.neb.com), eluted it in 60 µL buffer, and stored at −20°C until analysis. Filarial DNA detection targeted the internal transcribed spacer 1 (ITS1) region (Appendix Table 1). We performed screening with a published pan-filaria quantitative PCR (qPCR) (*23*) targeting a well-conserved sequence shared by all filarial species. Positive samples underwent a preamplification step of the ITS1 region following established protocols (*21*) to increase template availability for downstream assays.

We then conducted species-specific qPCRs for *M. streptocerca*, *M. perstans*, *Mansonella* sp. "DEUX," *O. volvulus*, and *L. loa*. Species-specific probes for *M. streptocerca* and *O. volvulus* nematodes were newly designed within the ITS1 region (Appendix). Each 20 µL reaction included buffer (SensiMix II Probe No-ROX [Meridian Bioscience, https://www.meridianbioscience.com] for pan-filaria and *L. loa* qPCR; 10× PCR Buffer [QIAGEN, https://www.qiagen.com] for preamplification; SensiFAST Probe No-ROX Mix [Meridian Biosciences] for all other reactions), primers (Integrated DNA Technologies, https://www.idtdna.com), and species-specific hydrolysis probes (Eurofins Genomics, https://eurofinsgenomics.com). Cycling consisted of an initial denaturation (95°C, 10 min), followed by 45 cycles of denaturation (95°C, 10 s) and annealing/extension (58°C, 60 s). For *Mansonella* sp. "DEUX" and *L. loa*, we performed annealing at 62°C. Positive controls consisted of synthetic plasmids carrying ITS1 inserts of the targeted species (*M. streptocerca*, *M. perstans*, *Mansonella* sp. "DEUX," *O. volvulus*) (Appendix Table 2). For *L. loa*, we used monoinfected DNA samples with low cycle quantification (Cq) values as controls. Negative controls included nuclease-free water and noninfected human DNA.

We screened a subset of *M. streptocerca*–positive samples for *Wolbachia* DNA by qPCR, according to published protocols (*19*,*24*). Assays targeted the *Wolbachia ftsZ* gene using species-specific primers and probes (Appendix Table 1) after a preamplification step. We selected the *Wolbachia* cell-division gene (*ftsZ*) as a highly conserved marker that enables detection across nematode-associated *Wolbachia* supergroups C, D, F, and J. Each reaction included *O. volvulus* DNA as a positive control and nuclease-free water as a negative control.

We performed all molecular assays in duplicate using a LightCycler 480 system (Roche, https://www.roche.com). Because the ITS1 region is multicopy and a preamplification step has been incorporated, we interpreted the Cq values as relative measures of

template abundance rather than as direct estimates of microfilarial density.

### Data Management and Statistical Analysis

We pseudonymized and analyzed all data in R version 4.5.0 (The R Project for Statistical Computing, https://www.r-project.org). We considered a sample positive if amplification occurred in ≥1 of 2 assay duplicates with a characteristic sigmoidal curve and any Cq value in qPCR.

We calculated prevalence estimates with exact (Clopper-Pearson) 95% CIs. We assessed associations between infection status and categorical variables (binary or multi-category) using the Pearson $\chi^2$ test of independence (or Fisher exact test when expected counts were <5). We defined age categories (18–34, 35–50, 51–62, ≥63 years) using quartiles to distribute participants evenly across categories and analyzed them as ordered variables using the Cochran-Armitage trend test to evaluate linear trends in prevalence across categories.

We tested ordinal questionnaire variables (e.g., frequency of reported symptoms, number of *Culicoides* midge bites, housing score) using trend tests or Mann-Whitney U tests as appropriate (Table 1). To account for potential collinearity, we evaluated dependence between key predictors (occupation, housing quality, sex, and rural/urban residence) using $\chi^2$ tests of independence (Table 1). We interpreted variables showing strong overlap with caution in multivariable models.

We analyzed independent predictors of *M. streptocerca* infection using multivariable logistic regression. We derived a parsimonious final model by stepwise Akaike information criterion selection and formally tested a sex/occupation interaction. We presented results as adjusted odds ratios (aOR) with 95% CIs and p values; we excluded missing responses. Analyses focused solely on *M. streptocerca* nematodes, the predominant species detected in skin snips.

## Results

We enrolled 1,007 adults from 51 sampling points. Participants were balanced by sex (49% female, 50% male) and were 18–97 years of age (Table 2). Most (63.9%) lived in rural areas, whereas 36.1% were from semiurban centers (Table 2). Agriculture and forest-related work predominated in rural villages, whereas semiurban residents were more often employed in commerce, health, or public services (Table 2).

Pan-filaria screening identified filarial DNA in 18.3% (median Cq 34.42) of skin snips. *M. streptocerca* was the most frequent nematode species at 14.2% (median Cq 19.38), followed by *O. volvulus* at 3.4% (median Cq 17.35). Blood-dwelling nematode species were occasionally detected in skin samples: *L. loa* in 4.1% (median Cq 22.80), *M. perstans* in 0.3% (median Cq 33.21), and *Mansonella* sp. "DEUX" in a single case (0.1% [median Cq 13.32]); 3.8% of the participants were co-infected with ≥2 species (Appendix Table 3, Figure 1). Of 67 monoinfected *M. streptocerca* nematode–positive samples, 19 (28.4%) tested positive for *Wolbachia* nematodes after preamplification. Median Cq values of *M. streptocerca* ITS1 qPCR were significantly lower in *Wolbachia*-positive samples than in *Wolbachia*-negative samples (12.77 vs. 18.20 by Wilcoxon rank-sum test; p<0.001), which is consistent with higher template abundance in *Wolbachia*-positive samples (Appendix Figure 2). However, given the preamplification step before the species-specific detection, Cq values should not be interpreted as direct quantitative measures of microfilaremia. To validate qPCR results, we sequenced the *Wolbachia ftsZ* target region in 11 samples and confirmed the expected sequence in 9 of them. We generated a consensus sequence from 4 *M. streptocerca* nematode–positive samples (GenBank accession nos. PZ173978–81) (Appendix). Compared with the published *Wolbachia ftsZ* sequence from *M. perstans* (GenBank accession no. KJ631375), the 438-bp consensus sequence obtained from *M. streptocerca* nematode–positive samples showed 8 nt differences.

Geographic mapping showed marked heterogeneity; filaria prevalence ranged from no cases to >60% for different sites (Figure 2, panel A; Appendix Table 4). The distribution of *M. streptocerca* nematodes (Figure 2, panel B) largely mirrored overall positivity, exceeding 40% in some rural sites and reaching up to 80% in Nzoghe-Bang. By contrast, some semiurban sites had no cases (e.g., Atongowanga). *M. streptocerca* nematode prevalence was 19.3% in rural areas (range 0%–80%) compared with 5.2% in semiurban areas (range 0%–23.1%), a highly significant difference (p<0.0001 by $\chi^2$ test). Infection was 4 times more likely in rural residents (odds ratio 4.34 [95% CI 2.63–7.16]); *O. volvulus* nematodes (Figure 2, panel C) displayed a highly focal pattern, confined almost entirely to 1 area (Sindara area).

Infection was significantly more common in men (102/504 [20.2%]) than in women (40/489 [8.2%]) (p<0.0001 by $\chi^2$ test) (Table 1). No significant linear trend was observed across age categories (p = 0.893 by Cochran-Armitage test). Occupational categories showed heterogeneous risks: nonagricultural manual laborers had the highest prevalence (19/82 [23.2%]) of the occupational categories, and that association was significant in univariate analysis (p = 0.0065). Agricultural workers had a slightly higher prevalence than

**Table 1.** Univariate analysis of associations between demographic, environmental, and clinical variables and *Mansonella streptocerca* infection in study of molecular epidemiology of skin-dwelling filariae and risk factors for *M. streptocerca* infection, Gabon*

| Category | No. participants | No. (%) *M. streptocerca* qPCR-positive | No. (%) *M. streptocerca* qPCR-negative | p value (test) |
|---|---|---|---|---|
| Total no. | 1,007 | 143 (14.2) | 864 (85.8) | |
| Age, y | | | | |
| 18–34 | 249 | 37 (25.9) | 212 (24.5) | 0.893 (Cochran-Armitage) |
| 35–50 | 261 | 34 (23.8) | 227 (26.3) | |
| 51–62 | 249 | 34 (23.8) | 215 (24.9) | |
| 63–100 | 231 | 35 (24.5) | 196 (22.7) | |
| Unknown | 17 | 3 (2.1) | 14 (1.6) | |
| Sex | | | | |
| M | 504 | 102 (71.3) | 402 (46.5) | **<0.001** ($\chi^2$) |
| F | 489 | 40 (28.0) | 449 (52.0) | |
| Unknown | 14 | 1 (0.7) | 13 (1.5) | |
| Occupation | | | | |
| Agriculture | 447 | 72 (50.3) | 375 (43.4) | **0.007** ($\chi^2$) |
| Nonagricultural manual labor | 82 | 19 (13.3) | 63 (7.3) | |
| Health and public sector | 86 | 14 (9.8) | 72 (8.3) | |
| Commerce | 49 | 3 (2.1) | 46 (5.3) | |
| Other | 328 | 33 (23.1) | 295 (34.1) | |
| No answer | 15 | 2 (1.4) | 13 (1.5) | |
| Comorbidities | | | | |
| Yes | 247 | 28 (19.6) | 219 (25.3) | 0.199 ($\chi^2$) |
| No | 739 | 110 (76.9) | 629 (72.8) | |
| No answer | 21 | 5 (3.5) | 16 (1.9) | |
| No. *Culicoides* midge bites/day | | | | |
| >50 | 382 | 47 (32.9) | 335 (38.8) | 0.440 (Mann-Whitney U) |
| 10–49 | 345 | 51 (35.7) | 294 (34.0) | |
| <10 | 208 | 33 (23.1) | 175 (20.3) | |
| Rare/never | 47 | 4 (2.8) | 43 (5.0) | |
| No answer | 25 | 8 (5.6) | 17 (2.0) | |
| Everyday life impacted by skin condition | | | | |
| A lot | 55 | 3 (2.1) | 52 (6.0) | 0.410 (Mann-Whitney U) |
| Sometimes | 116 | 12 (8.4) | 104 (12.0) | |
| Rarely | 181 | 23 (16.1) | 158 (18.3) | |
| Never | 330 | 25 (17.5) | 305 (35.3) | |
| No answer | 325 | 80 (55.9) | 245 (28.4) | |
| History of helminth infection within 1 y | | | | |
| No | 941 | 130 (90.9) | 811 (93.9) | 0.509 ($\chi^2$) |
| Yes | 43 | 8 (5.6) | 35 (4.1) | |
| No answer | 23 | 5 (3.5) | 18 (2.1) | |
| Anthelminthic treatment intake within 1 y | | | | |
| No | 906 | 124 (86.7) | 782 (90.5) | 0.219 ($\chi^2$) |
| Yes | 77 | 15 (10.5) | 62 (7.2) | |
| No answer | 24 | 4 (2.8) | 20 (2.3) | |
| Recent travel within 1 y | | | | |
| Yes | 718 | 96 (67.1) | 622 (72.0) | 0.377 ($\chi^2$) |
| No | 273 | 43 (30.1) | 230 (26.6) | |
| No answer | 17 | 4 (2.8) | 13 (1.5) | |
| Presence of animals inside the habitation | | | | |
| Yes | 813 | 98 (68.5) | 715 (82.8) | **<0.001** ($\chi^2$) |
| No | 176 | 42 (29.4) | 134 (15.5) | |
| No answer | 18 | 3 (2.1) | 15 (1.7) | |
| Filaria-related ocular symptoms | | | | |
| Yes | 322 | 41 (28.7) | 281 (32.5) | 0.313 ($\chi^2$) |
| No | 650 | 100 (69.9) | 550 (63.7) | |
| No answer | 35 | 2 (1.4) | 33 (3.8) | |
| Housing score | | | | |
| 4 | 133 | 5 (3.5) | 128 (14.8) | **0.011** (Mann-Whitney U) |
| 3 | 127 | 10 (7.0) | 117 (13.5) | |
| 2 | 249 | 23 (16.1) | 226 (26.2) | |
| 1 | 132 | 21 (14.7) | 111 (12.8) | |
| 0 | 53 | 4 (2.8) | 49 (5.7) | |
| No answer | 313 | 80 (55.9) | 233 (27.0) | |

*Bold p values indicate statistical significance (p<0.05). qPCR, quantitative PCR.

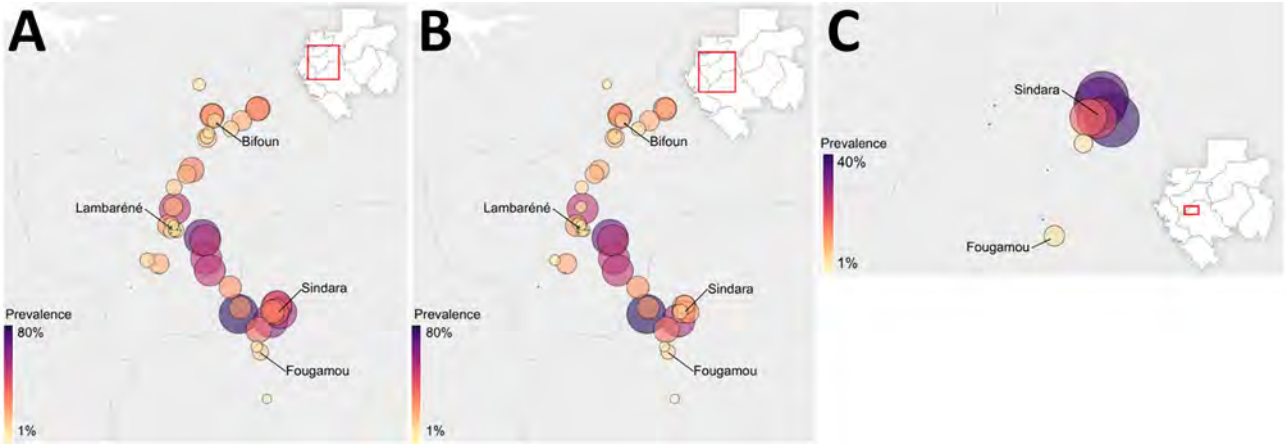


**Figure 2.** Geographic distribution of skin-dwelling filariae in central Gabon in study of molecular epidemiology of skin-dwelling filariae and risk factors for *Mansonella streptocerca* infection, Gabon. A) Overall filarial DNA prevalence; B) distribution of M. streptocerca nematodes; and C) distribution of *O. volvulus* nematodes, showing a focal hotspot around Sindara. Each circle represents 1 sampling area; size and color correspond to prevalence. Inset maps show locations of corresponding area in Gabon.

the general population (72/447 [16.2%]), although that difference did not reach statistical significance. Housing conditions were also associated with infection. Participants with lower housing scores, reflecting limited access to electricity, water, cement flooring, and sanitation, were more frequently infected (p = 0.0105), suggesting that improved infrastructure exerted a protective effect. Presence of animals inside the household had a protective effect against *M. streptocerca* infection; infected persons were less likely to report cohabitation with pets or domestic animals (p<0.0001). Other variables, including underlying conditions, travel history, recent antiparasitic treatment, and number of *Culicoides* midge bites reported per day, were not significantly associated with infection status.

Self-reported symptoms were examined for associations with *M. streptocerca* infection (Table 3). Joint pain, subcutaneous nodules, urticaria, and stomach pain were more frequent in infected participants, whereas no differences in fatigue, rash, and headaches were noted. Eye symptoms were included as exploratory variables but did not differ by infection status.

Multivariable logistic regression identified 3 independent predictors (Table 4). Male sex remained strongly associated with infection (aOR 2.9 [95% CI 1.6–5.4]; p = 0.001). Housing score also retained

**Table 2.** Population characteristics and prevalence of filarial DNA in 1,007 scapular skin snips in study of molecular epidemiology of skin-dwelling filariae and risk factors for *Mansonella streptocerca* infection, Gabon*

| | No. (%) participants | | | | |
|---|---|---|---|---|---|
| | | Age, y | | | |
| Category | Total | 18–34 | 35–50 | 51–62 | ≥63 |
| Total | 1,007 (100.0) | 249 (24.7) | 261 (25.9) | 249 (24.7) | 231 (22.9) |
| Sex | | | | | |
| F | 489 (48.6) | 111 (22.7) | 125 (25.6) | 129 (26.4) | 120 (24.5) |
| M | 507 (50.3) | 137 (27.0) | 136 (26.8) | 120 (23.7) | 111 (21.9) |
| Setting | | | | | |
| Rural | 643 (63.9) | 142 (22.1) | 151 (23.5) | 157 (24.4) | 180 (28.0) |
| Semiurban | 364 (36.1) | 107 (29.4) | 110 (30.2) | 92 (25.3) | 51 (14.0) |
| Occupation | | | | | |
| Agriculture and forestry | 447 (44.4) | 76 (17.0) | 121 (27.1) | 131 (29.3) | 118 (26.4) |
| Nonagricultural manual labor | 82 (8.1) | 20 (24.4) | 32 (39.0) | 18 (22.0) | 12 (14.6) |
| Health and public sector | 86 (8.5) | 14 (16.3) | 23 (26.7) | 25 (29.1) | 24 (27.9) |
| Commerce | 49 (4.9) | 9 (18.4) | 23 (46.9) | 14 (28.6) | 3 (6.1) |
| Other | 328 (32.6) | 130 (39.6) | 61 (18.6) | 61 (18.6) | 74 (22.6) |
| qPCR results | | | | | |
| Pan-filaria qPCR positive | 184 (18.3) | 47 (25.5) | 41 (22.3) | 47 (25.5) | 45 (24.5) |
| *M. streptocerca* qPCR positive | 143 (14.2) | 37 (25.9) | 34 (23.8) | 34 (23.8) | 35 (24.5) |
| *Loa loa* qPCR positive | 41 (4.1) | 9 (22.0) | 12 (29.3) | 15 (36.6) | 5 (12.2) |
| *O. volvulus* qPCR positive | 34 (3.4) | 11 (32.4) | 4 (11.8) | 10 (29.4) | 7 (20.6) |
| *M. perstans* qPCR positive | 3 (0.3) | 1 (33.3) | 0 | 1 (33.3) | 1 (33.3) |
| *Mansonella* sp. “DEUX” qPCR positive | 1 (0.1) | 0 | 0 | 1 (100.0) | 0 |
| Co-infections, ≥2 species) | 38 (3.8) | 9 (23.7) | 9 (23.7) | 14 (36.8) | 5 (13.2) |

*Totals may not sum to 100% due to missing or unknown responses, which are not displayed in the table. qPCR, quantitative PCR.

**Table 3.** Frequency of reported symptoms by infection status in study of molecular epidemiology of skin-dwelling filariae and risk factors for *Mansonella streptocerca* infection, Gabon*

| Symptoms | Total | No. (%) participants | | | | | | | | p value |
|---|---|---|---|---|---|---|---|---|---|---|
| | | Ms+ 4 | Ms+ 3 | Ms+ 2 | Ms+ 1 | Ms– 4 | Ms– 3 | Ms– 2 | Ms– 1 | |
| Urticaria | 976 | 57 (41) | 211 (25.2) | 17 (12.2) | 150 (17.9) | 15 (10.8) | 106 (12.7) | 50 (36) | 370 (44.2) | **0.003** |
| Fatigue or exhaustion | 971 | 40 (28.8) | 160 (19.2) | 20 (14.4) | 203 (24.4) | 17 (12.2) | 142 (17.1) | 62 (44.6) | 327 (39.3) | 0.727 |
| Cutaneous rash | 971 | 32 (22.9) | 117 (14.1) | 7 (5) | 113 (13.6) | 16 (11.4) | 97 (11.7) | 85 (60.7) | 504 (60.6) | 0.396 |
| Headaches | 978 | 48 (34.3) | 152 (18.1) | 14 (10) | 226 (27) | 26 (18.6) | 180 (21.5) | 52 (37.1) | 280 (33.4) | 0.266 |
| Stomach pain | 971 | 32 (23) | 85 (10.2) | 12 (8.6) | 116 (13.9) | 22 (15.8) | 171 (20.6) | 73 (52.5) | 460 (55.3) | **0.018** |
| Joint pain | 977 | 66 (47.5) | 325 (38.8) | 34 (24.5) | 152 (18.1) | 21 (15.1) | 115 (13.7) | 18 (12.9) | 246 (29.4) | **<0.001** |
| Subcutaneous nodules | 947 | 23 (16.7) | 46 (5.7) | 48 (34.8) | 128 (15.8) | 4 (2.9) | 45 (5.6) | 63 (45.7) | 590 (72.9) | **<0.001** |

*Ms+, PCR-positive for *M. streptocerca* (n = 143); Ms–, PCR-negative for *M. streptocerca* (n = 864). Numbers 1–4 indicate frequency of symptoms: 4, every day; 3, once a week; 2, once a month; 1, rarely/never. Bold p values indicate statistical significance (p<0.05).

significance; higher scores indicated protection (aOR 0.78 per unit increase [95% CI 0.61–0.98; p = 0.037). Urticaria frequency remained independently associated with infection (aOR 1.35 per category [95% CI 1.10–1.76]; p = 0.009). Among occupational groups, only the assigned group of other occupations showed lower odds than agriculture, whereas we detected no significant sex–occupation interaction (p = 0.24). Because the group was highly heterogeneous and the overall occupation variable did not remain significant after adjustment, that finding is unlikely to represent a true occupational effect.

To explore those confounding patterns, we tested collinearity between key predictors. Strong associations between occupation and both rural/urban residence (p<0.0001) and sex (p<0.0001) were demonstrated by $\chi^2$ tests of independence. Housing score was strongly correlated with place of residence (p<0.0001); poorer housing conditions were more common in rural areas. The small variation of housing scores by sex (p = 0.003) likely reflects differences in the sampling distribution between rural and semiurban households, rather than a true sex-related difference in housing conditions. Those results confirm that occupation and housing quality overlap strongly with structural demographic variables, which likely explains why occupation did not remain significant in the multivariable model. By contrast, housing retained an independent effect, indicating that even within rural or semiurban settings, better housing infrastructure conferred some protection.

## Discussion

This cross-sectional study shows that nearly 1 in 5 adults in central Gabon carried skin filariae; *M. streptocerca* nematodes dominated. Detected in 1 of 7 participants, *M. streptocerca* nematodes accounted for most filarial infections in scapular skin snips. Prevalence was highly uneven, exceeding 70% in some rural villages but remaining low in semiurban sites. This heterogeneity is consistent with earlier studies conducted in Gabon and Uganda where prevalences ranged from 5% to 90% depending on the region (*4*; J. Chandenier, doctoral thesis, University of Paris VI, 1983). By contrast, *O. volvulus* nematodes were confined to an epidemiologic hotspot (Sindara). As expected, blood-dwelling filariae such as *L. loa*, *M. perstans*, and *Mansonella* sp. "DEUX" were rarely identified. Detection was probably caused by a small amount of blood contaminating the snip during skin sampling or unusual localization of *L. loa* nematodes in the skin (*13*). Those data update the scarce epidemiologic information for skin-dwelling filaria for Gabon (J. Chandenier, doctoral thesis).

**Table 4.** Multivariate logistic regression analysis of potential risk factors associated with *Mansonella streptocerca* infection in study of molecular epidemiology of skin-dwelling filariae and risk factors for *M. streptocerca* infection, Gabon*

| Predictor | Category (reference) | Adjusted OR (95% CI) | p value |
|---|---|---|---|
| Sex | Male (female) | 2.86 (1.57–5.38) | **<0.001** |
| Occupation | Nonagricultural manual labor (agriculture) | 1.36 (0.59–3.00) | 0.458 |
| | Health/public (vs Agriculture) | 1.31 (0.45–3.37) | 0.599 |
| | Commerce (agriculture) | 0.81 (0.19–2.52) | 0.747 |
| | Other (agriculture) | 0.41 (0.19–0.82) | **0.014** |
| Housing score (0–4) | Per 1-unit increase† | 0.78 (0.61–0.98) | **0.037** |
| Urticaria frequency (1–4) | Per 1-category increase | 1.39 (1.10–1.76) | **0.009** |
| Stomach pain (1–4) | Per 1-category increase | 0.8 (0.58–1.12) | 0.195 |
| Joint pain (1–4) | Per 1-category increase | 1.03 (0.82–1.31) | 0.780 |
| Subcutaneous nodules (1–4) | Per 1-category increase | 1.07 (0.76–1.52) | 0.693 |
| Animals in the household | Yes (no) | 1.16 (0.49–2.74) | 0.730 |

*OR, odds ratio.
†For housing, adjusted OR <1 indicates that higher housing scores are protective (lower odds of infection). Bold p values indicate statistical significance (p < 0.05).

The predominance of *M. streptocerca* nematodes confirms the species' central role in filarial infections in rainforest regions of Central Africa (*3*,*4*). Infection prevalence was clearly influenced by setting, being almost 4 times higher in rural communities than in semiurban communities. Rural residents engage more often in forest-based activities and live in less-protected housing, conditions favoring exposure to *Culicoides* midges. Semiurban environments, by contrast, may reduce risk through fewer vector breeding sites. The *C. grahamii* midge is the only species so far confirmed as a vector (*25*).

The Sindara cluster of *O. volvulus* nematodes illustrates the focal nature of onchocerciasis transmission, linked to the breeding ecology of *Simulium* black flies (*26*). Outside that hotspot, prevalence was negligible, highlighting the need for updated fine-scale mapping in Gabon, where only a few recent studies have addressed the epidemiology of onchocerciasis (*21*,*27*). The focal detection of *O. volvulus* nematodes is consistent with the heterogeneous distribution of onchocerciasis previously reported in Gabon (*21*; J. Chandenier, doctoral thesis). Although *O. volvulus* nematodes were detected in a highly focal pattern restricted to the Sindara region, their presence has programmatic implications. One in 5 persons in Sindara carried *O. volvulus* nematodes, and even a limited cluster of onchocerciasis represents a substantial reservoir. Given the ongoing efforts of the WHO toward onchocerciasis elimination in Africa, such foci could threaten progress, especially if infected persons travel to areas where transmission is already under control (*28*,*29*).

Male sex emerged as one of the strongest predictors of *M. streptocerca* infection; men were >3 times as likely to be infected. This pattern is consistent with reports for other filarial parasites (*30*,*31*). Occupational exposure, outdoor activity, and less frequent use of protective clothing could explain some of the difference in filarial species prevalences between men and women (*32*,*33*), although biologic susceptibility has also been proposed (*16*,*34*). Occupation itself appeared associated in univariate analysis but was strongly correlated with sex and rural residence.

Housing quality was also independently protective. Higher housing scores, reflecting better infrastructure such as cement flooring, electricity, and improved sanitation, were linked to lower infection risk. Although housing remained independently associated with infection, the underlying mechanism is unclear. Better housing might reduce exposure to biting vectors, but housing quality might also reflect differences in the surrounding environment that influence vector abundance and transmission risk.

We observed an unexpected protective association between *M. streptocerca* infection and the presence of animals inside the household. That association might reflect a dilution effect if local *Culicoides* midges also feed on animals, although unmeasured confounding factors cannot be excluded. This finding should be interpreted with caution.

The absence of an association between self-reported number of *Culicoides* midge bites and infection status should also be interpreted cautiously. This variable might have been difficult for participants to estimate reliably in a setting with frequent biting exposure. In addition, *Culicoides* midge bites are nonspecific and might have been difficult to distinguish from mosquito bites or other pruritic skin conditions.

Clinical manifestations were limited, but urticaria remained significantly associated with infection after adjustment. That finding echoes previous descriptions of dermatological involvement (*3*,*4*). Other symptoms, including joint pain, nodules, and stomach pain, did not remain predictive.

We detected *Wolbachia* DNA in approximately one quarter of *M. streptocerca* monoinfected samples. Those endosymbionts are essential for the survival and reproduction of many filarial species, including *Wuchereria bancrofti*, *O. volvulus,* and *Mansonella* species (*M. perstans, M. ozzardi*, *Mansonella* sp. "DEUX"), but not *L. loa* (*35*). Low *Wolbachia* abundance in microfilariae is common; thus, samples with low microfilarial densities might approach the PCR detection limit, as reported previously (*19*,*24*). This finding suggests the presence of *Wolbachia* in *M. streptocerca* nematodes and the therapeutic relevance of doxycycline, which has proven effective in other filarial infections (*36*–*38*).

The first limitation of this study is that scapular skin snips might underestimate *O. volvulus* nematode presence compared with iliac crest samples (*39*). The cross-sectional design cannot capture temporal trends, and symptom data were self-reported because no medical examination was conducted as part of this study. In addition, convenience sampling without random selection might have introduced selection bias and limits the generalizability of our findings. *M. rodhaini* nematodes, previously reported in the region (J. Chandenier, doctoral thesis), were not included in our molecular assays because of lack of DNA sequence data. Last, because our study did not include children or adolescents, we could not assess early-life exposure. However, the similar prevalence across adult age groups suggests that infection is likely acquired in childhood or adolescence and persists over time.

In conclusion, our results confirm that *M. streptocerca* nematodes are highly prevalent but neglected in Gabon, and risk for infection is shaped by ecologic and socioeconomic factors. The protective role of better housing highlights the value of structural improvements within integrated control strategies. Urticaria was the only consistent clinical correlate, warranting further study. The focal detection of *O. volvulus* nematodes underlines the need for updated surveillance and entomological studies to be in line with the WHO goals on onchocerciasis control and elimination. Because most medical consultations in Gabon concern infectious diseases (*40*), addressing *M. streptocerca* and *O. volvulus* nematodes within national control frameworks could reduce their hidden burden. Operational research is needed to evaluate feasible interventions and guide integration into the broader skin-NTD agenda (*41*). Future work should clarify the clinical significance of *M. streptocerca* nematodes, particularly dermatologic and immunomodulatory effects, and their vectors and transmission hotspots.

### Acknowledgments

We thank all study participants for their voluntary participation in this study. We also thank the field workers and drivers at Centre de Recherches Médicales de Lambaréné and the village chiefs for their support during participant recruitment and sample collection.

Data are provided in the Appendix (https://wwwnc.cdc.gov/EID/article/32/7/25-1800-App1.pdf). Pseudonymized data and R scripts used for analysis will be shared upon request to the corresponding author.

This work was partly funded by the German Center for Infection Research (TTU 03.910). We acknowledge support by Open Access Publishing Fund from the University of Tübingen.

C.M.S., M.F., C.W., M.B., L.M., and E.M. performed sample collection. Methodology was designed by C.M.S., M.F., C.W., M.B., L.M., M. Rodi, and S.V.S. C.M.S., J.I., and J.H. supervised research. C.M.S. and J.H. performed analysis. C.M.S. and J.H. wrote the original draft. All authors participated in review and editing. Study infrastructure and logistical support were provided by A.K., P.B.M., M. Ramharter, S.T.A., and J.H.

An AI tool (ChatGPT, OpenAI) was used for assistance; prompts were limited to rephrasing text for language improvement and to support scripting for data handling and visualization in RStudio. All the study design, data analysis, and interpretation of the results were performed by the authors.

### About the Author

Ms. Sicard is a 5th-year PhD candidate at the Institute of Tropical Medicine of the University of Tübingen. Her research focuses on the molecular epidemiology of infectious diseases in Central Africa, more particularly filarial species and *Plasmodium*, combining clinical research with molecular diagnostics.

### References

1. Ta-Tang TH, Crainey JL, Post RJ, Luz SL, Rubio JM. Mansonellosis: current perspectives. Res Rep Trop Med. 2018;9:9–24. https://doi.org/10.2147/RRTM.S125750
2. Mackenzie CD, Homeida MM, Hopkins AD, Lawrence JC. Elimination of onchocerciasis from Africa: possible? Trends Parasitol. 2012;28:16–22. https://doi.org/10.1016/j.pt.2011.10.003
3. Meyers WM, Connor DH, Harman LE, Fleshman K, Moris R, Neafie RC. Human streptocerciasis. A clinicopathologic study of 40 Africans (Zairians) including identification of the adult filaria. Am J Trop Med Hyg. 1972;21:528–45. https://doi.org/10.4269/ajtmh.1972.21.528
4. Fischer P, Bamuhiiga J, Büttner DW. Occurrence and diagnosis of *Mansonella streptocerca* in Uganda. Acta Trop. 1997;63:43–55. https://doi.org/10.1016/S0001-706X(96)00607-9
5. Ritter M, Ndongmo WPC, Njouendou AJ, Nghochuzie NN, Nchang LC, Tayong DB, et al. *Mansonella perstans* microfilaremic individuals are characterized by enhanced type 2 helper T and regulatory T and B cell subsets and dampened systemic innate and adaptive immune responses. PLoS Negl Trop Dis. 2018;12:e0006184. https://doi.org/10.1371/journal.pntd.0006184
6. Medeiros JF, Crainey JL, Pessoa FAC, Luz SLB. Mansonelliasis. In: Marcondes CB, editor. Arthropod borne diseases. Cham (Switzerland): Springer International Publishing; 2017. p. 405–26.
7. Zouré HGM, Wanji S, Noma M, Amazigo UV, Diggle PJ, Tekle AH, et al. The geographic distribution of *Loa loa* in Africa: results of RAPLOA. PLoS Negl Trop Dis. 2011;5:e1210. https://doi.org/10.1371/journal.pntd.0001210
8. Murdoch ME, Asuzu MC, Hagan M, Makunde WH, Ngoumou P, Ogbuagu KF, et al. Onchocerciasis: the clinical and epidemiological burden of skin disease in Africa. Ann Trop Med Parasitol. 2002;96:283–96. https://doi.org/10.1179/000349802125000826
9. Enk CD. Onchocerciasis—river blindness. Clin Dermatol. 2006;24:176–80. https://doi.org/10.1016/j.clindermatol.2005.11.008
10. Winthrop KL, Furtado JM, Silva JC, Resnikoff S, Lansingh VC. River blindness: an old disease on the brink of elimination and control. J Glob Infect Dis. 2011;3:151–5. https://doi.org/10.4103/0974-777X.81692
11. Murdoch ME. Mapping the burden of onchocercal skin disease. Br J Dermatol. 2021;184:199–207. https://doi.org/10.1111/bjd.19143
12. Uslu U, Dik B. Chemical characteristics of breeding sites of *Culicoides* species (Diptera: Ceratopogonidae). Vet Parasitol. 2010;169:178–84. https://doi.org/10.1016/j.vetpar.2009.12.007
13. Nana-Djeunga HC, Fossuo-Thotchum F, Pion SD, Chesnais CB, Kubofcik J, Mackenzie CD, et al. Loa loa Microfilariae in skin snips: consequences for onchocerciasis monitoring and evaluation in *L. loa*–endemic areas. Clin Infect Dis. 2019;69:1628–30. https://doi.org/10.1093/cid/ciz172

14. Niamsi-Emalio Y, Nana-Djeunga HC, Chesnais CB, Pion SDS, Tchatchueng-Mbougua JB, Boussinesq M, et al. Unusual localization of blood-borne *Loa loa* microfilariae in the skin depends on microfilarial density in the blood: implications for onchocerciasis diagnosis in coendemic areas. Clin Infect Dis. 2021;72(Suppl 3):S158–64. https://doi.org/10.1093/cid/ciab255
15. Veletzky L, Hergeth J, Stelzl DR, Mischlinger J, Manego RZ, Mombo-Ngoma G, et al. Burden of disease in Gabon caused by loiasis: a cross-sectional survey. Lancet Infect Dis. 2020;20:1339–46. https://doi.org/10.1016/S1473-3099(20)30256-5
16. Van Hoegaerden M, Chabaud B, Akue JP, Ivanoff B. Filariasis due to *Loa loa* and *Mansonella perstans* in Gabon. Trans R Soc Trop Med Hyg. 1987;81:441–6. https://doi.org/10.1016/0035-9203(87)90163-5
17. Akue JP, Nkoghe D, Padilla C, Moussavou G, Moukana H, Mbou RA, et al. Epidemiology of concomitant infection due *to Loa loa* and *Mansonella perstans* in Gabon. PLoS Negl Trop Dis. 2011;5:e1329. https://doi.org/10.1371/journal.pntd.0001329
18. Boussinesq M, Gardon J, Kamgno J, Pion SDS, Gardon-Wendel N, Chippaux JP. Relationships between the prevalence and intensity of *Loa loa* infection in the Central province of Cameroon. Ann Trop Med Parasitol. 2001;95:495–507. https://doi.org/10.1080/00034983.2001.11813662
19. Sandri TL, Kreidenweiss A, Cavallo S, Weber D, Juhas S, Rodi M, et al. Molecular epidemiology of *Mansonella* species in Gabon. J Infect Dis. 2021;223:287–96. https://doi.org/10.1093/infdis/jiaa670
20. Rodi M, Gross C, Sandri TL, Berner L, Marcet-Houben M, Kocak E, et al. Whole genome analysis of two sympatric human *Mansonella*: *Mansonella perstans* and *Mansonella* sp "DEUX". Front Cell Infect Microbiol. 2023;13:1159814. https://doi.org/10.3389/fcimb.2023.1159814
21. Eyang-Assengone ER, Makouloutou-Nzassi P, Mbou-Boutambe C, Bangueboussa F, Atsame J, Boundenga L. Status of onchocerciasis elimination in Gabon and challenges: a systematic review. Microorganisms. 2023;11:1946. https://doi.org/10.3390/microorganisms11081946
22. Directorate General of Statistics of Gabon. 2013 general census of population and housing [in French]. Libreville (Gabon): The Directorate General; 2015.
23. Bassene H, Sambou M, Fenollar F, Clarke S, Djiba S, Mourembou G, et al. High prevalence of *Mansonella perstans* filariasis in rural Senegal. Am J Trop Med Hyg. 2015;93:601–6. https://doi.org/10.4269/ajtmh.15-0051
24. Gehringer C, Kreidenweiss A, Flamen A, Antony JS, Grobusch MP, Bélard S. Molecular evidence of *Wolbachia* endosymbiosis in *Mansonella perstans* in Gabon, Central Africa. J Infect Dis. 2014;210:1633–8. https://doi.org/10.1093/infdis/jiu320
25. Henrard C, Peel E. *Culicoides grahami* as a vector of *Dipetalonema streptocerca.* Ann Soc Belg Med Trop. 1949;29:127–43.
26. Brown AW. A survey of *Simulium* control in Africa. Bull World Health Organ. 1962;27:511–27.
27. Atsame J, Stapley JN, Ramani A, Mourou R, Ntsame E, Efame E, et al. Comparison of diagnostic tools to assess the feasibility of programmatic use of rapid diagnostic tests for onchocerciasis: a dataset from Gabon. Data Brief. 2024;57:110901. https://doi.org/10.1016/j.dib.2024.110901
28. Nikièma AS, Koala L, Post RJ, Paré AB, Kafando CM, Drabo F, et al. Onchocerciasis prevalence, human migration and risks for onchocerciasis elimination in the Upper Mouhoun, Nakambé and Nazinon river basins in Burkina Faso. Acta Trop. 2018;185:176–82. https://doi.org/10.1016/j.actatropica.2018.05.013
29. Mutono N, Basáñez MG, James A, Stolk WA, Makori A, Kimani TN, et al. Elimination of transmission of onchocerciasis (river blindness) with long-term ivermectin mass drug administration with or without vector control in sub-Saharan Africa: a systematic review and meta-analysis. Lancet Glob Health. 2024;12:e771–82. https://doi.org/10.1016/S2214-109X(24)00043-3
30. Debrah LB, Nausch N, Opoku VS, Owusu W, Mubarik Y, Berko DA, et al. Epidemiology of *Mansonella perstans* in the middle belt of Ghana. Parasit Vectors. 2017;10:15. https://doi.org/10.1186/s13071-016-1960-0
31. Noireau F, Carme B, Apembet JD, Gouteux JP. *Loa loa* and *Mansonella perstans* in the Chaillu mountains, Congo. Trans R Soc Trop Med Hyg. 1989;83:529–34. https://doi.org/10.1016/0035-9203(89)90280-0
32. Whittaker C, Walker M, Pion SDS, Chesnais CB, Boussinesq M, Basáñez MG. The population biology and transmission dynamics of *Loa loa.* Trends Parasitol. 2018;34:335–50. https://doi.org/10.1016/j.pt.2017.12.003
33. Pion DS, Gardon J, Kamgno J, Gardon-Wendel N, Chippaux JP, Boussinesq M. Structure of the microfilarial reservoir of *Loa loa* in the human host and its implications for monitoring the programmes of community-directed treatment with Ivermectin carried out in Africa. Parasitology. 2004;129:613–26. https://doi.org/10.1017/S0031182004005694
34. Wanji S, Tendongfor N, Esum M, Ndindeng S, Enyong P. Epidemiology of concomitant *Loa loa*, *Mansonella perstans*, and *Onchocerca volvulus.* Med Microbiol Immunol. 2003;192:15–21. https://doi.org/10.1007/s00430-002-0154-x
35. Desjardins CA, Cerqueira GC, Goldberg JM, Dunning Hotopp JC, Haas BJ, Zucker J, et al. Genomics of *Loa loa*, a *Wolbachia*-free filarial parasite of humans. Nat Genet. 2013;45:495–500. https://doi.org/10.1038/ng.2585
36. Turner JD, Tendongfor N, Esum M, Johnston KL, Langley RS, Ford L, et al. Macrofilaricidal activity after doxycycline only treatment of *Onchocerca volvulus* in an area of *Loa loa* co-endemicity: a randomized controlled trial. PLoS Negl Trop Dis. 2010;4:e660.
37. Coulibaly YI, Dembele B, Diallo AA, Lipner EM, Doumbia SS, Coulibaly SY, et al. A randomized trial of doxycycline for *Mansonella perstans* infection. N Engl J Med. 2009;361:1448–58. https://doi.org/10.1056/NEJMoa0900863
38. Batsa Debrah L, Phillips RO, Pfarr K, Klarmann-Schulz U, Opoku VS, Nausch N, et al. The efficacy of doxycycline treatment on *Mansonella perstans* infection: an open-label, randomized trial in Ghana. Am J Trop Med Hyg. 2019;101:84–92. https://doi.org/10.4269/ajtmh.18-0491
39. Taylor HR, Keyvan-Larijani E, Newland HS, White AT, Greene BM. Sensitivity of skin snips in the diagnosis of onchocerciasis. Trop Med Parasitol. 1987;38:145–7.
40. Manego RZ, Mombo-Ngoma G, Witte M, Held J, Gmeiner M, Gebru T, et al. Demography, maternal health and the epidemiology of malaria and other major infectious diseases in the rural department Tsamba-Magotsi, Ngounie Province, in central African Gabon. BMC Public Health. 2017;17:130. https://doi.org/10.1186/s12889-017-4045-x
41. World Health Organization. Ending the neglect to attain the sustainable development goals: a road map for neglected tropical diseases 2021–2030. Geneva: The Organization; 2020.

Address for correspondence: Jana Held, Institute of Tropical Medicine, University Hospital Tübingen, Wilhelmstr. 27, 72070 Tübingen, Germany; email: jana.held@uni-tuebingen.de

# Investigation of Donor-Transmitted *Strongyloides stercoralis* Infections in Solid Organ Transplant Recipients, United States, 2012–2024

Kerry R. Gainor, Dawn Blackburn, Pallavi Annambhotla, Sridhar V. Basavaraju, Katherine E. Bowden, Diana Martin, David A. Baran, Irene Frantzis, Irene D. Lytrivi, Julia Simkowski, Danielle Stanek, Susan P. Montgomery, Rebecca J. Chancey

*Strongyloides stercoralis* is a parasitic nematode endemic in tropical and subtropical regions, including parts of the southeastern United States, that can be transmitted via organ donation. As of October 2025, the Organ Procurement and Transplant Network implemented new policy for screening in deceased US organ donors to reduce the risk for donor-derived *Strongyloides* infection. To assess the potential effect of policy changes, we reviewed investigations of suspected transplant-related strongyloidiasis in the United States conducted by the Centers for Disease Control and Prevention and partners for solid organ transplants occurring during 2012–2024. During that period, 21 proven donor-derived strongyloidiasis cases originated from 15 unscreened donors. Of donors who were screened, 31 seropositive donors resulted in ivermectin prophylaxis for 77 recipients, none of whom had disease develop. Our findings support the effectiveness of universal organ donor screening and prophylactic ivermectin treatment of recipients to prevent donor-derived *Strongyloides* infection.

Solid organ transplantations are lifesaving; however, they can pose major risks for illness and death from transplant-related complications, including infection with the parasite *Strongyloides stercoralis*. *S. stercoralis* is a parasitic nematode endemic in tropical and subtropical regions, including parts of the southeastern United States, and is estimated to affect 300–600 million persons worldwide (*1*–*3*). Risk factors for acquiring *Strongyloides* infection include living in or traveling to endemic regions, activities involving direct skin contact with soil, living in long-term care or correctional facilities, and human T-lymphotropic virus 1 (HTLV-1) infection (*1*,*4*,*5*).

*S. stercoralis* nematodes have a unique autoinfection cycle that enables them to establish asymptomatic, chronic infections even in immunocompetent persons (*1*,*4*–*6*). Immunocompromised persons, including solid organ recipients, have increased risk for severe disease because of infection reactivation or donor-derived infection (*6*,*7*). Severe disease is characterized by hyperinfection syndrome or disseminated *Strongyloides* infection, or both, and can have high mortality rates that reach up to 90% (*8*,*9*). Ivermectin is the treatment of choice for strongyloidiasis and has high efficacy, achieving cure rates of up to 96% in clinical trials (*6*,*10*–*13*).

To reduce the risks associated with donor-derived infections, the Organ Procurement and Transplant Network (OPTN) in the United States added *S. stercoralis* screening to policy 2.9, Required Deceased Donor Infectious Disease Testing, as part of the initiative to improve deceased donor evaluation for endemic diseases (*14*). This policy requires organ procurement organizations (OPO) to obtain serologic testing for *S. stercoralis* infection as part of the deceased donor evaluation process. The policy was approved in June 2023 and implemented in October 2025; testing all donors in the interim was highly recommended (*15*). When new donor testing information indicating a positive test becomes available, the OPO must

Author affiliations: Centers for Disease Control and Prevention, Atlanta, Georgia, USA (K.R. Gainor, D. Blackburn, P. Annambhotla, S.V. Basavaraiu, K.E. Bowden, D. Martin, S.P. Montgomery, R.J. Chancey); Cleveland Clinic Florida, Weston, Florida, USA (D.A. Baran); Columbia University Irving Medical Center, New York, New York, USA (I. Frantzis, I.D. Lytrivi); Cleveland Clinic, Cleveland, Ohio, USA (J. Simkowski); Florida Department of Health, Tallahassee, Florida, USA (D. Stanek).

DOI: https://doi.org/10.3201/eid3207.260747

notify the transplant centers. When a potential donor-derived disease transmission event is identified in a recipient, the transplant center must notify the OPO. The OPO then reports the suspected donor-derived infection case to OPTN in accordance with OPTN policy 15. Potential donor-derived transmission events reported to OPTN are reviewed by the ad hoc Disease Transmission Advisory Committee (DTAC) (*16*,*17*). The Centers for Disease Control and Prevention (CDC), as a member of DTAC, works with partners to routinely investigate pathogens of special interest, including *S. stercoralis*, as a public health response to ensure the ongoing safety of organ transplantation.

To assess the potential effect of implementing OPTN policy 2.9, we reviewed CDC-led investigations of transplant-related strongyloidiasis in the United States from 2012–2024. In addition, cases of confirmed donor-derived strongyloidiasis from 2023 and 2024 are described to emphasize the critical clinical features of *S. stercoralis* infection in organ recipients.

## Methods

### Data Compilation for Cases, 2012–2024

We extracted and reviewed records of suspected transplant-related strongyloidiasis cases previously collected by CDC during routine public health investigations for information related to transplant procedures and infection status of organ donor recipients. Data sources for descriptive analysis included case summary reports, donor and recipient demographic and clinical information as provided by OPOs and transplant hospitals, and laboratory test results collected during CDC-investigated cases of transplant-related strongyloidiasis. Donor information included age, sex, birthplace, exposure risks, *Strongyloides* serology testing results, and organs transplanted. Recipient information included time of symptom onset, time of diagnosis, testing results, exposure risks, and outcome at follow-up. We extracted the data by using a standardized Microsoft Excel (Microsoft, https://www.microsoft.com) data abstraction template and compiled the data in a database for descriptive analysis.

### Data Analysis

We reviewed the database of CDC-led case investigations from 2012–2024 to assess the potential effect of OPTN policy 2.9 by examining donor screening practices, donor risk characteristics, and recipient characteristics and outcomes to evaluate how universal donor screening could address gaps in identifying infected donors. We analyzed the data by using Microsoft Excel to generate frequency counts and proportions of donor and recipient variables. Variables analyzed include the year of transplant; donor age, sex, and birthplace; donor and recipient pretransplant and posttransplant testing results; the number of recipients and type of organ transplanted; and the recipient's clinical course and outcome (Appendix Table 1, http://wwwnc.cdc.gov/EID/article/32/7/26-0747-App1.xlsx). We used the clinical, laboratory, and epidemiologic data to assign a case determination to each organ recipient according to our case definitions (Figure; Appendix Table 2). We applied this approach to maintain consistency in classification. Case determinations were assigned by 1 independent reviewer and reassessed by 2 other independent reviewers by using predefined criteria (Figure; Appendix Table 2). We resolved discrepancies by consensus. The case definitions were proven, probable, possible, inconclusive, excluded, intervention without documented transmission, and no intervention no disease transmission (Appendix Table 2). We excluded investigations that did not have sufficient evidence of *S. stercoralis* infection in the donor and recipients from analysis. For analytical purposes, we classified donors as originating from countries considered endemic for *S. stercoralis* nematodes on the basis of CDC and the World Health Organization epidemiologic descriptions of regions with documented sustained transmission.

We describe investigations assigned as proven donor-derived infections in 2023 and 2024 for each donor and transplant-related strongyloidiasis recipient, corresponding to the period after policy approval and before full implementation across OPOs. Descriptions included donor and recipient data such as demographics, exposure risk factors, *S. stercoralis* and other diagnostic testing, treatment, and clinical course and outcomes that were previously collected as routine reporting for transplant procedures. This activity was reviewed by CDC, deemed not research, and was conducted consistent with applicable federal law and CDC policy (45 CFR part 46.102(l)(2), 21 CFR part 56; 42 USC §241(d); 5 USC §552a; 44 USC §3501 et seq.).

## Results

### Investigations from 2012–2024

During 2012–2024, CDC led 72 investigations of potential transplant-related strongyloidiasis involving 72 donors and 227 solid organ recipients. For this report, we excluded 8 investigations from analysis for lack of supportive evidence of *S. stercoralis* infection in the donor and recipients. The remaining 64 investigations available for analysis involved 64 donors (63 deceased

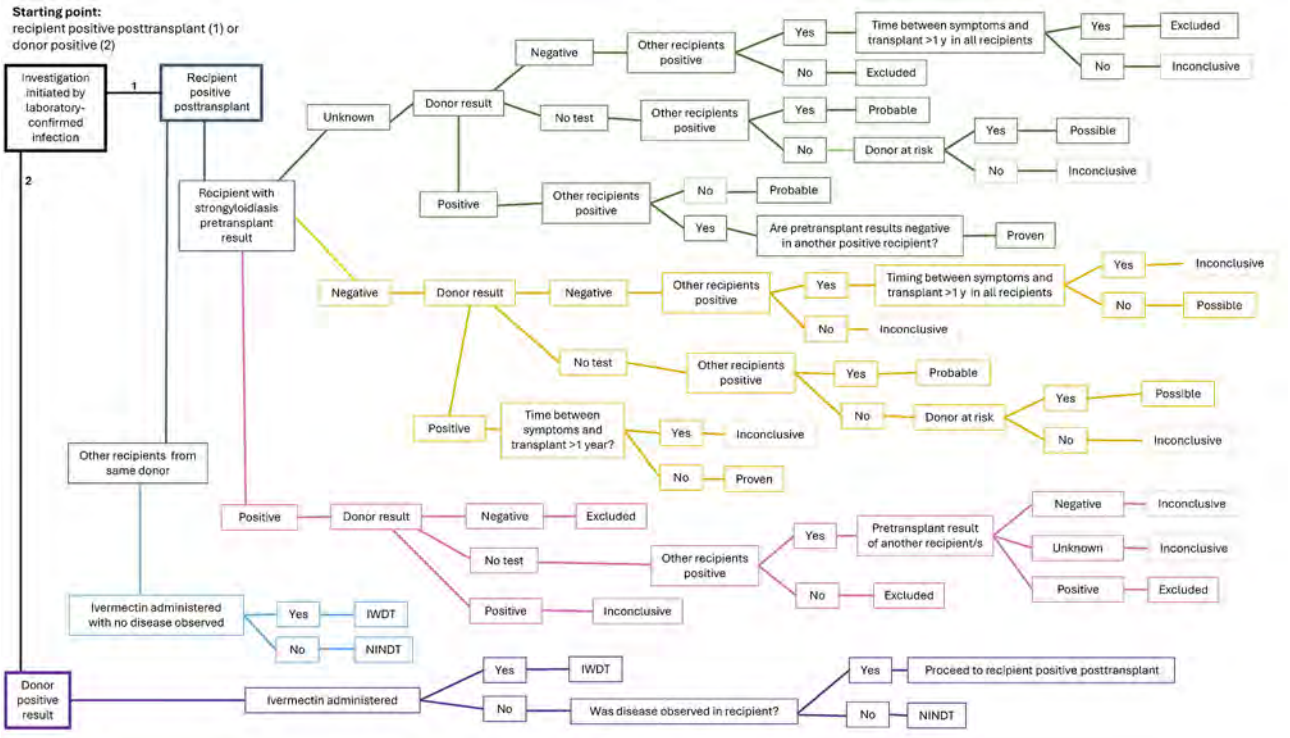


**Figure.** Case determination algorithm used for analysis in the Centers for Disease Control and Prevention investigations of potential donor-derived strongyloidiasis, United States, 2012–2024. Each investigation begins with a trigger, either recipient positive posttransplant (1) or donor positive (2), and follows the algorithm to a designated case determination based on clinical, laboratory, and epidemiologic data and our case definitions. Determination categories include proven, excluded, NINDT, IWDT, probable, possible, and inconclusive cases. IWDT, intervention without disease transmission; NINDT, no intervention and no disease transmission.

and 1 living) and 197 recipients (Table); Appendix Table 1). Among the donors, 69% (n = 44) were male and 31% (n = 20) were female. Donors were 13–67 (median 46) years of age. Of donors, 53% (n = 34) were from countries other than the United States with documented endemic transmission of *S. stercoralis* nematodes, 14% (n = 9) of donors were born in the southeastern United States, 17% (n = 11) of donors were born in other parts of the mainland United States, 9% (n = 6) of donors were from Puerto Rico, and 6% (n = 4) of donors had an unknown country of origin.

Specimens were submitted for serologic testing on 83% (n = 60) of the 72 donors. Of those, 53% (n = 32) were tested by the OPO referral laboratory at the time of organ procurement. Another 47% (n = 28) of specimens were tested by the OPO referral laboratory or CDC after transplant in response to reported recipient infection. For the remaining 4 of 64 investigations, donor specimens were not tested. Three of the 4 donor specimens were not tested because confirmatory serologic testing was unavailable at that time and because the samples did not meet the storage time requirements for testing at the OPO's contracted laboratory. For donor specimen 4, the OPO determined the recipient's infection was because of reactivation rather than donor-derived transmission and therefore did not test or send a sample to CDC for testing.

The investigations included 197 recipients who received solid organ transplants with a total of 212 organs transplanted (Table); Appendix Table 1). Among the recipients, 183 received a single organ and 14 received multiple organs during transplantation. The most frequently transplanted organs were the kidneys (55%, n = 108) and liver (24%, n = 48). A heart was transplanted in 24 patients (12% of total recipients), 21 as a single organ and 3 as part of a multiorgan transplant. Of the heart transplant recipients, 7 acquired donor-derived strongyloidiasis and 2 tested seropositive for *S. stercoralis* infection on serum samples collected before transplant, consistent with pretransplant infection, and subsequently experienced reactivation posttransplant. The remaining heart recipient outcomes are provided (Table 1). Less frequently transplanted organs include lungs and other multiorgan combinations.

On the basis of the case determination algorithm (Figure), 11% (n = 22) of cases met the definition of proven transmission, characterized by confirmed *S. stercoralis* infection in both the donor and ≥1 recipient, with documented absence of pretransplant infection

**Table.** Summary of investigations of potential donor-derived strongyloidiasis, United States, 2012–2024*

| Donor and recipient information | Total |
|---|---|
| Donors | 64 (100) |
| Median age (range), y | 46 (13–67) |
| Sex | |
| M | 44 (69) |
| F | 20 (31) |
| Birthplace | |
| International | 34 (52) |
| United States | 26 (41) |
| Unknown | 4 (6) |
| Serologic testing | |
| Yes | 60 (94) |
| No | 4 (6) |
| Total organs transplanted | 212 |
| Recipients | 197 (100) |
| Organs per recipient | |
| 1 | 183 (93) |
| 2 | 12 (6) |
| 3 | 1 (0.5) |
| 4 | 1 (0.5) |
| Recipients by organ types transplanted | |
| Right kidney | 50 (25) |
| Left kidney | 45 (23) |
| Liver | 44 (22) |
| Heart | 21 (11) |
| Lung, unspecified | 7 (4) |
| Right lung | 6 (3) |
| Left lung | 6 (3) |
| Kidney, unspecified | 4 (2) |
| Bilateral lung | 4 (2) |
| Left kidney and pancreas | 3 (1.5) |
| Liver and left kidney | 2 (1) |
| Kidney and pancreas | 1 (0.5) |
| Heart and left kidney | 1 (0.5) |
| Heart and lung | 1 (0.5) |
| Heart, liver, and left kidney | 1 (0.5) |
| Liver, left kidney, pancreas, and bowel | 1 (0.5) |
| Posttransplant strongyloidiasis diagnosis | |
| Positive | 43 (22) |
| Negative | 31 (16) |
| Unknown | 123 (62) |
| Case determination | |
| Proven | 22 (11) |
| Probable | 3 (1.5) |
| Possible | 1 (0.5) |
| Excluded | 10 (5) |
| No intervention, no disease transmission | 19 (10) |
| Intervention without disease transmission | 125 (64) |
| Inconclusive | 17 (9) |
| Outcome at follow-up | |
| Alive | 167 (85) |
| Deceased | 15 (8) |
| Unknown | 15 (8) |
| Heart transplant recipients | |
| Recipients | 24 |
| Single-organ | 21 |
| Multi-organ | 3 |
| Case determination among heart transplant recipients | |
| Excluded, reactivation | 2 |
| Proven | 7 |
| Inconclusive | 3 |
| Intervention without disease transmission | 10 |
| No intervention, no disease transmission | 1 |
| Excluded, unknown | 1 |

*Values are no. (%) except as indicated. Heart transplant recipients are presented separately for descriptive purposes and were not analyzed as a distinct risk group.

in the recipient. Three (2%) cases were classified as probable transmission because evidence strongly suggested donor origin but not all criteria for proven transmission were fulfilled. Possible transmission was identified in 1 (0.5%) case; transmission was suspected but the available evidence was insufficient to meet the criteria for proven or probable. Among the 26 proven, probable, and possible cases, the most frequently transplanted organ was the kidney (46%, n = 12 cases), followed by the heart (27%, n = 7 cases). We excluded 10 (5%) cases on the basis of evidence indicating the recipient had reactivated chronic infection acquired before transplant or new infection acquired posttransplant. The organs most frequently transplanted in the excluded cases were the lungs (40%, n = 4 cases). In 63% (n = 125) of cases, recipients received treatment posttransplant and had no observed transmission; we categorized those cases as intervention without disease transmission. In 9% (n = 17) of cases, we could not determine the strongyloidiasis cause or we assigned the case to another classification; we designated those cases as inconclusive. Of the inconclusive cases, kidneys (65%, n = 11 cases) were the most frequently transplanted organs. The remaining 10% (n = 19) of cases received no prophylaxis and no transmission was documented; we assigned those cases no intervention no disease transmission status. Complications related to strongyloidiasis resulted in the death of 5% (n = 10) of recipients.

In the proven and probable investigations, 15 donors were from non-US countries and 4 donors were from the United States and Puerto Rico. Among the 25 affected recipients, 32% (n = 8) died because of complications related to strongyloidiasis. Since the approval of policy 2.9 in 2023, there were 5 proven cases and 1 probable case of donor-derived infections involving 5 unscreened donors.

## Proven Donor-Derived Public Health Investigations, 2023–2024

The following select, proven investigations occurred after June 26, 2023, when OPTN approved policy 2.9, emphasizing ongoing gaps in screening protocols and the need to implement universal donor screening across all OPOs to prevent future donor-derived strongyloidiasis. Transplant case identifiers correspond to those listed in Appendix Table 1.

### Transplant Case Identification 2023-3

The donor was a 33-year-old man born in Guatemala. The OPO performed *S. stercoralis* serology at the time of death, and results were reported positive 3 days later. The transplant centers of all 4 recipients

were notified. Of the 4 recipients, the liver, right kidney, and left kidney recipients received prophylactic ivermectin; none reported disease development. The heart recipient did not receive prophylaxis. At 11 weeks posttransplant, the heart recipient reported a 2-week history of decreased appetite, abdominal pain, bloating, and diarrhea and was hospitalized. Fecal ova and parasite examination was positive for *S. stercoralis* infection. Upon receipt of the positive result, the heart recipient was administered ivermectin. Despite medical intervention, the recipient's condition declined, leading to death at 87 days posttransplant. The recipient's pretransplant serology was negative for *S. stercoralis* infection, supporting the absence of detectable infection before transplantation. The recipient was born in China and arrived in the United States 4 years before the heart transplant. Although the donor screening result was communicated 1 day posttransplant, the message did not reach the appropriate members of the heart transplant team, and prophylactic ivermectin was not administered. Corrective measures have been established to improve communication and follow-up in the future.

#### Transplant Case Identification 2024-1

The donor was a 52-year-old woman originally from Guatemala. She traveled to Guatemala most recently in 2022 and had no other travel history. She was not tested for *S. stercoralis* infection before the time of organ transplant in recipients. A serum sample from the donor was submitted for testing after the heart and left kidney recipients' diagnosis of strongyloidiasis. Results of *S. stercoralis* IgG ELISA testing were positive at both the OPO referral laboratory and CDC. Organs transplanted were heart, right and left kidneys, lung, and liver.

The heart recipient was born in OPTN region 1 (Northeast United States, New England region) and resided in region 10 (Midwest United States, Great Lakes region) at the time of transplant. The recipient traveled to a state in region 11 (Southeast United States, southern Atlantic region) and had no other recent travel or exposure risks. The result of a *S. stercoralis* antibody test in the heart recipient was negative pretransplant. On day 62 posttransplant, the heart recipient complained of worsening pain, nausea, and diarrhea. Intestinal biopsy on day 69 posttransplant and skin biopsies on day 75 posttransplant revealed acute duodenitis with *S. stercoralis* organisms and cutaneous strongyloidiasis. Serology and fecal ova and parasite microscopic examination were positive for *S. stercoralis* infection on day 75 posttransplant. Bronchoscopy with bronchoalveolar lavage (BAL) demonstrated diffuse alveolar hemorrhage, and *Strongyloides* larvae were observed in BAL cultures. The recipient was treated for disseminated strongyloidiasis with oral ivermectin before transitioning to subcutaneous ivermectin. Other conditions included vancomycin-resistant *Enterococcus* bacteremia, pneumonia, and suspected meningitis. As of 89 days posttransplant, the recipient remained in the intensive care unit requiring ventilator support. Abnormal mental status, encephalopathy, and delirium were observed. At follow-up 118 days posttransplant, the recipient continued to be hospitalized and was slowly improving.

The left kidney recipient was a resident of OPTN region 10, had no recent travel history and had pretransplant serology negative for *Strongyloides* antibodies. On day 67 posttransplant, the recipient reported complaints of intractable vomiting and nausea. *Strongyloides* larvae were observed in sputum cultures and fecal samples were positive for *S. stercoralis* larvae. The recipient was treated with oral albendazole for 27 days and oral ivermectin for 2 days, then subcutaneous ivermectin for 25 days. Complications experienced by the recipient included respiratory failure, septic shock, encephalopathy, bacteremia, and fluid accumulation around the transplanted kidney. At follow-up 97 days posttransplant, the recipient remained in the ICU.

Pretransplant and posttransplant serum samples from the right kidney and lung recipients were not tested, and both recipients were given ivermectin. The liver recipient's pretransplant and posttransplant serology were negative, and the recipient was also treated with ivermectin.

#### Transplant Case Identification 2024-2

The donor was a 33-year-old Hispanic man who was born in and resided in Honduras until 17 years of age, when he moved to the United States. Prior to organ donation, he was not screened for *S. stercoralis* infection. After notification of strongyloidiasis in the heart recipient, the archived donor serum was tested by the OPO referral laboratory with a positive result for *Strongyloides* antibodies and subsequently tested negative at CDC. This discordance is likely attributable to differences in assay methodologies, antigens used, and assay performance. Donor organs transplanted include heart, right and left kidneys, and liver.

The heart recipient was from OPTN region 9 (Northeast United Sates, including New York and western Vermont), did not have international travel or exposure risk for *S. stercoralis* infection, and had serum samples that were negative when tested pretransplant. At 161 days posttransplant, the heart recipient reported complaints of abdominal pain, nausea, and weight

loss. Clinical course was complicated by diffuse pulmonary disease characterized by extensive nodular and reticulonodular opacities, pulmonary hemorrhage, and multi–organ system involvement, including renal failure and anemia requiring blood transfusions. The recipient was treated with antimicrobial drugs and steroids for possible *Pneumocystis* pneumonia. A commercial metagenomic molecular test identified *S. stercoralis* DNA in plasma, which was confirmed by identification of *Strongyloides* larvae in a BAL sample. Treatment with oral ivermectin and albendazole was initiated 171 days posttransplant, and the patient was transitioned to subcutaneous ivermectin. After initiation of ivermectin therapy, the heart recipient experienced cerebral edema and poor neurologic function and was placed on veno-venous extracorporeal membrane oxygenation and continuous renal replacement therapy because of worsening clinical status. At 274 days posttransplant, the recipient had a tracheostomy, remained on continuous renal replacement therapy, regained consciousness, and could communicate.

Pretransplant serum from the left and right kidney recipients could not be tested, and posttransplant serology was negative. Both recipients received ivermectin. The liver recipient died from causes unrelated to strongyloidiasis and could not be tested.

## Discussion

Donor-derived infections are a rare but serious complication of solid organ transplantation (*17*–*19*). Parasitic infections, particularly with *S. stercoralis*, can be fatal in recipients, often because of delayed diagnosis (*2*,*8*,*17*). To reduce risk, professional society guidelines have recommended targeted screening of deceased donors on the basis of epidemiologic risk factors such as country of origin (*2*,*8*,*20*,*21*). However, adherence to screening protocols for *S. stercoralis* infection in organ donors remained suboptimal. In 2016, only 10% of OPOs reported screening donors on the basis of risk factors, and by 2019, only 24% had adopted either targeted or universal screening protocols (*22*,*23*). In the cases investigated (Appendix Table 1), 50% donors were not screened before transplant. Of those, 94% had epidemiologic risk factors, and 40% of donors transmitted *S. stercoralis* infection to 18 recipients, leading to 3 strongyloidiasis-related deaths.

More recently, the OPTN added universal *S. stercoralis* screening to policy 2.9 (*14*). Implementing universal screening, which involves testing all donors regardless of epidemiologic risk, could reduce variability in the application of screening guidelines. Testing all donors would also address the limitations of targeted screening, which might miss donors with unrecognized risk, and help prevent severe disease that is difficult to treat. In the time between policy 2.9 approval and implementation, donor-derived *Strongyloides* infections continued to occur, with 2 investigations involving donors from endemic regions who were not screened at the time of organ procurement. In both cases, multiple recipients had serious complications of hyperinfection and disseminated disease, including respiratory failure, sepsis, encephalopathy, and prolonged ICU stays.

In our investigations, 9 donors and 4 recipients were positive for *S. stercoralis* infection and lacked international travel history, suggesting *S. stercoralis* infection was acquired in the United States (Appendix Table 1). *S. stercoralis* nematodes have been documented in parts of the Appalachian region since the 1940s and more recently in several other US states (*24*–*31*). However, *S. stercoralis* infection is not nationally notifiable or reportable in any state, and current comprehensive national data remain scarce (*31*,*32*). Therefore, the true prevalence and geographic distribution are unknown, complicating accurate risk assessment and limiting the feasibility of targeted screening strategies. The 9 donors described here lived in US regions historically found to have *Strongyloides* transmission or had identifiable risk factors such as incarceration, communal living, or occupational exposure, and some had history of both US region residence and other risk factors. Donor histories might have been incomplete and lacked documentation of exposure risk factors and therefore donor screening was not undertaken (*19*,*33*). Screening all donors, even those with unrecognized risks, would help prevent donor-derived infection and identify potential donors who might have acquired *S. stercoralis* infection in the United States.

Screening for *S. stercoralis* infection enables early identification of seropositive donors. Organs from seropositive donors have been successfully transplanted without adverse outcomes when recipients received prophylactic treatment (*19*,*34*–*36*). Although serologic tests might produce false positives in a low prevalence population, this should not preclude safe organ use (*2*,*37*). Treating recipients with ivermectin is a well-tolerated and effective low-risk intervention (*6*,*15*,*38*,*39*). Our assessment identified 31 of 32 screened donors who were seropositive, prompting prophylactic ivermectin treatment in 77 recipients. No disease was reported in those recipients at follow-up. The success of universal screening is contingent on timely and accurate communication of positive results. In 3 investigations with a positive donor, communication errors led

to 4 recipients not receiving prophylactic ivermectin, resulting in deaths attributable to strongyloidiasis. In contrast, other recipients from the same donors were treated after donor screening and remained disease-free, suggesting that screening might have prevented donor-derived strongyloidiasis in these recipients. The recipient outcomes observed emphasize the importance of donor screening to identify seropositive donors, timely effective communication of results, and early ivermectin treatment.

The first limitation of our study is that the retrospective design of the analysis is limited by the availability and accuracy of historical records. Donor and recipient risk factors, travel histories, and testing results might have been incompletely documented. Those factors might have affected the ability to definitively assign appropriate case determination. Second, the scope of this report is limited to CDC-led investigations and might not represent all donor-derived strongyloidiasis cases in the United States from 2012–2024. Third, serology methods used for donor screening, although valuable, have inherent limitations. Sensitivity and specificity of commonly used serologic tests can vary by assay and reference standard. Reported sensitivities range approximately from 70% to 95%, whereas specificities are generally high, ranging from ≈90% to 99% (*40*–*42*). False positives can occur in low prevalence populations or from cross reactivity with other nematodes, whereas false negatives are possible in immunocompromised persons and hemodiluted samples. Last, our analysis primarily includes investigations conducted before the approval of policy 2.9, which limits our ability to determine the direct measurable effect of the policy on donor screening practices and recipient outcomes; however, the 2 cases described from 2023 and 2024 highlight the importance of screening donors.

In conclusion, universal screening of all donors, regardless of risk, is expected to reduce donor-derived strongyloidiasis in recipients by providing early detection, timely preventative intervention, and help reduce severe disease that is difficult to treat. Future comparative analyses should be performed to evaluate the effect of *S. stercoralis* screening implementation across OPOs prepolicy and postpolicy implementation and associated recipient outcomes. Our analysis confirms support of universal *S. stercoralis* screening of US solid organ donors.

### Acknowledgments

We acknowledge Anne Straily and Andrew Vogan for their contributions to the CDC case investigations.

### About the Author

Dr. Gainor is an Epidemic Intelligence Service Officer at the Centers for Disease Control and Prevention. Her research interests include emerging and reemerging zoonotic diseases, viral diversity and evolution, and One Health approaches to disease prevention and control.

### References

1. Lo NC, Addiss DG, Buonfrate D, Amor A, Anegagrie M, Bisoffi Z, et al. Review of the WHO guideline on preventive chemotherapy for public health control of strongyloidiasis. Lancet Infect Dis. 2025;25:e146–52. https://doi.org/10.1016/S1473-3099(24)00595-4
2. La Hoz RM, Morris MI, Infectious Diseases AST; AST Infectious Diseases Community of Practice. Intestinal parasites including *Cryptosporidium*, *Cyclospora*, *Giardia*, and *Microsporidia*, *Entamoeba histolytica*, *Strongyloides*, *Schistosomiasis*, and *Echinococcus*: guidelines from the American Society of Transplantation Infectious Diseases Community of Practice. Clin Transplant. 2019;33:e13618. https://doi.org/10.1111/ctr.13618
3. Buonfrate D, Bisanzio D, Giorli G, Odermatt P, Fürst T, Greenaway C, et al. The global prevalence of *Strongyloides stercoralis* infection. Pathogens. 2020;9:468. https://doi.org/10.3390/pathogens9060468
4. Nutman TB. Human infection with *Strongyloides stercoralis* and other related *Strongyloides* species. Parasitology. 2017;144:263–73. https://doi.org/10.1017/S0031182016000834
5. Yeh MY, Aggarwal S, Carrig M, Azeem A, Nguyen A, Devries S, et al. *Strongyloides stercoralis* infection in humans: a narrative review of the most neglected parasitic disease. Cureus. 2023;15:e46908. https://doi.org/10.7759/cureus.46908
6. Keiser PB, Nutman TB. *Strongyloides stercoralis* in the immunocompromised population. Clin Microbiol Rev. 2004;17:208–17. https://doi.org/10.1128/CMR.17.1.208-217.2004
7. Roseman DA, Kabbani D, Kwah J, Bird D, Ingalls R, Gautam A, et al. *Strongyloides stercoralis* transmission by kidney transplantation in two recipients from a common donor. Am J Transplant. 2013;13:2483–6. https://doi.org/10.1111/ajt.12390
8. Kim JH, Kim DS, Yoon YK, Sohn JW, Kim MJ. Donor-derived strongyloidiasis infection in solid organ transplant recipients: a review and pooled analysis. Transplant Proc. 2016;48:2442–9. https://doi.org/10.1016/j.transproceed.2015.11.045
9. Mobley CM, Dhala A, Ghobrial RM. *Strongyloides stercoralis* in solid organ transplantation: early diagnosis gets the worm. Curr Opin Organ Transplant. 2017;22:336–44. https://doi.org/10.1097/MOT.0000000000000428
10. Henriquez-Camacho C, Gotuzzo E, Echevarria J, White AC Jr, Terashima A, Samalvides F, et al. Ivermectin versus albendazole or thiabendazole for *Strongyloides stercoralis* infection. Cochrane Database Syst Rev. 2016;2016:CD007745. https://doi.org/10.1002/14651858.CD007745.pub3
11. Gann PH, Neva FA, Gam AA. A randomized trial of single- and two-dose ivermectin versus thiabendazole for treatment of strongyloidiasis. J Infect Dis. 1994;169:1076–9. https://doi.org/10.1093/infdis/169.5.1076
12. Datry A, Hilmarsdottir I, Mayorga-Sagastume R, Lyagoubi M, Gaxotte P, Biligui S, et al. Treatment of *Strongyloides stercoralis* infection with ivermectin compared with albendazole: results of an open study of 60 cases. Trans R Soc Trop Med Hyg. 1994;88:344–5. https://doi.org/10.1016/0035-9203(94)90110-4

13. Marti H, Haji HJ, Savioli L, et al. A comparative trial of a single-dose ivermectin versus three days of albendazole for treatment of *Strongyloides stercoralis* and other soil-transmitted helminths. Am J Trop Med Hyg. 1996;55:477–81. https://doi.org/10.4269/ajtmh.1996.55.477
14. Organ Procurement and Transplantation Network. Policy 2.9: improve deceased donor evaluation for endemic diseases. 2023 [cited 2025 Mar 12]. https://optn.transplant.hrsa.gov/media/lrxfreqj/dtac_endemics_policy-notice_june23bod.pdf
15. Ad Hoc Disease Transmission Advisory (DTAC). Recognizing seasonal and geographically endemic infections in organ donors: considerations during deceased and living donor evaluation. 2024 [cited 2025 May 29]. https://optn.transplant.hrsa.gov/media/q4xfi14u/policy_notice_dtac_endemic_guidance.pdf
16. Organ Procurement and Transplantation Network. Policy 15: identification of transmissible diseases. [cited 2025 Jul 15]. https://optn.transplant.hrsa.gov/media/eavh5bf3/optn_policies.pdf
17. Kaul DR, Vece G, Blumberg E, La Hoz RM, Ison MG, Green M, et al. Ten years of donor-derived disease: a report of the disease transmission advisory committee. Am J Transplant. 2021;21:689–702. https://doi.org/10.1111/ajt.16178
18. Ison MG, Nalesnik MA. An update on donor-derived disease transmission in organ transplantation. Am J Transplant. 2011;11:1123–30. https://doi.org/10.1111/j.1600-6143.2011.03493.x
19. Hogan JI, Mehta SA. *Strongyloides stercoralis* infection in solid organ transplant recipients. Curr Opin Infect Dis. 2024;37:367–75. https://doi.org/10.1097/QCO.0000000000001046
20. La Hoz RM. Minimizing the risk of donor-derived events and maximizing organ utilization through education and policy development. Infect Dis Clin North Am. 2023;37:443–58. https://doi.org/10.1016/j.idc.2023.05.002
21. Schwartz BS, Mawhorter SD, Infectious Diseases AST; AST Infectious Diseases Community of Practice. Parasitic infections in solid organ transplantation. Am J Transplant. 2013;13(Suppl 4):280–303. https://doi.org/10.1111/ajt.12120
22. Abanyie FA, Valice E, Delli Carpini KW, Gray EB, McAuliffe I, Chin-Hong PV, et al. Organ donor screening practices for *Strongyloides stercoralis* infection among US organ procurement organizations. Transpl Infect Dis. 2018;20:e12865. https://doi.org/10.1111/tid.12865
23. Theodoropoulos NM, Greenwald MA, Chin-Hong P, Ison MG. Testing deceased organ donors for infections: an organ procurement organization survey. Am J Transplant. 2021;21:1924–30. https://doi.org/10.1111/ajt.16552
24. Siddiqui AA, Berk SL. Diagnosis of *Strongyloides stercoralis* infection. Clin Infect Dis. 2001;33:1040–7. https://doi.org/10.1086/322707
25. Starr MC, Montgomery SP. Soil-transmitted helminthiasis in the United States: a systematic review—1940–2010. Am J Trop Med Hyg. 2011;85:680–4. https://doi.org/10.4269/ajtmh.2011.11-0214
26. Singer R, Sarkar S. Modeling strongyloidiasis risk in the United States. Int J Infect Dis. 2020;100:366–72. https://doi.org/10.1016/j.ijid.2020.09.002
27. Croker C, She R. Increase in reports of *Strongyloides* infection—Los Angeles County, 2013–2014. MMWR Morb Mortal Wkly Rep. 2015;64:922–3. https://doi.org/10.15585/mmwr.mm6433a8
28. Leapley A, Cruze A, Mejia-Echeverry A, et al.; Centers for Disease Control and Prevention. Notes from the field: *Strongyloides* infection among patients at a long-term care facility—Florida, 2010–2012. MMWR Morb Mortal Wkly Rep. 2013;62:844.
29. Berk SL, Verghese A, Alvarez S, Hall K, Smith B. Clinical and epidemiologic features of strongyloidiasis. A prospective study in rural Tennessee. Arch Intern Med. 1987;147:1257–61. https://doi.org/10.1001/archinte.1987.00370070071011
30. Jones JM, Hill C, Briggs G, Gray E, Handali S, McAuliffe I, et al. Notes from the field: strongyloidiasis at a long-term–care facility for the developmentally disabled—Arizona, 2015. MMWR Morb Mortal Wkly Rep. 2016;65:608–9. https://doi.org/10.15585/mmwr.mm6523a5
31. Singer R, Xu TH, Herrera LNS, Villar MJ, Faust KM, Hotez PJ, et al. Prevalence of intestinal parasites in a low-income Texas community. Am J Trop Med Hyg. 2020;102:1386–95. https://doi.org/10.4269/ajtmh.19-0915
32. Davis S, Bosserman E, Montgomery S, Woodhall D, Russell ES; Centers for Disease Control and Prevention. Notes from the field: Strongyloidiasis in a rural setting—southeastern Kentucky, 2013. MMWR Morb Mortal Wkly Rep. 2013;62:843.
33. White SL, Rawlinson W, Boan P, Sheppeard V, Wong G, Waller K, et al. Infectious disease transmission in solid organ transplantation: donor evaluation, recipient risk, and outcomes of transmission. Transplant Direct. 2018;5:e416. https://doi.org/10.1097/TXD.0000000000000852
34. Abanyie FA, Gray EB, Delli Carpini KW, Yanofsky A, McAuliffe I, Rana M, et al. Donor-derived *Strongyloides stercoralis* infection in solid organ transplant recipients in the United States, 2009–2013. Am J Transplant. 2015;15:1369–75. https://doi.org/10.1111/ajt.13137
35. Multani A, Deresinski S. Strongyloidiasis in solid organ transplantation. OBM Transplant. 2018;2:035.
36. Rosen A, Ison MG. Screening of living organ donors for endemic infections: understanding the challenges and benefits of enhanced screening. Transpl Infect Dis. 2017;19:e12633. https://doi.org/10.1111/tid.12633
37. Camargo JF, Simkins J, Anjan S, Guerra G, Vianna R, Salama S, et al. Implementation of a *Strongyloides* screening strategy in solid organ transplant donors and recipients. Clin Transplant. 2019;33:e13497. https://doi.org/10.1111/ctr.13497
38. Kottkamp AC, Filardo TD, Holzman RS, Aguero-Rosenfeld M, Neumann HJ, Mehta SA. Prevalence of strongyloidiasis among cardiothoracic organ transplant candidates in a non-endemic region: a single-center experience with universal screening. Transpl Infect Dis. 2021;23:e13614. https://doi.org/10.1111/tid.13614
39. Roxby AC, Gottlieb GS, Limaye AP. Strongyloidiasis in transplant patients. Clin Infect Dis. 2009;49:1411–23. https://doi.org/10.1086/630201
40. Bisoffi Z, Buonfrate D, Sequi M, Mejia R, Cimino RO, Krolewiecki AJ, et al. Diagnostic accuracy of five serologic tests for *Strongyloides stercoralis* infection. PLoS Negl Trop Dis. 2014;8:e2640. https://doi.org/10.1371/journal.pntd.0002640
41. Kalantari N, Chehrazi M, Ghaffari S, Gorgani-Firouzjaee T. Serological assays for the diagnosis of *Strongyloides stercoralis* infection: a systematic review and meta-analysis of diagnostic test accuracy. Trans R Soc Trop Med Hyg. 2020;114:459–69. https://doi.org/10.1093/trstmh/trz135
42. Buonfrate D, Formenti F, Perandin F, Bisoffi Z. Novel approaches to the diagnosis of *Strongyloides stercoralis* infection. Clin Microbiol Infect. 2015;21:543–52. https://doi.org/10.1016/j.cmi.2015.04.001

Address for correspondence: Rebecca Chancey, Centers for Disease Control and Prevention, 1600 Clifton Rd NE, Mailstop H16-4, Atlanta, GA 30329-4018, USA; email: nqw1@cdc.gov

# Discovery of *Cinchona* as Antimalarial, Viceroyalty of Peru, Circa 1630

Jesús Rojas-Jaimes, Stephanie Rodríguez-Gómez, Guido P. Lombardi

The empirical discovery of the therapeutic power of *Cinchona* tree bark in the 17th Century has been one of the most important achievements in the history of medicine in its fight against malaria. Only after 2 centuries, since the isolation of its main alkaloid, quinine, could other important antimalarials, such as chloroquine, be synthesized, all of which helped to save hundreds of millions of lives. In this historical review, we examine the evidence, accessed from early documentary sources, concerning the discovery of *Cinchona* and its therapeutic value as an antimalarial during the Viceroyalty of Peru.

The genus *Cinchona*, family Rubiaceae, comprises 23 tree species (*1*). Together, they are called *quina*, 15-meter-high trees native to South America whose bark, branches, and leaves hold an intense bitter taste (*2*). Authors such as Espinosa and Cobo have confused the *quina* trees of the *Cinchona* genus with the *quina-quina* tree of the genus *Myroxylon* (*3*).

*Cinchona*'s propensity to treat malaria came at an opportune time, when much of the population of southern Europe was experiencing this disease, during the 17th Century. Classified in 1742 by Carl Linnaeus, *Cinchona*'s processed bark was known as Peruvian, Jesuits', countess', Loja's, cardinal's, or Lugo's powders and also as Peruvian antitertian and bark of fevers (*1*).

*Cinchona* bark was discovered in the 1600s in the Viceroyalty of Peru as a treatment that could be used to treat fevers in general. In 1820, Pierre-Joseph Pelletier and Joseph Bienaimé Caventou managed to isolate 2 alkaloids in the *Cinchona* bark, to which they attributed the febrifuge and antiparasitic properties of the substance, calling them quinine and cinconine (*4*). However, quinine is the main active principle and alkaloid in *Cinchona* for treating malaria.

Later, in 1889, Charles Louis Alphonse Laveran (winner of the Nobel Prize in Physiology or Medicine in 1907) discovered the *Plasmodium* parasite, the causative agent of malaria, and in 1897, Ronald Ross discovered the *Anopheles* mosquito, the vector that transmits *Plasmodium*. In 1902, Robert Koch implemented massive chemoprophylaxis in New Guinea, emphasizing malaria-control measures, which were effectively used in World War I. Until then, treatment of malaria relied strongly on extracts from the bark of the *Cinchona* tree for their antimalarial effect. Not until 1944, with the discovery of quinine's molecular structure, could antimalarial drugs be synthesized on a commercial scale (*4*–*6*).

Although the initial discovery of *Cinchona*'s antimalarial effect in humans was empirical, the mechanism of action of the molecules responsible for this effect, such as the alkaloids involved in the schizonticidal effect, was subsequently elucidated. The molecules interfere with the parasite's ability to detoxify by using quinoline. In vitro studies have been fundamental in determining those mechanisms of action. The effect of quinine inhibiting the heme polymerase extracted from *P. falciparum* trophozoites and the mechanisms of action of specific alkaloids depend on the chemical structures of quinine, quinidine, 9-epiquinine, and 9-epiquinidine mediated by the geometry of the 9-hydroxyl group and the quinuclidine ring system, which are fundamentally determined by the hydroxyl and amino groups (*7*,*8*).

Unfortunately, *Cinchona*, popularly known in Spanish as *cascarilla*, was intensively exploited after its discovery as an antimalarial, which made the trees extremely vulnerable. In addition, the tree's trunk is not wide or robust, making it difficult to climb and therefore easy to fell with machetes,

Author affiliations: Universidad Privada del Norte, Lima, Peru (J. Rojas-Jaimes); Universidad Científica del Sur, Lima (J. Rojas-Jaimes); Universidad Continental, Lima Postgraduate School (J. Rojas-Jaimes); Universidad Nacional Federico Villarreal, Lima (S. Rodríguez-Gómez); Universidad Peruana Cayetano Heredia, Lima (G.P. Lombardi)

DOI: https://doi.org/10.3201/eid3207.260042

leading to trees being cut down to extract the precious *cascarilla* (*1*). Therefore, it is important to consider the harvesting, acquisition, and management of this valuable tree.

The beginning of the *Cinchona* story is less than clear. As Pratik Chakrabarti indicates, that uncertainty could have been driven by colonialist intellectual and material interests (*4*).

### Discovery of *Cinchona*'s Value as an Antimalarial

In terms of who discovered *Cinchona*'s value as an antimalarial, 2 basic assumptions exist: the natives discovered both its febrifuge and antimalarial properties consciously, and Jesuits discovered its antimalarial value after learning of its febrifuge use by the natives. Jesuit priest Sánchez Labrador tells how Loja natives learned about *Cinchona*'s value: they noticed that a man got cured of an intense fever after drinking from a bitter lake. The water had taken the flavor of fallen cinchona trees. To pinpoint the source of the cure, they soaked different tree parts, concluding that the medicinal part was the bark (*9*).

Nicolas Monardes, a 16th-Century protobotanist, provides a version:

> From the new kingdom they bring a bark, which they say is from a tree, which is of great size, which they say, bears heart-shaped leaves, and bears no fruit. This tree has a very solid and hard thick bark, which in this and in color resemble much the bark of the stick they call Guayacán: on the surface it has a thin whitish skin, broken all over it: it has the bark more than a finger thick, solid and heavy, which tasted has remarkable bitterness, like that of the gentian: it has a remarkable taste astriction, with some aromaticity, because at the end of the chewing it breathes a good smell. The Indians have the bark in abundance, and use it in all kinds of xamaras, whether with or without blood. The Spaniards, weary of this disease, on the advice of the Indians, have used this bark and have healed many of them with it. They take of it as much as a small bean made into powders, they are taken in red wine, or in appropriate water, as they have the fever or bad... (*10*).

A.W. Haggis, in his Fundamental Errors in the Early History of *Cinchona*: Part 1 (*3*), said that Antonio de la Calancha (1631) and Sebastiano Bado (1663) mention a "fever tree" from Loja, which has a thick cinnamon-colored bark and a bitter taste (*11*,*12*). Bado wrote, "When two reals of its powder, mixed with wine or another liquid, is ingested, it had the capacity to cure fevers and tertians" (*12*). However, he casts doubt on statements by Joseph de Jussieu, who said that a Jesuit was the first European to be cured of fever by quinquina at Malacatos, and Charles M. de La Condamine, who in 1600 referred to the use of quinquina as a remedy by Europeans living in Lima, because the actual remedy taken in both cited cases could have been *Myroxylon*, which also was used as a febrifuge (*3*). Moreover, Haggis indicates that Schedula Romana (1651), a famous apothecaries guide, was the oldest printed source citing the use of cinchona (*china della febre*) as a remedy for fever (*2*).

In contrast, Francisco Guerra considers Bollo's letter, cited by Bado in 1663, as the oldest reference to the use of *Cinchona* bark (*13*). The letter states that its febrifuge properties were known and profited by the natives, who prevented the Spaniards from finding out about it (*13*).

In 1663, Caldera reported that both the tree, which was abundant in the province of Quito, and its bark were called *quarango* (*12*). Its medicinal properties were noticed among natives of the Amazon River, who, on their way to a gold mine, swam across an icy river, having shivers afterwards. Drinking powdered *quarango* bark dissolved in hot water provided them immediate relief. When the Jesuits heard about this, they obtained all information from the natives (*14*). The perception that the natives were fully aware of *Cinchona*'s medicinal properties is reinforced by Diego de Herrera's testimony on his lost manuscript De Cortice Quinae Quinae (1699), cited by La Condamine in 1738 (*10*).

Father Bernabé Cobo noticed that Llano-y-Zapata referred to *Cinchona* as *Lacanna Perida*, a novel name of obscure origin. Cono added that Juan de Vega was the first to use the husk to counteract the fevers of the Viceroy in 1638 (*15*).

According to E. Augusto in 1943, the Spaniards adopted the use of *Cinchona* from Inca medicine (*16*). The first to get cured were Juan López de Cañizares (governor of Quito) and 2 Jesuits from Malacatos (*16*).

In 1963, Alfonso Anda Aguirre attributed *Cinchona* medicinal lore to the native Paltas, from whom the Spaniards took knowledge at Mercadillo (*17*). Regarding Pedro Leiva, chief of the native Paltas, healing the Corregidor de Cañizares (corregidors were political, administrative, and judicial authorities appointed directly by the Spanish Crown to govern a territory or province), Anda Aguirre rejects criticisms pointing out that the chief's Spanish name undermines the veracity of the story; Spaniards used to

name their subjects after themselves, meaning that the native Pedro Leiva could have taken the name of the Spaniard with whom he was socially connected, as was a custom (*17*).

Adding to our knowledge of the role of indigenous people on the discovery of the *Cinchona* tree, in 1995, Eduardo Estrella highlighted 2 important but little-known references (*18*). The first reference was Fernando de la Vega, a merchant and healer born in Loja, who wrote in 1752, at the age of 80 and upon request of Miguel de Santisteban, an extraordinary memoir: "Virtues of the cascarilla made from leaves, buds, bark, powder, and root bark," considered the first indigenous contribution about the medicinal properties of *Cinchona* (*18*). The second reference was Miguel de Santisteban, a soldier and superintendent of Bogota's mint, who, by royal order, reported on the situation of cinchona in 1752 and organized its regular shipment to the Royal Apothecary in Madrid. Upon visiting Loja in 1739, he wrote Noticias de la Cascarilla de Loja, an illustrated guide on the tree and its celebrated bark. He also proposed establishing *Cinchona* state-run stores to ensure its quality.

During the process of extracting the *Cinchona* (*cascarilla*), a trade route was marked out in the mountains of Vilcabamba (Figure 1). The Vilcabamba mountains were populated by *Cinchona* trees during the viceroyalty period, so this geographic region was a center for the use of *Cinchona* for trade and medicine. Jussieu, a botanist of the Catelnau expedition looking for *Cinchona calisaya* during 1843–1845), described how knowledge about the medicinal properties of *Cinchona* was first obtained:

> Thanks to the Indians of Malacatos, south of Loja; who suffered intermittent fevers due to the inconsistencies of the climate; they found it necessary to seek a cure and were botanical experts and connoisseurs of the virtues of various types of herbs; after experimenting with various plants they discovered that cinchona bark was the only remedy to cure intermittent fevers, so they called it Yara [tree] Chucchu or Cava [bark] Chucchu [cold]" (*19*).

José Arias agreed that the natives who discovered *Cinchona* in time immemorial were the Palta, indigenous to Loja (*20*). Early in the 17th Century, Chief Pedro Leiva used it to treat a Jesuit sick with malaria who, in turn, would use the remedy to cure the Corregidor de Cañizares in 1630. Two years later, Juan López would provide it to the wife of the Viceroy of Peru (*20*). Furthermore, previous sources have already demonstrated the presence of *cascarilla* during the Viceroyalty of Peru, both in Cusco and Lima (*21*,*22*) (Figure 2).

*Cinchona* was freely traded until 1752. A year earlier, the Spanish Crown had already intervened in its exploitation, implementing the demarcation of the forests of Loja. Its extraction, selection, collection, and transport were regulated, which had a positive effect on the economy (*20*). Likewise, according to the diary of Don Miguel de Santisteban, exports to Spain, which began around 1640, expanded to include Rome and Paris 10 years later (*23*).

The main sources of the Royal Spanish Apothecary were Loja (1750–1775), followed by Cuenca (1775–1787), after Loja's forests were depleted (*14*). Despite this event, Loja kept its role as the start point of the export routes, which proceeded from Loja to Catacocha to Celica to Tumbes to Piura and Malacatos to Tumbes to Guayaquil. The main destinations in Spain were the ports of Cádiz and El Ferrol (*24*).

## Set of Historical Contexts as Bases for the Discovery of *Cinchona* Bark (*Cascarilla*) for Treatment of Malaria

### Geographic Conext of *Cinchona* and Precolonial and Colonial Febrile Endemic Diseases in the Region

Although *Cinchona* originates ancestrally from the central-eastern Andes, historically it has been commercially exploited farther north, in the Andes between Ecuador and Peru. In that region, an important site is Mt. Caxanuma (Loja), described by La Condamine in 1737. Between that year and 1799, he verified the presence of *Cinchona* between Loja and the central Peruvian Amazon. It was most prevalent in Piura and Cajamarca, where the most frequently observed species were *C. pubescens* and *C. officinalis*. Subsequent studies have validated his observations (*25*,*26*). In the described area, on both sides of the mountain range, several important elements converged, including the presence of native communities and their medicinal plants, endemic malaria beginning with the arrival of the Spaniards, and the existence of a north–south trade route for *Cinchona* bark leading to Lima.

Malaria has only been present on the Piura Coast and in the Cajamarca and Amazonas' jungles since the viceroyalty period. The presence of *Plasmodium* parasites has been documented in a colonial-era mummy from Amazonas (*27*).

*Cinchona* thrives in so-called health axes areas (i.e., Loja, Ecuador–Piura–Cajamarca–Amazonas, and Peru). Those areas are ethnographic regions

where communities share concepts of health and principles of folk medicine, such as the "hot–cold" opposition, which is prevalent in Latin America. This method involved administering substances opposite to what they perceived in the patient (e.g., if healers perceived heat in the patient, they would administer a substance they considered cold, and in this way cure the patient) (*28*,*29*). Those areas have the most biodiverse centers worldwide. The relative low altitude of the Andes has enabled the exchange of flora and fauna from both slopes (the eastern rainforest and the western coast) since time immemorial.

In this region, which includes Peru's Piura–Huancabamba and Cajamarca regions and Ecuador's Loja and Zamora–Chinchipe regions, Carrion's disease, a febrile infection caused by *Bartonella* bacteria, has existed since pre-Columbian times, as demonstrated in a Huari mummy. Malaria became established in the valleys, as in the rest of the western tropics, starting in the late 15th Century. Of note, both diseases cause fever and anemia, and their presence overlapped in this region. Therefore, the indigenous people might have used *Cinchona* to treat malaria on the basis of their previous experience treating fevers caused by Carrion's disease (*30*,*31*). The use of *Cinchona* as febrifuge was documented in a nearly contemporary situation; the Spanish took advantage of the ancestral use of quinine by the Andaquí people (Caquetá, Colombia) to treat the intermittent fevers that afflicted them during their expedition from the Andes to the mouth of the Amazon River during 1541–1561, as described by chroniclers Gaspar de Carvajal, Francisco Vásquez, and Pedrarias de Almesto (*32*–*34*).

Previous studies have demonstrated the presence of *Plasmodium* parasites in Chachapoyas (a remote region in northern Peru) during 1437–1617. Although genomic analyses show similarity to current strains in Peru, those colonial cases undoubtedly represent infections within the context of the European invasion of the Americas (*31*,*35*–*38*). In


**Figure 1.** Loja, Peru, and the reserved Vilcabamba mountains where Cinchona trees grow, highlighting trade routes during the Viceroyalty of Peru. Source: General Archive of the Indies, Seville, Spain, 1773. Courtesy of José Carlos Arias.

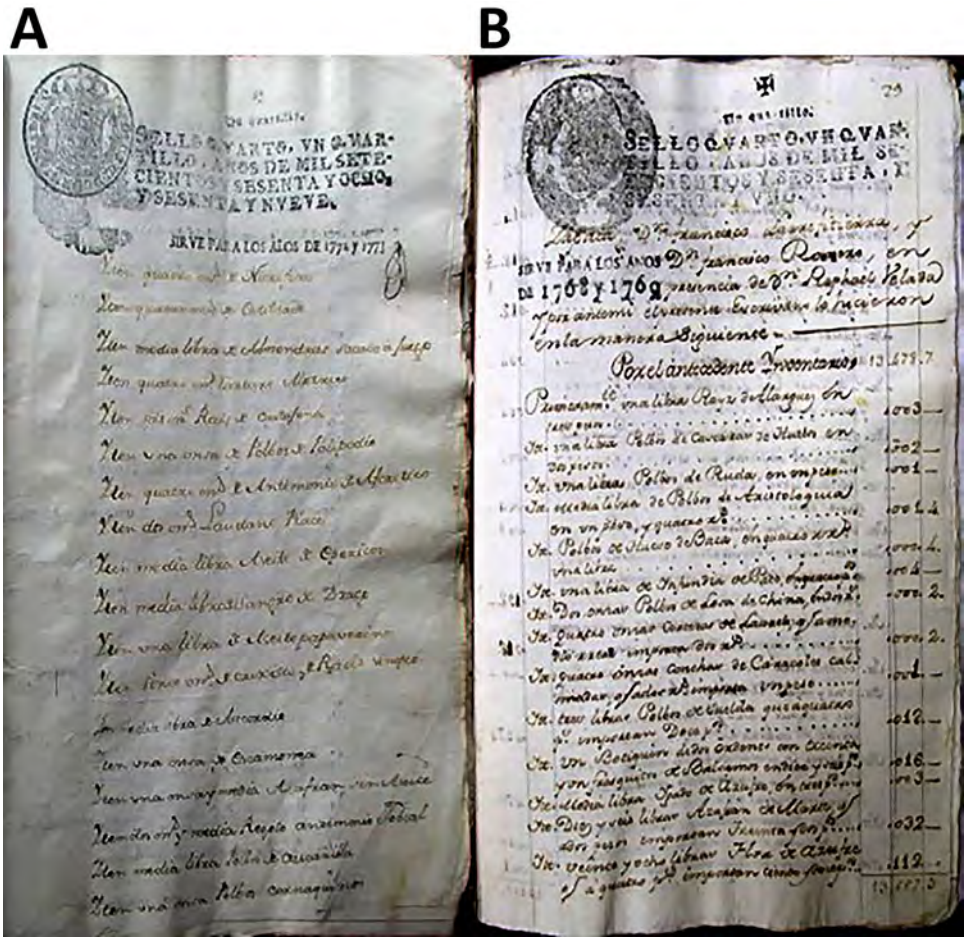


**Figure 2.** Documents from 1768 in archives of 2 very important locations for the Viceroyalty of Peru (Cuzco and Lima in present-day Peru) referring to "*cascarilla* powder" and "Loja powder" A) "Cascarilla powder" is mentioned in the Archive of the Colegio Ciencias: File 6, book 1, page 112, Cuzco. 1768–1769 (*21*). B) Page of the inventory of the apothecary of Saint Paul's College, where "Loja's powders of cinchona" is mentioned. Source: Velada R. National Archives of Peru, 1768 (*22*).

that case, the antimalarial effect of *Cinchona* might have been discovered because of the use of this plant to treat a febrile illness that causes anemia such as Carrion's disease.

### Ethnobotanical Knowledge and Cultural and Commercial Exchange with Respect to *Cinchona* Bark (*Cascarilla*)

From the perspective of local ethnomedicine, it is important to understand the use an appropriate treatment prescribes the opposite, as described previously (e.g., cold remedies to draw out the heat and hot remedies to draw out the cold of *Cinchona*) (*28*,*29*). Another principle used by traditional medicine is the sweet–bitter opposition. In ancient times, bitter concoctions, such as *Cinchona* bark solutions, were used to expel evil spirits to which ailments were attributed. Similarly, if an illness was accompanied by sweet fluids (e.g., blood or urine) because of secondary hyperglycemia (e.g., dehydration from fever or adrenergic stress), the condition could be counteracted by administering bitter substances such as *cascarilla*. The native Peruvian–Ecuadorian peoples might have discovered the fever-reducing properties of *Cinchona* within this context. A similar line of reasoning could have been to follow the principle of similarity, using bitter substances to treat fevers associated, for example, with liver disease and other ailments causing bilious vomiting (*39*,*40*). Of note, in Loja, Ecuador, ethnobotany has been used to treat fevers, as demonstrated through a study that documented 25 plants used to treat suspected malaria and other fevers (*39*). Some of those plants belong to the Rubiaceae family, to which the genus *Cinchona* belongs.

The well-documented trade route between northern Peru (Piura) and southern Ecuador (Loja) was the setting where information about the discovery and use of *Cinchona* as an antimalarial spread from the early viceroyalty. The Jesuits played a key role in that process, thanks to the development of their missions, from which they gathered and disseminated all possible knowledge. That role was particularly important for Loja, where Jesuits arrived at the beginning of the colonial period and founded the first secondary school in 1727 (*41*).

During that time, *Cinchona* was widely traded along various routes that swiftly connected Loja and Cuenca (Ecuador) with Piura and Lima (Peru) and, from there, with Spain. Such trade led to the emergence of a local elite, distinct from that of Lima (*42*). Families were linked through marriage and strengthened ties through business, such as the González de Salazar and Sánchez Navarrete Peninsular-Creole clan of *Cinchona* bark merchants operating between Guayaquil and Lima, through southern Ecuador and northern Peru. The clan established an annual shipment of cinchona bark from Loja to the royal pharmacy in Madrid, which departed from ports in present-day Peru and Ecuador (*43*,*44*). It is important to highlight the recognition of *Cinchona* in the medicinal, commercial, and historical contexts in Lima and Loja during the colonial period and present day (Figure 3)

*Cascarilla* also was obtained, in smaller quantities, in the northern highlands of Piura (Huancabamba and Ayabaca). The continuous trade involved corregidors Matías Joseph de Valdivieso (Piura) and Pedro Javier de Valdivieso (Loja), who also supplied the Royal Pharmacy of Madrid (*45*).

Spaniards such as Diego Vaca de Vega and Jesuit missionaries settled in Maynas (Loreto, Peru), a process during which they became more familiar with local medicinal plants. Vaca de Vega and soldiers from Loja founded the San Francisco de Borja School in 1619 (*46*). That collaboration highlights the relationship between military companies and the Jesuits. They arrived together, having knowledge of the malaria that caused fevers and the traditional medicines used by the native communities based on plants to treat the fevers; therefore, the colonists used the plants for the treatment of fevers and for their trade.

The intense social and administrative activity along the commercial axis between Cuenca, Loja, Piura, and Lima was dominated by Piura, from where *Cinchona* bark and textiles were also exported through the port of Paita (*47*,*48*). In 1778, *Cinchona* shipment began in Malacatos (Loja), where it was packed and transported to the ports of Tumbes (Peru) or Guayaquil (Ecuador), then on to the port of Callao (Peru), with the final destination being the port of Cádiz in Spain (*21*,*46*).

The documents describing the *Cinchona* trade reveal not only the use and importance of *Cinchona* bark but also its characteristics and the most sought-after and commercially traded varieties. Furthermore, they show the main routes by which this product and its use as an antimalarial spread from Peru to the world, through Europe. They also indicate problems that arose throughout the global distribution of *Cinchona* bark in terms of quality and price. The discovery of *Cinchona* unites aspects of distribution, ethnobotanical, epidemiologic, exchange, and commerce from the pre-Inca era to the Viceroyalty (Figure 4).

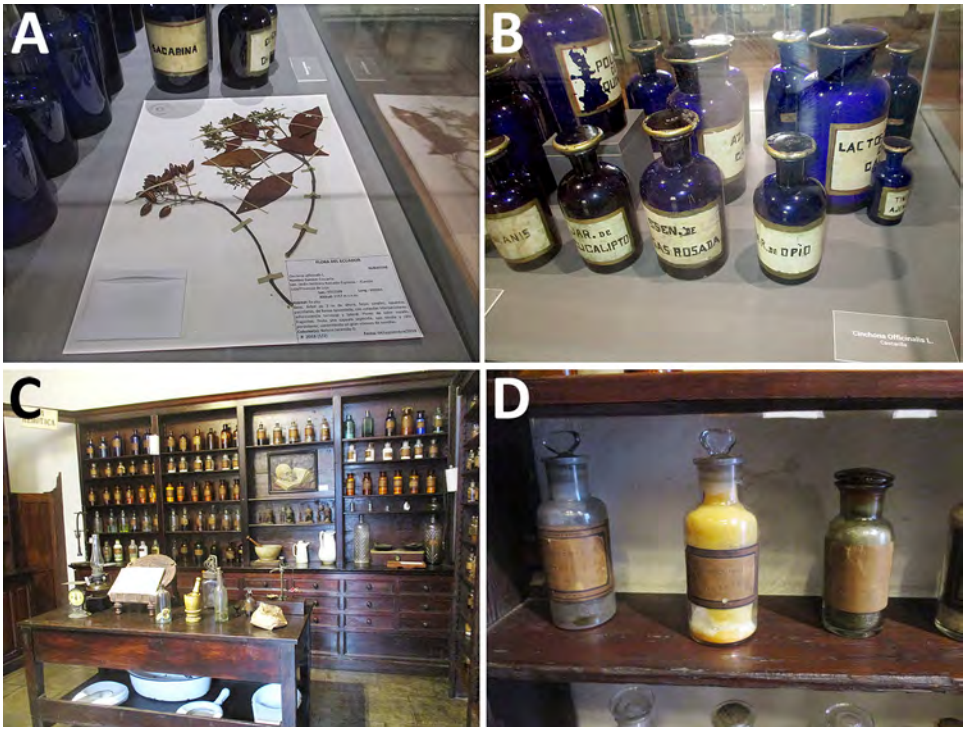


**Figure 3.** Presence of *Cinchona* in Loja, Ecuador, and Lima, Peru, and its use as powdered medicine. A) Herbarium file of *Cinchona officinalis*. Source: Museum and Cultural Center of Loja, Ecuador. B) Bottle labeled "quinine powder." Source: Museum and Cultural Center of Loja, Ecuador. C) Pharmacy and medication preparation area. Source: Museum of the Barefoot, Franciscan Order, Lima, Peru. D) Bottle of quinine. Source: Museum of the Barefoot, Franciscan Order, Lima, Peru.

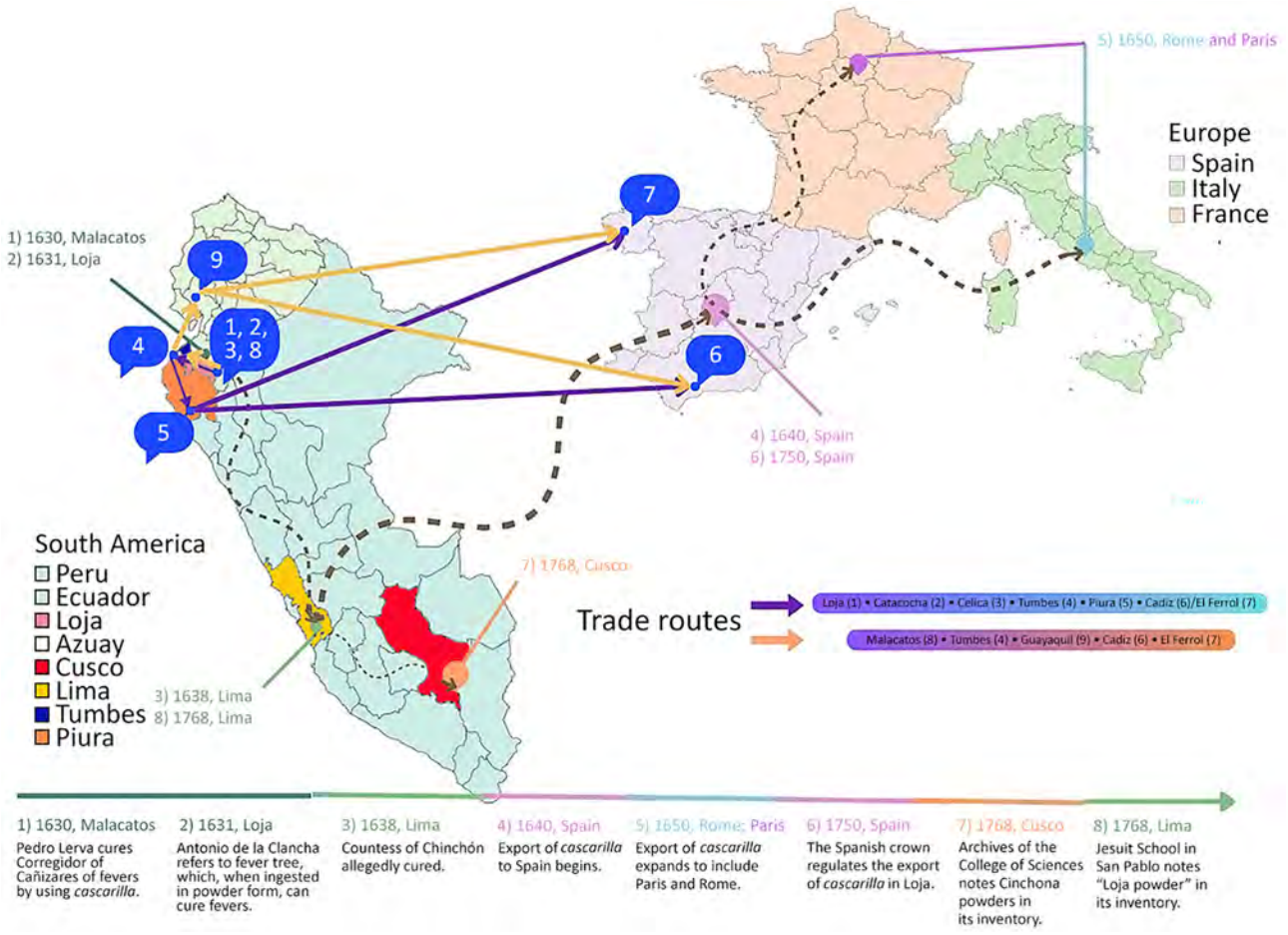


**Figure 4.** Chronologic and historical milestones of the *Cinchona* bark (also known as *cascarilla* or Loja's powder).

## Discussion

Unfortunately, despite having the *Cinchona* tree on Peru's national coat of arms, very little information exists about its discovery or early use in Peruvian archives, libraries, and the main headquarters of the Jesuit Order (the Basilica, the minor Convent of San Pedro, and the Apothecary of the Colegio de San Pablo were the main administrative centers and sites of *Cinchona* use by the Jesuit Order during the Viceroyalty of Peru). We do not consider the story about the Countess of Chinchón, which is depicted in a popular novel about the discovery of *Cinchona* as an antimalarial, because it lacks scientific veracity and most researchers now consider this story apocryphal (*2*). Information is limited about the discovery and early use of the *Cinchona* tree. This situation resulted from 3 events: the expulsion of the Jesuits in 1767, during which their documents were relocated or lost; the War of the Pacific during 1879–1884, when the National Library was looted (1881); and the National Library fire in 1943, when even more historical sources were lost.

Within the variety of references to the discovery of the therapeutic use of *Cinchona* bark, a common fact stands out: most authors highlight the indigenous people as the true discoverers. The oldest reference to that fact is from Nicolas Monardes in 1574 (*49*). Haggis, Calancha, and Bado indicate that the natives used *Cinchona* bark as a remedy for fevers (*3*,*11*,*12*). According to Bado, the natives acquired this knowledge late, between the arrival of the Spaniards and the discovery of this remedy by the Europeans (*12*). This observation is supported by a recent evaluation of the genomic variation of *P. vivax* in Latin America; all lineages can be traced to multiple introductions from Europe and Africa that occurred after contact between the natives and the Europeans (*50*).

The discovery of *Cinchona* as an antimalarial occurred because of the confluence of favorable factors that were present since pre-Hispanic times. Those factors include the geographic distribution and endemism of *Cinchona*, Amazonian ethnobotany conducive to treating fevers, endemic febrile diseases such

as bartonellosis, and mobility and cultural–commercial exchange.

## Conclusions

Loja was the axis of discovery and a center of supply and export of *Cinchona* in the 17th Century. Viceregal documents abound in this regard, especially highlighting the town of Malacatos and its leader, Chief Pedro Leiva, who raised the *Cinchona* to universal acceptance as a therapeutic intervention for malaria.

Chief Leiva revealed the secret of *Cinchona* as a febrifuge to a Jesuit missionary and, in turn, shared that information with the Corregidor Juan López Cañizares around 1630. From Loja, either by the Jesuits, an administrative, political, and judicial authority such as the Corregidor Juan López Cañizares, or both, the information arrived in Lima, capital of the Viceroyalty of Peru, seat of its political and religious authorities. From Lima, the effectiveness of the bark as an antimalarial expanded exponentially to the world.

Likewise, the Jesuits clearly maintained an early monopoly on the value and use of *Cinchona*. Of this fact there is testimony in different documents (recipe books in the apothecaries of San Pablo and the Jesuits of Santiago).

Both native and European characters played key roles in *Cinchona*'s heritage. The natives, in their long tradition of trial-and-error plant-based medicine, swiftly succeeded when confronted with a newly arrived disease (malaria). The Europeans were responsible for controlling the production and distribution of *Cinchona*, which, in the long run, saved millions of lives.

### Acknowledgments

With great gratitude to José Carlos Arias Álvarez, head of the Historical Archive of Loja, Ecuador; Akumi Analy of the historical archive of the San Antonio Abad University of Cusco, Peru; Alberto Baileti; Illa Rocconi de Quintanilla for her support in editing and improving the English writing of the article; the Jesuit José Rodriguez Rodriguez of the Jesuit Church Matriz San Pedro in Lima, Peru; and Catherine Cecilio of the Pasteur Institute of France for their great support in the search for the sources in this research.

## About the Author

Dr. Rojas-Jaimes is a research professor at Continental University, Lima-Perú. His primary research interests include One Health, discoveries of new and emerging pathogenic vectors, and the search for antimicrobial substances.

## References

1. Brack A. The Peruvian bark that saved millions of lives. A brief history of cinchona and quinine [in Spanish]. 1st edition. Lima (Peru): Powerful Mining Company; 2021.
2. Epiquién MA. Natural bicentennials. Stories of cinchona trees and vicuñas [in Spanish]. 1st edition. Lima (Peru): Black Box Publishing Group; 2021.
3. Haggis AW. Fundamental errors in the early history of Cinchona. Bull Hist Med. 1941;10:417–59 [cited 2026 Jun 8]. https://archive.org/details/b2982381x
4. Chakrabarti P. Empire and alternatives: *Swietenia febrifuga* and the cinchona substitutes. Med Hist. 2010;54:75–94. https://doi.org/10.1017/S0025727300004324
5. Rieckmann KH. The chequered history of malaria control: are new and better tools the ultimate answer? Ann Trop Med Parasitol. 2006;100:647–62. https://doi.org/10.1179/136485906X112185
6. Lowe D. Chloroquine, past and present. Science. 2020 Mar 20 [cited 2026 Apr 10]. https://www.science.org/content/blog-post/chloroquine-past-and-present
7. Slater AFG, Cerami A. Inhibition by chloroquine of a novel haem polymerase enzyme activity in malaria trophozoites. Nature. 1992;355:167–9. https://doi.org/10.1038/355167a0
8. Karle JM, Karle IL, Gerena L, Milhous WK. Stereochemical evaluation of the relative activities of the cinchona alkaloids against *Plasmodium falciparum*. Antimicrob Agents Chemother. 1992;36:1538–44. https://doi.org/10.1128/AAC.36.7.1538
9. Laval E. Pharmacy of the Jesuits of Santiago [in Spanish]. 1st edition. Santiago (Chile): Stanley; 1953 [cited 2026 Jun 8]. https://www.memoriachilena.gob.cl/602/w3-article-62244.html
10. Ortiz F. Monardes and Fragoso: two 16th-century protobotanists who dealt with New World plants and the implications of their writings on the European introduction of "quina" (cinchona) tree bark. In: Rios M, y Borgtoft H, editors. Use and management of plant resources: proceedings of the Second Ecuadorian Symposium on Ethnobotany and Economic Botany [in Spanish]. First edition. Quito (Ecuador): Abya-Yala; 1997. p. 347–60.
11. Calancha A. Moralized chronicle of the order of Saint Augustine in Perú [in Spanish]. 1639 [cited 2026 Jun 8]. https://estudiosindianos.up.edu.pe/en/biblioteca-indiana/coronica-moralizada-del-orden-de-san-agustin-en-el-peru
12. Bado S. Anastasis of the bark of Perú, or defense of the china-china [in Latin]. 1663 [cited 2026 Jun 8]. https://archive.org/details/Be.XVII.A.613.2.
13. Guerra F. The introduction of Cinchona in the treatment of malaria. Part I. J Trop Med Hyg. 1977;80:112–8.
14. Lopez JM, Calero F. On the febrifuge powder of the West Indies (1663) de Gaspar Caldera de Heredia and the introduction of quinine in Europe [in Spanish]. 1st edition. Valencia (Spain): Universidad de Valencia; 1992 [cited 2025 July 27]. https://digital.csic.es/bitstream/10261/90526/1/XXXIX_Pulvere_Febrifugo.pdf
15. Cobo B. Works of Father Bernabé Cobo [in Spanish]. 1st edition. Madrid: Atlas Editions; 1964.
16. Augusto E. Quinine in Peru [in Spanish]. 1st edition. Tambopata (Peru): Permanent Commission of Quina; 1943.
17. Anda Aguirre A. Quinine or cascarilla in Loja [in Spanish]. 1st edition. Loja (Ecuador): Editorial Office of the Private Technical University of Loja; 2002.
18. Estrella E. Enlightened science and popular knowledge in the understanding of quinine in the 18th century [in Spanish]. In: Cueto M, editor. Andean knowledge: science and technology in Bolivia, Ecuador, and Peru

[in Spanish]. Lima (Peru): Institute of Peruvian Studies; 1995. p. 37–57.
19. De Jussieu J. Description of the cinchona tree [in French]. 1st edition. Paris: Company for the Processing of Cinchonas; 1936.
20. Arias J. Barks of hope [in Spanish]. 1st edition. Loja (Ecuador): Hernandez Graphics; 2017.
21. Archive College of Sciences. File 6, notebook 1, shelves 112 [in Spanish]. Cuzco (Peru). 1768–1769, file 6.
22. Velada R. Inventory of the pharmacy of the Saint Paul's College, made as a result of the expatriation of the Fathers of the Society of Jesus [in Spanish]. Lima (Peru): National Archives of Peru; 1768.
23. Santisteban M. A thousand leagues through America. From Lima to Caracas, 1740–1741. Diary of Don Miguel de Santisteban [in Spanish]. Bogotá (Columbia): Bank of the Republic; 1992.
24. Cuvi N. Science and imperialism in Latin America: the Chinchona misión and the cooperative agricultural stations [in Spanish]. 1st edition. Barcelona (Spain): Autonomous University of Barcelona; 2009 [cited 2026 Jun 8]. http://www.tdx.cat/TDX-0121110-151121
25. García L, Veneros J, Chavez SG, Oliva M, Rojas-Briceño NB. World historical mapping and potential distribution of *Cinchona* spp. in Peru as a contribution for its restoration and conservation. J Nat Conserv. 2022;70:126290. https://doi.org/10.1016/j.jnc.2022.126290
26. Ireland KB, Kriticos DJ. Why Are plant pathogens under-represented in eco-climatic niche modelling? Int J Pest Manag. 2019;65:207–16. https://doi.org/10.1080/09670874.2018.1543910
27. Griffing SM, Gamboa D, Udhayakumar V. The history of 20th century malaria control in Peru. Malar J. 2013;12:303. https://doi.org/10.1186/1475-2875-12-303
28. Ramírez SE. The world upside down: cross-cultural contact and conflict in sixteenth-century Peru. Stanford (California): Stanford University Press; 1996.
29. Foster GM. Hippocrates' Latin American legacy: "hot" and "cold" in contemporary folk medicine. In: Wetherington R, editor. Colloquia in anthropology, volume 2. Dallas: Southern Methodist University, Fort Burgwin Research Center; 1978. p. 3–19.
30. Allison MJ, Pezzia A, Gerszten E, Mendoza D. A case of Carrion's disease associated with human sacrifice from the Huari culture of Southern Peru. Am J Phys Anthropol. 1974;41:295–300. https://doi.org/10.1002/ajpa.1330410212
31. Michel M, Skourtanioti E, Pierini F, Guevara EK, Mötsch A, Kocher A, et al. Ancient *Plasmodium* genomes shed light on the history of human malaria. Nature. 2024;631:125–33. https://doi.org/10.1038/s41586-024-07546-2
32. Albis MM. The Indians of Andaqui, New Granada. Notes of a traveler (Translated from the Spanish by J.S. Thrasher under the J.M. Vergara y Vergara & E. Delgado supervision). Bull. Am Ethnological Soc. 1855;1:53–72.
33. De Carvajal G, Toribio J, editors. Discovery of the Amazon River according to the hitherto unpublished account of the voyage of Francisco de Orellana [in Spanish]. Seville (Spain): E. Rasco Printing House; 1894.
34. Simón P. The expedition of Pedro de Ursua & Lope de Aguirre in search of El Dorado and Omagua in 1560–1. Cambridge: Cambridge University Press; 2010. https://doi.org/10.1017/CBO9780511697142
35. Cooper P, Guderian R, Paredes W, Daniels R, Perera D, Espinel M, et al. Bartonellosis in Zamora Chinchipe province in Ecuador. Trans R Soc Trop Med Hyg. 1996;90:241–3, 544–6. https://doi.org/10.1016/S0035-9203(96)90229-1
36. Legua LP. Malaria in Perú [in Spanish]. Heredian Medical Journal 2013;5(3) [cited 2025 Oct 19]. https://revistas.upch.edu.pe/index.php/RMH/article/view/436
37. Church WB, Von Hagen AC, Silverman H, Isbell WH, editors. Handbook of South American archaeology. New York: Springer; 2008.
38. Austin Alchon S. A pest in the land: New World epidemics in a global perspective. Albuquerque (NM): University of New Mexico Press; 2003.
39. Bussmann RW, Sharon D. Traditional medicinal plant use in Loja Province, southern Ecuador. J Ethnobiol Ethnomed. 2006;2:44. https://doi.org/10.1186/1746-4269-2-44
40. Aguilar CA, Xolalpa MS. Mexican herbal medicine in the treatment of diabetes [in Spanish]. Science (Mexico). 2002;53:24–35.
41. Jaramillo Alvarado, Pío. History of Loja and its province [in Spanish]. 4th edition. Guayaquil (Ecuador): Artes Gráficas Senefelder; 2001.
42. Hernadez E. The Piura elite and the independence of Peru: the struggle for continuity in the nascent republic (1750–1824) [in Spanish]. Lima (Peru): University of Piura, Riva–Agüero Institute; 2008.
43. Hernádez E. The Sánchez Navarrete and González de Salazar: a powerful family in the port of Paita in the second half of the 18th century [in Spanish]. Complutense Journal of American History. 2008;34:183–207.
44. General Archive of the Indies of Seville [in Spanish]. Quito (Ecuador). 246 No. 48. Year 1788. Fol. 9.
45. Hernadez E. The Piura elite and the independence of Peru: the struggle for continuity in the nascent republic (1750–1824) [in Spanish]. Lima (Peru): University of Piura, Riva-Agüero Institute; 2008.
46. Arias JC. Historic Loja [in Spanish]. First edition. Loja (Ecuador): International Congress of History; 2016 [cited 2024 Dec 23]. https://biblioteca.culturaypatrimonio.gob.ec/cgi-bin/koha/opac-detail.pl?biblionumber=248041
47. Departmental Archive of Piura, Cabildo, civil cases, leg. 8 exp. 154 [in Spanish]. 1796.
48. General Archive of the Nation, account Books, c15, leg. 177, exp. 880 [in Spanish]. 1796 [cited 2024 Dec 23]. https://fondosdocumentales.agn.gob.pe/index.php.
49. Monardes N. First, second, and third parts of the medicinal history of things brought from our West Indies [in Spanish]. First edition. 1574 [cited 2026 Jun 8]. https://estudiosindianos.up.edu.pe/en/biblioteca-indiana/primera-y-segunda-y-tercera-partes-de-la-historia-medicinal-de-las-cosas-que-se-traen-de-nuestras-indias-occidentales-de-nicolas-monardes
50. Lefebvre MJM, Degrugillier F, Arnathau C, Fontecha GA, Noya O, Houzé S, et al. Genomic exploration of the journey of *Plasmodium vivax* in Latin America. PLoS Pathog. 2025;21:e1012811. https://doi.org/10.1371/journal.ppat.1012811

Address for correspondence: Jesús Rojas-Jaimes, Universidad Continental, Calle Junín 355, Miraflores, Lima, Perú; email: jesus.rojas.jaimes@gmail.com

# *Phormia regina* Fly as Vector for *Ignatzschineria* spp. Bacteremia in Persons Experiencing Homelessness, Canada, 2025

Emma C.L. Finlayson-Trick, Awatif F. Alenazi, Yi Zhen Jia, Michael Payne, Gordon Ritchie, Aleksandra Stefanovic, Christopher F. Lowe, Samuel D. Chorlton, Nancy Matic, Patrick Tang, Victor Leung, David Harris, Marc G. Romney

*Ignatzschineria* spp. bacteria are emerging pathogens whose vectors historically have not been clearly identified. We used molecular methods to establish a relationship between the black blow fly (*Phormia regina*) and human *Ignatzschineria* bacteremia in persons experiencing homelessness in Vancouver, British Columbia, Canada, validating a novel transmission pathway in a vulnerable urban population.

*Ignatzschineria* bacteria are increasingly recognized as a cause of human infection (*1*). Four species have been described to date: *I. indica*, *I. larvae*, *I. ureiclastica*, and *I. cameli* (*1*). Historically, species associated with human wound and blood infection have shown a geographic distribution; *I. indica* predominates in North America, and *I. larvae*/*I. ureiclastica* predominates in Europe (*1*). The gram-negative, aerobic, nonmotile, and oxidase- and catalase-positive bacteria were originally isolated from the larvae and adult gastrointestinal tracts of *Wohlfahrtia magnifica* parasitic flies (*2*). Experimental and ecologic studies suggest that *Ignatzschineria* are part of the larvae microbiome through a combination of vertical transmission and environmental acquisition during feeding (*3*–*5*). Ultimately, host identity appears to shape overall abundance; blow fly species such as *Phormia regina* have a high abundance of *Ignatzschineria* (Appendix Figure 1, https://wwwnc.cdc.gov/EID/article/32/7/25-1914-App1.pdf) (*4*).

Although *W. magnifica* flies primarily cause myiasis in animals, blow flies are associated with facultative myiasis in humans (*6*). At least 3 case reports of *Ignatzschineria* bacteremia in humans have implicated the green blow fly (*Lucilia sericata*), but the methods used for identification have primarily relied on epidemiology and morphologic features (*1*,*7*). In general, the specific fly vectors associated with human urban myiasis are seldom confirmed molecularly.

We describe 2 cases of *Ignatzschineria* bacteremia in persons experiencing homelessness (PEH) in Vancouver, British Columbia, Canada. We used genomic approaches to characterize the bacterial isolates from both cases and performed vector identification on the fly associated with 1 of the cases. We obtained written consent from both patients for publication of their cases.

## The Study

Case 1 involved a 49-year-old man, a PEH with active substance use disorder (SUD) and chronic bilateral leg wounds, who sought care for worsening pain, swelling, and wound myiasis (Figure 1, panel A, B). We collected 2 aerobic and 2 anaerobic blood cultures, and within 24 hours, all 4 collection bottles grew gram-negative bacilli. After an additional 24 hours, small gray colonies appeared on sheep blood agar and clear colonies appeared on MacConkey agar (Appendix Figure 2). Matrix-assisted laser desorption/ionization time-of-flight mass spectrometry (MALDI Biotyper; Bruker, https://www.bruker.com) identified the isolates as *I. larvae*, *I. indica*, and *Fusobacterium varium*.

Author affiliations: University of British Columbia, Vancouver, British Columbia, Canada (E.C.L. Finlayson-Trick, A.F. Alenazi, Y.Z. Jia, M. Payne, G. Ritchie, A. Stefanovic, C.F. Lowe, N. Matic, P. Tang, V. Leung, D. Harris, M.G. Romney); St. Paul's Hospital, Vancouver (M. Payne, G. Ritchie, A. Stefanovic, C.F. Lowe, N. Matic, P. Tang, V. Leung, D. Harris, M.G. Romney); BugSeq Bioinformatics, Inc., Vancouver (S.D. Chorlton)

DOI: https://doi.org/10.3201/eid3207.251914


**Figure 1.** Leg wounds in case-patient 1 in pair of *Ignatzschineria* spp. bacteremia cases in persons experiencing homelessness, Vancouver, British Columbia, Canada, 2025. A) Bilateral leg wounds at time of admission; B) close-up of myiasis in exposed right tibialis anterior tendon.

Whole-genome sequencing (WGS) confirmed the species as *I. larvae* and *I. indica* (Appendix Figure 3).

We conducted antimicrobial susceptibility testing by using gradient strip diffusion method for several antibiotics (Table). We referenced the 2025 Clinical and Laboratory Standards Institute breakpoints for other non-Enterobacterales for interpretation of MICs (*8*). The genotypic antimicrobial resistance prediction for the *I. larvae* isolate was concordant with phenotype for all tested antimicrobials (Table). The *I. indica* isolate did not grow for phenotypic testing, but no genotypic resistance was detected for antibiotics of interest.

The patient underwent surgical debridement of both leg wounds and a split thickness skin grafting from the upper thigh. Computed tomography imaging of the right lower leg demonstrated periosteal reaction and irregularity of the underlying bone cortex. He was treated for osteomyelitis with 6 weeks of amoxicillin/clavulanate. After antimicrobial therapy, the leg wounds healed well and showed healthy granulation tissue. We performed no repeat imaging.

Shortly after case-patient 1 was admitted to hospital, a second patient (case-patient 2), a 36-year-old man who was a PEH and SUD, sought care for fevers and an erythematous right shin containing necrotic wounds heavily infested with fly larvae (Figure 2, panel A, B). His blood cultures grew *I. larvae* and *Pasteurella multocida*, which we confirmed by using WGS. The genotypic antimicrobial resistance prediction was concordant with phenotype for all antibiotics tested (Table). His orthopedic and plastic surgery physicians recommended wound care without

**Table.** Antibiotic MICs as determined by gradient strip diffusion method for *Ignatzschineria larvae* reported for case-patient 1 (blood culture) and case-patient 2 (blood and wound culture), Vancouver, British Columbia, Canada, 2025

| | MIC, μg/mL | | | |
|---|---|---|---|---|
| Antibiotic | Case-patient 1 blood culture | Case-patient 2 blood culture | Case-patient 2 wound culture | Interpretation |
| Amoxicillin/clavulanate | 0.032 | 0.047 | 0.047 | Susceptible |
| Ceftriaxone | <0.002 | <0.002 | <0.002 | Susceptible |
| Ciprofloxacin | 0.094 | 0.047 | 0.047 | Susceptible |
| Meropenem | 0.023 | 0.012 | 0.012 | Susceptible |
| Piperacillin/tazobactam | <0.016 | <0.016 | <0.016 | Susceptible |
| Trimethoprim/sulfamethoxazole | 0.023 | 0.06 | 0.008 | Susceptible |

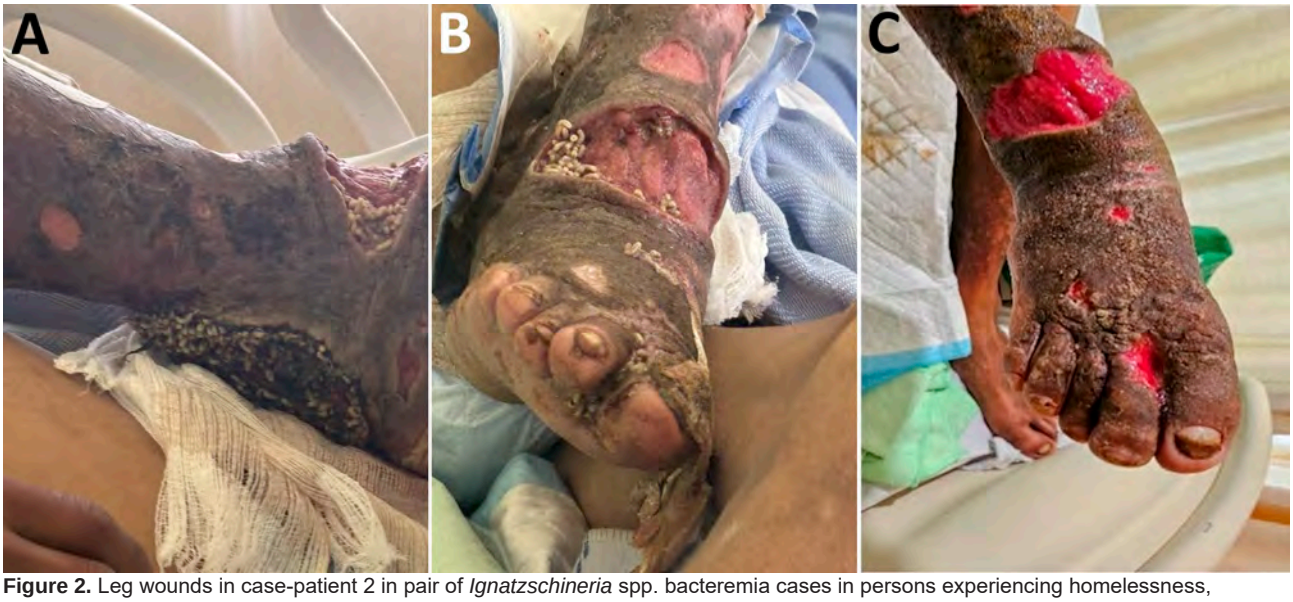


**Figure 2.** Leg wounds in case-patient 2 in pair of *Ignatzschineria* spp. bacteremia cases in persons experiencing homelessness, Vancouver, British Columbia, Canada, 2025. A, B) Lateral (A) and anterior (B) right leg wounds with visible myiasis at time of admission. C) Same wounds after 3 weeks of antibiotics and regular wound care.

surgical intervention. The plan was to complete 6 weeks of ceftriaxone for osteomyelitis, but the patient self-initiated discharge before completing therapy.

When case-patient 2 sought care, we recognized a pattern of myiasis-associated bacteremia. We collected fly larvae from the patient in a sterile container, stored them on blood agar, and observed them over time to document their development into adult flies (Figure 3). The third instar larvae (9–12 mm) were creamy white with distinct bands along the body covered in short spines. The prothoracic spiracles had ≥10 openings. We observed 2 incomplete peritremes on the posterior with three inner slits directed toward the median line ventrally. The adult flies (10–12 mm) were metallic green. Considered together, those features were suggestive of the Calliphoridae family and the *Phormia* genus (*9*). We confirmed the fly to be *P. regina* by sequencing the cytochrome c oxidase subunit I gene using universal primers (Appendix Figure 4) (*10*). To confirm the presence of *Ignatzschineria* spp. in the fly larvae, we washed a larva 3 times in phosphate-buffered saline, macerated the anterior portion of the larva in phosphate-buffered saline, and subjected the homogenate to mechanical disruption with glass beads before DNA extraction and 16S rRNA sequencing. We uploaded sequencing data to the CZ ID platform (https://czid.org) for metagenomic analysis (S.E. Simmonds et al., unpub. data, https://doi.org/10.1101/2024.02.29.579666). We identified *Ignatzschineria* spp. at a 16S rRNA read abundance of 0.1% from the larva bacterial microbiome, providing molecular evidence of vector colonization.

## Conclusions

We have established a relationship between *P. regina* fly wound myiasis and *I. larvae* bacteremia by identifying *P. regina* flies as the probable causative agent of myiasis, isolating *Ignatzschineria* bacteria in patients' blood cultures, and detecting the organism within the larval microbiome. Our findings fulfill the criteria for sequence-based determination of causation as proposed by Fredricks and Relman (*11*). Moreover, the larval microbiome results were consistent with the findings of Deguenon et al. (*12*), who identified *Ignatzschineria* bacteria in the microbiome of wild *P. regina* flies. Because *P. regina* blow flies are ubiquitous and widely distributed across North America, our results suggest that exposure risk could be far broader than previously assumed.

Both patients were at heightened risk for *Ignatzschineria* bacteremia because of their PEH status, SUD, chronic wounds, and competing health and social priorities (i.e., resuming everyday life versus receiving treatment and follow-up) (*13*). We hypothesize that the complexity of wounds and the magnitude of infestation might increase the risk for *Ignatzschineria* infection. Those cases also illustrate the value of a One Health perspective, in which human vulnerability, environmental exposure, and interactions with urban flies converge to create conditions for pathogen transmission. Clinicians should maintain a high index of suspicion and obtain blood cultures in patients with wound myiasis and systemic symptoms.

Accurate identification of *Ignatzschineria* bacteria remains a diagnostic challenge in the clinical

microbiology laboratory. In several cases, *Ignatzschineria* isolates were initially misidentified as other bacteria using phenotypic and molecular methods (*7*,*13*). We observed that the Bruker MALDI Biotyper successfully identified *I. indica* and *I. larvae/ureiclastica* but could not differentiate between *I. larvae* and *I. ureiclastica* because of the high degree of genetic similarity. Of note, the VITEK MS version 3.2 knowledge base (bioMérieux, https://www.biomerieux.com) does not include *Ignatzschineria* species. Most case reports have relied on molecular methods such as 16S rRNA gene sequencing for genus identification, but only WGS can truly provide species-level resolution (*14*). Those findings highlight a broader diagnostic gap in detecting emerging zoonotic pathogens and demonstrate the value of WGS for achieving species-level resolution.

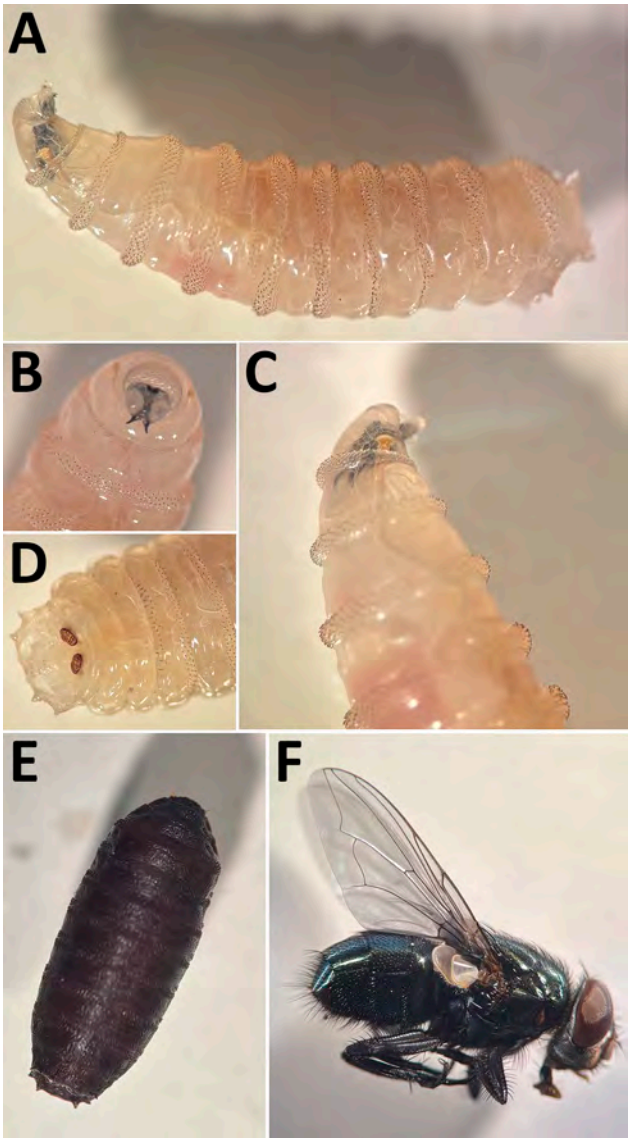


**Figure 3.** Development of black blow fly (*Phormia regina*) from larvae collected from case-patient 2 in pair of *Ignatzschineria* spp. bacteremia cases in persons experiencing homelessness, Vancouver, British Columbia, Canada, 2025. A–D) Third instar. E) Pupa. F) Adult. Key features of *P. regina* larvae include segmental spines (A), cephalopharyngeal skeleton (B), anterior spiracle (C), and peritremes (D).

Information on the antimicrobial susceptibility of *Ignatzschineria* is currently limited. Reported testing methods include disk diffusion, automated instruments, gradient strip diffusion, or some combination of those methods (*1*). Most published cases demonstrate that *Ignatzschineria* bacteria are susceptible to β-lactam antibiotics, which comprise the mainstay of therapy (*1*). Treatment typically includes appropriate antimicrobial therapy combined with larvae removal, wound care, debridement, amputation, or some combination of these interventions (*1*,*7*). Overall, patient outcomes have been favorable when both infection and underlying wounds are addressed (*13*).

### Acknowledgments

We thank Cherie Lai, Gillian Andersen, and the rest of the microbiology laboratory staff at St. Paul's Hospital who played an instrumental role in rearing the fly larvae.

Sequence data from this study are available in GenBank (BioProject accession no. PRJNA1438763).

Author contributions: review and editing, E.C.L.F.-T., A.F.A., Y.Z.J., M.P., G.R., A.S., C.F.L., S.D.C., N.M., P.T., V.L., D.H., and M.G.R.; supervision, M.G.R.; original draft, E.C.L.F.-T., A.F.A., Y.Z.J., M.P., A.S., C.F.L., and N.M.; methodology, E.C.L.F.-T., M.P., G.R., and P.T.; project administration, M.P., P.T., and M.G.R.; investigation, E.C.L.F.-T., M.P., G.R., A.S., C.F.L., S.D.C., N.M., P.T., and M.G.R.; formal analysis, E.C.L.F.-T., M.P., G.R., S.D.C., P.T., and M.G.R.; data curation, E.C.L.F.-T., M.P., G.R., S.D.C., and P.T.; conceptualization, E.C.L.F.-T., A.F.A., Y.Z.J., M.P., G.R., A.S., C.F.L., N.M., P.T., V.L., D.H., and M.G.R.

### About the Author

Dr. Finlayson-Trick is a third-year medical microbiology resident at the University of British Columbia, Vancouver. Her primary research interests include antimicrobial resistance with a focus on detection in the clinical microbiology laboratory, optimization of antimicrobial stewardship strategies, and advancement of novel therapeutics.

### References

1. Fear T, Richert Q, Levesque J, Walkty A, Keynan Y. *Ignatzschineria indica* bloodstream infection associated with maggot infestation of a wound in a patient from Canada. J Assoc Med Microbiol Infect Dis Can. 2020;5:193–200. https://doi.org/10.3138/jammi-2019-0027

2. Tóth E, Kovács G, Schumann P, Kovács AL, Steiner U, Halbritter A, et al. *Schineria larvae* gen. nov., sp. nov., isolated from the 1st and 2nd larval stages of *Wohlfahrtia magnifica* (Diptera: Sarcophagidae). Int J Syst Evol Microbiol. 2001;51:401–7. https://doi.org/10.1099/00207713-51-2-401
3. Long W, Pang J, Yan W, Hu N. Industrial-scale bioconversion of three-phase residue by *Musca domestica* larvae: dynamics of gut microbiota and their ecological driver. Insects. 2025;16:686. https://doi.org/10.3390/insects16070686
4. Mikaelyan A, Receveur J, Bernstein K, Babcock NJ, Pechal JL, Welsh MV, et al. Host-specific microbiomes of blow flies: ecological drivers and implications for pathogen carriage. Front Immunol. 2025;16:1673934. https://doi.org/10.3389/fimmu.2025.1673934
5. Tang H, Zhang X, Yang F, Zhang C, Ngando FJ, Ren L, et al. Effect of ciprofloxacin on the composition of intestinal microbiota in *Sarcophaga peregrina* (Diptera: Sarcophagidae). Microorganisms. 2023;11:2867. https://doi.org/10.3390/microorganisms11122867
6. Cardoso GA, Cunha VAS, Genevcius BC, Madeira-Ott T, Costa BMA, Rossoni DM, et al. Origins and diversification of myiasis across blowflies. Ecol Evol. 2025;15:e70993. https://doi.org/10.1002/ece3.70993
7. Barker HS, Snyder JW, Hicks AB, Yanoviak SP, Southern P, Dhakal BK, et al. First case reports of *Ignatzschineria* (*Schineria*) *indica* associated with myiasis. J Clin Microbiol. 2014;52:4432–4. https://doi.org/10.1128/JCM.02183-14
8. Clinical and Laboratory Standards Institute. Performance standards for antimicrobial susceptibility testing, 35th edition. Supplement M100. Wayne (PA): The Institute; 2025.
9. Centers for Disease Control and Prevention. Pictorial keys: arthropods, reptiles, birds, and mammals of public health significance. 2000 May 22 [cited 2025 Sep 23]. https://stacks.cdc.gov/view/cdc/60114
10. Folmer O, Black M, Hoeh W, Lutz R, Vrijenhoek R. DNA primers for amplification of mitochondrial cytochrome c oxidase subunit I from diverse metazoan invertebrates. Mol Mar Biol Biotechnol. 1994;3:294–9.
11. Fredricks DN, Relman DA. Sequence-based identification of microbial pathogens: a reconsideration of Koch's postulates. Clin Microbiol Rev. 1996;9:18–33. https://doi.org/10.1128/CMR.9.1.18
12. Deguenon JM, Travanty N, Zhu J, Carr A, Denning S, Reiskind MH, et al. Exogenous and endogenous microbiomes of wild-caught *Phormia regina* (Diptera: Calliphoridae) flies from a suburban farm by 16S rRNA gene sequencing. Sci Rep. 2019;9:20365. https://doi.org/10.1038/s41598-019-56733-z
13. Pomerantz E, Pericak O, Sokach C, Edathil J, Yeung HM. Two cases of maggot-associated *Ignatzschineria* bacteremia in xylazine-induced injection wounds: an emerging threat. Case Rep Infect Dis. 2024;2024:7684187. https://doi.org/10.1155/crdi/7684187
14. Belote A, Hawkinson D, Shoemaker DM. Myiasis as a vector for bacteremia: a unique case of *Helcococcus kunzii* and *Ignatzschineria ureiclastica/larvae* polymicrobial bacteremia from myiasis. Vector Borne Zoonotic Dis. 2024;24:788–91. https://doi.org/10.1089/vbz.2024.0005


Address for correspondence: Emma Finlayson-Trick, University of British Columbia Medical Microbiology Residency Program, Department of Pathology and Laboratory Medicine, University of British Columbia, 910 West 10th Ave, Vancouver, BC V5Z 1M9, Canada; email: emma.finlaysontrick@phc.ca

# Cat-Scratch Disease Associated with Acute Hearing Loss, Israel

Michal Yakubovsky, Michal Katzir, Alaa Atamna, Dana Yelin, Michal Landes, Gabriel Weber, Moshe Ephros, Michael Giladi

We report 5 patients in Israel with cat-scratch disease (CSD) who had unilateral sudden sensorineural hearing loss. Several mechanisms are plausible, but further research is needed to clarify pathogenesis. The cases highlight a previously underrecognized association between CSD and sudden sensorineural hearing loss, expanding the spectrum of cranial nerve neuropathies in CSD.

Cat-scratch disease (CSD), caused by *Bartonella henselae* bacteria, is a zoonotic infection primarily transmitted through contact with cats, mainly scratches or bites. Approximately 90% of cases, designated as typical CSD, are characterized by regional lymphadenitis. Atypical CSD manifestations are diverse and include fever of unknown origin (FUO), erythema nodosum, hepatosplenic involvement, neuroretinitis, and neurologic complications such as encephalitis, and cranial nerve neuropathy (*1*,*2*). Sudden sensorineural hearing loss (SSNHL) has been associated with viral and bacterial infections (*3*), but it is not a recognized sequela of CSD.

On the basis of data from a national CSD registry in Israel with long-term follow-up, we report 5 patients with CSD who had SSNHL. This case series suggests a potentially underrecognized association between CSD and SSNHL.

## The Study

We have conducted a surveillance study of CSD in Israel since 1991 (*4*). We defined CSD as illness in a patient with symptoms and signs consistent with CSD in the absence of another diagnosis and ≥1 confirmatory laboratory result: a positive serologic test for *B. henselae* antibodies (IgM, IgG, or both) or a positive PCR for *B. henselae* DNA. We performed serologic testing by using enzyme immunoassay (EIA) and interpreted results as previously described (*5*). We performed PCR on lymph node tissue as previously reported (*4*). We confirmed SSNHL by audiometry when the patient was admitted for care. Clinical outcome was based on patient-reported hearing because repeat audiometric testing was not available. We considered doxycycline, macrolides, and rifampin to be active against *B. henselae*. The Tel Aviv Sourasky Medical Center Institutional Review Board approved the study (approval no. TLV-0147-08). We collected follow-up data prospectively and obtained informed consent from all patients.

Five patients with CSD had unilateral SSNHL, confirmed by audiometric testing performed after an otolaryngologic evaluation. Two patients also reported tinnitus. All patients had ≥1 additional manifestations characteristic of CSD, including FUO (4/5), lymphadenitis (3/5), ocular CSD manifestations (3/5), erythema nodosum (1/5), and encephalitis (1/5). Among the 4 patients with FUO, fever was continuous or intermittent, lasting 3–12 weeks (median 6 weeks). The fifth patient had no fever but reported prolonged weakness (Table).

In 4 patients, SSNHL occurred 3–9 weeks after initial CSD diagnosis. The fifth patient, a musician, experienced severe, prolonged CSD, beginning with 3 months of intermittent fever and unilateral cervical lymphadenitis, during which he had onset of encephalitis eventually requiring hospitalization, followed by persistent fatigue. SSNHL occurred 9 months after CSD diagnosis. At the

Author affiliations: Tel Aviv University, Gray Faculty of Medical and Health Sciences, Tel Aviv, Israel (M. Yakubovsky, M. Katzir, A. Atamna, D. Yelin, M. Giladi); Tel Aviv Sourasky Medical Center, Tel Aviv (M. Yakubovsky, M. Giladi); Meir Hospital, Kfar Saba, Israel (M. Katzir); Beilinson Hospital, Rabin Medical Center, Petach Tiqva, Israel (A. Atamna); Sheba Medical Center, Ramat Gan, Israel (D. Yelin); Technion–Israel Institute of Technology, Rappaport Faculty of Medicine, Haifa, Israel (M. Landes, G. Weber, M. Ephros); Emek Medical Center–Clalit, Afula, Israel (M. Landes); Carmel Medical Center, Haifa (G. Weber)

DOI: https://doi.org/10.3201/eid3207.260592

**Table.** Characteristics of CSD patients with sudden sensoneuronal hearing loss, Israel*

| Characteristic | Patient no. | | | | |
|---|---|---|---|---|---|
| | 1 | 2 | 3 | 4 | 5 |
| Age, y | 35 | 47 | 71 | 15 | 35 |
| Sex | Female | Female | Male | Female | Male |
| Cat contact | Yes | Yes | Yes | Yes | Yes |
| Fever (duration, wks) | Yes (8) | Yes (3) | Yes (4) | No | Yes (12) |
| Lymphadenopathy | Not reported | Not reported | Retroperitoneal | Retro-auricular | Cervical |
| Atypical CSD manifestations | Neuroretinitis, CSD-FUO syndrome | Central retinal artery occlusion, chorioretinitis, CSD-FUO syndrome | CSD-FUO syndrome | Neuroretinitis | Erythema nodosum, encephalitis, CSD-FUO syndrome |
| Time from CSD onset to hearing loss, wks | 9 | 3 | 5 | 6 | 52 |
| Laboratory diagnosis of CSD | IgG 1:200; IgM positive | IgG 1:800; IgM negative | IgG 1:400; IgM negative | IgG 1:100 (IgG seroconversion); IgM negative; positive PCR (lymph node) | IgG 1:200; IgM borderline |
| Antibiotics | Doxycycline and rifampin | Doxycycline | None | None | Doxycycline and rifampin |
| Corticosteroids | Yes | Yes | Yes | No | No |
| Outcome | Partial recovery with residual hearing impairment | Partial recovery with residual hearing impairment | Recovery after 4 wks | Recovery after 10 wks | Partial recovery with residual hearing impairment |
| Duration of follow-up, mo | 107 | 75 | 58 | 85 | 29 |

*CSD, cat-scratch disease; FUO, fever of unknown origin.
†Based on the patients' own subjective perception of hearing ability because repeat audiometric testing was not available. For complete recovery, duration of hearing loss is shown; for partial recovery, hearing was assessed at last follow-up.

last follow-up, 29 months after SSNHL onset, he reported persistent hearing impairment but declined further evaluation.

Three patients received relevant antibiotics (none received azithromycin), 3 received oral corticosteroids, and 3 received no treatment (Table). After a median follow-up of 66 months (range 29–107 months), 3 (60%) of 5 patients reported partial recovery, with residual hearing impairment, and 2 reported complete recovery.

In this case series, we report 5 patients with CSD and SSNHL. A temporal association between active CSD and SSNHL was evident in 4 patients. In contrast, patient 5 had hearing loss 1 year after the onset of a prolonged CSD, making causality less certain.

SSNHL is a recognized but uncommon sequela of viral and bacterial infections (*3*). Our literature search identified only 2 early reports predating the identification of *B. henselae* as the etiologic agent of CSD in 1992 (*6*,*7*), suggesting this association may be underrecognized.

Although the diagnosis of CSD often is challenging, it was well supported in our patients by epidemiologic, clinical, and laboratory data: all patients reported cat contact and exhibited various CSD manifestations, including lymphadenopathy, FUO, encephalitis, erythema nodosum, and ocular findings (*1*), and all patients had serologic confirmation (Table). Of note, serodiagnosis of CSD usually is IgG-based, whereas IgM is short-lived and detectable in approximately half of CSD patients (*5*).

Ancillary testing for alternative infections (e.g., HIV and syphilis) was inconsistent and generally performed for other indications (e.g., prolonged fever), rather than the hearing loss. This approach aligns with current guidelines, which do not recommend routine laboratory testing in SSNHL because of limited yield (*8*). All cases predated COVID-19, and Lyme disease is not endemic in Israel; therefore, corresponding laboratory testing was not performed.

The pathogenesis of SSNHL in CSD remains unknown. In viral-associated SSNHL, such as herpes simplex, mumps, measles, rubella, HIV, and enteroviruses, proposed mechanisms include direct cochlear invasion, reactivation of latent virus, and immune-mediated injury (*9*). Similar processes have been suggested in COVID-19–associated hearing loss, and imaging findings supported cochlear inflammation and occasional nerve involvement (*9*). In bacterial infections, mechanisms are less defined. *Rickettsia* spp., known to be intracellular and endotheliotropic like *B. henselae*, have been associated with hearing loss, possibly mediated by immune-related vasculitic involvement of the cochlear or cochlear nerve vasculature (*10*).

Several observations in *Bartonella* infection provide biologic plausibility for the proposed mechanisms underlying SSNHL. In vitro studies show that *B. henselae* can infect feline microglial brain cells (*11*).

Animal studies further indicate dissemination to the central nervous system (CNS); in a feline model, *B. henselae* was recovered from brain tissue after intradermal inoculation (*12*), consistent with the potential for neural involvement. Clinical observations further support cranial nerve involvement and potential pathogenic mechanisms. *B. henselae* has been identified in human CNS tissue through autopsy, indicating direct invasion of neural structures (*13*). In addition, the endothelial tropism of *B. henselae* is evidenced by its association with vascular injury, including cerebral vasculitis, in human brain biopsy (*14*). Moreover, retinal vascular occlusion and ischemic optic neuropathy in CSD patients (*1*) suggest that microvascular injury might contribute to dysfunction of the cochlear or cochlear nerve, structures known to be highly vulnerable to ischemia. Furthermore, a pediatric case of CSD-associated peripheral facial nerve palsy demonstrated a granulomatous lesion at the internal auditory meatus that resolved with treatment (*15*). Given the intimate anatomic proximity of cranial nerves VII and VIII within this compartment, a similar inflammatory lesion could affect the cochlear nerve, causing neuritis, compressive neuropathy, or both. Our recent report of multiple cranial neuropathies in CSD, involving cranial nerve III, VI, VII, and IX (*2*), further supports the potential for *B. henselae* infection to involve cranial nerves and cause neuropathic manifestations. Immune-mediated inflammatory mechanisms could also contribute, although current evidence remains indirect (*3*).

Taken together, data support 3 non–mutually exclusive mechanisms for SSNHL in CSD: vascular or vasculitic injury of the cochlea or cochlear nerve, analogous to rickettsial disease; focal inflammatory involvement of the vestibulocochlear nerve within the internal auditory canal, potentially causing neuritis, compressive neuropathy, or both within this anatomically confined space; and immune-mediated cranial neuritis occurring in the context of systemic *Bartonella* infection. Although definitive proof is lacking, the ability of *B. henselae* to involve neural and neurovascular components of the CNS, together with its recognized associations with cranial neuropathies, provides a biologically plausible explanation for transient nerve VIII dysfunction and sudden hearing loss.

The small number of cases and the heterogeneity of treatment preclude therapeutic conclusions. Of note, none of the patients received azithromycin, excluding azithromycin-associated SSNHL as a confounder.

## Conclusions

We report a possible but underrecognized association between CSD and SSNHL that warrants further clinical awareness. Several mechanisms are plausible, but further research is needed to clarify the pathogenesis. All 5 patients had additional CSD manifestations, which, together with the sudden hearing loss, posed a diagnostic challenge. A history of cat exposure may serve as a critical clue prompting appropriate laboratory testing.

### Acknowledgments

We thank the patients for their kind cooperation and for granting permission to publish their clinical information as part of this study.

The data that support the findings of this study are available from the corresponding author upon reasonable request. Patient-level data are not publicly available because of privacy restrictions.

Author contributions: M.Y. and M.G. contributed substantially to the conception and design of the study, data interpretation, and manuscript drafting. All authors participated in data collection and provided critical revisions of the manuscript for important intellectual content. All authors approved the final version.

The authors used ChatGPT (GPT-5; OpenAI, https://www.openai.com) to assist with language editing and style refinement of the manuscript text. All content, data analysis, and interpretations were generated and verified by the authors.

## About the Author

Dr. Yakubovsky is a senior infectious disease physician at Tel Aviv Sourasky Medical Center, Tel Aviv, Israel. Her primary research interests focus on *Bartonella* infections and neurologic infectious diseases.

### References

1. Florin TA, Zaoutis TE, Zaoutis LB. Beyond cat scratch disease: widening spectrum of *Bartonella henselae* infection. Pediatrics. 2008;121:e1413–25. https://doi.org/10.1542/peds.2007-1897
2. Yakubovsky M, Kosman A, Kadar L, Paran Y, Grisaru-Soen G, Gadoth A, et al. Cranial nerve neuropathies: a rare manifestation of cat scratch disease. BMC Infect Dis. 2026;26:392. https://doi.org/10.1186/s12879-026-12628-9
3. Schreiber BE, Agrup C, Haskard DO, Luxon LM. Sudden sensorineural hearing loss. Lancet. 2010;375:1203–11. https://doi.org/10.1016/S0140-6736(09)62071-7
4. Goaz S, Rasis M, Binsky Ehrenreich I, Shapira L, Halutz O, Graidy-Varon M, et al. Molecular diagnosis of cat scratch disease: a 25-year retrospective comparative analysis of various clinical specimens and different PCR assays.

Microbiol Spectr. 2022;10:e0259621. https://doi.org/10.1128/spectrum.02596-21
5. Giladi M, Kletter Y, Avidor B, Metzkor-Cotter E, Varon M, Golan Y, et al. Enzyme immunoassay for the diagnosis of cat-scratch disease defined by polymerase chain reaction. Clin Infect Dis. 2001;33:1852–8. https://doi.org/10.1086/324162
6. Carithers HA, Margileth AM. Cat-scratch disease. Acute encephalopathy and other neurologic manifestations. Am J Dis Child. 1991;145:98–101. https://doi.org/10.1001/archpedi.1991.02160010104026
7. Ammar-Khodja A. Sudden deafness following a scratch-induced benign lymphoreticulosis [in French]. Rev Laryngol Otol Rhinol (Bord). 1982;103:63.
8. Chandrasekhar SS, Tsai Do BS, Schwartz SR, Bontempo LJ, Faucett EA, Finestone SA, et al. Clinical practice guideline: sudden hearing loss (update) executive summary. Otolaryngol Head Neck Surg. 2019;161(1_suppl):S1-S45. https://doi.org/10.1177/0194599819859885
9. Yamada S, Kita J, Shinmura D, Nakamura Y, Sahara S, Misawa K, et al. Update on findings about sudden sensorineural hearing loss and insight into its pathogenesis. J Clin Med. 2022;11:6387. https://doi.org/10.3390/jcm11216387
10. Tsiachris D, Deutsch M, Vassilopoulos D, Zafiropoulou R, Archimandritis AJ. Sensorineural hearing loss complicating severe rickettsial diseases: report of two cases. J Infect. 2008;56:74–6. https://doi.org/10.1016/j.jinf.2007.10.002
11. Muñana KR, Vitek SM, Hegarty BC, Kordick DL, Breitschwerdt EB. Infection of fetal feline brain cells in culture with *Bartonella henselae*. Infect Immun. 2001;69:564–9. https://doi.org/10.1128/IAI.69.1.564-569.2001
12. Guptill L, Slater L, Wu CC, Lin TL, Glickman LT, Welch DF, et al. Experimental infection of young specific pathogen-free cats with *Bartonella henselae*. J Infect Dis. 1997;176:206–16. https://doi.org/10.1086/514026
13. Gerber JE, Johnson JE, Scott MA, Madhusudhan KT. Fatal meningitis and encephalitis due to *Bartonella henselae* bacteria. J Forensic Sci. 2002;47:640–4. https://doi.org/10.1520/JFS15307J
14. Balakrishnan N, Ericson M, Maggi R, Breitschwerdt EB. Vasculitis, cerebral infarction and persistent *Bartonella henselae* infection in a child. Parasit Vectors. 2016;9:254. https://doi.org/10.1186/s13071-016-1547-9
15. Nakamura C, Inaba Y, Tsukahara K, Mochizuki M, Sawanobori E, Nakazawa Y, et al. A pediatric case with peripheral facial nerve palsy caused by a granulomatous lesion associated with cat scratch disease. Brain Dev. 2018;40:159–62. https://doi.org/10.1016/j.braindev.2017.09.001
16. Landes M, Maor Y, Mercer D, Habot-Wilner Z, Bilavsky E, Chazan B, et al. Cat scratch disease presenting as fever of unknown origin is a unique clinical syndrome. Clin Infect Dis. 2020;71:2818–24. https://doi.org/10.1093/cid/ciz1137

Address for correspondence: Michal Yakubovsky, Department of Infectious Diseases and Infection Control, Tel Aviv Sourasky Medical Center, 6 Weizmann St, Tel Aviv, Israel; email: michalya@tlvmc.gov.il

# etymologia revisited

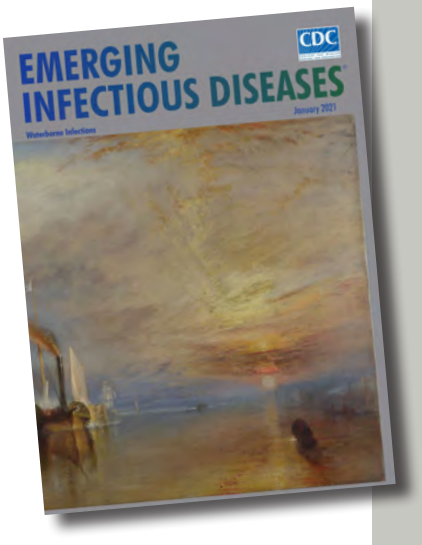


*Originally published in January 2021*

## Petri Dish
[pe'tre 'dish]

The Petri dish is named after the German inventor and bacteriologist Julius Richard Petri (1852–1921). In 1887, as an assistant to fellow German physician and pioneering microbiologist Robert Koch (1843–1910), Petri published a paper titled "A minor modification of the plating technique of Koch." This seemingly modest improvement (a slightly larger glass lid), Petri explained, reduced contamination from airborne germs in comparison with Koch's bell jar.

### References
1 Central Sheet for Bacteriology and Parasite Science [in German]. Biodiversity Heritage Library. Volume 1, 1887 [cited 2020 Aug 25]. https://www.biodiversitylibrary.org/item/210666#page/313/mode/1up
2. Petri JR. A minor modification of the plating technique of Koch [in German]. Cent für Bacteriol und Parasitenkd. 1887;1:279–80.
3. Shama G. The "Petri" dish: a case of simultaneous invention in bacteriology. Endeavour. 2019;43:11–6. DOIExternal
4. The big story: the Petri dish. The Biomedical Scientist. Institute of Biomedical Science [cited 2020 Aug 25]. https://thebiomedicalscientist.net/science/big-story-petri-dish

*https://wwwnc.cdc.gov/eid/article/27/1/et-2701_article*

# Cluster of Human Tanapox Cases in Wildlife Reserve, South Africa, 2024

Monica Birkhead, Antoinette A. Grobbelaar, Daniel Morobadi, Hlupi D. Mpangani, Julia Dabrowski, Kamini Govender, Lucille H. Blumberg, Mandla Zwane, Naazneen Moolla, Naume D. Tebeila, Nevashan Govender, Terry Marshall, Veerle Dermaux-Msimang, Wayne Grayson, Jacqueline Weyer

Tanapox is a rare, self-limiting, mosquitoborne viral zoonosis. During February–March 2024, we identified 11 human tanapox cases near Orpen in Kruger National Park, South Africa. We retrospectively identified 2 suspected cases from Pafuri from 2021, suggesting continued virus circulation. Public awareness of tanapox is essential for appropriate medical treatment.

Tanapox virus (TANV), a member of the genus *Yatapoxvirus* (Poxviridae), is associated with a rare zoonotic infection; only 1 human tanapox case has been reported globally since 2004 (*1*–*3*). That case originated in Skukuza, a subtropical area of Kruger National Park (KNP), a wildlife reserve in South Africa. That geographic location differed from all previously recorded tanapox cases from endemic countries in equatorial Africa, including Democratic Republic of the Congo, Kenya, Republic of Congo, and Sierra Leone, and from Tanzania in tropical east Africa (*4*–*9*). Skukuza is also south of the possible TANV distribution predicted by ecologic niche modeling (*9*).

Although geographic origins differ, the environmental and clinical features of all reported human tanapox cases are comparable. TANV is thought to be transmitted mechanically from wildlife hosts (nonhuman primates) to humans by hematophagous culicine mosquitoes (*4*–*10*). All previously reported cases originated from locations where human–wildlife interfaces were closely juxtaposed, after heavy rainfall and high temperatures that preceded the mosquito breeding season (*3*–*5*,*9*).

Generally, TANV infection presents as 1–3 nodules in exposed body areas where mosquitoes typically tend to bite, such as hands, elbows, lower limbs, and toes (*5*). Although the centrally umbilicated lesions are self-limiting, resolving without intervention over 6–8 weeks, TANV infection can cause symptoms consistent with a viraemia, including fever, fatigue, intense headaches, myalgia, lymphadenopathy, and viral exanthem. The lesions can be unsightly, painful, and pruritic and infrequently become secondarily infected after scratching (*2*,*4*,*5*,*8*). As yet, no human-to-human TANV transmission or infection from contact or fomites has been recorded, and no deaths or systemic infection have been reported (*2*,*5*,*11*). Given the self-limiting nature and mildness of the infection, underreporting by workers in wildlife areas is highly probable, but for persons who do seek medical assistance, a lack of familiarity with the disease could lead to misdiagnosis and inappropriate treatment. We describe a cluster of tanapox cases from in and around KNP, South Africa, a novel, subtropical location for TANV transmission.

## The Study

In February 2024, a patient (case 1) with several skin lesions sought care from a general practitioner in Hoedspruit, a small town ≈68 km west of KNP. The patient resided in KNP staff lodging near Orpen (Figure 1). On the advice of an infectious diseases expert familiar

Author affiliations: National Institute for Communicable Diseases, Johannesburg, South Africa (M. Birkhead, A.A. Grobbelaar, K. Govender, L.H. Blumberg, N. Moolla, N.D. Tebeila, N. Govender, V. Dermaux-Msimang, J. Weyer); Ampath Laboratories Ltd., Centurion, South Africa (D. Morobadi, T. Marshall, W. Grayson); Mpumalanga Department of Health, Mbombela, South Africa (H.D. Mpangani, M. Zwane); Hoedspruit Family Practice, Hoedspruit, South Africa (J. Dabrowski); Right to Care, Johannesburg (L.H. Blumberg); University of Stellenbosch, Stellenbosch, South Africa (L.H. Blumberg); University of Pretoria, Pretoria, South Africa (L.H. Blumberg, N. Moolla, J. Weyer); University of the Witwatersrand, Johannesburg (N. Moolla, W. Grayson, J. Weyer)

DOI: https://doi.org/10.3201/eid3207.251961

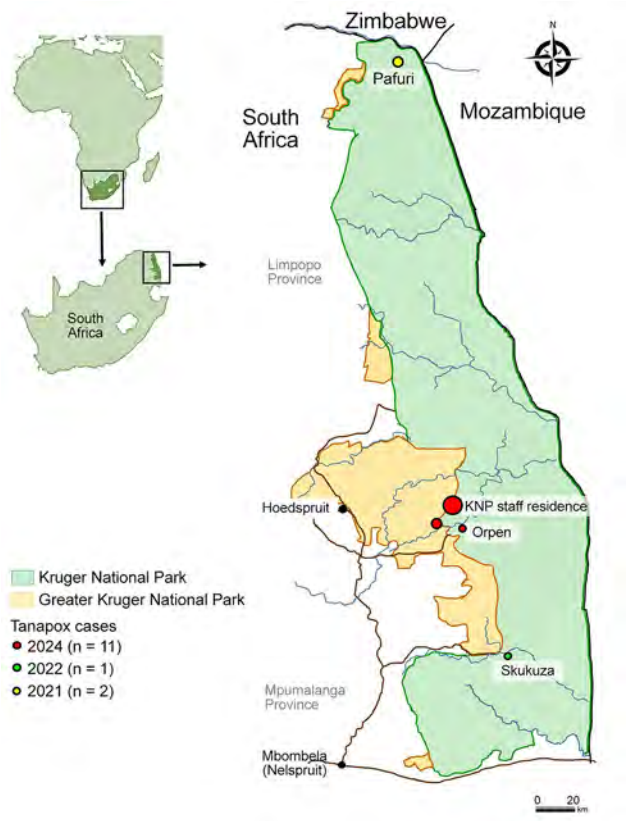


**Figure 1.** Locations of cases in a cluster of human tanapox cases in wildlife reserve, South Africa, 2024. Of 11 cases in 2024, nine were laboratory confirmed by PCR and sequencing, and 2 were suspected on the basis of clinical symptoms and epidemiologic links. In addition, one case was laboratory-confirmed in 2022. We also retrospectively identified 2 suspected cases from 2021 on the basis of lesion features, clinical symptoms, and suitable environmental parameters. Insets show location of KNP within South Africa and the continent. KNP, Kruger National Park.

with poxvirus infections, a lesion swab sample was sent to the Special Viral Pathogens Laboratory, Centre for Emerging Zoonotic and Parasitic Diseases, National Institute for Communicable Diseases (NICD), Johannesburg, South Africa, for poxvirus testing.

Using previously described methods (*3*), we performed molecular testing to identify the genus of poxvirus involved. We confirmed *Yatapoxvirus* TANV by sequencing, which we corroborated by transmission electron microscopy of a subsequent lesion biopsy (Table; Appendix Figure 1, https://wwwnc.cdc.gov/EID/article/32/7/25-1961-App1.pdf).

Two other persons (cases 2 and 3), household members of case-patient 1, also had pox-like nodules (Table). Consequently, we developed and distributed a questionnaire through established, community communication networks that link KNP and Greater KNP, a collection of private and community-owned wildlife reserves adjacent to the western boundary of KNP. We received 10 additional lesion swab samples (cases 2–11) for molecular confirmatory testing, among which 8 (cases 2–9) were accompanied by a completed questionnaire (Table). Of those 10 lesion swab samples, 8 were TANV-positive, and we submitted a representative example of the sequences to GenBank (accession no. PV816105). Two specimens, from cases 4 and 10, failed PCR amplification because the swabs were likely collected after the lesions had sufficiently healed and consequently no longer contained viral DNA. However, we included those 2 as suspected cases on the basis of epidemiologic and clinical features common to all 11 cases in the cluster.

All TANV cases occurred within 20 km of each other (Figure 1). Most case-patients were male (7 game rangers, 1 adult visitor, and 1 resident child); 2 were female (both KNP residents). Lesions and symptoms were consistent with those described in cases originating from equatorial Africa during 1957–2004 (*4*–*8*). Typically, case-patients had 1–3 umbilicated lesions coinciding with common sites for mosquito bites (Table). Case-patients noted that nodules initially were itchy; some mentioned that they thought

**Table.** Epidemiologic data of patients in a cluster of human tanapox cases in wildlife reserve, South Africa, 2024

| Case no. | Age, y/sex | Location | Symptom onset date | No. lesions | Body part affected | Laboratory-confirmed* |
|---|---|---|---|---|---|---|
| 1 | 12/M | KNP staff residence | Feb 8 | 8 | Elbow, hand, finger | Y |
| 2 | 33/F | KNP staff residence | Feb 8 | 1 | Shin | Y |
| 3 | 43/F | KNP staff residence | Feb 19 | 1 | Knee | Y |
| 4 | 41/M | KNP staff residence | Early Feb | 2 | Fingers | N |
| 5 | 38/M | KNP staff residence | Feb 10 | 1 | Back of knee | Y |
| 6 | 34/M | KNP staff residence | Feb 19 | 1 | Big toe | Y |
| 7 | 58/M | KNP staff residence | Feb 27 | 1 | Knee | Y |
| 8† | 47/M | Open camp, KNP | Mar 3 | 3 | Elbow, hand | Y |
| 9 | 33/M | KNP staff residence | Mar 13 | 1 | Hand | Y |
| 10‡ | >30/M | Private camp, greater KNP | Unknown | Unknown | Unknown | N |
| 11‡ | >30/M | Private camp, greater KNP | Unknown | Unknown | Unknown | Y |

*Confirmed by PCR and sequencing of dry swab sample of lesion, following previously described methods (*3*). KNP, Kruger National Park.
†Lesion swab sample accompanied by skin punch biopsy for electron microscopy.
‡No complete questionnaire submitted with lesion swab sample.

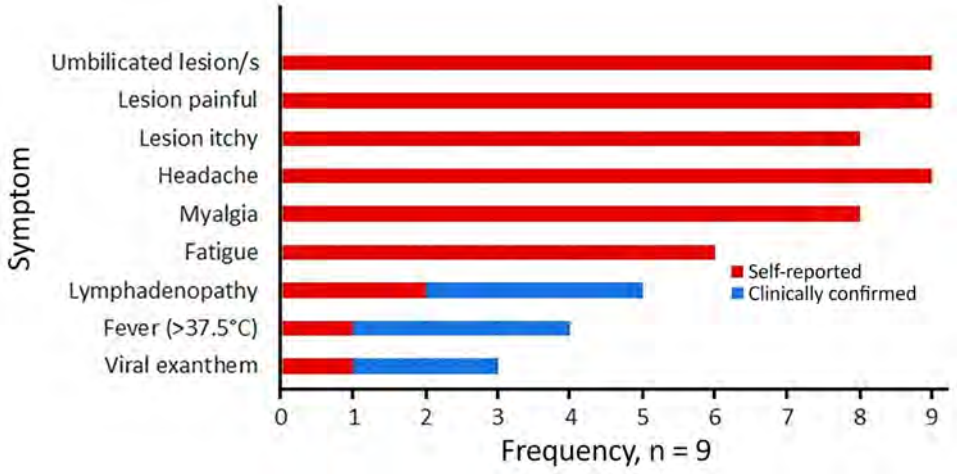


**Figure 2.** Clinical data from a cluster of human tanapox cases in wildlife reserve, South Africa, 2024. Data represent 9 laboratory-confirmed cases of 11 persons for whom lesion samples were submitted.

nodules were just mosquito or insect bites, but most case-patients said nodules later became painful (Figure 2). Case-patients reported other symptoms of TANV infection, most consistently headaches, myalgia, and fatigue (Figure 2). Among 3 case-patients who reported a maculopapular viral exanthem, 2 described a generalized distribution over the torso.

An initial misdiagnosis of impetigo in some patients prompted topical antibiotic treatment, and 1 person was treated with intravenous antibiotic drugs for a suspected superinfection associated with lymphadenitis. Lesion development described in questionnaires by 2 persons detailed the progression from an itchy bite to a firm, circular nodule with an erythematous base (Appendix Figure 2). The centrally umbilicated nodules, some of which enlarged to 20 mm diameter, remained firm and noncystic. Other nodules ulcerated at a diameter of ≤15 mm, forming craters with raised edges around a necrotic central area. Subsequent crusting and reepithelialization began around the circumference, and concurrent tissue granulation developed in the center. About 25 days after symptom onset, the central tissue dried to form a scab, which darkened and sloughed off ≈3 weeks later. The initial erythematous areola surrounding each lesion persisted for the duration of lesion development, with varying degrees of associated edema and inflammation. Extensive inflammation, for example affecting an entire forearm (Appendix Figure 2), was more likely to be associated with local lymphadenopathy.

NICD compiled tanapox information for online public dissemination (*12*). NICD also alerted regional stakeholders, including the provincial health department, private practitioners, managers of wildlife reserves, and training facilities in the area, and asked them to further distribute tanapox information.

Serendipitous feedback included the possibility of 2 tanapox cases acquired by visitors to the Pafuri area of KNP in February 2021 (Figure 1). On telephonic follow-up, we suspected clinical diagnoses of tanapox in the 2 adult male visitors on the basis of a suitable environment (omnipresent nonhuman primates and a perceived abundance of mosquito vectors after high rainfall recorded in previous weeks), lesion attributes (photographic evidence of number, placement, and appearance), as well as other recalled symptoms, including headaches, myalgia, and extreme fatigue. Both men sought medical assistance; 1 had his lesion excised, and the other was placed on intravenous antibiotic drugs because of apparent purulence of 1 of the lesions, possibly associated with a diabetically compromised immune system.

## Conclusions

This cluster of cases strongly suggests autochthonous TANV transmission is occurring in the KNP area. Therefore, residents, workers, and visitors to KNP and surrounding areas need to be aware of the possibility of tanapox during February and March, after peak summer rainfall. Because no evidence supports the assumption that inflammation associated with tanapox nodules is caused by a bacterial superinfection, clinicians should be aware of tanapox symptoms and pathogenesis and avoid antibiotic use. Instead, clinicians can provide more applicable patient management by reducing anxiety, unnecessary medical procedures, and expense. As with any mosquito-transmitted virus, persons at risk for mosquito exposure should follow recommendations for using mosquito repellents and bed nets, especially considering that no antiviral drugs or vaccines for TANV are available.

### Acknowledgments

We thank Danny Govender, Danie Pienaar, and Greg Bond for assisting in the collection of swabs, questionnaires, and epidemiological data. Theresa Sowry was pivotal in distributing and communicating tanapox knowledge and resources in the greater KNP area.

Ethics clearance (approval no. M210752) was obtained from the Faculty of Health Sciences, University of the Witwatersrand, Johannesburg, South Africa. Written photo consent was obtained from patients for the reproduction of lesion photographs.

Author contributions: J.W. and M.B. conceptualized the study; D.M., J.D., L.H.B., T.M., and W.G. conducted data and specimen collection; A.A.G., K.G., N.M., and J.W. performed laboratory testing; M.B. performed microscopy; J.D. and L.H.B. conducted case finding; H.D.M., J.W., L.H.B., N.G., N.T., M.Z., and V.D.-M. conducted outbreak investigation; J.W., M.B., N.T., and V.D.-M. obtained resources; J.W. and M.B. prepared original manuscript draft; A.A.G., D.M., H.D.M., J.B., J.W., K.G., L.H.B., N.G., N.M., N.T., M.Z., T.M., V.D.-M., and W.G. reviewed and edited the manuscript. All authors read and provided written consent to publish the current version of the manuscript.

### About the Author

Dr. Birkhead is an electron microscopist in the Centre for Emerging Zoonotic and Parasitic Diseases, National Institute for Communicable Diseases, South Africa. Her research interests are biological ultrastructure, particularly that of pathogens, and ultrastructural diagnosis of primary ciliary dyskinesia.

### References

1. McInnes CJ, Damon IK, Smith GL, McFadden G, Isaacs SN, Roper RL, et al. ICTV virus taxonomy profile: *Poxviridae* 2023. J Gen Virol. 2023;104:001849. https://doi.org/10.1099/jgv.0.001849
2. Obermeier PE, Buder SC, Hillen U. Poxvirus infections in dermatology—the neglected, the notable, and the notorious. J Dtsch Dermatol Ges. 2024;22:56–93. https://doi.org/10.1111/ddg.15257
3. Birkhead M, Grayson W, Grobbelaar A, Msimang V, Moolla N, Mathee A, et al. Tanapox, South Africa, 2022. Emerg Infect Dis. 2023;29:1206–9. https://doi.org/10.3201/eid2906.230326
4. Downie AW, Taylor-Robinson CH, Caunt AE, Nelson GS, Manson-Bahr PEC, Matthews TCH. Tanapox: a new disease caused by a pox virus. BMJ. 1971;1:363–8. https://doi.org/10.1136/bmj.1.5745.363
5. Jezek Z, Arita I, Szczeniowski M, Paluku KM, Kalisa R, Nakano JH. Human tanapox in Zaire: clinical and epidemiological observations on cases confirmed by laboratory studies. Bull. World Health Organ. 1985;63:1027–35.
6. Stich A, Meyer H, Köhler B, Fleischer K. Tanapox: first report in a European traveller and identification by PCR. Trans R Soc Trop Med Hyg. 2002;96:178–9. https://doi.org/10.1016/S0035-9203(02)90295-6
7. Croitoru AG, Birge MB, Rudikoff D, Tan MH, Phelps RG. Tanapox virus infection. Skinmed. 2002;1:156–7. https://doi.org/10.1111/j.1540-9740.2002.01778.x
8. Dhar AD, Werchniak AE, Li Y, Brennick JB, Goldsmith CS, Kline R, et al. Tanapox infection in a college student. N Engl J Med. 2004;350:361–6. https://doi.org/10.1056/NEJMoa031467
9. Monroe BP, Nakazawa YJ, Reynolds MG, Carroll DS. Estimating the geographic distribution of human tanapox and potential reservoirs using ecological niche modeling. Int J Health Geogr. 2014;13:34. https://doi.org/10.1186/1476-072X-13-34
10. Downie AW. Serological evidence of infection with Tana and Yaba pox viruses among several species of monkey. J Hyg (Lond). 1974;72:245–50. https://doi.org/10.1017/S0022172400023445
11. Suryawanshi YR, Zhang T, Razi F, Essani K. Tanapoxvirus: from discovery towards oncolytic immunovirotherapy. J Cancer Res Ther. 2020;16:708–12. https://doi.org/10.4103/jcrt.JCRT_157_18
12. National Institute for Communicable Diseases. Diseases A–Z index: tanapox [cited 2026 Mar 12]. https://www.nicd.ac.za/diseases-a-z-index/tanapox

Address for correspondence: Monica Birkhead, National Institute for Communicable Diseases, Private Bag X4, Sandringham, Johannesburg 2192, South Africa; email: monicab@nicd.ac.za

# Vascularized Iris Mass as Sentinel Manifestation of Syphilis in Patient with HIV Infection, Spain, 2025

Marta Caminal-Caramés, Jaume Sánchez-Serra, Jesus Díaz-Cascajosa, Albert Saladrigas, Santiago Conversa, Jose Ignacio Vela-Segarra

Vascularized iris masses are rare, yet highly suggestive of syphilis. We report a 51-year-old man in Spain with HIV infection who had painful vision loss, rash, and an iris mass. Laboratory testing confirmed syphilis; ocular manifestations resolved with intravenous ceftriaxone and penicillin. Early recognition of syphilis can prevent vision loss and neurologic complications.

Syphilis has experienced an alarming global resurgence over the past 2 decades, evolving into a major public health concern across developed nations (*1*). Ocular syphilis, known as the great masquerader, can involve any ocular structure and can occur at any stage of the disease; ocular syphilis frequently serves as the sentinel manifestation of an undiagnosed HIV infection (*2*,*3*). Although uveitis is the most common manifestation of ocular syphilis, vascularized iris masses, spanning a clinical spectrum from iris roseola and papulosa to iris nodosa and gummata, represent an exceptionally rare and poorly characterized phenotype (*4*). Fewer than 15 cases have been reported in English-language literature (*5*–*8*), and paradoxically, despite the synergy between syphilis and HIV infection, iris lesions are even more infrequent in persons with advanced immunosuppression (*9*).

The formation of structured nodules or gummata typically represents an inadequate or failed delayed-type hypersensitivity (DTH) reaction (*8*). Differential diagnosis is challenging because the lesions can mimic other inflammatory, neoplastic, or opportunistic fungal processes in patients with HIV. Multimodal ultrasound biomicroscopy (UBM) imaging and anterior segment optical coherence tomography (AS-OCT) can aid in lesion characterization, defining depth, internal composition, vascularity, and stromal involvement (*5*,*8*). We report a case of iris papulosa as a sentinel sign of syphilis in a patient in Spain with HIV infection.

## The Case

In 2025, a 51-year-old man with a history of HIV, depression, and substance abuse (amphetamines and cocaine) sought care for 3 days of right-eye pain and vision loss. Facial maculopapular rash suggested secondary syphilis (Figure 1, panel A). Best-corrected visual acuity was hand motion in the right eye and 20/20 in the left eye. Intraocular pressures were 8 mm Hg in the right eye and 10 mm Hg in the left eye. Slit-lamp examination of the right eye revealed marked conjunctival hyperemia, a vascularized nonpigmented iris base mass, corneal edema, mutton-fat keratic precipitates, posterior synechiae, and 3+ anterior chamber cells and flare (Figure 1, panel B). Ocular ultrasonography ruled out vitreous inflammation and retinal detachment. UBM revealed a well-defined, homogeneous hyperechoic iris stromal mass with ciliary body involvement and iris pigment epithelium disruption (Figure 2, panel A). AS-OCT demonstrated a homogeneous lesion with irregular hyperreflective anterior surface, internal hyperreflectivity, posterior shadowing, iris pigment epithelium disruption, keratic precipitates, and anterior chamber cells (Figure 2, panel B).

Ocular syphilis was confirmed by rapid plasma regain (titer 1:256) and positive *Treponema pallidum* microparticle enzyme immunoassay. Lumbar puncture was performed, and cerebrospinal fluid tested *T. pallidum*–negative. HIV viral load was 25 copies/mL; CD4+ cell count was 13% (300 cells/μL). HIV history was unavailable because of poor follow-up; the patient reported intermittent, poorly adherent antiretroviral therapy but was taking it during uveitis diagnosis, which explains viral suppression despite

Authors affiliation: Hospital Sant Pau, Barcelona, Spain

DOI: https://doi.org/10.3201/eid3207.260388

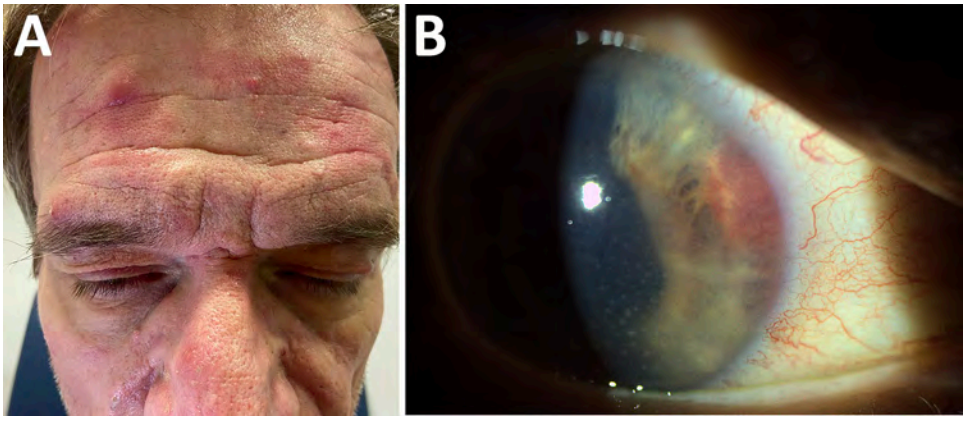


**Figure 1.** Clinical findings of a vascularized iris mass as sentinel manifestation of syphilis in patient with HIV infection, Spain, 2025. A) Maculopapular facial rash consistent with secondary syphilis. B) Slit-lamp photograph demonstrating a nonpigmented, vascularized iris base mass with conjunctival hyperemia, corneal edema, and mutton-fat keratic precipitates.

persistent immunosuppression. No viral loads or CD4 counts were available from the previous year. Serologic tests for tuberculosis, sarcoidosis, hepatitis, and toxoplasmosis were negative.

We administered intravenous ceftriaxone (2 g/d for 5 d) as an initial bridging therapy at home while we arranged logistics for in-home intravenous penicillin G (18 million units/d for 10 d) (*10*). Adjunctive therapy included 1% topical prednisolone acetate (4×/d), 1% cycloplegic agent (atropine; 2×/day, and systemic prednisone initiated at 30 mg/day and tapered over 2 weeks. At 1 month, best-corrected visual acuity recovered to 20/20, and repeat UBM and AS-OCT confirmed complete lesion resolution in the right eye.

Ocular syphilis most commonly occurs during the secondary stage of *T. pallidum* infection (*6*). Among its diverse phenotypes, vascularized iris masses, including iris roseola, papulosa, nodosa, and gummata, are considered exceptional but highly suggestive of treponemal disease (*5*,*6*). Such lesions are thought to result from *T. pallidum* capillary engorgement or focal inflammatory infiltration, representing a spectrum of progressively intensifying inflammatory responses (*6*). Iris roseola, the earliest manifestation in secondary syphilis, consists of dilated capillaries or vascular tufts and can evolve into iris papulosa, single or multiple nodules, and subsequent iris nodosa, reflecting increasing granulomatous stromal infiltration (*5*,*7*,*11*). In contrast, iris gummata typically occur in later stages, presenting as poorly vascularized nodules with central degeneration that represent chronic granulomatous inflammation associated with impaired cellular immune control (*5*,*6*,*8*).

In a comprehensive review of reports published in English, we identified only ≈13 cases of vascularized iris masses documented since 1915 (*5*–*9*) (Appendix Table, https://wwwnc.cdc.gov/EID/article/32/7/26-0388-App1.pdf). One case of a large syphilitic iris granuloma in a patient with HIV infection has been highlighted in recent reviews,

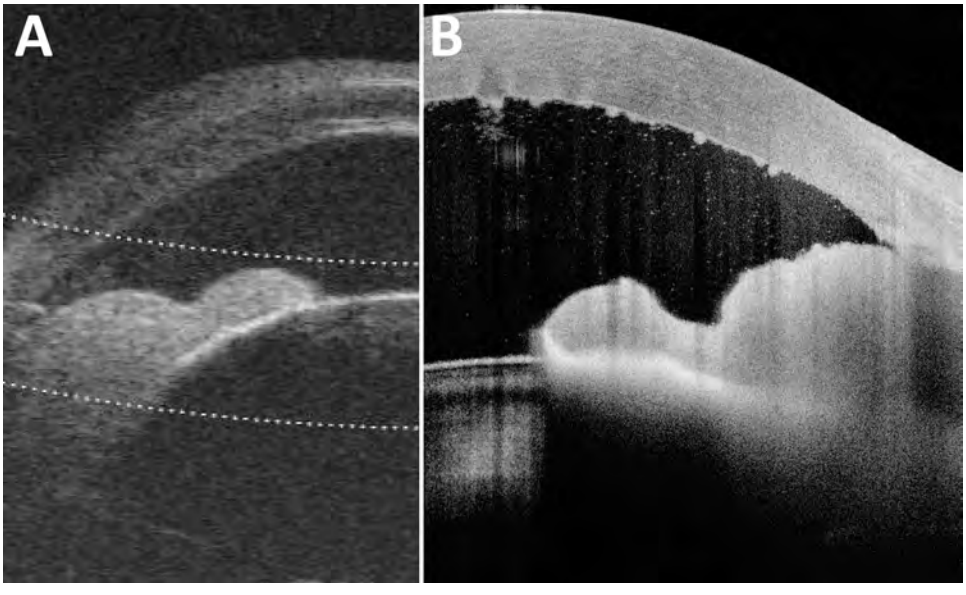


**Figure 2.** Imaging for a vascularized iris mass as sentinel manifestation of syphilis in patient with HIV infection, Spain, 2025. A) Ultrasound biomicroscopy revealing a well-defined hyperechoic iris mass with ciliary body involvement. B) Anterior segment optical coherence tomography showing a homogeneous hyperreflective stromal lesion with keratic precipitates and inflammatory cells in the anterior chamber.

whereas most published cases occurred in patients without HIV or with unreported HIV status (*9*) (Appendix Table).

The co-occurrence of syphilitic iris nodules and HIV infection appears paradoxically rare. Despite the epidemiologic synergy between HIV and syphilis, iris granulomas are reported less often among persons with HIV infection than in immunocompetent hosts (*12*). Gummata represent chronic granulomatous lesions arising from a failure of effective DTH reaction to *T. pallidum*, reflecting impaired cellular immune control (*8*). In HIV infection with CD4+ depletion, the immune system might lack the capacity for such granulomatous responses (*13*). Consequently, syphilis in patients with HIV more frequently manifests as severe, diffuse inflammation or posterior segment involvement, rather than discrete iris nodules (*12*,*13*). The pronounced granulomatous iris mass in this patient, despite CD4+ of 300 cells/μL, suggests residual capacity for granuloma formation despite DTH impairment, possibly due to partial immune reconstitution or localized immune responses.

In patients with HIV, a solitary vascularized iris mass substantially broadens the differential diagnosis. Syphilitic nodules must be distinguished from neoplastic entities, other infections, or inflammatory causes (*8*,*14*). Among neoplastic causes, iris nevus typically presents as a flat or minimally elevated, well-circumscribed pigmented lesion with slow growth and is usually asymptomatic, whereas iris melanoma tends to be more elevated and might exhibit intrinsic vascularity, corectopia, uveal ectropion, and progressive enlargement. Iris metastases are typically amelanotic and often identified in patients with a known primary tumor (*15*). Intraocular lymphoma, although less common, can appear as diffuse iris infiltration, often accompanied by chronic inflammation. Infectious causes of iris granulomas include ocular tuberculosis in the setting of chronic granulomatous uveitis, often with systemic involvement (*5*,*15*).

Anterior segment imaging can support diagnostic evaluation by helping define lesion depth and internal characteristics, thereby contributing to the differential diagnosis among inflammatory, neoplastic, and alternative infectious causes. However, the diagnosis of ocular syphilis remains primarily clinical and serologic, and imaging findings can further aid in lesion characterization and monitoring treatment response (*5*,*6*).

## Conclusions

Vascularized iris masses represent an exceptionally rare manifestation of ocular syphilis; only ≈13 cases have been reported in the literature, and just 1 previous case was described in a patient with HIV coinfection. Our case demonstrates that, even in HIV infection, syphilis manifestations can present as a localized anterior segment mass rather than diffuse ocular inflammation. Internists and infectious disease physicians should be aware that an unexplained iris mass, particularly in patients at risk for sexually transmitted infections, could represent syphilis. Prompt serologic testing and appropriate parenteral therapy are essential to preventing irreversible visual and neurologic complications.

The authors certify that they obtained all appropriate patient consent forms. In the form, the patient gave consent for his images and other clinical information to be reported in the journal, signing a written informed consent. All procedures were performed in accordance with the principles expressed in the Declaration of Helsinki.

## About the Author

Dr. Caminal-Caramés is an ophthalmologist at Hospital Sant Pau, Barcelona, Spain. Her research interests include retina, uveitis and ocular inflammation diseases, retinal dystrophies, and pediatric retina disorders.

## References

1. Zhou LR, Kirupaharan N, Berkenstock MK. Incidence and prevalence of syphilitic uveitis and associated ocular complications in the TriNetX database. Am J Ophthalmol. 2025;277:387–94. https://doi.org/10.1016/j.ajo.2025.05.048
2. Lee SY, Cheng V, Rodger D, Rao N. Clinical and laboratory characteristics of ocular syphilis: a new face in the era of HIV co-infection. J Ophthalmic Inflamm Infect. 2015;5:56. https://doi.org/10.1186/s12348-015-0056-x
3. Amaratunge BC, Camuglia JE, Hall AJ. Syphilitic uveitis: a review of clinical manifestations and treatment outcomes of syphilitic uveitis in human immunodeficiency virus-positive and negative patients. Clin Exp Ophthalmol. 2010;38:68–74. https://doi.org/10.1111/j.1442-9071.2010.02203.x
4. Schulz DC, Orr SMA, Johnstone R, Devlin MK, Sheidow TG, Bursztyn LLCD. The many faces of ocular syphilis: case-based update on recognition, diagnosis, and treatment. Can J Ophthalmol. 2021;56:283–93. https://doi.org/10.1016/j.jcjo.2021.01.006
5. Rosenberg CR, Pasadhika S. A vascularized iris mass in ocular syphilis: a case report and review of literature. Ocul Immunol Inflamm. 2024;32:1648–54. https://doi.org/10.1080/09273948.2023.2276298
6. Chen JL, Tessema R, Emami-Naeini P, Lim MC. A vascular syphilitic iris lesion. Am J Ophthalmol Case Rep. 2023;31:101858. https://doi.org/10.1016/j.ajoc.2023.101858
7. de Jong Y, Haverkort ME, van Sorge AJ, Jansen C, Luyten GP, Joosse M. A translucent vascularised iris granuloma in a patient with secondary syphilis. Lancet Infect Dis. 2017;17:255–6. https://doi.org/10.1016/S1473-3099(17)30071-3

8. Michaelov E, Iqbal MM, Hooper PL. Uveal mass, uveitis, and diffuse rash in a woman in her 50s. JAMA Ophthalmol. 2018;136:704–5. https://doi.org/10.1001/jamaophthalmol.2017.5560
9. Yang P, Zhang NI, Li F, Chen Y, Kijlstra A. Ocular manifestations of syphilitic uveitis in Chinese patients. Retina. 2012;32:1906–14. https://doi.org/10.1097/IAE.0b013e3182509796
10. Workowski KA, Bachmann LH, Chan PA, Johnston CM, Muzny CA, Park I, et al. Sexually transmitted infections treatment guidelines, 2021. MMWR Recomm Rep. 2021;70:1–187. https://doi.org/10.15585/mmwr.rr7004a1
11. Bociąga-Kożuch M, Raczyńska A, Trela D, Garlicki A, Berus T. Diagnostic riddle—case report of ocular syphilis. J Ophthalmic Inflamm Infect. 2025;15:33. https://doi.org/10.1186/s12348-025-00488-4
12. Balba GP, Kumar PN, James AN, Malani A, Palestine AG, Welch JN, et al. Ocular syphilis in HIV-positive patients receiving highly active antiretroviral therapy. Am J Med. 2006;119:448.e21–5. https://doi.org/10.1016/j.amjmed.2005.11.016
13. Carlson JA, Dabiri G, Cribier B, Sell S. The immunopathobiology of syphilis: the manifestations and course of syphilis are determined by the level of delayed-type hypersensitivity. Am J Dermatopathol. 2011;33:433–60. https://doi.org/10.1097/DAD.0b013e3181e8b587
14. Tasnim S, Dave D, Tawfeeq Y, Naguib T, Rasheed W. A case of ocular neurosyphilis in a patient with HIV. Southwest Respir Crit Care Chron. 2021;9:44–6. https://doi.org/10.12746/swrccc.v9i41.931
15. Moshirfar M, Rageh A, Ronquillo Y. Benign and malignant iris tumors. In: StatPearls. Treasure Island (FL): StatPearls Publishing; 2024.

Address for correspondence: Marta Caminal-Caramés, Ophthalmology Department, Hospital Sant Pau, C/Sant Quintí 89, Barcelona 08025, Spain; email: martacaminalcarames@gmail.com

# Nipah Virus Shedding in Urine from Fruit Bats, Sri Lanka, 2018–2019

Claudia Kohl,[1] Sahan Siriwardana,[1] Therese Muzeniek, Thejanee Perera, Dilara Bas, Mizgin Öruc, Annika Brinkmann, Beate Becker-Ziaja, Franziska Schwarz, Hamsananthy Jeevatharan, Jagathpriya Weerasena, Shiroma Handunnetti, Inoka C. Perera, Gayani Premawansa, Sunil Premawansa, Wipula Yapa, Andreas Nitsche

Nipah virus causes outbreaks in humans with high case-fatality rates. In this study, we confirmed the presence of Nipah virus in Sri Lanka in *Pteropus medius* fruit bats, one of the known natural reservoir species. Sequences we generated were genetically related to Nipah virus strains from outbreaks in southern India.

Nipah virus (NiV; *Henipavirus nipahense*) and Hendra virus (*H. hendraense*) are species within the genus *Henipavirus* of the family Paramyxoviridae (*1*). Several paramyxoviruses, including measles virus and respiratory syncytial virus, cause serious respiratory illnesses and are often highly transmissible through the air. NiV can cause severe outbreaks in humans; its clinical symptoms range from subclinical infection to severe encephalitis, respiratory diseases, and death (*2*). Reported case-fatality rate (CFR) of NiV encephalitis is 61% (95% CI 45.7%–75.4%) (*2*,*3*).

NiV emerged in 1998 in Malaysia and Singapore (*4*). Subsequent outbreaks were reported from Bangladesh, the Philippines, and India; they resulted in >643 laboratory-confirmed infections and 380 deaths (*2*). Bats (flying foxes, *Pteropus* spp.) are the known reservoir hosts of NiV (*5*). Transmission from bat to human occurs via exposure to urine, either through consumption of raw palm sap contaminated with bat excreta, direct contact with infected intermediate hosts (e.g., swine), or direct contact with bat urine (*5*). In 2023 several cases of Nipah virus were reported from Kozhikode, Kerala district, India, and in Dhaka, Rajbari, and Shariatpur districts in Bangladesh (*6*). The shortest distance between Mannar Island, Sri Lanka, and Natarajapuram, India, is <55 km; *Pteropus* spp. bats are reported to migrate >450 km with ease (*7*). In this study, we monitored urine excreted by several colonies of *P. medius* bats in Sri Lanka for the presence of viruses using molecular techniques. Our focus was to investigate if NiV is present in Sri Lanka and to determine the measures required to prevent spillover into humans. We obtained ethics approval for this study from the Institute of Biology, Sri Lanka (WL/3/2/05/18) and necessary clearance from the Department of Wildlife Conservation, Sri Lanka.

## The Study

During March 2018–June 2019, we monitored *P. medius* bat colonies for shedding of pathogens in Colombo, Mannar, Anuradhapura, and Badulla, Sri Lanka. We laid clean sampling sheets below roosting trees in the early morning and transferred excreted urine drop by drop to sterile microtiter plates in the morning using disposable pipettes. We conducted all work while wearing appropriate personal protective equipment (PPE) as previously described (*5*).

We collected a total of 2,218 urine samples and combined them into 32 pools with ≤8 urine specimens each. We extracted RNA from the individual pools using the QIAamp Viral RNA Mini Kit (QIAGEN, https://www.qiagen.com). We performed Nipah virus screening using real-time PCR targeting the phosphoprotein (P) gene, as previously described (*8*). As an additional confirmation, we developed a real-time PCR targeting the nucleocapsid protein of the Nipah virus genome (Table 1).

We used Illumina HiSeq (https://www.illumina.com) to sequence the NiV positive pools S3_P02 and S18_P08 (2 of 32 pools). We trimmed using Trimmomatic (*9*) and mapped to NiV strain MCL-18-H-1088

Author affiliations: Robert Koch Institute, Berlin, Germany (C. Kohl, T. Muzeniek, T. Perera, D. Bas, M. Öruc, A. Brinkmann, B. Becker-Ziaja. F. Schwarz, A. Nitsche); University of Colombo, Columbo, Sri Lanka (S. Siriwardana, T. Perera, J. Weerasena, S. Handunetti, I.C. Perera, S. Premawansa, W. Yapa); Ministry of Health, Colombo (H. Jeevatharan); Colombo North Teaching Hospital, Ragama, Sri Lanka (G. Premawansa)

DOI: https://doi.org/10.3201/eid3207.251567

[1]These first authors contributed equally to this article.

**Table 1.** Primers and cycling conditions for quantitative PCR assay developed for study of NiV shedding in urine from fruit bats, Sri Lanka, 2018–2019

| Component | Conditions |
|---|---|
| Primers | |
| NiV_F | AAA TCA AGT TGC AGA ACT CGC T |
| NiV_R | CTC CRA TGA GCA CAC CTC CTG |
| NiV Probe | FAM-CTT CCT GCT GAT GTT TC- MGB |
| Protocol† | AgPath-ID One-Step RT-PCR Kit,‡ 6 µL $H_20$, 12.5 µL RT buffer, 1 µL NiV_F (10 µM), 1 µL NiV_R (10 µM), 0.5 µL NiVN_probe (10 µM), 1.0 µL enzyme mix (25×) |
| Cycling conditions | 45°C for 900 s, 95°C for 600 s, 95°C for 15 s for 45 cycles, 60°C for 45 s |
| Cycler types | Light Cycler 480,§ ABI 7500,‡ Bio-Rad CFX 96¶ |

*F, forward primer; FAM, fluorescein amidites; MGB, minor groove binder; NiV, Nipah virus; R, reverse primer.
†The primers listed are all included in the mix.
‡Applied Biosystems, https://www.thermofisher.com.
§Roche Life Science, https://lifescience.roche.com.
¶Bio-Rad Laboratories, https://www.bio-rad.com.

(accession no. MHK523642; Kerala, India) as a reference strain. In addition, we developed an AmpliSeq primer panel, NiVliSeq, spanning the whole NiV genome using Primer3 version 2.3.7 (Figure 1; Appendix Table, https://wwwnc.cdc.gov/EID/article/32/7/25-1567-App1.xlsx). We sequenced corresponding PCR products on the MinIon platform as described previously (*10,11*). We submitted draft genomes to GenBank (accession nos. PP893186–9) and aligned them with NiV strains and type species of paramyxovirus genomes indicated by the International Committee on Taxonomy of Viruses and available in GenBank. We calculated phylogenetic molecular clock reconstruction with MrBayes version 0.39 software (https://nbisweden.github.io/MrBayes) using Markov chain Monte Carlo approach of molecular clock reconstruction based on the general time reversible model with the parameters set at 1 million replicates, 4 chains, and burn in at 10% (partial large sequence 7,977 nt; coding for the RNA-dependent RNA polymerase gene, of the subfamily Orthoparamyxovirinae).

We collected pool S3_P02 and pool S18_P08 in Colombo; both tested positive for NiV using the henipavirus quantitative PCR (qPCR) targeting the P gene (*8*). The NiV qPCR (targeting the nucleocapsid gene) further confirmed NiV in the same sample pools (Table 2). Sequencing revealed corresponding NiV reads in the 2 sample pools that we mapped over the entire NiV genome (Table 2), providing additional confirmation. The NiVliSeq approach revealed 93% of the NiV genome from pool S3_P02 and 98% of NiV genome for pool S18-08, (Table 2). Comparison of the NiV genomes with the GenBank database revealed the highest identity to a strain collected from a human patient during the 2018 outbreak in Kerala, India (accession no. MH396625); the genomes from pool S3_P02 and pool S18-08 each had 98% nucleotide identity to the Kerala strain. We named the Sri Lanka NiV strains in accordance with the system used for the India strains: NiV strain C-18-B-0302 Sri Lanka (accession

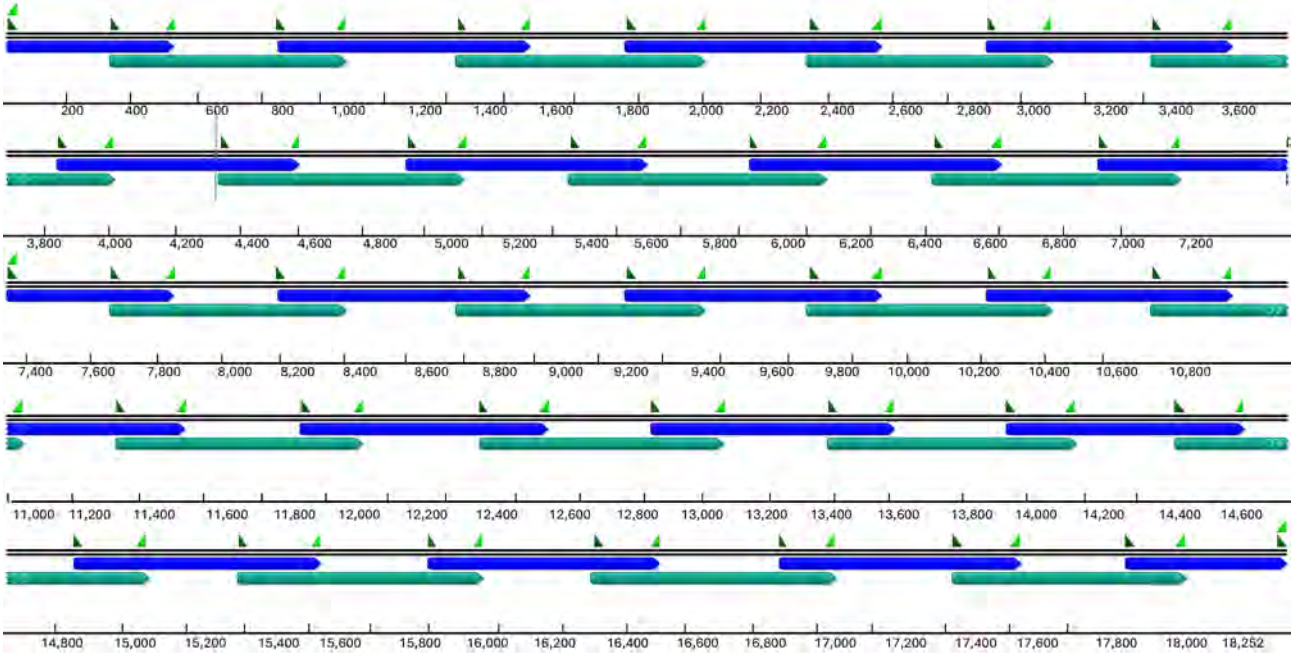


**Figure 1.** Positions of primers used for NiVliSeq amplification panel in study of Nipah virus shedding in urine from fruit bats, Sri Lanka, 2018–2019. Blue and green represent 2 nonoverlapping primer pools to which the primers were added.

**Table 2.** Sequencing results for NiV-positive bat urine samples in study of NiV shedding in urine from fruit bats, Sri Lanka, 2018–2019*

| Characteristic | Bat urine pools tested positive for NiV | |
|---|---|---|
| | S03-P2 | S18-08 |
| Origin | *Pteropus medius*, Colombo | *P. medius*, Colombo |
| Sampling date | June 2018 | March 2019 |
| PCR | | |
| Henipa PCR | | |
| Ct value | 33 | 35 |
| Mean duplicates | 8 | 6 |
| NiV in-house | | |
| Ct value | 32 | 37 |
| Mean duplicates | 3 | 7 |
| Illumina sequencing, shotgun† | | |
| Trimmed reads | 5,094,516 | 5,633,085 |
| NiV reads | 128 | 20 |
| Longest contig | 481 nt (accession no. PP893187.1) | 255 nt (accession no. PP893189.1) |
| Highest % ID nt | 98.96% MCL-18-H-1088 (accession no. MHK523642)‡ | 99.61% (accession no. MN549404.1)§ |
| NiVliSeq, amplicon-based approach¶ | | |
| Genome length and coverage | 93% query, 189-fold average (>10-fold) | 98% query, 8,783-fold average (>10-fold) |
| Highest % ID nt | 98.34%‡ | 98.43%‡ |
| Novel strain | Nipah virus strain C-18-B-0302 Sri Lanka (accession no. PP893186.1) | Nipah virus strain C-19-B-1808 Sri Lanka (accession no. PP893188.1) |

*Ct, cycle threshold; NiV, Nipah virus; % ID, percentage identity of nucleotide and amino acid sequence between pool and reference strain.
†Illumina, https://www.illumina.com.
‡Reference strain MH396625 (GenBank accession no.) from a human patient during the 2018 outbreak in Kerala, India.
§Reference strain from a bat in India.
¶ AmpliSeq primer panel spanning the whole NiV genome using Primer3 version 2.3.7 (Figure 1; Appendix Table, https://wwwnc.cdc.gov/EID/article/32/57/25-1567-App1.xlsx).

no. PP893186.1) and NiV strain C-19-B-1808 Sri Lanka (accession no. PP893188.1). In that nomenclature, C denotes Colombo, 18 and 19 indicate the years 2018 and 2019, B denotes bat, and the remaining numbers represent the sample number.

Phylogenetic analysis allocated the novel Nipah virus strains C-18-B-0302 Sri Lanka and C-19-B-1808 Sri Lanka to the species Nipah virus (*H. nipahense*) within the genus *Henipavirus* (Figure 2). Both are clustering monophyletically with the strains sampled from humans during the outbreaks in Kerala region, India in 2007, 2018, 2019, 2021, and 2023.

## Conclusions

This study demonstrated the presence of NiV strains in Sri Lanka. The qPCR and NiVliSeq sequencing approach we developed validated previously obtained results and represented valuable tools that can be used in further studies. The identified strains have highest similarities to human-pathogenic strains causing recent outbreaks in India (2007, 2018, 2019, and 2023). However, NiV is still a rare disease, and transmission rates are comparably low. Furthermore, the detection of a certain virus in a bat population does not necessarily mean that transmission occurs; diverse strains of henipaviruses can be found in *Pteropus* spp. bats across the whole distribution range.

The initial prevention of any infection should be one of the major goals and could include protection of the bats and their roosts. Bat colonies are vital for healthy ecosystems and should be protected for several reasons, including the ecosystem services they provide such as pollination and seed dispersal. Moreover, *Pteropus* spp. bats are threatened by extinction (*12*). The World Health Organization (WHO) has recognized the need for research and diagnosis of NiV within the distribution range of *Pteropus* spp. (*13*).

Understanding the mechanisms influencing shedding of NiV will likely prevent further spread; NiV shedding likely also follows seasonal and temporal pulses previously reported for Hendra virus (*14*–*15*). We recognize that disease emergence might be a result of disturbance within ecologic systems and hence cannot be alleviated by further disturbance. As a tropical country, Sri Lanka has complex and diverse ecosystems; its resilience to climate change may be better than other regions of the world.

The potential of zoonotic bat-to-human transmission of NiV could be minimized by preventive measures. Such measures could include education of healthcare workers to raise appropriate awareness for NiV, equipment and training for the early detection of NiV RNA in clinical specimens, preparation for clinical management of NiV-positive patients, and messaging the public about avoidance of known infection routes to prevent transmission (i.e., circular fencing of trees with roosting bats).

This article was preprinted at https://www.biorxiv.org/content/10.1101/2024.07.31.605971v1.

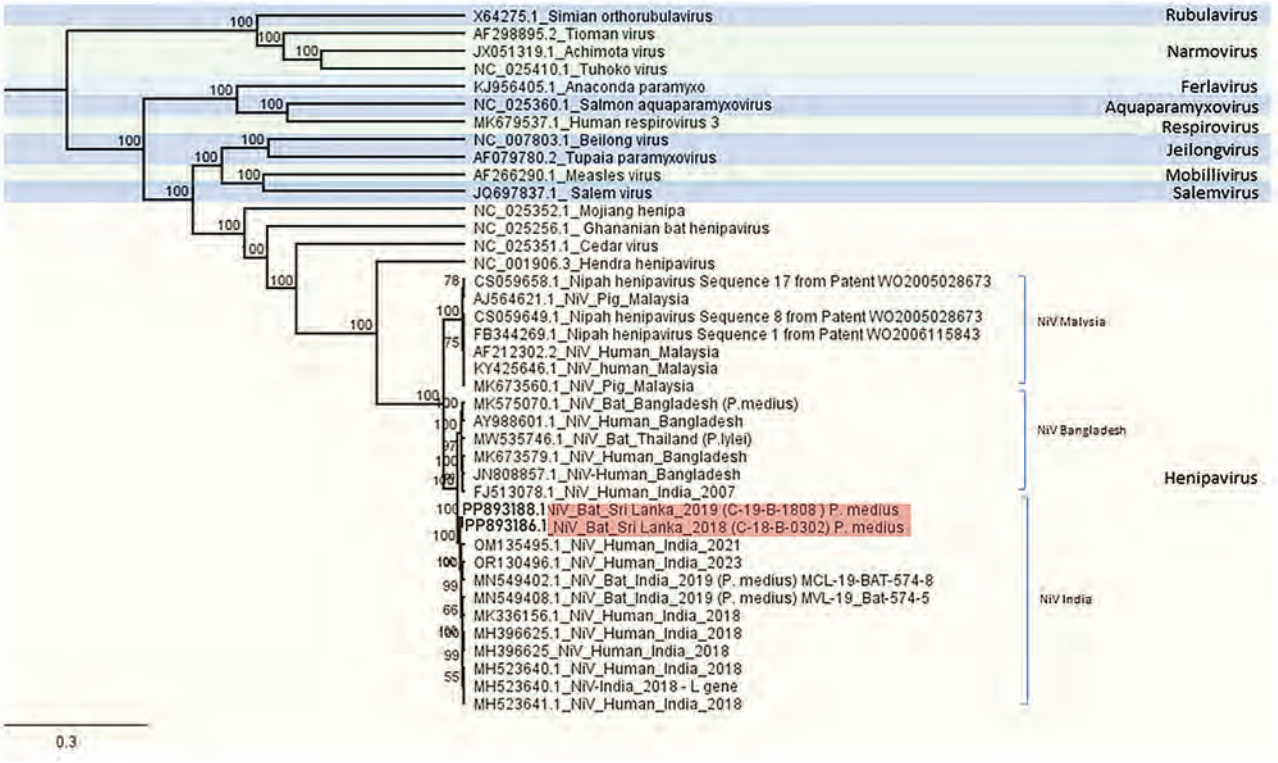


**Figure 2.** Phylogenetic reconstruction of subfamily Orthoparamyxovirinae viruses in study of NiV shedding in urine from fruit bats, Sri Lanka, 2018–2019. The alignment is based on the partial large gene (7,977 nt) coding for the RNA-dependent RNA polymerase. Calculation was done using a MrBayes Markov chain Monte Carlo approach of molecular clock reconstruction based on the general time reversible model with the parameters set at 1 million replicates, 4 chains, and burn-in at 10%. Blue shading and green shading indicate distinct genera of paramyxoviruses. Red shading highlights the novel strains from Sri Lanka. Node numbers indicate posterior probability. We used a simian orthorubulavirus as an outgroup. Scale bar indicates branch length. NiV, Nipah virus; *P. medius*, *Pteropus medius*.


## Acknowledgments

We thank the Genome Competence Center at the Robert Koch Institute for Illumina sequencing and Ursula Erikli for copyediting. We also thank the Federal Ministry of Health, Germany (Bundesministerium für Gesundheit, BMG) for funding and Department of Wildlife Conservation, Sri Lanka, for necessary approvals and permits. We also thank Colombo Municipal Council for granting permission and access to conduct the research in the public park.


The study involved non-invasive sampling (sheet sampling of bat droppings and urine). However, research has been approved by appropriate human or animal subjects research review boards. This research was conducted according to the guidelines of the Fauna and Flora Protection Ordinance (FFPO) of Sri Lanka under permit no. WL/3/2/05/18, issued by the Department of Wildlife Conservation, Sri Lanka, January 10, 2018. Collection of bat urine under roosting trees was carried out according to relevant guidelines and regulations of the Fauna and Flora Protection Ordinance, Sri Lanka.

The results reported in this study were obtained without the conduction of animal experiments. All bat samples were collected non-invasively (bat droppings) and bats were not handled for sampling procedure. Relevant guidelines for animal research in vivo are not applicable.

This study was supported by the Federal Ministry of Health, Germany, under the Identification of Emerging Agents (IDEA) project within the Global Health Protection Programme. S.S., T.M., and T.P. received funding from the IDEA project. The authors declare no competing interests. The funders had no role in the design of the study; in the collection, analyses, or interpretation of data; in the writing of the manuscript; or in the decision to publish the results.

## About the Author

Dr. Kohl is a scientist at the Robert Koch Institute in Berlin, Germany, at the Centre for Biological Threats and Special Pathogens. Her research interests are the detection of emerging and reemerging viruses and the characterization of novel pathogens, especially from bats.

## References


1. Rima B, Balkema-Buschmann A, Dundon WG, Duprex P, Easton A, Fouchier R, et al.; ICTV Report Consortium. ICTV virus taxonomy profile: *Paramyxoviridae.* J Gen Virol. 2019;100:1593–4. https://doi.org/10.1099/jgv.0.001328
2. Sharma V, Kaushik S, Kumar R, Yadav JP, Kaushik S. Emerging trends of Nipah virus: a review. Rev Med Virol. 2019;29:e2010. https://doi.org/10.1002/rmv.2010
3. Kenmoe S, Demanou M, Bigna JJ, Nde Kengne C, Fatawou Modiyinji A, Simo FBN, et al. Case fatality rate and risk factors for Nipah virus encephalitis: A systematic review and meta-analysis. J Clin Virol. 2019;117:19–26. https://doi.org/10.1016/j.jcv.2019.05.009
4. Chua KB, Goh KJ, Wong KT, Kamarulzaman A, Tan PS, Ksiazek TG, et al. Fatal encephalitis due to Nipah virus among pig-farmers in Malaysia. Lancet. 1999;354:1257–9. https://doi.org/10.1016/S0140-6736(99)04299-3
5. Chua KB. A novel approach for collecting samples from fruit bats for isolation of infectious agents. Microbes Infect. 2003;5:487–90. https://doi.org/10.1016/S1286-4579(03)00067-4
6. As AK, Sahay RR, Radhakrishnan C, P S, Kandath S, Patil DY, et al. Clinico-epidemiological presentations and management of Nipah virus infection during the outbreak in Kozhikode district, Kerala state, India 2023. J Med Virol. 2024;96:e29559. https://doi.org/10.1002/jmv.29559
7. Roberts BJ, Catterall CP, Eby P, Kanowski J. Long-distance and frequent movements of the flying-fox *Pteropus poliocephalus*: implications for management. PLoS One. 2012;7:e42532. https://doi.org/10.1371/journal.pone. 0042532
8. Feldman KS, Foord A, Heine HG, Smith IL, Boyd V, Marsh GA, et al. Design and evaluation of consensus PCR assays for henipaviruses. J Virol Methods. 2009;161:52–7. https://doi.org/10.1016/j.jviromet.2009.05.014
9. Bolger AM, Lohse M, Usadel B. Trimmomatic: a flexible trimmer for Illumina sequence data. Bioinformatics. 2014;30:2114–20. https://doi.org/10.1093/bioinformatics/btu170
10. Brinkmann A, Ulm SL, Uddin S, Förster S, Seifert D, Oehme R, et al. AmpliCoV: rapid whole-genome sequencing using multiplex PCR amplification and real-time Oxford Nanopore MinION sequencing enables rapid variant identification of SARS-CoV-2. Front Microbiol. 2021;12:651151. https://doi.org/10.3389/fmicb.2021.651151
11. Brinkmann A, Pape K, Uddin S, Woelk N, Förster S, Jessen H, et al. Genome sequencing of the mpox virus 2022 outbreak with amplicon-based Oxford Nanopore MinION sequencing. J Virol Methods. 2024;325:114888. https://doi.org/10.1016/j.jviromet.2024.114888
12. International Union for Conservation of Nature and Natural Resources. IUCN Red List: Indian flying fox. 2021 [cited 2019 Aug 14]. https://doi.org/10.2305/IUCN.UK.2020-3.RLTS.T18725A194134899.en
13. World Health Organization. WHO South-East Asia Regional Strategy for the prevention and control of Nipah virus infection 2023–2030. 2023 [cited 2024 Feb 3] https://www.who.int/publications/i/item/9789290210849
14. Plowright RK, Peel AJ, Streicker DG, Gilbert AT, McCallum H, Wood J, et al. Transmission or within-host dynamics driving pulses of zoonotic viruses in reservoir-host populations. PLoS Negl Trop Dis. 2016;10:e0004796. https://doi.org/10.1371/journal.pntd.0004796
15. Plowright RK, Eby P, Hudson PJ, Smith IL, Westcott D, Bryden WL, et al. Ecological dynamics of emerging bat virus spillover. Proc Biol Sci. 2015;282:20142124. https://doi.org/10.1098/rspb.2014.2124


Address for correspondence: Claudia Kohl, Centre for Biological Threats and Special Pathogens, Robert Koch Institute, Seestraße 10, 13352 Berlin, Germany; email: kohlc@rki.de

# Recurrent Facial Folliculitis Caused by *Klebsiella aerogenes* Sequence Type 117 in Men who Have Sex with Men

Gentiane Monsel, Alexandre Bleibtreu, François Durupt, Brigitte Rached, Nicolas Yin, Delphine Martiny, Jonathan Krygier, Olivier Chosidow, Landon Porter, Matthieu Godinot, Erwan Turquier, Estelle Hau, Jean-Noël Dauendorffer, Maxime Bonjour, Marie Jachiet, Mathilde Liberge, Béatrice Berçot, Valérie Pourcher, Vincent Bérot, Marion Levast, Olivier Dauwalder, Romain Salle, Sébastien Fouéré, Cécile Brin, Laurent Dortet, Cécile Emeraud

We describe 17 cases of recurrent facial folliculitis caused by *Klebsiella aerogenes* bacteria in men who have sex with men in France, Belgium, and the United States. Whole-genome sequencing showed all isolates belonged to sequence type 117 or related lineages. Our findings suggest sexual transmission and highlight emerging clinical and public health concerns.

*Klebsiella aerogenes* (formerly *Enterobacter aerogenes*) is a gram-negative bacillus present in the environment and human gut microbiota and is an uncommon cause of community-acquired skin and soft tissue infections. Since 2025, a pattern of relapsing facial folliculitis caused by *K. aerogenes* has been reported in France, Belgium, and Spain (*1*–*3*). Those cases occurred exclusively among men who have sex with men (MSM), which strongly suggests that *K. aerogenes* could be an emerging sexually transmissible pathogen within that population (*1*–*3*). Whole-genome sequencing (WGS) of 4 isolates from Belgium revealed they all belonged to sequence type (ST) 117 (*2*), suggesting the emergence of a particular clone. Unfortunately, isolates reported in France and Spain were not sequenced, precluding confirmation of that hypothesis (*1*,*3*). We describe a multinational case series of 17 MSM with recurrent *K. aerogenes* facial folliculitis (KAFF) and analyze their epidemiologic, clinical, microbiologic, and genomic characteristics to assess the emergence of a specific lineage.

## The Study

We retrospectively identified cases through clinician notification within the Dermatologic Infectiology and Sexually Transmitted Infections Working Group in

Author affiliations: Pitié Salpêtrière Hospital, APHP, Paris, France (G. Monsel, A. Bleibtreu, B. Rached, E. Turquier, V. Pourcher, V. Bérot); Dermatologic Infectiology and Sexually Transmitted Infections Working Group of the French Society of Dermatology, Paris (G. Monsel, F. Durupt, J. Krygier, O. Chosidow, J.-N. Dauendorffer, M. Jachiet, V. Bérot, R. Salle, S. Fouéré, C. Brin); Croix Rousse Hospital, Hospices Civils de Lyon, Lyon, France (F. Durupt, M. Godinot, M. Bonjour, O. Dauwalder); Laboratoire Hospitalier Universitaire de Bruxelles–Universitair Laboratorium Brussel, Université Libre de Bruxelles, Brussels, Belgium (N. Yin, D. Martiny); University of Mons, Mons, Belgium (D. Martiny); St. Pierre University Hospital, Université Libre de Bruxelles, Brussels (J. Krygier); Ambroise Paré-UVSQ and Bicêtre-Paris Saclay Hospitals, APHP, Paris (O. Chosidow); University of Texas at Austin, Austin, Texas, USA (L. Porter); Edouard Herriot Hospital, Hospices Civils de Lyon, Lyon ( M. Godinot); Saint Louis Hospital, Paris Cité University, APHP, Paris (E. Hau, J.-N. Dauendorffer, M. Jachiet, M. Liberge, B. Berçot, S. Fouéré); Sorbonne University, INSERM UMR S 1136, Pierre Louis Epidemiology and Public Health Institute, Paris (V. Pourcher); Savoie Metropole Hospital, Chambéry, France (M. Levast, C. Brin); Centre National de Référence des Staphylocoques, Lyon (O. Dauwalder); Centre for Genital and Sexually Transmitted Diseases, Hôtel-Dieu Hospital, APHP, Paris (R. Salle); Kremlin Bicêtre Hospital, APHP, Le Kremlin Bicêtre, France (L. Dortet, C. Emeraud); Associated French National Reference Center for Antibiotic Resistance: Carbapenemase-Producing Enterobacteriaceae, Le Kremlin-Bicêtre (L. Dortet, C. Emeraud); IHU SEPSIS Comprehensive Sepsis Center, Université Paris-Saclay, Le Kremlin Bicêtre (L. Dortet, C. Emeraud)

DOI: https://doi.org/10.3201/eid3207.260572

Paris, Lyon, and Chambéry, France; Brussels, Belgium; and Austin, Texas, USA. We extracted clinical data from medical records. We defined disease duration as the time from symptom onset to healing or last follow-up. We recovered 24 *K. aerogenes* isolates from 17 patients, with multiple isolates in cases of recurrence or longitudinal sampling.

All 17 patients were MSM; median age was 35 years (interquartile range [IQR] 31.5–45.5 years) (Appendix 1 Table, https://wwwnc.cdc.gov/EID/article/32/7/26-0572-App1.xlsx). None of the patients were HIV-positive or immunocompromised; 9 were receiving HIV preexposure prophylaxis (PrEP). Ten patients reported history of sexually transmitted infections (STIs); 11 had a remote history (>10 years earlier) of acne treated with isotretinoin, doxycycline, or both, followed by a prolonged symptom-free interval before the folliculitis. Eight patients reported regular attendance at communal facilities (hot tubs, saunas, swimming pools, or gyms). We classified lesions as superficial for follicular pustules or inflammatory papules, deep for painful purulent nodules indicating deeper follicular involvement, or mixed. Lesions were exclusively facial, predominantly in the beard and mustache areas (Figure 1).

The median time from lesion onset to diagnosis was 7 (IQR 1.5–16) months. Before *K. aerogenes* identification, patients received antimicrobial drugs targeting gram-positive cocci without improvement. In recurrent or persistent cases, repeated cultures consistently yielded *K. aerogenes*. Nasal swab cultures were positive in 8 (73%) of 11 tested patients. Mycologic samples remained negative, thereby excluding tinea barbae. Median disease duration was 23 (IQR 9–54) months. Thirteen patients initially responded to targeted antimicrobial therapy but relapsed within 1–3 weeks after discontinuation. Overall, 12 patients did not achieve cure, 2 achieved sustained remission, 2 were still under treatment, and 1 did not complete follow-up care.

We performed WGS on all 24 isolates using short-read technology (Hiseq; Illumina, https://www.illumina.com). We conducted multilocus sequence typing (MLST) and resistome analysis using PubMLST (https://pubmlst.org) and ResFinder (https://genepi.food.dtu.dk/resfinder) databases. All folliculitis isolates belonged to ST117, except 1 ST117-like isolate (1FOLC4) with 1 nucleotide variation in *rplB*. One isolate (1FOLB1) acquired the *sul2* gene, conferring sulfamethoxazole resistance, which was absent in earlier isolates from the same patient; no other acquired resistance genes were detected.

We assessed genetic diversity and relatedness phylogenetic analysis using SNIppy version 4.6.0 (https://github.com/tseemann/snippy); reference genome was strain 1FOLA5. Analysis included 4 additional *K. aerogenes* ST117 isolates from the French National Reference Center for carbapenem resistance, which were unrelated to folliculitis cases and genomes from a previous study (2). Folliculitis-associated isolates were highly divergent from unrelated ST117 isolates (>520 single-nucleotide polymorphisms [SNPs])

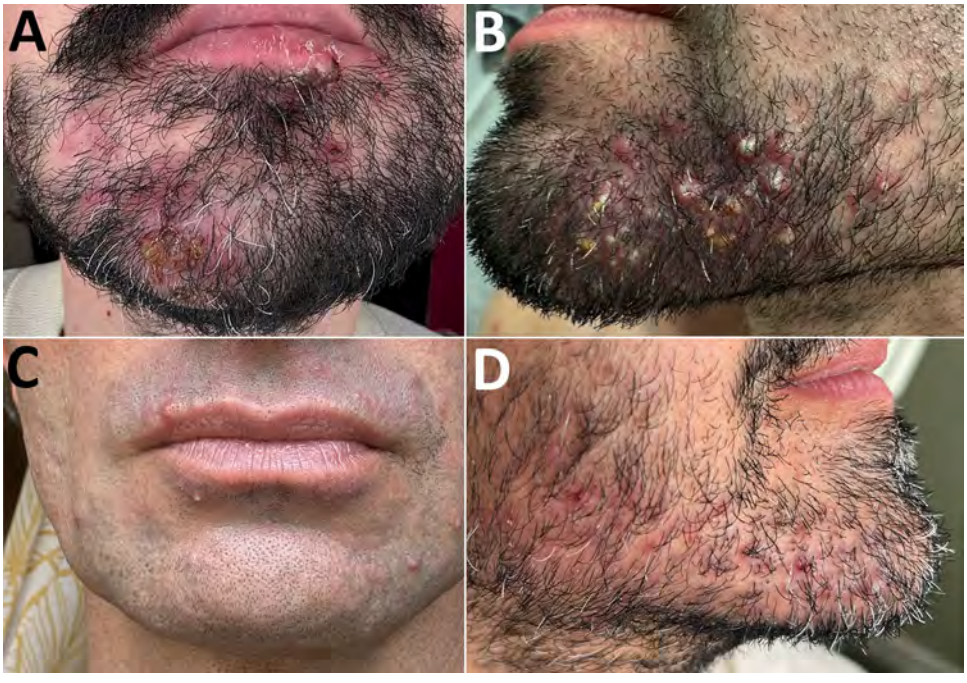


**Figure 1.** Clinical appearance of patients in study of *Klebsiella aerogenes* sequence type 117 facial folliculitis in men who have sex with men in France, Belgium, and the United States. A) Beard sycosis with painful purulent lesions (deep folliculitis). B) Papulopustular lesions in the beard region, consistent with both superficial and deep folliculitis. C) Pustular lesions of the mustache and beard area (superficial folliculitis). D) Multiple erythematous papules and pustules involving the right cheek and chin (superficial folliculitis).

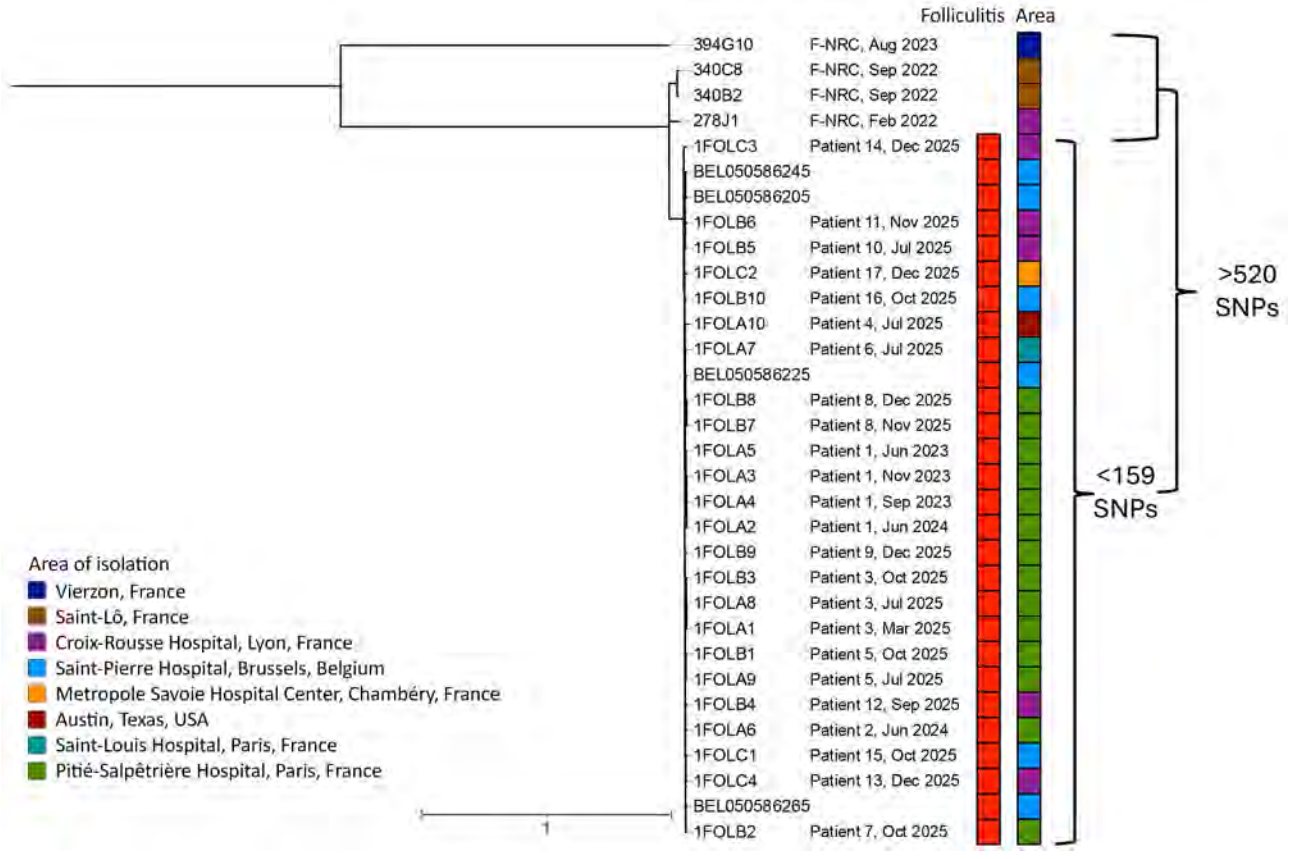


**Figure 2.** SNP-based phylogeny of *Klebsiella aerogenes* sequence type (ST) 117 and related isolates from study of facial folliculitis in men who have sex with men in France, Belgium, and the United States. Phylogenetic tree shows 24 folliculitis-associated isolates from 17 patients, 4 unrelated ST117 isolates from the French National Reference Center not implicated in folliculitis, and 4 ST117 folliculitis isolates collected in Belgium in 2025 (*2*). An expanded version of this figure is available online (https://wwwnc.cdc.gov/EID/article/32/7/26-0572-App2.pdf). F-NRC, French National Reference Center; SNP, single-nucleotide polymorphism.

but clustered together regardless of geographic origin (Figure 2; Appendix 2 Figure). Within that cluster, pairwise distances were 1–159 SNPs; for most isolates they were 60–80 SNPs (Figure 2; Appendix 2 Figure). Given an estimated evolutionary rate of 7–10 SNPs per year in Enterobacterales (*4*), those observed distances suggest a recent common ancestor and support the recent emergence and international dissemination of this lineage within interconnected MSM sexual networks.

## Conclusions

Although *K. aerogenes* is not considered a sexually transmitted pathogen, our findings support transmission through intimate contact: all cases occurred in MSM, many patients had previous STIs or were receiving PrEP, and the distribution of lesions is compatible with exposure during oro-anal contact. However, direct evidence of sexual transmission is lacking, no contact tracing was conducted, no documented transmission events were identified, and alternative routes including shared environmental exposures cannot be excluded. The emergence and intercontinental dissemination of enteric pathogens in MSM, such as *Shigella* spp., *Campylobacter jejuni*, and extended-spectrum β-lactamase–producing Enterobacterales, have been well documented (*5*–*7*). Rectal swab specimens were collected from some patients to assess potential enteric carriage, but *K. aerogenes* was not identified within the fecal Enterobacterales flora. Similarly, sexually transmissible dermatophytes, such as *Trichophyton mentagrophytes* internal transcribed spacer genotype VII, as well as monkeypox virus, illustrate the expanding spectrum of pathogens transmitted through intimate contact (*8*,*9*). Because half of the patients in this investigation reported exposure to communal water facilities, nonsexual transmission may also occur. The condition might be better classified as sexually transmissible, rather than strictly sexually transmitted (*10*).

KAFF appears to be an uncommon and likely underrecognized condition, consistent with previous

reports of gram-negative folliculitis in patients who had acne after prolonged antibiotic exposure (*11*,*12*). Because *K. aerogenes* is not a recognized skin pathogen, it may be overlooked in cutaneous samples, which contributes to underdiagnosis. The broad clinical spectrum, from superficial to disfiguring folliculitis, suggests a major role for host factors (*11*). Its strict facial localization points to regional determinants such as sebum composition and the follicular microenvironment (*13*). Previous use of systemic antimicrobial drugs can disrupt the cutaneous and nasal microbiome, reducing colonization resistance and promoting the emergence of gram-negative organisms such as *K. aerogenes* (*2*,*11*–*13*).

We observed nasal colonization consistent with previous descriptions of gram-negative folliculitis (*11*,*12*), supporting the hypothesis that the nasal cavity is a reservoir for *K. aerogenes* (*2*,*3*,*12*). However, its clinical significance and role in recurrence remain unclear. A study in Guangzhou, China, reported nasal carriage rates of ≈30% among MSM; that study identified 2 ST117 strains, supporting international dissemination of that lineage (*14*). In several patients, relapses occurred despite elimination of predisposing factors, suggesting persistence in a difficult-to-eradicate reservoir (*1*). Dysbiosis of skin microbiota and bacterial factors such as virulence traits or biofilm formation might also contribute to persistence and treatment failure (*13*,*14*,*15*).

Therapeutic management of KAFF remains challenging (*1*–*3*). Although trimethoprim/sulfamethoxazole or fluoroquinolones often lead to apparent clinical cure, relapses commonly occur soon after treatment discontinuation (*1*–*3*). Those recurrences have prompted consideration of nonantimicrobial approaches such as oral isotretinoin (*1*,*3*), which might act by reducing sebum production and follicular reservoirs rather than through direct antibacterial activity (*12*). By limiting repeated antimicrobial exposure and associated cutaneous dysbiosis, isotretinoin could help restore microbial balance (*13*), although its mechanisms and clinical effectiveness in KAFF remain uncertain. The emergence of the recurrent treatment-refractory ST117 clone in MSM is particularly concerning in the context of increasing antimicrobial pressure from routine STI management and implementation of doxycycline postexposure prophylaxis.

Our observations highlight the need for further research into the virulence determinants of *K. aerogenes* ST117, its reservoirs, and its modes of transmission. Studies integrating clinical data, microbiology, and microbiome analyses will be crucial to clarify the role of host factors, antimicrobial exposure, and skin ecosystem disruption in the pathogenesis and persistence of that pathogen and determine the optimal therapeutic strategy. Surveillance in sexual health clinics and dermatology care will better define the burden of KAFF and guide prevention strategies.

### Acknowledgments

We thank Célestin Mairesse for technical assistance with the sequencing of the Belgian strains.

All patients gave signed informed consent for publication of their case details and clinical photographs. Given the noninterventional nature of the study, approval from a patient protection committee was not required. This study was conducted in compliance with the reference methodology 004 in accordance with French law (no. 78-17, Computers, files and liberties, 6 January 1978).

Sequence data from this study were deposited in the National Center for Biotechnology Information Sequence Read Archive (BioProject no. PRJNA1427417). Sequence data from the previously published Belgium study (*2*) were deposited under BioProject no. PRJNA1250536.

The SEPSIS Comprehensive Center–IHU SEPSIS was supported by the French National Research Agency–France 2030 programme (grant no. ANR-23-IAHU-0004)

Author contributions: conceptualization: G.M., C.E., and A.B.; data collection: G.M., A.B., O.C., L.P., B.L., N.Y., J.K., D.M., O.D., F.D., M.G., J.N.D., M.B., V.B., E.H., M.J., E.T., B.R., Ma Li, Ma Le, C.B., R.S., S.F.; data analysis and interpretation: G.M. and C.E.; literature search: G.M. and C.E.; phylogenetic analysis: C.E.; writing original draft: G.M. and C.E.; figures and table: G.M. and C.E.; funding acquisition: L.D.; manuscript revision: all authors.

## About the Author

Dr. Monsel is an infectious diseases specialist and dermatologist at Pitié-Salpêtrière Hospital, Paris, France. Her clinical and research interests include infectious dermatology and sexually transmitted infections.

### References

1. Bérot V, Monsel G, Dauendorffer J-N, Aubry A, Nebbad B, Schneider P, et al.; Groupe Infectiologie Dermatologique et Infections Sexuellement Transmissibles (GrIDIST) de la Société Française de Dermatologie. *Klebsiella aerogenes*-related facial folliculitis in men having sex with men: a hypothetical new STI? J Eur Acad Dermatol Venereol. 2025;39:e10–2. https://doi.org/10.1111/jdv.20008
2. Yin N, Krygier J, Mairesse C, Libois A, Quoilin S, Martiny D. *Klebsiella aerogenes* ST117 causing folliculitis in men having sex with men, Belgium, February 2025. Euro Surveill. 2025;30:2500304. https://doi.org/10.2807/1560-7917.ES.2025.30.20.2500304
3. García Muñoz N, Sáez Vicente A, Feito Sancho L, Santa Cruz Martín A, Folcrá González M, Tarín Vicente EJ,

et al. Beard folliculitis by *Klebsiella aerogenes* in a young man: an emergent sexually transmitted infection? Int J STD AIDS. 2026;37:76–8. https://doi.org/10.1177/09564624251369576
4. Emeraud C, Mahamat A, Jousset AB, Bernabeu S, Goncalves T, Pommier C, et al. Emergence and rapid dissemination of highly resistant NDM-14–producing *Klebsiella pneumoniae* ST147, France, 2022. Euro Surveill. 2023;28:2300095. https://doi.org/10.2807/1560-7917.ES.2023.28.42.2300095
5. Mason LCE, Greig DR, Cowley LA, Partridge SR, Martinez E, Blackwell GA, et al. The evolution and international spread of extensively drug resistant *Shigella sonnei*. Nat Commun. 2023;14:1983. https://doi.org/10.1038/s41467-023-37672-w
6. Surgers L, Chiarabini T, Royer G, Rougier H, Mercier-Darty M, Decré D, et al. Evidence of sexual transmission of extended-spectrum β-lactamase–producing Enterobacterales: a cross-sectional and prospective study. Clin Infect Dis. 2022;75:1556–64. https://doi.org/10.1093/cid/ciac218
7. Gaudreau C, Rodrigues-Coutlée S, Pilon PA, Coutlée F, Bekal S. Long-lasting outbreak of erythromycin- and ciprofloxacin-resistant *Campylobacter jejuni* subspecies *jejuni* from 2003 to 2013 in men who have sex with men, Quebec, Canada. Clin Infect Dis. 2015;61:1549–52. https://doi.org/10.1093/cid/civ570
8. Jabet A, Dellière S, Seang S, Chermak A, Schneider L, Chiarabini T, et al. Sexually transmitted *Trichophyton mentagrophytes* genotype VII infection among men who have sex with men. Emerg Infect Dis. 2023;29:1411–4. https://doi.org/10.3201/eid2907.230025
9. Allan-Blitz LT, Gandhi M, Adamson P, Park I, Bolan G, Klausner JD. A position statement on mpox as a sexually transmitted disease. Clin Infect Dis. 2023;76:1508–12. https://doi.org/10.1093/cid/ciac960
10. Raccagni AR, Castagna A, Nozza S. When is it a sexually transmitted infection? Intimate contact transmission of pathogens not traditionally defined as STIs. Curr Opin Infect Dis. 2025;38:65–70. https://doi.org/10.1097/QCO.0000000000001072
11. Neubert U, Jansen T, Plewig G. Bacteriologic and immunologic aspects of gram-negative folliculitis: a study of 46 patients. Int J Dermatol. 1999;38:270–4. https://doi.org/10.1046/j.1365-4362.1999.00688.x
12. James WD, Leyden JJ. Treatment of gram-negative folliculitis with isotretinoin: positive clinical and microbiologic response. J Am Acad Dermatol. 1985;12:319–24. https://doi.org/10.1016/S0190-9622(85)80043-8
13. Dreno B, Dekio I, Baldwin H, Demessant AL, Dagnelie MA, Khammari A, et al. Acne microbiome: from phyla to phylotypes. J Eur Acad Dermatol Venereol. 2024;38:657–64. https://doi.org/10.1111/jdv.19540
14. Cheng Q, Ma Z, Gong Z, Liang Y, Guo J, Ye X, et al. Whole-genome sequencing analysis of *Klebsiella aerogenes* among men who have sex with men in Guangzhou, China. Front Microbiol. 2023;14:1102907. https://doi.org/10.3389/fmicb.2023.1102907
15. Feng Y, Yang Y, Hu Y, Xiao Y, Xie Y, Wei L, et al. Population genomics uncovers global distribution, antimicrobial resistance, and virulence genes of the opportunistic pathogen *Klebsiella aerogenes*. Cell Rep. 2024;43:114602. https://doi.org/10.1016/j.celrep.2024.114602

Address for correspondence: Cécile Emeraud, Hopital Bicêtre, Bacteriology EA7361, 78 rue du général Leclerc, Le Kremlin-Bicêtre, Île-de-France 94270 France; email: cecile.emeraud@aphp.fr

# Trends in Congenital Syphilis Cases by Maternal Country of Birth, Spain, 2016–2024

Victoria Hernando, Carmen Montaño, Ana Fernandez, Laura Molina, Guillermo Perez, Luis Viloria, Raquel Morales, Henar Marcos, Evelin Lopez-Corbeto, Paula Silvestre, Santiago Vicente, Olaia Perez-Martinez, Laura Montero, M. Isabel Barranco-Boada, Jesus Castilla, Pello Latasa, Eva Martinez, Ninoska Lopez, Daniel Castrillejo, Ana Roldan, Asuncion Diaz; STIs Group of National Epidemiological Surveillance Network[1]

The number of congenital syphilis cases in Spain remains low; 40 cases were confirmed during 2016–2024. However, a slight increase has been observed, particularly in children born to migrant mothers. Young maternal age, migrant status, and social disadvantages are warning signs that underscore the need to strengthen prenatal screening.

Congenital syphilis is preventable through antenatal screening and treatment of pregnant women (*1*); however, a resurgence of congenital syphilis has been observed (*2*). During 2018–2022, rates surged by 599% in Canada (*3*) and 81.8% in the United States (*4*); slight increases were also noted in Europe (*5*). That increase stems from multiple factors, including limited healthcare access, substance use, and migration (*6*), which can introduce legal, cultural, and language barriers that heighten vulnerability (*7*). We analyzed trends in congenital syphilis in Spain during 2016–2024 by maternal country of birth.

## The Study

We analyzed confirmed cases of congenital syphilis in children <2 years of age reported to the National Epidemiologic Surveillance Network. In Spain, congenital syphilis has been a notifiable disease since 1997, although changes were made to the maternal variables collected in 2016. We categorized cases according to maternal country of birth: women born in Spain and women born elsewhere. We calculated annual incidence rates per 100,000 live births for each group using the annual number of live births in Spain as the denominator. We used the $\chi^2$ test to

Author affiliations: National Centre of Epidemiology, Carlos III Health Institute, Madrid, Spain (V. Hernando, A. Diaz); CIBER in Infectious Diseases (CIBERINFEC), Instituto de Salud Carlos III, Madrid (V. Hernando, A. Diaz); Dirección General de Salud Pública del Gobierno de Aragón, Servicio de Vigilancia en Salud Pública, Zaragoza, Spain (C. Montaño); Dirección General de Salud Pública y Atención a la Salud Mental, Servicio Vigilancia Epidemiológica, Oviedo, Spain (A. Fernandez); Dirección General de Salud Pública, Servicio de Epidemiología, Palma de Mallorca, Spain (L. Molina); Dirección General de Salud Pública, Servicio Canario de Salud, Servicio de Vigilancia y Prevención, Las Palmas de Gran Canarias, Spain (G. Perez); Dirección General de Salud Pública Servicio de Vigilancia Epidemiologica, Santander, Spain (L. Viloria); Dirección General Salud Pública, Toledo, Spain (R. Morales); Dirección General Salud Pública, Valladolid, Spain (H. Marcos); Centro de Estudios Epidemiológicos sobre las ITS y Sida de Cataluña, Badalona, Spain (E. Lopez-Corbeto); Dirección General de Salud Pública, Servicio de Vigilancia y Control Epidemiológico, Valencia, Spain (P. Silvestre); Servicio Extremeño de Salud, Dirección General de Salud Pública, Mérida, Spain (S. Vicente); Dirección Xeral de Saúde Pública, Servizo de Vixilancia Epidemiolóxica, Santiago de Compostela, Spain (O. Perez-Martinez); Dirección General Salud Publica, Subdirección General de Vigilancia en Salud Pública Programas de Vigilancia de Infecciones de Transmisión Sexual, Madrid (L. Montero); Consejeria de Salud, Murcia, Spain (M.I. Barranco-Boada); Instituto de Salud Pública de Navarra-IdiSNA, CIBERESP, Pamplona, Spain (J. Castilla); Dirección General de Salud Pública, Servicio de Epidemiologia y Vacunación, San Sebastian, Spain (P. Latasa); Dirección General de Salud Pública, Consumo y Cuidados, Logroño, Spain (E. Martinez); Consejería de Sanidad, Servicio de Epidemiologia, Ceuta, Spain (N. Lopez); Dirección General de Salud Pública, Servicio de Vigilancia Epidemiológica, Melilla, Spain (D. Castrillejo); Consejería de Sanidad, Presidencia y Emergencias, Servicio de Vigilancia y Salud Laboral, Sevilla, Spain (A. Roldan)

DOI: https://doi.org/10.3201/eid3207.260146

[1]STIs Study Group team members are listed at the end of this article.

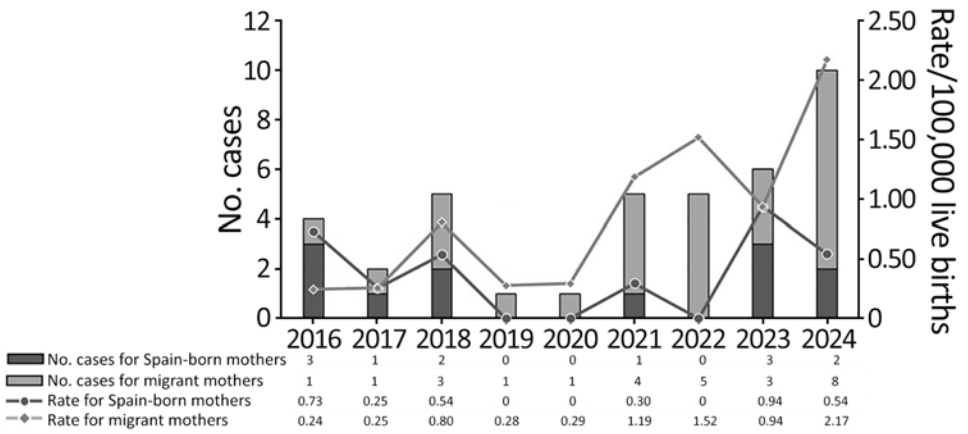


**Figure.** Number of congenital syphilis cases and rates per 100,000 live births by mother's place of birth, Spain, 2016–2024.

compare proportions and the Kruskal-Wallis test to compare medians.

Forty confirmed cases were reported during the study period. One case was excluded because of missing information on maternal country of birth. Of the 39 remaining cases, 12 (30.8%) cases involved children born to women born in Spain, whereas 27 (69.2%) cases involved infants of women born elsewhere (Figure). All children were born in Spain; no cases were classified as imported. From 2020 onward, incidence rates increased among women born outside Spain.

Of the infants born to women born in Spain, 75.0% (n = 9) were boys, compared with 44.4% (n = 12) for women born elsewhere (p = 0.096). Median age at diagnosis was 2 days in both groups; interquartile range (IQR) was 1–28 days for children of women born in Spain and 1–7 days for children of women born elsewhere (p = 0.817). Symptoms were present in 50.0% (n = 6) of infants of women born in Spain and 55.5% (n = 15) of infants of women born elsewhere (p = 0.950) (Table 1). No differences were observed in clinical manifestations.

Hospitalization percentages were similar in both groups: 83.3% (n = 10) among infants of women born in Spain and 81.5% (n = 22) among infants of women born elsewhere (p = 0.792). Complications were also comparable, occurring in 25.0% (n = 3) of children born to women in Spain and 22.2% (n = 6) of children born to women born elsewhere (p = 0.241). Two deaths were reported; both were children born to women born in Spain.

A total of 38 women were included in this analysis; 11 (28.9%) were born in Spain and 27 (71.0%) outside Spain. One woman born in Spain gave birth to twins; congenital syphilis was diagnosed in both. Among women born outside Spain, most originated from countries in Latin America (n = 22), including Paraguay (n = 8) and Colombia (n = 4). Three were from Eastern Europe and 1 from Western Europe; in 1 case, country of origin was not specified.

Women born in Spain were younger at the time of delivery than women born elsewhere (Table 2). Syphilis screening had not been performed during pregnancy in 9.1% (n = 1) of women born in Spain and 11.1% (n = 3) of women born elsewhere. Adequate treatment was recorded for 36.4% (n = 4) of women born in Spain and 22.2% (n = 6) of women born elsewhere. Of the 39 women included in the analysis, 11

**Table 1.** Clinical manifestations of congenital syphilis cases by mother's place of birth, Spain, 2016–2024

| Manifestation | No. (%) cases | | p value* |
|---|---|---|---|
| | Child born to woman born in Spain | Child born to woman born outside Spain | |
| Symptomatology | | | |
| Asymptomatic | 2 (16.7) | 4 (14.8) | 0.950 |
| Symptomatic | 6 (50.0) | 15 (55.6) | |
| Unknown | 4 (33.3) | 8 (29.6) | |
| Clinical manifestations, symptomatic cases only† | | | |
| Hepatosplenomegaly | 4 (66.7) | 8 (53.3) | 0.577 |
| Mucocutaneous lesions | 3 (50.0) | 4 (26.7) | 0.306 |
| Anemia | 3 (50.0) | 3 (50.0) | 0.169 |
| Central nervous system involvement | 1 (16.7) | 5 (33.3) | 0.445 |
| Jaundice | 3 (50.0) | 2 (13.3) | 0.075 |
| Nephrotic syndrome | 1 (16.7) | 1 (6.7) | 0.481 |
| Others | 3 (50.0) | 9 (60.0) | 0.676 |

*$\chi^2$ was used to calculate p values.
†Clinical manifestations are nonexclusive categories.

**Table 2.** Maternal characteristics in study of trends in congenital syphilis cases by maternal country of birth, Spain, 2016–2024*

| Characteristic | Value | | p value† |
|---|---|---|---|
| | Mother born in Spain† | Mother born outside Spain | |
| Total no. women | 11 (28.9) | 27 (71.1) | |
| Median age at delivery (IQR), y | 21.5 (19–33) | 25 (22–29) | 0.421 |
| Syphilis screening during pregnancy | | | 0.877 |
| First trimester | 3 (27.3) | 8 (29.6) | |
| Third trimester | 0 | 2 (7.4) | |
| First and third trimester | 2 (18.2) | 2 (7.4) | |
| Not documented | 2 (18.2) | 4 (14.8) | |
| Not performed | 1 (9.1) | 3 (11.1) | |
| Unknown | 3 (27.3) | 8 (29.6) | |
| Syphilis treatment | | | 0.284 |
| Without treatment | 4 (36.4) | 11 (40.7) | |
| Appropriate treatment | 4 (36.4) | 6 (22.2) | |
| Inappropriate treatment | 0 | 4 (14.8) | |
| During labor or delivery | 3 (27.3) | 2 (7.4) | |
| Not documented | 0 | 3 (11.1) | |
| Unknown | 0 | 1 (3.7) | |
| Maternal risk for syphilis | | | 0.318 |
| Yes | 6 (54.6) | 8 (29.6) | |
| None | 1 (9.1) | 6 (22.2) | |
| Unknown | 4 (36.4) | 13 (48.2) | |
| Risk factors, women with maternal risk for syphilis‡ | | | |
| Disadvantaged situation | 2 (33.3) | 8 (100) | 0.006 |
| Engagement in sex work | 1 (16.7) | 1 (12.5) | 0.825 |
| Drug use | 3 (50.0) | 1 (12.5) | 0.124 |
| Unspecified factors | 4 (66.7) | 1 (12.5) | 0.036 |
| Maternal HIV coinfection | | | 0.430 |
| Yes | 0 | 0 | |
| No | 9 (81.8) | 23 (85.2) | |
| Not testing | 0 | 2 (7.4) | |
| Unknown | 2 (18.2) | 2 (7.4) | |

*Values are no. (%) except as indicated.
†$\chi^2$ was used to calculate p values.
‡Risk factors are nonexclusive categories.

were living in socially or economically disadvantaged circumstances. In 1 case, the mother's syphilis was diagnosed after the diagnosis of congenital syphilis in the child; that woman was born in Spain.

## Conclusions

Although the absolute number of congenital syphilis cases remains low in Spain, an increase has been observed in recent years, particularly among women born outside Spain. The observed increase in cases might be considered a consequence of the rising number of syphilis cases among young women. Previous studies in Spain have shown that the greatest increases in syphilis occurred among women 20–34 years of age (*8*) and women from Latin America (*9*). However, data are unavailable on the percentage of women with syphilis who were pregnant at the time of diagnosis or whose condition was diagnosed during delivery.

Of the confirmed congenital syphilis cases in this study, two thirds were in infants of women born outside Spain, whereas pregnancies among women born elsewhere accounted for only 25.6% of all pregnancies in 2024 (*10*). That difference might indicate unmet needs in antenatal care for migrant women, which pose risks to both child and maternal health, even though access to pregnancy, childbirth, and postpartum care is guaranteed to all women in Spain regardless of administrative status (*11*). Therefore, ensuring that migrants receive comprehensive information regarding their own health and prenatal care during pregnancy, such as screening tests, is essential to guaranteeing adequate follow-up care.

Most women in this study originated from countries in Latin America, which also represents the largest region of origin among migrants in Spain (*10*). Migration during pregnancy is not rare and poses a challenge for timely diagnosis and treatment of syphilis in pregnant women.

Other factors, such as younger maternal age, might also contribute to increased vulnerability. National data show a rising trend in maternal age in Spain. Among women born in Spain, the mean age at delivery increased from 32.5 years in 2016 to 33.1 years in 2023, whereas among women born elsewhere it rose from 29.5 years to 30.5 years over the same period (*10*). In contrast, the mothers in this analysis were younger; median age was 21.5 years for women born in Spain and 25 years for women born elsewhere.

Adverse birth outcomes related to congenital syphilis are closely linked to inadequate access to timely screening and treatment during pregnancy (*12*). Screening has also been shown to reduce syphilis-related deaths by up to 50% (*13*). In this analysis, the percentage of women whose condition was adequately diagnosed and treated was very low in both groups, underscoring the need for improved implementation of existing recommendations. Serologic screening for syphilis during pregnancy is recommended at the first prenatal visit, and additional testing should be performed during the third trimester and at delivery for women at high risk of acquiring syphilis (e.g., because of sex work, drug use, disadvantaged social conditions, or other sexually transmitted infections during pregnancy) or if no test was performed during the first trimester (*14*,*15*). Although information on predisposing factors was available for a limited number of women, more than half (14/26) were in disadvantaged situations, highlighting the role of broader social determinants of health.

Epidemiologic surveillance data provide a comprehensive overview of trends in the general population but have limitations. Under case definitions in Europe, only children <2 years of age are included, and fetal deaths or stillbirths caused by congenital syphilis are excluded, potentially leading to underdiagnosis. In addition, maternal information in surveillance records is often incomplete. Enhancing those data could help elucidate existing gaps in prenatal care for pregnant women and identify groups that are more vulnerable to syphilis.

Our findings highlight the importance of ensuring timely, accessible, and respectful prenatal care and syphilis screening for all pregnant women, particularly when social or structural vulnerabilities are present. Strengthening epidemiologic surveillance and reinforcing person-centered approaches in maternal care are essential steps toward preventing congenital syphilis and promoting maternal and child health.

Members of the STIs Study Group of National Epidemiological Surveillance Network: Andalucía: Isabel Maria Vázquez Rincón, Esperanza Carmona Fernández, Ana Roldán Garrido, Nicola Lorusso; Aragón: Carmen Montaño Remacha, Ana Delia Cebollada Gracia, Miriam García Vazquez; Asturias: Ana M Fernández Verdugo, Sara Iglesias Martinez, Maria del Campo San Emeterio, Ana Fernandez Ibañez; Baleares: Laura Molina Núñez, M Magdalena Salom Castell; Canarias: Oscar Guillermo Pérez Martín, Carles Barres Giménez, Fabiola González Rancel, Ricardo Jesús Moreno Saavedra, Álvaro Torres Lana; Cantabria: Luis Viloria; Castilla La Mancha: Carmen Morales, Raquel Morales; Castilla y León: Maria Henar Marcos Rodríguez, Maria del Mara Anreu Román, Maria Yolanda Vallejo Ramos, Cristina Ruiz Sopeña, Mª Isabel Carramiñana Martinez, José Antonio Aguilera Mellado, Loreto Mateos Baruque, Isabel González Vara, Rafael Villanueva Agero, Rosa Maria Moralejo Vicente, Maria Trinidad Romo Cortina, Clara Berbel Hernández, Marta Allúe Tango, Irene Andrés García, Maria José Cordero Maestre; Cataluña: Evelin Lopez Corbeto, Jordi Casabona, en nombre del grupo de trabajo de las ITS de la comisión de vigilancia epidemiológica de Cataluña y los profesionales de las secciones de Epidemiologia de los Servicios Territoriales; Comunidad Valenciana: Mª Elena Vidal Montañana, Begoña Medina Cortés, Katja Villatoro Bongiorno, Empar Giner Ferrando, Francisco Javier Roig Sena; Extremadura: Santiago Vicente Iglesias, Maria del Mar López-Tercero Torvisco, Noa Batalla Rebollo, Juan Antonio Linares Dopido; Galicia: Olaia Pérez Martínez, Miguel Conde Rodriguez, Cristina Estévez Dávila, Alberto Fernández Martínez, Mª Carmen Marrero Flores, María Blanca Vázquez Rodríguez; Madrid: Ángel Miguel Benito, Laura Montero Morales; Murcia: Isabel Barranco Boada, Encarnación Vicente Martinez, Encarnación Gutiérrez Pérez, Alonso Sanchez-Migallón Naranjo; Navarra: Jesús Castilla, Mercedes Herranz-Aguirre, Arantza de Miguel; País Vasco: Larraitz Etxebarriarteun Aranzabal, Madealen Oribe Amores, Idurre Ayala Izaguirre, Patricia Sancho Uriarte, Pello Latasa Zamalloa; La Rioja: Ana Carmen Ibáñez Pérez, Angela Blanco Martinez, Eva Martínez Ochoa; Ceuta: Ninoska Lopez Berrios, Violeta Ramos Martin; Melilla: Atanasio Gómez Anés, Daniel Castrillejo.

### Acknowledgments

We thank the epidemiologic surveillance professionals in the autonomous regions, as well as all those who contribute to the reporting and improving the quality of the data of the National Epidemiological Surveillance Network.

## About the Author

Dr. Hernando is an epidemiologist and senior scientist at the National Epidemiology Centre of the Carlos III Health Institute in Madrid, Spain. Her research interests include sexually transmitted infections, HIV infection, and viral hepatitis, especially in aspects related to surveillance and public health.

### References

1. Medoro AK, Sánchez PJ. Syphilis in neonates and infants. Clin Perinatol. 2021;48:293–309. https://doi.org/10.1016/j.clp.2021.03.005
2. Gilmour LS, Walls T. Congenital syphilis: a review of global epidemiology. Clin Microbiol Rev. 2023;36:e0012622. https://doi.org/10.1128/cmr.00126-22

3. Public Health Agency of Canada. Infectious syphilis and congenital syphilis in Canada, 2022–2023 [cited 2026 Jun 12]. https://www.canada.ca/content/dam/phac-aspc/documents/services/reports-publications/canada-communicable-disease-report-ccdr/monthly-issue/2023-49/issue-10-october-2023/ccdrv49i10a04a-eng.pdf
4. US Centers for Disease Control and Prevention. Sexually transmitted infections surveillance, 2024–2025 [cited 2026 Jun 12]. https://www.cdc.gov/sti-statistics/annual/index.html
5. European Centre for Disease Prevention and Control. Congenital syphilis. Annual epidemiological report for 2023–2025 [cited 2026 Jun 12]. https://www.ecdc.europa.eu/sites/default/files/documents/congenital-syphilis-annual-epidemiological-report-2023.pdf
6. Tetteh A, Moore V. The rise of congenital syphilis in Canada: threats and opportunities. Front Public Health. 2025;12:1522698. https://doi.org/10.3389/fpubh.2024.1522698
7. Adrian Parra C, Stuardo Ávila V, Contreras Hernández P, Quirland Lazo C, Bustos Ibarra C, Carrasco-Portiño M, et al. Structural and intermediary determinants in sexual health care access in migrant populations: a scoping review. Public Health. 2024;227:54–62. https://doi.org/10.1016/j.puhe.2023.11.031
8. Hernando V, Lorusso N, Montaño C, Boone AL, Garí A, Perez G, et al.; STIs Study Group of National Epidemiological Surveillance Network. Increased trends in reported sexually transmitted infections according to age groups and sex in Spain, 2016-2022. Infect Dis (Lond). 2025;57:247–55. https://doi.org/10.1080/23744235.2024.2417241
9. Hernando V, Simón L, Díaz A. Grupo de estudio de ITS de la RENAVE, Sífilis y gonococia notificada en España, 2023. Diferencia según sexo y región de nacimiento. XLIII Reunión anual de la Sociedad Española de Epidemiología (SEE) y XX Congresso da Associacao Portugesa de Epidemiología (APE); Las Palmas de Gran Canaria: Gaceta Sanitaria; 2025. p. 8.
10. Instituto Nacional de Estadistica. Demography and population [cited 2026 Jun 12]. https://ine.es/dyngs/INEbase/en/categoria.htm?c=Estadistica_P&cid=1254734710984
11. Agencia Estatal Boletín Oficial del Estado. Royal decree-law 7/2018, on universal access to the National Health System [in Spanish] [cited 2026 Jun 12]. https://www.boe.es/buscar/doc.php?id=BOE-A-2018-10752
12. Korenromp EL, Rowley J, Alonso M, Mello MB, Wijesooriya NS, Mahiané SG, et al. Global burden of maternal and congenital syphilis and associated adverse birth outcomes-Estimates for 2016 and progress since 2012. PLoS One. 2019;14:e0211720. https://doi.org/10.1371/journal.pone.0211720
13. Hawkes S, Matin N, Broutet N, Low N. Effectiveness of interventions to improve screening for syphilis in pregnancy: a systematic review and meta-analysis. Lancet Infect Dis. 2011;11:684–91. https://doi.org/10.1016/S1473-3099(11)70104-9
14. Janier M, Unemo M, Dupin N, Tiplica GS, Potočnik M, Patel R. 2020 European guideline on the management of syphilis. J Eur Acad Dermatol Venereol. 2021;35:574–88. https://doi.org/10.1111/jdv.16946
15. Salomè S, Cambriglia MD, Montesano G, Capasso L, Raimondi F. Congenital syphilis: a re-emerging but preventable infection. Pathogens. 2024;13:481. https://doi.org/10.3390/pathogens13060481


Address for correspondence: Victoria Hernando, National Centre of Epidemiology, Carlos III Health Institute, Avda. Monforte de Lemos, 5. 28029 Madrid, Spain; email: vhernando@isciii.es

# Household Transmission of Enterovirus D68, Washington and Oregon, United States, 2022–2024

Pavitra Roychoudhury, Erica Wetzler, Anna Elias-Warren, Katherine L. Hoffman, Alex Harteloo, Hyeong Geon Kim, Kevin Kong, Hong Xie, Jolene Gov, Margaret G. Mills, Collrane Frivold, Madison Hollcroft, Mark Drummond, Tara Hatchie, Erica Clark, Brenna Ehmen, Peter D. Han, Luis Gamboa, Sally Grindstaff, Jeremy Stone, Alexander L. Greninger, Lea M. Starita, Christina Lockwood, Janet A. Englund, Marco Carone, Ana A. Weil, Sacha L. Reich, Richard A. Mularski, Mark A. Schmidt, Jennifer L. Kuntz, Allison L. Naleway, Helen Y. Chu

During 2022–2024, a total of 35 of 1,040 households had a distinct symptomatic index case of enterovirus D68; estimated symptomatic secondary infection rate was 13.6%. Sequences from patients within households clustered closely; we observed 0–2 pairwise nucleotide differences between household cases 6–14 days apart.

Enterovirus D68 (EV-D68) typically causes respiratory illness with symptoms such as difficulty breathing, fever, wheezing, and respiratory distress (*1*). Interest in EV-D68 has grown since 2014 because of associations with acute flaccid myelitis in children (*2*) and recent outbreaks in the United States and Europe (*3*). In a descriptive epidemiologic study of the 2014 US outbreak of medically attended EV-D68, children <16 years of age accounted for >80% of severe respiratory illness cases (*4*); however, community-based assessments of EV-D68 incidence and age distribution remain limited. In congregate settings like homeless shelters, EV-D68 transmission occurred primarily in adult and not family shelters (*5*). No specific treatments or vaccines are available for nonpolio enteroviruses, and the epidemiology of EV-D68, including risk factors for household transmission, are not well understood (*6*).

Few studies have incorporated genomic sequencing to confirm transmission patterns or quantify viral evolution between transmission events (*7*,*8*). Our study aimed to characterize the epidemiology and household transmission of EV-D68 using specimens and data collected as part of a community-based prospective CASCADIA cohort (*9*).

## The Study

The CASCADIA study included active surveillance for respiratory viruses among enrolled households with children and adults in metropolitan Seattle, Washington, USA, and Portland, Oregon, USA during June 2022–March 2024 (Appendix, https://wwwnc.cdc.gov/EID/article/32/7/25-1733-App1.pdf). Participants completed surveys and self-collected nasal swab samples weekly, regardless of symptoms. We subsequently tested swab specimens from participants who reported symptoms ≤72 hours of collection (Appendix), as well as specimens with a positive or inconclusive result for SARS-CoV-2, influenza, or respiratory syncytial virus (RSV), by using a multiplex assay for 26 targets, including EV-D68. To rule out false-positive results caused by cross-reactivity of the multiplex assay target described previously (*5*), we selected specimens that tested positive for EV-D68 with relative cycle threshold (Crt) <28 for EV-D68–specific reverse transcription PCR. We sequenced samples by hybridization probe capture using a panel that covers ≈80 viral targets (Appendix).

Author affiliations: Fred Hutchinson Cancer Center, Seattle, Washington, USA (P. Roychoudhury); University of Washington, Seattle (P. Roychoudhury, E. Wetzler, A. Elias-Warren, K.L. Hoffman, A. Harteloo, H.G. Kim, K. Kong, H. Xie, J. Gov, M.G. Mills, C. Frivold, M. Hollcroft, M. Drummond, T. Hatchie, E. Clark, B. Ehmen, P.D. Han, L. Gamboa, S. Grindstaff, J. Stone, A.L. Greninger, L.M. Starita, C. Lockwood, J.A. Englund, M. Carone, A.A. Weil, H.Y. Chu); Brotman Baty Institute for Precision Medicine, Seattle (L. Gamboa); Seattle Children's Research Institute, Seattle (J.A. Englund); Kaiser Permanente Center for Health Research, Portland, Oregon, USA (S.L. Reich, R.A. Mularski, M.A. Schmidt, J.L. Kuntz, A.L. Naleway)

DOI: https://doi.org/10.3201/eid3207.251733

After excluding 179 single-person households, we included 1,040 multiperson households in our analysis (Appendix Figure 1). We detected a distinct EV-D68 index case in 35 (3.4%) households (Tables 1, 2). We identified potential secondary transmission, defined as detection of EV-D68 in a symptomatic household contact 1–14 days after a distinct index case, among 7 (20%) households. Those households included 15 household contacts, 14 of whom were tested because they reported symptoms. The 28 households with unlikely secondary transmission included 51 household contacts, 21 of whom were tested because they reported symptoms. Among 66 household contacts of the 35 identified index cases, 9 contacts were infected; we estimated the symptomatic secondary infection rate for EV-D68 as 13.6%

**Table 1.** Characteristics of index cases in study of household transmission of enterovirus D68, Washington and Oregon, United States, 2022–2024*

| Characteristics | Potential secondary transmission† | Unlikely secondary transmission‡ | Total |
|---|---|---|---|
| No. index cases | 7 | 28 | 35 |
| Median age, y (range) | 11 (3–34) | 8.5 (1–48) | 9 (1–48) |
| Age range | | | |
| 6 mo–1 y | 0 | 2 (7.1) | 2 (5.7) |
| 2–4 y | 1 (14.3) | 8 (28.0) | 9 (25.7) |
| 5–12 y | 3 (42.9) | 8 (28.6) | 11 (31.4) |
| 13–50 y | 3 (42.9) | 10 (35.7) | 13 (37.1) |
| Sex | | | |
| F | 3 (42.9) | 17 (60.7) | 20 (57.1) |
| M | 4 (57.1) | 11 (39.3) | 15 (42.9) |
| Race or ethnicity | | | |
| Asian | 0 (0.0) | 1 (3.6) | 1 (2.9) |
| White | 3 (42.9) | 22 (78.6) | 25 (71.4) |
| Multiracial | 3 (42.9) | 4 (14.3) | 7 (20.0) |
| Other | 1 (14.3) | 1 (3.6) | 2 (5.8) |
| Hispanic | 0 (0.0) | 3 (10.7) | 3 (8.6) |
| Child attending school or daycare | 5 (71.4) | 18 (64.3) | 23 (65.7) |
| Any smoking | 0 | 0 | 0 |
| Any underlying conditions§ | 1 (14.3) | 8 (28.6) | 9 (25.7) |
| Masking in public at baseline | | | |
| Any | 7 (100) | 23 (82.1) | 30 (85.7) |
| Never | 0 | 5 (17.9) | 5 (14.4) |
| Relative cycle threshold | | | |
| Median (range) | 18.8 (13.6–21.8) | 16.0 (9.6–22.5) | 17.3 (9.6–22.5) |
| Overall median ≥17.3 | 2 (28.6) | 17 (60.7) | 19 (54.3) |
| Viral co-detections¶ | | | |
| Any | 7 (100) | 26 (92.9) | 33 (94.3) |
| SARS-CoV-2 | 0 | 1 (3.6) | 1 (2.9) |
| Adenovirus | 1 (14.3) | 0 (0) | 1 (2.9) |
| RSV | 0 | 1 (3.6) | 1 (2.9) |
| HPIV | 1 (14.3) | 0 | 1 (2.9) |
| ARI symptoms# | | | |
| ≥2 ARI symptoms | 7 (100) | 19 (67.9) | 26 (74.3) |
| Cough, rhinorrhea, or both | 7 (100) | 28 (100) | 35 (100) |
| Any care seeking during illness** | 0 | 3 (10.7) | 3 (8.6) |
| Any behavior change to reduce transmission in the air†† | 3 (42.9) | 11 (39.3) | 14 (40.0) |
| Any behavior change to reduce transmission on surfaces‡‡ | 3 (42.9) | 10 (35.7) | 13 (37.1) |

*Values are no. (%) except as indicated. ARI, acute respiratory illness; EV, enterovirus; HPIV, human parainfluenza virus; RSV, respiratory syncytial virus.
†Occurring when EV-D68 is detected in a secondary household member 1–14 days after index case.
‡Unlikely secondary transmission defined as occurring when only 1 EV-D68 case is detected in the household or when ≥2 EV-D68 cases are in a household but secondary case detected >14 days after index case.
§Underlying conditions include asthma, chronic obstructive pulmonary disease (including chronic bronchitis and emphysema), sleep apnea, heart disease, congenital heart disease, heart failure, Down syndrome, hypertension (high blood pressure), diabetes (high blood sugar), liver condition, weak or failing kidneys, cancer or malignancy, arthritis, stroke, deep vein thrombosis or pulmonary embolism, sickle cell disease or thalassemia, weakened immune system, depression, anxiety, thyroid issues, or other health diagnosis.
¶Rhinovirus target was detected in 32 (91.4%) samples but is not shown because of cross-reactivity between that target and EV-D68 and several other enterovirus species (assay ID Vi99990016_po, Thermo Fisher [https://www.thermofisher.com]).
#Symptoms reported ≤7 days of the individual EV-D68 illness episode's first positive specimen collection, including fever, cough, sore throat, shortness of breath, myalgia, rhinorrhea, or a combination of symptoms. All persons included reported ≥1 symptom.
**Self-reported care seeking defined as seeking healthcare from a healthcare provider during illness.
††Includes masking, sleeping separately, covering cough or sneeze before or during illness episode.
‡‡Includes handwashing, cleaning, disinfecting.

**Table 2.** Characteristics of households and household contacts in study of household transmission of enterovirus D68, Washington and Oregon, United States, 2022–2024*

| Characteristics | Potential secondary transmission† | Unlikely secondary transmission‡ | Total |
|---|---|---|---|
| No. households | 7 | 28 | 35 |
| Household density§ | | | |
| 2–4 persons | 6 (85.7) | 24 (85.7) | 30 (85.7) |
| ≥5 persons | 1 (14.3) | 4 (14.3) | 5 (14.3) |
| Housing type | | | |
| House, condo, or townhouse | 7 (100) | 27 (96.4) | 34 (97.1) |
| Missing | 0 | 1 (3.6) | 1 (2.9) |
| Household enrollment | | | |
| Median no. participants (range) | 3 (2–4) | 3 (2–4) | 3 (2–4) |
| No children <5 y | 5 (71.4) | 17 (60.7) | 22 (62.9) |
| Child <5 y, but no childcare | 1 (14.3) | 2 (7.1) | 3 (8.6) |
| Child <5 y in childcare¶ | 1 (14.3) | 9 (32.1) | 10 (28.6) |
| Income ≥$100,000 | 3 (42.9) | 22 (78.6) | 25 (71.4) |
| Smoker in household | 1 (14.3) | 2 (7.1) | 3 (8.6) |
| Study site | | | |
| Kaiser Permanente Northwest | 4 (57.1) | 12 (42.9) | 16 (44.4) |
| University of Washington | 3 (42.9) | 16 (57.1) | 19 (54.3) |
| No. household contacts | 15 | 51 | 66 |
| No. swab samples tested from symptomatic participants | 14 | 20 | 34 |
| Median age, y (range) | 42 (2–48) | 38 (3–49) | 38.5 (2–49) |
| Age range | | | |
| 6 mo–1 y | 0 | 0 | 1 (1.4) |
| 2–4 y | 1 (6.7) | 1 (2.0) | 1 (1.7) |
| 5–12 y | 3 (20.0) | 17 (33.3) | 22 (31.4) |
| 13–50 y | 11 (73.3) | 33 (64.7) | 45 (64.3) |
| Female sex at birth | 9 (60.0) | 30 (58.8) | 39 (59.1) |
| Sex | | | |
| F | 9 (60.0) | 29 (56.9) | 38 (57.6) |
| M | 6 (40.0) | 21 (41.2) | 27 (40.9) |
| Other | 0 | 1 (2.0) | 1 (1.5) |
| Race or ethnicity | | | |
| Asian | 2 (13.3) | 2 (3.9) | 4 (6.1) |
| White | 11 (73.3) | 44 (86.3) | 55 (83.3) |
| Multiracial | 2 (13.3) | 5 (9.8) | 7 (10.6) |
| Hispanic | 0 | 4 (7.8) | 4 (6.1) |
| Any smoking | 1 (6.7) | 2 (3.9) | 3 (4.5) |
| Any underlying conditions# | 10 (66.7) | 23 (45.1) | 33 (50.0) |
| Masking in public | | | |
| Any | 14 (93.3) | 48 (94.1) | 62 (93.9) |
| Never | 1 (6.1) | 3 (5.9) | 4 (6.1) |

*Values are no. (%) except as indicated. ARI, acute respiratory illness; EV, enterovirus; HPIV, human parainfluenza virus; RSV, respiratory syncytial virus.
†Occurring when EV-D68 is detected in a secondary household member 1–14 days after index case.
‡Unlikely secondary transmission defined as occurring when only 1 EV-D68 case was detected in the household or when ≥2 EV-D68 cases were in a household but secondary case detected >14 days after index case.
§Household density represents the number of household members regardless of enrollment in the study; thus, numbers might be greater than the number of participants enrolled in the study, if not all household members were enrolled.
¶Daycare or school attendance among ≥1 child <5 years in the household as reported at enrollment.
#Underlying conditions include asthma, chronic obstructive pulmonary disease (including chronic bronchitis and emphysema), sleep apnea, heart disease, congenital heart disease, heart failure, Down syndrome, hypertension (high blood pressure), diabetes (high blood sugar), liver condition, weak or failing kidneys, cancer or malignancy, arthritis, stroke, deep vein thrombosis or pulmonary embolism, sickle cell disease or thalassemia, weakened immune system, depression, anxiety, thyroid issues, or other health diagnosis.

(95% CI 6.8%–27.5%). Median detection interval between index and secondary cases was 7 (range 6–14) days. Households with secondary transmission (n = 7) were less likely to have children <5 years of age than households without secondary transmission (n = 28); 28.6% of the households with secondary transmission had young children, compared with 39.3% of those without secondary transmission (p = 0.38 by Fisher exact test). Compared with households with unlikely secondary transmission, index cases in households with secondary transmission were older (median age 11 vs. 9 years) and more frequently reported ≥2 acute respiratory illness (ARI) symptoms (100% vs. 68%; p = 0.01 by $\chi^2$ test). Among households with secondary transmission, median age of household contacts was older (42 vs. 26 years of age)

than in households with unlikely secondary transmission. Households with secondary transmission had lower household income than those without (42.9% vs. 78.6% had income lower than the median income threshold). A greater percentage of contacts reported underlying conditions in households with secondary transmission than in households with unlikely secondary transmission (67% vs. 45%). We conducted sensitivity analysis including only households with complete enrollment of all members; we observed no difference (Appendix Table 3).

Samples from adults with either a primary or secondary infection (n = 18) tended to have lower minimum Crt values (mean 16.3, SD 4.27) compared with children 6 months to 4 years of age (n = 11; mean Crt 17.5, SD 3.73) and children 5–17 years of age (n = 15; mean Crt 17.1, SD 3.74). Participants who reported ≥2 ARI symptoms (n = 35) had similar Crt values (mean 16.8, SD 4.12), compared with those reporting a single symptom (n = 9; mean Crt 16.8, SD 3.11). Household contacts with ≥2 ARI symptoms (n = 9) had lower Crt (mean 16.4, SD 5.17) compared with index cases (n = 26; mean Crt 17.0, SD 3.81) (Appendix Figure 2).

We recovered high-quality EV-D68 whole-genome sequences for ≥2 persons within a household in a total of 11 households. All sequenced samples in this study (Appendix Table 1) fell within the B3 clade with other GenBank sequences from the United States and Europe; sequences from the same household clustered closely (Figure; Appendix Figure 3). Among those 11 households, 6 had samples collected from different members (co-primary cases) on the same day and the within-household pairwise nucleotide (nt) distance between sequences was 0–1 (median 0.5) nt. In 4

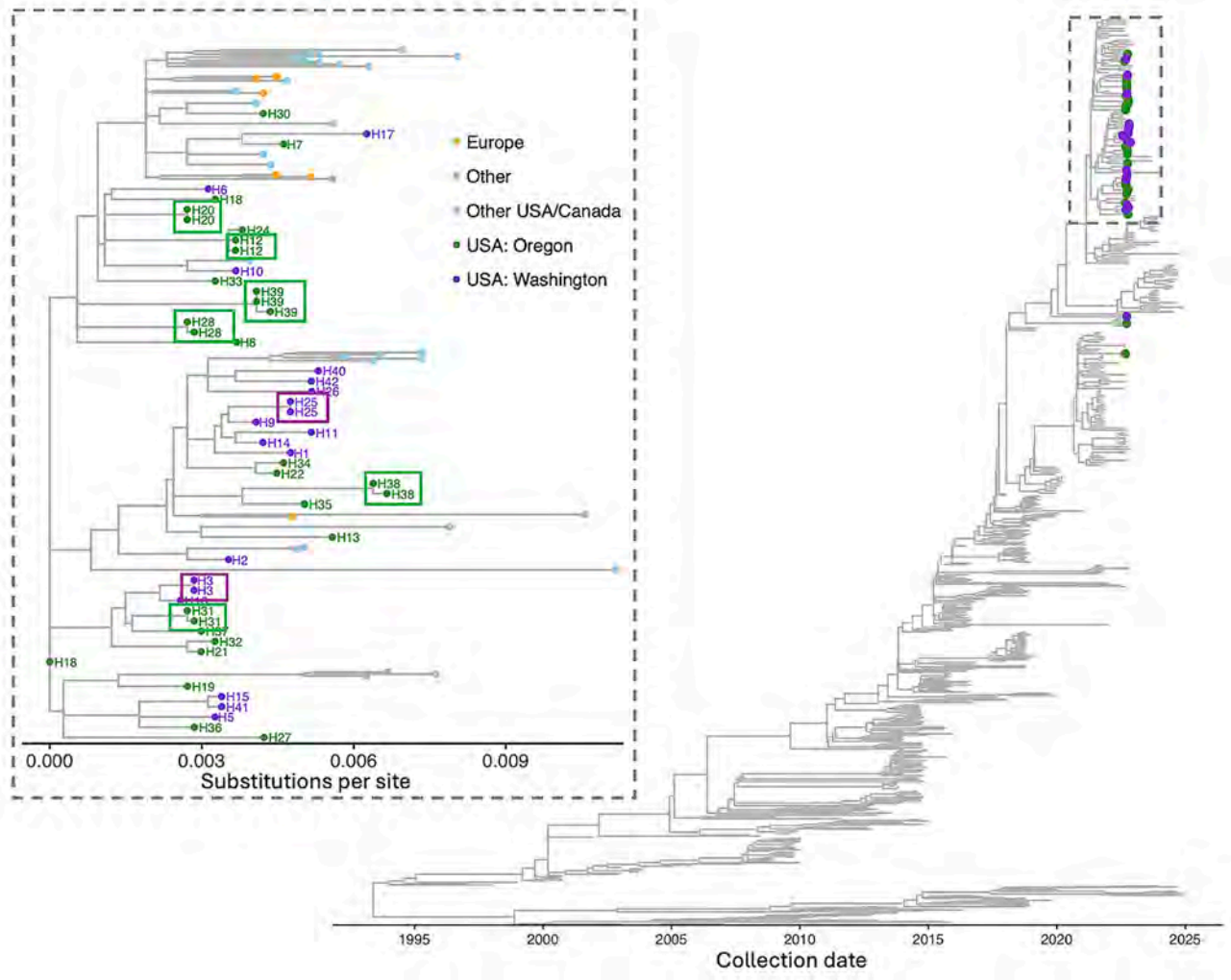


**Figure.** Maximum-likelihood time-resolved phylogenetic tree from study of household transmission of enterovirus D68, Washington and Oregon, United States, 2022–2024. Tree shows study samples from Washington (purple tips) and Oregon (green tips) and publicly available global sequences. Inset shows a divergence tree by substitutions per site. Purple and green boxes around tips highlight close clustering of sequences from the same household.

households, samples were collected 6–14 days apart; the within-household pairwise distance was 0–3 (median 1) nt. In 1 household with samples collected 148 days apart, sequences confirmed distinct introductions into the household. Among the 10 households with samples collected 0–14 days apart, sequences from children tended to be more basal in the tree relative to the sequences from adults in the same household; adult sequences contained ≥1 additional nucleotide substitutions (Appendix Figure 3), suggesting transmission from child to adult. Because we used a hybridization capture–based method for sequencing, enriching for respiratory viruses (Appendix), we identified a coinfecting pathogen in 3 samples: SARS-CoV-2 in a sample from an adult and adenovirus and human parainfluenza virus in 2 samples from children <5 years of age.

Transmission of symptomatic infection appears to be from younger school-aged children (5–12 years of age) to adults, suggesting introductions to the household from children attending school; however, we are limited by our small sample size. Other limitations of our study were the inability to precisely measure the duration of viral detection or to detect asymptomatic shedding because we collected specimens weekly and tested only swab specimens from symptomatic participants. Because participants swabbed weekly and we did not collect symptom onset dates, we were unable to report serial interval, and we could not determine the exact illness onset date. The estimated median detection interval of 7 days is slightly higher than reported serial intervals for other viruses; a reason could be that our study used weekly sampling, compared with other studies that conducted daily sampling. Our threshold of 14 days for identifying symptomatic secondary infections is supported by our genomic analysis and consistent with other studies that have estimated the duration of EV-D68 shedding in the respiratory tract (*8*); in rare cases, it might miss late transmission events.

## Conclusions

In our 2-year community respiratory virus surveillance study, we found relatively few cases of symptomatic EV-D68 in households compared with other respiratory viruses, such as RSV, in the same cohort of households during an overlapping timeframe, July–November 2022 (*10*) (Appendix Figure 4). Overall, our work adds to the body of literature on enterovirus household transmission and confirms that in households with young children, EV-D68 is a less common source of symptomatic respiratory viral illness than other pathogens such as RSV, influenza virus, and SARS-CoV-2.

This article was preprinted at https://doi.org/10.64898/2026.02.16.26346322.

### Acknowledgments

The authors thank the following individuals for supporting this study: Deralyn Almaguer, David Amy, Britt Ash, Allison Bianchi, Cassandra Boisvert, Stacy Bunnell, Joseph Cerizo, Evelin Coto, Phil Crawford, Robin Daily, Lantoria Davis, Stephen Fortmann, Kendall Frimodig, Lisa Fox, Holly Groom, Tarika Holness, Matt Hornbrook, Terry Kimes, Keelee Kloer, Dorothy Kurdyla, Bryony Melcher, John Ogden, Jennifer Rivelli, Katrina Schell, Emily Schield, Meagan Shaw, Martin Simer, Britta Torgrimson-Ojerio, Alexandra Varga, Mica Werner, Neil Yetz, Rebecca Ziebell (Kaiser Permanente Center for Health Research); Ariana Magedson, Denise McCulloch, Natalie Lo, Kyle Luiten, Devon McDonald, Sarah Cox, Jenni Logue, Melissa MacMillan, Grace Marshall, Jean Mernaugh, Daniel Nguyen, Zarna Marfatia, Amanda Casto, Chidozie Iwu, Julia Bennett, Jordan Opsahl, Kathryn McCaffrey, David Reinhart, Ben Cappodano, Sarah Heidl, Zack Acker, Lani Regelbrugge, Leslie Rodriguez-Salas, Ailyn Perez, Sean Ellis, Hanna Edgar (University of Washington); and Dallas Haws, Hanna Grioni, Josh Sanders, Irem Onalan, Laura Ostrina Restrepo (Seattle Children's Hospital).

The CASCADIA study was funded by the Centers for Disease Control and Prevention (research contract no. 75D30121C12297 to Kaiser Foundation Hospitals). The funders were not involved in the design of the study and do not have any ownership over the management and conduct of the study, the data, or the rights to publish. Computational analyses were supported by Fred Hutch Scientific Computing (National Institutes of Health Office of Research Infrastructure Programs grant no. S10OD028685) and University of Washington Laboratory Medicine Informatics. This analysis was funded by the Washington State Department of Health Northwest Pathogen Genomics Center of Excellence (WA DOH contract no. HED29377-1, federal grant no. NU50CK000630).

H.Y.C. reports consulting with Roche and Vir outside of the submitted work. P.R. reports contracts to University of Washington from Aicuris and Arisan Therapeutics outside of the submitted work. J.A.E. reports consulting with Abbvie, Ark Biopharmaceuticals, Sanofi Pasteur, Moderna, Meissa Vaccines, AstraZeneca, and Pfizer, Inc. outside of the submitted work and has received research funding from AstraZeneca, Merck, GlaxoSmithKline, and Pfizer. J.L.K. reported research funding not related to the submitted work from Pfizer, Novartis, and Vir Biotechnology. A.L.G. reports contract testing to UW from Abbott, Cepheid, Novavax, Pfizer, Janssen, and Hologic and research support from Gilead outside of the described work.

## About the Author

Dr. Roychoudhury is a research assistant professor in the Department of Laboratory Medicine and Pathology at the University of Washington and affiliate investigator in the Vaccine and Infectious Disease Division at the Fred Hutchinson Cancer Center. Her primary research interests are pathogen genomics and mathematical models of viral evolution and host-pathogen interactions.

## References

1. Clopper BR, Lopez AS, Goldstein LA, Ng TFF, Toepfer AP, Staat MA, et al. Enterovirus D68–associated respiratory illness in children. JAMA Netw Open. 2025;8:e259131. https://doi.org/10.1001/jamanetworkopen.2025.9131
2. Dyda A., Stelzer-Braid S., Adam D., Chughtai A.A., MacIntyre C.R. The association between acute flaccid myelitis (AFM) and enterovirus D68 (EV-D68)—what is the evidence for causation? Euro Surveill. 2018;23:17-00310. https://doi.org/10.2807/1560-7917.ES.2018.23.3.17-00310
3. Park SW, Pons-Salort M, Messacar K, Cook C, Meyers L, Farrar J, et al. Epidemiological dynamics of enterovirus D68 in the United States and implications for acute flaccid myelitis. Sci Transl Med. 2021;13:eabd2400. https://doi.org/10.1126/scitranslmed.abd2400
4. Midgley CM, Watson JT, Nix WA, Curns AT, Rogers SL, Brown BA, et al.; EV-D68 Working Group. Severe respiratory illness associated with a nationwide outbreak of enterovirus D68 in the USA (2014): a descriptive epidemiological investigation. Lancet Respir Med. 2015;3:879–87. https://doi.org/10.1016/S2213-2600(15)00335-5
5. Cox SN, Casto AM, Franko NM, Chow EJ, Han PD, Gamboa L, et al. Clinical and genomic epidemiology of coxsackievirus A21 and enterovirus D68 in homeless shelters, King County, Washington, USA, 2019–2021. Emerg Infect Dis. 2024;30:2250–60. https://doi.org/10.3201/eid3011.240687
6. Cassidy H, Poelman R, Knoester M, Van Leer-Buter CC, Niesters HGM. Enterovirus D68—the new polio? Front Microbiol. 2018;9:2677. https://doi.org/10.3389/fmicb.2018.02677
7. Grunnill M, Eshaghi A, Damodaran L, Nagra S, Gharouni A, Braukmann T, et al. Inferring enterovirus D68 transmission dynamics from the genomic data of two 2022 North American outbreaks. Npj Viruses. 2024;2:34. https://doi.org/10.1038/s44298-024-00047-z
8. Nguyen-Tran H, Thompson C, Butler M, Miller KR, Pyle L, Jung S, et al. Duration of enterovirus D68 RNA shedding in the upper respiratory tract and transmission among household contacts, Colorado, USA. Emerg Infect Dis. 2023;29:2315–24. https://doi.org/10.3201/eid2911.230947
9. Babu TM, Feldstein LR, Saydah S, Acker Z, Boisvert CL, Briggs-Hagen M, et al. CASCADIA: a prospective community-based study protocol for assessing SARS-CoV-2 vaccine effectiveness in children and adults using a remote nasal swab collection and web-based survey design. BMJ Open. 2023;13:e071446. https://doi.org/10.1136/bmjopen-2022-071446
10. Cox SN, Roychoudhury P, Frivold C, Acker Z, Babu TM, Boisvert CL, et al. Household transmission and genomic diversity of respiratory syncytial virus in the United States, 2022–2023. Clin Infect Dis. 2026;81:1159–69. https://doi.org/10.1093/cid/ciaf048

Address for correspondence: Pavitra Roychoudhury, University of Washington, 1100 Fairview Ave N, E5-110, Seattle WA 98109-1024, USA; email: proychou@uw.edu

# *Angiostrongylus cantonensis* Rat Lungworm Detected in Rats, Madagascar, 2022–2023

Santatriniaina F. Randrianarisoa, Elise N. Paietta, Rachel A. Johnston, Tahina T. Razanamahenina, Antsa Ramboninarimalala, Toussaint G. Raherinirina, Laurent Raveloson, Nina L. Finley, Eric Baitchman, Arvind Varsani, Fidisoa T. Rasambainarivo

*Angiostrongylus cantonensis*, the rat lungworm, is a zoonotic parasite that causes eosinophilic meningitis in humans; the parasite is maintained in rat definitive hosts and transmitted through gastropod intermediate hosts. We report *A. cantonensis* prevalence and mitochondrial genome from oral swab specimens from rats in Madagascar, supporting swabs for noninvasive detection of this parasite.

*Angiostrongylus cantonensis*, the rat lungworm, is a zoonotic nematode and a leading cause of eosinophilic meningitis in humans and other mammals (*1*). Originally described in rats in China in 1935, *A. cantonensis* lungworm is now reported in >30 countries globally (*2*). Distribution has expanded because of globalization, human activity, and range expansion of definitive and intermediate hosts (*2*,*3*).

Adult *A. cantonensis* worms inhabit the pulmonary arteries of rats (definitive hosts), including black rats (*Rattus rattus*) and brown rats (*Rattus norvegicus*), where eggs hatch into first-stage larvae shed in feces. Those larvae infect intermediate hosts such as snails and slugs, where they develop into third-stage larvae and can be transmitted via paratenic hosts (including reptiles and amphibians), where larvae can persist for extended periods, and through transient hosts (e.g., crustaceans and insects), where larvae survive for only a short time (*4*). Rats acquire infection by ingesting those hosts, completing the life cycle (*5*). Humans are infected accidentally through consumption of raw or undercooked intermediate or paratenic hosts or via contaminated food and water (*6*). After ingestion, the larvae migrate from the intestines to the brain, causing meningitis and neurologic complications (*4*,*7*).

Madagascar is one of the world's most expansive biodiversity hotspots, where humans and an exceptional diversity of endemic wildlife frequently interact with nonnative animals across the island (*8*). Although *A. cantonensis* worms have been reported in the region (*9*), genomic data and epidemiologic insights remain limited. In this study, we used metagenomic sequencing of oral swabs to characterize mitochondrial genomes and estimate prevalence of *A. cantonensis* lungworm in black rats from southeastern Madagascar.

## The Study

As part of a broader One Health study (*10*), we collected oral swab samples from 125 wild black rats that were captured, anesthetized, and euthanized during October 2022 and July 2023 in the Manombo Special Reserve (MSR), southeastern Madagascar (Figure 1, panels A, B). The samples were collected in 3 different habitats: littoral forest (n = 76 samples), lowland rainforest (n = 22 samples), and village-edge (n = 27 samples).

We conducted DNA extraction by using the Roche HighPure Viral Nucleic Acid Kit (Roche, https://www.roche.com). We followed our previously published pipeline for library preparation, sequencing, bioinformatic processing, quality trimming, de novo assembly, and contig screening by using standard tools and the National Center for Biotechnology Information (NCBI)

Author affiliations: Mahaliana Labs, Antananarivo, Madagascar (S.F. Randrianarisoa, F.T. Rasambainarivo); Duke University, Durham, North Carolina, USA (E.N. Paietta); Arizona State University, Tempe, Arizona, USA (E.N. Paietta, A. Varsani); Broad Institute, Cambridge, Massachusetts, USA (R.A. Johnston); Zoo New England, Boston, Massachusetts, USA (R.A. Johnston, E. Baitchman); University of Antananarivo, Antananarivo (T.T. Razanamahenina, A. Ramboninarimalala); Centre ValBio, Ranomafana, Madagascar (T.G. Raherinirina); Health In Harmony-Fahasalamana Mirindra, Farafangana, Madagascar (L. Raveloson, N.L. Finley); London School of Hygiene and Tropical Medicine, London, UK (N.L. Finley); University of Cape Town, Cape Town, South Africa (A. Varsani); East Carolina University, Greenville, North Carolina, USA (F.T. Rasambainarivo)

DOI: https://doi.org/10.3201/eid3207.260142

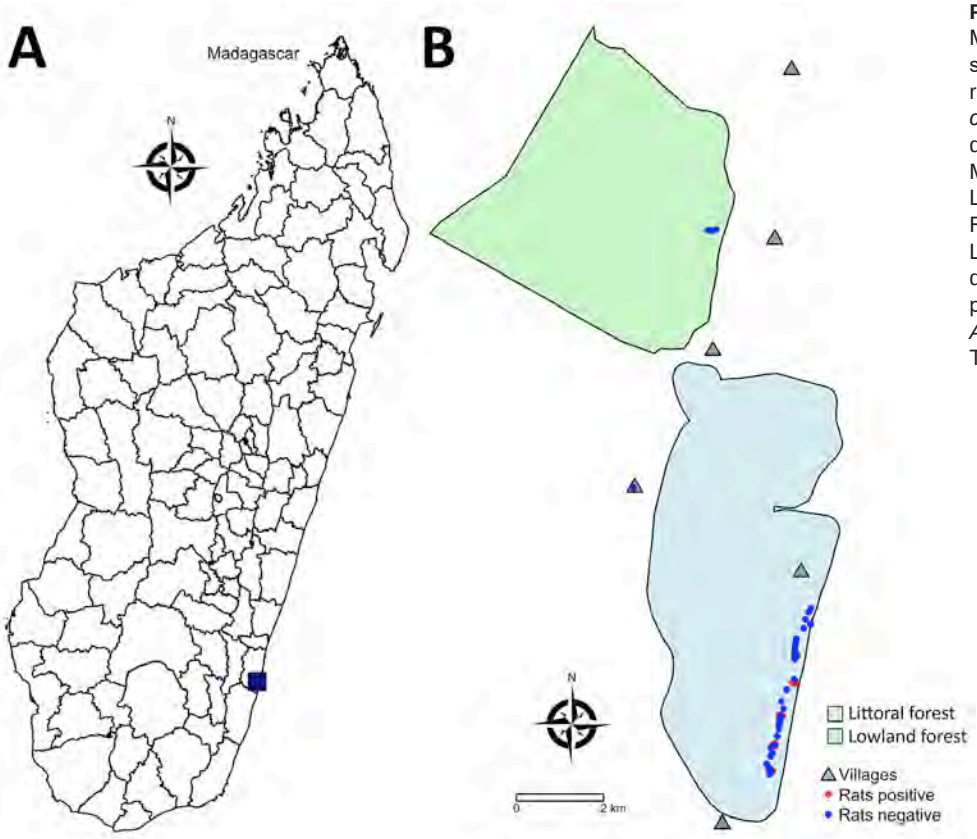


**Figure 1.** Geographic location of Manombo Special Reserve and spatial distribution of sampled rats in a study of *Angiostrongylus cantonensis* rat lungworm detection in rats in southeastern Madagascar, 2022–2023. A) Location of Manombo Special Reserve (black square). B) Locations of sampled rats; red dots indicate *A. cantonensis*–positive rats; blue dots indicate *A. cantonensis*–negative rats. Triangles indicate villages.

mitochondrial RefSeq database (*11*). We annotated mitochondrial genomes by using reference genomes of *A. cantonensis* (NCBI Sequence Read Archive accession no. GQ398121) with manual curation.

For phylogenetic analysis, we aligned complete mitochondrial genomes with publicly available *A. cantonensis* sequences. We constructed a maximum-likelihood tree by using IQ-Tree 2 (*12*) to determine the genetic relationships of our samples and haplotype placement.

Because metagenome-assembled *A. cantonensis* mitogenomes were highly similar, we mapped raw reads to a representative mitogenome by using CoverM (*13*) with a minimum read identity of 95%. We used a read coverage threshold of ≥75% to determine presence or absence of *A. cantonensis* genomes in each sample, providing a high-confidence proxy for infection status and calculated prevalence accordingly. To identify predictors of infection, we performed a generalized linear model in R version 4.4.1 (The R Project for Statistical Computing, https://www.r-project.org), testing age, sex, location, body condition, weight, and year of sampling.

All procedures were approved by Duke University Institutional Animal Care and Use committee (approval no. A075-23-03), Zoo New England ethics board, and the Madagascar Ministry of the Environment (approval nos. 286/22 and 215/23/MEDD/SG/DGGE/DAPRNE/SCBE.Re). We deposited all raw sequencing data in the NCBI Sequence Read Archive. Taxonomic classification revealed that 26.26%–51.43% of reads per sample were assigned to known taxa, including bacteria (15.01%–47.72%), eukaryotes (0.53%–4.62%), and viruses (0.04%–18.78%). Viral sequences mainly comprised anelloviruses and bacteriophages (*10*).

We detected 5 complete *A. cantonensis* mitochondrial genomes from black rat oral swab specimens, de novo assembled with high coverage (GenBank accession nos. PX571103–7) (Figure 2). All 5 mitochondrial genomes were 13,503 nt in length with 26.8% guanine and cytosine content, in comparison with published *A. cantonensis* mitogenomes that were 13,497–13,519 nt in length with 26.7%–26.8% guanine and cytosine content. The mitogenomes from Madagascar revealed 99.96%–100% sequence similarity among themselves and 96.44%–99.99% similarity compared with global sequences. Of note, the genomes from Madagascar demonstrated >99.98% similarity to sequences from Valencia, Spain (GenBank accession no. PP748572). Phylogenetic analysis placed all sequences from

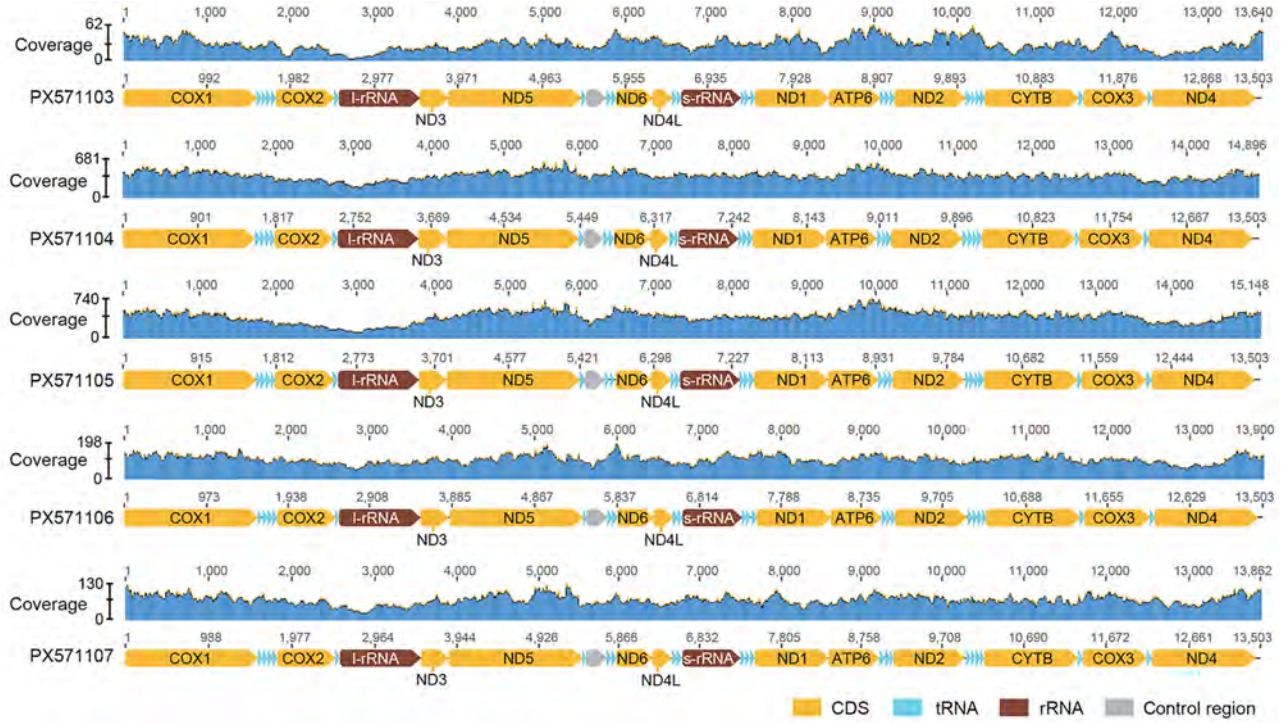


**Figure 2.** Mitochondrial genome organization and sequence coverage maps of *Angiostrongylus cantonensis* rat lungworm from black rat oral swab specimens in southeastern Madagascar, 2022–2023.

Madagascar within clade II, grouping with the Val-II haplotype and clustering with the haplotype Ac8 from Brazil (Figure 3) (*14*).

*A. cantonensis* prevalence in black rat oral swabs was determined to be 10.4% (95% CI 6.2%–16.9%; 13/125 samples). All positive rats were from the

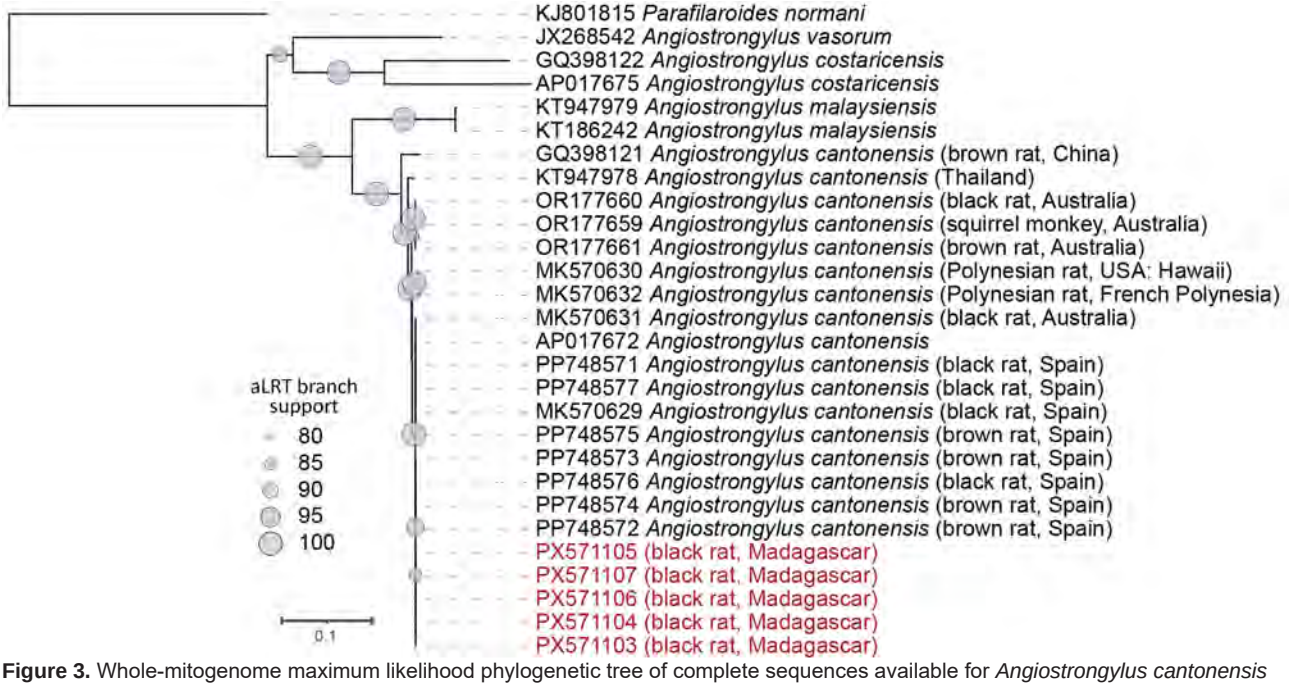


**Figure 3.** Whole-mitogenome maximum likelihood phylogenetic tree of complete sequences available for *Angiostrongylus cantonensis* rat lungworm and 3 related *Angiostrongylus* species along with the sequences identified in study of *A. cantonensis* lungworm detection in rats in Madagascar, 2022–2023. Red text indicates black rat oral swab specimens. GenBank accession numbers are indicated. For deposited sequences with available metadata, the host species and geolocation of the sample collected is included in parentheses. The tree was rooted with a representative mitogenome of *Parafilaroides normani.*

littoral forest of the MSR (Figure 1, panel B). Positive cases were detected in both sampling years, with no significant difference in prevalence between years: 9.67% (95% CI 4.5%–19.6%; 6/62) in 2022 and 11.11% (95% CI 5.5%–21.4%; 7/63) in 2023. Logistic regression analysis identified age as the only significant predictor of infection. Young rats had significantly lower odds of infection compared to adults (odds ratio 0.13, 95% CI 0.02–0.77; p = 0.03) (Table). We observed no significant associations for sex, body condition, weight, or year of sampling (Table).

**Table.** Multivariable logistic regression analysis of factors associated with *Angiostrongylus cantonensis* detection in *Rattus rattus* captured in the littoral forest in southeastern Madagascar, 2022–2023*

| Variable | Odds ratio (95% CI) | p value |
|---|---|---|
| Age | | |
| Adult | Referent | |
| Young | 0.13 (0.02–0.77) | **0.03** |
| Sex | | |
| F | Referent | |
| M | 1.13 (0.29–4.59) | 0.85 |
| Body condition, continuous | 1.97 (0.62–7.07) | 0.26 |
| Weight, continuous | 0.96 (0.93–1.00) | 0.06 |
| Year | | |
| 2022 | Referent | |
| 2023 | 0.46 (0.09–1.88) | 0.26 |

*Bold indicates statistically significant value.

## Conclusions

The 5 mitogenomes we obtained were nearly identical to each other (99.96%–100% similarity), indicating a highly conserved parasite population within the MSR littoral forest and low genetic diversity of *A. cantonensis* lungworm in Madagascar, which is similar to another report (*3*). Phylogenetic analysis further demonstrated that all the sequences cluster within clade II and specifically group with the Val-II haplotype, previously reported in Europe and associated with haplogroup Ac8 from Brazil (*14*). That pattern supports the hypothesis of recent or historical introductions mediated by human activities, particularly through the movement of invasive rats and intermediate hosts via trade and transport networks (*3*,*14*).

The overall prevalence in rats in the current study was 10.4% (95% CI 6.2%–16.9%; 13/125 rats), higher than the 2.7% prevalence previously reported in rats from central-eastern Madagascar (n = 78) (*9*). All positive rats were from the littoral forests. Host-related factors also contributed to infection patterns. Age was the only significant predictor; young rats showed markedly lower odds of infection compared with adults. That finding reflects cumulative exposure over time, because older rats have more opportunities to encounter infected intermediate or paratenic hosts (*15*). We observed no significant effects for sex, body condition, weight, or year, suggesting that exposure-driven processes might be more necessary than intrinsic host factors in shaping infection risk. No positive detections were observed in the lowland rainforest or village-edge habitats, potentially because of intermediate host distribution (*5*).

This study provides metagenomic-based mitochondrial genome characterization and prevalence estimates of *A. cantonensis* lungworm from black rats in southeastern Madagascar. Because of the parasite's life cycle, oral swab specimens likely capture first-stage larvae expelled from the respiratory tract, which are known to be present in the oral cavity during patent infections. However, because necropsy data were not systematically collected for parasitologic examination, we could not assess the relationship between larval detection in oral swab specimens and adult worm burden in the pulmonary vasculature. Future studies combining oral swab specimens with necropsy or quantitative parasitologic methods would help validate this relationship. Nevertheless, our findings demonstrate that complete *A. cantonensis* mitochondrial genomes can be recovered from oral swab specimens, supporting their use as a complementary, minimally invasive approach for molecular detection and genomic characterization of this parasite.

## Acknowledgments

We gratefully acknowledge Zoo New England for their continued funding support and dedication to One Health and biodiversity conservation research at MSR.

We also extend our appreciation to the local guides, cooks, and Madagascar National Parks staff who assisted with fieldwork during the 2022 and 2023 sampling efforts. We thank Health In Harmony-Fahasalamana Mirindra for fostering strong relationships with communities, providing communication about our research activities, and serving as an essential bridge between researchers and community members. Our sincere gratitude goes to each village's Mpanjaka (the King or Queen of the village) and the communities of all 31 villages for granting us access to their forests. We likewise acknowledge the Centre ValBio research technicians who contributed to rodent sampling in both years. We appreciate the support of the Madagascar Ministry of the Environment and Sustainable Development and the Duke University Institutional Animal Care and Use Committee for granting research permissions. Finally, we thank Madagascar Institute for the Conservation of Tropical Ecosystems, with special acknowledgment to Tiana Vololona, for their valuable assistance in coordinating research logistics and permits.

The sequences described in this study are deposited in GenBank (accession nos. PX571103–7). The raw reads for the black rat oral swab samples are deposited in the NCBI Sequence Read Archive (BioProject no. PRJNA1290322; Biosample nos. SAMN49916503, SAMN49916584, SAMN49916600, SAMN49916604, and SAMN49916608; Sequence Read Archive accession nos. SRR34496630, SRR34496775, SRR34496757, SRR34496753, and SRR34496748).

This study was supported in part by a grant from the Wild Animal Health Fund of the American Association of Zoo Veterinarians to Zoo New England and Mahaliana Labs. Additional funding for E.N.P. was provided by Duke University.

## About the Author

Dr. Randrianarisoa is a wildlife veterinarian and laboratory manager at Mahaliana Labs in Antananarivo, Madagascar. His research focuses on zoonotic pathogens, antimicrobial resistance, and wildlife health at the human–animal–environment interface in Madagascar.

## References

1. Centers for Disease Control and Prevention. *Angiostrongyliasis cantonensis*. 2019 [cited 2025 Nov 10]. https://www.cdc.gov/dpdx/angiostrongyliasis_can/index.html
2. Barratt J, Chan D, Sandaradura I, Malik R, Spielman D, Lee R, et al. *Angiostrongylus cantonensis*: a review of its distribution, molecular biology and clinical significance as a human pathogen. Parasitology. 2016;143:1087–118. https://doi.org/10.1017/S0031182016000652
3. Červená B, Modrý D, Fecková B, Hrazdilová K, Foronda P, Alonso AM, et al. Low diversity of *Angiostrongylus cantonensis* complete mitochondrial DNA sequences from Australia, Hawaii, French Polynesia and the Canary Islands revealed using whole genome next-generation sequencing. Parasit Vectors. 2019;12:241. https://doi.org/10.1186/s13071-019-3491-y
4. Galán-Puchades MT, Gómez-Samblás M, Osuna A, Sáez-Durán S, Bueno-Marí R, Fuentes MV. Update on the first finding of the rat lungworm, *Angiostrongylus cantonensis*, in *Rattus* spp. in continental Europe, Valencia, Spain, 2022. Pathogens. 2023;12:567. https://doi.org/10.3390/pathogens12040567
5. Cowie RH. Biology, systematics, life cycle, and distribution of *Angiostrongylus cantonensis*, the cause of rat lungworm disease. Hawaii J Med Public Health. 2013;72(Suppl 2):6–9.
6. Wang QP, Lai DH, Zhu XQ, Chen XG, Lun ZR. Human angiostrongyliasis. Lancet Infect Dis. 2008;8:621–30. https://doi.org/10.1016/S1473-3099(08)70229-9
7. Li T mei, Liu Y hua, Fang W, Zhao S hua, Li T, Jiang L, et al. Monitoring the trends of *Angiostrongylus cantonensis* infection in humans and *Pomacea* spp. snails in Dali, Yunnan, China, 2007–2021. PLOS Neglected Tropical Diseases. 2025;19:e0013065.
8. Rasambainarivo F, Goodman SM. Disease risk to endemic animals from introduced species on Madagascar. Fowler's Zoo and Wild Animal Medicine Current Therapy. 2019;9:292–7. https://doi.org/10.1016/B978-0-323-55228-8.00043-6
9. Maminirina LA, Bodoarison ZI, Rajerison M, Ferdinand S, Ramasindrazana B. *Angiostrongylus cantonensis* lungworms in definitive and intermediate hosts, Madagascar, 2024. Emerg Infect Dis. 2025;31:2054–6. https://doi.org/10.3201/eid3110.241741
10. Paietta EN, Johnston RA, Randrianarisoa SF, DeSisto CMM, Kraberger S, Martin D, et al. Host-anellovirus interactions in an island ecosystem: non-human primates and rodents in Madagascar harbour diverse, rich anellovirus populations. Microb Genom. 2026;12:001681. https://doi.org/10.1099/mgen.0.001681
11. Paietta EN, Randrianarisoa SF, Razanamahenina TT, Ramboninarimalala A, Raherinirina TG, Raveloson L, et al. Complete mitochondrial DNA sequences of *Eliurus webbi* and *Eliurus minor*, endemic tufted-tailed rats in Madagascar. Mitochondrial DNA B Resour. 2026;11:561–6. https://doi.org/10.1080/23802359.2026.2638673
12. Minh BQ, Schmidt HA, Chernomor O, Schrempf D, Woodhams MD, von Haeseler A, et al. IQ-TREE 2: new models and efficient methods for phylogenetic inference in the genomic era. Mol Biol Evol. 2020;37:1530–4. https://doi.org/10.1093/molbev/msaa015
13. Aroney STN, Newell RJP, Nissen JN, Camargo AP, Tyson GW, Woodcroft BJ. CoverM: read alignment statistics for metagenomics. Bioinformatics. 2025;41:btaf147. https://doi.org/10.1093/bioinformatics/btaf147
14. Gómez-Samblás M, Navarro-Dominguez B, Sáez-Durán S, Osuna A, Bueno-Marí R, Galán-Puchades MT, et al. Analysis of the mitochondrial genome to determine the origins and pathways of entry of *Angiostrongylus cantonensis* in continental Europe (Valencia, Spain). Parasitology. 2024;151:1364–70. https://doi.org/10.1017/S0031182024001318
15. Rivory P, Bedoya-Pérez M, Ward MP, Šlapeta J. Older urban rats are infected with the zoonotic nematode *Angiostrongylus cantonensis*. Curr Res Parasitol Vector Borne Dis. 2024;5:100179. https://doi.org/10.1016/j.crpvbd.2024.100179

Address for correspondence: Santatriniaina F. Randrianarisoa, Mahaliana Labs, Lot II B 55 G Amboditsiry, Antananarivo 101, Madagascar; email: santatrarandria6@gmail.com

# New World Ocular Dirofilariasis Caused by *Dirofilaria repens* Infection, United States

Ben J. Glasgow, Mackenzie Collins, Luke Helminiak, Joshua A. Lieberman, Blaine A. Mathison, Shangxin Yang

Author affiliations: University of California Los Angeles David Geffen School of Medicine, Los Angeles, California, USA (B.J. Glasgow, M. Collins, L. Helminiak, S. Yang); University of Washington, Seattle, Washington, USA (J.A. Lieberman); ARUP Laboratories and University of Utah, Salt Lake City, Utah, USA (B.A. Mathison)

DOI: https://doi.org/10.3201/eid3207.251596

We describe an infection caused by *Dirofilaria repens* nematodes in California, USA. A firm nodule developed after an insect bite on a patient's eyelid. Excision with morphologic and molecular analysis confirmed *D. repens* infection. Our findings confirm the necessity of both molecular and histological studies to identify nematode infections.

Dirofilariasis is caused by *Dirofilaria* (family Onchocercidae) nematodes. Old World infections are commonly caused by *Dirofilaria repens* nematodes. New World infections are generally caused by species other than *D. repens*, such as *D. immitis*, *D. tenuis*, *D. subdermata*, *D. striata*, and *D. ursi* (*1*). Canids, felids, and raccoons are the definitive hosts for most zoonotic infections, and mosquitoes serve as intermediate vectors. In humans, ocular dirofilariasis, which includes eyelid, subconjunctival, orbital, and intraocular infections, accounts for ≤35% of all cases (*2*). The eyelid and orbit are the sites of ≈42% of ocular dirofilariasis cases (*3*). The species causing ocular dirofilariasis have distinct geographic associations (*3*). We describe ocular dirofilariasis caused by *D. repens* nematodes in California, USA.

A 74-year-old man from California was bitten by an insect on his left lower eyelid. Initially, he experienced transient pain, swelling, and weeping at the wound. Six weeks later, his dermatologist noted an 8-mm diameter, firm, nontender subcutaneous nodule at this site. The patient had no medical history or recent travel of note. After referral to an ophthalmologist, magnetic resonance imaging of the orbits confirmed a well-circumscribed cystic lesion on the eyelid (Figure 1, panel A). The mass persisted for 5 months, and an excisional biopsy was performed. The mass was dissected from closely adherent surrounding tissue and submitted to pathology in formalin. The patient was asymptomatic 6 months after the surgery.

The tissue was processed routinely and sectioned after paraffin embedding. Microscopy revealed a parasite surrounded by fibrosis with marked chronic inflammation. The cross section of the parasite revealed features of a nematode consistent with *Dirofilaria* sp. (Figure 1, panel B).

The formalin-fixed paraffin-embedded tissue was sent to the University of Washington Reference Laboratories (Seattle, WA, USA) for species identification, where we conducted broad-range 28S and internal transcribed spacer (ITS) rDNA PCR and sequencing (*4*). We detected *D. repens* DNA. We conducted an in-house ITS-based targeted next-generation sequencing assay on the same formalin-fixed paraffin-embedded

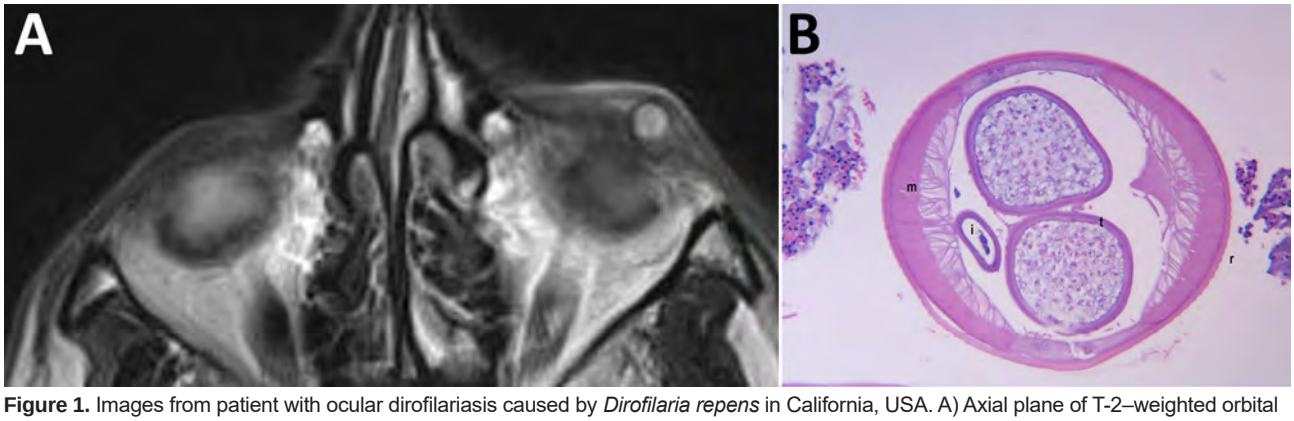


**Figure 1.** Images from patient with ocular dirofilariasis caused by *Dirofilaria repens* in California, USA. A) Axial plane of T-2–weighted orbital magnetic resonance imaging revealing a well circumscribed cystic lesion in the left lower eyelid. The center of the lesion is hyperintense and circumscribed by a hypointense signal. The interpretation was a benign inflammatory lesion. B) Histopathologic image from hematoxylin and eosin–stained slide that reveals a 500-micron diameter cross section of a nematode with a thick cuticular wall featuring external cuticular ridges (indicated by r) and vertically oriented muscle (indicated by m) extending toward the internal cavity (coelomyarian) that are numerous per quadrant (polymyarian), as well as paired reproductive tubes (indicated by t), and simple intestine (indicated by i).

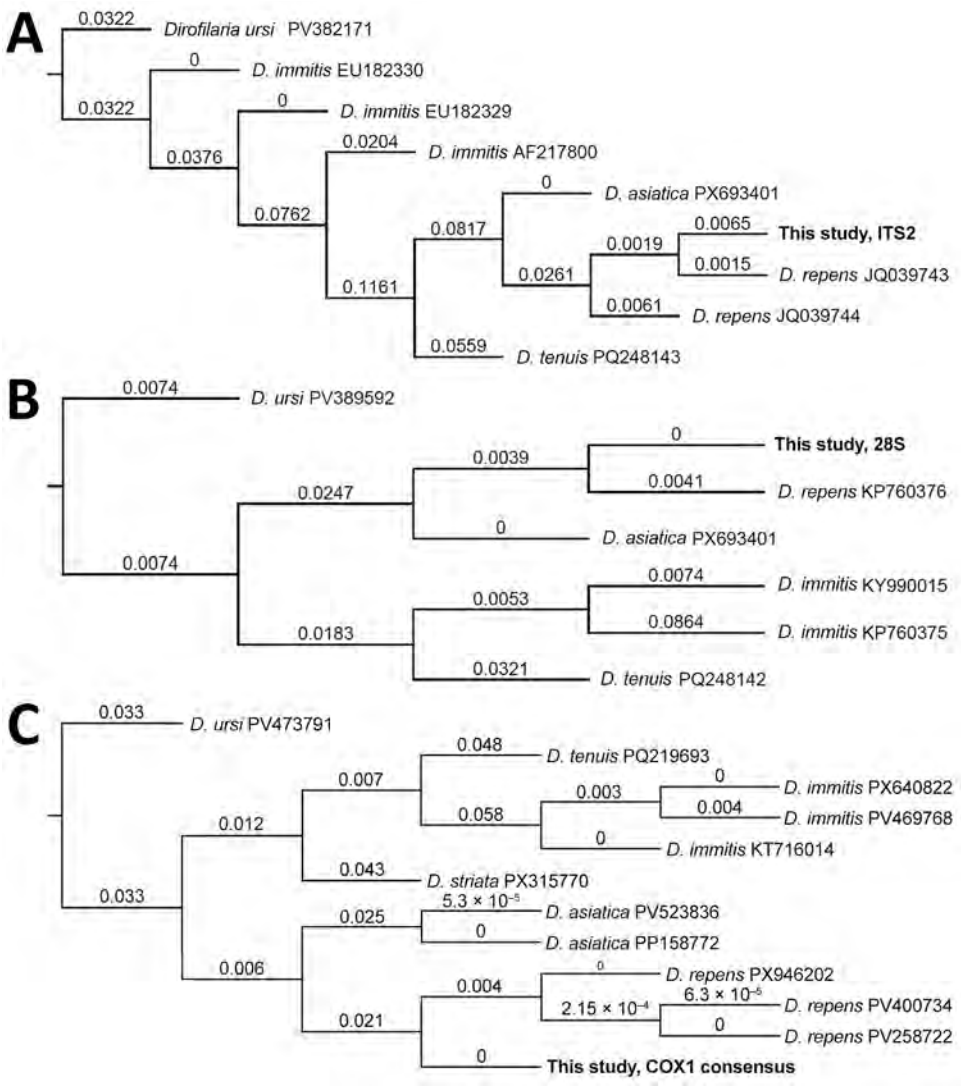


**Figure 2.** *Dirofilaria repens* phylogenetic trees from study of ocular dirofilariasis in California, USA. A) ITS gene sequences; B) 28S gene sequences; C) COX1 gene sequences. All 3 marker gene comparisons confirmed the study sample belonged to *D. repens*. Genbank accession numbers are indicated. Branch numbers indicate nucleotide substitutions per site. ITS, internal transcribed spacer.

tissue, as previously described (*5*), confirming the species as *D. repens*. The ITS sequence matched reference sequences from GenBank with 100% pairwise identity. In addition, we conducted shotgun sequencing by using Illumina Miseq (Illumina, https://www.illumina.com) to acquire more genetic information about the parasite. We submitted raw sequence reads to Chan Zuckerberg ID (https://czid.org) for metagenomic analysis, gathering reads aligning to *Dirofilaria* species. We generated consensus sequence of the COX1 gene by mapping the aligned reads to a *D. repens* mitochondrial DNA reference (GenBank accession no. KX265049). We conducted phylogenetic analysis on the basis of all 3 marker genes (ITS, 28S, and COX1), which further confirmed the species identification (Figure 2).

The identification of *D. repens* infection in the United States is noteworthy because of the parasite's previous absence. Microfilariae of *D. repens* have been reported in ring-tailed coati in Brazil and Chile (*6*,*7*). A nationwide survey of domestic hosts in the United States identified *D. immitis* parasites in 6.3% of 1,080 dogs and 0.3% of 1,254 cats, but all samples were negative for *D. repens* parasites (*8*). The case-patient's chronology of infection is consistent with the development of infective third-state larvae into juvenile worms, ≈50 days (2). Infection from a domestic host is likely. The recently increased population of *Aedes* mosquitoes in southern California might have contributed, but the lack of available *D. repens* surveys in wildlife hosts from California hampers conclusive findings.

Most cases of ocular dirofilariasis and all previous cases of dirofilariasis infections of the eyelid reported in the United States were attributed to *D. tenuis* infection (*3*). *D. repens* is the most common

infection of the eyelid in the Old World, with only rare cases of *D. asiatica* infection reported (*9*). Various species share common characteristics including a multilayered cuticle, coelomyarian or polymyarian muscle cells, simple intestine, paired sterile reproductive tubes, and internal lateral ridges (*3*). *D. tenuis* and *D. repens* nematodes both have external ridges, which *D. immitis* nematodes lack. For cases in which speciation was on the basis of morphologic assessment alone, we cannot exclude possible errors.

Most previous *D. repens* eyelid infections were localized and did not result in patent infection. Young adult nematodes are usually seen in the human, an unsuitable or accidental host. Of note, rare exceptions exist in which the worm was able to mature subcutaneously and produce microfilariae (*10*).

Eyelid dirofilariasis frequently masquerades as other entities, such as a neoplasm, chalazion, or benign cyst. In this case, a chalazion was suspected. Prior cases in the literature of dirofilariasis have shown similar cystic changes with enhancement on magnetic resonance imaging (Figure 1). Other parasitic infections, such as cysticercosis, leishmaniasis, and rarely loiasis, can produce single eyelid cysts.

We report a case of *D. repens* human infection in California, USA. Suspicion of this disorder is predicated on a careful history of the environment with mosquitos, raccoons, canids, or felids. The identification of *D. repens* nematodes in the United States warrants continued surveillance. Careful histologic examination and molecular studies are critical for parasite identification.

The consensus COX1 gene sequence was deposited to into GenBank (accession no. PZ357936).

This study was supported by the Edith and Lew Wasserman Professorship in Ophthalmology awarded to B.J.G.

## About the Author

Dr. Glasgow is an eye pathologist at the Jules Stein Eye Institute, University of California, Los Angeles, California, USA. His research interests include ocular diseases.

## References

1. Dantas-Torres F, Otranto D. Dirofilariosis in the Americas: a more virulent *Dirofilaria immitis?* Parasit Vectors. 2013;6:288. https://doi.org/10.1186/1756-3305-6-288
2. Simón F, Siles-Lucas M, Morchón R, González-Miguel J, Mellado I, Carretón E, et al. Human and animal dirofilariasis: the emergence of a zoonotic mosaic. Clin Microbiol Rev. 2012;25:507–44. https://doi.org/10.1128/CMR.00012-12
3. Camacho M, Antonietti M, Sayegh Y, Colson JD, Kunkler AL, Clauss KD, et al. Ocular dirofilariasis: a clinicopathologic case series and literature review. Ocul Oncol Pathol. 2024;10:43–52. https://doi.org/10.1159/000533340
4. Cao XZ, Mi TY, Li L, Vermeer MA, Zhang CC, Huang N, et al. HPLC-FLD determination of NBD-cholesterol, its ester and other metabolites in cellular lipid extracts. Biomed Chromatogr. 2013;27:910–5. https://doi.org/10.1002/bmc.2881
5. Larkin PMK, Lawson KL, Contreras DA, Le CQ, Trejo M, Realegeno S, et al. Amplicon-based next-generation sequencing for detection of fungi in formalin-fixed, paraffin-embedded tissues: correlation with histopathology and clinical applications. J Mol Diagn. 2020;22:1287–93. https://doi.org/10.1016/j.jmoldx.2020.06.017
6. Moraes MFD, da Silva MX, Magalhães-Matos PC, de Albuquerque ACA, Tebaldi JH, Mathias LA, et al. Filarial nematodes with zoonotic potential in ring-tailed coatis (*Nasua nasua* Linnaeus, 1766, Carnivora: Procyonidae) and domestic dogs from Iguaçu National Park, Brazil. Vet Parasitol Reg Stud Reports. 2017;8:1–9. https://doi.org/10.1016/j.vprsr.2017.01.003
7. López J, Valiente-Echeverría F, Carrasco M, Mercado R, Abarca K. Morphological and molecular identification of canine filariae in a semi-rural district of the Metropolitan Region in Chile [in Spanish]. Rev Chilena Infectol. 2012;29:248–89. https://doi.org/10.4067/S0716-10182012000300006
8. Smith R, Murillo DFB, Chenoweth K, Barua S, Kelly PJ, Starkey L, et al. Nationwide molecular survey of *Dirofilaria immitis* and *Dirofilaria repens* in companion dogs and cats, United States of America. Parasit Vectors. 2022;15:367. https://doi.org/10.1186/s13071-022-05459-5
9. Tirakunwichcha S, Sansopha L, Putaporntip C, Jongwutiwes S. Case report: an eyelid nodule caused by *Candidatus* Dirofilaria hongkongensis diagnosed by mitochondrial 12s rrna sequence. Am J Trop Med Hyg. 2021;106:199–203. https://doi.org/10.4269/ajtmh.21-0800
10. Blaizot R, Receveur MC, Millet P, Otranto D, Malvy DJM. Systemic infection with *Dirofilaria repens* in southwestern France. Ann Intern Med. 2018;168:228–9. https://doi.org/10.7326/L17-0426

Address for correspondence: Ben J. Glasgow, University of California Los Angeles David Geffen School of Medicine, 100 Stein Pl, Los Angeles, CA 90095, USA; email: bglasgow@mednet.ucla.edu

# Human Pulmonary Dirofilariasis, North Queensland, Australia, 2023[1]

Kimberley Murray, Emily Grahn, Andrew Stacey, Carly Hughes, Harsha Sheorey, Constantin Constantinoiu, Leslie Kuma, Richard S. Bradbury

Author affiliations: Townsville University Hospital, Townsville, Queensland, Australia (K. Murray, A. Stacey, C. Hughes, L. Kuma); James Cook University, Townsville (E. Grahn, C. Hughes, C. Constantinoiu, R.S. Bradbury); St Vincent's Hospital Melbourne, Melbourne, Victoria, Australia (H. Sheorey); Royal Melbourne Hospital, Melbourne (H. Sheorey).

DOI: https://doi.org/10.3201/eid3207.260280

*Dirofilaria* nematodes, a common cause of canine filarial disease, are increasingly recognized as emerging human pathogens. We report a case of human pulmonary dirofilariasis in the lung of a man from Northern Australia with pulmonary adenocarcinoma. This case highlights the risk for zoonotic transmission in regions with high canine heartworm prevalence.

*Dirofilaria immitis* is a mosquitoborne filarial nematode that causes canine filarial disease. Although this parasite primarily affects canids, human dirofilariasis caused by several canine *Dirofilaria* spp. nematodes are increasingly being reported, especially in Europe and Asia (*1*-*4*). Humans are accidental hosts for *D. immitis* nematodes and become infected after the bite of a mosquito carrying *D. immitis* larvae. Larvae migrate through the circulatory system and die within the pulmonary vasculature, where they infarct small vessels, leading to a surrounding pulmonary granuloma (*5*). Those granulomatous nodules are often diagnosed incidentally on routine chest radiography and appear as single or multiple 0.5–4.5 cm round, dense, and opaque coin lesions in the lungs, which can be mistaken for primary or metastatic pulmonary malignancy (*1*,*5*).

Human pulmonary dirofilariasis (HPD) caused by *D. immitis* infection is typically asymptomatic and self-limiting, and specific treatment is generally not necessary (*1*). Most cases of HPD are asymptomatic; wheezing, cough, hemoptysis, fever, chest pain, arthralgia, and malaise can develop (*1*). HPD is rarely reported (*2*,*3*), possibly underdiagnosed (*3*), and commonly misdiagnosed (*1*,*3*). We describe a case of HPD caused by *D. immitis* infection, identified incidentally in conjunction with primary pulmonary adenocarcinoma.

The male patient was 75 years of age and living in the tropical city of Townsville, Queensland, Australia; he was seen at a trauma visit in 2023. He reported a 100 pack/year smoking history, an occupational exposure to asbestos and silica, and a chronic and nonproductive cough. During his visit, imaging revealed a spiculated mass lesion measuring 35 × 28 mm in the right upper lobe that obstructed the posterior segmental bronchus and was closely associated with a separate nodule.

The patient underwent a right upper lobectomy and mediastinal lymph node sampling for suspected primary pulmonary malignancy. Histopathologic and immunohistochemical evaluation of the pulmonary nodule confirmed a 34-mm solid-predominant primary adenocarcinoma. Gross dissection of the specimen revealed an additional nodule (Figure 1). Initial findings suggested multifocal disease; microscopy of the sample revealed a helminthic co-infection. We sought consultation for helminth characterization. The morphology of the worm within the second granulomatous nodule was most consistent with *D. immitis* (Figure 2). No further intervention was required for the *Dirofilaria* infection, although the patient continued management of the lung carcinoma.

Identification of the helminthic parasite relied on characteristic morphologic features because DNA extraction and sequencing from the paraffin embedded specimen was not possible. However, *D. immitis* is the only canine *Dirofilaria* species known to occur in Australia (*6*,*7*). *D. roemeri*, a parasite of kangaroos and wallabies, is found in Queensland but is morphologically distinct in histological cross-sections (*5*,*7*).

Human infection remains rare in Australia; only 19 cases of *D. immitis*–related HPD were reported through 2012 (*3*), and only 1 additional case has been published since, also from North Queensland (*8*). A recent serosurvey of shelter dogs in Townsville revealed a high prevalence of *D. immitis* infection (≤32%) (*9*), which could lead to increased zoonotic transmission.

*D. immitis* nematodes infect not only domestic dogs and cats but also wild canids (*2*). The widespread prevalence of heartworm in domestic dogs in Townsville might be attributable to dingoes (wild dogs of Australia) being common in bushland on the urban fringe of the city. Dingoes likely act as a sylvatic reservoir for infection of domestic dogs in Townsville (*9*). Previous necropsy surveillance studies of dingoes

[1]This case was presented at the 2024 Royal College of Pathologists of Australasia Pathology Update Conference; Adelaide, Australia; 2024 Mar 1–3.

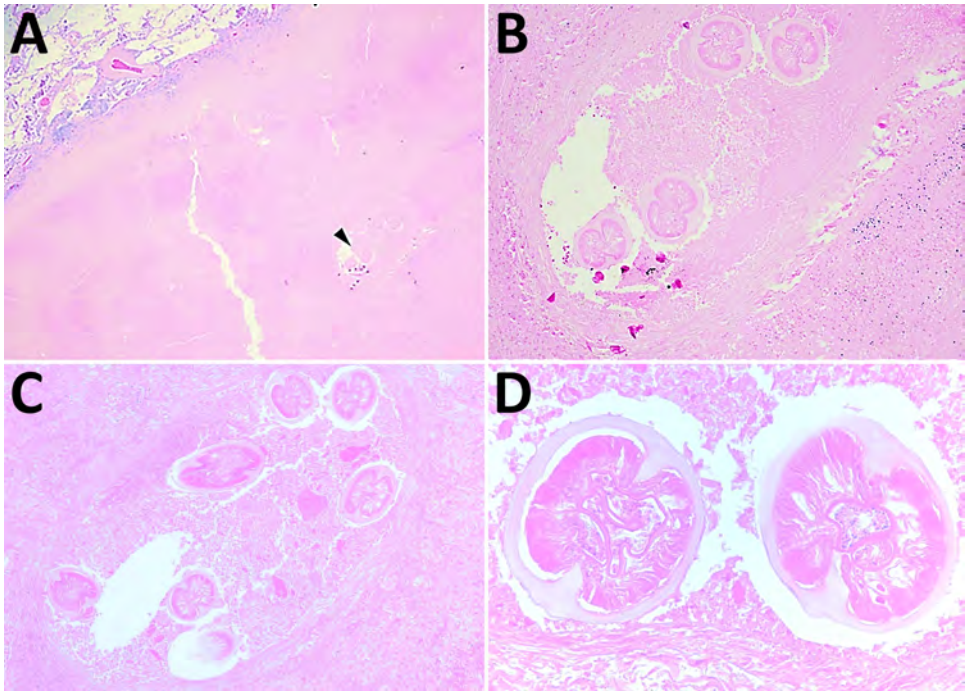


**Figure 1.** *Dirofilaria* organisms recovered from a patient with human pulmonary dirofilariasis in North Queensland, Australia, 2023. A) Degenerate *D. immitis* nematode (black arrow) within a necrotic human lung granuloma and adjacent parenchyma. Original magnification ×2. B, C) Deeper cuts of the same region at 100× magnification. D) Cross-section of 2 regions of the coiled worm at 400× magnification. Hematoxylin and eosin stains.

from the Townsville area found a heartworm prevalence of 75% (*9*).

We describe a case of *D. immitis* HPD in conjunction with primary adenocarcinoma. Similar coincidental findings of *D. immitis* infection and concurrent lung cancer have been previously reported in Texas, USA (*6*). Although those diagnoses were incidental, the overlapping clinical and radiologic features of lung cancer and pulmonary dirofilariasis pose a diagnostic challenge for clinicians and radiologists. Our report highlights the importance of preresection biopsy, meticulous gross dissection, and histologic sampling of the resection specimen for accurate diagnosis. Without those steps, the entire necrotic mass could have been included in the tumor measurement, potentially altering the tumor-nodes-metastasis stage and the associated prognosis.

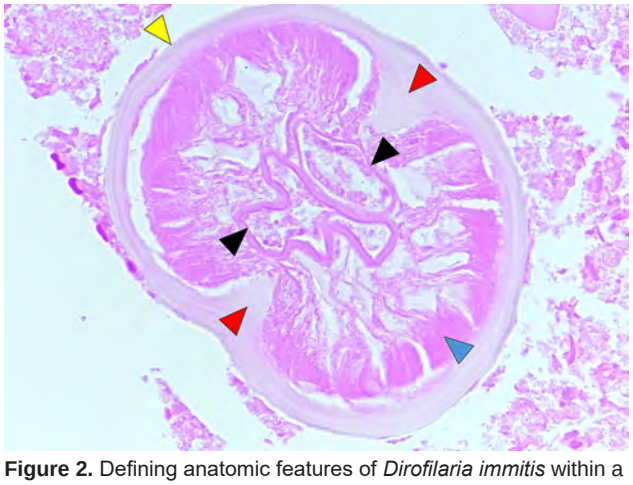

**Figure 2.** Defining anatomic features of *Dirofilaria immitis* within a small blood vessel (arteriole) in a necrotic human lung granuloma, recovered from a patient with human pulmonary dirofilariasis in Queensland, Australia, 2023. Yellow arrowhead indicates inflated necrotic smooth cuticle, without cuticular ridges; blue arrowhead indicates degenerate coelomyarian muscle structure; red arrows indicate inflated and necrotic internal cuticular ridges; and black arrows indicate degenerate paired uterine tubes. Hematoxylin and eosin stain; original magnification is ×600.

Clinicians, radiologists, and pathologists practicing in regions where canine heartworm is endemic should consider HPD in the differential diagnosis of pulmonary nodules. This case adds to the limited literature describing HPD caused by *D. immitis* nematodes in Australia and highlights the value of a One Health approach when evaluating emerging zoonotic infections in an endemic setting.

## About the Author

Dr. Murray is a senior anatomical pathology trainee currently completing her specialist training with Queensland Health. Her interests include soft tissue, pulmonary, and neuropathology conditions.

## References

1. Saha BK, Bonnier A, Chong WH, Chieng H, Austin A, Hu K, et al. Human pulmonary dirofilariasis: a review for the clinicians. Am J Med Sci. 2022;363:11–7. https://doi.org/10.1016/j.amjms.2021.07.017
2. Perles L, Dantas-Torres F, Krücken J, Morchón R, Walochnik J, Otranto D. Zoonotic dirofilariases: one, no one, or more than one parasite. Trends Parasitol. 2024;40:257–70. https://doi.org/10.1016/j.pt.2023.12.007

3. Simón F, Siles-Lucas M, Morchón R, González-Miguel J, Mellado I, Carretón E, et al. Human and animal dirofilariasis: the emergence of a zoonotic mosaic. Clin Microbiol Rev. 2012;25:507–44. https://doi.org/10.1128/CMR.00012-12
4. Colella V, Young ND, Manzanell R, Atapattu U, Sumanam SB, Huggins LG, et al. *Dirofilaria asiatica* sp. nov. (Spirurida: Onchocercidae)—defined using a combined morphological-molecular approach. Int J Parasitol. 2025;55:461–74. https://doi.org/10.1016/j.ijpara.2025.04.006
5. Orihel TC, Ash LR. Parasites in human tissues. Chicago: ASCP Press; 1995.
6. Mulanovich EA, Mulanovich VE, Rolston KVI. A case of *Dirofilaria* pulmonary infection coexisting with lung cancer. J Infect. 2008;56:241–3. https://doi.org/10.1016/j.jinf.2008.01.007
7. Spratt DM. Histological morphology of adult *Dirofilaria roemeri* and anatomy of the microfilaria. Int J Parasitol. 1972;2:193–200. https://doi.org/10.1016/0020-7519(72)90006-9
8. Theodore SG, Sawkins HJ, Mathew M, Yadav S, Norton R. Human pulmonary dirofilariasis: an unexpected differential diagnosis for a solitary lung lesion. Med J Aust. 2023;219:455–6. https://doi.org/10.5694/mja2.52115
9. Constantinoiu C, Croton C, Paterson MBA, Knott L, Henning J, Mallyon J, et al. Prevalence of canine heartworm infection in Queensland, Australia: comparison of diagnostic methods and investigation of factors associated with reduction in antigen detection. Parasit Vectors. 2023;16:63. https://doi.org/10.1186/s13071-022-05633-9

Address for correspondence: Richard Bradbury, PHTM, Building 41, James Cook University, 1 James Cook Dr, Townsville, QLD 4814, Australia; email: richard.bradbury@jcu.edu.au

# Detection of and Early Genomic Insights into Chikungunya Virus, Bolivia, 2025

Joel Alejandro Chuquimia Valdez,[1] Natalia R. Guimarães,[1] Vagner Fonseca,[1] Cleidy Orellana Mendoza, Sebastián Sasías Martínez, Sara Cândida F. Santos, Gilson Carlos Soares, Mariela Martínez Gómez, Leticia Franco, Lionel Gresh, Jairo Méndez-Rico, Luiz Carlos J. Alcantara,[2] Marta Giovanetti,[2] Leidy Roxana Loayza Mafayle[2]

Author affiliations: Centro Nacional de Enfermedades Tropicales, Santa Cruz de la Sierra, Bolivia (J.A.C. Valdez, C.O. Mendoza, S.S. Martinez, L.R. Loayza Mafayle); Fundação Ezequiel Dias, Belo Horizonte, Brazil (N.R. Guimarães, S.C.F. Santos); Instituto René Rachou, Belo Horizonte (N.R. Guimarães, S.C.F. Santos, L.C.J. Alcantara); Universidade do Estado da Bahia, Salvador, Brazil (V. Fonseca); Stellenbosch University, Stellenbosch, South Africa (V. Fonseca); Universidade Federal de Minas Gerais, Belo Horizonte, (S.C.F. Santos, G.C. Soares); Pan American Health Organization, Washington, DC, USA (M. Martínez Gómez, L. Franco, L. Gresh, J. Méndez-Rico); Università Campus Bio-Medico di Roma, Rome, Italy (M. Giovanetti); Instituto Oswaldo Cruz, Rio de Janeiro, Brazil (M. Giovanetti).

DOI: https://doi.org/10.3201/eid3207.260540

We report the detection and genomic characterization of chikungunya virus, an arbovirus, during a 2025 outbreak in Bolivia. We identified the circulating chikungunya virus lineage and the transmission dynamics by using genomic surveillance and phylogenetic analyses. Our findings highlight the utility of sustained genomic surveillance for monitoring emerging arboviruses.

Chikungunya virus (CHIKV) is a positive-sense RNA virus belonging to the genus *Alphavirus* (family Togaviridae), primarily transmitted by *Aedes aegypti* and *A. albopictus* mosquitoes. CHIKV is comprised of 3 major lineages: West African, Asian, and East/Central/South African (ECSA). The Asian lineage was introduced into the Americas in 2013, and the ECSA lineage was introduced in 2014. Those introductions gave rise to the Asian-American and ECSA-American sublineages (*1*). Chikungunya infection is typically characterized by acute febrile illness with polyarthralgia, although severe manifestations, including neurologic complications, can occur (*1*). Globally, CHIKV has expanded greatly, with an estimated 16.9 million cases annually and >5.6 billion persons living in at-risk areas (*1*). The Asian-American lineage was first detected in Bolivia in 2015, followed by outbreaks in 2016 and 2017 (*2*). In 2025, a major CHIKV outbreak took place in Bolivia after several years without any reported cases. That outbreak included 4,696 confirmed cases, and most cases (90.8%) were in Santa Cruz (*3*). This resurgence highlights the vulnerability of previously affected regions to new CHIKV outbreaks and underscores the need for sustained surveillance.

This work is part of the routine arbovirus genomic surveillance implemented in Bolivia. Samples used in this study were obtained anonymously from

[1]These first authors contributed equally to this article.
[2]These senior authors contributed equally to this article.

material exceeding routine arbovirus diagnostics within Bolivia's public health laboratory network. To investigate the origin and transmission dynamics of the 2025 outbreak, we implemented genomic surveillance of CHIKV in Bolivia. We selected 78 quantitative reverse transcription PCR–positive samples (cycle threshold [Ct] ≤30), collected from February–June 2025 from 4 departments (Chuquisaca, Cochabamba, Santa Cruz, and Tarija) for our analysis on the basis of Ct value and available metadata (Figure 1).

We used a multiplex PCR approach to amplify CHIKV RNA (*4*), and we sequenced CHIKV by using Illumina (Illumina, https://www.illumina.com) and Oxford Nanopore (Oxford Nanopore, https://nanoporetech.com) platforms. We generated consensus genomes by using combined de novo and reference-based approaches (*5*). We conducted a phylogenetic analysis by using genomes from the 78 selected samples together with the 972 publicly available ECSA sequences from the National Center for Biotechnology Information database, which included complete sequences, sampling date, and geographic origin. We performed multiple sequence alignment by using MAFFT (*6*), and we inferred maximum-likelihood phylogenies by using IQ-TREE (*7*). We assessed temporal signal by using root-to-tip regression, yielding a correlation coefficient of 0.52, consistent with sufficient temporal structure for molecular clock inference (*8*). We performed time-scaled phylogeographic reconstruction by using BEAST (*9*) under a relaxed molecular clock model, with an estimated mean evolutionary rate of 2.18 × $10^{-3}$ substitutions/site/year.

Samples were collected from patients 0–90 years of age, with the highest proportion of samples from patients 0–9 years of age (19.2%, n = 15), followed by samples from patients 20–29 years of age (16.7%, n = 13), and 30–39 years of age (16.7%, n = 13). Most (52.6%, n = 41) samples were from female patients (Appendix 1 Figure 1, http://wwwnc.cdc.gov/EID/article/32/7/26-0540-App1.pdf; Appendix 2 Table, http://wwwnc.cdc.gov/EID/article/32/7/26-0540-App2.xlsx). Most patients had acute febrile illness (n = 60), and 18 cases were classified as severe, including 1 encephalitis case and 1 fatal outcome (Appendix 1 Figure 2).

The sequenced samples had Ct values ranging from 10 to 28 (mean 18.5) (Appendix 1 Figure 3). Sequencing generated 78 near-complete CHIKV genomes with an average genome coverage of 95.9%. All genomes were classified as the ECSA lineage. All CHIKV genomes from Bolivia formed a well-defined monophyletic clade, with the closest ancestry linked to viruses circulating in Midwest Brazil

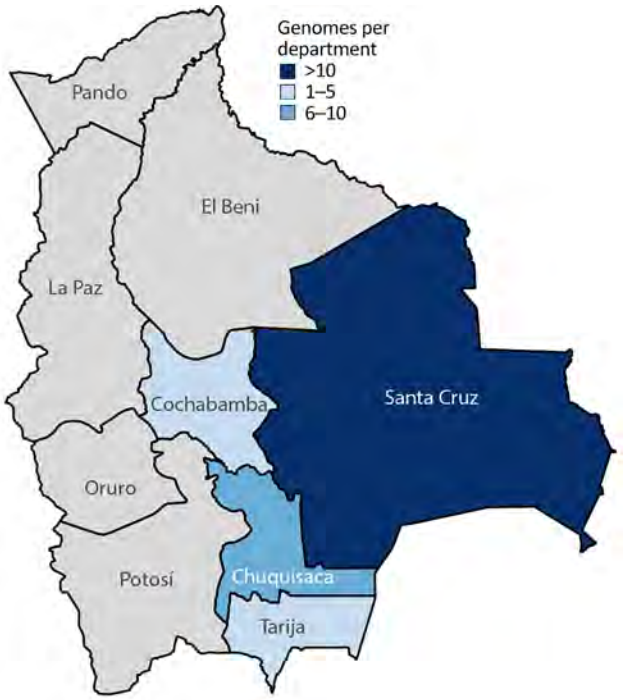


**Figure 1.** Geographic distribution of sequenced chikungunya virus genomes in a study of chikungunya virus in Bolivia, 2025. Colors indicate the numeric range of genomes per department.

(Figure 2, panel A). This genomic analysis suggests that the 2025 CHIKV outbreak in Bolivia was driven by a single introduction event followed by sustained local transmission. Time-scaled phylogeographic analysis estimated CHIKV introduction around November 2024 (95% CI late October–early November). The earliest transmission was inferred in Chuquisaca, followed by dissemination to Santa Cruz and subsequent spread to Tarija and Cochabamba (Figure 2, panel B). The inferred directional spread toward more densely populated regions further supports the role of human mobility and urban transmission networks in enabling rapid geographic expansion (*10*).

Our results reveal the genetic similarity of CHIKV strains circulating in Bolivia during the 2025 outbreak and provides evidence indicating a single introduction of CHIKV from Midwest Brazil, with subsequent spread across multiple departments. Our findings improve our knowledge of CHIKV transmission dynamics in Bolivia; however, limitations in temporal and geographic sampling coverage might have limited full characterization of viral diversity. Our findings also demonstrate how integrating genomic surveillance into outbreak investigations enables identification of introduction events and reconstruction of transmission pathways, providing critical insights to inform public health interventions. Because of increasing arboviral activity across the Americas,

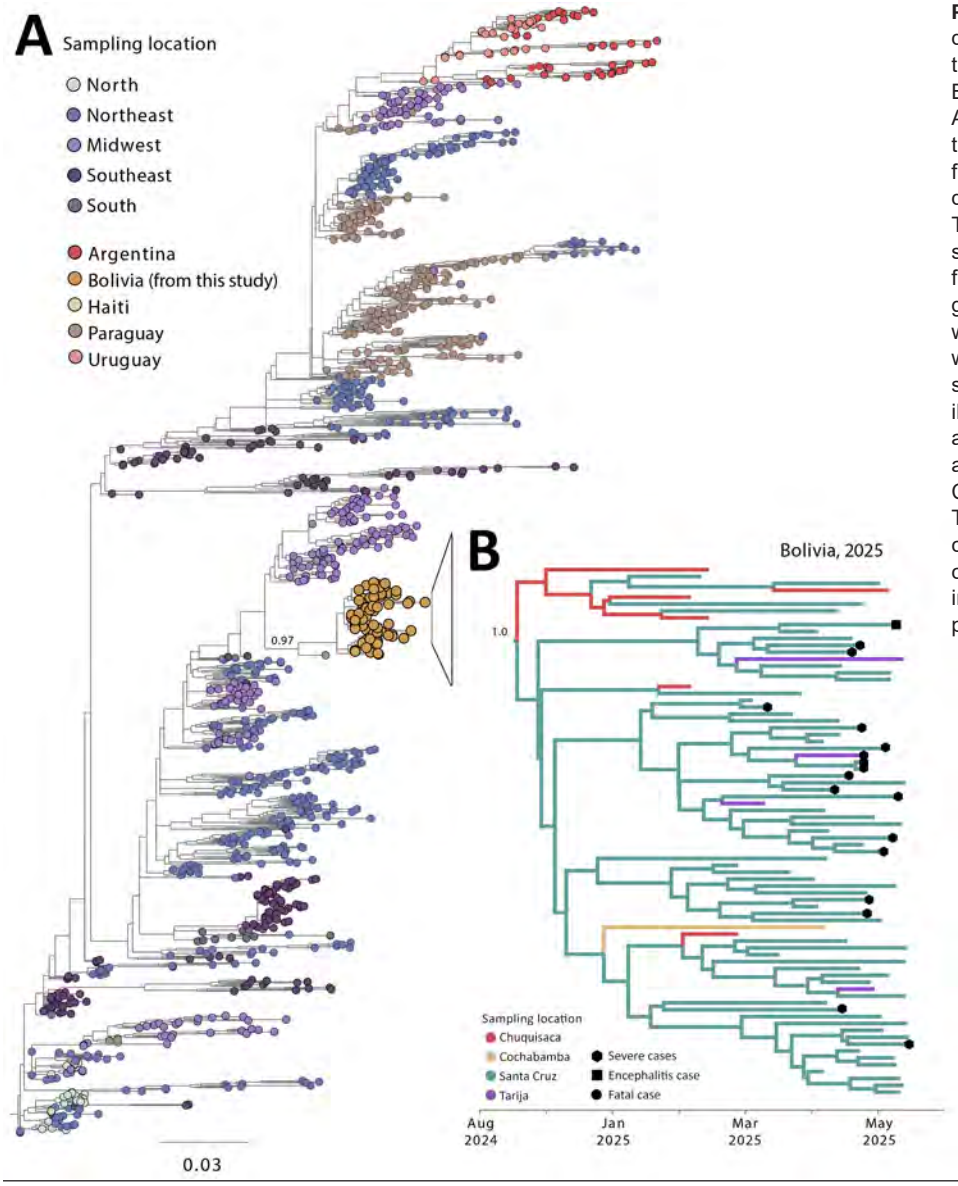


**Figure 2.** Regional genetic diversity and temporal spread of the chikungunya virus outbreak in Bolivia within the Americas, 2025. A) Phylogenetic tree showing the placement of genomes from Bolivia within the broader diversity across the Americas. Tips are colored according to sampling origin, and sequences from Bolivia are highlighted. The genomes from Bolivia cluster in a well-supported group, consistent with local expansion. B) Time-scaled tree of the Bolivian clade illustrating temporal progression and geographic distribution across departments (Chuquisaca, Cochabamba, Santa Cruz, and Tarija). Symbols indicate severe cases (including 1 encephalitis case and 1 fatal case). Scale bar indicates nucleotide substitutions per site.

those approaches are essential to improve early detection and guide timely response strategies.


## Acknowledgments

We thank Dina Condori Choque and Alinda Nilda Espinoza Quevedo for their support in providing epidemiological data at the national level. We thank the departmental reference laboratories of Cochabamba, Tarija, and Chuquisaca for collecting and sending serum samples for molecular diagnosis and genomic surveillance of chikungunya to the National Center for Tropical Diseases.

The XML file (https://github.com/genomicsurveillance/chikv_bolivia) and raw sequencing data and associated metadata (BioProject accession no. PRJNA1460444) are available.

N.R.G. was supported partially by the Fundação de Amparo à Pesquisa do Estado de Minas Gerais (project no. RED-00234-23). V.F. was supported by the Conselho Nacional de Desenvolvimento Científico e Tecnológico, Brazil (grant nos. 444903/2024-0 and 314941/2025-8). This work was supported by the Centers for Disease Control and Prevention award (cooperative agreement no. CK000639) to the Pan American Health Organization (PAHO), by the Novo Nordisk Foundation (award no. NNF24OC0094346), and by the Pandemic Response Optimization Through Engaged Communities and Territories project. PROTECT project, led by 7 countries including Bolivia, is supported by a grant from the Pandemic Fund, a multilateral financing mechanism dedicated exclusively to strengthening pandemic prevention, preparedness, and response capacities

in low- and middle-income countries. Project implementation is supported by 2 implementing entities: PAHO and the World Bank.

## About the Author

Dr. Valdez is a researcher at the Centro Nacional de Enfermedades Tropicales (CENETROP) in Santa Cruz, Bolivia, where he is responsible for genomic surveillance activities.

## Reference


1. de Souza WM, Lecuit M, Weaver SC. Chikungunya virus and other emerging arthritogenic alphaviruses. Nat Rev Microbiol. 2025;23:585–601. https://doi.org/10.1038/s41579-025-01177-8
2. França CMB, Loayza R, Roca Y, Montaño Arias AM, Tinajeros F, Loaiza JR, et al. Genome sequences of chikungunya virus isolates from Bolivia. Microbiol Resour Announc. 2020;9:e00230–20. https://doi.org/10.1128/MRA.00230-20
3. Pan American Health Organization. Epidemiological alert: chikungunya. 2026 [cited 2026 Mar 27]. https://www.paho.org/en/documents/epidemiological-alert-chikungunya-10-february-2026
4. Quick J, Grubaugh ND, Pullan ST, Claro IM, Smith AD, Gangavarapu K, et al. Multiplex PCR method for MinION and Illumina sequencing of Zika and other virus genomes directly from clinical samples. Nat Protoc. 2017;12:1261–76. https://doi.org/10.1038/nprot.2017.066
5. Vilsker M, Moosa Y, Nooij S, Fonseca V, Ghysens Y, Dumon K, et al. Genome Detective: an automated system for virus identification from high-throughput sequencing data. Bioinformatics. 2019;35:871–3. https://doi.org/10.1093/bioinformatics/bty695
6. Katoh K, Standley DM, Yamada KD. MAFFT multiple sequence alignment software version 7: improvements in performance and usability. Mol Biol Evol. 2013;30:772–80. https://doi.org/10.1093/molbev/mst010
7. Nguyen LT, Schmidt HA, von Haeseler A, Minh BQ. IQ-TREE: a fast and effective stochastic algorithm for estimating maximum-likelihood phylogenies. Mol Biol Evol. 2015;32:268–74. https://doi.org/10.1093/molbev/msu300
8. Rambaut A, Lam TT, Max Carvalho L, Pybus OG. Exploring the temporal structure of heterochronous sequences using TempEst (formerly Path-O-Gen). Virus Evol. 2016;2:vew007. https://doi.org/10.1093/ve/vew007
9. Baele G, Ji X, Hassler GW, McCrone JT, Shao Y, Zhang Z, et al. BEAST X for Bayesian phylogenetic, phylogeographic and phylodynamic inference. Nat Methods. 2025;22:1653–6. https://doi.org/10.1038/s41592-025-02751-x
10. Chadsuthi S, Althouse BM, Iamsirithaworn S, Triampo W, Grantz KH, Cummings DAT. Travel distance and human movement predict paths of emergence and spatial spread of chikungunya in Thailand. Epidemiol Infect. 2018;146:1654–62. https://doi.org/10.1017/S0950268818001917


Address for correspondence: Marta Giovanetti, Fundação Oswaldo Cruz (Fiocruz), Av. Brasil 4365, Manguinhos, Rio de Janeiro, RJ 21040-900, Brazil; email: giovanetti.marta@gmail.com

# Ophthalmomyiasis Outbreak Caused by *Oestrus ovis* Infection, Algeria, 2025

Yuyang Zeng,[1] Hongkuan Yang,[1] Xin Li, Hongzheng Yang, Yunyun Zhou

Author affiliations: Spencer Center for Vision Research Department of Ophthalmology, Byers Eye Institute at Stanford University School of Medicine, Palo Alto, California, USA (Y. Zeng); Renmin Hospital of Wuhan University Research Department of Ophthalmology, Wuhan, China (Y. Zeng, Y. Zhou); Tongji Hospital of Huazhong University of Science and Technology Department of Anesthesiology, Wuhan (Hongkuan Yang); Hubei Cancer Center Hospital of Huazhong University of Science and Technology Department of Anesthesiology, Wuhan (X. Li); Renhe Hospital Affiliated with China Three Gorges University Department of Medical Cosmetology, Yichang, China (Hongzheng Yang)

DOI: https://doi.org/10.3201/eid3207.260552

Ophthalmomyiasis is a rare eye infestation caused by fly larvae and more often seen in rural areas. We report an outbreak of 17 patients in Algeria with ophthalmomyiasis after sheep exposure. All patients fully recovered after removal of ocular *Oestrus ovis* larvae and topical therapy, highlighting the effectiveness of early detection and treatment.

Ophthalmomyiasis is a rare ocular infestation in modern clinical settings. *Oestrus ovis*, the sheep nasal bot fly, is the most common cause of human cases (*1*). Because *O. ovis* larvae primarily infect sheep and goats, human infection occurs predominantly in rural settings, although urban cases have been reported (*2*–*4*). Ophthalmomyiasis is classified as external, internal, or orbital, on the basis of infestation site. External ophthalmomyiasis is limited to the ocular surface, involving the conjunctiva and cornea (*5*). Internal ophthalmomyiasis affects intraocular structures including the anterior chamber, choroid, and vitreous (*6*). Last, orbital ophthalmomyiasis involves the orbital cavity and adjacent tissues. Larval migration and intraocular involvement can cause structural damage and vision loss (*7*).

We report a case series of 17 patients with acute external ophthalmomyiasis caused by *O. ovis* infection after sheep exposure during ritual sacrifice for Eid al-Adha in Algeria during June 6–8, 2025. Patients were 26–45 years of age; 10 were men and 7 were women.

[1]These first authors contributed equally to this article.

Sixteen patients reported exposure during Eid al-Adha, whereas 1 patient denied direct or indirect sheep exposure but suspected a foreign body in the eye. The time from exposure to hospital visit ranged from 5 to 32 hours, and symptom onset occurred 1–10 hours after exposure (Appendix Table, http://wwwnc.cdc.gov/EID/article/32/7/26-0552-App1.pdf).

Clinical manifestations included palpebral edema, conjunctival hyperemia, pruritus, foreign body sensation, epiphora, chemosis, photophobia, and pricking pain (Figure 1, panels A–C). All cases were unilateral. Slit-lamp examination revealed numerous and motile larvae on the cornea, bulbar conjunctiva, and upper and lower conjunctival fornices with active movement (Figure 1, panels D and E; Video, http://wwwnc.cdc.gov/EID/article/32/7/26-0552-V1.htm). Conjunctivitis-like signs included conjunctival congestion or edema, mucous discharge, and punctate keratitis (Figure 1, panels F–I). Corneal impairment was observed in 10 of 17 cases, including punctate keratitis in most and epithelial defects in 3 severe cases. Larvae measured ≈1–2 mm (Figure 2, panels A, B), and 4–22 larvae were identified per affected eye. Intraocular pressure was normal in all patients. Funduscopic examination and optical coherence tomography did not reveal posterior segment abnormalities (Appendix Figure).

We rinsed and immersed extracted specimens in phosphate-buffered saline before submission for parasitologic analysis at the Parasitology Laboratory, Tongji Medical College, Huazhong University of Science and Technology (Wuhan, China). We treated the specimens with lactic acid–phenol, and microscopic examination revealed internal larval structures that included body segments, spines, spicules, cephalic oral hooks, valves (shape and number of stomata), and the cephalopharyngeal skeleton, consistent with *O. ovis* larvae (Figure 2, panels C–E).

We removed all visible larvae from infected patients and subsequently treated the patients with topical antimicrobial drug eye drops (4×/d for 1 wk) and neomycin/polymyxin B/dexamethasone ophthalmic ointment (1×/d for 1 wk), except in patients with corneal lesions. All patients achieved complete clinical resolution within 1–2 weeks without complications.

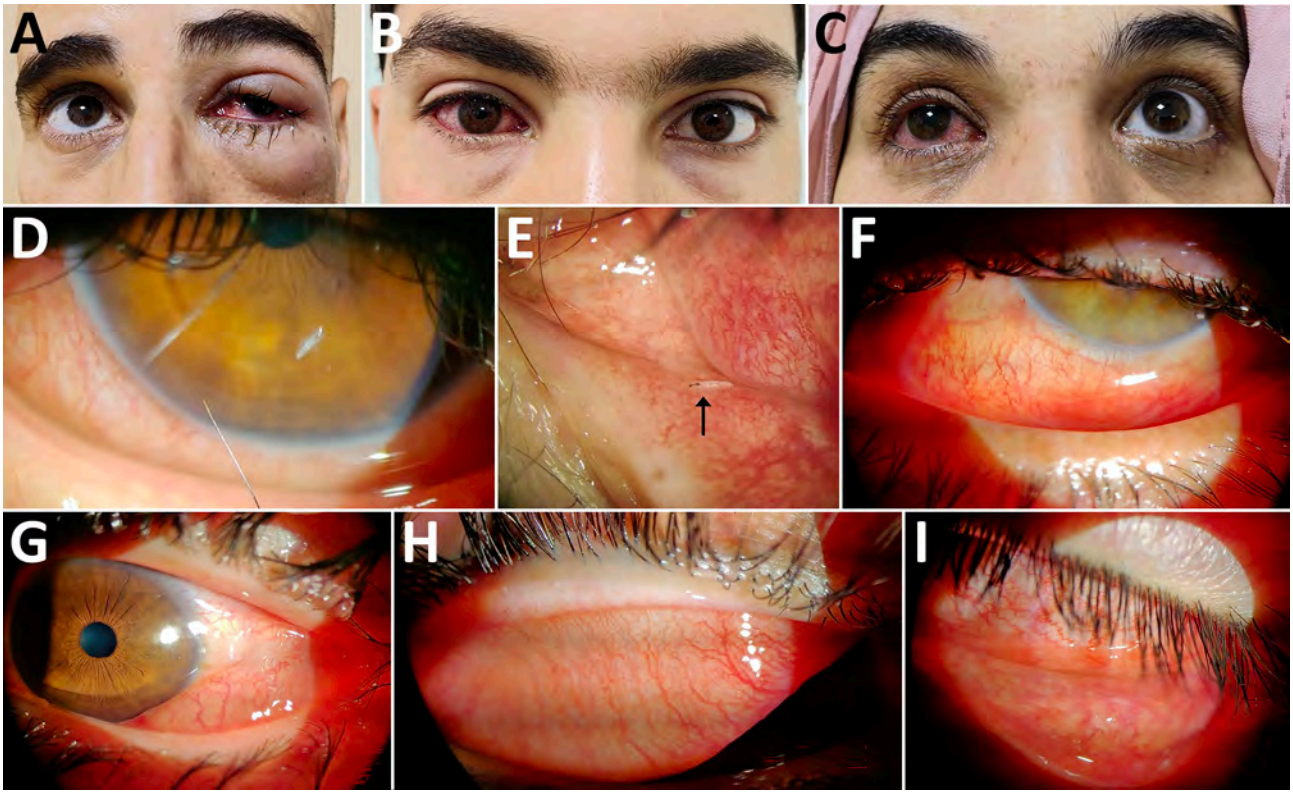


**Figure 1**. Clinical ocular findings in patients with acute external ophthalmomyiasis caused by *Oestrus ovis* infection after sheep exposure during Eid al-Adha, Algeria, 2025. A–C) Representative external ocular photographs show acute conjunctivitis-like findings, including palpebral edema, conjunctival hyperemia, and mucous discharge. D, E) Slit-lamp examination images show motile larvae on the corneal surface and in the lower conjunctival fornix. F–I) Slit-lamp examination images show conjunctival inflammation, including conjunctival congestion, edema, and mucous discharge. Black arrow in panel E indicates the location of an *O. ovis* larva.

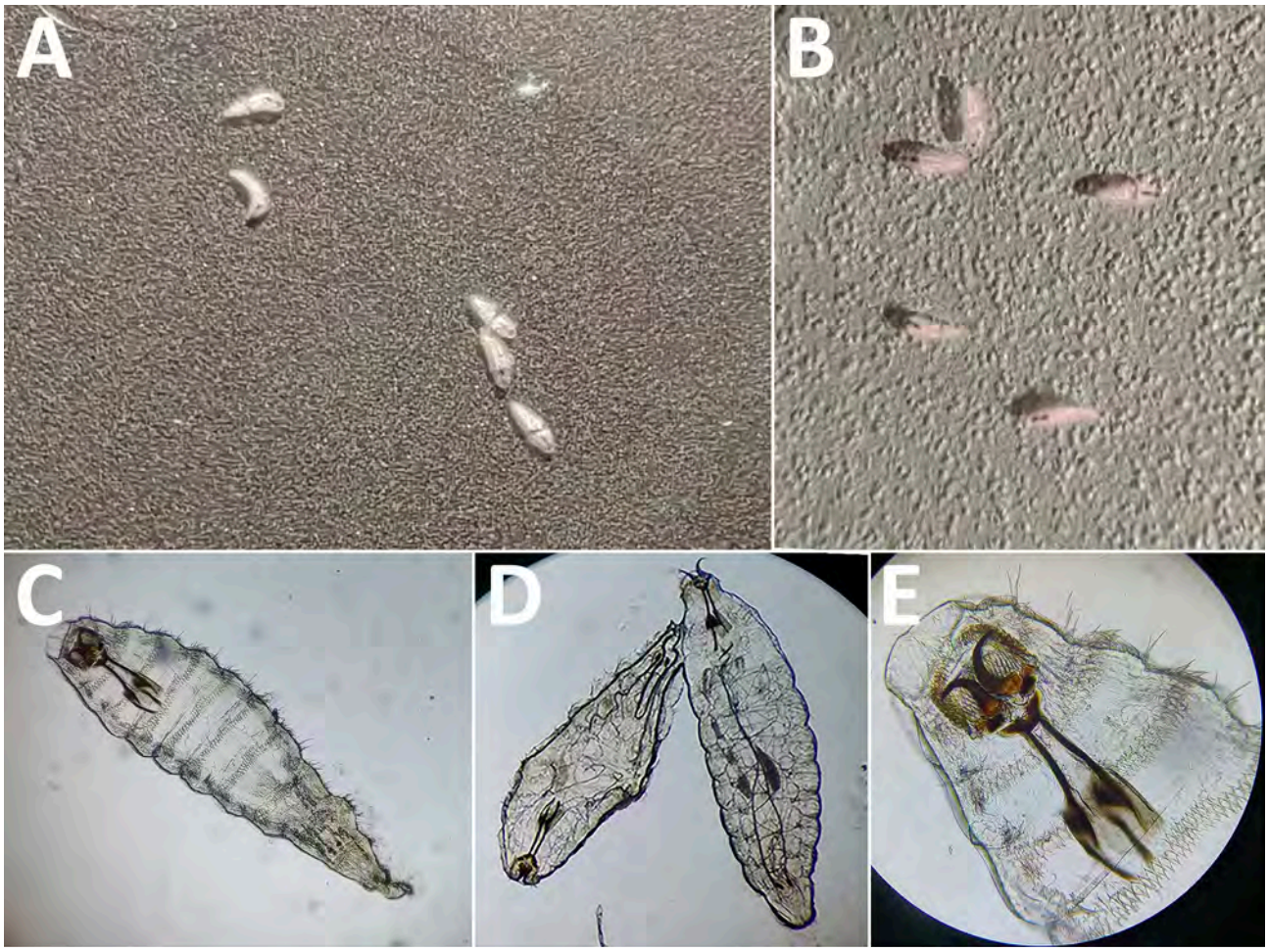


**Figure 2.** Morphologic identification of *Oestrus ovis* larvae extracted from patients with acute external ophthalmomyiasis after sheep exposure during Eid al-Adha, Algeria, 2025. A, B) Extracted first-instar larva from the ocular surface is shown grossly. C–E) Microscopic examination demonstrates characteristic features of *O. ovis*, including prominent oral hooks connected to the internal cephalopharyngeal skeleton and multiple rows of spiny projections. Original magnification ×40 (panel C), ×10 (panel D), and ×100 (panel E).

From our investigation, we believe that *O. ovis* larvae entered the patients' eyes when adult flies deposited first-stage larvae. The substantial larval burden contributed to conjunctival inflammation and superficial corneal abrasions through cephalic oral hooks and body spicules.

*O. ovis* ophthalmomyiasis is traditionally associated with sheep- and goat-rearing areas in warm, dry Mediterranean climates (*8*). However, recent European reports (*2*–*4*) suggest broader geographic distribution; cases have been described in temperate or urban areas (*9*) and sometimes without clear livestock exposure. External ophthalmomyiasis might be overlooked because it closely mimics acute viral or bacterial conjunctivitis or nonspecific inflammatory ocular irritation (*1*,*10*). Thorough ocular examination and detailed livestock exposure history are therefore essential for timely diagnosis. Prompt mechanical removal of all larvae is critical to prevent intraocular involvement. This large cluster of 17 patients with ophthalmomyiasis underscores the potential for zoonotic ocular infestation from unprotected sheep contact during seasonal religious rituals. Public education, eye protection, and hygiene practices during ritual slaughter might help reduce similar outbreaks in endemic regions.

**Acknowledgments**

We thank the administration and clinical staff of El Moudjahid Madjen Benmira Hospital for their support in enabling this study. We also acknowledge the patients who participated and contributed to this research.

This work was supported by the Open Research Fund of Hubei Key Laboratory (award no. 2021KFY057 to Y.Z.).

### About the Author

Dr. Zeng is a clinician-scientist in the Department of Ophthalmology at Stanford University School of Medicine and an ophthalmologist with residency training in ophthalmology. Her research focuses on translational studies of a broad range of eye diseases, including glaucoma, therapeutic strategies to protect retinal ganglion cells and preserve vision, retinal neurodegeneration, and ocular infectious diseases.

### Reference


1. Martinez-Rojano H, Huerta H, Sámano R, Chico-Barba G, Mier-Cabrera J, Plascencia-Nieto ES. Ophthalmomyiasis externa and importance of risk factors, clinical manifestations, and diagnosis: review of the medical literature. Diseases. 2023;11:180. https://doi.org/10.3390/diseases11040180
2. Tamponi C, Pasini C, Ahmed F, Dessì G, Contu E, Porcu F, et al. External ophthalmomyiasis by *Oestrus ovis* in tourists visiting Italy. Report of three cases and a literature review. Travel Med Infect Dis. 2022;46:102279. https://doi.org/10.1016/j.tmaid.2022.102279
3. Vedpathak M, Chatterjee N, Baradkar V, Shastri J. Ophthalmomyiasis externa: a case report. Trop Parasitol. 2020;10:147–9. https://doi.org/10.4103/tp.TP_2_20
4. Rosenberg R, Halimi E, Benayoun Y, Khadimallah Y, Robert PY. External ophthalmomyiasis (botfly larval infestation) in urban France [In French]. J Fr Ophtalmol. 2013;36:466–7.
5. Abihaidar N, Garcin T. External ophthalmomyiasis due to *Oestrus ovis*. N Engl J Med. 2022;386:e35. https://doi.org/10.1056/NEJMicm2115416
6. Rodger DC, Kim EL, Rao NA. Ophthalmomyiasis interna. Ophthalmology. 2016;123:247.
7. Singh P, Tripathy K. Ophthalmomyiasis. StatPearls. 2023 [cited 2025 Aug 25]. https://www.ncbi.nlm.nih.gov/books/NBK576408
8. Dunbar J, Cooper B, Hodgetts T, Yskandar H, van Thiel P, Whelan S, et al. An outbreak of human external ophthalmomyiasis due to *Oestrus ovis* in southern Afghanistan. Clin Infect Dis. 2008;46:e124–6.
9. D'Assumpcao C, Bugas A, Heidari A, Sofinski S, McPheeters RA. A case and review of ophthalmomyiasis caused by *Oestrus ovis* in the central valley of California, United States. J Investig Med High Impact Case Rep. 2019;7:2324709619835852.
10. Balamurugan R, Gupta PC, Dhingra D, Ram J. External ophthalmomyiasis by *Oestrus ovis* larvae. QJM. 2020;113:751.


Address for correspondence: Yunyun Zhou, Renmin Hospital of Wuhan University, 238 Jiefang Rd, Wuchang District, Wuhan, Hubei 430060, China; email: zhouyunyun@whu.edu.cn

# Molecular Confirmation of Autochthonous *Taenia saginata* Infection, Timor-Leste, 2019

Hanna Jin, Sung-Tae Hong, Merita Antonio Armindo Monteiro, Endang da Silva, Odete da Silva Viegas, Felix dos Santos Lopes, Dong Hee Kim, Sung Hye Kim

Author affiliations: Seoul National University College of Medicine, Jongno-gu, South Korea (H. Jin, S.-H. Hong, D.H. Kim); National Institute of Public Health, Dili, Timor-Leste (M.A. Armindo Monteiro, E. da Silva); Ministry of Health, Dili (O. da Silva Viegas); World Health Organization, Timor-Leste Country Office, Dili (F. dos Santos Lopes); Hanyang University College of Medicine, Seongdong-gu, South Korea (S.H. Kim)

DOI: http://doi.org/10.3201/eid3207.252034

We report a case of autochthonous *Taenia saginata* infection in Timor-Leste. Screening of 1,121 schoolchildren revealed a 0.4% prevalence of human taeniasis. Genetic analysis of the mitochondrial *cox1* gene identified group A lineage. Our findings fill a considerable geographic data gap and highlight the need for integrated One Health control strategies.

Human taeniasis is a foodborne neglected tropical disease caused by 3 species of tapeworms: *Taenia solium*, *Taenia saginata*, and *Taenia asiatica*. Although the parasites are endemic across Africa and the Americas, Asia is unique for the sympatric distribution of all 3 species, particularly in rural areas where traditional livestock rearing persists (*1*). Among these species, the *T. saginata* beef tapeworm is the most common zoonotic tapeworm globally; infection occurs through the consumption of raw or undercooked beef containing cysticerci (*2*). The epidemiologic landscape in Southeast Asia is complex because of the genetic relationship between *T. saginata* and *T. asiatica* tapeworms (*3*). Recent molecular analyses have revealed that the 2 are sister species that are not completely reproductively isolated; consequently, many adult worms circulating in the region, including those in Indonesia, are hybrid-derived descendants (*4*).

Timor-Leste, a Southeast Asia nation sharing the island of Timor with Indonesia, has long represented a considerable geographic data gap. A 2020 systematic review covering 1990–2017 found no retrievable data for the country (*2*), leaving its endemic status unconfirmed, despite cultural

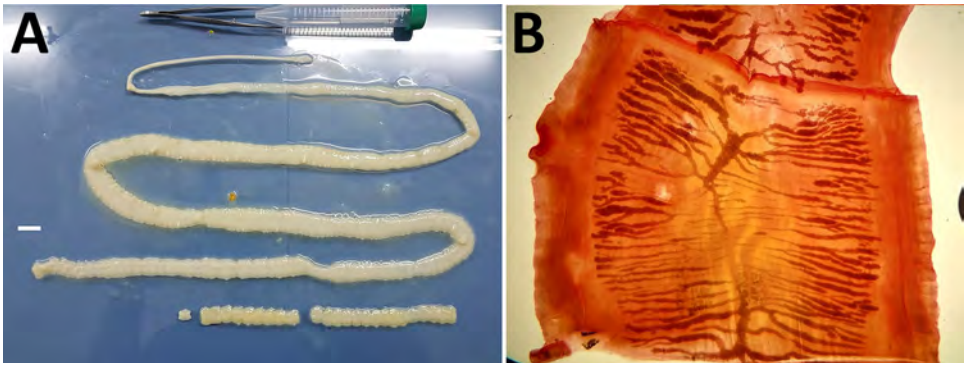


**Figure 1.** Proglottids of *Taenia saginata* beef tapeworm collected from an 11-year-old girl in Dili, Timor-Leste, informing an investigation focused on molecular confirmation of autochthonous *T. saginata* infection, Timor-Leste, 2019. A) Gross morphology of proglottids, showing flat, creamy-white segments, measuring 12–15 mm in length. The scolex was confirmed to lack rostellar hooks on gross examination. Scale bar = 1 cm. B) Acetocarmine-stained proglottid showing 18–20 lateral uterine branches, morphologically consistent with *T. saginata* tapeworm and excluding *T. solium* tapeworm.

practices favoring beef consumption and a population of ≈225,000 cattle (*5*).

In early 2019, as part of a national monitoring program for soil-transmitted helminthiasis, we collected fecal samples from 1,121 schoolchildren across 6 schools in Timor-Leste. Initial screening using the Kato-Katz thick-smear technique identified 4 children as *Taenia* spp. egg–positive, representing an overall prevalence of 0.4%, which is consistent with regional pediatric data from countries such as Myanmar (*6*). After the identification of eggs, we administered a single oral dose of praziquantel (10 mg/kg) to affected children, followed by a purge with a mild laxative solution (Colonlyte powder; Dream Pharma [now Alvogen Korea], https://www.alvogenkorea.com) so that we could recover intact tapeworm segments. We successfully recovered intact proglottids from an asymptomatic 11-year-old girl residing in the capital, Dili. Of note, the patient had no history of international travel, confirming that the infection was autochthonous.

The recovered tapeworm segments were flat and creamy-white and measured 12–15 mm in length (Figure 1). Acetocarmine staining revealed 18–20

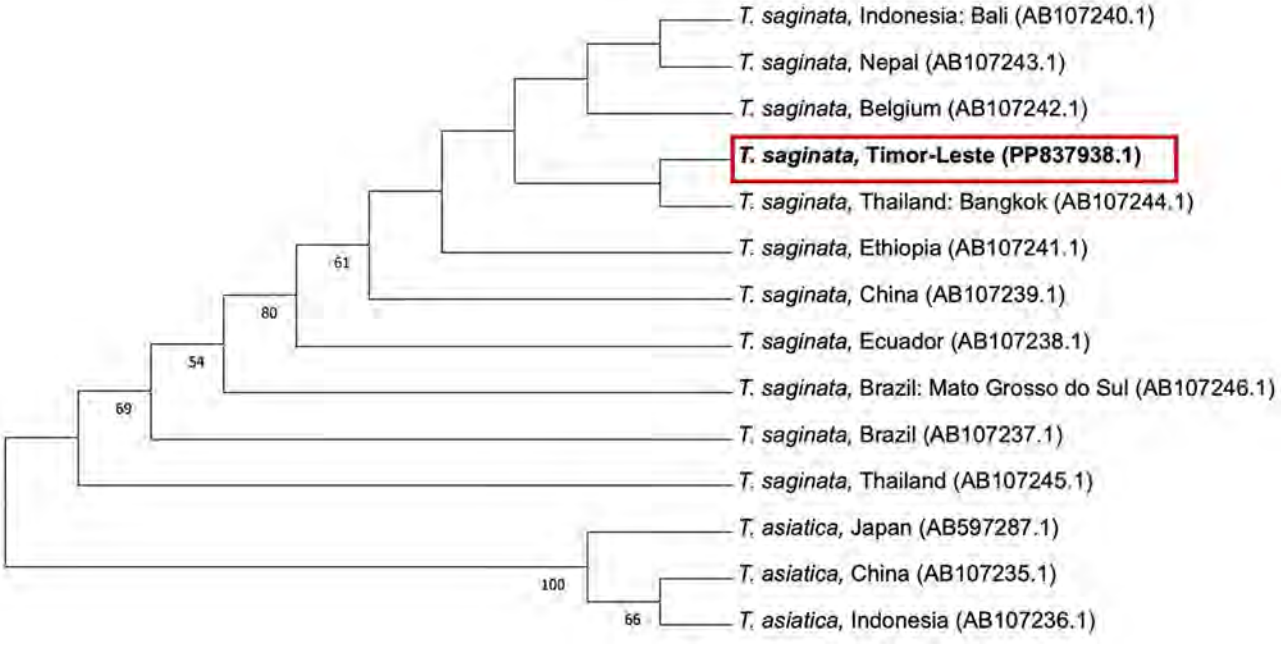


**Figure 2.** Phylogenetic analysis of the *cox1* gene from a child with taeniasis in a study revealing molecular confirmation of autochthonous *Taenia saginata* infection, Timor-Leste, 2019. Phylogenetic tree of *T. saginata* and related taxa was based on partial mitochondrial *cox1* gene sequences (458 bp). The evolutionary history was inferred by the neighbor-joining method with 1,000 bootstrap replicates; bootstrap values (≥50%) are shown at branch nodes. Evolutionary distances computed using Kimura 2-parameter model. Analyses performed in MEGA 11 (https://www.megasoftware.net). The Timor-Leste isolate (GenBank PP837938.1, red box) clusters within the group A clade of *T. saginata*, distinct from *T. asiatica* (outgroup) and *T. solium* lineages. GenBank accession numbers are shown in parentheses.

lateral uterine branches and a lack of rostellar hooks on the scolex, which served to morphologically exclude the *T. solium* pork tapeworm. To achieve definitive species identification, we extracted genomic DNA using the DNeasy Blood & Tissue Kit (QIAGEN, https://www.qiagen.com) and targeted a fragment of the mitochondrial *cox1* gene for PCR amplification using T1F and T1R primers as described previously (*7*). Sequencing of the amplicons showed a 99.58% identity with *T. saginata* (GenBank AB984348.1) and a marked genetic divergence from *T. solium*. Phylogenetic analysis using the neighbor-joining method placed the Timor-Leste isolate firmly within the group A clade, distinct from *T. asiatica* and *T. solium* lineages (Figure 2; Appendix, https://wwwnc.cdc.gov/EID/article/32/7/25-2034-App1.pdf). The high bootstrap support (>90%) for those nodes reinforces the isolate's genetic alignment with regional *T. saginata* populations rather than the hybrid-derived descendants of *T. asiatica* and *T. saginata* tapeworms found in nearby North Sumatra (Figure 2).

Combined with the emergence of a concurrent *T. solium* infection that was molecularly confirmed in a 10-year-old child in Dili during the same surveillance period (*7*), our results confirm the co-endemicity of *T. saginata* and *T. solium* tapeworms in Timor-Leste. Although the *T. saginata* isolate is linked to regional Southeast Asian genotypes (group A), the *T. solium* case showed homology with Madagascar lineages, suggesting different historical introduction routes for the 2 species (*7*). The detection of the parasites in schoolchildren suggests transmission risks within the home environment and the early cultural integration of beef consumption (*1*,*8*).

The reliance on Kato-Katz smears in regional surveillance remains a hurdle, because this analysis cannot differentiate between *Taenia* species. Furthermore, the documented presence of hybrid-derived descendants in neighboring Indonesia (*4*) suggests that future surveillance should incorporate nuclear markers to complement mitochondrial genotyping. Such a dual-marker approach is essential to detect potential interspecific hybridization or introgression that may be masked by mitochondrial analysis alone. Nevertheless, the confirmation of endemicity for both *T. saginata* and *T. solium* tapeworms warrants enhanced integrated surveillance to accurately identify co-circulating *Taenia* species. The concurrent detection of *T. solium* tapeworm in this pediatric cohort underscores the need for species-discriminating molecular diagnostics and cross-border cooperation to prevent neurocysticercosis, the public health consequences of which far exceed those of *T. saginata* taeniasis (*9*).

This work was supported by the Korea International Cooperation Agency's "Project of Integrated Control and Elimination of Neglected Tropical Diseases in Timor-Leste" and the Education and Research Encouragement Fund of Seoul National University Hospital.

## About the Author

Dr. Jin is a doctoral student at the Department of Tropical Medicine and Parasitology, Seoul National University College of Medicine. Her research focuses on public health and neglected tropical diseases, with an emphasis on the development of point-of-care diagnostics.

## References

1. Ito A, Li T, Wandra T, Dekumyoy P, Yanagida T, Okamoto M, et al. Taeniasis and cysticercosis in Asia: a review with emphasis on molecular approaches and local lifestyles. Acta Trop. 2019;198:105075. https://doi.org/10.1016/j.actatropica.2019.105075
2. Eichenberger RM, Thomas LF, Gabriël S, Bobić B, Devleesschauwer B, Robertson LJ, et al. Epidemiology of Taenia saginata taeniosis/cysticercosis: a systematic review of the distribution in East, Southeast and South Asia. Parasit Vectors. 2020;13:234. https://doi.org/10.1186/s13071-020-04095-1
3. Jeon HK, Eom KS. *Taenia asiatica* and *Taenia saginata:* genetic divergence estimated from their mitochondrial genomes. Exp Parasitol. 2006;113:58–61. https://doi.org/10.1016/j.exppara.2005.11.018
4. Zein U, Siregar S, Janis I, Pane AH, Purba JM, Sardjono TW, et al. Identification of a previously unidentified endemic region for taeniasis in North Sumatra, Indonesia. Acta Trop. 2019;189:114–6. https://doi.org/10.1016/j.actatropica.2018.10.004
5. Ministry of Agriculture and Fisheries. Timor-Leste Agriculture Census 2019 National Report. 2023 [cited 2025 Dec 25]. https://inetl-ip.gov.tl/2023/03/16/2241/
6. Won EJ, Jung B-K, Song H, Kim M-S, Kim H-S, Lee KH, et al. Molecular diagnosis of Taenia saginata tapeworm infection in 2 schoolchildren, Myanmar. Emerg Infect Dis. 2018;24:1156–8. https://doi.org/10.3201/eid2406.180217
7. Jin H, Hong S-T, Monteiro MAA, da Silva E, da Silva Viegas O, Dos Santos Lopes F, et al. Molecular confirmation of *Taenia solium* taeniasis in child, Timor-Leste. Emerg Infect Dis. 2024;30:1964–7. https://doi.org/10.3201/eid3009.240238
8. Wandra T, Ito A, Swastika K, Dharmawan NS, Sako Y, Okamoto M. Taeniases and cysticercosis in Indonesia: past and present situations. Parasitology. 2013;140:1608–16. https://doi.org/10.1017/S0031182013000863
9. Food and Agriculture Organization of the United Nations. Transforming the livestock sector through the Sustainable Development Goals. Rome, 2018. Licence: CC BY-NC-SA 3.0 IGO [cited 2025 Dec 25]. https://openknowledge.fao.org/server/api/core/bitstreams/d67a99fb-66ca-42a0-b5ac-3f907b35f09f/content

Address for correspondence: Sung Hye Kim, Hanyang University College of Medicine, 222 Wangshipni-ro, Seongdong-gu, Seoul, South Korea; email: sunghyekim@hanyang.ac.kr

# Emergence of West African Human T-Lymphotropic Virus 1aC Subgroup, Brazilian Amazon

Jean de Melo Silva, Emmily Myrella Vasconcelos Mourão, Enzo Miranda Santos, Luma Silva Mineiro, Paulo Henrique Rodrigues de Souza, Leonardo Calheiros de Oliveira, Jacqueline da Silva Batista, Giselle Moura Guimarães Marques, Carolina Rosadas de Oliveira, Graham P. Taylor, Antonio Carlos Rosário Vallinoto, Gemilson Soares Pontes

Author affiliations: Institute of Biological Science, Federal University of Amazonas, Manaus, Brazil (J. de Melo Silva, G.S. Pontes); Leônidas and Maria Deane Institute–ILMD/Fiocruz Amazônia, Manaus (E.M.V. Mourão); Foundation of Hematology and Hemotherapy of Amazonas, Manaus (E.M. Santos); National Institute of Amazonian Research, Manaus (L.S. Mineiro, P.H.R. de Souza, L.C. de Oliveira, J. da Silva Batista, G.M. Guimarães Marques, G.S. Pontes); Faculty of Medicine, Imperial College London, London, UK (C.R. de Oliveira, G.P. Taylor); National Centre for Human Retrovirology, St. Mary's Hospital, Imperial College Healthcare NHS Trust, London (G.P. Taylor); Federal University of Pará, Belém, Brazil (A.C.R. Vallinoto)

DOI: https://doi.org/10.3201/eid3207.260372

In a cross-sectional survey of 1,397 residents of Manaus, Brazil, we found a seroprevalence of 0.3% for human T-lymphotropic viruses (HTLVs) 1/2 and identified HTLV type 1aC by phylogenetic analysis. Those findings provide evidence of introduction of West African HTLV-1aC into the Brazilian Amazon and highlight regional limitations in genomic surveillance.

Epidemiologic surveillance is essential for defining the burden, geographic distribution, and transmission patterns of human T-lymphotropic viruses (HTLVs) 1 and 2 (HTLV-1/2), particularly in underserved settings such as the Brazilian Amazon. Although Brazil is estimated to harbor the largest absolute number of HTLV-1 infections worldwide, data from urban Amazonian populations remain scarce (*1*,*2*). In this context, molecular surveillance is also critical because HTLV genetic diversity is geographically structured, could have clinical relevance, and helps refine understanding of lineage distribution and viral dissemination (*3*). We therefore investigated HTLV-1/2 infection in the metropolitan region of Manaus in the Amazonas state of Brazil and performed phylogenetic and phylogeographic analyses.

During May 2021–November 2023, we conducted a cross-sectional study of 1,397 residents of metropolitan Manaus recruited by convenience sampling across different city zones at universities, community centers, polyclinics, and primary healthcare units. Eligible participants were Manaus residents ≥7 years of age who voluntarily agreed to participate and provided written informed consent; for minors, we obtained parental or guardian consent and assent when applicable. We screened plasma samples for HTLV-1/2 antibodies by ELISA and confirmed seroreactive samples by Western blot or line immunoassay; indeterminate samples underwent molecular testing. We collected sociodemographic and behavioral data through a standardized questionnaire.

We amplified the 5′ long terminal repeat (LTR) region of HTLV-1 (579 bp) and HTLV-2 (788 bp) by nested PCR and sequenced the amplicons by Sanger sequencing. We inferred phylogenetic relationships by maximum-likelihood analysis in MEGA12 (https://www.megasoftware.net) using the Kimura 2-parameter model with 1,000 bootstrap replicates and a geographically diverse panel of HTLV-1 and HTLV-2 reference sequences retrieved from GenBank from a previously assembled dataset. We deposited sequences generated in this study into GenBank (accession nos. PV647910 for sequence WDM1168_BrMao, PV647909 for sequence WQC1199_BrMao, PV647908 for sequence SSS850_BrMao, and PV742404 for sequence JDC1001_BrMao). To investigate the timing and geographic history of HTLV-1 lineages, we performed Bayesian time-scaled phylogenetic and discrete phylogeographic analyses in BEAST X version 10.5 (https://beast.community).

Overall HTLV-1/2 seroprevalence was 0.3% (95% CI 0.11%–0.73%; 4/1,397 participants), comprising 3 HTLV-1 and 1 HTLV-2 infections. All seropositive participants were >40 years of age and shared a profile of socioeconomic vulnerability: 75% were female, earned no more than minimum wage, had only elementary education, lacked marital partnerships, and relied on government assistance (Appendix, https://wwwnc.cdc.gov/EID/article/32/7/26-0372-App1.pdf). Phylogenetic analysis classified sequence SSS850_BrMao as HTLV-1aC, the West African subgroup, providing evidence of this lineage in the Brazilian Amazon (Figure 1, panel A). The remaining isolates were HTLV-1aA (WDM1168_BrMao and WQC1199_BrMao) and HTLV-2c (JDC1001_BrMao), indicating co-circulation of distinct HTLV lineages in this population (Figure 1).

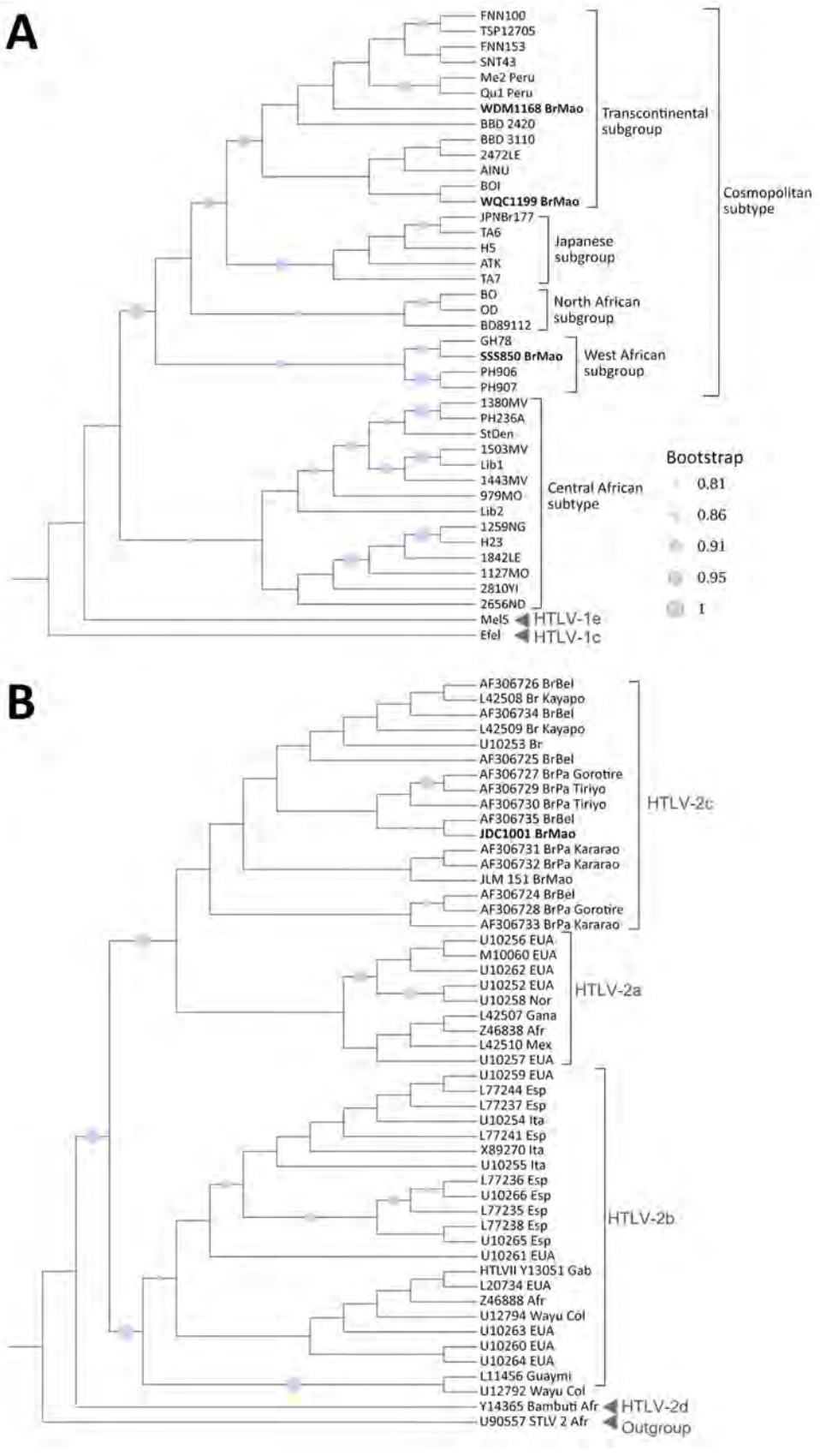


**Figure 1.** Phylogenetic tree of HTLV isolates in study of emergence of West African HTLV-1aC subgroup, Brazilian Amazon. A) HTLV-1 sequences obtained in this study (bold text) were analyzed with 38 reference sequences from GenBank. The Manaus isolates clustered within the Cosmopolitan subtype, including the Transcontinental subgroup (WDM1168_BrMao and WQC1199_BrMao) and the West African subgroup (SSS850_BrMao). B) The HTLV-2 sequence identified in Manaus (JDC1001_BrMao, bold text) was analyzed with 49 reference sequences from GenBank (accession numbers provided) and clustered within subtype HTLV-2c. Trees were inferred using the maximum-likelihood method under the Kimura 2-parameter substitution model. The best-scoring trees (log-likelihood −14,610.1 for panel A and −2,247.45 for panel B) were selected through heuristic searches initiated with neighbor-joining and maximum parsimony starting topologies. Branch support was assessed with 1,000 bootstrap replicates. HTLV, human T-lymphotropic virus.

After we identified the HTLV-1aC lineage, we performed Bayesian time-scaled phylogenetic and discrete phylogeographic analyses to infer its introduction and evolutionary history (Figure 2). Our results demonstrate that strain SSS850_BrMao clusters robustly within the HTLV-1aC clade, supporting its introduction into Amazonas around 2015 without evidence of intermediate dispersal through Pará. In contrast, 2 HTLV-1aA sequences clustered with reference sequences from Japan, indicating a separate

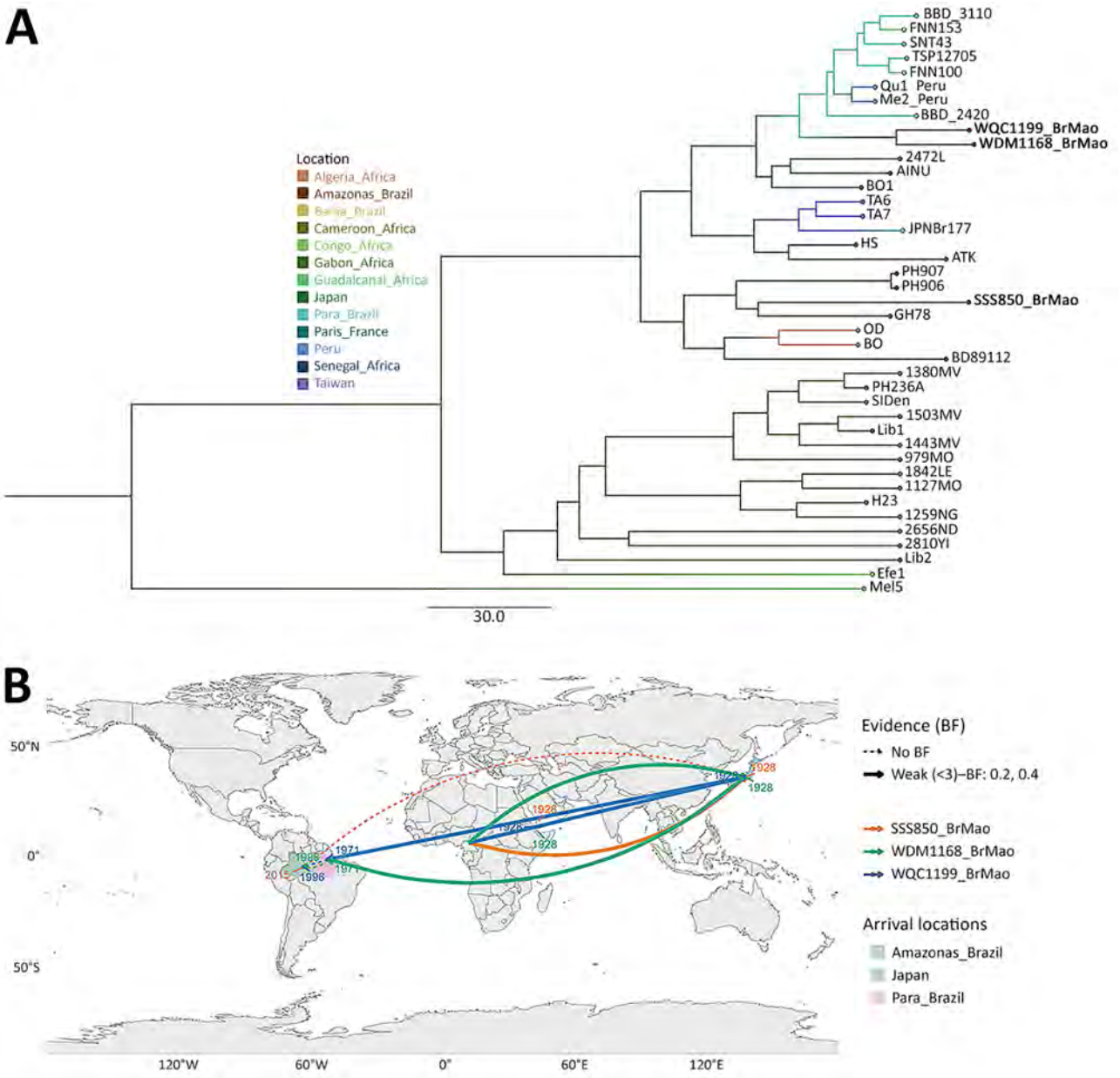


**Figure 2.** Time-scaled phylogeny and discrete phylogeographic diffusion of HTLV-1 lineages in study of emergence of West African HTLV-1aC subgroup, Brazilian Amazon. A) Time-calibrated maximum clade credibility tree inferred in BEAST version 10.5 (https://beast.community) from the long terminal repeat (LTR) dataset (3 sequences from this study plus reference sequences), using sampling year as tip date, a strict molecular clock, and discrete geographic-state reconstruction under a continuous-time Markov chain model with Bayesian stochastic search variable selection. Branches and tips are colored by inferred location (see key); bold text indicates sequences generated in this study. B) Spatiotemporal diffusion reconstructed from Markov jumps. Trajectory colors correspond to each Manaus lineage: orange, SSS850_BrMao; green, WDM1168_BrMao; blue, WQC1199_BrMao. Numbers indicate posterior median year of first arrival (labels shown for years ≥1970; Cameroon→Japan step, ≈1928, is retained for context). Line style indicates support: dashed, no Bayers factor recovered; solid, weak support (<3; here, 0.2–0.4). Shaded polygons indicate inferred arrival locations (Amazonas and Pará states, Brazil, and Japan). HTLV, human T-lymphotropic virus.

introduction into northern Brazil via Pará (≈1971) followed by spread to Amazonas (≈1996). Together, those findings reveal ≥2 subtype-stratified introductions and identify HTLV-1aC as an epidemiologically relevant lineage in the region. However, because the phylogeographic inferences were based on a ≈579-bp 5′ LTR region fragment, they should be interpreted cautiously.

We observed a HTLV-1/2 prevalence in metropolitan Manaus, lower than estimates from other regions of Brazil, including Salvador and Mato Grosso do Sul (*4*,*5*). However, comparisons should be made with caution because sampling strategies and population composition differ across studies. Beyond prevalence, the key finding was detection of HTLV-1aC. Although this subgroup has previously been reported in Brazil by restriction fragment length polymorphism analysis (*6*), our study provides phylogenetically supported evidence of HTLV-1aC's occurrence in the country and places it in phylogeographic context. This result broadens the known distribution of HTLV-1aC and suggests that viral diversity in northern Brazil may be greater than previously recognized, despite evidence that HTLV-1aA predominates nationwide (*7*,*8*). Phylogeographic analyses supported ≥2 subgroup-specific introductions into the region, highlighting HTLV-1aC as an epidemiologically relevant lineage. We also identified HTLV-2c in an urban resident, reinforcing evidence that this subtype is not restricted to Indigenous populations and might circulate across multiple epidemiologic settings in northern Brazil (*9*,*10*).

The first limitation of our study is that we used convenience sampling at multiple sites, rather than a population-based design. Therefore, the sample might not fully represent the city's general population. The small number of positive participants precluded robust inference on risk factors or transmission routes. Phylogeographic reconstruction was further constrained by use of a short 5′ LTR fragment from a slowly evolving virus and by uneven regional sequence availability, reducing temporal and geographic resolution.

Despite those limitations, detection of HTLV-1aC in Manaus has surveillance relevance because rare lineages might remain unnoticed in settings with limited molecular monitoring. Broader epidemiologic surveillance combined with longer genomic regions and regionally representative sampling will be essential to refine lineage dispersion patterns, strengthen transmission hypotheses, and support HTLV prevention, diagnosis, and care policies tailored to the Brazilian Amazon.

**Acknowledgments**

We thank the Amazonas State Research Support Foundation, the Coordination for the Improvement of Higher Education Personnel (CAPES), the National Council for Scientific and Technological Development (CNPq), the Pan American Health Organization, the World Health Organization, the Ministry of Health, and the Ministry of Science, Technology and Innovation for their support of this project. We also thank SEMSA (Municipal Health Department) and SES-AM (Amazonas State Health Department) for help with participant recruitment. In addition, we are grateful to the Federal University of Amazonas, as well as the staff of the laboratory of Virology and Immunology-INPA, for their valuable assistance, particularly with sample collection.

Ethical approval was granted by the National Commission for Ethics Research and the INPA Human Research Ethics Committee on October 21, 2020 (CAAE: 39320120.2.3000.0106).

The data that support the findings of this study are available from the corresponding author upon reasonable request.

This work was supported by the Amazonas State Research Support Foundation, the Coordination for the Improvement of Higher Education Personnel Brazil (grant nos. 88881.933595/2024-01 and PROCAD AMAZONIA 88881.200581/201801), and the National Council for Scientific and Technological Development (grant nos. 401569/2023-3 and 302935/2021-5).

J.M.S. conceived and designed the study, collected blood samples, performed laboratory assays, curated and analyzed data, and prepared the original draft. G.S.P. conceived and designed the study, supervised all activities, secured funding, managed the project, interpreted data, and contributed to writing and critical revision of the manuscript. A.C.R.V. secured funding, supported study oversight and data interpretation, and contributed to writing and revision of the manuscript. C.R.O. and G.P.T. contributed to the study design and data interpretation and also participated in writing and critical revision of the manuscript. J.S.B. and G.M.G.M. performed sample purification and HTLV-1/2 LTR amplicon sequencing, curated sequencing data, and supported laboratory quality control. E.M.S., E.M.V.M., L.S.M., P.H.R.S., and L.C.O. collected blood samples and field data and assisted with data curation. All authors reviewed and approved the final version of the manuscript.

## About the Author

Dr. de Melo Silva is a biomedical scientist with the Institute of Biological Science, Federal University of

Amazonas, Manaus, Brazil. His research interest is the epidemiology of viral infections, particularly emerging viruses, in the Brazilian Amazon.

## References


1. Brazil Ministry of Health. Clinical management guide for HTLV infection. 2021 [in Portuguese] [cited 2026 Feb 24]. https://www.gov.br/aids/pt-br/central-de-conteudo/publicacoes/2021/guia-de-manejo-clinico-da-infeccao-pelo-htlv
2. Rosadas C, Espinosa Miranda A, Gonçalves DU, Caterino-de-Araujo A, Assone T, Ishak R. Prevalence of HTLV-1/2 infection in Brazil [in Portuguese]. Bol Epidemiol (Porto Alegre). 2020;51:25–33.
3. Furukawa Y, Yamashita M, Usuku K, Izumo S, Nakagawa M, Osame M. Phylogenetic subgroups of human T cell lymphotropic virus (HTLV) type I in the tax gene and their association with different risks for HTLV-I-associated myelopathy/tropical spastic paraparesis. J Infect Dis. 2000;182:1343–9. https://doi.org/10.1086/315897
4. Dourado I, Alcantara CJ, Barreto ML, Da M, Teixeira G, Galvão-Castro B. HTLV-I in the general population of Salvador, Brazil: a city with African ethnic and sociodemographic characteristics. J Acquir Immune Defic Syndr. 2003;34:527–31. https://doi.org/10.1097/00126334-200312150-00013
5. Amianti C, Bandeira LM, Cardoso WM, da Silva ASP, de Jesus MDS, Ibañez R, et al. HTLV infection in urban population from Mato Grosso do Sul, Central Brazil. Retrovirology. 2024;21:18. https://doi.org/10.1186/s12977-024-00650-1
6. Segurado AA, Biasutti C, Zeigler R, et al. Identification of human T-lymphotropic virus type I (HTLV-I) subtypes using restricted fragment length polymorphism in a cohort of asymptomatic carriers and patients with HTLV-I-associated myelopathy/tropical spastic paraparesis from São Paulo, Brazil. Mem Inst Oswaldo Cruz. 2002;97:329–33. https://doi.org/10.1590/s0074-02762002000300009
7. Afonso PV, Cassar O, Gessain A. Molecular epidemiology, genetic variability and evolution of HTLV-1 with special emphasis on African genotypes. Retrovirology. 2019;16:39. https://doi.org/10.1186/s12977-019-0504-z
8. Amoussa AER, Wilkinson E, Giovanetti M, de Almeida Rego FF, Araujo TH, de Souza Gonçalves M, et al. HTLV-1aA introduction into Brazil and its association with the trans-Atlantic slave trade. Infect Genet Evol. 2017;48:95–101. https://doi.org/10.1016/j.meegid.2016.12.005
9. Pontes GS, Ribeiro HHF, Toro DM, Moura Neto JP, Souza V, Almeida MEM, et al. HTLV-2 infection in Manaus, Brazil: first description of HTLV-2c subtype in an urban area of the Western Amazon region. Rev Soc Bras Med Trop. 2020;54:e20200066. https://doi.org/10.1590/0037-8682-0066-2020
10. Vallinoto ACR, Ishak MOG, Azevedo VN, Vicente AC, Otsuki K, Hall WW, et al. Molecular epidemiology of human T-lymphotropic virus type II infection in Amerindian and urban populations of the Amazon region of Brazil. Hum Biol. 2002;74:633–44. https://doi.org/10.1353/hub.2002.0059


Address for correspondence: Gemilson Soares Pontes, Laboratory of Virology and Immunology, National Institute of Amazonian Research (INPA), Av. André Araújo, 2.936–Petrópolis, Manaus, Amazonas, Brazil; email: pontesbm1@gmail.com or gemilson.pontes@inpa.gov.br

# Neurologic Alveolar Echinococcosis in Postpartum Zoo-Housed Gorilla, the Netherlands, 2024

Laura A.N. Derks, Marieke Opsteegh, Denise Hoek-van Deursen, Jorrit J. Hofstra, Christine Kaandorp-Huber, Jooske IJzer, Erik A.W.S. Weerts, Volker H. Hackert, Anna R. Tellegen, Vanessa X.N. Visser, Joke W.B. van der Giessen

Author affiliations: Centre for Infectious Disease Control, National Institute for Public Health and the Environment, Bilthoven, the Netherlands (L.A.N. Derks, M. Opsteegh, D. Hoek-van Deursen, J.J. Hofstra, J.W.B. van der Giessen); GaiaZOO, Kerkrade, the Netherlands (C. Kaandorp-Huber); Veterinary Pathology Diagnostic Centre, Utrecht University, Utrecht, the Netherlands (J. IJzer, E.A.W.S. Weerts); Public Health Service South Limburg, Heerlen, the Netherlands (V.H. Hackert); Faculty of Veterinary Medicine, Utrecht University, Utrecht, (A.R. Tellegen); Dutch Food and Consumer Product Safety Authority, Utrecht (V.X.N. Visser)

DOI: http://doi.org/10.3201/eid3207.260136

We report a case of postpartum alveolar echinococcosis in a zoo-housed gorilla in the Netherlands in 2024, with cerebral involvement causing neurologic symptoms. Infection was likely acquired via contaminated feed. This case highlights diagnostic challenges, public health risks, and the need for preventive feed hygiene and surveillance in endemic regions.

*Echinococcus multilocularis*, a zoonotic tapeworm with foxes as the main definitive host and rodents as intermediate hosts, was first detected in foxes in the Netherlands in 1996 (*1*) and is considered an emerging parasitic pathogen (*2*). Humans and other primates can be infected via contaminated food or fomites, risking potentially fatal alveolar echinococcosis (AE). We describe a case of neurologic AE in a postpartum, zoo-housed gorilla in the Netherlands, complicated by pregnancy and neonatal care.

In April 2024, a 25-year-old female western lowland gorilla (*Gorilla gorilla gorilla*), born in England and transferred to GaiaZOO (Kerkrade, the Netherlands) in 2013, gave birth to her second young. The gorilla had no prior health issues. After parturition, lethargy and intermittent anorexia developed, followed by intermittent neurologic symptoms in 1 arm (hemiplegia) and both legs (paraplegia).

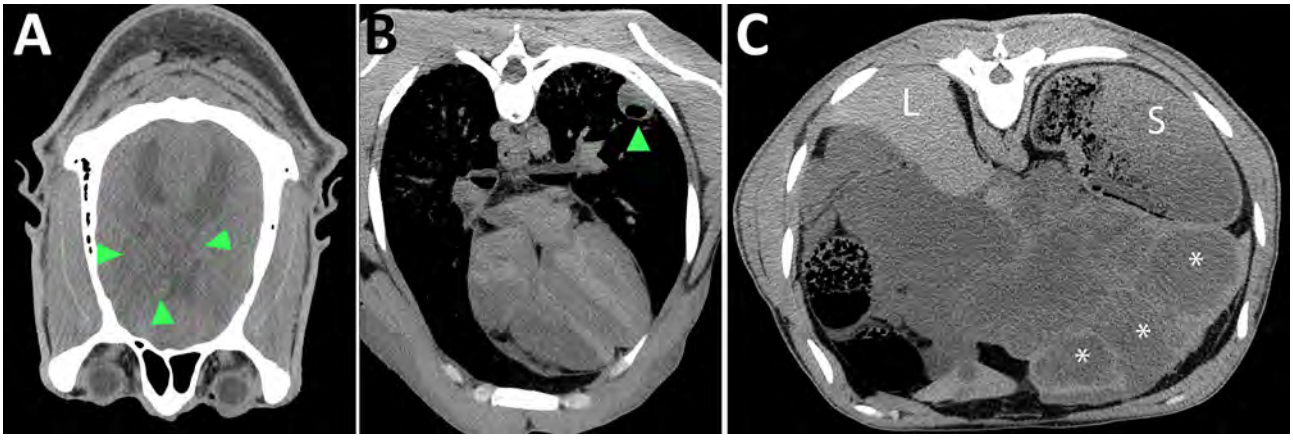


**Figure 1.** Postmortem computed tomography images in soft tissue window from a case of neurologic alveolar echinococcosis in postpartum zoo-housed gorilla, the Netherlands, 2024. A) Transverse view of the brain (anterior is bottom, right is left of image). Green arrows show space-occupying lesion within right hemisphere of cerebrum. B) Transverse view of the lung shows fluid- and gas-filled lesion within the left lung lobe (arrow). C) Transverse view of the liver shows multiple thick-walled, fluid-filled lesions (asterisks). L indicates normal liver tissue; S indicates stomach.

Parasitologic and bacteriologic stool diagnostics yielded no results. Because the gorilla was caring for a newborn, we initially withheld anesthesia-requiring diagnostics and initiated empirical treatment for various differential diagnoses, including *Balamuthia mandrillaris* infection. When symptoms progressed, we performed abdominal ultrasonography and blood sampling under sedation, revealing abscess-like liver lesions. Fine-needle aspiration biopsy yielded bacteriologically and mycologically negative purulent material, negative for *B. mandrillaris* by PCR (Erasmus Medical Center, Rotterdam, the Netherlands). After blood tests and cytology yielded no diagnosis, we submitted serum for *E. multilocularis* serology (Laboklin, Bad Kissingen, Germany).

While awaiting results, we noted stiffness and worsening of hemiparesis in the gorilla. We postponed euthanasia for the newborn to learn to drink from a bottle and bond with another female gorilla. By August 2024, the infected gorilla was unable to walk, prompting euthanasia. Simultaneously, serologic results revealed *E. multilocularis* infection. Imaging and necropsy showed lesions in the brain (Figure 1, panel A; Figure 2, panel A), lungs (Figure 1, panel B), and liver (Figure 1, panel C; Figure 2, panel B). Molecular (12S and COX1) and serologic tests confirmed *E. multilocularis* infection, acquired after 2016 (Appendix, https://wwwnc.cdc.gov/EID/article/32/7/26-0136-App1.pdf), leading to a final diagnosis of disseminated alveolar echinococcosis with liver, lung, and cerebral lesions.

Prior reports have described AE in gorillas (*3*,*4*), noting clinical similarities of progressive apathy, anorexia, and fibrous abdominal adhesions (*3*–*5*). In the case we describe, disease progressed in 4 months from onset to marked deterioration, a more rapid course than the 2-year progression described in cases from Switzerland and Germany, both of which lacked neurologic involvement. A case involving neurologic symptoms was reported in a gorilla in Japan that died after 9 months (*4*). In gorillas, cerebral lesions seem to accelerate disease progression and could be considered a marker of terminal AE, similar to humans (*6*).

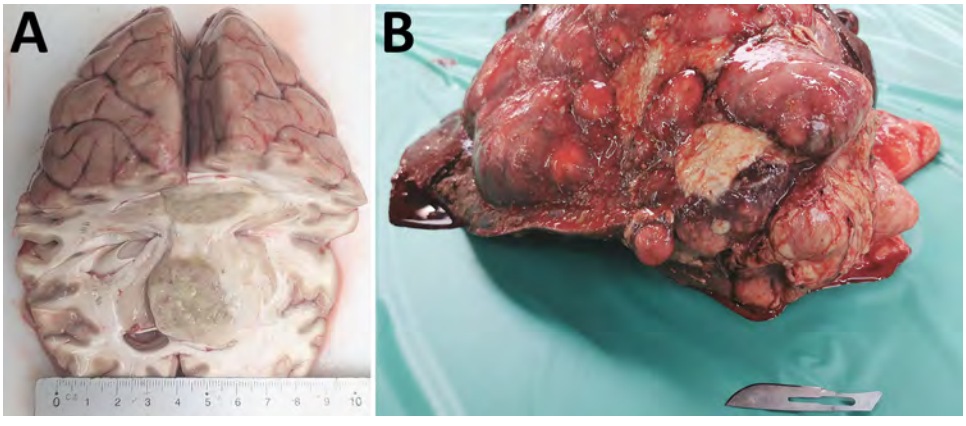


**Figure 2.** Necropsy brain and liver tissue from a case of neurologic alveolar echinococcosis in postpartum zoo-housed gorilla, the Netherlands, 2024. A) Cut surface of the cerebrum. Right hemisphere contains a 3.5-cm diameter, space-occupying tissue mass with ill-defined borders and secondary dislocation of preexisting structures. B) Surface of the liver. The parenchyma is largely replaced by multiple variably sized confluent nodules.

Reports of AE in humans have noted an association between brain metastasis, occurring in 1%–3% of cases (*6*), and immune suppression, which, depending on the host's cellular immunity and cytokine profiles, increases the host's susceptibility to infection and parasitic growth rate. Researchers reporting an AE case in a woman residing in a highly endemic region of China hypothesized pregnancy as a predisposing factor for rapid disease progression in humans, including brain metastasis (*7*). Another report noted rapid disease progression during pregnancy in a woman with cystic echinococcosis (*8*).

Born in England, a country free of *E. multilocularis* parasites, the gorilla we describe was housed in the Netherlands from 2013 and was still serologically negative in 2016, implying local infection. Foxes entering the enclosure seemed unlikely because of physical barriers; therefore, foodborne infection seemed plausible. The gorilla's diet included locally grown fresh produce, leaves, and branches. A prior study investigating fruit from this endemic region found some to contain *E. multilocularis* DNA (*9*). In addition, research conducted in a zoo in Switzerland revealed fresh produce from the primate diet to be contaminated with fox-specific cestodes (*10*), suggesting contact between fox feces and primate feed.

Strategies to minimize infection risks associated with AE include feed hygiene measures, such as thermo-treatment of branches, hard vegetables, and fruits, and purchasing leafy and soft vegetables from nonendemic areas (*10*). Feed should be stored indoors, with minimal contact with the ground. Foxes should be kept out where possible, and fox feces on zoo grounds should be removed, particularly because feces from infected foxes also pose a zoonotic risk to visitors and employees. To monitor foxes roaming the GaiaZOO, zoo staff now regularly collect droppings found on zoo grounds, which are then sent out and tested for *E. multilocularis* parasites.

The rapid deterioration due to cerebral involvement in the gorilla we describe illustrates the aggressive course AE can take when the brain is affected and demonstrates the importance of including AE in the differential diagnosis of neurologic disease, especially in immunocompromised or pregnant individuals in endemic areas. Foodborne transmission from locally grown products seemed the most probable infection source, which implies a risk for humans consuming fresh produce from endemic areas. Education and preventive measures could minimize infection risks for zoo animals and other consumers. Our case highlights the clinical and ethical complexities of managing AE in zoologic settings and reinforces the need for surveillance and prevention strategies at the human–animal–environment interface.

### Acknowledgments

We thank Emile Prins and Ruby Wagensveld for providing us with various samples and information and Stefanie Veraa for the computed tomography scan report. We also thank Chesley van Buuren for performing the DNA extractions and, finally, Pieter Jacobs and Léon Labout for their active involvement in this case.

### About the Author

Ms. Derks is a veterinarian with a master's degree in One Health. She is currently working at the Dutch National Institute for Public Health and the Environment, pursuing her PhD on the epidemiology and public health risks of *Echinococcus multilocularis* in the Netherlands.

### References

1. van der Giessen JW, Rombout YB, Franchimont JH, Limper LP, Homan WL. Detection of *Echinococcus multilocularis* in foxes in The Netherlands. Vet Parasitol. 1999; 82:49–57. https://doi.org/10.1016/S0304-4017(98)00263-5
2. van der Giessen JW, Rombout Y, Teunis P. Base line prevalence and spatial distribution of *Echinococcus multilocularis* in a newly recognized endemic area in the Netherlands. Vet Parasitol. 2004;119:27–35. https://doi.org/10.1016/j.vetpar.2003.11.001
3. Rehmann P, Gröne A, Lawrenz A, Pagan O, Gottstein B, Bacciarini LN. *Echinococcus multilocularis* in two lowland gorillas (*Gorilla g. gorilla*). J Comp Pathol. 2003;129:85–8. https://doi.org/10.1016/S0021-9975(02)00159-7
4. Kondo H, Wada Y, Bando G, Kosuge M, Yagi K, Oku Y. Alveolar hydatidosis in a gorilla and a ring-tailed lemur in Japan. J Vet Med Sci. 1996;58:447–9. https://doi.org/10.1292/jvms.58.447
5. Rehmann P, Gröne A, Gottstein B, Sager H, Müller N, Völlm J, et al. Alveolar echinococcosis in the zoological garden Basle. Schweiz Arch Tierheilkd. 2005;147:498–502. https://doi.org/10.1024/0036-7281.147.11.498
6. Bresson-Hadni S, Vuitton D-A, Bartholomot B, Heyd B, Godart D, Meyer J-P, et al. A twenty-year history of alveolar echinococcosis: analysis of a series of 117 patients from eastern France. Eur J Gastroenterol Hepatol. 2000;12:327–36. https://doi.org/10.1097/00042737-200012030-00011
7. Yang YR, Vuitton DA, Jones MK, Craig PS, McManus DP. Brain metastasis of alveolar echinococcosis in a hyperendemic focus of *Echinococcus multilocularis* infection. Trans R Soc Trop Med Hyg. 2005;99:937–41. https://doi.org/10.1016/j.trstmh.2005.04.020
8. Kain KC, Keystone JS. Recurrent hydatid disease during pregnancy. Am J Obstet Gynecol. 1988;159:1216–7. https://doi.org/10.1016/0002-9378(88)90451-6
9. Umhang G, Bastien F, Cartet A, Ahmad H, van der Ark K, Berg R, et al. Detection of *Echinococcus* spp. and other taeniid species in lettuces and berries: Two international multicenter studies from the MEmE project. Int J Food Microbiol. 2025;430:111059. https://doi.org/10.1016/j.ijfoodmicro.2025.111059

10. Wenker C, Hoby S, Wyss F, Mengiardi B, Vögtli R, Posthaus H, et al. Alveolar echinococcosis in western lowland gorillas (*Gorilla gorilla gorilla*): albendazole was not able to stop progression of the disease. J Zoo Wildl Med. 2019;50:243–53. https://doi.org/10.1638/2018-0064

Address for correspondence: Laura Derks, Centre for Infectious Disease Control, National Institute for Public Health and the Environment, Antonie van Leeuwenhoeklaan 9, 3721MA Bilthoven, the Netherlands; email: laura.derks@rivm.nl

# *Dracunculus* sp. PantanalBr Infection in Florida Panthers and Bobcat, Florida, USA

Michael J. Yabsley, Alexander Perez, Kayla B. Garrett, Christopher A. Cleveland, Mark Cunningham, Peter Sebastian, Bambi Clemons, Jeff M. Gruntmeir, Heather D.S. Walden

Author affiliations: Warnell School of Forestry and Natural Resources and Southeastern Cooperative Wildlife Disease Study, University of Georgia, Athens, Georgia, USA (M.J. Yabsley); University of Georgia, Athens (M.J. Yabsley, K.B. Garrett, C.A. Cleveland); University of Florida, Gainesville, Florida, USA (A. Perez, J.M. Gruntmeir, H.D.S. Walden); Florida Fish and Wildlife Commission, Fish and Wildlife Research Institute, Gainesville (M. Cunningham, P. Sebastian, B. Clemons)

DOI: http://doi.org/10.3201/eid3207.260514

We used morphologic and genetic methods to analyze subcutaneous worms removed from endangered Florida panthers and a bobcat in Florida, USA, identifying *Dracunculus* sp. PantanalBr and several *Dirofilaria* spp. worms. *Dracunculus* sp. PantanalBr had been previously reported in a domestic dog and a jaguar in Brazil.

*Dracunculus* (Spirurida:Dracunculoidea) are large subcutaneous nematodes that can be found in mammals and reptiles (*1*). The life cycle of the parasites involves ingestion of infected cyclopoid copepods via drinking water, although consumption of paratenic or transport hosts (amphibians, fish) may also be involved (*1*,*2*). Female *Dracunculus* nematodes are morphologically indistinguishable by species and more commonly detected than the much smaller male nematodes, so sequence analysis is necessary for species identification (*1*).

Six of 15 *Dracunculus* species infect mammals, and most studies focus on the human Guinea worm, *Dracunculus medinensis*, in Africa (*1*). In North America, studies have reported 4 mammalian *Dracunculus* spp. nematodes: *D. insignis* (in various wild carnivores, dogs, cats), *D. lutrae* and an undescribed species (in river otters [*Lontra canadensis*]), and another undescribed species (in a Virginia opossum [*Didephis virginianus*], a river otter [USA], and a dog [Spain]) (*1*,*3*–*5*). Researchers have reported 3 *Dracunculus* nematode species in South America: *D. jaguape* (in a neotropical otter [*Lontra longicaudis*]), *D. fuelleborni* (in a big-eared opossum [*Didelphis aurita*]), and an undescribed species (*Dracunculus* sp. PantanalBr) (in dogs and a jaguar [*Panthera onca*] in Brazil) (*6*,*7*).

The Florida panther (*Puma concolor coryi*) is an endangered North American puma (*P. c. couguar*) subspecies restricted to South Florida. As part of mortality investigations, Florida Fish and Wildlife Conservation Commission veterinarians perform necropsies on panthers and bobcats (*Lynx rufus*). This study reports the findings related to worms collected from panthers and a bobcat, including detection of *Dracunculus* sp. PantanalBr.

We removed subcutaneous or internal parasites from 12 Florida panthers and 1 bobcat collected in Florida during 2002–2025, preserving the samples in formalin or 70% ethanol (Figure 1, panel A; Appendix 1 Table, https://wwwnc.cdc.gov/EID/article/32/7/26-0514-App1.pdf). We morphologically identified and genetically characterized all worms collected (Appendix 1).

Most worms were fragments, so we based identification on a combination of sequence analysis and morphology (characteristic first-stage larvae) (Figure 1, panel B). We noted 5 panthers and the bobcat to be infected with *Dracunculus* sp. nematodes, subsequently identifying parasites from 2 of those panthers and the bobcat as *Dracunculus* sp. PantanalBR. We identified *Dirofilaria* spp. nematodes in 7 panthers (Appendix 1).

We obtained partial *Dracunculus* cytochrome oxidase subunit I (COI) and 18S rRNA sequences from 2 Florida panthers and the bobcat. The two 657-bp COI sequences from Florida panthers were identical and were 99.7% similar to *Dracunculus* sp. PantanalBR identified in a jaguar and 98.8% similar to *Dracunculus* sp. PantanalBR detected in a dog (Appendix 2 Table 1, https://wwwnc.cdc.gov/EID/article/32/7/26-0514-App2.xlsx). The bobcat worm sequence was 99.5%

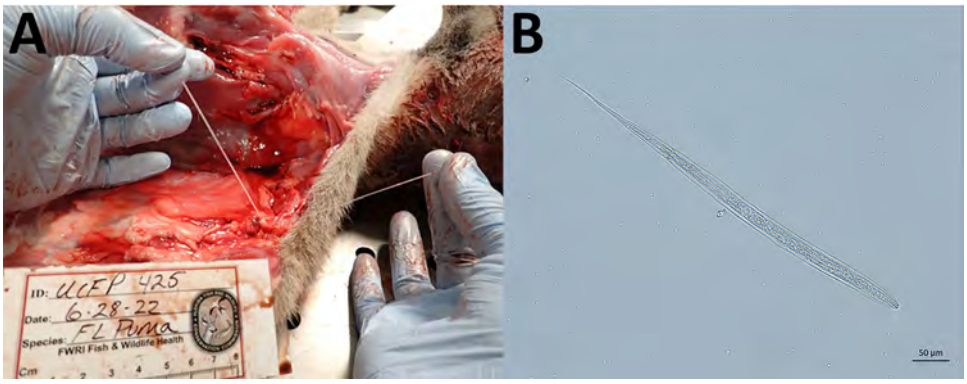


**Figure 1.** *Dracunculus* sp. PantanalBR nematode samples collected in investigation of *Dracunculus* sp. PantanalBr infection in Florida panthers and a bobcat, Florida, USA. A) Female *Dracunculus* sp. PantanalBR nematode was detected in subcutaneous tissues of a Florida panther (*Puma concolor coryi*). B) First-stage larvae of female *Dracunculus* sp. PantanalBR from a Florida panther. Original magnification ×200.

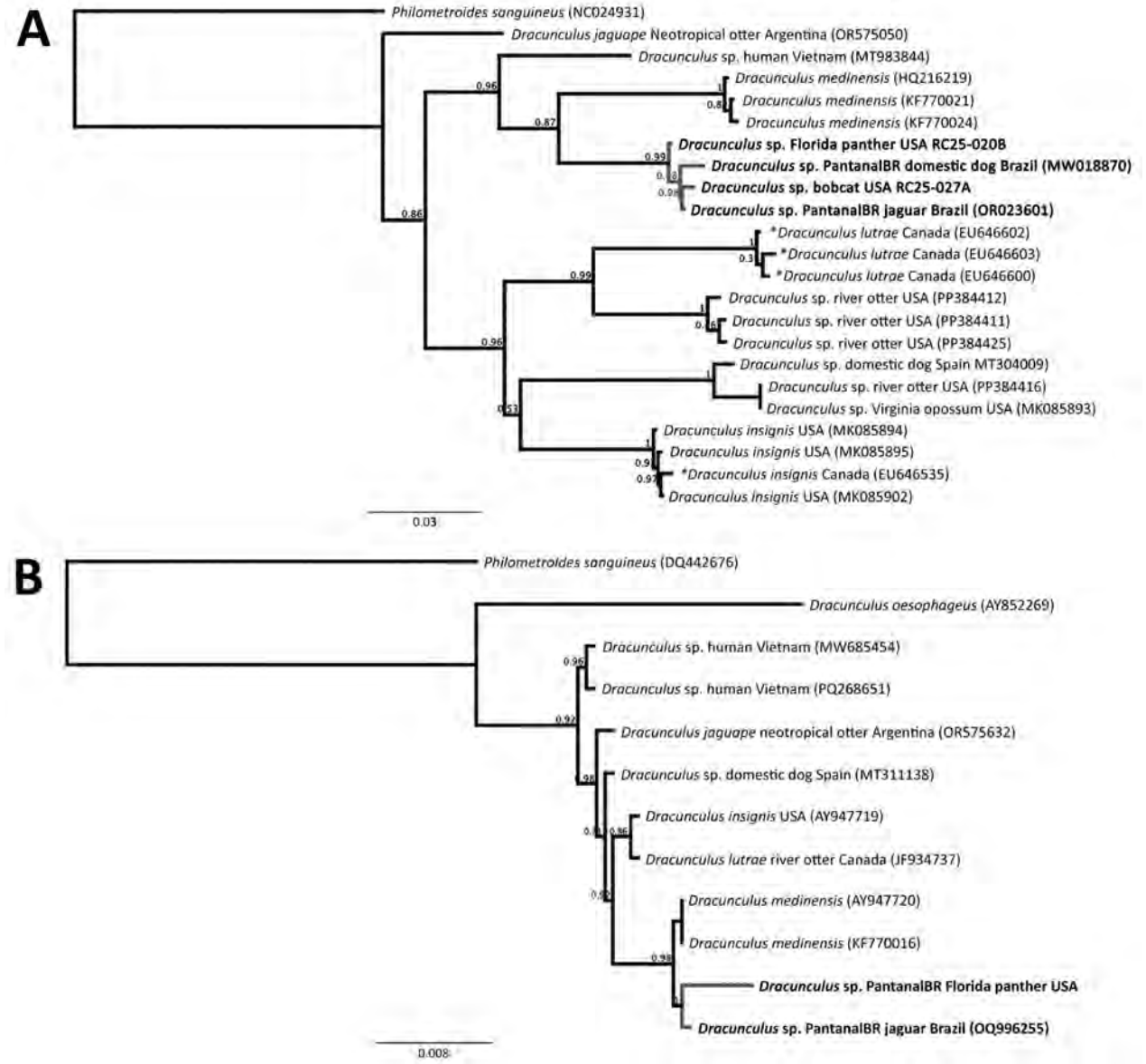


**Figure 2.** Phylogenetic tree of *Dracunculus* sp. PantanalBr nematodes collected from Florida panthers and a bobcat, Florida, USA. A) Genetic relationships of *Dracunculus* sp. PantanalBR from a Florida panther (*Puma concolor coryi*) and a bobcat (*Lynx rufus*) compared with other *Dracunculus* spp. based on partial cytochrome c oxidase subunit 1 gene sequences. B) Genetic relationships of *Dracunculus* sp. PantanalBR from Florida panther compared with other *Dracunculus* spp. based on partial 18S rRNA gene sequences. Boldface text represents specimens analyzed in this study. Scale bars indicate substitutions per site.

(654/657 bp) similar to the Florida panther sequences. Phylogenetically, the Florida panther and bobcat worm sequences grouped with the 2 *Dracunculus* sp. PantanalBR sequences (Figure 2, panel A). The 18S rRNA sequences (956 base pair) from the 2 Florida panthers and bobcat were identical and 99.9% similar to *Dracunculus* sp. PantanalBR (806/807 bp) (Appendix 2 Table 2). Phylogenetic analysis produced a similar tree to the COI gene (Figure 2, panel B). Larvae from *Dracunculus* sp. PantanalBR from 1 panther measured 601.67 μm long and 25.56 μm wide.

Our data confirm *Dracunculus* sp. PantanalBR nematodes in North America. A prior report of female *Dracunculus* nematodes in Florida panthers was reported as *D. insignis* in 2 Florida panthers from Monroe County in 1989–1990; however, that investigation included no genetic analysis to confirm species (*8*). Thus, it is unknown if Florida panthers are hosts for *Dracunculus* sp. PantanalBR and *D. insignis* nematodes, although *D. insignis* nematode infects domestic cats (*5*). Before our report, researchers reported 3 *Dracunculus* nematode species in Florida, including 2 undescribed *Dracunculus* clades in 2 river otters and unspeciated female *Dracunculus* nematodes in a domestic dog and raccoons (*1*,*3*,*4*). However, because *Dracunculus* sp. PantanalBR infects dogs and *D. insignis* nematode is only presumed to occur in Florida, worms from dogs and cats should be genetically characterized to determine species.

The *Dracunculus* sp. PantanalBR life cycle is unknown, but *Dracunculus* nematode species use copepods as intermediate hosts, and some species may use aquatic paratenic hosts (*1*,*2*). Further studies are needed to determine if this parasitic species is transmitted through ingestion of copepods or through a paratenic host. We discovered the subcutaneous parasites in the animals we studied during routine necropsy, and no lesions were noted, but researchers have observed ulceration and edema in other *Dracunculus*-infected hosts (*1*,*3*–*7*). *Dracunculus* infections can cause lameness in some hosts, but observation of clinical signs in free-ranging wildlife might be difficult.

The Florida panther is restricted to southern Florida, and the source of *Dracunculus* nematodes in the population is unknown. Genetic testing of panthers in Florida identified a unique lineage in the Everglades National Park that appeared to be of South American origin (*9*,*10*). Researchers presumed the origin of this unique genotype was the introduction of 7 captive pumas in the 1950–1960s to the park, all of which were brought from Central America (*9*,*10*). Although that history suggests a possible introduction route for *Dracunculus* sp. PantanalBR nematodes, additional surveillance of canids and felids in the Americas is needed to further clarify distribution and risk for infection.

Support was provided by the wildlife management agencies of the Southeastern Cooperative Wildlife Disease Study member states through the Federal Aid to Wildlife Restoration Act (50 Stat. 917) and by a U.S. Department of the Interior Cooperative Agreement. Florida Fish and Wildlife Conservation Commission veterinarians collected Florida panther samples using funding from the Florida Panther Research and Management Trust Fund.

## About the Author

Dr. Yabsley is the Mace Distinguished Professor of wildlife disease ecology, University of Georgia, Athens, Georgia. His research interests include vectorborne, parasitic, and zoonotic pathogens of wildlife and domestic animals.

## References

1. Cleveland CA, Garrett KB, Cozad RA, Williams BM, Murray MH, Yabsley MJ. The wild world of Guinea worms: a review of the genus *Dracunculus* in wildlife. Int J Parasitol Parasites Wildl. 2018;7:289–300. https://doi.org/10.1016/j.ijppaw.2018.07.002
2. Box EK, Yabsley MJ, Garrett KB, Thompson AT, Wyckoff ST, Cleveland CA. Susceptibility of anurans, lizards, and fish to infection with *Dracunculus* species larvae and implications for their roles as paratenic hosts. Sci Rep. 2021;11:11802. https://doi.org/10.1038/s41598-021-91122-5
3. Williams BM, Cleveland CA, Verocai GG, Swanepoel L, Niedringhaus KD, Paras KL, et al. *Dracunculus* infections in domestic dogs and cats in North America; an under-recognized parasite? Vet Parasitol Reg Stud Reports. 2018;13:148–55. https://doi.org/10.1016/j.vprsr.2018.05.005
4. Yabsley MJ, Garrett KB, Thompson AT, Box EK, Giner MR, Haynes E, et al. Otterly diverse—a high diversity of *Dracunculus* species (Spirurida: Dracunculoidea) in North American river otters (*Lontra canadensis*). Int J Parasitol Parasites Wildl. 2024;23:100922. https://doi.org/10.1016/j.ijppaw.2024.100922
5. Cleveland CA, Eberhard ML, Garrett KB, Thompson AT, Swanepoel L, Miller EA, et al. *Dracunculus* species in meso-mammals from Georgia, United States, and implications for the Guinea Worm Eradication Program in Chad, Africa. J Parasitol. 2020;106:616–22. https://doi.org/10.1645/18-178
6. Fagundes-Moreira R, Bezerra-Santos MA, May-Junior JA, Baggio-Souza V, Rampim LE, Sartorello LR, et al. The jaguar (*Panthera onca*) as a potential new host of *Dracunculus* sp. Parasitol Res. 2023;122:2951–6. https://doi.org/10.1007/s00436-023-07984-3
7. Paiva F, de Souza Piazzalunga P, Pereira FB, Borghesan TC, Soares P, Tavares LER. Dracunculiasis in a domestic dog in Brazil. Parasitol Res. 2021;120:1371–7. https://doi.org/10.1007/s00436-021-07098-8
8. Forrester DJ. Parasites and diseases of wild mammals in Florida. Gainesville (FL): University Press of Florida; 1992.
9. US Fish & Wildlife Service. Species status assessment for the Florida panther. 2020, version 1.0. September 2020.

Vero Beach, Florida [cited 2026 June 12] https://www.researchgate.net/publication/355077988_Species_Status_Assessment_for_the_Florida_Panther
10. Saremi NF, Supple MA, Byrne A, Cahill JA, Coutinho LL, Dalén L, et al. *Puma* genomes from North and South America provide insights into the genomic consequences of inbreeding. Nat Commun. 2019;10:4769. https://doi.org/10.1038/s41467-019-12741-1

Address for correspondence: Michael Yabsley, Southeastern Cooperative Wildlife Disease Study, College of Veterinary Medicine, University of Georgia Wildlife Disease Building, Athens, GA 30605, USA; email: myabsley@uga.edu

# *Ancylostoma ceylanicum* Hookworm, Rural Papua New Guinea, 2020

Jessica L. Scott, Daniel Pelowa, Wayne Melrose, Jeffrey M. Warner, Catherine M. Rush

Author affiliations: James Cook University College of Medicine and Dentistry, Townsville, Queensland, Australia (J.L. Scott, W. Melrose, J.M. Warner, C.M. Rush); James Cook University Australian Institute of Tropical Health and Medicine, Townsville (J.L. Scott, J.M. Warner, C.M. Rush); Balimo District Hospital, Balimo, Papua New Guinea (D. Pelowa)

DOI: https://doi.org/10.3201/eid3207.251567

We conducted a cross-sectional study of zoonotic hookworm *Ancylostoma ceylanicum* in humans in Western Province, Papua New Guinea, confirmed by internal transcribed spacer sequencing. Overall hookworm prevalence was 54.9%; *A. ceylanicum* hookworms were present in 3.3% of specimens. One Health approaches are needed for hookworm control in Papua New Guinea.

Hookworm infections pose a major public health challenge in Papua New Guinea (PNG). Historic national estimates suggest that up to three quarters of the population may be infected (*1*); a 2025 study reported prevalence ≥80% for the anthropophilic hookworm species *Necator americanus* in Madang Province (*2*). In 2018, the zoonotic hookworm *Ancylostoma ceylanicum* was confirmed in a migrant worker returning from Manus Island by using molecular methods (*3*). However, since that initial report, no data have been published on the prevalence of *A. ceylanicum* hookworm among local populations in PNG. We report molecular evidence of locally acquired *A. ceylanicum* infections in a rural community in PNG, alongside a high overall prevalence of hookworm infection.

We conducted a cross-sectional study in collaboration with the Balimo District Hospital (Balimo, PNG) during January 2020. We recruited community members >16 years of age through convenience sampling from Balimo, which is situated in the Delta Fly District of the Western Province of PNG (Appendix Figure 1, https://wwwnc.cdc.gov/EID/article/32/7/25-1657-App1.pdf). We preserved fecal specimens in sodium-acetate 5% formalin (SAF) and separately in guanidinium thiocyanate within 8 hours of submission. We examined SAF-preserved specimens for hookworm ova by microscopy, using direct unconcentrated and ethyl acetate–concentrated fecal smears.

We extracted genomic DNA from guanidinium thiocyanate–preserved fecal specimens using the Zymo Quick-DNA Fecal/Soil Microbe Miniprep Kit (Zymo Research Corporation, https://www.zymoresearch.com). We detected 3 hookworm species, *N. americanus*, *A. ceylanicum*, and *A. duodenale*, using TaqMan quantitative PCR (qPCR) (Integrated DNA Technologies, https://sg.idtdna.com) (Appendix Table). We Sanger sequenced all *Ancylostoma* qPCR-positive samples targeting the internal transcribed spacer region, using custom primers (forward 5′-GAATGCCGCCTTACTGCTTG-3′ and reverse 5′-CGATTCAGCAGCAACAACGAG-3′) (Appendix).

Among the 122 participants who submitted a fecal specimen, microscopy detected hookworm ova in 28 (22.9%), whereas qPCR identified 64 (52.5%) as positive. Combining both methods yielded an overall hookworm prevalence of 54.9% (67/122) (Table). Three (4.5%) samples that tested positive by microscopy were negative by qPCR. *N. americanus* was the predominant hookworm species detected by qPCR, identified in 64 (52.5%) participants. We detected *Ancylostoma* spp. hookworm in 4 (3.3%) samples; all *Ancylostoma*-positive participants were also infected with *N. americanus*. All sequences identified in this study (GenBank accession nos. PV530493–6) formed a distinct cluster with *A. ceylanicum* sequences, including the positive template control isolate (accession no. PV530497) and the PNG isolate previously identified from the migrant worker (accession no. LC036567), confirming all 4 cases as *A. ceylanicum* hookworm

**Table.** Prevalence of hookworm infections found in study of *Ancylostoma ceylanicum* hookworm, rural Papua New Guinea, 2020*

| Method | No. (%) | | |
|---|---|---|---|
| | Hookworm | *Necator americanus* | *Ancylostoma* spp. |
| Microscopy | 28 (22.9) | NA | NA |
| TaqMan qPCR† | 64 (52.5) | 64 (52.5) | 4 (3.3) |
| Total | 67 (54.9) | 64 (52.5) | 4 (3.3) |

*NA, not applicable; qPCR, quantitative PCR.
†Integrated DNA Technologies, https://sg.idtdna.com.

(Figure). We detected no *A. duodenale* cases (Appendix Figure 2).

This study provides molecular evidence of *A. ceylanicum* hookworm in a rural community in Western Province, PNG. Our findings further support the recognition of *A. ceylanicum* as the second most common human hookworm in the Asia-Pacific region (*4*); however, in our study it accounted for only a small proportion of the overall hookworm burden compared with *N. americanus*.

The absence of *A. duodenale* hookworm prompts reconsideration of earlier hookworm surveys in PNG. Previous studies relied on larval culture for species identification; however, the close morphologic similarity between *A. duodenale* and *A. ceylanicum* larvae might have led to misclassification, raising the possibility that *A. ceylanicum* infections were historically present but attributed to *A. duodenale*. Whether that is the case or that *A. ceylanicum* hookworm was more recently introduced remains unclear. A study in Madang Province found neither *A. ceylancium* nor *A. duodenale* hookworm despite high hookworm prevalence, indicating geographic variation could also exist (*2*). Conditions in Balimo, including free-roaming dogs that serve as household guardians, may favor potential zoonotic transmission of *A. ceylanicum* hookworms. At the time of our study, veterinary services and deworming programs were absent, creating

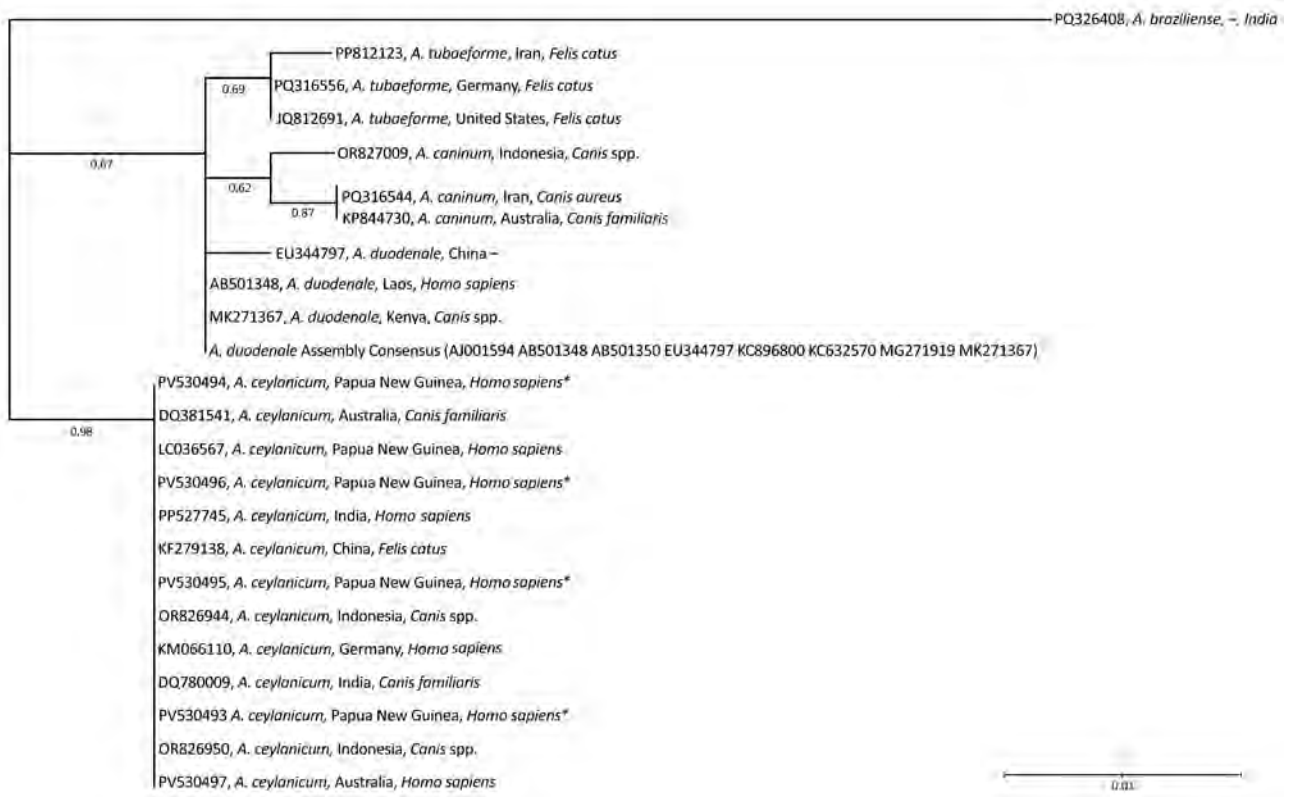


**Figure.** Phylogenetic analysis of *Ancylostoma* spp. in study of *A. ceylanicum* hookworm, rural Papua New Guinea, 2020. Analysis is based on the internal transcribed spacer sequence regions 1 and 2 and conducted with the maximum-likelihood method, using the Kimura 2-parameter model. Model selection was based on penalized-likelihood information criteria. The phylogenetic tree was visually adjusted using Interactive Tree of Life version 7.2.2 (https://itol.embl.de). Values at branch nodes indicate bootstrap support values (1,000 replicates). *A. braziliense* was used as an outgroup to root the tree. GenBank accession numbers are shown; asterisks (*) denote sequences identified in this study (accession nos. PV530493–96). We used *A. ceylanicum* (accession no. PV530497) as a positive control. Dash (–) indicates that no information was available for a particular attribute of the strain. Scale bar represents 0.01 substitutions per site.

opportunities for parasite persistence at the human–animal–environment interface. Nevertheless, without concurrent sampling of local dogs and cats, the contribution of animal reservoirs and the directionality of transmission remain unclear.

Delayed specimen processing might have resulted in lysis of hookworm ova, thereby reducing the sensitivity of microscopy in our study. Furthermore, hookworm ova are morphologically similar to those of *Strongyloides fuelleborni* subspecies *fuelleborni*, which is known to occur in the region (*5*); strongyloidiasis has been detected in the same community in which we conducted our study (*6*). That overlap in egg morphology might represent one of several factors contributing to the discrepancy observed between microscopy-positive and qPCR-negative specimens. In addition, the modest sample size and convenience sampling of participants >16 years of age limit the generalizability of our findings to the wider community and surrounding areas. Given that untreated hookworm infection can persist long term, prevalence estimates may also be influenced by chronic infections within the sampled population.

In summary, the presence of *A. ceylanicum* hookworms in this region requires a One Health approach to addressing both human infections and animal reservoirs. Traditional deworming programs targeting only humans are insufficient for preventing reinfection and achieving sustainable elimination where zoonotic transmission may occur.

### Acknowledgments

We thank the participants and community members of the Balimo region, whose invaluable contribution was fundamental to this research. We thank Angela Slatcher for her technical guidance in participant recruitment and specimen processing.

Approval for this study was obtained from the Middle Fly District Health Service, Evangelical Church of PNG Health Services, James Cook University Human Research Ethics Committee (H6432 and H8015), and the PNG Medical Research Advisory Committee (MRAC 19.21). Informed consent was obtained from all participants.

J.L.S. has been supported through the Australian Government Research Training Program Scholarship. Primary funding provided by the HOT NORTH—Pilot Project was awarded to C.M.R. and J.M.W.

During the preparation of this work, J.L.S. used Claude Opus (Claude 3.5 Sonnet) and Grammarly for Microsoft Office (version 6.8.263) to check grammar and spelling. After using this tool, the author reviewed and edited the content as needed and takes full responsibility for the publication's content.

## About the Author

Ms. Scott is a PhD candidate at James Cook University, Australia, with a background in biomedical sciences. Her primary research interests are intestinal parasitic infections and tuberculosis co-infections.

### References

1. Kline K, McCarthy JS, Pearson M, Loukas A, Hotez PJ. Neglected tropical diseases of Oceania: review of their prevalence, distribution, and opportunities for control. PLoS Negl Trop Dis. 2013;7:e1755. https://doi.org/10.1371/journal.pntd.0001755
2. Tobon Ramos JA, Maure T, Carias L, Lew D, Goss C, Samuel A, et al. Impact of mass drug administration with ivermectin, diethylcarbamazine, and albendazole for lymphatic filariasis on hookworm and *Strongyloides stercoralis* infections in Papua New Guinea. PLoS Negl Trop Dis. 2025;19:e0012851. https://doi.org/10.1371/journal.pntd.0012851
3. Yoshikawa M, Ouji Y, Hirai N, Nakamura-Uchiyama F, Yamada M, Arizono N, et al. *Ancylostoma ceylanicum*, novel etiological agent for traveler's diarrhea—report of four Japanese patients who returned from Southeast Asia and Papua New Guinea. Trop Med Health. 2018;46:6. https://doi.org/10.1186/s41182-018-0087-8
4. Tenorio JCB, Tabios IKB, Inpankaew T, Ybañez AP, Tiwananthagorn S, Tangkawattana S, et al. *Ancylostoma ceylanicum* and other zoonotic canine hookworms: neglected public and animal health risks in the Asia-Pacific region. Anim Dis. 2024;4:11. https://doi.org/10.1186/s44149-024-00117-y
5. Zhao H, Haidamak J, Noskova E, Ilik V, Pafčo B, Ford R, et al. Insights into infant strongyloidiasis, Papua New Guinea. Emerg Infect Dis. 2025;31:1793–801. https://doi.org/10.3201/eid3109.241923
6. Scott J, Emeto TI, Melrose W, Warner J, Rush C. Seroepidemiology of *Strongyloides* spp. infection in Balimo, Western Province, Papua New Guinea. Am J Trop Med Hyg. 2023;108:346–52. https://doi.org/10.4269/ajtmh.22-0408

Address for correspondence: Catherine Rush, Australian Institute of Tropical Health & Medicine, James Cook University, Mount Stuart St, Bldg 48 Rm 104, Douglas, Townsville, QLD 4811, Australia; email: catherine.rush@jcu.edu.au

# Autochthonous Neurocysticercosis Brain Lesions Mimicking Metastatic Disease, Spain

Elena Hernández-Sánchez, Paloma Monllor, Maria Gil-Fortuño, Edelmira Guillamón

Author affiliation: Hospital de La Plana, Vila-real, Castellón, Spain

DOI: http://doi.org/10.3201/eid3207.260587

Autochthonous neurocysticercosis is exceptionally rare in Western Europe. We describe multiple brain lesions, initially mimicking metastases, in a 60-year-old man in Spain without travel history. We confirmed diagnosis by neuroimaging and positive serology. Our study highlights cryptic local *Taenia solium* cestode transmission risks and diagnostic challenges in nonendemic regions.

A 60-year-old man, a lifelong resident of Castellón (Valencian Community), Spain, sought treatment for a 2-week history of progressive headache and subtle behavioral changes. He had no history of international travel or immunosuppression. Neurologic examination revealed mild psychomotor slowing without focal deficits. Initial laboratory tests were unremarkable except for an elevated total serum IgE of 200 IU/mL (reference <100 IU/mL). A noncontrast head computed tomography scan revealed multiple ill-defined intra-axial lesions with marked vasogenic edema, initially suspected to represent metastatic disease (Figure, panel A). We initiated dexamethasone (8 mg/d), rapidly resolving his symptoms. Extensive oncologic workup, including whole-body, contrast-enhanced computed tomography, colonoscopy, and fluorine-18 fluorodeoxyglucose positron emission tomography/computed tomography showed no primary malignancy. A subsequent brain magnetic resonance imaging scan demonstrated numerous solid-cystic lesions diffusely distributed throughout both hemispheres, displaying ring enhancement (Figure, panel B). Of note, several cystic lesions contained internal nodular components suggestive of a scolex (Figure, panel C).

Both the patient we report and his household contacts lacked travel history to *Taenia*-endemic regions, and results of stool examinations for ova and parasites for the patient and his household contacts were negative. However, the man had previously worked as a construction laborer until retiring 10 years prior. In that occupation, he frequently shared meals and communal sanitary facilities with migrant coworkers from regions endemic for *Taenia solium* tapeworms, presenting a potential setting for cryptic fecal–oral transmission.

Given the pathognomonic imaging features and the patient history, we evaluated serum antibodies against *T. solium* by using enzyme-linked immunoelectrotransfer blot at the Spanish National Centre for Microbiology (Instituto de Salud Carlos III, Madrid), the national reference laboratory. The official report confirmed a positive diagnostic result. After noting fulfillment of 2 major Del Brutto diagnostic criteria (*1*,*2*), we established a definitive diagnosis of neurocysticercosis (NCC). We treated the patient successfully with albendazole (400 mg 2×/d) and praziquantel (1,200 mg 3×/d) (*3*), alongside dexamethasone taper, without complications.

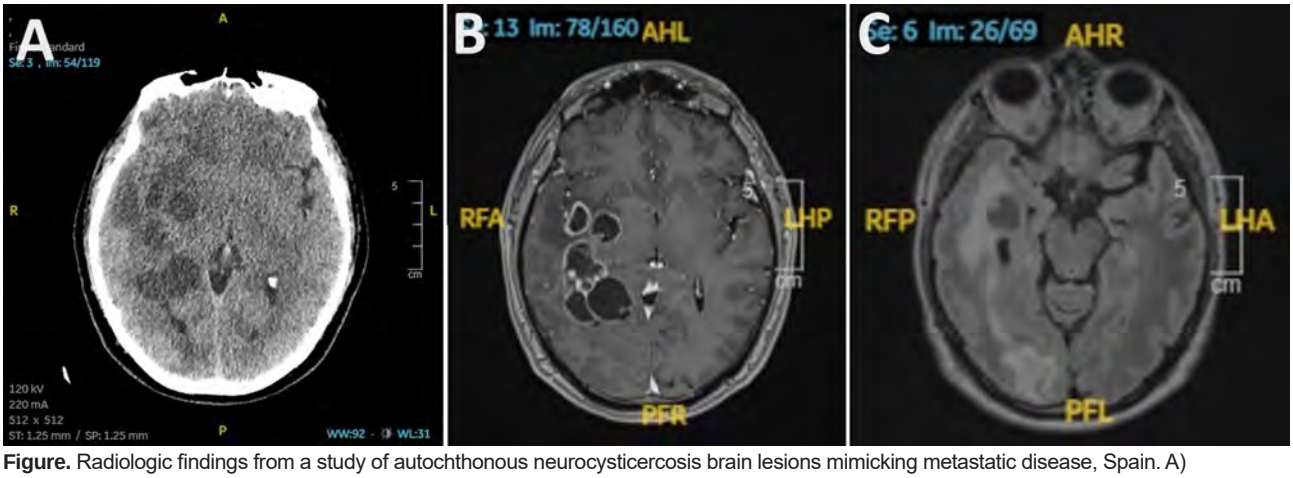


**Figure.** Radiologic findings from a study of autochthonous neurocysticercosis brain lesions mimicking metastatic disease, Spain. A) Noncontrast head computed tomography demonstrating multiple intra-axial lesions with surrounding vasogenic edema. B) Axial T1-weighted magnetic resonance imaging sequence with gadolinium showing multiple ring-enhancing lesions. C) Axial T2-FLAIR magnetic resonance imaging sequence revealing cystic lesions with internal nodular components suggestive of a scolex, surrounded by extensive edema.

In Europe and the United States, NCC is a disease seen predominantly in migrants and returning travelers. Autochthonous transmission is exceptionally rare. In the United States, domestically acquired cases account for <2% of all NCC diagnoses, usually linked to close contact with a household employee or family member from an endemic area (*4*). In Europe, a comprehensive systematic review identified only 18 confirmed autochthonous cases of NCC across Western Europe in 1990–2011 (*5*). More recent data confirm this rarity; during 2000–2019, reports of autochthonous cases across all European Union member states totaled <30 (*6*,*7*). In Spain, Herrador et al. identified 1,912 hospital discharges with cysticercosis during 1997–2014, with hospitalization rates paralleling external migration trends (*8*).

Our case emphasizes that the absence of travel history should not preclude NCC from the differential diagnosis of multiple ring-enhancing brain lesions, even in regions where metastatic cancer is statistically much more likely. Early recognition of specific neuroimaging markers, such as the scolex, coupled with confirmatory enzyme-linked immunoelectrotransfer blot testing, can prevent unnecessary invasive oncologic procedures and lead to prompt, targeted antiparasitic therapy.

### Acknowledgment

We are very grateful to the patient and his family, who consented to the publication of this report and the accompanying anonymized radiologic images.

### About the Author

Dr. Hernández-Sánchez is an internal medicine resident at Hospital Universitari de La Plana, Vila-real, Spain. Her primary interests include humanitarian medicine and neglected tropical diseases.

### References

1. Del Brutto OH, Nash TE, White AC Jr, Rajshekhar V, Wilkins PP, Singh G, et al. Revised diagnostic criteria for neurocysticercosis. J Neurol Sci. 2017;372:202–10. https://doi.org/10.1016/j.jns.2016.11.045
2. Garcia HH, Del Brutto OH. *Taenia solium* cysticercosis. Infect Dis Clin North Am. 2000;14:97–119, ix. https://doi.org/10.1016/S0891-5520(05)70220-8
3. White AC Jr, Coyle CM, Rajshekhar V, Singh G, Hauser WA, Mohanty A, et al. Diagnosis and treatment of neurocysticercosis: 2017 Clinical Practice Guidelines by the Infectious Diseases Society of America (IDSA) and the American Society of Tropical Medicine and Hygiene (ASTMH). Clin Infect Dis. 2018;66:e49–75. https://doi.org/10.1093/cid/cix1084
4. O'Neal SE, Flecker RH. Hospitalization frequency and charges for neurocysticercosis, United States, 2003-2012. Emerg Infect Dis. 2015;21:969–76. https://doi.org/10.3201/eid2106.141324
5. Zammarchi L, Strohmeyer M, Bartalesi F, Bruno E, Muñoz J, Buonfrate D, et al.; COHEMI Project Study Group. Epidemiology and management of cysticercosis and *Taenia solium* taeniasis in Europe, systematic review 1990-2011. PLoS One. 2013;8:e69537. https://doi.org/10.1371/journal.pone.0069537
6. Laranjo-González M, Devleesschauwer B, Trevisan C, Allepuz A, Sotiraki S, Abraham A, et al. Epidemiology of taeniosis/cysticercosis in Europe, a systematic review: Western Europe. Parasit Vectors. 2017;10:349. https://doi.org/10.1186/s13071-017-2280-8
7. Devleesschauwer B, Allepuz A, Dermauw V, Johansen MV, Laranjo-González M, Smit GSA, et al. *Taenia solium* in Europe: Still endemic? Acta Trop. 2017;165:96–9. https://doi.org/10.1016/j.actatropica.2015.08.006
8. Herrador Z, Fernandez-Martinez A, Benito A, Lopez-Velez R. Clinical Cysticercosis epidemiology in Spain based on the hospital discharge database: What's new? PLoS Negl Trop Dis. 2018;12:e0006316. https://doi.org/10.1371/journal.pntd.0006316

Address for correspondence: Elena Hernández, Department of Internal Medicine, Hospital Universitari de La Plana, Vila-real Ctra. Vila-Real a Burriana km 0.5, 12540, Castelló, Spain; email: hernandez_elena@gva.es

# Chikungunya Outbreak, Cuba, July 2025

Melissa M. Perez,[1] Sonia Resik,[1] Berta Maria Bello Rodriguez, Ariamys Companioni, Daniel Gonzalez, Ana Julia Benitez, Yanet Martinez, Mónica Sanchez, Mayling Alvarez, Denelsys Hernandez, Jose Raul de Armas, Aliuska Batista Serrano, Madelaine Rivera, Carilda Peña, Liannet Domínguez Ramos, Silvia Serrano, Rosario Gravier, Lorena Vazquez, Vivian Kourí, Maria G. Guzman

Author affiliations: Pedro Kouri Tropical Medicine Institute, Havana, Cuba (M.M. Perez, S. Resik, A. Companioni, D. Gonzalez, A.J. Benitez, Y. Martinez, M. Sanchez, M. Alvarez, D. Hernandez, S. Serrano, R. Gravier, L. Vazquez, V. Kourí, M.G. Guzman); Matanzas Provincial Center for Hygiene, Epidemiology and Microbiology, Matanzas, Cuba (B.M. Bello Rodriguez); Ministerio de Salud Pública, Havana (J.R. de Armas, M. Rivera, C. Peña); Polyclinic 30th Anniversary, Perico Municipality, Matanzas (A. Batista Serrano, L. Domínguez Ramos)

DOI: https://doi.org/10.3201/eid3207.260344

[1]These authors contributed equally to this article.

Chikungunya transmission was confirmed in Perico, Matanzas Province, Cuba. Initial research confirmed the presence of East/Central/South African genotype related to Brazil 2025 strains in serum samples and in *Aedes aegypti* mosquito pools from transmission areas. Our findings underscore the need for surveillance and signal potential spread to other regions.

In 2004, the global epidemiology of chikungunya shifted, when the virus spread from Kenya to islands in the Indian Ocean. By 2013, transmission reached the French Caribbean and subsequently expanded throughout the Americas. In 2025, the Pan American Health Organization reported 631,720 suspected chikungunya cases, primarily in Brazil, Bolivia, Argentina, and Paraguay (*1*). Viral persistence in the Americas is driven by a combination of climatic, economic, social, demographic, and entomovirologic factors (*2*).

Cuba maintains a national dengue surveillance system for acute febrile illness (AFI) of unknown etiology. Serum samples are routinely tested for dengue IgM at local laboratories, and molecular testing by quantitative reverse transcription PCR (qRT-PCR) is conducted at the Arbovirus National Reference Laboratory of the Institute of Tropical Medicine Pedro Kouri (*3*).

On July 16, 2025, an increase in AFI cases was reported in España Republicana, Perico Municipality, Matanzas Province. Serum samples from AFI cases collected for dengue IgM detection tested negative at Perico laboratory. On July 21, the reference laboratory received 12 serum samples from patients with AFI from España Republicana and tested extracted RNA by qRT-PCR using QIAmp Viral RNA Mini Kit (QIAGEN, https://www.qiagen.com) and VIASURE multiplex test (Certest Biotec, https://www.certest.es) for dengue (DENV), Zika, chikungunya (CHIKV), Mayaro, Oropouche, and yellow fever viruses (*4*). Eight (66.7%) samples tested positive for CHIKV and 1 (8.3%) for DENV.

Confirmed chikungunya patients experienced high-grade fever lasting 48–72 hours and unresponsive to antipyretics, and severe disabling joint pain, predominantly in the hands, ankles, and back. Inflammation of the affected joints and a pruritic maculopapular rash were observed at various stages of the illness. Additional symptoms included oral lesions, vomiting, nausea, loss of appetite, diarrhea, and malaise. Median age was 46 (range 15–72) years. An equal number of male and female patients were affected. No severe or fatal cases were identified in that initial cluster.

**Table.** Characteristics of samples collected from symptomatic patients during chikungunya outbreak, Matanzas Province, Cuba, 2025*

| Municipality | No. tested | Epidemiologic week collected | Mean (range) days of sample collection† | CHIKV-positive | | DENV-positive | |
|---|---|---|---|---|---|---|---|
| | | | | No. (%) | Mean (range) Ct value‡ | No. (%) | Mean Ct value‡ |
| Perico | 12 | 29 | 6.5 (2–11) | 8 (67) | 30.40 (24.25–35.03) | 1 (6.6) | 37.8 |
| | 15 | 30 | 1 (1–3) | 15 (100) | 23.05 (19.10–30.50) | 1 (6.6) | 39.7 |
| Cardenas | 2 | 28–29 | 6 (6–6) | 0 | NA | 0 | NA |
| Jovellanos | 3 | 28–30 | 6 (6–8) | 0 | NA | 1 (33.3) | 39.3 |
| Colon | 27 | 27–30 | 6 (6–6) | 0 | NA | 0 | NA |
| Limonar | 3 | 28 | 6 (6–10) | 0 | NA | 0 | NA |
| Matanzas city | 4 | 28 | 4 (1–9) | 0 | NA | 1 (25) | 39.6 |
| Total | 66 | NA | 5.07 (1–9) | 23 (34.8) | NA | 4 (6.06) | NA |

*Internal control was positive for all tested samples by quantitative reverse transcription PCR. One sample from Perico municipality tested positive for both CHIKV and DENV. CHIKV, chikungunya virus; Ct, cycle threshold; DENV, dengue virus; NA, not applicable.
†Days of sample collection from illness onset.
‡Ct threshold was ≤40 for both CHIKV and DENV by quantitative reverse transcription PCR.

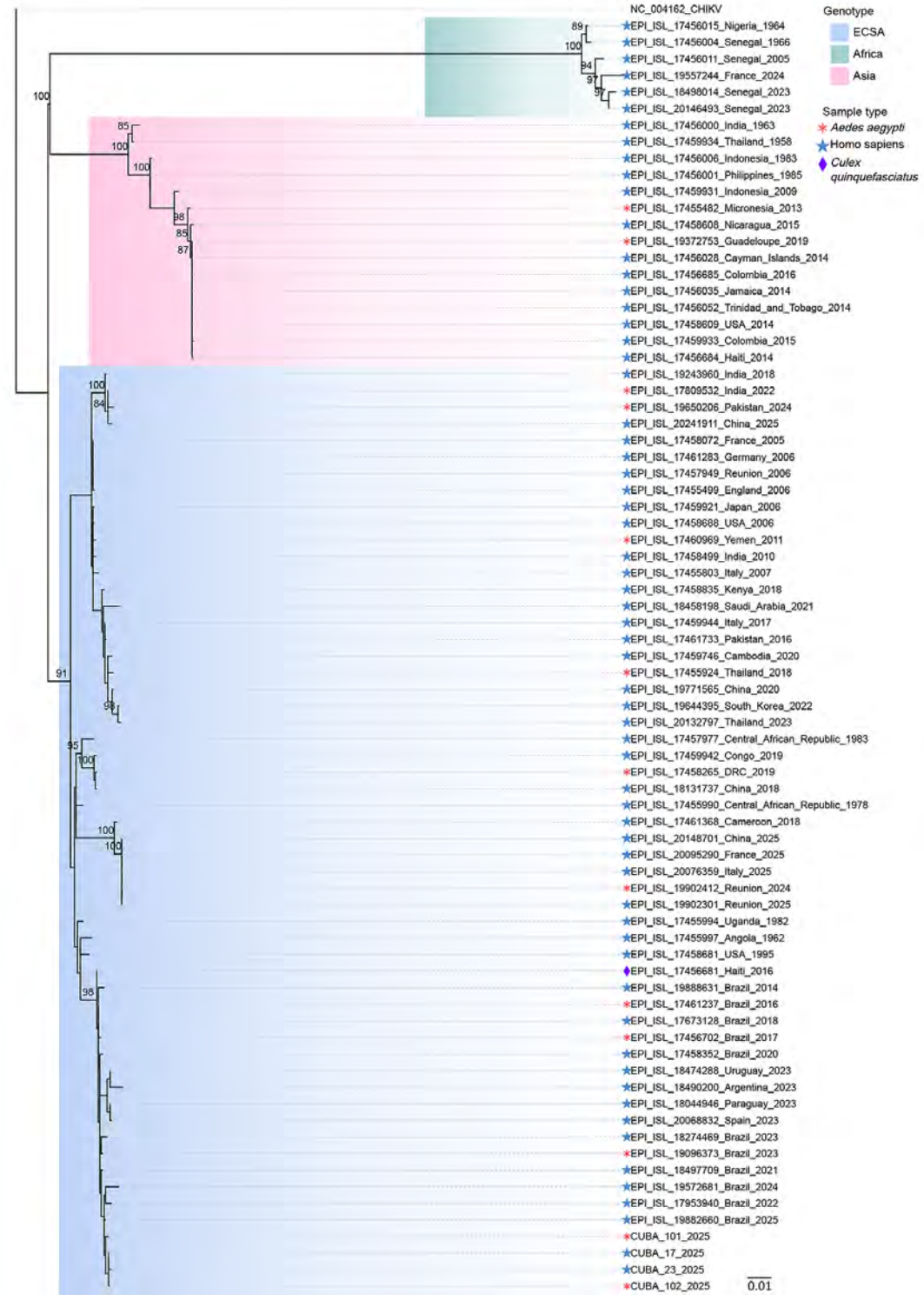


**Figure.** Molecular phylogenetic analysis of chikungunya virus from outbreak in Matanzas Province, Cuba, 2025. We obtained all available chikungunya virus sequences from GISAID, then filtered the sequences to ensure dataset and genetic diversity. We inferred evolutionary history by maximum-likelihood method by using the Tamura-Nei model (*6*). We applied the neighbor-joining method to a matrix of estimated pairwise distances to obtain initial trees and used a discrete gamma distribution to model evolutionary rate differences among sites. We conducted evolutionary analyses in MEGA version 6 (*7*). Numbers at branches indicate the percentage of trees in which associated taxa clustered together. Scale bar indicates number of substitutions per site. DRC, Democratic Republic of the Congo; USA, United States.

To assess the extent of transmission, we collected acute serum samples from AFI patients in Perico (15 samples) and neighboring municipalities (39 samples) on July 23 (Table). All samples tested negative for dengue IgM. All Perico samples tested positive for CHIKV; 1 case had DENV co-infection. No CHIKV was detected in neighboring municipalities, although 2 samples were positive for DENV.

After confirming CHIKV transmission, national surveillance was intensified through active AFI case finding; standardized case definitions for suspected and confirmed cases were implemented (*5*). By epidemiologic week 52, transmission was confirmed in 15 provinces and 147 municipalities, including 49,258 suspected cases, 1,959 confirmed cases, and 46 deaths. Severe cases included neurologic complications (encephalitis, Guillain-Barré syndrome, meningoencephalitis), cardiovascular manifestations (acute myocarditis, decompensation of preexisting conditions, pulmonary thromboembolism), and perinatal or neonatal transmission.

We conducted entomologic investigations in the home of the first identified case from a town in Perico and 9 neighboring households. We collected a total of 16 *Culex quinquefasciatus* and 8 *Aedes aegypti* mosquitoes and grouped them into 3 pools: 10 engorged *Cx. quinquefasciatus,* 3 engorged *Ae. aegypti*, and 2 nonengorged *Ae. aegypti*. All pools tested positive for CHIKV by qRT-PCR. Cycle threshold cutoff was 40; values were 36.1 in the *Cx. quinquefasciatus* pool, 39.6 in the engorged *Ae. aegypti* pool, and 21.7 in the nonengorged *Ae. aegypti* pool (Appendix Table, https://wwwnc.cdc.gov/EID/article/32/7/26-0344-App1.pdf).

The detection of CHIKV in engorged mosquitoes of both species suggests the presence of the virus in the blood of residents. Detection in nonengorged *Ae. aegypti* mosquitoes supports active viral replication and ongoing transmission. We ruled out contamination, because all extraction and PCR negative controls were negative and mosquito samples were processed separately from human specimens.

For genetic characterization, we sequenced CHIKV from 2 human serum samples and 2 mosquito pools (engorged and nonengorged *Ae. aegypti*) using the MinION (Oxford Nanopore Technologies, https://nanoporetech.com), achieving >80% genome coverage. Phylogenetic analysis showed that the Cuba sequences formed a monophyletic clade, sharing a most recent common ancestor with Brazil sequences from 2021 and 2025, and clustering with sequences from Uruguay, Paraguay, and Argentina from 2023 (Figure; Appendix). We classified the virus within genotype II ECSA, consistent with strains circulating in the Americas (Chikungunya Typing Tool version 3.72 (Genome Detective, https://www.genomedetective.com). We did not detect the E1-A226V mutation associated with increased infectivity in *Ae. albopictus* (*8*). We deposited sequences in GISAID (accession nos. EPI_ISL_20294022–25).

Our findings document a chikungunya outbreak in Cuba. A previous outbreak occurred in Santiago de Cuba Province in 2015 and was successfully contained; no subsequent transmission was detected (*3*). This outbreak underscores the importance of strengthening arbovirus surveillance systems. Early detection was achieved in a small town where the virus had not been previously reported, despite the presence of competent vectors and substantial travel exchange with other countries in the region.

In conclusion, chikungunya incidence might be increasing globally because of favorable climatic and environmental conditions, as well as the accumulation of susceptible populations. The Cuba outbreak highlights the need for integrated clinical, epidemiologic, virologic, and entomologic surveillance to explore additional mutations and clarify introduction pathways of arboviruses in the Americas.

**Acknowledgments**

We thank Jairo Mendez, Leticia Franco, Lionel Gresh Vagner Fonseca, Oswaldo Cruz Foundation, Belo Horizonte, Brazil University, for their useful comments, and Yosiel Molina Gómez, translator and language editor. We thank all health workers and the affected population of the province of Matanzas.

The ethics committee of the Pedro Kouri Tropical Medicine Institute reviewed and approved this project (no. 2505001). The samples processed in this study were obtained anonymously from material exceeding that used in the routine diagnosis of arboviruses.

This work was funded by the Cuban Ministry of Health. Real-time PCR reagents were provided by the Pan American Health Organization (PAHO).

Author contributions: M.G.G., S.R., and V.K. coordinated and designed the study, analyzed the results, and drafted and reviewed the manuscript. M.M.P., M.A., and R.G. conducted the laboratory work, analyzed the results, and cleaned data. M.M.P., A.J.B., S.S., M.P., and D.H. performed all real-time PCR assays. M.M.P. and R.G. performed the genetic characterization. A.C., Y.M., M.S., and M.R. conducted the field and laboratory vector studies. J.R.A., C.P., M.R., D.G., B.M.B.R., A.B.S., and

L.D.R. coordinated the clinical, epidemiologic, and field studies. B.M.B.R., A.B.S., L.D.R., and L.V. collected the clinical and epidemiological data. All authors reviewed the draft and approved the final version.

## About the Authors

Dr. Pérez is head of genomic surveillance of arboviruses at the virology department, Pedro Kouri Tropical Medicine Institute. Her main research interests are the diagnosis of viral diseases by molecular biology methods and the sequencing of viral genomes. Dr. Resik is head of the virology department at Pedro Kouri Tropical Medicine Institute. Her main research interests are in polio and nonpolio enteroviruses, as well as other viruses including herpes, HIV, rubella, measles, rabies, mumps, arbovirus, and respiratory viruses.

## References


1. Pan American Health Organization. Chikungunya: analysis by country. 2025 [cited 2025 Dec 5]. https://www.paho.org/es/arbo-portal/chikunguna-datos-analisis/chikunguna-analisis-por-pais
2. de Souza WM, Ribeiro GS, de Lima STS, de Jesus R, Moreira FRR, Whittaker C, et al. Chikungunya: a decade of burden in the Americas. Lancet Reg Health Am. 2024;30:100673. https://doi.org/10.1016/j.lana.2023.100673
3. Guzmán MG, Vázquez S, Álvarez M, Pelegrino JL, Amores DR, Martínez PA, et al. Laboratory surveillance of dengue and other arboviruses in Cuba, 1970–2017 [in Spanish]. Rev Cubana Med Trop. 2019;71:1–31.
4. Naveca FG, Nascimento VAD, Souza VC, Nunes BTD, Rodrigues DSG, Vasconcelos PFDC. Multiplexed reverse transcription real-time polymerase chain reaction for simultaneous detection of Mayaro, Oropouche, and Oropouche-like viruses. Mem Inst Oswaldo Cruz. 2017;112:510–3. https://doi.org/10.1590/0074-02760160062
5. General Directorate of Public Health of Havana. MINSAP. Cuban chikungunya protocol. 2025 [cited 2026 Mar 10]. https://temas.sld.cu/chikungunya/files/2025/12/protocolo-cubano-chikungunya-1.3.pdf
6. Kimura M. A simple method for estimating evolutionary rates of base substitutions through comparative studies of nucleotide sequences. J Mol Evol. 1980;16:111–20. https://doi.org/10.1007/BF01731581
7. Tamura K, Stecher G, Peterson D, Filipski A, Kumar S. MEGA6: Molecular Evolutionary Genetics Analysis version 6.0. Mol Biol Evol. 2013;30:2725–9. https://doi.org/10.1093/molbev/mst197
8. Tsetsarkin KA, Vanlandingham DL, McGee CE, Higgs S. A single mutation in chikungunya virus affects vector specificity and epidemic potential. PLoS Pathog. 2007;3:e201. https://doi.org/10.1371/journal.ppat.0030201


Address for correspondence: Maria G. Guzman, Instituto Medicina Tropical Pedro Kouri, Autopista Novia del Mediodía Km 6 1/2, Havana, Lisa 11600, Cuba; email: lupe@ipk.sld.cu

# etymologia revisited

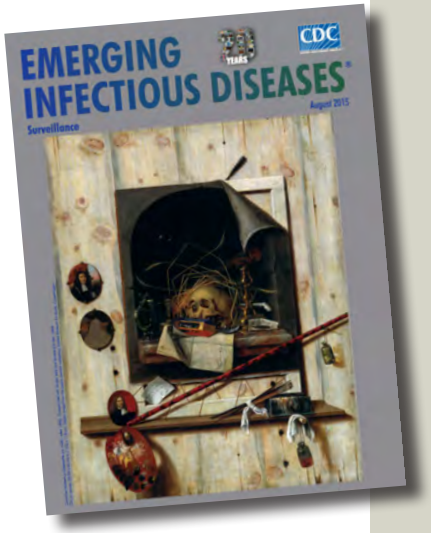


***Originally published in August 2015***

## *Escherichia coli*

[esh”ə-rik’e-ə co’lī]

A gram-negative, facultatively anaerobic rod, *Escherichia coli* was named for Theodor Escherich, a German-Austrian pediatrician. Escherich isolated a variety of bacteria from infant fecal samples by using his own anaerobic culture methods and Hans Christian Gram’s new staining technique. Escherich originally named the common colon bacillus *Bacterium coli commune*. Castellani and Chalmers proposed the name *E. coli* in 1919, but it was not officially recognized until 1958.

**References:**


1. Oberbauer BA. Theodor Escherich—Leben und Werk. Munich: Futuramed-Verlag; 1992.
2. Shulman ST, Friedmann HC, Sims RH. Theodor Escherich: the first pediatric infectious diseases physician? Clin Infect Dis. 2007;45:1025–9 .


**https://wwwnc.cdc.gov/eid/article/21/8/et-2108_article**

**Sherri Richards (1955–), *An Everlasting Love*, 2024** (detail). Acrylic and oil on gallery-wrapped canvas. 36 in x 36 in (91.44 cm x 91.44 cm). Used with permission of the artist.

# Jimmy Carter and Eradication of Guinea Worm Disease

Shannon O'Connor, Donald Hopkins, Vitaliano A. Cama

This month's cover, *An Everlasting Love* by Sherri Richards, features former US President Jimmy Carter (1924–2024) and his wife, Rosalynn (1927–2023). The painting, inspired by a photograph Mrs. Richards' husband, Dr. Frank Richards, took of the Carters on a trip to Ethiopia in 2007, depicts the Carters walking along a red dirt path that winds through a field of flowers and trees.

"The road had a reddish color, like the red clay of Georgia, and President and Mrs. Carter were walking up that road," Mrs. Richards recalled. "[The Carters] going up the path hand-in-hand was me seeing them walking to heaven together" (S. Richards, pers. comm., interview, 2026 Apr 13).

Mrs. Richards lives in Atlanta, Georgia, USA, and holds a fine arts degree from Georgia State University. Her husband, a public health expert on the elimination of parasitic diseases, worked for The Carter Center until he retired in 2024. *An Everlasting Love* was created that same year in response to an invitation from The Carter Center to donate a painting for its annual donor retreat and auction, as she had done in previous years.

Shown from behind, in casual clothes, the Carters' figures are instantly familiar. In the background, Mrs. Richards included some of Mrs. Carter's favorite flowers and butterflies. *An Everlasting Love* captures

Author affiliations: Centers for Disease Control and Prevention, Atlanta, Georgia, USA (S. O'Connor, V.A. Cama); The Carter Center, Atlanta (D. Hopkins)

DOI: https://doi.org/10.3201/eid3207.AC0746

the love and kindness for humanity and each other that the Carters shared, which helped lead to their founding of The Carter Center in 1982.

The Carter Center was created with a focus on human rights and peace but also established programs to eliminate or reduce certain tropical diseases because the Carters championed health as a fundamental human right. Since its founding, The Carter Center has improved the lives of millions of people affected by diseases neglected by public health systems around the world. The Carter Center's first executive director, appointed in 1986, was Dr. William Foege (1936–2026); Carter had appointed Dr. Foege director of the then-named Center for Disease Control (CDC) in 1977, during his presidency.

In the history of public health, only 2 diseases have been globally eradicated. First was smallpox in 1980, during Dr. Foege's tenure at CDC and in which he had a critical role; that accomplishment is heralded as one of mankind's greatest achievements. The second was rinderpest, a devastating veterinary disease with high mortality rates in cattle and wildlife, declared eradicated in 2011. Eradication of smallpox and rinderpest permanently relieved the world of 2 deadly infectious threats. Now, thanks to the work of President Carter and The Carter Center, another centuries-old illness might soon be added to that short list: dracunculiasis, also known as Guinea worm disease.

Guinea worm disease, a tropical disease of poverty, is caused by the nematode *Dracunculus medinensis*. Humans contract infections when they drink water contaminated with copepod crustaceans infected with Guinea worm larvae. When the copepod is digested, larvae penetrate the digestive tract, migrate into the body, and develop into adults. After ≈1 year, the gravid adult female worm makes its way to the skin, where it causes a burning and painful blister. Infected people seeking relief immerse the affected limb in water (often a nearby pond), which triggers the worm to emerge and eject larvae, contaminating the water. Copepods then ingest the larvae, perpetuating the life cycle.

During worm emergence, infected people experience intense pain, ulcer formation, and allergic reactions. Other symptoms include infections of the wound, general malaise, fever, and gastrointestinal symptoms. If the worm breaks during emergence, severe allergic reactions can result. Potential long-lasting complications include chronic inflammation, pain, and, in severe cases, disability resulting from joint damage.

Dracunculiasis is an ancient disease and was first called Guinea worm disease by Europeans who saw it along the Gulf of Guinea in West Africa. The organism has been found in an Egyptian mummy and likely was referenced by the Greek writer Agatharchides (2nd Century BCE). An anonymous medieval illustration depicting Saint Roch pointing his forefinger at a worm emerging from a wound on his inner thigh probably portrays dracunculiasis (Figure).

In 1980, after smallpox eradication, the Guinea Worm Eradication Program (GWEP) began at CDC. By 1982, the World Health Organization and the US Agency for International Development convened the first international meeting on Guinea worm eradication; in 1986, the World Health Assembly called for

**Figure.** An image of Saint Roch, a French pilgrim and plague saint from the 14th Century, by an unknown painter (ca. 15th–16th Century). The painting shows what is likely a Guinea worm emerging from his leg. Source: Wikimedia Commons.

elimination of Guinea worm disease, a goal that it later upgraded to global eradication. Also in 1986, aided by Carter's leadership and unique diplomatic skills, The Carter Center became the leading partner for the GWEP. Over the past 4 decades, CDC has provided technical support for those efforts, which have been endorsed by the World Health Organization, implemented by national programs of endemic countries, and backed by many other partners and benefactors.

The Carter Center and its partners' ongoing work to fight Guinea worm disease has yielded astounding results. In 1986, an estimated 3.5 million human cases of Guinea worm disease occurred across 21 countries in Asia and Africa. By the end of 2025, that number had dwindled to just 10 cases in 3 countries. That dramatic decrease was accomplished without drugs or vaccines, instead focusing on clean water, behavior modification, vector control, and other nonpharmaceutical interventions. However, in 2023, parasite persistence in animals led to redefinition of worldwide eradication by the International Commission for the Certification of Dracunculiasis Eradication as "confirmed absence of the emergence of adult female worms (defined as compatible with the interruption of transmission of *D. medinensis*) in humans and animals for three consecutive years or longer at the global level." Approximately 700 cases were detected in animals in 6 countries in 2025.

The GWEP has pioneered several interventions to support Guinea worm eradication efforts. Carter himself recruited many strategic partners that committed to support GWEP until eradication is accomplished. Those long-lasting partnerships ensured sustainability of key program interventions, such as filtering water through cloth to remove copepods, using variant straw-type filters for drinking water directly from ponds, and chemically treating water to reduce copepod infestation. In 2025, The Carter Center produced a documentary, *The President and the Dragon*, highlighting Carter's work behind the scenes toward the goal of dracunculiasis eradication.

The Carter Center has also spearheaded peace efforts to support health initiatives. In 1995, Carter brokered a cease fire in the Sudan civil war that enabled the GWEP to work in the conflict areas, while also providing urgently needed medical support and immunizations. Those efforts became the model for other similar peace for health initiatives. On the epidemiologic side, the GWEP established a reward system to improve detection of infections and postelimination surveillance. Most of those initiatives became established thanks to direct support from Carter. The Carter Center has also established health programs for elimination of diseases including river blindness (onchocerciasis), lymphatic filariasis, malaria, schistosomiasis, and trachoma.

Late in his life, President Carter stated he hoped to outlive Guinea worm disease. He did not reach that milestone, but his long years of support for interventions and research helped bring Guinea worm eradication within reach. When he accepted the Nobel Peace Prize in 2002, Carter said, "The bond of our common humanity is stronger than the divisiveness of our fears and prejudices. God gives us the capacity for choice. We can choose to alleviate suffering." Long after President Carter's death, the Carters' legacy at The Carter Center will continue to alleviate suffering and advance public health by fighting to eradicate Guinea worm disease and other neglected diseases.

## Bibliography


1. Biswas G, Sankara DP, Agua-Agum J, Maiga A. Dracunculiasis (Guinea worm disease): eradication without a drug or a vaccine. Philos Trans R Soc Lond B Biol Sci. 2013;368:20120146. https://doi.org/10.1098/rstb.2012.0146
2. The Carter Center. Guinea worm disease reaches all-time low: only 10 human cases reported in 2025. 2026 Jan 30 [cited 2026 Feb 17]. https://www.cartercenter.org/news/guinea-worm-announcement/
3. The Carter Center. International Task Force for Disease Eradication [cited 2026 Feb 17]. https://www.cartercenter.org/international-task-force-for-disease-eradication
4. The Carter Center. The President and the dragon. 2025 Sep 1 [cited 2026 Apr 16]. https://www.cartercenter.org/stories/documentary-debut-the-president-and-the-dragon
5. Centers for Disease Control and Prevention. History of smallpox. 2024 [cited 2026 Feb 19]. https://www.cdc.gov/smallpox/about/history.html
6. Eberhard ML, Ruiz-Tiben E, Hopkins DR, Farrell C, Toe F, Weiss A, et al. The peculiar epidemiology of dracunculiasis in Chad. Am J Trop Med Hyg. 2014;90:61–70. https://doi.org/10.4269/ajtmh.13-0554
7. Gaeta R, Bruschi F, Giuffra V. The painting of St. Roch in the picture gallery of Bari (15th century): an ancient representation of dracunculiasis? J Infect. 2017;74:519–21. https://doi.org/10.1016/j.jinf.2017.02.002
8. Hopkins DR, Weiss AJ, Yerian S, Ortega YR, Zhao Y, Eneanya OA, et al. Progress toward eradication of dracunculiasis (Guinea worm disease)—worldwide, January 2024–June 2025. MMWR Morb Mortal Wkly Rep. 2026;74:648–54. https://doi.org/10.15585/mmwr.mm7442a2
9. International Commission for the Certification of Dracunculiasis Eradication. Outcomes of 12th meeting [cited 2026 Jun 2]. https://www.who.int/groups/international-commission-for-the-certification-of-dracunculiasis-eradication
10. Morens DM, Holmes EC, Davis AS, Taubenberger JK. Global rinderpest eradication: lessons learned and why humans should celebrate too. J Infect Dis. 2011;204:502–5. https://doi.org/10.1093/infdis/jir327


Address for correspondence: Shannon O'Connor, Centers for Disease Control and Prevention, 1600 Clifton Rd NE, Mailstop H16-2, Atlanta, GA 30329-4018, USA; email: fue7@cdc.gov

# EMERGING INFECTIOUS DISEASES®

## Upcoming Issue • August 2026
## Foodborne and Other Enteric Diseases

- Western Equine Encephalitis Virus in Blood Donors during Outbreak, Argentina, 2023–2024
- Use of *Salmonella* Typhi Hemolysin E and Lipopolysaccharide IgA to Identify Enteric Fever Cases, South Asia
- Epidemiologic, Entomologic, and Virologic Findings during the Reemergence of Western Equine Encephalitis Virus in Argentina
- Qualitative Risk Assessment of Infectious Agents Associated with Canine Importation into Canada
- Occupationally Exposed and General Population Antibody Profiles to Influenza A Viruses Circulating in Swine as an Indication of Zoonotic Risk
- Rapid Expansion of Highly Pathogenic Avian Influenza A(H5N1) Clade 2.3.4.4b Genotype D1.1 Virus across Flyway Regions, North America, Fall 2024
- Evaluation of Virulence of *Burkholderia pseudomallei* Strains from the Western Hemisphere and Africa in the BALB/c and C57BL/6 Mouse Models of Inhalational Melioidosis
- Systemic Distribution and Protracted Detection of Clade 2.3.4.4b Highly Pathogenic Avian Influenza A (H5N1) D1.2 in Swine after Experimental Inoculation
- Entomologic Surveillance and Pathogen Detection Focussing on *Aedes* (*Stegomyia*) *aegypti* and Dengue Virus in an Arid Urban Environment
- Detection of Congenital Syphilis Case via Digital PCR and Next-Generation Sequencing, Colombia
- Hepatitis A Outbreak Associated with Frozen Blueberries, the Netherlands, November 2024–February 2025
- Antibodies Cross-Reactive with Bundibugyo Virus in Ferrets Vaccinated with Ebola Virus Vaccine
- Genomic Epidemiology of Emergent Multisource, Multiseason *Vibrio parahaemolyticus* Acute Gastroenteritis Outbreaks in Aotearoa New Zealand, 2019–2022
- Respiratory Syncytial Virus Suppression through Public Health and Social Measures, Hong Kong, China, 2020–2023
- Human Cases of *Borrelia miyamotoi* Disease, Slovenia, 2025
- Outbreak of *Salmonella enterica* Serovar Reading Linked to Dried Bovine Meat, Australia, 2023
- Identification of Camel Prion Disease in Tataouine, Tunisia, 2019-2021:
- Filovirus Surveillance in Communities Bordering Cameroon, Equatorial Guinea Marburg Outbreak, 2023
- Infectious Highly Pathogenic Avian Influenza H5N1 Virus Isolated from Fetal Bovine Serum
- Association of Medically-Attended Infections in Infancy with Long-Term Weight Gain and Obesity among Children in Southern California, USA
- Hepatitis A Outbreak in a Skilled Nursing Facility, Los Angeles County, California, USA, 2025
- Human *Lactococcus garvieae* Bloodstream Infection Complicated by Spondylodiscitis, Germany
- Updated Passive Surveillance of Human-Parasitizing Ticks and Tickborne *Borrelia*, *Ehrlichia*, and *Rickettsia* spp. in Texas, USA, 2014–2021
- Extragenital Antimicrobial Resistance Patterns in *Neisseria gonorrhoeae*, US Military Medical Centers, 2022–2024
- Multifarm Outbreak of Novel Parvovirus in Pigs Associated with Exophthalmos and Erythema, the Netherlands, 2024
- Detection of a $bla_{OXA-23}$-positive *Proteus mirabilis* Isolate through the CDC Antimicrobial Resistance Laboratory Network, United States, 2024

**Complete list of articles in the August issue at http://www.cdc.gov/eid/#issue-334**

## Earning CME Credit

To obtain credit, you should first read the journal article. After reading the article, you should be able to answer the following, related, multiple-choice questions. To complete the questions (with a minimum 75% passing score) and earn continuing medical education (CME) credit, please go to http://www.medscape.org/journal/eid. Credit cannot be obtained for tests completed on paper, although you may use the worksheet below to keep a record of your answers.

You must be a registered user on http://www.medscape.org. If you are not registered on http://www.medscape.org, please click on the "Register" link on the right hand side of the website.

Only one answer is correct for each question. Once you successfully answer all post-test questions, you will be able to view and/or print your certificate. For questions regarding this activity, contact the accredited provider, CME@medscape.net. For technical assistance, contact CME@medscape.net. American Medical Association's Physician's Recognition Award (AMA PRA) credits are accepted in the US as evidence of participation in CME activities. For further information on this award, please go to https://www.ama-assn.org. The AMA has determined that physicians not licensed in the US who participate in this CME activity are eligible for *AMA PRA Category 1 Credits*™. Through agreements that the AMA has made with agencies in some countries, AMA PRA credit may be acceptable as evidence of participation in CME activities. If you are not licensed in the US, please complete the questions online, print the AMA PRA CME credit certificate, and present it to your national medical association for review.

## Article Title

### Trichinellosis Outbreak Linked to Undercooked Bear Jerky, North Carolina, USA, 2024

## CME Questions

**1. Which of the following statements regarding trichinellosis is most accurate?**

A. There were 106 cases of trichinellosis reported in North Carolina between 1991 and 2022
B. Complete freezing of wild game meat will eliminate the risk for trichinellosis
C. There were no motile *Trichinella spiralis* larvae noted after freezing meat in the current study
D. Seroconversion in trichinosis can occur weeks after infection

**2. What were 3 of the symptoms required to define clinical trichinellosis in the current study?**

A. Fever, periorbital edema, eosinophilia
B. Fever, rash, transaminitis
C. Myalgia, headache, neutropenia
D. Myalgia, diarrhea, acute kidney injury

**3. What was the overall attack rate of trichinellosis after the consumption of bear jerky in the current study?**

A. 10%
B. 30%
C. 50%
D. 90%

**4. What was the median incubation period for trichinellosis in the current study?**

A. 4 days
B. 8 days
C. 14 days
D. 33 days